

Directed Evolution of an Fe^{II}-Dependent Halogenase for Asymmetric C(sp³)-H Chlorination

This dissertation is submitted for the degree of
Doctor of natural science
(Dr. rer. nat.)

presented to the Department of Chemistry
of the Philipps-University Marburg

by Sabine Düwel, M.Sc.
from Saarbrücken, Germany

Marburg/Lahn 2018

Die vorliegende Dissertation entstand in der Zeit von September 2015 bis September 2018 am Fachbereich Chemie der Philipps-Universität Marburg in der Arbeitsgruppe Hoebenreich und unter der Betreuung von Frau Dr. Sabrina Hoebenreich.

Vom Fachbereich Chemie der Philipps-Universität Marburg (Hochschulkennziffer 1180)
Dissertation am 19.12.2018 angenommen.

Erstgutachterin: Dr. Sabrina Hoebenreich

Zweitgutachter: Prof. Dr. Eric Meggers

Tag der mündlichen Prüfung: 19.12.2018

You never lose. Either you win, or you learn.

Nelson Mandela

Erklärung

Ich erkläre, dass eine Promotion noch an keiner anderen Hochschule als der Philipps-Universität Marburg, Fachbereich Chemie, versucht wurde.

Ich versichere, dass ich meine vorgelegte Dissertation „Directed Evolution of an Fe^{II}-Dependent Halogenase for Asymmetric C(sp³)-H Chlorination“ selbst und ohne fremde Hilfe verfasst, nicht andere als die in ihr angegebenen Quellen oder Hilfsmittel benutzt, alle vollständig oder sinngemäß übernommenen Zitate als solche gekennzeichnet sowie die Dissertation in der vorliegenden oder einer ähnlichen Form noch bei keiner anderen in- oder ausländischen Hochschule anlässlich eines Promotionsgesuchs oder zu anderen Prüfungszwecken eingereicht habe.

Marburg, den

Sabine Düwel

Zusammenfassung

Im Rahmen dieser Arbeit wurde Chlorinase *Wi-WelO15* von *Westiella intricata* UH HT-29-1 bezüglich ihrer Anpassungsfähigkeit an nicht-natürliche Substrate sowie ihre biokatalytische Anwendung getestet.

Organohalogene spielen eine wichtige Rolle als Pharmazeutika, Agrarchemikalien oder synthetische Intermediate. Jedoch ist die selektive Chlorierung aliphatischer Kohlenstoffe an komplexen Molekülen unter milden, nicht giftigen Bedingungen noch immer eine große Herausforderung in der chemischen und enzymatischen Katalyse.

2014 wurde eine neue Klasse aliphatischer Halogenasen entdeckt, die ein großes Potential als Biokatalysator für late-stage Chlorierung hat. Die Enzymklasse gehört zu einer großen Familie von nicht-Häm-Eisen Oxygenasen. Eine zuvor gefundene Unterklasse von aliphatischen Halogenasen ist abhängig davon, dass die Substrate an ein Acyl-Carrier-Protein gebunden sind. Im Gegensatz dazu, können Mitglieder der neuen Halogenasen-Unterklasse freistehende Substrate halogenieren. Synthetische Methoden, die von Chemikern benutzt werden um gewünschte Substrate herzustellen, können als Synthese-Werkzeugkoffer verstanden werden. Wenn diese Klasse von Halogenasen so angepasst werden kann, dass nicht-natürliche Substrate selektiv chloriert werden und die Enzyme im Labor einfach produziert und verwendet werden können, können sie als neue Methode zum Werkzeugkoffer hinzugefügt werden um Halogene zu einem späten Synthesestadium an komplexe Moleküle hinzuzufügen..

Wi-welO15 and *Hw-welO15* (von *Hapalosiphon welwitschii* UH IC-52-3) wurden aus der entsprechenden genomischen DNA amplifiziert und in ein Plasmid, welches mit hoher Kopienanzahl in der Zelle vorliegt, eingefügt. Durch heterologe Expression in *E. coli* konnten die Halogenasen in guten Ausbeuten von 60-80 mg/L Zellkultur hergestellt werden. Aufreinigung wurde durch Affinitäts-Chromatographie und wenn nötig auch Größenausschlusschromatographie erreicht. Kristallisation der Variante *Wi-0*, der Startpunkt für die gerichtete Evolution, wurde erreicht und die Enzymstruktur konnte gelöst werden. Um die Chlorierungsaktivität an nicht-natürlichen Substraten zu untersuchen, wurde eine Anzahl nicht natürlicher Substrate synthetisiert, die eine Keto-Funktion, anstelle des natürlich vorkommenden Isonitriles, tragen. Diese wurden durch die Wildtyp Enzyme unter initialen Bedingungen nicht chloriert.

Zunächst, als keine Strukturinformationen vorhanden waren, wurde ein Enzym-Model mit Hilfe von SwissModel kreiert um *Hw-WelO15* zufällig zu mutieren. Als die Enzymstruktur von *Wi-0* gelöst war, wurde gerichtete Evolution mittels semi-rationaler und rationaler Mutagenese angewendet. Innerhalb von 4 Generationen wurde die Halogenase an das ausgewählte Leitmolekül angepasst. Eine Anzahl an Chlorinasen wurden als Zellysate sowie als aufgereinigt Enzyme getestet und die besten Varianten zeigten 87% Produktbildung unter optimierten Bedingungen, während die Startvariante *Wi-0* Produktbildung von <1% zeigt. Modifikationen

am Leitmolekül wurden teilweise akzeptiert und insgesamt wurde die regio- und diastereoselektive Chlorierung von fünf nicht-natürlichen Substraten, mit Chemoselektivitäten von 96-99% ermöglicht. Weitere fünf Substrate wurden in komplexe Produktmixe transformiert. Unter allen gebildeten Produkten konnte nur ein chloriertes Produkt gefunden werden.

Wenn nicht-natürliche Substrate von Halogenasen umgesetzt werden, werden häufig vor allem hydroxylierte Produkte gebildet. Eine Enzymvariante, die während der gerichteten Evolution gefunden wurde, hatte eine verringerte Chemoselektivität von 68% Chlorierung und 32% Hydroxylierung. Mit dem Ziel Biokatalysatoren zu erschaffen, die nur Hydroxylierung erzielen, wurden mehrere Varianten erstellt, diese hatten jedoch keine Aktivität. Stattdessen wurde die Monooxygenase P450_{BM3} verwendet um vier neue, hydroxylierte und epoxidierte Produkte herzustellen.

Halogenasen, die während verschiedenen Stufen der gerichteten Evolution gefunden wurden, wurden bezüglich ihrer kinetischen Eigenschaften untersucht. Dabei zeigte sich, dass die beste Variante eine 93-fache Verbesserung im Vergleich zum niedrigsten, messbaren k_{cat}/K_m hatte. Die beiden Varianten mit höchster Produktbildung unterschieden sich jeweils in ihren Eigenschaften. Während *Wi-11* mit einem k_{cat} von 0.64 min^{-1} die höchste Umsatzrate hat, kann *Wi-12* die Substrate besser binden mit dem niedrigsten K_m von $20 \mu\text{M}$.

Weiterhin wurde die Stabilität der Halogenasen untersucht und stabilisierte *Wi-WelO15* Varianten, die von dem PROSS Server vorgeschlagen wurden, hergestellt. Zum Auslesen der Stabilität wurde die Schmelztemperatur (T_m) der Enzyme bestimmt. Es zeigte sich, dass die Halogenasen mit T_m von $62 \text{ }^\circ\text{C}$ für *Hw-WelO15* und $54 \text{ }^\circ\text{C}$ für *Wi-WelO15* schon recht stabil sind. Die hergestellten Varianten während des Aktivitätsscreening zeigten im Vergleich zur Startvariante generell schon eine leichte Verbesserung in ihrer thermischen Stabilität und Kombination aus stabilitäts- sowie aktivitätsverbessernden Mutationen resultierte in der stabilsten *Wi-WelO15* Variante *Wi-5P3* mit $T_m=61 \text{ }^\circ\text{C}$. Inkubation der aufgereinigten Enzyme in Puffer bei verschiedenen Temperaturen mit anschließender SDS-PAGE Analyse zeigte, dass für die stabilste Variante nach 4 h bei $65 \text{ }^\circ\text{C}$ immer noch lösliches Enzym vorhanden war. Aktivitätstests bei erhöhten Temperaturen zeigten überdies eine Restaktivität von 90% bei Reaktionen, die bei $45 \text{ }^\circ\text{C}$ gemacht wurden sowie 85% Restaktivität in Anwesenheit von 5% Ethanol.

Abstract

Within this thesis, the chlorinase *Wi-WelO15* from *Westiella intricata* UH strain HT-29-1 was explored for its evolvability towards non-natural substrates and its biocatalytic applicability.

Organohalogens play an important role as pharmaceuticals and agricultural chemicals or synthetic intermediates. However selective aliphatic chlorination under mild and non-hazardous conditions at complex molecules is still a formidable challenge in chemical and enzymatic catalysis.

A new class of aliphatic halogenases, which carries a great potential as useful biocatalysts for late stage chlorination, was discovered in 2014. The enzyme class belongs to a big superfamily of non-heme iron oxygenases. A previously found subclass of aliphatic halogenases are dependent on an acyl-carrier protein, in contrast to that, the new subclass is able chlorinate free-standing substrates. Synthetic methods, available to chemists, can be imagined as a toolbox which is used to create molecules of interest. If this class of halogenases can be engineered to chlorinate selectively non-natural substrates and can be produced and used under convenient conditions in the lab, they can be added to the synthesis toolbox enabling late-stage chlorination at complex molecules.

Within this thesis, *Wi-welO15* and *Hw-welO15* (from *Hapalosiphon welwitschii* UH IC-52-3) were amplified from genomic DNA, and inserted into a high copy plasmid, resulting in great amounts of 60-80 mg enzyme/L expression culture by heterologous expression in *E. coli*. Purification of the halogenase was achieved by immobilized metal affinity chromatography and if necessary, also size exclusion chromatography. Crystallization of the starting variant *Wi-0* for directed evolution was achieved and a structure of the enzyme could be solved by molecular replacement. To test the evolvability of the halogenases towards non-natural substrates, a lead molecule was chosen that contains a ketone instead of the naturally occurring isonitrile functionality, which was not converted by both halogenases, with initial reaction conditions.

First random mutagenesis of *Hw-WelO15*, based on a model created by SwissModel, was pursued while no structural information was available. After we solved the structure of *Wi-0*, directed evolution via semi-rational and rational mutagenesis was applied to evolve the halogenase in 4 generations to accept the chosen lead molecule. A panel of chlorinases was tested as lysates as well as isolated enzymes. Hereby the best variants revealed up to 87% product formation under optimized conditions while <1% product formation was present with *Wi-0*. Modifications at the lead structure were partially accepted and in total five non-natural substrates were chlorinated with >99.9% regio- and diastereoselectivity and chemoselectivities of up to 96-99%. In addition, transformation of a range of seven substrates were transformed into complex mixtures of novel products.

Hydroxylation by aliphatic halogenases is described, if non-native substrates are used. One variant found in the directed evolution already has a decreased chlorination selectivity and produces 32% hydroxylated side product. With the goal to increase the hydroxylation selectivity, several variants were created. Because these catalysts completely lost their activity, instead the monooxygenase P450_{BM3} was used to produce four new, oxygenated products of the lead structure.

Our discovered halogenases from different states of the engineering process were characterized for their kinetic properties, revealing that the best variant *Wi-12* has a 93-fold improvement in comparison to *Wi-2*, which has the lowest measurable k_{cat}/K_m . The two variants with highest product formation each have their own kinetic profile. While *Wi-11* is most active with a k_{cat} of 0.64 min^{-1} , *Wi-12* has the lowest K_m of $20 \text{ }\mu\text{M}$ for the lead substrate.

Furthermore, the stability of the halogenases was examined and stabilized variants proposed by the PROSS server created. As read out, melting temperatures were determined revealing a high thermal stability for the wild types with T_m of $62 \text{ }^\circ\text{C}$ for *Hw-WelO15* and $54 \text{ }^\circ\text{C}$ for *Wi-WelO15*. Created variants generally showed an improve in thermal stability and combination of stability with activity improving mutations resulted in a melting temperature of $61 \text{ }^\circ\text{C}$ for *Wi-5P3*. Incubation of purified enzymes in buffer at different temperatures with subsequent SDS-PAGE analysis showed that after incubation at $65 \text{ }^\circ\text{C}$ for 4 h, still soluble enzyme of the stabilized variants remains. Activity assays at increased temperatures or solvent ratios, showed a residual activity of 90% at $45 \text{ }^\circ\text{C}$ with *Wi-5P3* and 85% residual activity in the presence of 5% ethanol.

Danksagung

Ein großes Dankeschön an Dr. Sabrina Hoebenreich, für die Betreuung und Unterstützung in den letzten Jahren, die erfolgreiche Zusammenarbeit und die Einführung in die Welt der Biokatalyse.

Ich danke Herrn Professor Meggers für die Übernahme des Zweitgutachtens und die Unterstützung während meiner Promotion.

Ein herzliches Dankeschön auch an die Professoren Reetz und Meggers, sowie an alle Gruppenmitarbeiter für das Teilen von Geräten und die Einladungen zu gemeinsamen Gruppenaktivitäten. Hier möchte ich insbesondere Adriana, Dr. Sun, Majia, Qie, Jie und Xiaoshanq nennen, die eine interessante, angenehme, internationale Zusammenarbeit ermöglicht haben. Des Weiteren möchte ich Erik, Yvonne, Lissi, Conni, Thomas M. und Thomas C. danken, die als Labornachbarn immer offen für Diskussionen und nette Gespräche waren.

Ich danke allen ehemaligen Mitgliedern des Arbeitskreises Hoebenreich für die angenehme, kreative Arbeitsatmosphäre. Insbesondere Nati, für die gemeinsame Zeit und Unterstützung. Luca, Henrik, Max und Nikolai, danke für die vereinte Arbeitskraft im Halogenasenprojekt.

Olalla I would like to thank you for advices and support in the last years. Your open door means a lot to me. Auch allen Gruppenmitgliedern des Vázquez Arbeitskreises möchte ich danken, insbesondere Bene, Greta und Lea die mit Nati und mir den Kern der chemischen Biologie gebildet haben.

Den Korrekturlesern Nati, Bene und Erik möchte ich danken für Kommentare und Vorschläge.

Thanks to Prof. Dr. Rajesh Viswanathan for synthesis of substrates and plasmids of WelI1, WelI3 and WelP3.

Für die finanzielle Unterstützung während meiner Promotion danke ich dem LOEWE Schwerpunktprojekt SynChemBio. Ebenso dem DAAD sowie der GDCh, die mir die Teilnahme an mehreren Konferenzen ermöglicht haben.

Dank an alle Serviceabteilungen des Fachbereichs Chemie der Philipps-Universität Marburg, im Speziellen Dr. Srinivasan und Ralf Pöschke, Dr. Harms sowie Frau Dr. Xie.

An alle meine Vertiefungs- und Masterstudenten: Phuong, Alex, Luca, Henrik, Max, Sascha, Simon, Niklas, Erik, Dominik, Rebecca, Nora, Daniel, Tabea und Nikolai ein großes Dankeschön, eure Mitarbeit an den Projekten und die Diskussionen haben den Arbeitsalltag interessant gemacht.

Abschließend möchte ich vor allem meiner Familie für die immerwährende Unterstützung danken.

Publikationen

Zeitschriftenartikel

S. Duetzel, L. Schmermund, K. Harms, T. Faber, V. Srinivasan, S. Hoebenreich (2018) *Directed Evolution of an Fe(II)-Dependent Halogenase for Asymmetric C(sp³)-H Chlorination*, submitted.

N. Nett, S. Duetzel, L. Schmermund, G. E. Benary, K. Ranaghan, D. J. Opperman, A. Mulholland, S. Hoebenreich, (2018) *A Robust and Stereocomplementary Panel of Ene-Reductase Variants for Gram-Scale Asymmetric Hydrogenation*, Manuscript in preparation.

N. Nett*, S. Duetzel*, A. A. Richter, S. Hoebenreich, (2017) *Revealing Additional Stereo-complementary Pairs of Old Yellow Enzymes by Rational Transfer of Engineered Residues*, ChemBioChem, *equal contribution

Posterpräsentationen

S. Duetzel, L. Schmermund, V. Srinivasan, S. Hoebenreich, (2018), *Novel Enzymes 2018*, Darmstadt, Deutschland, Asymmetric C(sp³)-H Chlorination Through Engineered Halogenases

S. Duetzel, L. Schmermund, H. Mueller, R. Viswanathan, V. Srinivasan, S. Hoebenreich, (2017), *134th International Summer Course*, BASF, Ludwigshafen, Deutschland, Expanding the Substrate Scope of Fe(II) dependent Halogenase WelO15 by Directed Evolution

S. Duetzel, L. Schmermund, H. Mueller, R. Viswanathan, V. Srinivasan, S. Hoebenreich, (2017), *Biotrans*, Budapest, Expanding the Substrate Scope of Fe(II) dependent Halogenase WelO15 by Directed Evolution

Vorträge

S. Duetzel, (2017), *Fachbereichstag Chemie 2017*, Philipps-Universität Marburg, Marburg, Deutschland, Biokatalytische C(sp³)-H Funktionalisierung durch Halogenasen

Content

1. Introduction.....	1
1.1 Relevance of Organohalogens	1
1.2 Halogenation Methods	2
1.2.1 Chemical Halogenation	3
1.2.2 Biological Halogenation	5
1.3 Non-Heme Iron, α -Ketoglutarate Dependent Enzymes	8
1.3.1 Crystal Structure.....	9
1.3.2 Mechanism	11
1.3.3 Halogenation versus Hydroxylation	13
1.3.4 Halogenase <i>Wi-WelO5</i>	15
1.4 Biocatalysis	17
1.4.1 Green Chemistry.....	18
1.4.2 Enzyme Engineering and Directed Evolution.....	19
2. Thesis Goal	23
3. Results and Discussion	25
3.1 Biosynthetic Pathway of Hapalindole-type Alkaloids.....	26
3.1.1 Recloning and Heterologous Expression of <i>WelP1</i> , <i>HpI1</i> and <i>HpI3</i>	27
3.1.2 Cloning and Heterologous Expression of Oxygenases <i>WelO11</i> - <i>WelO19</i>	28
3.1.3 Characterization of Aliphatic Halogenases <i>Wi-WelO15</i> and <i>Hw-WelO15</i>	30
3.2 Halogenase Production and Purification.....	32
3.2.1 Structural Analysis of Halogenases <i>Wi-0</i> and <i>Hw-WelO15</i>	37
3.3 Syntheses of Hapalindole Derivatives and Biotransformation.....	41
3.4 Engineering of Halogenase <i>WelO15</i>	45
3.4.1 Random Mutagenesis	45
3.4.2 Structure Guided Directed Evolution of <i>Wi-WelO15</i>	49
3.5 Handling the Halogenase and Optimization of Protocols.....	62
3.5.1 Temperature of Heterologous Expression	62
3.5.2 Whole Cell Biotransformation	63
3.5.3 Influence of Additives in Lysate Transformations	64
3.5.4 Influence of Additives in Transformations with Purified Enzymes	65
3.5.5 Final Reaction Conditions	70
3.6 Substrate Scope	72
3.6.1 Biotransformation with <i>Wi-0</i> and <i>Hw-WelO15</i> and Small Molecule Isonitriles.....	72
3.6.2 Biotransformation with <i>WelO15</i> variants and Hapalindole-like Ketones	74
3.6.3 Hapalindole-like Nitrile, Isothiocyanate and Isonitriles.....	83
3.6.4 Hydroxylation of Screening Substrate 54.....	85

Content

3.7 Preparative Scale Reactions with Halogenase <i>Wi-WelO15</i>	94
3.7.1 Characterization of Chlorinated Products	94
3.7.2 Characterization of Unselective Reactions.....	97
3.8 Kinetic Analysis.....	98
3.9 Temperature and Solvent Stability of <i>WelO15</i>	100
3.9.1 Temperature Stability	101
3.9.2 Solvent Stability	106
4. Summary and Conclusion.....	108
5. Outlook	114
6. Material.....	117
6.1 Organisms and Genes.....	117
6.2 Media and Buffer.....	118
6.3 Primer.....	119
6.4 Programs and Online Tools	122
6.5 Devices	123
6.6 Chemicals.....	124
7. Methods	125
7.1 Biological Experiments	125
7.1.1 Cloning with Polymerase Chain Reaction	125
7.1.2 Mutagenesis with Polymerase Chain Reaction	126
7.1.3 Agarose Gel Electrophoresis.....	134
7.1.4 DpnI Digestion and Dialysis.....	135
7.1.5 Electrotransformation	135
7.1.6 Preparation of Electrocompetent Cells ^[437]	136
7.1.7 Plasmid Preparation.....	136
7.1.8 Cultivation of Precultures and Preparation of Glycerol Stocks.....	136
7.1.9 Heterologous Expression for Enzyme Production	137
7.1.10 Purification of Enzymes and Determination of Concentration	139
7.1.11 Sodium Dodecyl Sulfate Polyacrylamide Gel Electrophoresis	142
7.1.12 Determination of Intact Protein Mass (performed by Mass Department)	143
7.1.13 Tryptic Digestion (performed by Mass department)	144
7.1.14 Crystallization.....	144
7.1.15 Circular Dichroism Spectroscopy.....	148
7.1.16 Docking.....	148
7.2 Biotransformation.....	149
7.2.1 General Information.....	149
7.2.2 Biotransformation and Analysis of Substrate Scope - <i>Hw-WelO15</i> and <i>Wi-0</i>	150
7.2.3 Screening of Libraries in Cell Lysate	152

Content

7.2.4 Analysis of Reaction Conditions with <i>Wi-WelO15</i> Variants.....	153
7.2.5 Analysis of Substrate Scope with Optimized Reaction Conditions	155
7.2.6 Kinetic Analysis of Halogenase Variants	157
7.2.7 Screening of P450 Libraries	158
7.3 Preparative Scale Biotransformation	159
7.3.1 Halogenase	159
7.3.2 Oxygenase P450 _{BM3}	169
7.3.3 Reductase <i>TsER</i>	172
7.4 Chemical Synthesis.....	174
7.4.1 General Information.....	174
7.4.2 (<i>S</i>)-2,2-dimethyl-5-(prop-1-en-2-yl)cyclohexan-1-one (64)	175
7.4.3 (<i>5S,6S</i>)-6-(1 <i>H</i> -indol-3-yl)-2,2-dimethyl-5-(prop-1-en-2-yl)cyclohexan-1-one (54) ..	176
7.4.4 (<i>5S,6S</i>)-2,2-dimethyl-6-(5-methyl-1 <i>H</i> -indol-3-yl)-5-(prop-1-en-2-yl)cyclohexan-1-one (76)	177
7.4.5 (<i>5S,6S</i>)-6-(5-methoxy-1 <i>H</i> -indol-3-yl)-2,2-dimethyl-5-(prop-1-en-2-yl)cyclohexan-1-one (77).....	178
7.4.6 (<i>5S,6S</i>)-2,2-dimethyl-6-(6-methyl-1 <i>H</i> -indol-3-yl)-5-(prop-1-en-2-yl)cyclohexan-1-one (78)	179
7.4.7 (<i>5S,6S</i>)-6-(1 <i>H</i> -indol-3-yl)-2-methyl-5-(prop-1-en-2-yl)cyclohex-2-en-1-one (84)	180
7.4.8 (<i>S</i>)-2-(1 <i>H</i> -indol-3-yl)-3-methyl-6-(propan-2-ylidene)cyclohexan-1-one (8).....	180
7.4.9 6-(1 <i>H</i> -indol-3-yl)-2-methylcyclohex-2-en-1-one (85).....	181
7.4.1 6-(1 <i>H</i> -indol-3-yl)-2-methyl-5-(prop-1-en-2-yl)cyclohex-2-en-1-one (86)	182
7.4.1 (1 <i>H</i> -indol-3-yl)-6-methyl-3-(prop-1-en-2-yl)cyclohexan-1-one (87)	182
7.5 Analytical Methods	184
7.5.1 GC Measurements	184
7.5.2 HPLC Measurements	184
7.5.3 LC-MS	185
7.5.4 Preparative HPLC Purification.....	186
7.5.5 Mass Analysis	186
8. Appendix	188
8.1 List of Abbreviations.....	188
8.2 Names of Enzyme Variants.....	190
8.3 Biological Part	191
8.3.1 Cloning Information.....	191
8.3.2 Genes	193
8.3.3 Fast Protein Liquid Chromatography	200
8.3.4 Crystallization.....	203
8.3.5 Circular Dichroism and Stability.....	205

Content

8.3.6 Docking.....	214
8.4 Mutagenesis.....	216
8.4.1 Mutations in Sequenced Clones after Error Prone PCR.....	216
8.4.2 Quick Quality Control after Semi-Rational Mutagenesis	217
8.5 Biotransformation.....	221
8.5.1 SDS-PAGE Analysis of Whole Cells	221
8.5.2 SDS-PAGE Analysis of OD ₆₀₀ normalized Cell Lysate	221
8.5.3 SDS-PAGE Analysis of Purified Enzymes	222
8.5.4 HPLC Chromatograms of Biotransformation	223
8.5.5 Selectivities of Hapalindole-like Ketones.....	225
8.5.6 Hydroxylation with P450 _{BM3}	226
8.5.7 Kinetics.....	227
8.6 Analytic of Compound Characterization.....	229
8.6.1 NMR and HPLC/GC Chromatograms of Compounds 53-87.....	229
9. Literature	270

1. Introduction

1.1 Relevance of Organohalogens

In 1968 only 24 naturally occurring organohalogens were known. Until today the number increased to over 5000 and is continuously growing.^[1] Nearly one-quarter of pharmaceuticals and agrochemicals currently used are halogenated.^[2,3] Hence, these compounds are important in everyday life. The halogen within the molecule increases the thermal and oxidative stability, as well as the biological membrane permeability, resulting in a higher efficacy. These properties are inevitable for molecules used as drugs.^[3-5] Likewise, many found molecules carry astonishing biological activities such as anticancer, antibiotic, cytotoxic, herbicidal and insecticidal properties.^[2,5,6]

Even though organohalogens are found in terrestrial and marine organisms, the majority is found in marine sources. This can be explained by the high concentration of chloride and bromide in the ocean. Terrestrial halogens are mostly present in insoluble form which hinders the uptake by living organisms.^[1-3,7]

The diversity of identified organohalogens produced by nature ranges from chloroform to terpenes, complex macrocycles and peptides. The molecules are produced as secondary metabolites and their contribution to growth, reproduction, and defense play a primary role for the survival of the organisms. Chlorometabolites (51%) and bromometabolites (45%) are dominating while organoiodines (2%) and organofluorides (2%) are less common, however some orders of brown algae use iodination over chlorination and bromination.^[2,3,8-10] Often more than one halogen atom is present. In figure 1, some examples of naturally occurring organohalogens with biogenic properties are shown. Aureomycin (**1**), chloramphenicol (**2**) and vancomycin (**3**) are antibiotics, produced by bacteria.^[11-13] Further examples are 12-*epi*-hapalindole E (**4**), an inhibitor for bacterial RNA polymerase,^[14] (+)chlorolissoclimide (**5**), a potent cytotoxic labdane diterpenoid,^[15] and jamaicamide A (**6**), a sodium channel blocker.^[16]

The importance of the halogen within medicinal compounds has been demonstrated for example on the dechlorinated vancomycin molecule, where the antibiotic activity decreases about 70%.^[17] Also the human cathepsin L inhibitor has an increased binding affinity of factor 13 in comparison to its unsubstituted derivative.^[18] The increased efficacy is based on a halogen bond between a covalently bonded halogen atom (e.g. C-X, X=Cl, Br, I) and a nucleophile (e.g. Lewis base). In proteins, carbonyl groups of the amino acid backbone or polar amino acids can be the nucleophile, that can interact with a positively charged electrostatic region on the extension of the C-X bond which is due to the anisotropy of the charge distribution.^[19] Because of its enhancing effect of the ligand-acceptor interaction, halogen bonds have attracted more attention in drug discovery within the last years.^[20-22]

Introduction

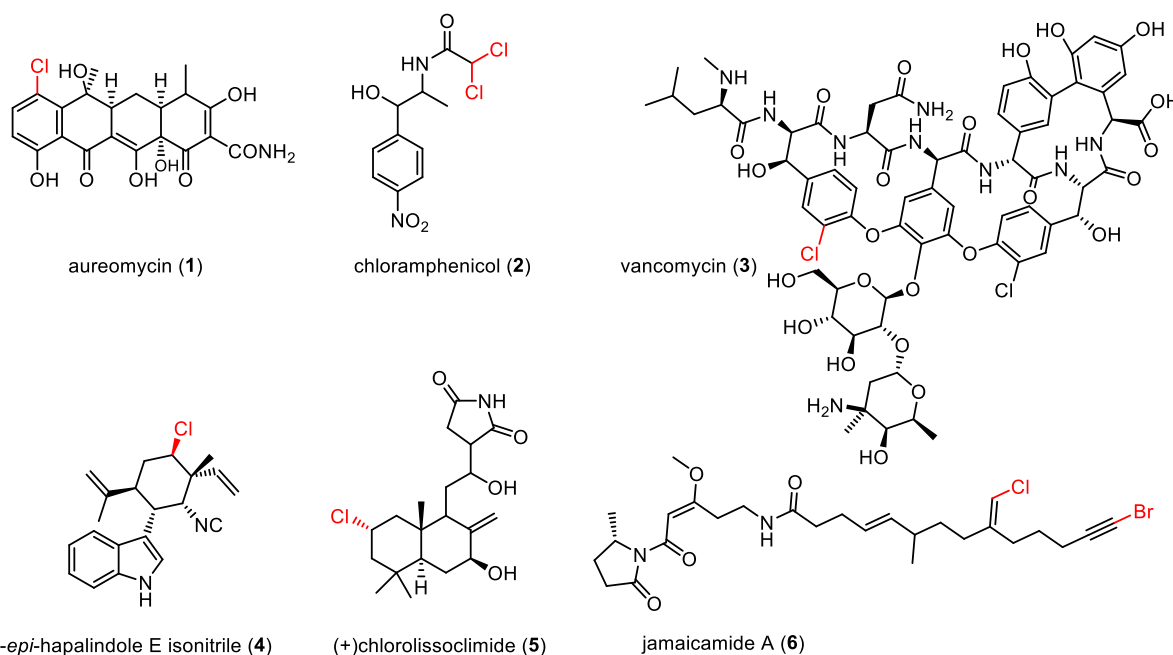


Figure 1. Examples of biogenic organohalogens. Aureomycin (1), chloramphenicol (2) and vancomycin (3) are antibiotics, produced by bacteria. 12-*epi*-hapalindole E (4) is an inhibitor for bacterial RNA polymerase, (+)chlorolissoclimide (5) is a potentially cytotoxic labdane diterpenoid, and jamaicamide A (6) is a sodium channel blocker.^[11–16]

The indispensable need of biogenic organohalogens in clinical medicine can be seen on high selling drugs as chloramphenicol (2) and vancomycin (3). In the last years, also the number of preclinical anticancer lead compounds originating from marine organisms increased.^[4] The importance of organohalogens is irrefutable but the general trend for increasing complexity is pushing organic synthesis to its limits. General synthetic methods for direct and selective functionalization of non-activated, aliphatic C(sp³)-H bonds are especially sought-after.^[23]

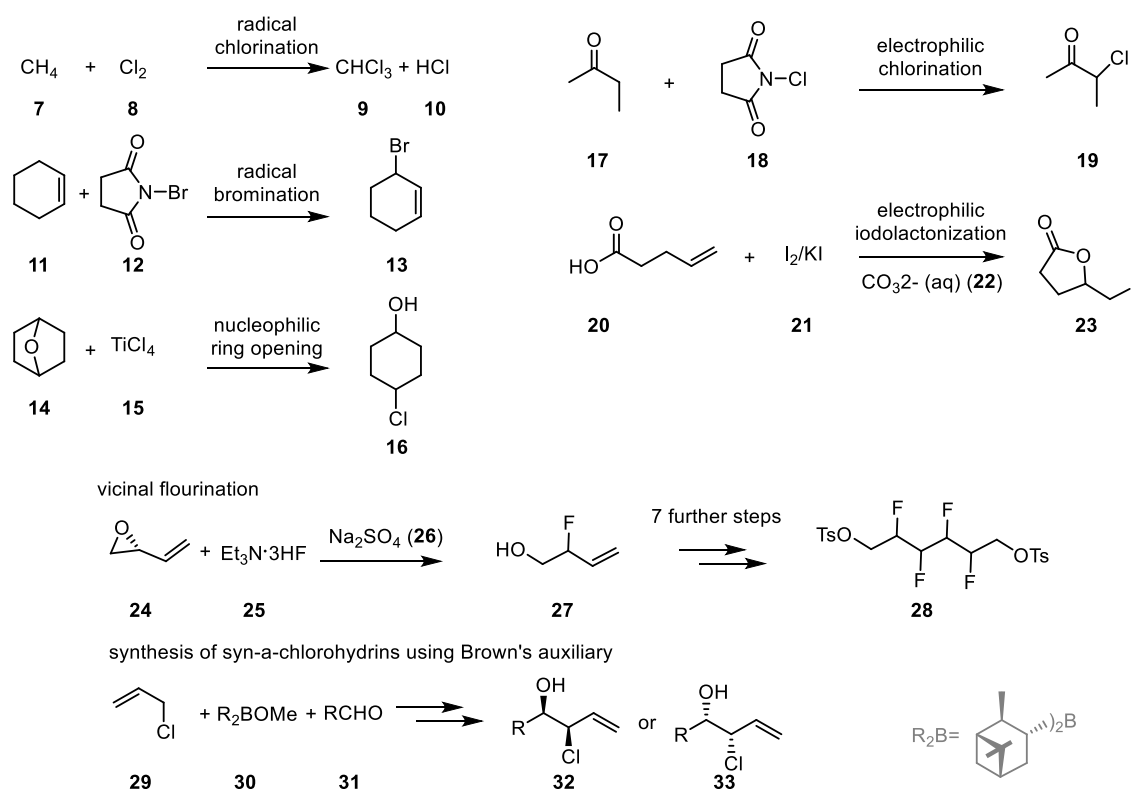
Next to their potential as pharmaceuticals and agrochemicals, organohalogens also possess a high synthetic value for further transformations. Especially transition metal-catalyzed cross-coupling reactions have become an indispensable tool in the synthesis of complex molecules, which use halogenated molecules as starting materials. Via these coupling reactions, formation of C-C, C-F, C-N and other C-heteroatom bonds are possible.^[24–31] Methods for robust and selective halogenation in the absence of directing groups are essential in today's synthesis toolbox.^[23,32] In the next chapter, several halogenation methods are described.

1.2 Halogenation Methods

If natural products are used in agrochemical or pharmaceutical industry, suitable molecules must be accessible in huge amounts. Often, only a few mg of secondary metabolites can be extracted from the natural producing hosts, typically below 0.1 % of dry bacterial weight.^[33,34] Therefore, robust synthetic routes must be developed. Especially the introduction of halogen species in a regio- and stereoselective manner can be problematic. Some chemical and enzymatic halogenation reaction will be discussed in the following chapters.

1.2.1 Chemical Halogenation

Examples of previously described halogenation reactions are shown in scheme 1. Traditional halogenation with elementary chlorine possess a high importance for industrial production of organohalogens since many years.^[35,36] The reactions have to be performed under harsh conditions with high reactivity of starting materials and in acidic environment. Especially with more complex molecules – larger or functionalized, in comparison to small hydrocarbons- this results in polyhalogenation and poor regio- and stereoselectivity.^[37,38] Bromination in contrast to chlorination is more often regioselective for the weakest C-H bond.^[39] Reagents with the halogen bound to a nitrogen of a small molecule, such as succinimide or methylamines, increase the selectivity in the reaction.^[39,40] The use of N-halide amides as halogen donor was developed over the years and combined for example to visible light to produce complex molecules in good regio- and stereoselectivity.^[41,42] Another method to introduce chlorine stereoselectively, is the nucleophilic ring opening of ethers which was first published with TiCl_4 ^[43] in 1986 followed by alternative opening reagents as BCl_3 ^[44], acetyl chloride^[45] and HCl ^[46]. This technique can be used in total syntheses such as (-)-N-methylwelwitindolinone B.^[47]



Scheme 1. Examples of halogenation reactions in organic chemistry.^[36,39,43,48–51]

Asymmetric halogenation at olefins and activated carbons is possible by nucleophilic attack at the α -position of aldehydes, carbonyls and 1,3-dicarbonyl compounds after activating the carbonyl compounds with an organocatalyst.^[49,52–58] Another important transformation at olefins is the electrophilic addition that transforms one functional group into two, with formation of new stereocenters.^[59] The olefin is hereby activated by the halogen in presence of a nucleophile

and both, halogen and nucleophile are added which typically results in the *trans* product.^[60] One important variation of this reaction is the intramolecular cyclization reaction, in which unsaturated acids are turned into lactones.^[50] The first iodocyclization was already described in 1904.^[61] Until today it belongs to the synthetic useful and important processes of organic chemistry.^[62]

Of recent interest is also the development of fluorination reactions. The first breakthrough was in 2002 and since then several strategies were published.^[63–65] Vicinal fluorination as well as vicinal chlorination methods were developed for polyhalogenation of alkanes^[48,66] and chlorosulfolipids^[67,68]. Stereoselective introduction of halogens with chiral auxiliars was shown by Evans in 1987.^[69,70] The use of auxiliars in halogenation reactions is nowadays an established methodology for example in the synthesis of *syn*-vinylchlorohydrins^[51,71,72] and the combination of halogenation with lactamization.^[73]

In recent years progress has been made in the field of halogenation. Even though many possible routes are known, the transformations are still highly challenging. A vast majority of reactions use conditions that are impractical and lack generality because the substrate scope is extremely limited and mechanistic understanding of the reactions is often not explored.^[59] Halogenation of unactivated, aliphatic carbons is a substantial challenge for chemists.^[74–78] To synthesize complex molecules, the halogen atom is currently introduced quite early and the remaining synthesis has to be planned with proper care to not eliminate the halogen, once introduced. Weires *et al.* and Reyes *et al.* have discussed these issues in the total synthesis of (-)-N-methylwelwitindolinone B isothiocyanate.^[47,79] Especially while developing new pharmaceuticals it is often necessary to adjust the properties such as reactivity, permeability or ligand-target interaction by testing different stereoisomers of a certain molecule once the core structure is synthesized. Therefore, late stage halogenation would be of advantage since the synthesis of the core substance has to be performed once and selective C-H bond functionalization in the absence of directing groups in further steps would greatly simplify synthesis^[23,32,78] and enable late-stage diversification of the complex molecules.^[80–82]

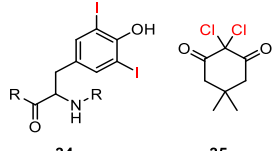
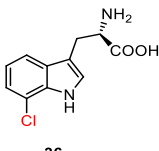
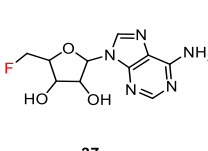
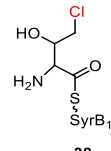
A different approach for halogenation is the use of enzymes which is described in detail in the next chapter. Additional to enzymes, which have a high complexity, high molecular weight and often low stability, some groups started to build synthetic mimics of the catalytic center of enzymes, which could be a versatile alternative to enzymes, once the catalysts are established. So far, halogenation of several alkyl moieties was achieved with the help of a manganese porphyrin catalyst.^[83,84] Cyclohexane as well as toluene were halogenated by the use of hexacoordinated iron catalysts that mimic the active site of non-heme iron (NHI) dependent halogenases.^[85] In both cases problems with chemoselectivity occur which results in hydroxylated by-products. The challenge of higher chemoselectivity needs to be tackled by further catalyst engineering.

1.2.2 Biological Halogenation

Biological halogenation occurs on a diverse array of organic scaffolds, from volatile hydrocarbons to indoles, terpenes, peptides, phenols, polyketides and nonribosomal peptides. Within these scaffolds, halogen atoms are incorporated on aliphatic carbons, olefinic centers and a wide variety of aromatic and heterocyclic rings.^[77,86]

The activity of the first halogenating enzyme was verified in 1959 when the biosynthesis of chlorinated metabolites, such as caldariomycin, of *Caldariomyces fumago* was investigated.^[87] Nowadays four different enzyme classes, haloperoxidases, flavin dependent halogenases (Fl-Hal), nucleophilic halogenases and non-heme iron (NHI) dependent halogenases are known. In table 1, characteristics are compared for the enzyme classes.

Table 1. Comparison of four halogenase classes.^[86,88] Haloperoxidases and NHI dependent halogenases can be classified again into two subclasses. Haloperoxidases can either have a catalytic center containing vanadate or heme. One subclass of NHI dependent halogenases can only transform substrates, that are bound to an acyl carrier protein, while the other subclass acts on freestanding substrates. VCPO – vanadium chloroperoxidase, CPO – chloroperoxidase.

	haloperoxidases		flavin dep. halogenases	nucleophilic halogenases	NHI dep. halogenase	
activated halogen	X ⁺			X ⁻	X [•]	
accepted halogens	Cl, Br, I		Cl, Br	F ⁻ , Cl ⁻	Cl [•] , Br [•]	
representatives	VCPO	CPO	PrnA RebH	FDAS SalL	ACP dep. SyrB2 CurA	WelO5, AmbO5 Wi-WelO15
cofactor	vanadate, H ₂ O ₂	heme, H ₂ O ₂	FADH ₂ , O ₂		Fe ^{II} /αKG, O ₂	
substrate requirements	electron rich arenes or enolates			electrophilic, good leaving group, SAM	aliphatic, unactivated	
examples of natural products						

As shown in table 1, each halogenase class requires their own cofactors and has quite different substrates as well as individual reaction mechanisms. In the next chapters, the halogenases will be described in detail.

1.2.2.1 Haloperoxidases

The first halogenase was discovered in 1966 and is a heme dependent chloroperoxidase (CPO).^[89] Later, more haloperoxidases were found that either contain heme or vanadium as cofactor and use halides (Cl, Br, I) and hydrogen peroxide to form hypohalous acid or hypohalite as freely diffusible halogenating agent. Due to that, they possess a flexible substrate scope,^[90] and the reaction, works without any regioselectivity.^[91] This results in generation of mono-, di- and trihalogenated products.^[92] It was shown that few members of this enzyme family show a specific reaction by binding their substrates^[93-95] or performed regio- and enantioselective reactions by trapping the hypohalite.^[96,97] Brominations and iodinations are possible for these enzymes, too. In this case a high ratio of bromide versus chloride is important to achieve bromination, as could also be shown for other types of halogenases.^[98-101]

Haloperoxidases generally have a poor stability at high temperatures and high concentration of its substrate hydrogen-peroxide.^[102] The enzyme stability can be enhanced by immobilization as was shown several times either by adsorption on talc^[103], mesoporous materials^[104-108] or amino-agarose gel^[109] or covalent attachment with mesoporous silica^[105,106,110,111], methacrylate^[112], chitosan membranes^[113], magnetic beads^[114] or others^[109,115]. But because of leaking from the surface or sterically hindrance by the attached surface, these methods need further improvement. By entrapping CPO in silica gel, doped with chitosan polysaccharide, the biocatalyst showed increased reusability and thermal stability.^[102] Successful application has been demonstrated by Merck that obtains indene oxide, an intermediate in the synthesis of the HIV-1 protease inhibitor Crixivan through biotransformation with a haloperoxidase.^[116]

1.2.2.2 Flavin dependent Halogenases

Flavin dependent halogenases (Fl-Hal) belong to the superfamily of flavin dependent monooxygenases.^[117,118] The tryptophan halogenase PrnA from *Pseudomonas fluorescens* was discovered as first representative of this enzyme class in the year 2000.^[119] Since then, several members were discovered. The most extensively studied halogenases are tryptophan halogenases which introduce chlorine in position 7 (PrnA, RebH), 6 (KtzR, ThalL) and position 5 (PyrH) in tryptophan.^[120] As in chloroperoxidases, first hypohalous acid is produced which is generated by the reaction of reduced flavin with molecular oxygen. However, unlike the other halogenase class, the hypohalous acid is not the halogenation agent. It is presumed that the hypohalous acid reacts with a lysine (Lys79, RebH) to form a chloramine which acts as final chlorination species. In comparison to the hypohalous acid it is more stable and therefore less reactive. The lysine is located between the flavin binding site and the binding site of the substrate which are about 10 Å apart, so that the chlorination occurs in a regioselective way.^[121] Also known but less extensively studied are flavin dependent pyrrole and phenolic halogenases, that halogenate either freestanding substrates or substrates tethered to a carrier protein.^[120]

Introduction

Fl-Hal have been shown to halogenate a range of synthetic as well as natural aromatic compounds. The exquisite regioselectivity makes them potentially useful biocatalysts.^[122–125] However, the application of Fl-Hal in vitro has been hampered by their poor catalytic activity and lack of stability. These drawbacks can be overcome by directed evolution.^[126,127] By formation of cross-linked enzyme aggregates, regioselective bromination up to gram scale could be developed.^[128] Also the finding of a thermostable Fl-Hal is of advantage for biocatalysis.^[127] Furthermore it could be shown that sequential or tandem halogenation/cross-coupling is possible to transform C-H into C-C, C-N or C-O bonds.^[120,129–132] Of special interest is the development of a high-throughput screening method with fluorescent output published 2016, that combines enzymatic halogenating of tryptophan with bioorthogonal Pd mediated cross-coupling to produce fluorescent products, which makes further enzyme engineering more facile.^[133] All these recent developments prove the high biocatalytic potential of Fl-Hal. However only halogenation on electron rich or activated systems are possible and the reaction system additionally needs a NADPH-dependent reductase, that reduces FAD to FADH₂ and a third enzyme that recycles NADP⁺ since NADPH as stoichiometric reagent is far too expensive.^[134,135]

1.2.2.3 Fluorinases

Fluorinated metabolites could only be isolated from plants and bacteria so far.^[136] In 2004, 5'FDAS from *Streptomyces cattleya*, the first enzyme able to fluorinate substances, was identified. The fluorinase works with a nucleophilic mechanism and uses S-adenosyl methionine as substrate to produce 5'-fluoro-5'-deoxyadenosine.^[137] The fluorinase can also perform chlorination, although the dechlorination is thermodynamically favored. A found homologue enzyme SalL is only able to chlorinate but not fluorinate.^[138,139] Until now only four more fluorinases have been identified.^[140–142]

The nucleophilic halogenase FDAS has already proven its usefulness as biocatalyst in the production of [¹⁸F]fluorine-labeled molecules for positron emission tomography. Because the enzymatic reaction is performed in aqueous solution, it eliminates the need to secure dry [¹⁸F]fluoride.^[143,144] Fluorinases are able to accept non-native substrates but often with a lower activity.^[144–147] Rational design and directed evolution have already been successfully applied to increase the activity towards non-native substrates.^[146,148] In the same study it was shown that the enzyme in general seem to be quite stable and good evolvable, as the fluorinase FIA1 has a higher activity at 42 °C and variants are active even at 47 °C.^[148] These recent findings suggest the fluorinase as great candidate for usage as biocatalyst especially since selective fluorination is such an important transformation and under mild conditions difficult to enable chemically.^[148]

1.2.2.4 Non-Heme Iron dependent Halogenases

The fourth family of halogenases, which was recently discovered are non-heme iron (NHI) or Fe^{II} and α -ketoglutarate (Fe^{II}/ α KG) dependent halogenases. Their ability to work on unactivated, aliphatic substrates makes them special since the addition of halogens in stereoselective manner of unactivated (sp³)-carbons is quite difficult for organic chemistry as well. The first, in 2005 discovered and so far best investigated member is SyrB2 from *Pseudomonas syringae*.^[149] The enzyme family belongs to the mononuclear Fe^{II}/ α KG dependent oxygenases, one of the largest subfamilies of non-heme iron enzymes. NHI halogenases can be further classified based on their substrate. The first subclass need their substrate to be tethered to an acyl-carrier protein (ACP),^[149–154] while the other class can transform freestanding substrates.^[155–158] The halogen addition works radically while the halide can originate from salts like sodium chloride.

Unlike the other halogenases, few investigations were conducted to test the biocatalytic potential of this enzyme class. Naturally these enzymes chlorinate their substrate, but in absence of chloride and with a high excess of bromide, also bromination can be performed.^[98,99] If the substrate positioning is improper, hydroxylation instead of chlorination will occur.^[159] Hydroxylation can furthermore be triggered with mutation in the 1st (G166D, WelO5) and 2nd (S189A, WelO5) sphere around the catalytic center,^[160] as well as by mutation in the substrate binding site.^[158] Also, for NHI-dependent hydroxylases to date, few engineering studies are published, the best studied member is TauD from *Escherichia coli*.^[161–166] This may be based on their low activity. Only a turnover number of 7 is described for SyrB2.^[149] The first directed evolution study with NHI dependent halogenases was performed in the Hoebenreich group within this thesis.^[158] It was shown that the halogenase *Wi-WelO15* from *Westiella intricata* can be engineered to accept non-native substrates. This proves the power of directed evolution to evolve the members of this challenging enzyme class and that activity problems can be overcome.^[158] In the next chapter, this halogenase class will be described in detail, followed by chapters about biocatalysis and directed evolution.

1.3 Non-Heme Iron, α -Ketoglutarate Dependent Enzymes

Fe^{II}/ α KG dependent enzymes encompass a large family of oxidative enzymes, which are wide spread along all kinds of organisms, as can be mentioned, humans, plants and prokaryotes. Variations to a common mechanism are used to hydroxylate structural proteins, regulate the hypoxic response, modulate histone methylation, repair alkylated DNA/RNA and synthesize or degrade a range of natural products. Hereby chemical transformations like halogenation, demethylation, desaturation, O-cyclization, ring expansion and epimerization are catalyzed. Substrate oxidation is coupled with reductive activation of molecular oxygen and decarboxylation of α KG to succinate.^[162,167–177]

In vitro reconstitution of aliphatic halogenases require halogenase, Fe^{II} and cosubstrates α KG and Cl⁻. For the reaction furthermore O₂ is needed. NHI dependent halogenases share

similarities in structure and mechanism to well-studied hydroxylases.^[149,178] Mutagenesis of an hydroxylase enabled the chlorination of its substrate while a chlorinase could also hydroxylate its substrate. This reversal of activity however is not possible for all members of this enzyme class. Structure and mechanism of both, halogenase and hydroxylase, will be discussed in detail in the next chapters. The chapter will focus on aliphatic halogenase *Wi-WelO15* which is used within this thesis^[158] and its homologue *WelO5*, which was characterized by the group of Liu.^[99,155,156,160]

1.3.1 Crystal Structure

Structurally, the enzymes share a jelly-roll motif that defines the cupin superfamily and is composed of an eight-stranded antiparallel beta sandwich containing an Fe^{II} in the active center (figure 2).^[77,160] The versatility of NHI dependent enzymes is possible since the iron is coordinated by only two or three protein ligands and thus has three to four sites available to coordinate substrates. Hydroxylases share a facial triade consisting of His(X_m)Asp/Glu(X_n)His for iron binding. Crystal structures of *SyrB2*^[149,178], *CytC3*^[153,179] and *WelO5*^[160] revealed that the facial triade in halogenases consists of His(X_m)Gly/Ala(X_n)His. The substitution of Asp/Glu by Ala/Gly creates an open space at the iron center for the chloride to bind (figure 2a).^[149,178,180]

Halogenase *WelO5* exclusively produces the hydroxylated fischerindole if mutation G166D is introduced instead of the chlorinated product^[160], while hydroxylase *SadA* halogenates its substrate when mutation D157G is present.^[181] However mutation of Ala to Asp in halogenase *SyrB2*^[178] and Asp to Ala in hydroxylase *TauD*^[182] failed to convert enzyme activities. Structural studies of halogenase *CytC3* revealed that numerous additional interactions with the protein environment are critical in ensuring chlorine can bind to the iron center, which explains the failure in modifying the enzyme activity.^[179] A nearby Arg residue located 15-22 residues beyond His2 in the sequence provides additional stabilization to the C-1 carboxylate in the cases of *TauD*, *AtsK*, *CAS*, *CarC* and *AlkB*.^[167]

Crystallization of several enzymes revealed that the structure seems to be quite flexible. The loops, covering the active site of *SyrB2* have higher B-factors, indicating that they have some degree of mobility^[178]. It is assumed that once iron and chloride bind, the protein closes around the active site. This closure involves motions of two loops and a beta hairpin. The phosphopantetheine arm with substrate enters the active site through the remaining narrow tunnel above.^[178] The structure of *CurA* could be solved in five different states.^[183] Also, the structure of *WelO5* was solved in an open and a closed conformation (figure 2b)^[160] and *Wi-WelO15*^[158] which differs only in 2 amino acids to *WelO5* shows a third structural state in its crystallized form (figure 2c). Even though the crystal structure of some halogenases are oligomers, e.g. *WelO5* is a monomer in solution^[160] with no known subunit interaction. While *CurA* is a dimer in solution which is consistent with the dimeric architecture of PKS modules.^[183]

Introduction

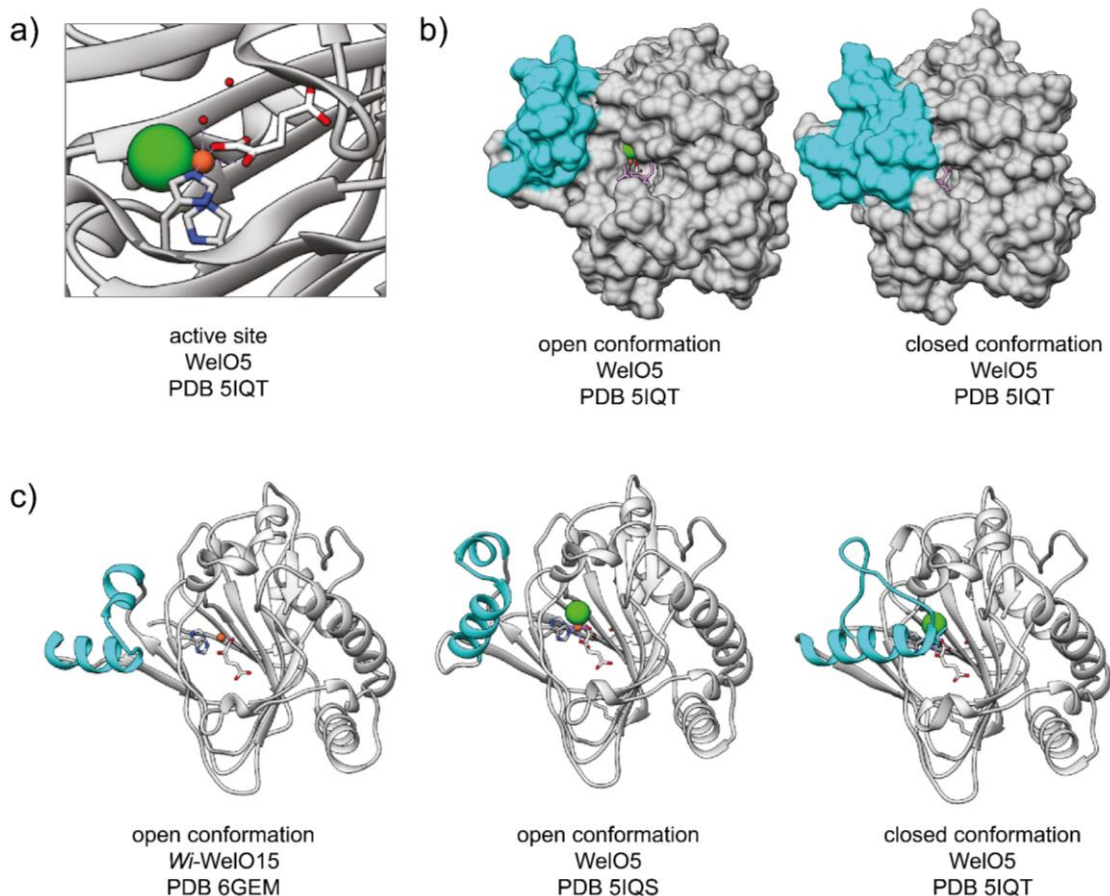


Figure 2. a) Active site of halogenase WelO5, shows the octahedral coordinated iron center (green ball). b) Compares open and closed conformation of WelO5, shown as surfaces. While the open structure has the substrate binding tunnel quite open and it can be seen to the iron center, while in the closed conformation, the center is shielded. In cyan, the lid is shown which can close over the active site. c) Comparison of three different crystallization states of *Wi-0* (PDB 6GEM)^[158] and WelO5 (PDB 5IQT)^[160]. The lid (cyan) can adapt in three different conformations

The stability of the structure seems to depend on the enzyme. Some members are readily isolable in apo form and adopt in the same overall conformation as the holo enzymes,^[168] as could be shown by some crystal structures in apo form (*AtsK*,^[184] *P3H*,^[185] *DAOCS*,^[186] *CAS*^[187]). However there is evidence that at least in some cases, the overall structure of enzymes becomes more ordered when Fe^{II} and α KG is added.^[188,189] Apo *SyrB2* has a low affinity for Fe^{II} and yields only ~35% incorporation while reconstitution with α KG followed by Fe^{II} yields 90% incorporation.^[149] *TauD* abolishes its activity in the presence of EDTA^[162] while for *XanA* it was shown that activity remains in the presence of EDTA which shows that cofactor binding differs depending on the enzymes.^[190] Since ferrous ion is required for all enzymatic activities of α KG enzymes the addition of a reducing agent as ascorbic acid to the reaction can increase the activity.^[158,162]

When Fe^{II} is present together with α KG, the metalcenter exhibit a characteristic metal-to-ligand charge transfer transition^[191-194] resulting in a lilac color to this state of enzyme. The rate of chromophore formation is independent of the concentration of Fe^{II} -*TauD* or α KG. This is consistent with α KG binding to the protein followed by a conformational change that gives

rise to the absorption.^[195] The lilac-colored α KG-TauD complex reacts with O_2 in the absence of added substrate to generate a transient yellow species $\lambda_{\max} = 408$ nm, which was identified as a tyrosyl radical on the basis of EPR studies, which is formed after α KG decomposition.^[196] Another species is observed if Fe^{II} is added to an anaerobic sample of apoprotein TauD. A weak and broad absorption band near 650 nm arises which is attributed to an Fe^{III} -catecholate species.^[182] The green color originates from the electron transfer from Fe^{II} to an ortho-quinone at position Tyr73 (TauD) where the oxidized side chain is derived from intracellular enzyme self-hydroxylation during aerobic cell growth followed by oxidation of the catechol to quinone state during further growth and protein purification.^[195] Self-oxidation is a common problem reported for many related Fe^{II}/α KG dependent dioxygenases leads to destruction of activity.^[196-198] This was also shown for SyrB2, which only catalyzed 7 turnovers before inactivation.^[149]

1.3.2 Mechanism

Fe^{II}/α KG-dependent enzymes encompass a large family of oxidative enzymes that use variations to a common mechanism to transform a wide range of molecules.^[195] The enzymes catalyze a two-electron oxidation. The two reducing equivalents required for the four-electron reduction of oxygen are often provided by a cosubstrate. This cosubstrate include α KG^[167], tetrahydrobiopterin^[199], reduced nicotinamides^[200], and ascorbic acid^[201]. Few enzymes oxidize their substrates by four electrons and thus do not require a reducing cosubstrate.^[200,202,203] The versatility of NHI dependent enzymes is possible since the iron is coordinated by only two protein ligands and thus has four sites available to coordinate substrates.

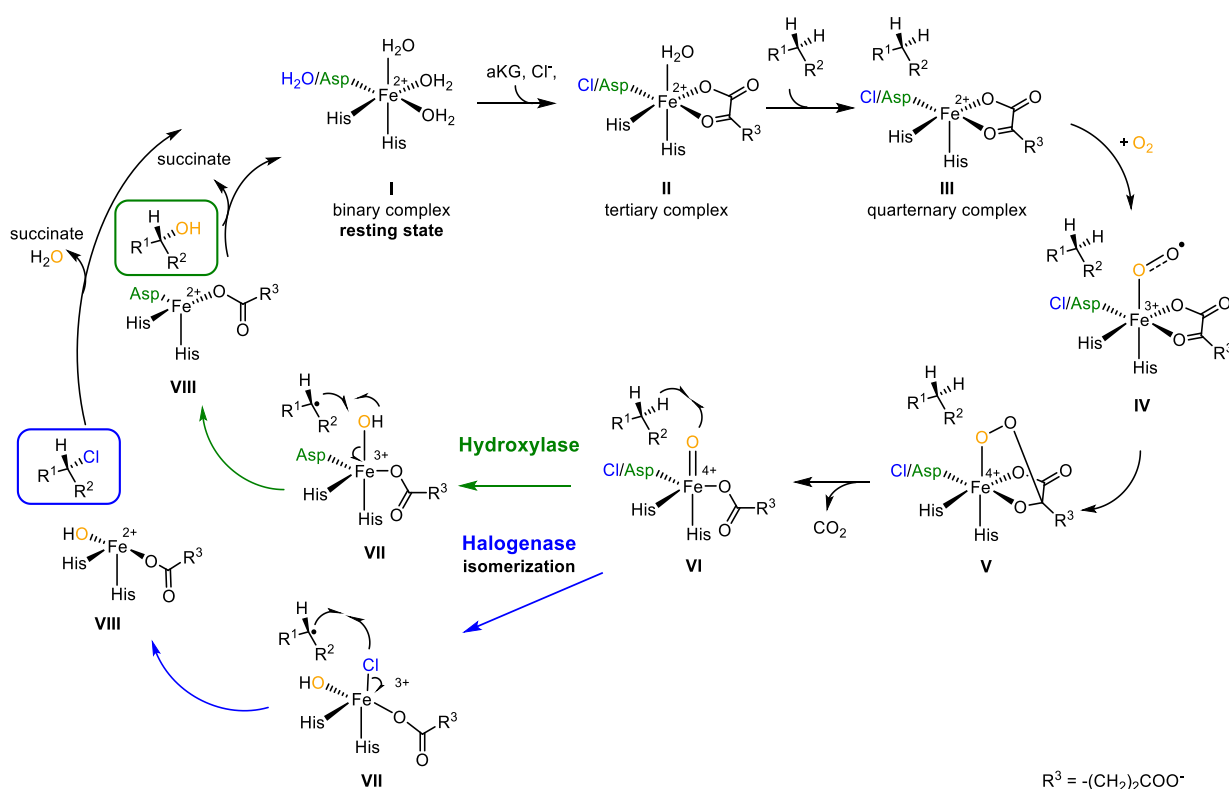
The proposed reaction mechanisms include several intermediates following the addition of oxygen to the Fe^{II} center.^[200,204,205] Almost 30 years ago, Hanauske-Abel and Günzler proposed a theoretical reaction mechanism for 4-prolyl hydroxylase.^[206,207] In the last years, studies of several α KG-dependent enzymes lead to the characterization of non-heme iron-oxo intermediates providing some insight into the reaction mechanism. Important roles played the taurine hydroxylase TauD^[208,209] and the halogenases SyrB2^[210,211] and CytC3^[74,212].

Halogenases and hydroxylases belong to the same class of oxidoreductases, however, since the sequence identity of some of the enzymes is quite low, it can be assumed that not all these genes evolved from a common ancestor but they developed by convergent evolution.^[162,172] Hydroxylation as well as halogenation reactions involve activation of the substrates through H-atom abstraction of the target C-H bond by the Fe^{IV} -oxo intermediate to yield a substrate radical and an Fe^{III} -OH complex. Followed by a rebound which formally involves recombination of a coordinated radical (hydroxyl or chloride) with the substrate radical to yield the product and a coordinatively unsaturated Fe^{II} center.^[213] Alternative reactions that do not involve radical recombination involve for example abstraction of a second H-atom to yield desaturated

Introduction

or cyclized products and an $\text{Fe}^{\text{II}}\text{-OH}_2$ complex. Significant insight into the geometric and electronic structures of high-valent non-heme Fe-oxo complexes and their reactivity was obtained from studies of inorganic complexes^[214–217] and quantum mechanism calculation^[211,218–222].

The observation of non-heme $\text{Fe}^{\text{IV}}\text{-oxo}$ intermediates and Fe^{II} containing product complexes with almost identical spectroscopic parameters in the reactions of two distantly related αKG dependent hydroxylases suggest that this subfamily follow a conserved mechanism for substrate hydroxylation.^[213] Although the mechanism of O_2 activation, leading to the highly-reactive $\text{Fe}(\text{IV})=\text{O}$ intermediate (with spin $S=2$), are thought to be similar for all αKG -dependent NHI enzymes, there is notable divergence in their subsequent catalytic cycles.^[223] The mechanisms of hydroxylase and halogenase are shown in scheme 2. Halogenation versus hydroxylation within the reaction will be discussed in the next chapter.



Scheme 2. General accepted reaction mechanism of αKG dependent enzymes.^[213] Proposed halogenase mechanism, with different conformation of $\text{Fe}^{\text{IV}}\text{-oxo}$ species is shown in comparison to proposed conformation of hydroxylase.^[213,222,223]

The catalytic cycle starts formally with a binary complex, which represents the enzyme in its apo form (I). When αKG and Cl^- are inserted in the active center, the tertiary complex (II) is formed. The crystal structure of SyrB2 showed, that the halide binds to iron before decarboxylation.^[178] The substrate does not bind directly to the metal but its coordination to the $\alpha\text{KG}\text{-Fe}^{\text{II}}$ enzyme complex induces the displacement of water which was shown to serve as a trigger to create an O_2 binding site,^[178,224] so that the quaternary complex (III) reacts with O_2 .

Two types of intermediates have been proposed: First a Fe coordinated (su)peroxo complexes (IV) with an intact O-O bond, $[\text{Fe}-\text{O}_2]^{2+/3+}$, which could not be detected so far. The attack

of the superoxide on the carbonyl carbon of α KG yields a peroxohemiketal bicyclic complex (V). Which decomposes to eliminate CO_2 and a bound succinate at an Fe^{IV} -oxo ($[\text{Fe}=\text{O}]^{4+}$) complex (VI), the second proposed intermediate, which could be confirmed by spectroscopic measurements.^[212,225–227] This Fe^{IV} -oxo complex in TauD revealed a unusual high-spin ($S \frac{1}{2} 2$) configuration.^[164] The large kinetic isotope effect on its decay in the presence of deuterated substrate identified this intermediate as the species that cleaves the C-H bond.^[228,229] The hydrogen abstraction occurs via hydrogen atom transfer from the C-H bond of the substrate, yielding a Fe^{III} -OH and a substrate radical (VII).^[74,230]

Comparable analysis of the halogenase CytC3 revealed the formation of at least two Fe^{IV} complexes upon reaction with O_2 . Both are Fe^{IV} complexes which are in a rapid equilibrium and are believed to be two distinct conformers.^[74] The existence of these two conformers of the Fe site may be the key factor accounting for the divergence of the halogenase reaction from the hydroxylation pathway after C-H bond cleavage.^[213] Recent studies^[223,231,232] propose the Fe^{IV} -oxo complex (VII) to be in a quintet state in which the oxido oxygen points away from the substrate (π -orientation of the oxo group, relative to the native C-H bond) as shown in scheme 2 (halogenase pathway) and scheme 3.^[223] For hydroxylases, rebound occurs with the axial positioned hydroxyl group while for halogenases, the hydroxyl group originating from oxygen isomerizes in a equatorial formation. If the chlorine rebound occur from a equatorial or axial position is not completely clear yet,^[222,231,232] but it was shown that in halogenases, hydroxylation and halogenation do not compete. Substrate positioning directs the reaction toward halogenation or hydroxylation (see next chapter hydroxylation).^[159]

Efforts to purposely generate a Fe^{III} -OH species and a taurine radical failed. Considering calculations, it is likely that the lack of intermediates is due to the nature of the substrate, not the protein environment. The lack of a stable Fe^{III} -OH species is consistent with spectroscopic studies which identified an Fe^{II} intermediate following the Fe^{IV} -oxo species.^[164] After the rebound is performed, the product is released and the iron complex can be regenerated.

Selective hydroxylation of unactivated carbons is of interest as well as the differentiation between halogenation and hydroxylation and therefore recent findings of hydroxylases and halogenases will be compared in the following chapter.

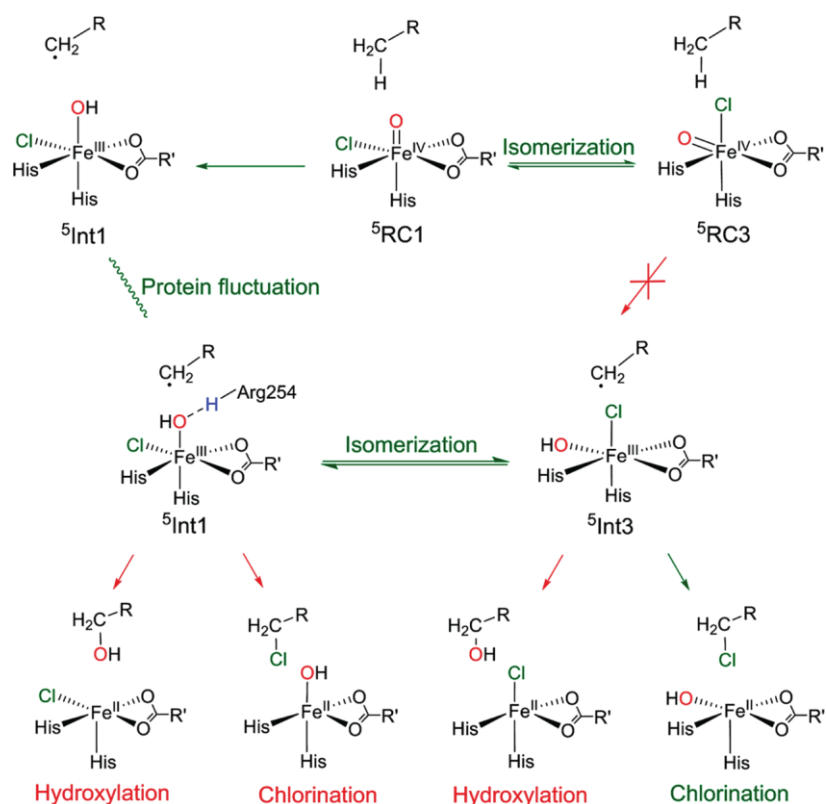
1.3.3 Halogenation versus Hydroxylation

After the discussion of general mechanistic intermediates above, a closer look on the differences between hydroxylation and halogenation will be taken in this chapter. No hydroxylation side reaction has been detected for SyrB2 with native substrate L-Thr, indicating that Cl radical transfer is greatly favored,^[149] while non-native substrates are preferably hydroxylated.^[227] Until today it remains largely unknown how the enzymes avoid potentially competing hydroxylation outcomes. There are several possible explanation including positioning of the substrate in the active site^[223] or lower potential of Cl radical versus OH radical^[223], as has been proposed

Introduction

to explain similar reactivity in model complexes.^[149,233] Recent studies^[223,231,232] propose the Fe^{IV}-oxo complex to be in a quintet state in which the oxido oxygen points away from the substrate (π -orientation of the oxo group, relative to the native C-H bond). The presence of this intermediate is supported by the crystal structure of WelO5 which shows a H-bond between carboxylate group of α KG and Ser189.^[160]

Recent findings by QM/MM studies from Huang *et al.*^[222] revealed the existence of three Cl-Fe^{IV}-oxo isomers which interconvert (scheme 3).



Scheme 3. Reaction network of the selective halogenation by SyrB2 starting from the Fe^{IV}=O species. The green pathway is the sole pathway for halogenation of L-Thr.^[222]

Only the one pointing its oxo ligand towards the target C-H bond is active during the hydrogen atom abstraction. It was shown, that an isomerization of the Cl-Fe^{IV}-oxo species is possible with an overall energy barrier of 16 kcal/mol (scheme 3, first row). In further optimization steps, RC3 always isomerizes back to RC1. Also, all attempts of hydrogen abstraction from the substrate led back to RC1, which leads to the conclusion that RC1 is the sole reactive species in the C-H activation (scheme 3).^[222]

After H-abstraction, the Fe^{III} species can undergo an isomerization which has only an energy barrier of 6 kcal/mol (scheme 3, middle).^[222] The crystal structure of WelO5 also indicated a relocation of the oxo unit from the axial position to the equatorial plane, defined by the chloride and the α KG, which would draw the oxo group further away from the substrate. This transition is apparently aided by a hydrogen bonding interaction with the hydroxyl group of

Ser189 in Fe^{II} secondary sphere. Mutation of Ser189 to Ala led to an equal portion of hydroxylation and chlorination products.^[160,234]

A hydrogen bonding between Arg254(SyrB2) and the OH ligand of Cl-Fe^{III}-OH intermediate not only prevents the OH ligand from participating in the reaction, but also facilitates the isomerization of the Cl-Fe-OH so that the Cl is directing towards the alkyl radical. Experimental data support the importance of the Arg residue in CurA, since mutation of Arg241 and Arg247 mutant completely suppress activity.^[183]

Calculations by Srnc and Solomon^[232] reveal that substrate orientation strongly influences if chlorination or hydroxylation happens. Their results are in agreement with experimental observations of Bollinger and Krebs.^[159] Hydroxylation is thermodynamically favored, but chlorination intrinsically more reactive.^[232] Selectivity is then determined by the orientation of the substrate C with respect to the HO-Fe-Cl plane. Especially non-native substrates are often hydroxylated rather than halogenated which supports a change in positioning with respect to the Fe center.^[159,227,235] Positioning of the alkyl group of a substrate away from the oxo/-hydroxy ligand and closer to halogen ligand sacrifices H abstraction proficiency for halogen rebound selectivity.^[227] This interesting reactivity and selectivity has been examined by theoretical groups, but so far most of the calculations do not reflect the experimental data.^[210,211,218,220,222]

Results within this thesis showed that also by mutations in the substrate binding site, chemoselectivity for transformation of non-native hapalindole derivatives can be changed from 98% chlorination to 68% chlorination (32% hydroxylation) by introducing mutation I84H (*Wi-WelO15*), see chapter 3.6.4.1.^[158]

The observation, that some halogenases are able to hydroxylate, if their chloride binding site is filled and vice versa, but other members are not able to change their transformation potential shows, that the mechanistic understanding of hydroxylation versus halogenation is far from being understood.

1.3.4 Halogenase *Wi-WelO5*

After general discussion of Fe^{II}/ α KG dependent halogenases and hydroxylases, a closer look will be taken to halogenase *Wi-WelO15*, which was mainly analyzed in this thesis. *Wi-WelO15* belongs to the recently discovered, new class of non-heme iron halogenases, that act on free-standing substrates and therefore has a high potential as biocatalyst.^[155] Today, five representatives of this enzyme class are known, which all originate from the gene clusters of cyanobacterial strains subsection V (Stigonematales).^[236] Whereby the classification of subsections is based on cyanobacteria morphology.^[237] Cyanobacteria (blue green algae) occur in terrestrial and aquatic ecosystems. They produce a large number of bioactive substances with a diverse range of biological activities. The two major alkaloids biosynthesized by cyanobacteria are saxitoxin and hapalindoles.^[238,239] The family of hapalindole natural products is a group of iso-

Introduction

prenoid-indole alkaloids, found exclusively in the subsection V cyanobacteria. Over 80 variations belong to this substrate class, which are divided in subfamilies including hapalindoles, welwitindolinones, fischerindoles and ambiguines. All contain either an isonitrile or isothiocyanate with an indole alkaloid skeleton and one or more cyclized isoprene units.^[236] Interestingly, some substances were isolated from cyanobacteria cultures as chlorinated and dechlorinated substance.^[236] Representative members of hapalindoles are shown in figure 3.

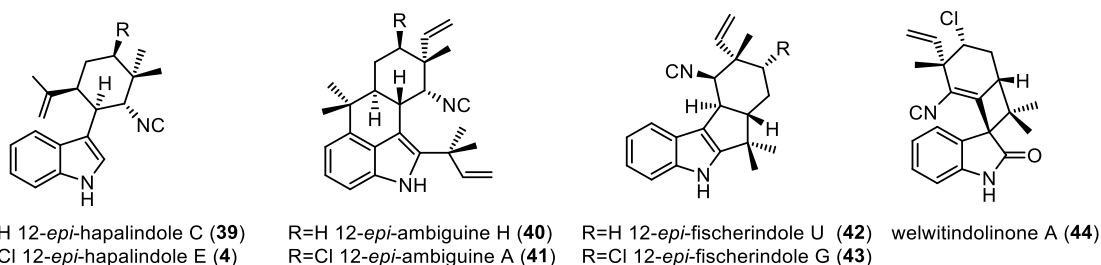


Figure 3. Examples for hapalindoles, isolated from cyanobacteria strains.^[236] Hapalindole-type alkaloids are a large group of indole monoterpoids with broad spectrum antimicrobial and antitumor activities.^[236]

Each substance has unique bioactivities, ranging from antitumor, anticancer, antialgal, antimycotic to antituberculosic activities.^[33,236,240] Gene clusters responsible for the biosynthesis of these natural products were identified^[236,241,242] and key biosynthetic steps towards the formation of hapalindoles were characterized.^[243–247] Next to other genes, several oxygenase genes were identified and numbered O1-19 combined with abbreviation for the gene cluster.^[236] Further information about the gene clusters is given in chapter 3.1, table 3. The oxygenases of the five gene clusters with their host organism are given in the following.

- *welO1-5*, *Hapalosiphon welwitschii* UTEX B1830,
- *ambO1-7* *Fischerella ambigua* UTEX 1903,
- *welO11-19* *Westiella intricata* UH strain HT-29-1,
- *welO11-17* *Hapalosiphon welwitschii* UH strain IC-52-3,
- *hpiO4-10* *Fischerella* sp. PCC 9339

Since *welO11-17* are present in *Westiella intricata* UH strain HT-29-1 and *Hapalosiphon welwitschii* UH strain IC-52-3, genes and proteins will be named *Wi-welOX* and *Hw-welOX*. Numbering was made based on sequence identity. Protein sequences with an identity greater than 90% were believed to be homologous proteins and labelled with the same number.^[236] *WelO5* and its homologues *AmbO5*, *HpiO5*, *Wi-WelO15* and *Hw-WelO15* were first suggested and later proven to be Fe^{II}/αKG dependent halogenases, responsible for the halogenation of 12-*epi*-hapalindole C and 12-*epi*-fischerindole U.^[155] *AmbO5* was shown to have an even broader substrate scope.^[156] The in vitro halogenase activity for *WelO5*, *AmbO5*, *Hw-WelO15*^[157] and *Wi-WelO15*^[158] was shown, while no in vitro characterization was performed so far for *HpiO5*. In figure 4, all-natural substrates that are accepted by the halogenases are shown.

Introduction

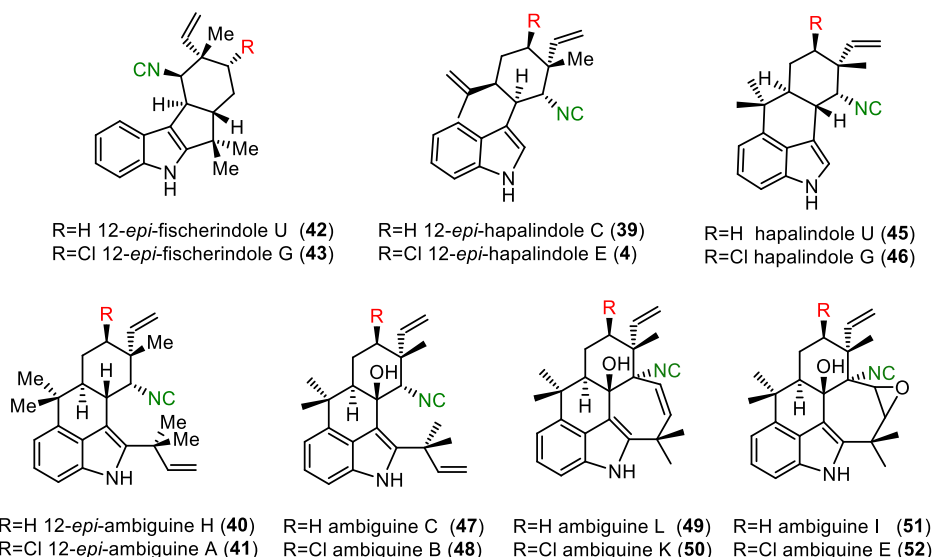


Figure 4. Natural substrate scope of halogenases WelO5 and AmbO5. Substrates are sorted by their acceptance. **42**, is accepted best, while **51** is accepted worse.^[156]

The halogenases stereo specifically replace the pro *R* hydrogen at the C13 of the substrates. Aligning the sequences, the highest difference in sequence appears in the part of the lid region which is assumed to be partially responsible for substrate recognition (ch. 3.1.3, figure 10).^[156] It was shown that by creating chimeras from AmbO5 and WelO5, the substrate scope of WelO5 could be enlarged albeit with reduced activity.^[156] Enzymes performing fascinating reactions as the selective halogenation of unactivated sp³-carbons are considered highly interesting for further use in biocatalysis. However the overall activity of the best substrate is still only 75 turnovers, which is 5-10 times greater than that of CmaB and SyrB2.^[155] To overcome the limit of a small substrate scope and low activity, enzyme engineering can be used to change properties of enzymes.

1.4 Biocatalysis

“Biocatalysis is the application of enzymes and microbes in synthetic chemistry.”^[248] Nature’s catalysts are applied for new purposes, for which enzymes have not evolved.^[248] In the last years, scientific and technological advances have established biocatalysis as a practical and environmentally friendly alternative to traditional metallo- and organocatalysis in chemical synthesis, in laboratory and industrial scale.^[248,249]

Focusing on halogenation, even though synthetic ways for halogenation reactions are known today (ch. 1.2.1), chemists often struggle with problems to halogenate unactivated carbons. To regio- and stereoselective introduce halides, many additional synthetic steps must be performed and once, the halogen is introduced, attention of further reaction conditions must be paid to not eliminate it again.^[47,79] But nature has developed a variety of elegant mechanisms to produce all these organohalogenes, in an environmental friendly way selectively. Reducing the risk potential and increasing sustainability in chemistry has been an important topic in the last years, which will be further discussed in the next chapter.

1.4.1 Green Chemistry

Starting 20 years ago, in the 1997, the concept of green chemistry was defined for the first time.^[250] The „design of chemical products and processes to reduce or eliminate the use and generation of hazardous substances“^[251] strives to work at the molecular level to achieve sustainability.^[252] Chemistry is often associated with toxicity, the first step in the lab to reduce personal risk is to use protective gear. However, in 1998, twelve principles were set by Paul Anastas and John Warner as a guiding framework for the design of new chemical products and processes.^[253] The rules should be applied to all aspects of the process life-cycle, from the raw materials used to efficiency and safety of the transformation, as well as toxicity and biodegradability of used products and reagents. The goal is to reduce intrinsic hazards to a minimum and limit the risks for accidents and damage for human and environment.^[252] In table 2, the twelve rules are overviewed.

Table 2. Twelve principles of green chemistry. For detailed explanation see Anastas and Eghbali.^[252]

Twelve Principles of Green Chemistry	
waste prevention	use of renewable feedstocks
atom economy	reduce derivatives
less hazardous chemical synthesis	catalytic reagents rather than stoichiometric reagents
designing safer chemicals	design for degradation: (products should break down into innocuous degradation products)
safer solvents and auxiliaries	real-time analysis for pollution prevention
design for energy efficiency (ambient temperature and pressure)	accident prevention

The twelve principles were not meant to be twelve independent goals but rather an integrated cohesive system of design. Only if all principles are applied a truly sustainable process can be achieved.^[252] Using one catalyst for various independent reactions or achieving an entire synthesis in one pot, would bring chemistry to a new level, as more complex molecules could be made with higher material and energy efficiency.^[252]

The typical reaction conditions for enzymatic transformations is aqueous reaction media at ambient temperatures, using renewable enzymes as catalysts.^[128] Mainly the latter named reagents are non-toxic, while conventional halogenation chemistry is often a noxious, environmentally hazardous process that requires harsh reaction conditions involving toxic reagents and solvents.^[254] One example is the carcinogenic solvent CCl₄, which is now forbidden in many countries because of its toxicity.^[120,255–257] However it must be taken into account that biocatalytic processes are sometimes run at low concentrations, producing huge amounts of waste-water.^[258] Water as solvent and high substrate loadings can often come together with solubility problems. Concentrations are reduced to a low millimolar range, which yield poor economic performances. Therefore, it can be of advantage to use a two-phase system, with one

aqueous and a second either organic phase or a solid resin. In this way, the substrate loading can be increased, while product inhibition most likely is prevented, since the organic phase serves as substrate reservoir and product sink.^[258] But the solvent and the high substrate concentration must be tolerated by the enzyme.

Stability against temperature, solvents and a variable pH range make enzymes attractive as biocatalysts. While in the lab, activity assays are mostly performed at 30 °C and individually chosen pH, in big processes, several factors like waste heat and economic profitability must be considered.^[259] The efficiency of some enzymes relative to analogous chemical processes has led to an increased use as biocatalysts in preparative and industrial applications. Furthermore, unlike small molecule catalysts, enzymes can be systematically optimized via directed evolution for a particular application and can be expressed *in vivo* to augment the biosynthetic capability of living organisms.^[260] Today there are already some biocatalytic processes that outperform conventional processes with regard to quality and economic profitability.^[259,261–263] In the past, an enzyme-based process was designed around the limitations of the enzyme; today, the enzyme can be engineered to fit the process specifications.^[248]

1.4.2 Enzyme Engineering and Directed Evolution

Protein or enzyme engineering describes the process of altering the structure of an existing protein to improve its properties.^[264] Even though enzymes in their natural substrate scope are often quite limited, successful enzyme engineering studies showed that the substrate scope of many enzymes can be enlarged or changed by adapting the active site to different molecule shapes.^[158,265–267] In contrast to classical synthetic chemistry, the structures of enzymes are able to imprint selectivities, overwrite electronic and steric properties of compounds which makes them excellent starting points for catalyst development and enable reactions that are not possible chemically.^[268] Also, low stability in general, against temperature or organic solvents could be overcome in several studies.^[249,269–272] If enzymes with low activity are used for biotransformation, large amounts of proteins are needed, reducing yield and hamper work-up because of emulsion formation.^[248] Adapting enzymes by engineering, and the use of isolated enzymes in contrast to lysate, is often considered more economic and practical because less mass is added and usually the product is easier to isolate.^[248] Purified enzymes tolerate harsher conditions, eliminate potential diffusion limitations caused by cell membranes and are easier to ship around the world. Improved enzymes with a long shelf life and good activity and stability in organic solvents should help biocatalysis to spread further into industrial laboratories.^[248]

Looking in the past, the use of living organisms and enzymes to transform natural products into new natural products is used for many decades, e.g. wine and beer fermentation, preparation of bread and cheese or natural antibiotic production.^[248] Components of living cells were already applied for useful chemical transformations more than a century ago.^[273,274]

Introduction

Over the years, the use of natural occurring catalysts changed. An important limitation is the stability of biocatalysts which can cause trouble also in today's processes. This can partially be overcome by immobilization of the enzyme, which also facilitates the reuse of the catalyst.^[248] The term directed evolution was first used in 1972, while the pH optimum of the acid phosphatase in baker's yeast (*Saccharomyces cerevisiae*) was changed.^[275]

Since X-ray diffraction of protein crystals^[276,277] became more and more established, the number of protein structures grows steadily, resulting in an increased number of structure based protein engineering. The substrate range of enzymes could be extended, which allowed the synthesis of unusual synthetic intermediates, fine chemicals and pharmaceuticals.^[278,279] In the late 1990s, directed evolution of proteins became popular in several groups and Reetz^[280], Stemmer^[281] and Arnold^[282] published modifications of an in vitro version of the Darwinian evolution. The process is based on iterative cycles of variation (amino acid changes = library creation), selection of variants with improved enzyme properties (library screening) and amplification (template chosen for next round of randomization). The process is shown in figure 5.

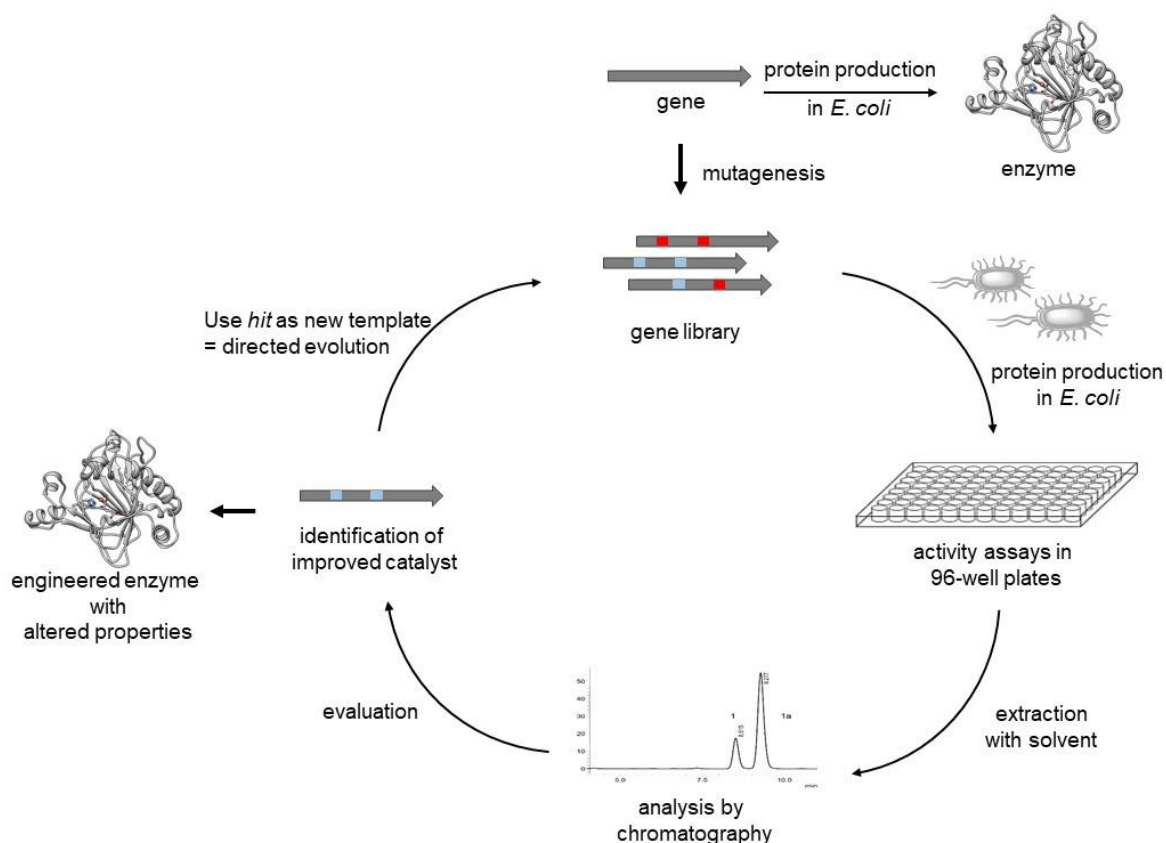


Figure 5. Protein or enzyme engineering describes the process of altering the structure of an existing protein to improve its properties.^[264] The gene is mutated to create a library of mutations, which is heterologously expressed in *E. coli*. The enzymes are examined in activity assays in 96-well plates and after extraction, their performance is read out by chromatography. An improved variant (hit) can be used as template in the next round of mutagenesis, if this engineering circle is run through several times, the process is called directed evolution.

Introduction

Previously, most directed evolution studies started with error prone PCR^[283,284] or DNA shuffling^[281,285]. However, soon it was emphasized that focused libraries usually are favorable since they decrease the screening effort. Key developments, enabling the creation of focused libraries, were an increasing number of protein crystal structures, bioinformatic tools, computer modelling and sequence analysis. Positions for mutation can be chosen from crystal structures, bioinformatic consensus information such as alignments or exploratory NNK-based saturation. Variant creation and screening are the bottleneck of all directed evolution studies since all produced variants must be examined for their properties.^[248,286–289]

Randomization of several residues simultaneously with an NNK codon, which corresponds to all 20 amino acids, adds up to library sizes with astronomical numbers. Large improvements of the enzymes' properties usually need multiple amino-acid substitutions because this results in bigger impact to the protein structure.^[248] However, substituting simultaneous multiple amino-acid creates exponentially more variants for testing. There are 7,183,900 possibilities for two substitutions anywhere in a 200 amino-acid protein and 9,008,610,600 possibilities for three substitutions. Therefore, it is useful to restrict library size to smaller alphabets.^[248,286] A molecular understanding of proteins helps to choose positions and alphabets as smart as possible.^[248,249] The design of the libraries can and should be supported by informatic tools.^[290–294] Until today, an important limitation in enzyme engineering is the unknown structure-function relationship, which makes prediction difficult.^[248,289]

In the early 2000s, 1–5 mutations were typical, whereas by 2010, 30–40 amino-acid were not unusual.^[261,295,296] Enzyme engineering is much faster than it was ten years ago, but changing 30–40 amino acids and screening tens of thousands of candidates still requires a large research team. Many, if not all, engineering strategies will yield improved variants, but some will yield better variants and find them faster.^[248] In 2005, the Reetz group described a strategy called CAST - combinatorial active-site saturation test.^[297] Here individually chosen residues are grouped into CAST randomization sites. These small libraries are tested individually. Found mutations can then be combined in iterative saturation mutagenesis (ISM).^[298] Both strategies combined are a good possibility to expand the substrate scope or change the enantioselectivity of a chosen enzyme.^[298]

CAST is of advantage, because simultaneously mutagenesis of several position also includes synergistic effects. Often it is assumed, that beneficial mutations are mostly additive,^[299] but often the contributions have unexpected behavior. For example, Weinreich and co-workers^[300] found in the evolution of a β -lactamase that a mutation A increased the reaction rate but destabilized the β -lactamase. The overall effect was slightly beneficial. Mutation B by itself had no effect because it did not affect the rate but stabilized the β -lactamase. Together, mutations A and B were highly beneficial because the β -lactamase was faster and maintained its stability. In the study all 120 possible paths were tested to attain an improved variant and only 18 of the tested paths improved resistance at each stage. Similarly, Reetz and Sanchis^[301] showed that

Introduction

only 8 out of 55 possible paths lead to an increased enantioselectivity of an epoxide hydrolase at each step. Both studies show the importance of cooperative effects, leading to the creation of smart libraries, consisting of several positions with small codons.^[302] Mutating stepwise, while taking always the best improved variant (hit) leads possibly to a dead end. The creation of small but smart libraries, takes synergistic effects into account and reduces screening effort and oversampling.^[303,304]

At the same time, high quality libraries are needed since they require less screening effort.^[305] Hence it is always necessary to check the library quality by performing Quick Quality Control (QQC), to make sure the expected diversity has been created.^[306] Furthermore statistics can be taken into account. Especially since screening is the bottleneck of engineering, it can be considered, if perhaps one out of the best three hits will be sufficient for the users need, then screening can be reduced effectively.^[307,308]

Another trend that developed in the last years is to remodel the purpose of enzymes or to design synthetic enzymes from scratch. The rationally designed biocatalysts are made for transformation that were accessible only with synthetic catalysts.^[287,288,309–312]

Today, the best approach to alter properties of enzymes, is to generate libraries containing multiple mutation sites with reduced amino-acid alphabets and to test them simultaneously. The positions to be mutated are chosen structure guided and the library design should, if possible, be supported by informatic methods. At the same time new methods for high-throughput screening are developed constantly, facilitating the screening of larger mutant libraries.^[248,249,286–288,293,294,303,310,313,314] Engineered enzymes can overcome problems like low activity and narrow substrate scopes. Stability for solvents and temperatures opens the door for industrial processes.^[248,249,315,316]

2. Thesis Goal

Goals of this thesis are to first show the evolvability of aliphatic halogenases towards non-natural substrates and to second test the properties of the created catalyst. Ultimately creating a new biocatalyst for direct and asymmetric C(sp³)-H chlorination under mild and non-hazardous conditions.

To achieve the first goal, two members, *Wi-WelO15* from *Westiella intricata* UH strain HT-29-1 and *Hw-WelO15* from *Hapalosiphon welwitschii* UH strain IC-52-3, of the 2014 discovered subclass of non-heme iron (NHI) dependent halogenases were cloned from the genomic DNA and heterologous expressed in *E. coli*. To analyze the substrate scope of the wild-type enzymes, commercially available, non-natural isonitriles and isothiocyanates are tested. To broaden the substrate scope, structure guided directed evolution is desirable, therefore, crystallization of the enzyme will be pursued to gain detailed insight into the active site of the enzymes. In parallel, random mutagenesis via error prone polymerase chain reaction (epPCR) is performed until an enzymatic structure will be available. The halogenases should be engineered to accept user defined non-natural substrates with a ketone (**54**) instead of the isonitrile group (**53**). To ensure the activity of the enzyme, a simplified derivative (**53**) of 12-*epi*-hapalindole C (**39**) will be synthesized (figure 6).

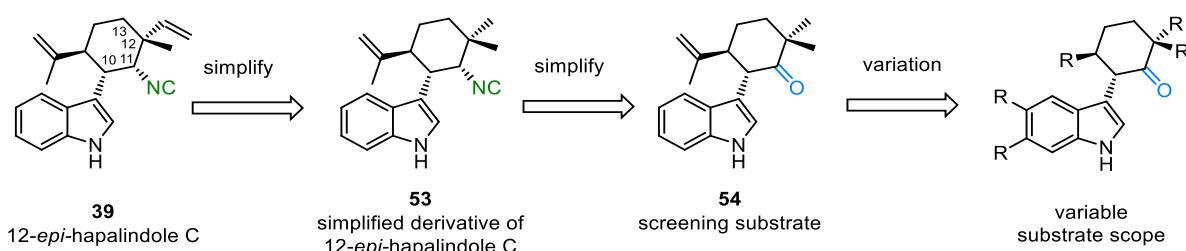


Figure 6. 12-*epi*-hapalindole C (**39**) is a natural substrate of the family of NHI dependent halogenases. To test the activity of the two representatives, used in this project, a simplified derivative of the hapalindole is synthesized (**53**). For the directed evolution towards non-natural substrates, the naturally rare occurring and instable isonitrile is substituted with a ketone functionality which simplifies the synthesis from 6 to 3 steps. When active variants are found, the substrate scope can further be tested with variations of the screening substrate (**54**).

In directed evolution studies, usually medium to high throughput screening is performed, in which several thousand created variants are tested for their chlorination activity towards the target molecule (in this case **54**), hence more than 2 g of substrate is required. Therefore, a simple and robust synthesis or cheap access should be granted. Because this is not the case for isonitriles which also occur rarely as intermediates, the ketone was chosen as functionality in position C11. Together with the substitution of the chiral center in position C10, to a simplified achiral dimethyl-function, the chosen screening substrate (**54**) can be synthesized in a 3-step synthesis (scheme 5).

Thesis Goal

The enzyme will be engineered within several generations. Screening is performed in cell lysate, where different reaction conditions have to be established that grant good enzyme activity and prevent fast iron(II) oxidation. Further reaction conditions for purified enzymes should be analyzed as well. With increased knowledge of the enzymatic system, smarter libraries can be created. Kinetic analysis of selected variants with **54** will help to gain a deeper understanding of the catalytic system and perhaps the effect of the targeted amino acid residues.

The second goal includes examination if the halogenase is applicable for a general use as chlorination method, which includes testing a larger non-natural substrate scope, increasing the reaction scale to a preparative level and determination of the enzyme's stability.

After finding one or more active variants in the screening, the substrate scope can further be tested with substrates containing variation in its structure at the indole as well as terpene ring. These substrates will be synthesized within this project and the master thesis of L. Schmermund.^[317] To characterize products and to test the biocatalytic applicability, the scale of the biocatalytic reaction should be increased from <0.5 mL and nanogram range in the screening to several milligram in flask.

Because stability of the biocatalysts is an important factor for possible future applications and projects, the melting temperature of several variants will be measured to get an idea of the overall enzyme stability. Important variants – with high selectivity and product formation – will then be tested for their stability in the presence of solvents and their activity at elevated reaction temperatures.

Next to halogenation, also the usage as hydroxylase will be examined. NHI dependent halogenases are close related to NHI dependent hydroxylases and in few cases, the reactivity can be interchanged by modifying one amino acid close to the iron center.^[160,181] This amino acid, G166 (*Wi-WelO15* numbering), will be mutated to see if a hydroxylation of the new substrates is possible. Furthermore, also oxygenase P450 from *Bacillus megaterium* will be tested if hydroxylation of the screening substrate **54** is possible. Within this project, existing oxygenase libraries in the group will be screened and from gained knowledge of this screening, a small new library of P450 will be created and selective variants will be used for preparative scale reactions to obtain products in mg-yield to characterize the new products.

3. Results and Discussion

This thesis deals with the biocatalytic halogenation of non-activated C(sp³)-H bonds with the help of engineered enzymes. As catalysts, halogenases *Wi-WelO15* and *Hw-WelO15* originating from cyanobacteria are used, which have hapalindole-type alkaloids as natural substrates. These indole monoterpene substrates are structurally fascinating molecules with interesting biological activities as anticancer properties of N-methylwelwitindolinone C isothiocyanate (**55**),^[318,319] or anti-tuberculosis activity of ambigunes K and M, fischambiguine B (**48**) as well as hapalindoles X and A(**56**).^[320–322] Today over 80 variations of the isonitrile- or isothiocyanate-containing indole alkaloid skeleton with a cyclized isoprene unit are known.^[236] The structural diversity is generated in the pattern of terpene by cyclization, chlorination, methylation, oxidation/reduction and additional prenylation.^[236] The numbering of hapalindoles differs from IUPAC nomenclature, therefore a short overview of the atom numbers in hapalindoles is given in figure 7 together with some of the mentioned structures.^[239]

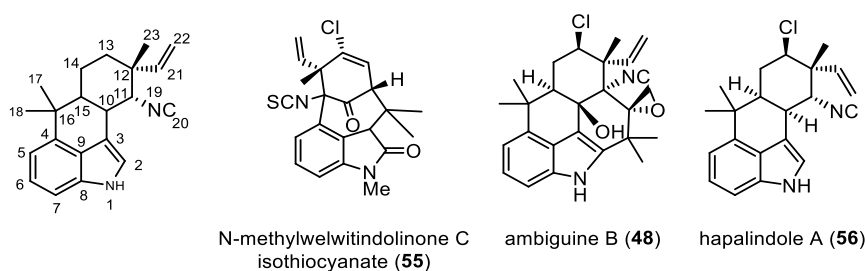


Figure 7. Numbering of atoms in hapalindoles and some examples of structures.^[239]

The results and discussion of experiments are described in several subchapters. First, the biosynthetic pathway of hapalindoles is shortly discussed. The cloning of several genes is described in chapter 3.1 including the halogenase *welO15*, which was further examined (ch. 3.2). To test the halogenase activity, analogues of the natural substrate were synthesized (ch. 3.3). The halogenase *Wi-WelO15* was then engineered by directed evolution to achieve the acceptance of a non-natural hapalindole, containing a ketone (**54**) instead of an isonitrile functionality (ch. 3.4). Different reaction conditions were tested to optimize the halogenation (ch. 3.5). The activity of the halogenase variants were analyzed with a broader, non-natural, substrate scope (ch. 3.6). Hydroxylation as side reaction was observable for some variants within the engineering process. To increase the hydroxylation selectivity, first rational designed variants of the halogenase were created and tested, but also the oxygenase P450_{BM3} was analyzed and engineered to transform **54** (ch. 3.6.4). Biocatalytic halogenation in large scale was conducted (ch. 3.7) and kinetic analysis were performed for selected enzyme substrate pairs (ch. 3.8). Furthermore, promising variants were analyzed on their stability towards an increased temperature and solvents (ch. 3.9).

3.1 Biosynthetic Pathway of Hapalindole-type Alkaloids

The biosynthesis of these natural products is quite interesting and at the onset of this thesis, different gene clusters responsible for ambigua (*amb*)^[236,241], welwitindolinone (*wel*)^[236,242] and hapalindole (*hpi*)^[236] biosynthesis were identified from different cyanobacteria strains. Comparing the gene clusters, a core set of 19 genes were identified which share greater than 92% sequence identity at the protein level.^[236] Blast analysis of the genes proposed their function: oxygenases O1-19, tryptophan biosynthesis genes T1-5 and C2, isonitrile biosynthesis genes I1-3, isoprenoid biosynthesis genes D1-4, geranyl pyrophosphate synthase gene P2, hapalindole-specific aromatic prenyltransferase gene P1, the regulatory protein-encoding genes R1 and R2, as well as C1 and C3.^[236] In figure 8 an illustration by Micallef *et al.*^[236] of the gene clusters is given.

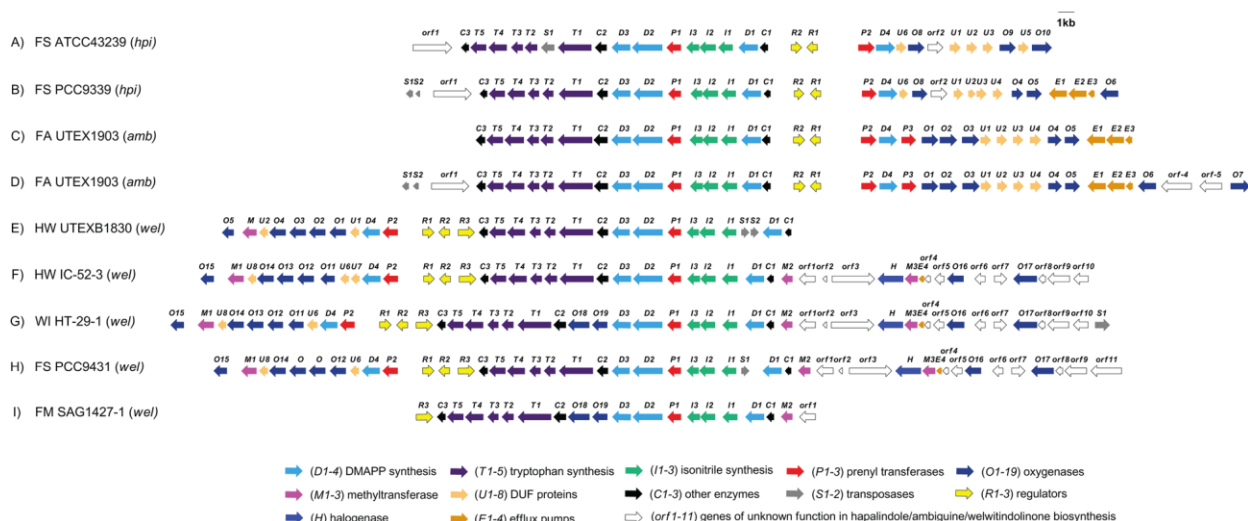
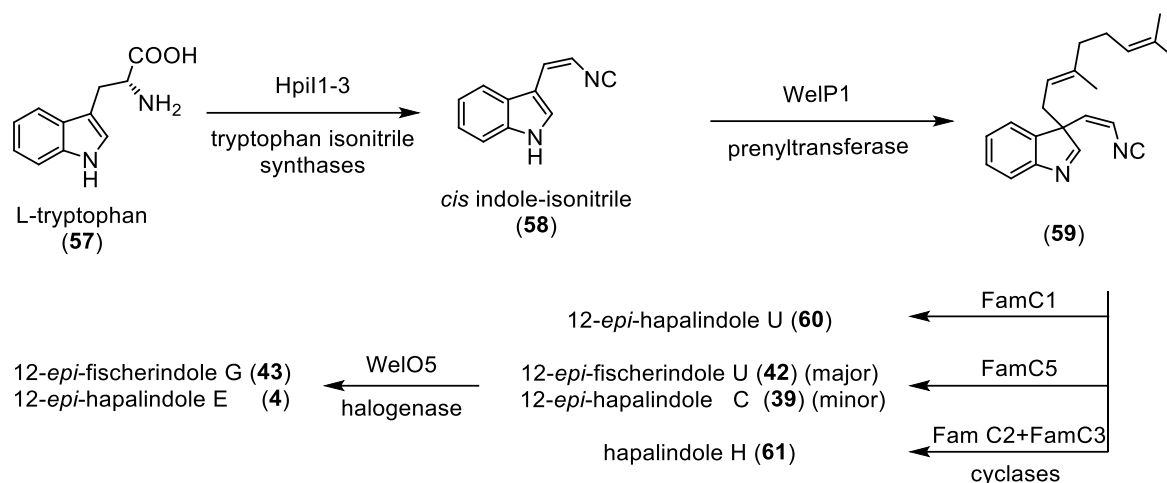


Figure 8. Illustration of the hapalindole (*hpi*), ambigua (*amb*) and welwitindolinone (*wel*) biosynthetic gene clusters. A) *hpi* gene cluster from *Fischerella sp.* ATCC 43239. B) *hpi* gene cluster from *Fischerella sp.* PCC 9339. C) *amb* gene cluster from *Fischerella ambigua* UTEX 1903. D) *amb* gene cluster from *Fischerella ambigua* UTEX 1903. E) *wel* gene cluster from *Hapalosiphon welwitschii* UTEX B1830. F) *wel* gene cluster from *Hapalosiphon welwitschii* UH strain IC-52-3. G) *wel* gene cluster from *Westiella intricata* UH strain HT-29-1. H) *wel* gene cluster from *Fischerella sp.* PCC 9431. I) *wel* gene cluster from *Fischerella muscicola* SAG 1427-1.^[236]

Key biosynthetic steps forming the monoterpene indole core structure were identified by biochemical characterization of some of these enzymes.^[155–157,236,238,241–247,323,324] Functional decorating enzymes -like the oxygenases- are still unexplored. In scheme 4 a proposed biosynthetic pathway is shown based on current knowledge.^[155,238,241,242,247]



Scheme 4. Proposed biosynthetic pathway for the production of some hapalindole-type alkaloids.^[155,238,241,242,247] Depending on literature, the cyclase genes, responsible to form the terpene ring, are either described as *famC1-5*^[244] or *ambU1-5* genes^[236].

As shown in scheme 4, the biosynthesis starts with tryptophan which is transformed by the tryptophan isonitrile synthases HpiI1-3 to build *cis* indole-isonitrile. The isonitrile functionality is characteristic for all hapalindole alkaloids. With the prenyltransferase WelP1, geranyl diphosphate is introduced into the molecule to add necessary carbons and to build the basis for cyclization.^[238] Several cyclases were found in the *amb*, *hpi* and *wel* gene cluster, able to produce different hapalindoles.^[244,325] Different oxygenases are proposed to do late-stage modification, mainly hydroxylation and indole oxidation. Amongst the oxygenases, an α KG/Fe^{II} dependent enzyme was identified as halogenase WelO5, followed by characterization of homologue halogenases WelO15 and AmbO5. The enzymes were shown to halogenate hapalindoles 39 and 42, while 60 and 61 have not yet been tested as substrates of WelO5. Several genes of the *wel* and *hpi* clusters were available in the Hoebenreich group and conducted experiments are described in the following chapters.

3.1.1 Recloning and Heterologous Expression of WelP1, HpiI1 and HpiI3

Codon optimized genes of prenyltransferase *welP1* and tryptophan isonitrile synthases *hpiI1* and *hpiI3* were received from R. Viswanathan.^[236] *welP1* was already in a suitable vector (pJExpress) for gene expression in a construct with C-terminal His₆-tag. The prenyltransferase could be produced by heterologous expression in *E. coli*. Purification via IMAC was performed by N. Braun. Elution with imidazole containing buffer (analogous to the protocol in chapter 7.1.10.1) resulted in a broad signal consisting of at least two peaks, while SDS-PAGE analysis (figure 9) of the eluted fractions showed two main signals and further impurities in low concentration. The signal at 35 kDa corresponds to the mass of WelP1, showing that the used conditions are suitable and enzyme production in *E. coli* works quite well.

Results and Discussion

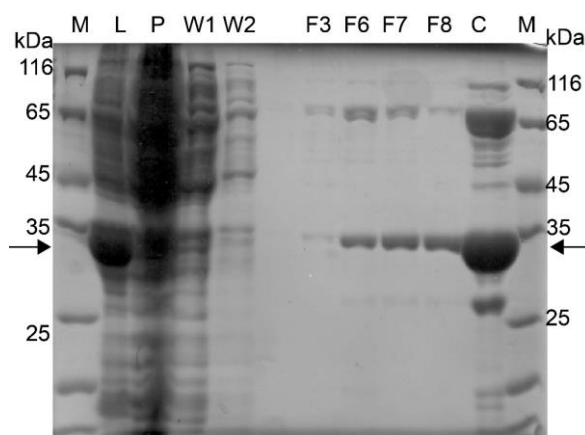


Figure 9. SDS-PAGE analysis of IMAC purification process via Ni-NTA of WelP1. M=Marker 26610 by Thermo Fischer, L=lysate, P = pellet, F3-8 are fractions collected while eluting with imidazole containing buffer, C= combined, concentrated fractions. WelP1 has a calculated mass of 34.9 kDa (Protparam^[326]). The protein band marked by an arrow contains WelP1 which was confirmed by mass analysis with a sequence coverage of 50% corresponding to 15 peptides. Other bands are assumed to be proteins from the host organism *E. coli* BL21-DE3(Gold), however no proteins could be assigned by mass.

If WelP1 should be further analyzed and purified, a modification of the purification protocol should be carried out. *hpl1*, *hpl3* were received in an unknown plasmid, sequencing revealed furthermore that no his-tag was present, which would simplify the purification process. Therefore, the genes were cloned with restriction free cloning (rf-cloning, ch. 7.1.1.3) into the pRSF-Duet vector to create an open reading frame with N-terminal His₆-tag. Since characterization of the oxygenases were in the main focus of this project, no heterologous expression was performed with the new created plasmids. WelP1 as well as HpI1 and HpI3 were characterized by other groups and recently the crystal structure of AmbP1 was published.^[236,245]

3.1.2 Cloning and Heterologous Expression of Oxygenases WelO11-WelO19

Synthetic oxidative C-H functionalizations are challenging reactions, where success highly depends on the structure and presence of functional groups. Especially challenging is control of stereo- and enantioselective introduction of hydroxy or halogen groups in complex molecules. Enzymes mostly perform reactions quite selective albeit with a limited substrate scope. If the substrate scope can be altered, enzymes as selective biocatalysts are a great alternative to chemical catalysts. The gene clusters responsible for hapalindole-like alkaloid production, which are not dependent on polyketide synthases or non-ribosomal peptide synthetases, carry a great potential to contain useful biocatalysts. Since the diversity of hapalindoles is huge, a variety of different transformations, such as hydroxylation, oxidation, desaturation must be possible with these enzymes.

In table 3 an overview of oxygenases in *hpi*, *wel* and *amb* clusters is given by Micallef *et al.*^[236]. Until now, few is known about the oxygenases. In 2014 and following years, WelO5/AmbO5/Wi-WelO15/Hw-WelO15/HpiO5, were published to be members of a new class of halogenases. These halogenases are non-heme iron (NHI) dependent and chlorinate

Results and Discussion

freestanding substrates.^[155–158] The enzymes in table 3 are sorted based on their sequence identity. Also, HpiO5/AmbO5 and the WelO15 enzymes are highly related with a sequence identity of 78-80%.

Table 3. List of encoded oxygenase enzymes from the *hpi*, *amb* and *wel* biosynthetic gene clusters.^[236] The halogenases HpiO5, AmbO5, WelO5 and WelO15 are highlighted in purple. Organisms which are abbreviated in the table: *Fs*=*Fischerella sp.*, *Fa*=*Fischerella ambigua*, *Hw*=*Hapalosiphon welwitschii*, *Wi*=*Westiella intricata*.^[236,242]

organism:	<i>Fs</i>	<i>Fa</i>	<i>Hw</i> UTEX	<i>Hw</i>	<i>Wi</i>	<i>Fs</i>
	PCC	UTEX	1803	IC-52-3	HT-29-1	PCC
oxygenases	9339	1903				9431
Rieske oxygenase		AmbO1	WelO1	WelO11	WelO11	
Rieske oxygenase		AmbO2	WelO2	WelO12	WelO12	WelO12
Rieske oxygenase		AmbO3	WelO3	WelO13	WelO13	
Rieske oxygenase	HpiO4	AmbO4	WelO4	WelO14	WelO14	WelO14
oxidoreductase, α KG/Fe ^{II} oxygenase family	HpiO5	AmbO5	WelO5	WelO15	WelO15	WelO15
alkanesulfonate monooxygenase	HpiO6	AmbO6	-			
oxidoreductase, FAD dependent pyridine nucleotide disulfide	-	AmbO7	-			
indoleamine 2,3 dioxygenase			-	WelO16	WelO16	WelO16
choline dehydrogenase-like flavoprotein			-	WelO17	WelO17	WelO17
monooxygenase			-		WelO18	
Rieske oxygenase			-		WelO19	

The genomic DNA of two cyanobacterial strains *Hapalosiphon welwitschii* UH strain IC-52-3 (*Hw*) and *Westiella intricata* UH strain HT-29-1 (*Wi*) were received from Michelle Moffit.^[236] All oxygenases from the *wel* gene cluster were amplified by polymerase chain reaction (PCR) and cloned by a restriction free cloning method^[327] into the high copy pRSF-Duet vector. By cloning, a His₆-tag was added to the N-terminus of all enzymes. The genes and enzymes will be named after their organism, combined with the cluster and numbering. For example, *Wi*-WelO15 represents the oxygenase 15 of the *wel* cluster occurring in *Westiella intricata* UH strain HT-29-1.

For the restriction free cloning, primers were designed with a partial overlap of the vector on one side and with the gene on the other side. These primers were used to amplify the genes from the genomic DNA. Due to the amplification with the primers, the gene carries overlap-

ping areas with the pRSF-Duet vector at the 3' and 5' end and can further be used as megaprimer for the amplification of the whole vector. Successful cloning was confirmed by sequencing and the plasmid incorporated in *E. coli* BL21-Gold(DE3). Cloning of oxygenases WelO11-19 of *Westiella intricata* and WelO11-WelO17 of *Hapalosiphon welwitschii* (except *Hw*-WelO14) was successful. In attempts to amplify *Hw*-welO14, only sequences of *Hw*-welO13 could be found, due to a high sequence similarity. In further attempts to clone *Hw*-welO14 new primers should be designed. Sequences of the genes are given in ch. 8.3.2 and additional information about cloning, mutations in the genes and silent mutations are listed in table 36 (ch. 8.3.1).

For genes *Wi*-welO11-14, test expressions were performed by S. Grobe (ch. 7.1.9.3). SDS-PAGE analysis showed that the enzymes could be produced best in LB-medium but seem to be mainly insoluble in the cell pellet under tested conditions. No further optimization of expression conditions, as shorter incubation times or different production temperatures, were tested. J. Pilgram tested the production of *Hw*-WelO16-WelO17 and *Wi*-WelO16-WelO18 (ch. 7.1.9.5) in *E. coli*, which was successful, but purification attempts indicated that the enzymes seem to be very instable since precipitation after purification was noticed already overnight. In contrast to that, the halogenase *Hw*-WelO15 and *Wi*-WelO15 were overexpressed in *E. coli* BL21-Gold(DE3), purified in high yields (~60 mg/L) and seemed to be quite stable (ch. 7.1.9.1).

3.1.3 Characterization of Aliphatic Halogenases *Wi*-WelO15 and *Hw*-WelO15

If the nucleotide sequence of *Wi*-WelO15 is analyzed with the nucleotide blast tool of the National Center for Biotechnology Information (NCBI)^[328], 13 sequences are found with a sequence identity >80%. The highest identity exists with *welO5* (99% similarity and identity), a gene from *Hapalosiphon welwitschii* UTEX B 1830 which was published in 2014 as aliphatic halogenase, dependent on Fe^{II}, alpha-ketoglutarate (α KG) and O₂ which belongs to a new class of halogenases that works on freestanding substrates.^[242] Therefore it can be assumed, that the halogenases *Wi*-WelO15 and *Hw*-WelO15 also belong to the class of non-heme iron (NHI) dependent halogenases. This new halogenase class is of special interest since they perform chemo-, regio- and stereoselective C-Cl bond formation under mild and non-hazardous conditions, which is still a formidable challenge in chemical^[57,84,329-332] and enzymatic catalysis,^[101,120,148,333-336] especially by direct functionalization of unactivated C(sp³)-H bonds.^[78,81,337,338]

Therefore, the two halogenases *Wi*-WelO15 and *Hw*-WelO15 enzymes should be explored for their biocatalytic potential within this thesis. The project was started by amplifying *Wi*-WelO15 and *Hw*-WelO15 from their respective genomic DNA. Identical primers were used, resulting in two mutations V6I and D284N in *Wi*-WelO15 which therefore is not the wild type but a starting variant, in the following named *Wi*-0. Figure 10 shows an amino acid alignment of all those Fe^{II}/ α KG dependent halogenases that so far have been cloned and recombinantly expressed. The two mutations introduced in *Wi*-0 are highlighted with blue boxes. The two

Results and Discussion

amino acids that differ between *Wi*-WelO15 and WelO5 are highlighted with red boxes. The green box highlights the area in which all enzymes differ most. After the crystal structure was solved it became clear that this area is a helical lid which closes over the active site and is partially responsible for substrate recognition.^[156]

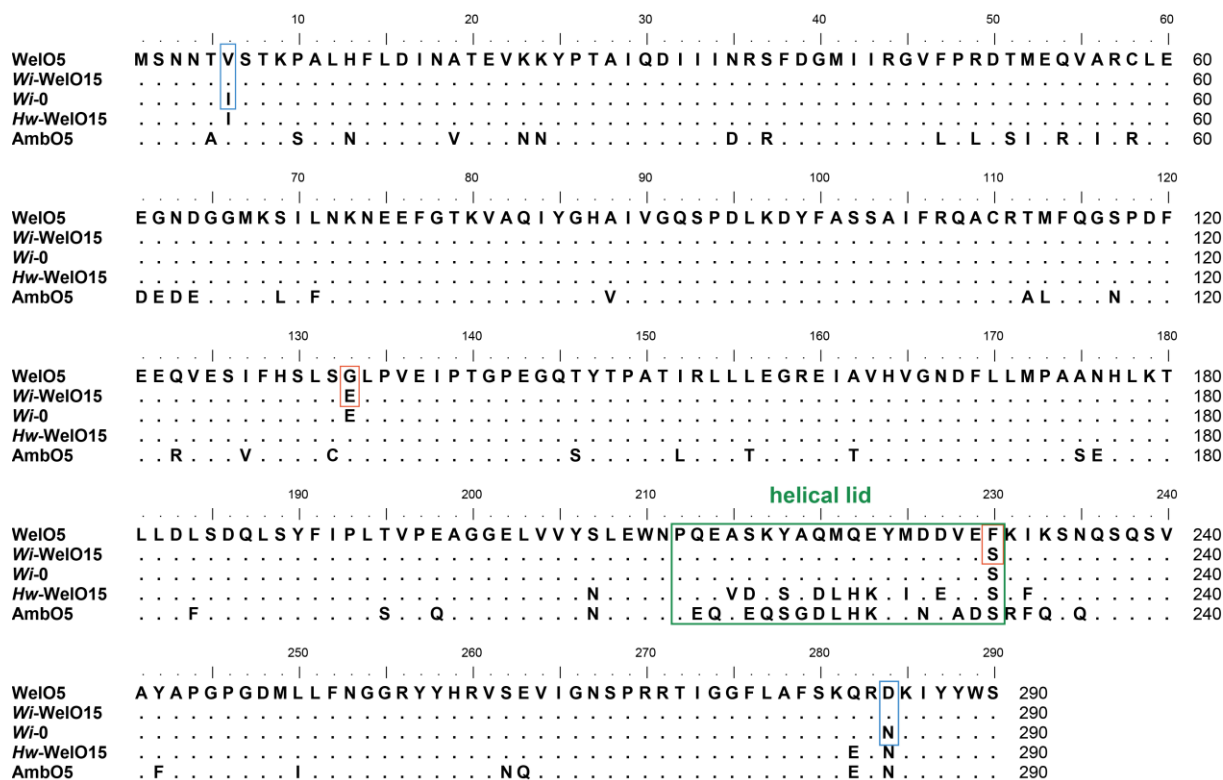


Figure 10. Alignment of cloned and recombinantly expressed Fe^{II}/αKG dependent halogenases which are able to chlorinate free-standing substrates. N-terminal His₆-tag and linker are not shown for clarity. *Wi*-0 is a variant of *Wi*-WelO15 from *Westiella intricata* HT-29-1, containing mutations V6I and D284N from primer design (blue boxes) and represents the starting point of this directed evolution study. *Hw*-WelO15 from *Hapalosiphon welwitschii* IC-52-3.^[236] WelO5 from *Hapalosiphon welwitschii* UTEX B1830^[242] and AmbO5 from *Fischerella ambigua* UTEX 1903.^[241] Red boxes highlight naturally occurring differences between *Wi*-0 and WelO5. The green box highlights the α-helices forming an active site lid.

The alignment shows that the amino acid sequences share a high identity with most differences in the part of the helical lid. AmbO5 has with 77% the lowest sequence identity to WelO5 and comparing the substrate scope, AmbO5 chlorinates more hapalindole alkaloids than WelO5.^[156] Comparison of sequences reveal 99% identity and similarity between *Wi*-WelO15 and WelO5 and 94% identity and 97% similarity between *Hw*-WelO15 and WelO5.^[339] In the following chapter, the expression and purification (ch. 3.2) as well as the activity of the halogenases *Wi*-0 and *Hw*-WelO15 (ch. 3.3 ff) will be analyzed.

3.2 Halogenase Production and Purification

Hw-WelO15 and *Wi-0* (*Wi-WelO15* V6I/D284N, mutations originate from primer design) were produced with N-terminal His₆-tag in *E. coli* BL21-Gold(DE3). In the beginning, different expression conditions were tested including TB and LB medium as well as IPTG concentrations in the range of 20 μ M to 1 mM. The following conditions worked best and were further used throughout this thesis: 0.5 L LB-medium containing 50 μ g/mL kanamycin and 50 μ M FeCl₃ in 2 L baffled flask. The medium was inoculated with 5 mL preculture and let grown at 37 °C until an OD₆₀₀ reached 0.4, gene expression was induced by adding IPTG to a final concentration of 20 μ M and the temperature was reduced to 22°C. After further shaking for 16 h the cells were harvested by centrifugation, the pellet was resuspended in buffer containing 50 mM HEPES, 10 mM NaCl, 10% glycerol with pH 7.4 and stored at -20°C until further usage.

In figure 11, an SDS-PAGE analysis of lysates, containing *Hw-WelO15*, *Wi-0* and *Wi-WelO15* V6I, is shown. Since the C-terminus points into the active site (see ch. 3.2.1.2 and figure 19) it could be possible that a mutation in this region effects folding or activity. Cells were normalized to OD₆₀₀ before lysis. Cleared lysate was applied to the SDS-polyacrylamide gel to compare the levels of soluble halogenase, which can be seen in the band at around 34.5 kDa, marked by an arrow. Lane 3 shows *Wi-WelO15* V6I, where mutation D284N from *Wi-0* was reversed to the wild-type sequence, to see if it has an effect on the expression level.

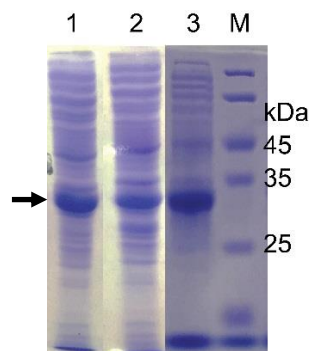


Figure 11. SDS-PAGE analysis of OD₆₀₀ normalized *E. coli* BL21-Gold(DE3) cells induced with IPTG after lysis with lysozyme. 1) *Hw-WelO15* 2) *Wi-0* and 3) *Wi-WelO15* V6I. The halogenases have a calculated molecular weight of 34.4 kDa (*Hw-WelO15*) and 34.5 kDa (*Wi-WelO15*), the band corresponding to the halogenase, is marked by an arrow.

Expression levels of *Hw-WelO15*, *Wi-0* and *Wi-WelO15* V6I are comparable. Because of the His₆-tag, simple one step immobilization metal ion chromatography (IMAC) purification was possible. Therefore, the cells were lysed by sonication and insoluble cell debris removed by centrifugation. An Äkta purification system with Ni-NTA column in combination with a Tris buffer was used. As can be seen in figure 12 the elution profile of both *WelO15* enzymes did not show a Gaussian distribution as expected but a very strong tailing. This also persisted while washing with buffer containing 0.5 M imidazole.

Results and Discussion

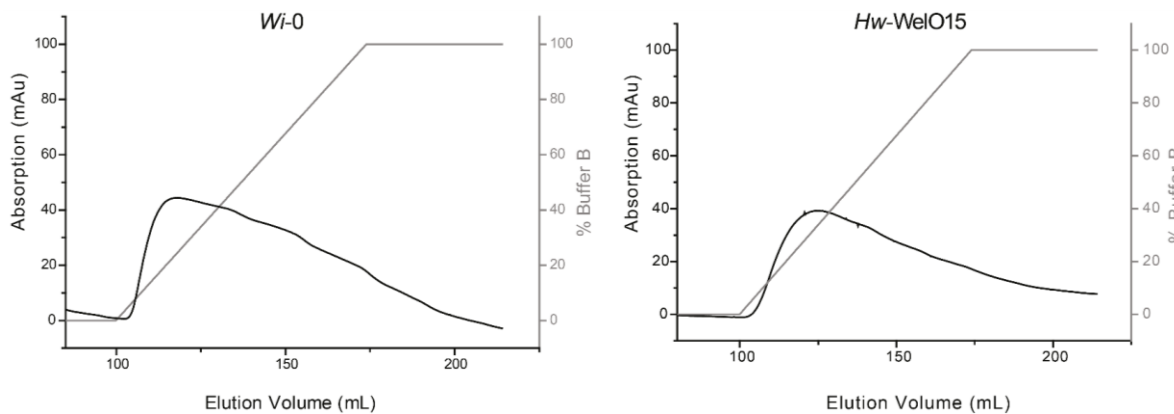


Figure 12. Elution profile of affinity chromatography of *Wi-0* and *Hw-WelO15*. To load the enzyme to the nickel resin buffer, buffer Tris A (50 mM Tris, pH=7.4, 500 mM NaCl, 0.1% Tween-20, 20 mM imidazole, 10 mM β -mercaptoethanol) was used. After washing unbound enzymes from the column, elution was performed by a gradient increasing the concentration of buffer Tris B (50 mM Tris, pH=7.4, 500 mM NaCl, 250 mM imidazole, 10 mM β -ME). The purification process is described in ch. 7.1.10.1.

From the elution profile, it appears that the enzyme binds strongly to the column material, which leads to the observed strong tailing. It could be possible that polar surface residues interact with the Ni-ions or that the enzyme is quite flexible and the iron binding site containing two histidines, in the active center, interacts with the column material. The ability of this enzyme class to bind nickel was shown for oxygenase TauD and halogenase WelO5 as both enzymes are inhibited by divalent ions Co^{2+} and Ni^{2+} .^[155,340] However, this strong interaction with the resin resulted in pure enzyme solution, as can be seen from the SDS-PAGE analysis in figure 13.

Batch purification with the same resin was tested by M. Biermeier but the yield decreased dramatically, therefore this purification approach was omitted.^[341] The exchange from Nickel resin to Talon, a cobalt based resin, was tested and lead to a low binding under similar buffer conditions. The enzyme was detected by SDS-PAGE analysis to be in the flow-through fraction.

In another approach to minimize tailing, the Ni-NTA column was run with phosphate buffer pH 6 (100 mM potassium phosphates, 500 mM NaCl, 20 mM imidazole to 250 mM imidazole). Less tailing was observed, however the enzyme eluted at higher imidazole concentration in a broad peak. While concentrating the enzyme, precipitation could be observed, therefore it was concluded that this buffer is not suitable for storage of the halogenase. Dialysis into another buffer was tried but activity assays showed a lower turnover than halogenase, purified with Tris buffer. In figure 13, the samples are shown, taken at different steps during the purification process.

Sample I (lane 2, figure 13a) represents the cell culture when IPTG is added. After 16 h growth time, the cells were harvested (H). After applying the lysate to the column, unbound samples are washed from the column (W). For elution, the concentration of imidazole was raised to 250 mM by a linear gradient and 5 mL fractions are collected (1-5).

Results and Discussion

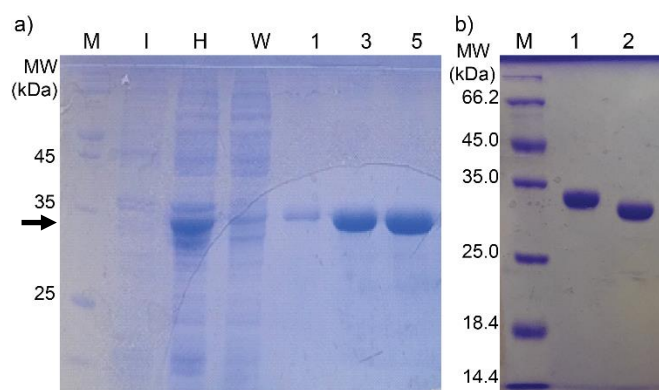


Figure 13. a) SDS-PAGE analysis of IMAC purification of *Wi-0*, the protein band of *Wi-0* is marked by an arrow. The shown samples were taken at I =induction with IPTG, H=harvest, W=wash fraction of IMAC, 1-5 = elution fractions. Marker (M) 26610, Thermo Fisher. b) Purified halogenases, concentration determined via Bradford Assay. Lane 1: *Hw-WelO15*, lane 2 *Wi-0*, each line contains 3.3 μg protein.

Figure 13b) shows 3.3 μg isolated *Hw-WelO15* (lane 1) and *Wi-0* (lane 2), after concentration determination with Bradford Assay. Protein production followed by IMAC purification yielded a reproducible yield of 60-65 mg/L of bacteria culture. In comparison to published yields of 25 mg/L,^[155] the yield could be increased by a factor of 2.5. Since a different vector and *E. coli* strain in combination with changed cell growth conditions as well as purification procedures were used, no conclusion can be drawn if one factor or several changes in the protocol lead the increased yield.

For crystallographic experiments, size exclusion chromatography (SEC) was performed afterwards using a Superdex26/60 column. Therefore, the enzyme was concentrated to 1 mL and applied to the column via a loop. It could be seen that the enzyme did not precipitate at concentrations up to 1.7 mM (60 mg/mL) in the presence of 10% glycerol, while the absence of glycerol in the purification buffers causes precipitation at lower enzyme concentrations. With isocratic elution by HEPES 2 buffer (50 mM HEPES, 10 mM NaCl, 10% glycerol, 0.5 mM DTT, pH 7.4), the enzyme eluted at 227 mL as can be seen in figure 14.

Samples were taken from the main peak that were analyzed by SDS-PAGE (figure 14a). To exclude, that the small band at about 25 kDa is an impurity, both bands (A and B, figure 14b) were analyzed by tryptic digestion, followed by mass analysis. Both showed the highest fragment coverage with *Wi-0*, which leads to the assumption that the smaller band is a fragment of the enzyme that cannot be separated with this chromatography step or originates from SDS-PAGE sample preparation. To see if it results from sample preparation for SDS-PAGE analysis, a native PAGE could be run, where no boiling with SDS for linearization is necessary.

After purification by chromatography, which include a dialysis step against EDTA containing buffer to remove metal ions (Fe^{III} or Ni^{II}), the enzyme solution is colorless. When αKG and iron are added, the color of the solution turns lilac, as can be seen in figure 14c.

Results and Discussion

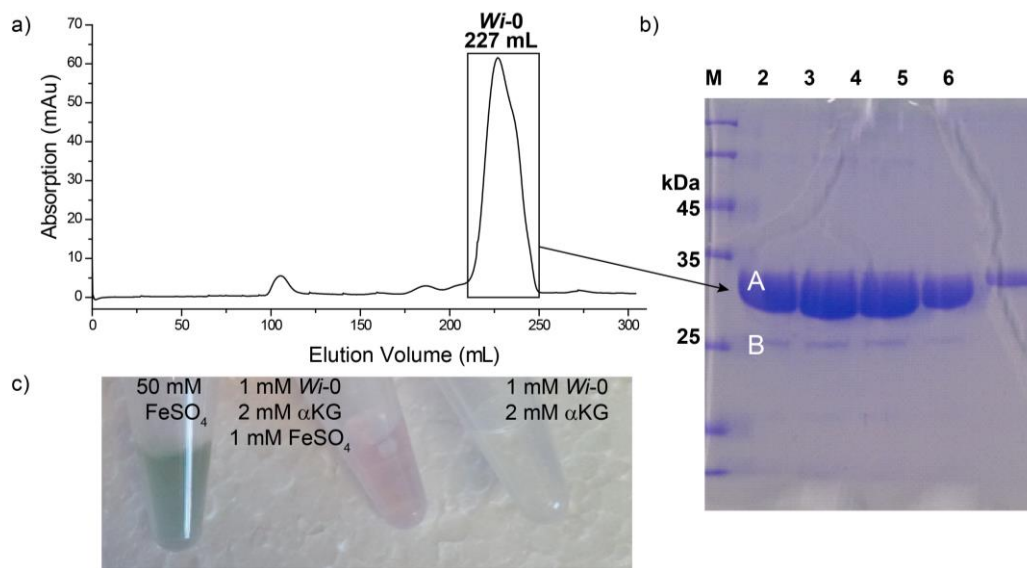


Figure 14. a) *Wi-0* elution profile from size exclusion chromatography (SEC). SEC was performed with an isocratic flow of 1.5 mL/min and 50 mM HEPES, pH 7.4, 10 mM NaCl, 10% glycerol, 0.5 mM DTT. b) SDS-PAGE gel of fractions that eluted in the main peak with a maximum at 227 mL. Gel bands A and B were cut and analyzed by tryptic digestion, followed by mass analysis. Both bands are from *Wi-0*. c) Freshly prepared reagent solutions for crystallization are shown, for color comparison. Iron sulfate was dissolved in N₂ purged buffer and has a greenish color, while the 1 mM *Wi-0* solution containing iron and αKG has a lilac color. The metal free enzyme solution is colorless.

The color is based on a charge transfer complex that is formed between αKG and Fe^{II} inside of the enzyme, as it is also described for TauD.^[191,192,224] This behavior could only be observed for *Wi-0*, but not for *Hw-WelO15* so far. The color intensity however is quite weak, as for TauD an extinction coefficient of only $\epsilon_{530} = 140 \text{ M}^{-1} \text{ cm}^{-1}$ was determined.^[342] In figure 14c a 1 mM enzyme solution with iron and αKG is shown in comparison to an iron-free sample. Storage of the lilac enzyme solution overnight lead to color change. The yellowish color of the solution indicate that Fe^{II} is oxidized to Fe^{III} by oxygen from air.

For some non heme iron dependent hydroxylases, for example TfdA (Trp113)^[163], AlkB homologue hABH3 (Leu177)^[343] and TauD (Tyr73, Trp 128, Trp240, Trp248)^[163,196,344] it was shown that the enzyme performs self-hydroxylation in the absence of a substrate. For the NHI dependent halogenase SyrB2 this was also supposed because of an overall low turnover number of 7 when chlorinating its natural substrate L-Thr-S-SyrB1.^[149,198,345] All cofactors, αKG, NaCl, Fe^{II/III} and O₂ are present in the growth media, therefore, it also could be possible that a long expression time results in self-hydroxylation which might inactivate the enzyme. To rule this out, samples with purified enzyme were submitted to the mass department to analyze the denatured mass. In figure 15, the received mass spectra (time of flight combined with electro spray ionization in positive ion mode (TOF-ESI⁺)) of *Wi-0* are shown, the ones of *Hw-WelO15* can be found in the attachment (ch. 8.3.3).

Results and Discussion

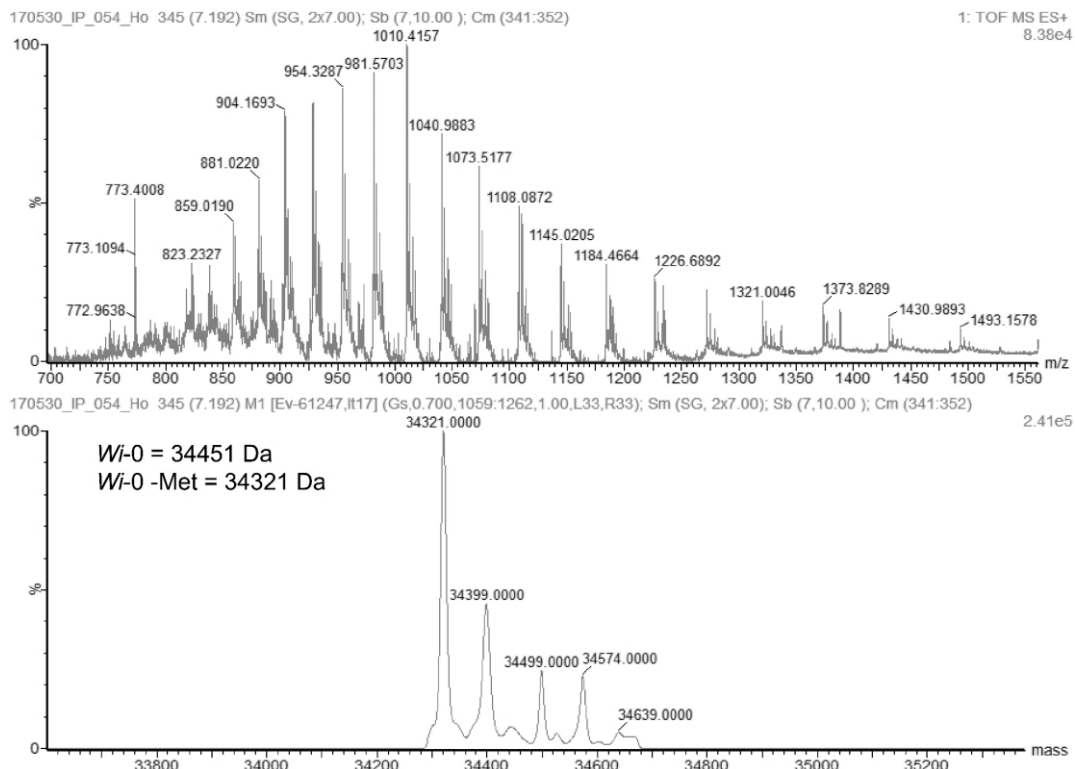


Figure 15. Mass spectrum of the isolated, denatured *Wi-0*. The denatured enzyme was measured via HPLC-TOF-ESI⁺ by the mass department of the Philipps-University Marburg. The theoretical mass of *Wi-0* is 34451 Da, calculated with ExPASy ProtParam.^[326] Further peaks correspond to adducts with ions or solvents (+78 = 2K⁺, +100 = 2K⁺, 1Na⁺,

With mass analysis no autooxidation could be detected for enzymes after heterologous expression and purification under standard conditions (ch. 7.1.9.1, ch. 7.1.10.1). But no information is available if this autooxidation happens during biotransformation.

Enzyme production and purification worked reliably with good yields and excellent purity. For the goal to do directed evolution, it is necessary to know as much about the enzyme as possible. Therefore, experiments regarding structural information and stability were conducted. On the one hand, this includes circular dichroism to examine melting temperatures of the halogenase, with which information about the effect of different buffers and presence of its cofactors should be examined. On the other hand, crystallization experiments were made to solve the structure of the enzyme, which was unknown at that time.

3.2.1 Structural Analysis of Halogenases *Wi-0* and *Hw-WelO15*

3.2.1.1 Circular Dichroism

For further stability and folding information, circular dichroism (CD) measurements were performed. Folding of both enzymes were measured in HEPES and KPi buffer to check if the folding is influenced by the buffer but no remarkable differences could be seen. It was observable that iron phosphate precipitated when FeSO_4 was added to the enzyme solution in KPi, therefore the enzyme was only used in HEPES afterwards.

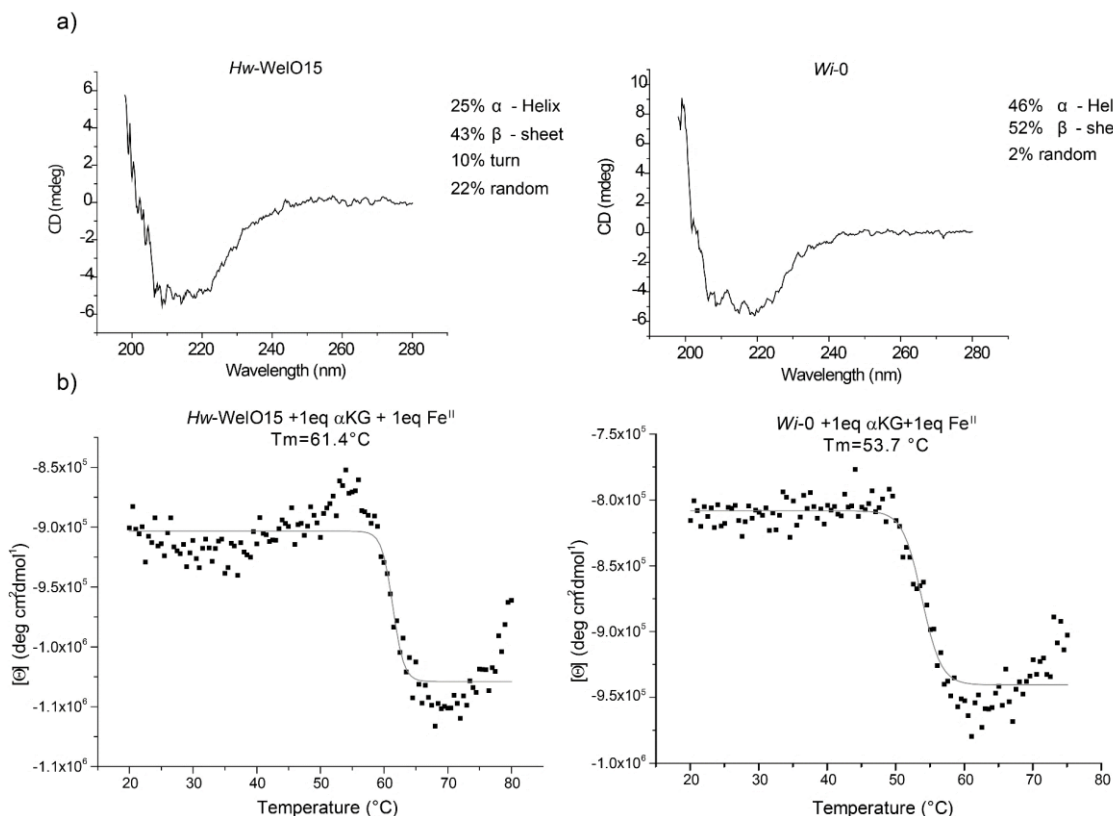


Figure 16. CD measurements of *Wi-0* and *Hw-WelO15*. a) 5 μM enzyme solution was measured in buffer which was diluted 1-10 with H_2O to reduce background by high salt concentrations (final concentration: 5 mM HEPES, 1 mM NaCl, pH 7.4). b) To see the unfolding a concentration of 25 μM enzyme in 5 mM HEPES, 1 mM NaCl, pH 7.4 was needed.

From the obtained data it could be seen, that quite high differences in folding were measured for the two enzymes, even though they are thought to have a quite similar structure based on a high sequence identity of 98%. From the later published crystal structure of WelO5 it could be seen, that WelO5 has 28% helical structures and 24% beta sheet,^[160] which differs from both obtained data sets. The folding was determined by triplicate measurements. But within different enzyme concentrations, folding changes of up to 10% for one motive could be observed. High errors in the range of 6-10% often occur and can be lead back to errors in concentration determination.^[346,347]

Measurement of melting curves showed that the melting temperature of *Hw*-WelO15 with 61.4 °C is about 8 °C higher than that of *Wi*-0 with 53.7 °C. Five-time measurement of a sample gave a standard deviation of only 0.3 °C. It can be assumed that the results from melting temperatures are more reliable since these values are independent from enzyme concentration or environmental influences since the measurement observes the change in millidegree at one fixed wavelength. Further results to melting curves and CD measurement can be found in chapter 3.9.1.

3.2.1.2 Crystallization

For enzyme engineers, it is less effective to engineer a system without knowing the structure. In cooperation with the MarXTal, the crystallography department of the Philipps-University, a crystallization screening was performed. Commercially available 96-well crystallization screening plates from Quiagen were used to test different crystallization conditions. Therefore, *Wi*-0 was isolated by affinity and size exclusion chromatography. In total ten 96-well plates were pipetted (all given in table 29, chapter 7.1.14) and with each well, two crystallization conditions can be screened. A 1 mM solution of *Wi*-0 in 50 mM HEPES, 10 mM NaCl, 10% glycerol and 0.5 mM DTT was used for crystallization. As cofactors, one sample contained additionally 2 mM α KG, while the second sample contained 2 mM α KG and 1 mM $\text{FeSO}_4 \cdot 7 \text{H}_2\text{O}$. Already after three days some crystals were formed in the set-up with iron (figure 17a). The measurement at the synchrotron in Grenoble was done by Dr. V. Srinivasan. The obtained data set resulted in a resolution of about 3.5 Å. Refinement and repetition of screening conditions, pipetted by hand, could not reproduce crystal growth. However, in the same plate but conditions without iron, more crystals with hexagonal shape grew within several months (figure 17b). Even though they had a diffraction of around 2 Å, the structure could not be solved because the molecules were twinned within the crystals. A third kind of crystals grew (figure 17c), which did not diffract in measurements at the synchrotron.

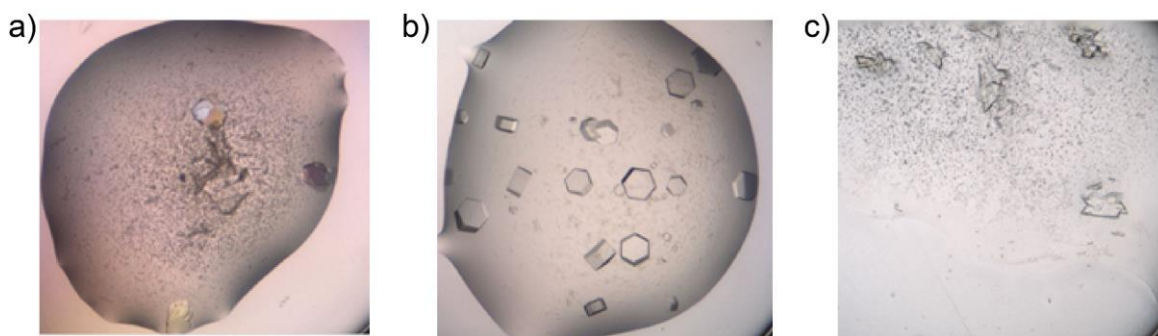


Figure 17. Crystals of *Wi*-0. a) The enzyme crystallized aerobically within 3 days. A stock solution of 32.5 mg/mL *Wi*-0, 2 mM α KG and 1 mM FeSO_4 was mixed 1-1 with reservoir buffer (0.2 M KOAc, 2.2 M AmSO_4). b) The aerobic growth of these crystals took about 3 months. A stock solution of 32.5 mg/mL *Wi*-0, 2 mM α KG was mixed 1-1 with reservoir buffer (0.1 M Tris pH 8.5, 2.4 M AmSO_4). c) The aerobic growth of these crystals took about 10 months. A stock solution of 32.5 mg/mL *Wi*-0, 2 mM α KG was mixed 1-1 with reservoir buffer (0.1 M Bicine, 1.6 M AmSO_4).

Results and Discussion

The structure of the first crystals (figure 17a) could be solved with a resolution of 3.46 Å, based on molecular replacement using the structure of WelO5^[160] which was published while crystals of *Wi-0* were measured at the synchrotron.

To reproduce crystal growth, a new enzyme stock was prepared (new purification without previous freezing) and four plates were prepared, three that resulted in crystals last time and one, which contains a variety of different divalent metal ions (table 29, chapter 7.1.14). These plates were pipetted and incubated aerobically and anaerobically. After about 6 months, few crystals grew as shown in figure 17c. Some crystals were soaked with a 1 mM solution of hapalindole Q in EtOH, but all tested crystals did not diffract. Interestingly all conditions that resulted in crystal growth had ammonium sulfate as salt present, which suggests its importance for the enzyme.

Also, *Hw-WelO15* was tried for crystallization. Therefore, it was purified by affinity and size exclusion chromatography and three crystallization screening plates, which resulted in crystals for *Wi-0*, were pipetted by the crystallization department, however, no crystal grew within 2 years.

The solved structure of *Wi-0* (PDB 6GEM) shows the typical jelly-fold with iron center which is bound to His₁₆₄ and His₂₅₉. In figure 18 the structure of *Wi-0* is shown in comparison to the 3 known states of WelO5.

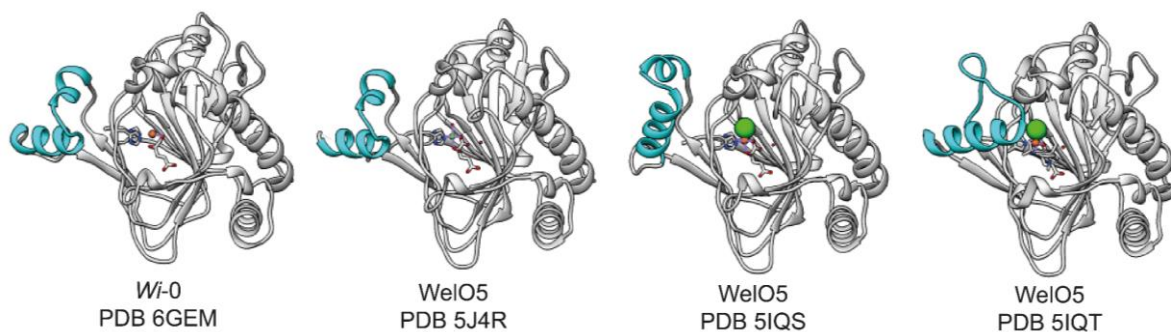


Figure 18. Crystal structure of *Wi-0* (*Wi-WelO15* V6I/D284N) in comparison to different crystallization states of WelO5.^[158,160,348] The α -helical lid, which can close over the active site, is shown in cyan.

The structure of *Wi-0* contains the cofactor α KG, however, no electron density could be detected, where the chloride is supposed to be sitting. In comparison to the published WelO5 structures, the α -helical lid is shifted. Liu and coworkers solved WelO5 in two conformations, an open and a closed form.^[160] *Wi-0* shows a third conformation, which was also observed by Schofield and coworkers who solved the structure of WelO5 with nickel as metal center instead of iron (PDB 5J4R).^[348] Their structure is without chloride, too. This indicates that the chloride might be responsible for the different conformation. Since the metal center is different in the two structures (PDB 6GEM and 5J4R), no clear assumption can be drawn. WelO5 struc-

Results and Discussion

tures of Mitchell *et al.* were soaked with 12-*epi*-fischerindole U before measuring and the structure with substrate could successfully be solved. Interestingly, the substrate was detected to be sitting in the enzyme with either open or closed conformation (figure 18, PDB 5IQS and 5IQT chain).^[160]

The two halogenases *Wi*-WelO15 and WelO5 share an identity of 99% and only differ in 2 amino acids S230F and E133G (*Wi*-WelO15 numbering). During amplification of *Wi*-WelO15, two more mutations were introduced namely V6I and D284N resulting in the variant *Wi*-0. The positions of these four mutations in comparison to WelO5 could have an effect on structure and the activity. In figure 19, these positions are highlighted.

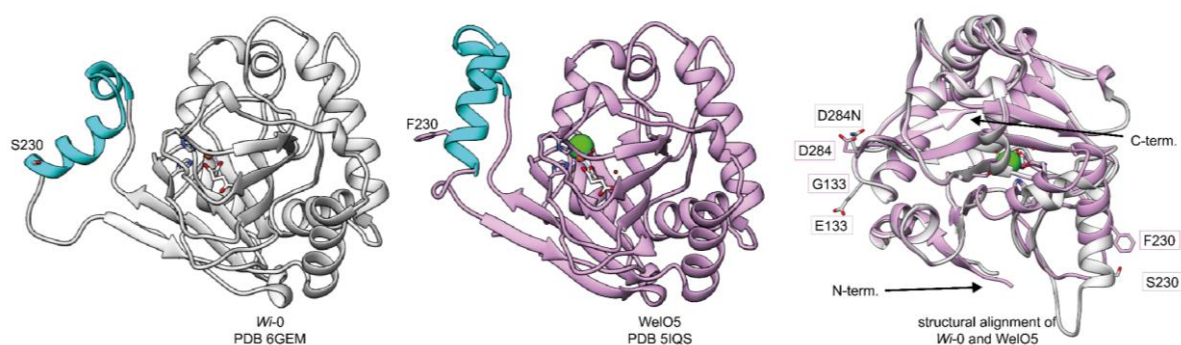


Figure 19. Highlight of amino acids differences between *Wi*-0 (left, shown in grey) and WelO5 (middle, shown in purple). The structures of both halogenases were aligned (right). Amino acid differences are shown as linkers and are named with one letter code and position. Mutation at position V6 is not visible since the N-terminus (highlighted on the right) was not dissolved. However, it is assumed that this position has the same effect as the N-terminal His₆-tag. The α -helical lid, which can close over the active site is shown in cyan.

The three amino acids S230, E133 and D284N (*Wi*-0) in comparison to F230, G133 and N284 (WelO5) are located on the enzyme surface and have no detectable effect on the enzyme conformation in the crystal. The fourth amino acid V6, is not solved in the crystal structure but it can be assumed that it has a similar effect as the His₆-tag which is also connected to the N-terminus of the enzyme. The effect of mutation D284N was further tested in activity assays (ch. 3.3) and it was seen that no activity influencing effect is present.

3.3 Syntheses of Hapalindole Derivatives and Biotransformation

Natural substrates of these aliphatic halogenases are hapalindole-like alkaloids. For WelO5, different natural alkaloids were tested and so far, 12-*epi*-fischerindole U (**42**) and 12-*epi*-hapalindole C (**39**) are converted best (figure 20), with a preference for **42**.^[155,156]

Extraction of natural products from their host organisms often require several month of culturing the organism and generally result in a low yield with below 0.1% of dry bacterial weight.^[33,34] Even though S. Doehring could show, that a simplified cultivation of cyanobacteria is possible without artificial light cycles and aeration with CO₂, the growth is slow and it took several month to increase cell mass.^[349] It was not tested if the natural products were produced but even if, few milligrams yield are expected, therefore access to these compounds via extraction is hardly possible.

The synthesis for some hapalindoles requires seven or more steps.^[350–353] So far, no synthesis routes to 12-*epi*-fischerindole U isonitrile (**42**) or 12-*epi*-hapalindole C (**39**) were published. To have a close derivative of the natural products, which can be synthesized in a simpler way, in a first step the stereocenter at C12 was simplified to a dimethylated, non-chiral group. The simplified isonitrile analogue **53** (figure 20) is available via 6-step synthesis and an overall yield of about 4%.

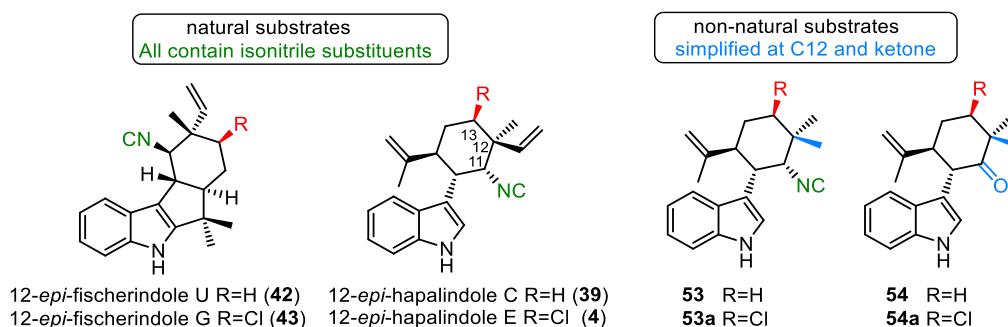
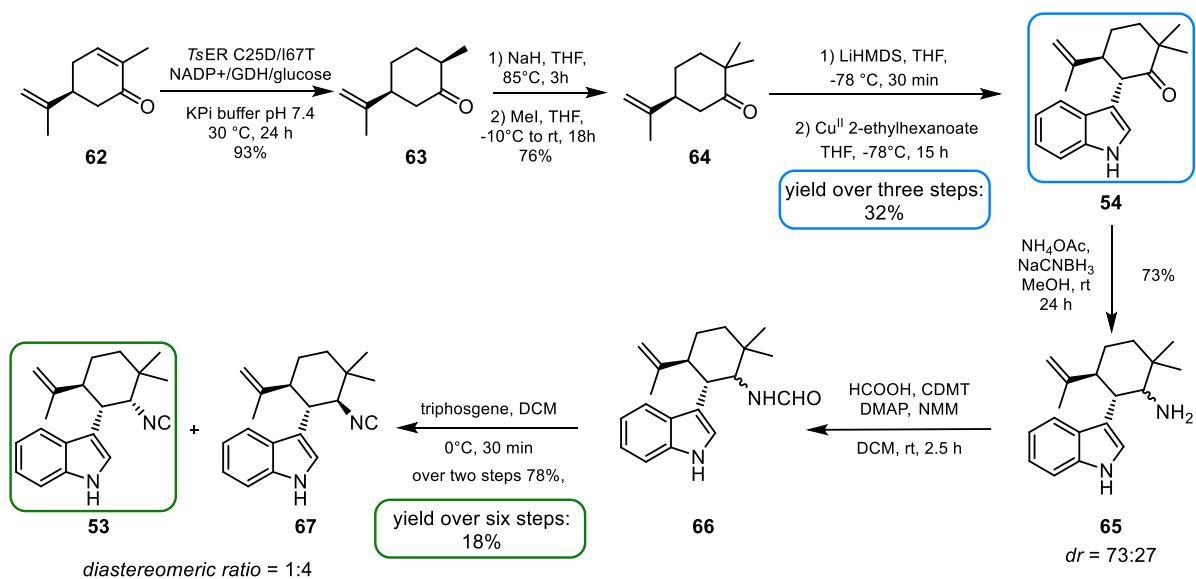


Figure 20. Natural substrates 12-*epi*-fischerindole U (**42**) and 12-*epi*-hapalindole C (**39**) were both shown to be chlorinated by NHI dependent halogenases.^[155–157] Starting from **39**, the molecule was simplified stepwise, first by replacing the vinyl group by a methyl group (**53**) and further by replacing the isonitrile with a ketone (**54**).

53 was used as reference to test if the enzyme is active and if the activity is in the same order of magnitude as the one of close homolog WelO5. In a second step, the halogenase should be adapted to non-natural substrates. Instead of the rare isonitrile function, ketone **54** (figure 20) was chosen as target molecule to screen enzyme libraries in the directed evolution of the enzyme. The ketone occurs more common within natural and synthetic compounds and is more stable in comparison to the isonitrile. The synthesis of **53** and **54** is shown in scheme 5.

Results and Discussion



Scheme 5. Synthesis of simplified hapalindole C derivative **53**. TsER = ene-reductase from *Thermus scotoductus* SA01, CDMT = 2-chloro-4,6-dimethoxy-1,3,5-triazine. DMAP = N,N-dimethylaminopyridin, NMM = N-methylmorpholin.

Both molecules, **53** and **54** crystallized upon freezing at -20°C in EtOH. **53** was stored as 50 mM stock and **54** had to be stored as saturated solution. The crystal structures of the molecules confirmed the stereocenters, assigned by NMR in the first place.

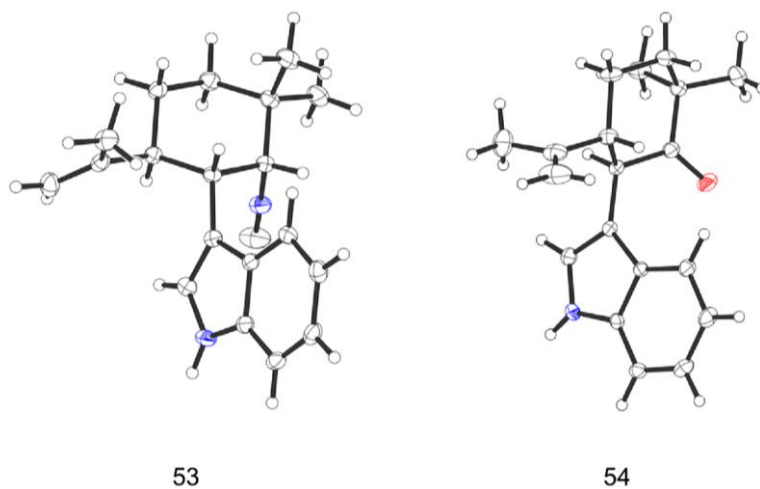


Figure 21. Crystal structures of isonitrile **53** and ketone **54**.

Comparing the molecule structures (figure 21 and figure 83, chapter 8.3.6.2), it is important to notice that the carbonyl group and the isonitrile group point in different directions, based on the different hybridization of C-11. Also, the terpene ring has a changed position.

Both substrates, **53** and **54** were tested in biotransformation to see if the reaction conditions are suitable for library screening. Results were furthermore compared with published values for *Hw*-WelO15 and WelO5 with 12-*epi*-fischerindole U (**42**) and 12-*epi*-hapalindole C (**39**).^[157] The biotransformations were performed in 202 μL in 2.2 mL 96 deep-well-plates (dw-plates).

Results and Discussion

A HEPES buffer was used as solvent including sodium chloride, α -ketoglutarate, iron ammonium sulfate and ascorbic acid (ch. 7.2.5). The buffer was flushed with nitrogen gas prior to the reaction to remove oxygen and to prevent fast oxidation of Fe^{II}, which is needed inside the active site of the enzyme. Both halogenases *Hw*-WelO15 and *Wi*-0 were tested with **53** and **54** as purified enzymes (table 4 and table 5) and as lysates (table 5). The enzyme or lysed cell pellet was prepared in a volume of 100 μ L and either added to a 2.2 mL squared dw-plate or a 2 mL reaction tube. A 2x reaction buffer containing the cofactors were prepared freshly and added to the plate. Finally, 2 μ L substrate were added from a 50 mM stock solution in EtOH to the reaction. The reaction was incubated at 30 °C. To stop the reaction, it was extracted with ethyl acetate. The organic phase was transferred into glass plates or plastic vials for HPLC measurements and placed at room temperature in a clean fume-hood overnight to evaporate all ethyl acetate. Remaining dry samples were dissolved in 100 μ L acetonitrile and analyzed via HPLC with UV detection at 280 nm. The results are shown in table 4 and table 5.

Table 4: Turnover frequency (TOF) of halogenases.

formed products	isonitrile 43 *	isonitrile 4 *	ketone 53a **	ketone 54a **
enzyme	TOF (min ⁻¹)			
WelO5	1.8	0.7	na	na
<i>Wi</i> -0	na	na	0.4	<1
<i>Hw</i> -WelO15	1.9	1.8	1.8	<1

*Biotransformation performed by Zhu *et al.*^[157]; 100 μ L scale with 20 μ M enzyme, 10 mM NaCl, 50 mM HEPES, pH 7.4, 0.5 mM (NH₄)₂Fe(SO₄)₂, 0.5 mM DTT, 0.5 mM substrate. TOF determined after 2 min. **Reactions performed within this thesis: 202 μ L scale with 10 μ M enzyme, 10 mM NaCl, 50 mM HEPES, pH 7.4, 0.5 mM (NH₄)₂Fe(SO₄)₂, 0.5 mM DTT, 0.5 mM **53** or **54**. TOF determined after 20 min. na= not available

12-*epi*-fischerindole U (**42**) as well as 12-*epi*-hapalindole C (**39**) were both tested with *Hw*-WelO15 and WelO5 by Zhu *et al.*^[157] and activities were reported as observed velocity k_{obs} , which actually represents the turnover frequency (TOF). In their transformations, *Hw*-WelO15 showed the same turnover for both substrates in 20 min. The TOF was determined after 2 min and *Hw*-WelO15 achieved 1.8 and 1.9 min⁻¹ for **42** and **39**, respectively. WelO5 had the same turnover for **42** (k_{obs} =1.8 min⁻¹), but less than half for **39** (k_{obs} =0.73 min⁻¹). In a biotransformation with *Hw*-WelO15 and **53** with slightly different reaction conditions (10 μ M enzyme instead of 20 μ M and 200 μ L reaction volume instead of 100 μ L, 20 min reaction time instead of 2 min), a TOF of 1.8 was achieved, showing that the missing methyl group does not influence the acceptance of the substrate. *Wi*-0 also shows a lower k_{obs} (0.4 min⁻¹) than *Hw*-WelO15 and as seen by WelO5 (0.7 min⁻¹), therefore the question arises whether the two mutations have an influence on the activity or the difference is based on the error in measurement. Since the reaction time to determine k_{obs} differed between WelO5 and *Wi*-0, it is also possible that the

Results and Discussion

reaction velocity slows down after the first two minutes, based on a fast oxidation of the Fe^{II} located in the active center.

After the reaction conditions were optimized to 100 mM NaCl and 2.5 mM ascorbic acid, the conversion increased. Ascorbic acid can work as recycling system for iron, if Fe^{II} is oxidized to Fe^{III}.^[354,355] Under these optimized conditions (ch. 7.2.5.2), both purified enzymes showed about the same conversion in 8 h (table 5). The values obtained for transformation in lysate however suggest, that the acceptance of **53** by *Hw-WelO15* is better than that of *Wi-0* (table 5).

Table 5: Biotransformation of *Hw-WelO15* and *Wi-0* as well as *Wi-WelO15 V6I* with **53** and **54**. Final reaction conditions: 202 µL volume in 2.2 mL 96 dw-plates sealed with a plastic lid, 50 mM HEPES, 100 mM NaCl, 2.5 mM ascorbic acid, 0.5 mM (NH₄)₂Fe(SO₄)₂, 0.5 mM substrate, 8 h, 30 °C, 200 rpm (Infors HT shaker). Either lysed cell pellet normalized to OD₆₀₀=5.0 and 2.5 mM αKG or 10 µM purified halogenase with 5 mM αKG were used.

substrate	isonitrile 53		ketone 54	
	conv. ^[a] cell lysate	conv. ^[a] purified enzyme	conv. ^[a] cell lysate	conv. ^[a] purified enzyme
<i>Hw-WelO15</i>	56	91	11	11
<i>Wi-0</i>	35	93	<1	<1
<i>Wi-WelO15 V6I</i>	34	nt	nt	nt

[a] relative conversion (% HPLC), nt= not tested

Wi-0 showed a similar conversion of **53** as *Hw-WelO15* as isolated enzyme but produced less chlorinated product in cell lysate. Both enzymes have a lower conversion in cell lysate than in its isolated form. It seemed that the isonitrile is instable in cell lysate because low signals (<20 mV) were detected by HPLC measurements. The same concentration of **53** in assays with purified enzymes or incubated in buffer resulted in signals between 150 and 200 mV.

To exclude an insufficient extraction, also the aqueous phase was measured but there, tailing peaks with signals below 10 mV were detected. At last, the organic phase was evaluated. Furthermore, mutation D284N of *Wi-0* was reversed to D284 and tested in a lysate-based biotransformation. It could be shown that the mutation D284N has no activity influencing property.

In contrast to isonitrile **53**, ketone **54** is hardly converted by *Wi-0*. *Hw-WelO15* achieved 11% conversion under optimized reaction conditions (100 mM NaCl and 2.5 mM ascorbic acid). Under initial conditions, also a low product formation of <1% was obtained for *Hw-WelO15*. With increasing activity, a hydroxylated side-product (**54b**) was detected with a chemoselectivity of 70% for **54a** and 30% **54b**. To increase the low conversion of **54**, the halogenases were engineered, which will be described in the next chapter.

3.4 Engineering of Halogenase WelO15

In an enzyme engineering process, different approaches are possible. Hereby the amount of information that is known about the enzyme and the screening method is a critical point. The time effort for screening must be balanced with the library size. However, the library size is also dependent on the probability to find an improved variant (hit). The dependency of screening effort versus information intensity was illustrated by Behrens *et al.*^[356] and several representative methods are given depending on the amount of available information.

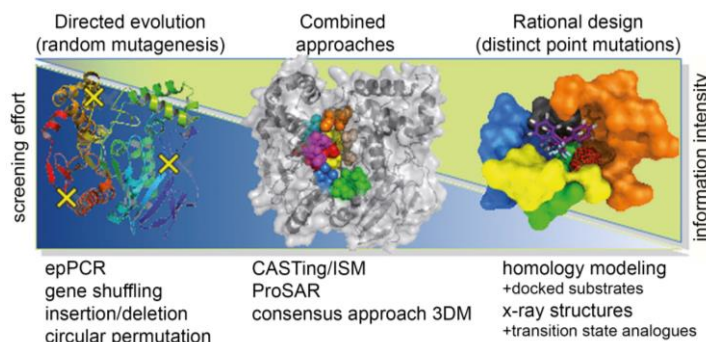


Figure 22. Overview of approaches for protein engineering methods. When only few information is available, methods like error prone PCR (epPCR) with a high screening effort have to be chosen. If more information is available, combined approaches like CASTing (combinatorial active-site saturation testing) or iterative saturation mutagenesis (ISM) can be performed. Rational design with distinct point mutations can only be applied if the information intensity is high.^[356]

When the project was started, error prone polymerase chain reaction (epPCR) was chosen as mutation strategy (ch. 3.4.1) because no enzyme structure was available. At the same time, crystallization trials of *Wi-0* were pursued. M. Biermeier furthermore analyzed *Hw-WelO15* with Hydrogen-Deuterium exchange (HDX) analysis with the goal to identify residues that interact with the substrate.^[341] HDX analysis did not yield information about the substrate binding, however two parts of the enzyme were identified that showed a high flexibility. These were the N-terminus as well as the lid area (amino acids 210-240).

In 2016, the structure of WelO5 was published,^[160] based on the structure, also the structure of *Wi-0* could be solved by molecular replacement. Therefore, random mutagenesis was stopped which did not lead to any success at that point and combined approaches with CASTing/ISM as well as rational design were used instead (ch. 3.4.2).

3.4.1 Random Mutagenesis

3.4.1.1 Creation of a *Hw-WelO15* Model with SwissModel

If no structure of the target enzyme is known, random mutagenesis has to be performed which includes a high screening effort.^[248] To minimize this effort, not the whole gene was planned to be mutated but a user defined, by modeling chosen, region should be mutated. To avoid mutation of the vector during epPCR the mutated gene parts were incorporated into the wt

DNA after the mutagenesis. Since rf-cloning worked well for cloning of the genes, this attempt was also chosen to combine the mutated gene and the vector.

The only sequence information about this enzyme class was the iron binding site which is a shared characteristic with two histidines (His₁₆₄ and His₂₅₉) in the active site in non-heme iron oxygenases/halogenases. To get some ideas about the structure, models were built with Swiss-Model.^[357–361] Therefore, the sequence of *Hw*-WelO15 was used and templates were chosen from the proposals given by the webpage. Three models were built. The templates were chosen by: 1) Highest overall coverage (0.82), (putative uncharacterized protein PDB 3W21). 2) Highest coverage with a non-heme iron dependent halogenase which is SyrB2 (coverage of 0.75, PDB 2FCU). 3) Highest coverage with an enzyme that has α KG and Fe²⁺ as ligands Phytanoyl-CoA dioxygenase (coverage of 0.78, PDB 2AX1).

From the build models it could be seen, that each of the active site of the three models with the two histidines, responsible for coordination of the iron was built correctly. A substrate and

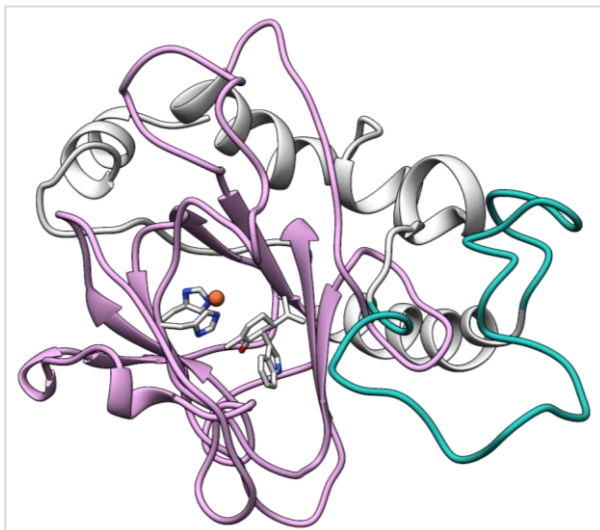


Figure 23. Model of *Hw*-WelO15 build with SwissModel based on template PDB 2FCU. In the active site the substrate is shown as grey sticks as well as the two histidines His₁₆₄ and His₂₅₉ with bound Fe (orange). In turquoise, the assumed lid area is shown while the assumed active site is shown in purple.

α KG were drawn in ChemDraw 3D, imported to PyMol, and by hand positioned into the enzyme pockets. The area within 5 Å was marked and the residues listed with Pymol. All these interaction positions were marked in the amino acid sequence and chosen as active site region (aa 120 – 290 shown in purple in figure 23).

Since for SyrB2 and CurA, two non-heme iron dependent halogenases, a lid mechanism is known, it was hypothesized that also WelO15 possibly works with a lid mechanism.^[178,183] Therefore a second region was chosen (aa 60-140, shown in turquoise, figure 23), that seem to form a lid, close to the active

site. In figure 23 the model with substrate (gray) and iron (orange) is shown.

Results and Discussion

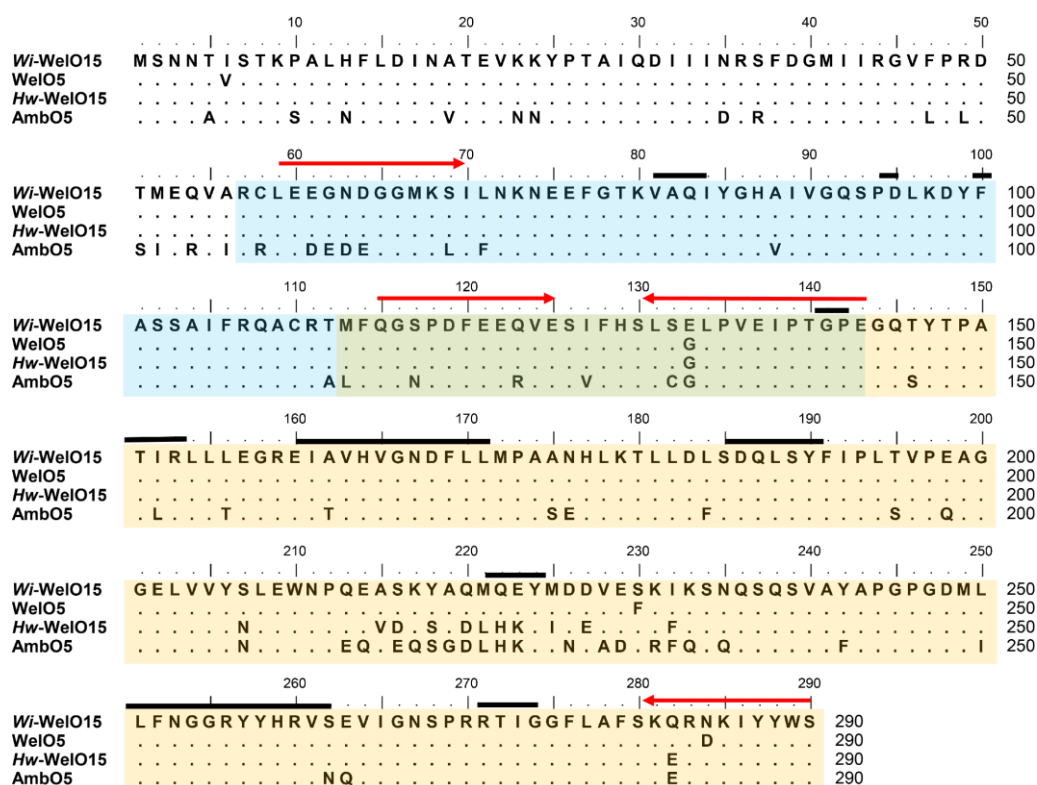


Figure 24. Amino acid alignment non-heme iron halogenases. In blue, the assumed lid region is highlighted and in orange the assumed active site region is marked. Primers that were used for error prone PCR mutagenesis are shown in red, these limit the mutation regions. Amino acids in a range of 5 Å to the substrate are marked with a black bar above.

Generally, the sequences have a quite high identity, except in the range of 213 and 235, where *Hw-WelO15* and *AmbO5* have several different amino acids. Based on the model, this area would be positioned in the active site. Several studies showed the extraction of quite different hapalindole-like alkaloids which support the hypothesis that the active site has to have a different shape to accept different substrates.^[236,239]

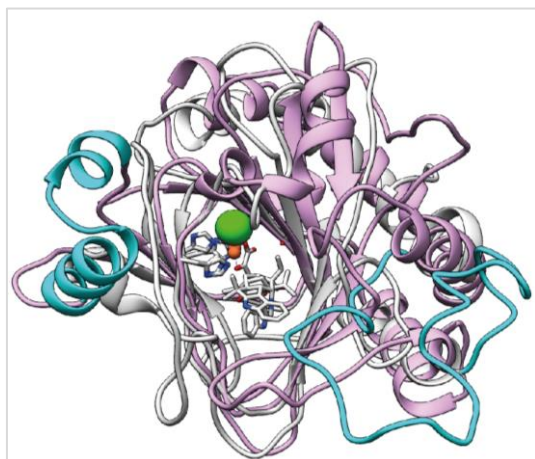


Figure 25. Alignment of *Hw-WelO15* model, based on template 2FCU made with SwissModel (grey) and the structure of WelO5 UTEX (5IQT, purple). 12-*epi*-fischerindole U (42) and 54 are shown as grey sticks. The active site with iron (orange) and chloride (green) are shown with the two histidines shown as grey sticks.

After the crystal structure was solved, a new model of *Hw-WelO15* was made based on the structure of WelO5 and compared to the previously used model. While the two histidines with iron and the substrate were positioned quite correctly, the lid area was assumed incorrect. The lid was thought to be positioned in the range of amino acids 90-110 (shown in turquoise, figure 25, right side). Alignment of the two structures followed by analysis with MatchMaker by Chimera 1.11.2, gives a RMSD of 1.269 Å between 74 pruned atom pairs, while across all 253 atom pairs it is 9.418 Å. The alignment and the 74 pruned atoms are shown

in figure 84. Interestingly, the area containing most amino acid substitutions within this enzyme class (aa 213-235) forms the α -helical lid (shown in turquoise, figure 25, on the left side). It was also shown that a chimera enzyme based on WelO5 combined with the lid area of AmbO5 broadens the substrate scope of the naturally more limited WelO5 to the one of AmbO5, proving that the lid is important for substrate recognition. Mutation of the loop region and the active site was performed individually and resulted in a variation of mutants. Individual error prone PCR conditions had to be developed for each library which is described in the next chapter.

3.4.1.2 Random Mutagenesis via Error Prone PCR and Screening

For error prone polymerase chain reaction (epPCR) it is important that well-chosen PCR conditions are used, since user defined amounts of mutations per gene are created. An average of 2-5 mutations per gene was set as goal. Based on the protocol, published in Current Protocols in Molecular Biology^[362] two different conditions were calculated for active site and lid. For the only 297 base pair long gene part of the lid region, 15 rounds of amplification should be performed in the PCR, while for the 482 base pair long part of the active site only 8 amplification steps should be used based on the protocol.

Eight polymerase chain reactions in 50 μ L scale were prepared. To see the amplification product, it was necessary to apply 25 μ L PCR product in an agarose gel, because only few amplification rounds were performed. Mutation of the lid region worked without any further optimization and yielded 560 ng DNA.

For the gene part containing the assumed active site, standard conditions were not applicable, therefore the reaction was optimized, so that the Taq polymerase was only added after the hot start and 13 amplification rounds were used instead of 8. To produce sufficient DNA 10x50 μ L PCRs were prepared. 1032 ng mutated gene could be purified by purification kit. Via rf-cloning the mutated gene parts were incorporated into the vector.

To prove the success of the random manner and the distribution of mutations within the gene, six clones of both mutation studies were sequenced. Sequencing revealed that 50% variants of the lid area and 66% variants of the active site contain mutations without having any frameshifts or stop codon. In figure 26 all positions of mutated amino acids which were found in the sequenced clones are shown in blue (found mutations are listed in table 39).

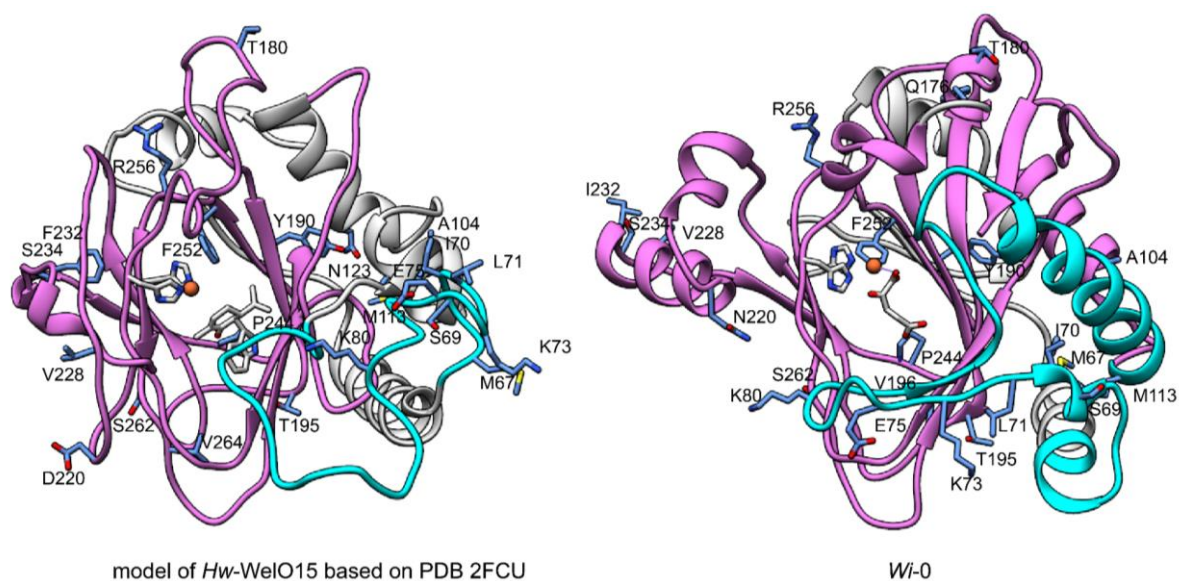
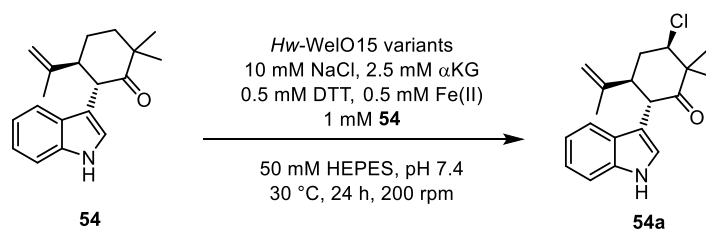


Figure 26. Positions that were mutated within the error prone PCR are highlighted within the model of *Hw-WelO15* and the crystal structure of *Wi-0*. The mutated amino acids are shown as sticks in blue. The assumed lid region is shown in turquoise and the active site region in purple. Iron is shown as orange ball. The mutations are distributed over the enzyme but just in those areas that should be mutated.

As can be seen in figure 26, the sequenced variants carry mutations distributed in the enzyme parts that were desired, however 50% and 34% had either a frameshift or an early stop codon and are likely to be inactive. In total 1100 variants of the lid-library and 650 variants of the active site-library were analyzed in lysate-based biotransformation with substrate **54** as shown in scheme 6, but no product formation could be detected.



Scheme 6. Reaction performed with libraries created by epPCR. The reaction was performed in 202 μ L volume with 50 mM HEPES, 10 mM NaCl, 0.5 mM DTT, 0.5 mM $(\text{NH}_4)_2\text{Fe}(\text{SO}_4)_2$, 1 mM substrate, 24 h, 30 $^\circ\text{C}$, 200 rpm (Infors HT shaker).

The plates were pooled, so that the cells from four plates were suspended, combined and pelleted again. Then, the cells were lysed, and the reaction performed. However, no product formation could be detected by HPLC. After the first library screening of epPCR-variants, the crystal structures of WelO5 was published^[160] and simultaneously the one of *Wi-0* solved, so that the engineering could be pursued in a more rational manner.

3.4.2 Structure Guided Directed Evolution of *Wi-WelO15*

After the crystal structure of WelO5 (99% identity) was published^[160] the previously not solvable data set of *Wi-0* (*Wi-WelO15* V6I/D284N) could be solved by molecular replacement and a structure guided directed evolution strategy could be started. *Wi-0* was used as starting

point. The ketone **54** was docked into the enzyme with Yasara by Henrik Müller.^[363] In figure 27, both structures are shown. Figure 27a) shows the structure of *Wi-0* with docked **54**. *Wi-0* crystallized in an open conformation, while 27b) shows the closed structure of WelO5 with soaked, natural substrate 12-*epi*-fischerindole U (**42**). Docking of 12-*epi*-hapalindole C revealed, that it is positioned in the same way as **42** (figure 81, ch. 8.3.6.1).

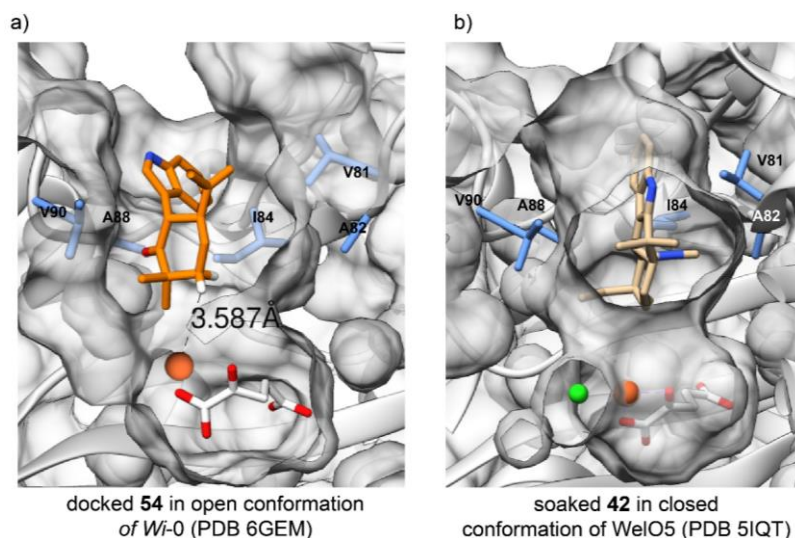


Figure 27. a) shows the structure of *Wi-0* with docked **54**. *Wi-0* crystallized in an open conformation, while b) shows the closed structure of WelO5 with natural substrate 12-*epi*-fischerindole U (**42**).

For docking of **54** and *Wi-0* the receptor was prepared using the standard settings of Dock Prep tool from UCSF Chimera, Version 1.11.2. This program deletes the solvent, fixes incomplete side chains and adds hydrogens and charges to the protein and the bound ligands. In the prepared receptor-file, α KG had a charge of -2 and the Fe-ion a charge of +2. The results were visually analyzed using Chimeras ViewDock-tool. Of 25 outputs, the indole pointed 18 times in the direction of the iron, which should not result in any chlorination. Only 3 poses (11, 16, 22, figure 82, ch. 8.3.6.2) had C₁₃-H(R) pointed in direction of the active site, however in poses 11 and 22, the indole flipped so that the conformation differs from the crystal structure of the small molecule. Pose 16 (figure 27a) was therefore chosen as the most probable binding mode.

Since all hapalindole-like alkaloids contain either isonitrile or isothiocyanate it can be suggested that these residues play a major role in native substrate recognition.^[160] By replacing it with a carbonyl function, the H-bond acceptor feature was kept, even though the docking results showed that the orientation of the carbonyl group points in the opposite direction. Crystallization of **53** and **54** also revealed that the isonitrile and the carbonyl group each are positioned in different indole half-sides (figure 83, ch. 8.3.6.2).

Amino acids pointing towards the six-membered ring, as for example V81, A82, I84, A88, V90 were interesting to be mutated, since the substrate was modified in this part. State of the

art directed evolution strategies suggest preparing small but smart libraries, proposing to mutate several positions at the same time.^[303] The bottle neck of directed evolution is the screening effort which means that enzyme libraries cannot be created in any size, since the time effort necessary for screening is technically not possible. For example, screening two positions with an NNK codon, two times 20 possible codons, leads to 400 possible variants with three or four different positions, even 8000 and 160000 possible variants are suggested to be screened, if aiming for 95% coverage, which is barely possible in HPLC screenings. Therefore, the number of variants has to be limited which is described as smart libraries. Reduction of screening is especially possible if libraries of high quality are prepared.^[302,303,364] High quality means in this case that incorporation of the desired codons actually worked and no template is left. The combined effects of enzyme dynamic, flexibility, allosteric effects, electrostatic preorganization make prediction of mutational effects difficult. Instead of saturation of positions, information from previous screenings or rational thinking are considered and, reduced codons are incorporated which leads to a reduced number of possible variants. In this way, synergistic effects of the amino acids are considered, and possible dead ends in single-step mutagenesis are avoided.

For this enzyme class however only one engineering study was made, which involves the creation of AmbO5/WelO5 chimeras to enlarge the substrate scope of WelO5. The lid area of WelO5 was substituted by the lid of AmbO5 which lead to the acceptance of more hapalindoles albeit with reduced activity in comparison to AmbO5.^[156] No structure guided engineering was performed for this enzyme class before and no non-natural substrates were tested. To start the structure guided directed evolution, first several positions should be saturated to gain initial information about this system. In a second generation of variants, the collected information will be used to prepare smart libraries that allow cooperative effects.^[297] The preparation include appropriate statistical analysis to prevent oversampling by reducing the screening effort to the probability to find one out of the three best variants.^[307,308,365,366] The results will be described in the next chapter.

3.4.2.1 Creation and Screening of 1st Generation Libraries

To individually check the effect of amino acid positions, eight libraries with an NNK saturation were created. Positions N74, F77, A82, I84, V90, F169 were chosen because of their close contact to the substrate, while M221 and M225 are assumed to be anchoring residues responsible to close the lid over the active site. Furthermore, a library with reduced codons of A82

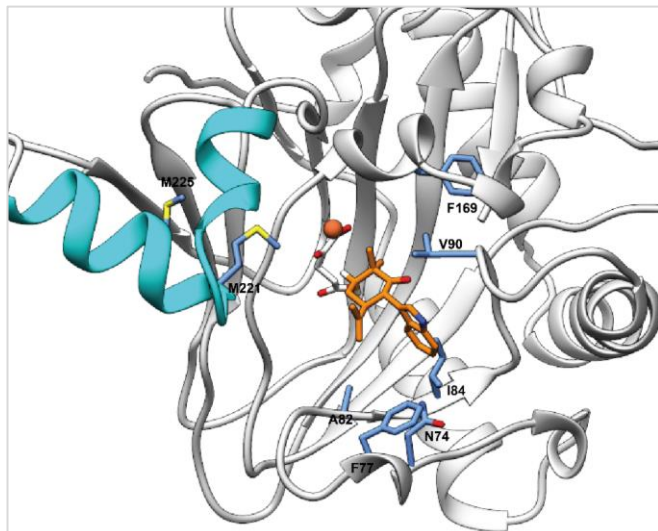


Figure 28. Wi-0 with docked 2. Positions, chosen for mutagenesis are highlighted in blue. The lid is shown in cyan.

and I84 were created. Mutation was performed via QuikChange PCR.^[367,368] In contrast to the original method, primers were designed that only partially overlap. This prevents primer-dimer formation and yields better success in site-directed mutagenesis.^[369] To check the quality of the mutation, quick quality control (QQC) was performed.^[306]

Generally, created libraries yielded a quite bad degeneracy. Therefore, the plasmid mix, resulting from the first mutation round was used for the next PCR

as template because it was assumed, that primers that did not bind to the template DNA might bind better to the mutated DNA. This procedure increased the degeneracy even though no desired distribution of bases could be achieved. For M221, no sufficient degeneracy could be achieved, therefore no further attempts were pursued. The chromatograms resulting from sequencing of single site libraries are shown in figure 85, ch. 8.4.1.1. If large libraries are being created, the number of screening variants is reduced to have a 95% to find one out of the three best hits. In the case of these first libraries however much information should be collected about the system therefore a larger number of colonies were analyzed, also based on the unsatisfied degeneracy. Since 145 colonies would be a 99% chance to pick all variants, two plates (190 colonies) for each NNK library were screened.

The following selected amino acids were chosen to be incorporated. For A82: D, Q, E, H, N, I, F, A, L, M, S, T, V. For I84: D, Q, E, H, N, I, S, T. To achieve this tailor-made set of amino acids with minimal redundancy, the DC_Analyzer^[370] was used, resulting in codons AWC, DYG, SAM for position A82 and SAM, ANC for position I84. To create this mutation a combination of 8 pairs of primer had to be bought and was introduced individually in 8 different PCR reactions, so in total 8 libraries were created. Initial difficulties in mutagenic PCR occurred. Impurity in the sequenced chromatograms after the primer binding site indicated that a frameshift happened. This problem could be overcome by decreasing the betaine concentration to maximal 0.5 M combined with an increased annealing time (previously 30 s, improved

60 s). With a second round of PCR on the mutated product from the first mutation, the degeneracy could be improved, however no optimal incorporation of the degenerated codons was possible (figure 86, ch.8.4.1.1). Often small amounts of template DNA remained as well as small amounts of impurities in the background sequence. For library A82TTC/I84ANC high amounts of impurities were present, but the incorporation of the mutations could not be optimized further and out of practical reasons, the screening was performed to see, if despite the presence of impurities also active variants were created. To cover all variants despite imperfect libraries, the number of colonies was calculated to cover >99% of all produced variants, if a perfect library would be present. 760 colonies were screened for a library consisting of 104 variants. In figure 86 the chromatograms from sequenced libraries are shown. To receive libraries with better degeneration, it might be beneficial to buy primer with a higher purity. It was shown that depending on the primer supplier and the purity there can be significant differences in library quality.^[371]

To screen the library, *E. coli* BL21-Gold(DE3) was transformed with the plasmid mix and plates on LB-agar plates. Single colonies were picked into 2.2 mL dw-plates and grown over night as preculture and finally transferred into expression medium. After heterologous expression overnight (ch. 7.1.9.2), the cells could be harvested, and the pellets used for activity assays (ch. 7.2.3.2). Therefore, the cells were lysed and all needed cofactors as well as the substrate were added to the reaction. After 24 h the reaction was stopped by extracting with ethyl acetate. The organic phase was dried, resolved in acetonitrile and analyzed via HPLC screening.

Within the screening two new peaks appeared in HPLC/UV-Vis measurements that later were further analyzed since no references were available. After scaling the reaction to preparative scale, the products could be assigned to one chlorinated (**54a**) and one hydroxylated (**54b**) product. Hydroxylation as side reaction is known for this enzyme class to happen if non-natural substrates are converted.^[159] The reaction conditions are described in figure 29a. While screening the first libraries, several variants were found that produced only the chlorinated product **54a** or chlorinated **54a** and hydroxylated **54b** products (figure 29c). The best enzymes (>1.5% prod. form.) from the first screening were sequenced, whereby some of the enzymes were found twice or three times. No variant was found that solely produced the hydroxylated product. In single site libraries, beneficial mutations A82L (*Wi-1*, formation of 4% **54a**), N74R (*Wi-2*, formation of 3.5% **54a**) and V90P (*Wi-3*, formation of 0.4% **54a**) were found. In the two-site library also A82V was found. Double mutants contain L, M, V and I in position 82 in combination with S, T or wild-type amino acid I. In summary, unpolar amino acids in position A82 as single variant or in combination with polar amino acids in position I84 chlorinate **54**. In figure 29b representative chromatograms are shown.

Results and Discussion

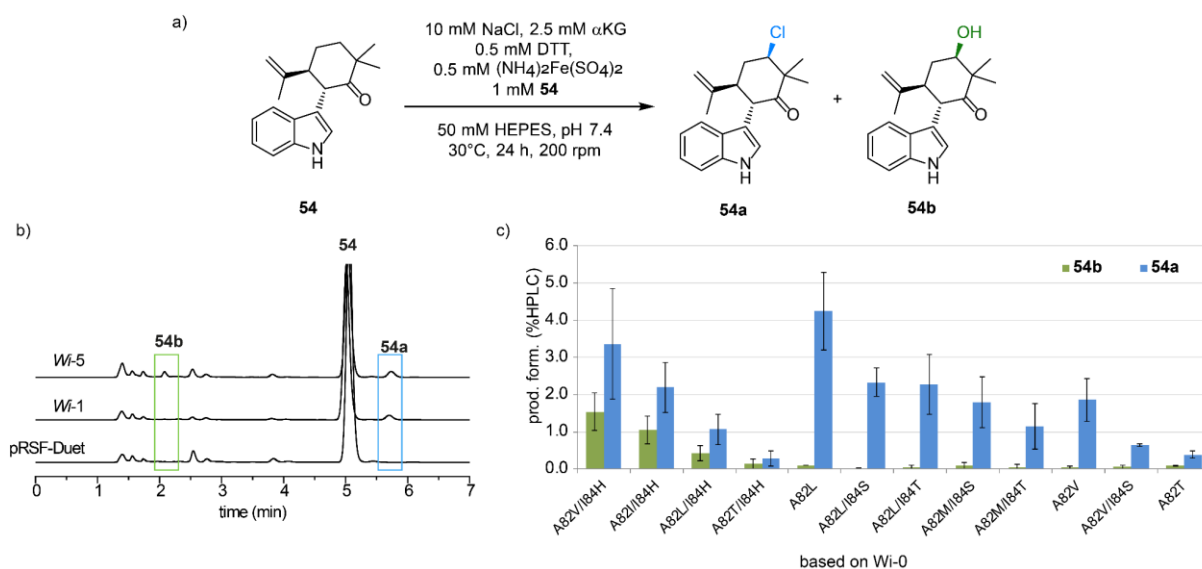


Figure 29. a) Reaction conditions of the screening are shown. The reaction was performed in a volume of 200 μ L. b) HPLC chromatogram of reaction with variants *Wi-1* (*Wi*-WelO15 V6I/A82L/D284N) and *Wi-4* (*Wi*-WelO15 V6I/A82V/I84H/D284N) and **54**. c) Product formation with variants found in the screening. All variants are based on *Wi-0* (*Wi*-WelO15 V6I/D284N). The averaged results from quadruple measurements in a hit plate. Variants that carry position I84H produce next to the chlorinated (**54a**) also a hydroxylated product (**54b**) with a chemoselectivity of about 70% for **54a**.

All variants producing **54b** contain I84H in combination with unpolar amino acids (V, L, T, I) in position A82. The variant with the highest activity, *Wi-4*, is *Wi*-WelO15 V6I/A82V/I84H/D284N and has a chemoselectivity of 68% for **54a**. That only small changes in the amino acid sequence of the active site can switch the chemistry was also shown, when two quite homologue enzymes SnoN and SnoK (38% sequence identity) were characterized and SnoK catalyzes a carbocyclization and SnoN an epimerization reaction.^[372]

N74R in contrast to the remaining found variants sits in the outer rim of the enzyme structure. This leads to the suggestion, it interacts with the indole part of the substrate. Information gained within these first libraries, was then used to create small and smarter libraries, one with three positions and one with five positions mutated at the same time.

3.4.2.2 Creation and Screening of 2nd Generation Libraries

Based on these first results, two libraries of A82L/V90NNK as well as A82L/F77NNK were created however the activity background of the template variant was so high, that only one variant showed clear increased activity which was *Wi*-WelO15 V6I/A82L/V90P/D284N (*Wi-5*) with 5.5% product formation, which is the most active variant from the first-generation libraries.

Considering the results in comparison to the docking results, it is not surprising, that bigger, unpolar amino acids in position 82 fill the gap that is present if no isonitrile functionality is present in the substrate. Since the carbonyl group points in the opposite direction, no polar residue is necessary in this position but the proline in V90P could perform some interaction with the carbonyl group. Reciprocal interaction of C=O – C=O have attracted attention recently

and are described to appear in proteins mainly in polyproline helices.^[373] Also in a study it was shown that 15% of prolines performing H-bonds.^[374] In all further screenings only Pro was found as substitution for V90 for ketone substrates, which indicates a strong positive effect on the acceptance for this kind of substrates.

After collecting initial information, two multi-site libraries were designed and created to find variants with higher chlorination activity.

In the first library of the 2nd generation, position A88 should be saturated combined with V90P and three amino acids in position I84 (I,S,T). In the first generation, the chosen mutations I84S and I84T as well as V90P had an activity increasing effect. The created library showed low conversion of **54**, the only active variant is *Wi-WelO15* V6I/A88V/V90P/D284N (*Wi-6*) with 1.5% product formation and 0.5 mM **54**.

In the second library, five positions around the substrate were chosen which were mutated simultaneously, so that also synergistic effects are considered during the screening. Positions that should be mutated are V81, A82, I84, A88 and V90. Since these positions are quite close to each other on the DNA sequence, a primer design was chosen, in which only three positions are incorporated in one primer. The design is visualized in figure 30.

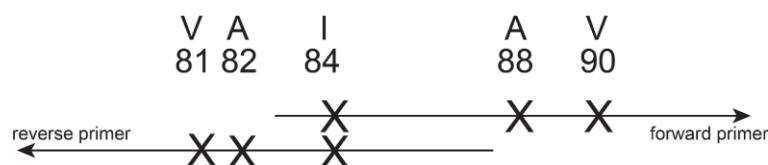


Figure 30. Primer design for QuikChange PCR to create the five-site library. Forward primer in the same length but other codons was also used for the three-site library in combination with the cloning reverse primer.

N74R which was also found as single variant was not included in this library because of primer design reasons. The effect of that mutation was further analyzed in the third generation of variants.

The five-residue library was planned as smart library. For all five positions only 3-5 amino acids should be introduced including the wild-type amino acid and a screening effort of maximum of 12 plates should be needed. Finally, for each position, two reduced codons were chosen except for position I84, where only one was needed (table 6).

Results and Discussion

Table 6. Overview of chosen residues and amino acids to be incorporated. Codons that have to be incorporated into the primers. B=C,G,T; M=A,C; Y=C,T; W=T,A; R=A,G

position	amino acids	nucleotide codon
V81	V, L, T, N, F	BTT, AMC
A82	A, L, M, V	GYG, AWG
I84	I, S, T	ABC
A88	A, N, S, V	GYG, ARC
V90	V, P, M, Q	RTG, CMG

Giving a theoretical library size of 960 variants without redundancy. To achieve a 95% chance to find one out of the best three hits, 1008 clones have to be tested. This corresponds to a sequence space of 65%.^[307]

To make sure, that amplification of the whole gene and mutation of all five positions works with this strategy, first a PCR with only two primers was performed, giving slight degenerations in all desired positions. Based on this result, further mutation with all primers in the same PCR were performed, based on the first plasmid pool (plasmid pool 1), until a complete absence of wild-type gene was seen. Plasmid pool 2 and 3 were achieved with different PCR conditions, both based on plasmid pool 1. Quick quality control revealed absence of thymine in the 1st base of position 81 in pool indicating that Phe will be missing in the library. Similarly, a very low presence of adenine and guanine in the 2nd base of A88 was observed. Therefore, a fourth round of PCR was set on plasmid pool 2 with primers especially encoding V81BTT and A88ARC (primer 77 and 79), creating plasmid pool 4 (figure 87). Colonies for screening were picked from pools 2-4 in equal parts. In total 1080 colonies were picked. The screening was performed with 0.5 mM substrate concentration. The active hits were measured in triplicate and the best ones sequenced.

Three variants were found with an increased formation of **54a**. Based on *Wi-0* following mutations were beneficial: V81T/A82M/A88V/V90P (*Wi-7*: 7% form. of **54a**), V81T/A82V/I84T/A88V/V90P (4% form. of **54a**), V81T/A82M/I84T/A88V/V90P (4% form. of **54a**) in comparison to 6% formation of **54a** by *Wi-1*. In the next step, the effect of N74R on the best variants found so far as well as scaffold sampling between *Wi-WelO15* and *Hw-WelO15* was tested.

3.4.2.3 Scaffold Sampling and Fine Tuning with N74R: 3rd Generation

Next, 2nd generation hits were rationally fine-tuned by adding mutation N74R (figure 31), a residue on the outer rim of the active site. Due to the position in the sequence and numerical reasons, the residue was not included into the multi-site library but found hits rational combined. In total, the mutation N74R was added to seven hit-variants. Often it is assumed, that beneficial mutations are mostly additive^[299] however in this case, only one variants shows in-

Results and Discussion

creased formation of **54a** with the combination of those mutations while all others show decreased activity. In figure 31, the two variants are in direct comparison. The reactions were performed in triplicate and 0.5 mM **54**.

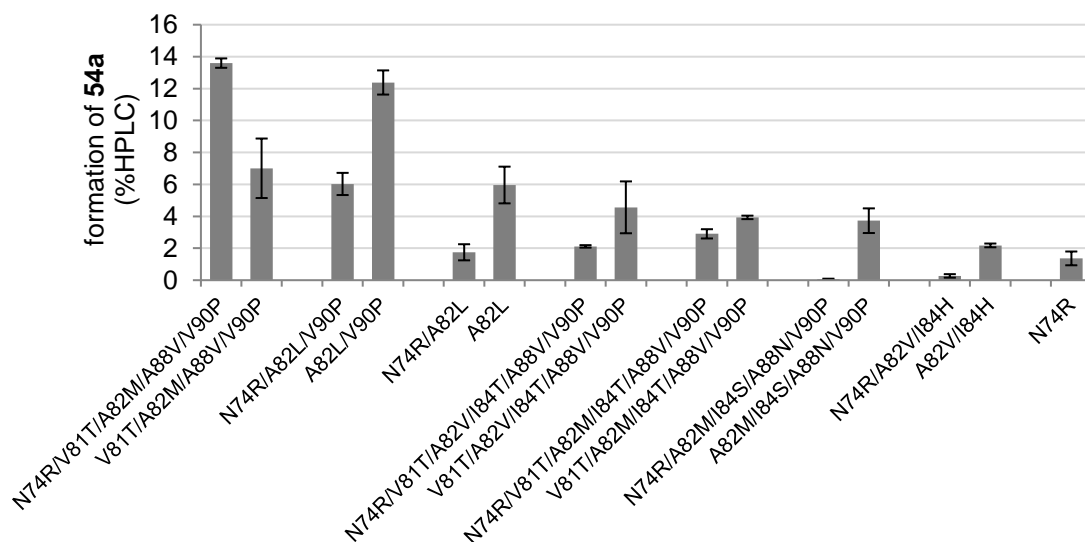


Figure 31. Comparison of variants carrying N74R and without. All variants carry additional mutations V6I and N284D. Lysate-based biotransformation with cells from 0.8 mL cell culture. Final reaction conditions: 200 μ L volume in 2.2 mL 96 dw-plates sealed with a plastic lid, 50 mM HEPES, 10 mM NaCl, 2.5 mM α KG, 0.5 mM DTT, 0.5 mM $(\text{NH}_4)_2\text{Fe}(\text{SO}_4)_2$, 0.5 mM **54**, 8 h, 30 $^\circ\text{C}$, 200 rpm (Infors HT shaker).

As can be seen in figure 31, V81T/A82M/A88V/V90P (*Wi-7*), combined with N74R to N74R/V81T/A82M/A88V/V90P (*Wi-8*) leads to an increase of product formation and results in the best variant that was found so far, with a product formation of 14% in a lysate based reaction. In all other created variants, the addition of N74R decreased the product formation which shows that this position has an important synergistic effect on the substrate positioning which cannot generally be mutated to N74R to achieve an increase in chlorination activity.

The strategy of scaffold sampling^[315,375] examines the transfer of mutations within homologous protein structures. Generally, it could be assumed that a found mutation that has an activity increasing effect on one enzyme could have the same positive effect on a close homologue which is structurally quite similar. If this would be applicable, especially directed evolution studies could be shortened dramatically because knowledge gained within one enzyme can be transferred to a whole class. However it was found that this is not so easy and even though in some cases it works, for other homologues it does not.^[315,375]

Building chimera enzymes by transfer of the lid-amino acids from AmbO5 to WelO5 enlarges the substrate scope of WelO5 to more natural hapalindole-like alkaloids albeit with reduced activity.^[156] Therefore it would be interesting to see the individual effect of transferring single amino acids to another member of the same enzyme class. The scaffold sampling strategy was used inspired by two facts: Despite the high sequence identity of 95%, *Wi-0* produces

Results and Discussion

<1% while *Hw-WelO15* forms 11% **54a**. The two halogenases mainly differ in the α -helical active site lid which was shown to control the native substrate scope.^[156] The lid residues L221 and I225 of *Hw-WelO15*, which point towards the substrate,^[160] were transferred to *Wi-0* and *Wi-5*, substituting M221 and M225. The new created variants are named *Wi-9*: V6I/M221L/M225I/D284N and *Wi-10*: V6I/A82L/V90P/M221L/M225I/D284N. Additionally it should be tested if the activity improving residues A82L/V90P have a beneficial influence on *Hw-WelO15*. During mutagenesis of *Hw-WelO15*, *Hw-1* (A82L) and *Hw-2* (A82L/V90P) were created.

The mutants were heterologous expressed and while harvesting, OD₆₀₀ normalized. Cell pellets of an OD₆₀₀=5 were lysed and the soluble halogenase content of cleared lysate was compared by SDS-PAGE analysis (figure 32).

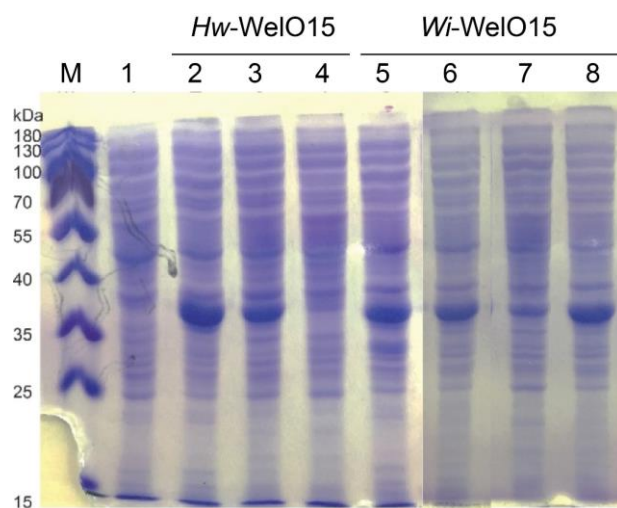


Figure 32. SDS-PAGE analysis of OD₆₀₀ normalized *E. coli* BL21-Gold(DE3), induced with IPTG and growth for 16 h at 22 °C. After lysis with lysozyme, insoluble cell debris was removed by centrifugation and cleared lysate was applied to a gel (12% separation gel, 5% stacking gel). The applied volume represents 4.4% of the enzyme mix present in the assay 1) pRSF-Duet 2) *Hw-WelO15* 3) *Hw-1* 4) *Hw-2* 5) *Wi-0* 6) *Wi-5* 7) *Wi-9* 8) *Wi-10*.

As can be seen in figure 32, the transfer variants *Hw-1* (lane 3), *Hw-2* (lane 4) and *Wi-9* (lane 7) show reduced expression levels. Biotransformations were made with variants and their template variants *Hw-WelO15*, *Wi-0* and *Wi-5*.

Results and Discussion

Table 7. Biotransformation of halogenase variants with **53** and **54**. Final reaction conditions: 200 μ L volume in 2.2 mL 96 dw-plates sealed with a plastic lid, 50 mM HEPES, 100 mM NaCl, either lysed cell pellet normalized to OD₆₀₀=5.0 and 2.5 mM α KG or 10 μ M purified halogenase with 5 mM α KG, 2.5 mM ascorbic acid, 0.5 mM (NH₄)₂Fe(SO₄)₂, 0.5 mM substrate, 8 h, 30 °C, 200 rpm (Infors HT shaker).

enzymes	53	54	54a	54	54a
	conv. ^[a] pur. enzyme	conv. ^[a] cell lysate	chemo- select.	conv. ^[a] pur. enzyme	chemo- select.
Wi-0	93	<1	nd	<1	nd
Wi-9	93	1	nd	2	nd
Wi-1	67	32	98	28	96
Wi-5	27	59	98	70	97
Wi-10	60	30	95	18	93
<i>Hw</i> -WelO15	91	11	70	11	73
A82L	nt	18	86	nt	nt
A82L/V90P	nt	3	nd	nt	nt

nt = not tested, nd = not determined, pur. = purified

Hw-WelO15 and *Wi*-0 convert **53** with 91-93%, therefore, no difference in activity is expected for *Wi*-9. Indeed, biotransformation with selected variants show, that the transfer of L221 and I221 to *Wi*-0 result in no activity change for **53**. However, a decrease in conversion is expected for *Wi*-10 since the mutations A82L/V90P (*Wi*-5) decrease the ability to chlorinate **53**. Comparing *Wi*-5 and *Wi*-10 however, it is noticeable, that the conversion for *Wi*-10 is twice as high as for *Wi*-5 which shows that the mutation M221L/M225I increases the chlorination activity **53**. **53** was only tested with purified enzymes. Due to their low expression level, no purification of *Hw*-WelO15 variants was performed, therefore only results with **54** are available.

For non-natural ketone **54**, it could be expected, that the introduction of L221 and I221 to *Wi*-variants increases the formation of **54a**, since *Hw*-WelO15 wild type already produces **54a** which is not the case for *Wi*-0. However, *Wi*-9 does not show a higher conversion than *Wi*-0 and *Wi*-10 shows a great loss in activity in comparison to *Wi*-5.

Mutation of A82L and A82L/V90P in *Wi*-WelO15 enables the chlorination of **54**. Since the sequence identity is quite high (95%) and especially the active site, except the α -helical lid, is identical (figure 10) it was expected that the two positions could be transferred and would lead to an increased formation of **54a** within *Hw*-WelO15. This is the case for *Hw*-WelO15 A82L. A higher conversion as well as chemoselectivity was achieved. *Hw*-WelO15 A82L/V90P however, only produces 3% **54a**, which can be explained by a low concentration of soluble halogenase in the lysate (figure 32).

Summarizing it can be said that scaffold sampling within these two halogenases albeit their high sequence identity in the above chosen positions cannot be performed. Mutants show low

expression level and even though *Hw*-WelO15 A82L has a higher formation of **54a** in comparison to its wild-type enzyme, the formation is still lower than with *Wi*-1. Hence, the engineering strategy based on residue transfer was abandoned.

3.4.2.4 4th Generation: Library for Active Site Entrance

As *Wi*-8, containing N74R, is the best variant found so far, it was surprising that incorporation of N74R to all other variants resulted in a lower activity. Therefore, it can be assumed that N74 is an important position, but R is not the right amino acid to combine for some variants. To

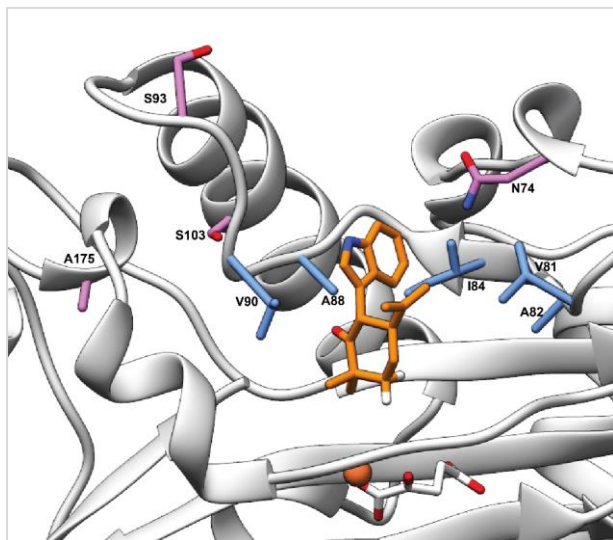


Figure 33. Active site of *Wi*-0 with amino acids (shown as sticks) that are chosen for mutagenesis. Amino acids shown in blue have been mutated in first- and second-generation libraries. Amino acids shown in purple are chosen to be mutated in the fourth generation.

incorporate the outer rim of the active site more (amino acids shown in purple in figure 33), two more libraries were created based on the best variants found so far: *Wi*-5 and *Wi*-8. *Wi*-5 should be mutated in four positions: N74, S93, S103 and A175 while *Wi*-8 which already includes N74R was only mutated in S93, S103 and A175. In both libraries positions 93,103 and 175 were mutated with the same codons incorporating amino acids N, H, D, A, S, V, L. Hereby 343 variants are created in the library based on *Wi*-8. The library design of *Wi*-5 consists of additional N74 N, S, Q, R, which corresponds to 864 combinations. Thereby first mutations in positions

N74 were incorporated and in a second PCR the three remaining positions were mutated. Because N74R/A82L/V90P showed a decreased activity to A82L/V90P, also 32 colonies of the small library of N74(N, S, Q, R)/A82L/V90P were tested which opens the possibility to gain more information about position N74. However, no hits were found for N74 NSQR/A82L/V90P.

Mutation was enabled by QuikChange (position N74) and megaprimer PCR (93,103, 175). After two rounds of PCR, satisfying degeneration was reached (figure 88) and the library based on *Wi*-8 was screened. Four plates were tested, with 368 colonies which correspond to a 95% chance to find one out of the three best hits. In the created libraries several variants with comparable conversion to the template were found however, no variants had a big increase in activity. Therefore, only eight plates for the second library based on *Wi*-5 were produced, corresponding to a sequence space coverage of 56%.

Under optimized reaction conditions (ch. 7.2.5), the template variants showed a conversion of 40% and 55% formation of **54a**, *Wi*-5 and *Wi*-8, respectively. Therefore, variants that had a

product formation of >30% based on *Wi-5* and >40% based on *Wi-8* were measured in triplicates (figure 89, ch. 8.4.1.3). From 48 analyzed variants, 14 variants were found that produce more **54a** than the template variants (table 8). Only mutated positions are given with the template variant. Amino acids that still contain the template amino acids are shown in grey, mutated residues are shown in black.

Mutating N74 alone based on *Wi-5* gave no new hits. However, in the library, variants could be found containing N74Q, N74R and N74N. While S103 was found to be only wild-type amino acid S or substituted by A, positions S93 and A175 showed more variety in their sequence.

Table 8. Variants that have a higher formation of **54a** in comparison to their template variants. For position N74, Q, R, S and N were introduced while for position S93, S103 and A175 amino acids N, H, D, A, S, V, L were possible. Amino acids shown in black are mutated in comparison to the wild type. Amino acids shown in grey are still the template, without mutation in this position.

N74Q/A82L/V90P			N74R/A82L/V90P			Wi-5			Wi-8		
S93	S103	A175	S93	S103	A175	S93	S103	A175	S93	S103	A175
S	A	A	D	S	A	D	S	A	D	S	A
D	A	H	A	A	N	L	S	N	N	A	S
H	S	A	S	A	N	S	S	N	D	A	A
			H	A	N				L	A	A

In summary, the activity improvement in this variant generation is 40% from *Wi-5* to *Wi-12* from 43% to 60% product formation and 17% from *Wi-8* to *Wi-11*, from 47% to 55% respectively.

Of all variants with improved activity, 13 *Wi-0* variants as well as two *Hw-WelO15* variants were chosen to test with further hapalindole-like ketones (ch. 3.6). In the next chapter, different conditions while handling the halogenase during heterologous expression and biotransformation are compared.

3.5 Handling the Halogenase and Optimization of Protocols

The halogenase *Wi-0* was engineered from no detectable product formation to 87% formation of **54a**. However not only the enzyme was adapted to the new substrate, but also different ways of heterologous expression and reaction conditions were tested and optimized. Since the synthesis of isonitrile derivative **53** was tedious and combined with low yields and furthermore the compound seems to be quite instable in reactions. Combined with almost full conversion by *Hw-WelO15* and *Wi-0* under tested conditions, it was not the appropriate substrate for reaction optimization. In the beginning of this project, ketone **54** was not chlorinated by both halogenases. Several conditions were tested however no product formation could be detected. Therefore, the chlorinase was engineered before reaction conditions for the halogenation were optimized. Screening and initial biotransformations were performed, using conditions based on published data for *WelO5*.^[155] After finding several variants that chlorinate **54**, heterologous expression was analyzed again (ch. 3.5.1) with product formation as read out, as well as several ways of biotransformation. The addition of several cofactors and additives were further analyzed in 3.5.3 and 3.5.4. The final reaction conditions are described in chapter 3.5.5 Influence of Additives in Lysate Transformations.

3.5.1 Temperature of Heterologous Expression

Two different conditions of heterologous expression were tested in 96 dw-plates including hit variants from library generations 1-3. One plate was inoculated in the morning and incubated at 30 °C for 7 h, while the other plate was inoculated in the afternoon and incubated for 2 h at 37 °C followed by further incubation at 22 °C for 15 h (standard protocol so far). Both plates were harvested each and frozen at -80 °C. To test the activity of the enzymes, a biotransformation with **54** was started. The results are shown in figure 34.

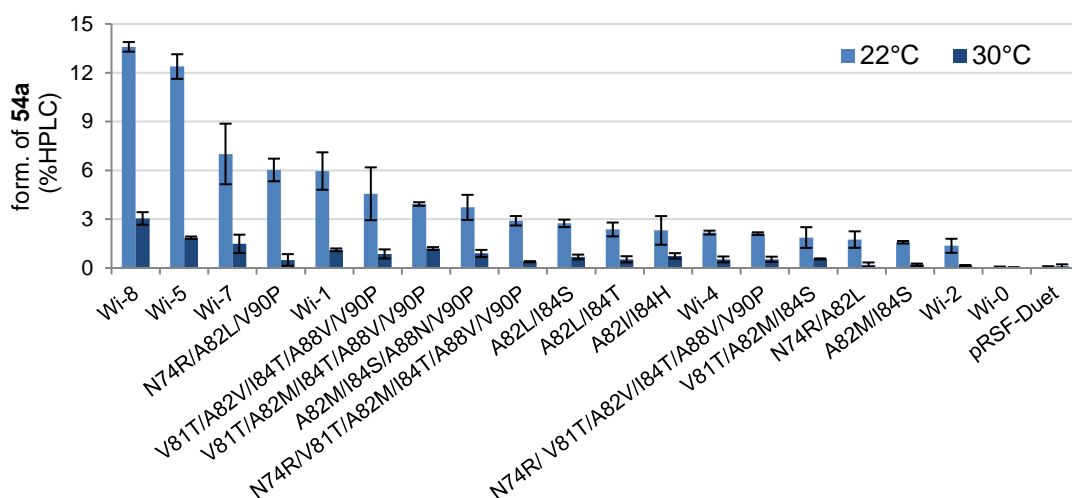


Figure 34. Comparison of formation of **54a** after heterologous expression at 30 °C or 22 °C. Final reaction conditions: 200 μ L volume in 2.2 mL 96 dw-plates sealed with a plastic lid, 50 mM HEPES, 10 mM NaCl, 2.5 mM α KG, 0.5 mM DTT, 0.5 mM $(\text{NH}_4)_2\text{Fe}(\text{SO}_4)_2$, 0.5 mM substrate, 8 h, 30 °C, 200 rpm (Infors HT shaker).

The results show that formation of **54a** after enzyme production at 30 °C is significantly lower. *Wi-8* and *Wi-5* produce less than 25% product than after enzyme production at 22 °C. To test if a shorter time during heterologous expression at 30 °C works better, another 96 dw-plate was prepared and incubated at 30 °C. Here, two variants were tested, *Wi-1* and *Wi-4*. *Wi-4* produced the hydroxylated side product **54b**. The cell culture was taken out after 4, 5, 6, 7 and 24 h. The samples were centrifuged, the supernatant discarded, and the cell pellet frozen. All pellets were thawed, lysed and a biotransformation with **54** conducted. The analysis showed that the highest product formation is present in the range of 5 h (*Wi-1*) to 7 h (*Wi-4*), while a longer expression time resulted in lower product formation (figure 35).

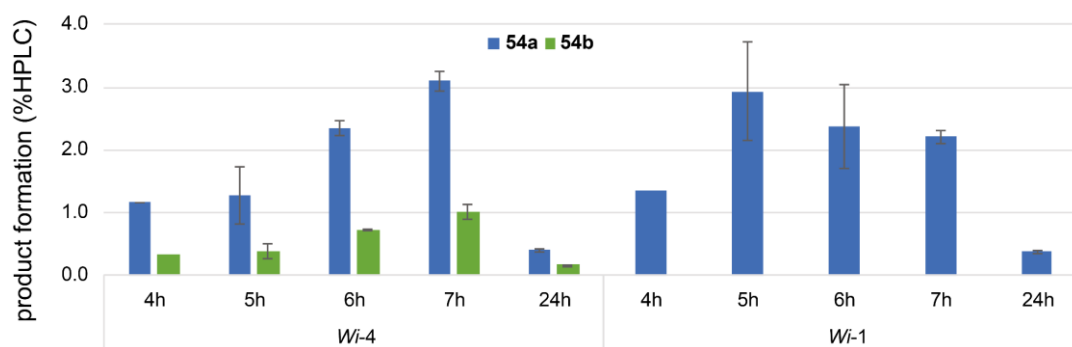


Figure 35. Formation of **54a** dependent on the time of heterologous expression at 30 °C. The reaction was performed in 200 μ L volume, 50 mM HEPES, 10 mM NaCl, 2.5 mM α KG, 0.5 mM DTT, 0.5 mM $(\text{NH}_4)_2\text{Fe}(\text{SO}_4)_2$, 0.5 mM **54**, 8 h, 30 °C, 200 rpm (Infors HT shaker).

While the formation of **54a** with *Wi-4* after 7 h growth is slightly better than the results after expression at 22 °C (figure 34), *Wi-1* shows only 3% formation of **54a** within this experiment, while 6% could be achieved after growth at 22 °C. Therefore, the standard conditions for heterologous expression with incubation for 2 h at 37 °C and subsequent reduction of the temperature to 22 °C with a further incubation of around 15 h is performed.

3.5.2 Whole Cell Biotransformation

The easiest and fastest way to perform biotransformations would be to add the substrate during cell growth and heterologous expression. This procedure was tested using *Wi-1* as catalyst. The experiments were conducted in triplicates in LB and in TB medium containing 50 μ g/mL kan, 20 μ M IPTG and 50 μ M FeCl_3 .

Two plates were analyzed in parallel, one was inoculated with 1/100 and the other with 1/10 preculture/medium, respectively. After 2h or 4h growth time, substrate and α KG were added to a final concentration of 1 mM and 2.5 mM, respectively and the plates incubated at 30 °C, 200 rpm (Infors HT shaker) for 4 h or overnight. None of the tested conditions showed product formation, which suggests that the substrate may not pass the cell membrane and lysis of the cells is essential for chlorination activity.

3.5.3 Influence of Additives in Lysate Transformations

Biotransformations in cell lysate were generally prepared by lysis of the cells with 100 μL lysis buffer (50 mM HEPES, 10 mM NaCl, pH 7.4, 1 mg/mL lysozyme). The pellet was resuspended by vortexing and the cells lysed by incubation of the plates at 37 $^{\circ}\text{C}$ for 30 min. A 2x reaction buffer containing all reaction components was freshly immediately prior to addition. The reaction was started by adding 2 μL of substrate solution (stock solutions in EtOH: 25, 50 and 100 mM, final EtOH conc. 1%).

To test different reducing agents as well as the influence of the substrate concentration, a cell pellet of *Wi-1* from a heterologous expression in a 2 L flask was thawed, diluted to 47.5 mL and 0.5 mL cell suspension was aliquoted in each well of a 2.2 mL- 96 dw-plate. Substrate concentrations of 0.25, 0.5 and 1 mM were used in combination of DTT, ascorbic acid and without a reducing agent. After different reaction times the reaction was stopped by extraction and analyzed by HPLC/UV-Vis. The results sorted by reducing agent and substrate concentration are shown in figure 36. For better comparison the formation of **54a** is presented, instead of conversion (%HPLC).

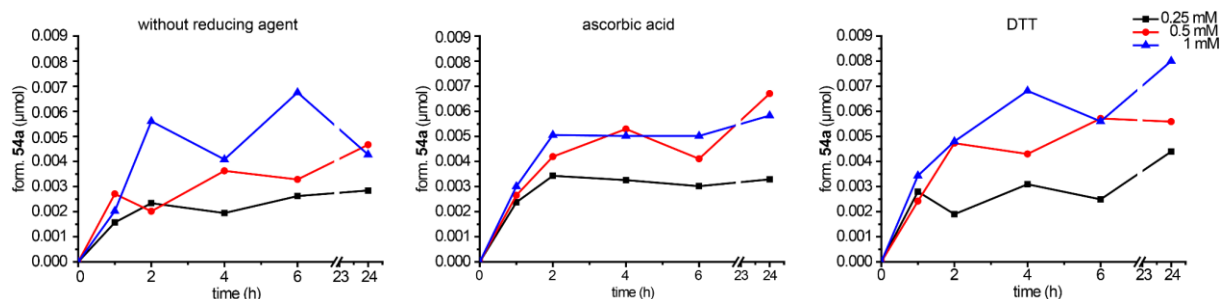


Figure 36. Comparison of formation of **54a** in dependence of different substrate concentrations (0.25 mM black, 0.5 mM red, 1 mM blue) and different reducing agents (without left, ascorbic acid middle, DTT right). Formation of **54a** was determined from duplicate measurements and is given in μmol to directly compare the different substrate concentrations.

The error in these lysate measurements is quite high in the range of 0.002 μmol which corresponds to 30% of the values. Which explains fluctuation within the time dependent product formation. The reason for the high error is probably based on the reaction set-up. After individual reaction times, the reactions are stopped and extracted by ethyl acetate. Then the organic phase was transferred into HPLC vials and the solvent evaporated. The remaining dry sample were dissolved in acetonitrile and measured via HPLC.

Despite the fluctuation it can be seen that a higher substrate concentration results in a higher turnover. With presence of 0.25 mM **54**, a lower formation of **54a** was detected while the difference between 0.5 mM and 1 mM is not clearly visible. From this experiment it can be concluded that no substrate inhibition occurs within the range of 0.25-1 mM. However, since the turnover with the 0.25 mM **54** is the lowest, it could be possible that a product inhibition

takes place. In the beginning, screening was performed with 1 mM **54**, however since substrate availability is a limiting factor, it was reduced to 0.5 mM later.

It is important to notice that half of the transformation occurs within the first hour and in the remaining 23 h less than 50% conversion happens. Furthermore, the addition of reducing agent increases the conversion slightly. After 24 h, the reactions with DTT did have a slightly better product formation than ascorbic acid. Therefore, in the beginning, while screening the variant libraries, DTT was used. After a certain time, the reducing agents were tested again, with purified enzymes and a new package of ascorbic acid, which resulted in a higher product formation than DTT.

3.5.4 Influence of Additives in Transformations with Purified Enzymes

The influence of various additives and reaction conditions were tested with purified enzymes. Different concentrations of cofactors α KG and Fe^{II} in combination with various enzyme concentrations. Furthermore, several approaches were tested to increase the stability of Fe^{II} in solution by addition of different reducing agents, catalase to destroy potentially formed hydrogen peroxide^[376–379] and glycerol to stabilize the protein. In addition, the effect of storage conditions was tested: Freezing at $-80\text{ }^{\circ}\text{C}$ or storage at $4\text{ }^{\circ}\text{C}$ overnight, as well as IMAC purification with a phosphate buffer at pH 6 in comparison to Tris buffer at pH 7.4 was compared as well.

After first experiments in cell lysate, the concentration of cofactors in comparison to the enzyme concentration was analyzed, therefore purified *Wi-1* was used. Also, the reducing agents were tested again. Therefore, enzyme concentrations of $50\text{ }\mu\text{M}$ and $100\text{ }\mu\text{M}$ were used with 2.5 eq $(\text{NH}_4)_2\text{Fe}(\text{SO}_4)_2$ and 12.5 or 25 eq α KG based on 0.5 mM **54**. In figure 37, the formation of **54a** under the different reaction conditions is compared. As in previous reactions the addition of a reducing agent results in the highest product formation.

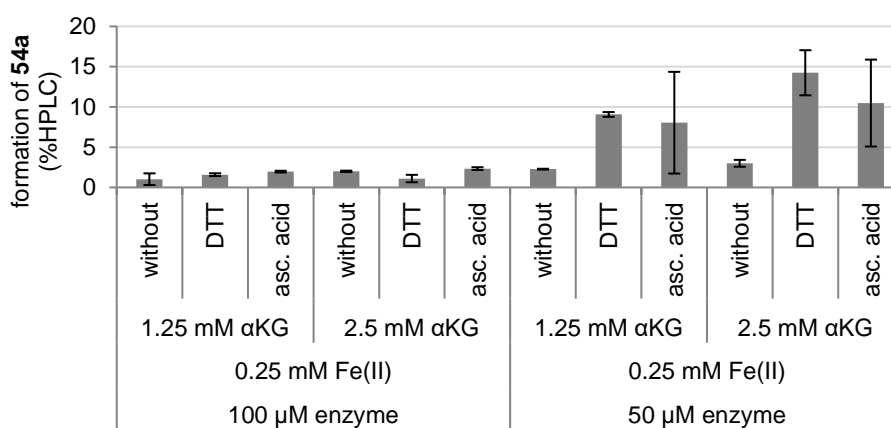


Figure 37. Formation of **54a** dependent on different reducing agents (0.5 mM). The reaction was performed in a 2.2 mL 96-dw plate with 300 μL reaction volume. Different cofactor concentrations were used as given above. A concentration of 0.5 mM **54** was used with a final concentration of 1% EtOH. The reaction was incubated for 4 h at $30\text{ }^{\circ}\text{C}$ at 200 rpm (Infors HT shaker) and stopped by extraction with ethyl acetate.

Results and Discussion

Interestingly, a higher enzyme concentration produces less product. It is possible that a higher excess of α KG and Fe^{2+} is needed to achieve the same turnover number as with the lower enzyme concentration. To confirm this, the reaction was repeated with doubled concentrations of α KG and $(\text{NH}_4)_2\text{Fe}(\text{SO}_4)_2$. However, a low catalyst concentration generally is desirable, therefore the reaction conditions were further optimized using lower enzyme concentrations. In the following experiment 0.5 mM DTT was used and conversions of 60% could be achieved with 100 μM enzyme and 5 mM α KG and 0.5 mM $(\text{NH}_4)_2\text{Fe}(\text{SO}_4)_2$ which supports the assumption that the excess of Fe^{2+} and α KG has to be quite high. For better comparison, in figure 38 the turnover number (TON) is compared which is independent of the enzyme concentration.

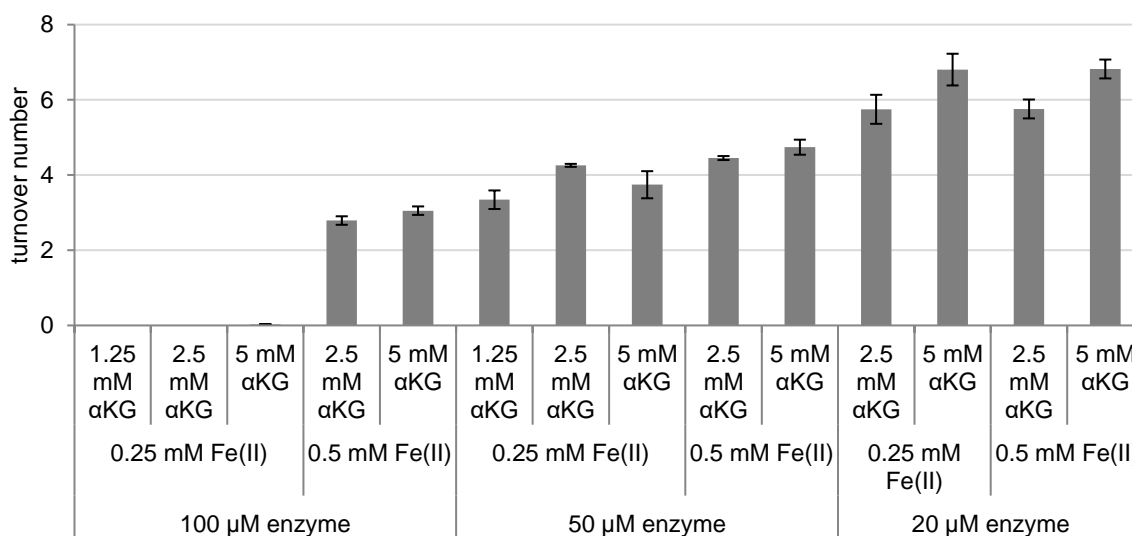


Figure 38. Turnover number of **54** to **54a** dependent on different cofactor concentrations and different concentrations of *Wi-1*. The reaction was performed in a 2.2 mL 96-dw plate with 200 μL reaction volume. Different cofactor concentrations were used as given above. A concentration of 0.5 mM **54** was used with a final concentration of 0.5% EtOH. The reaction was incubated for 24 h at 30 $^{\circ}\text{C}$ at 200 rpm (Infors HT shaker) and stopped by extraction with ethyl acetate.

Comparing the turnover numbers, again, the lowest enzyme concentration achieves the highest turnover number. This could be based on the excess of α KG since 20 μM enzyme with 0.25 mM $(\text{NH}_4)_2\text{Fe}(\text{SO}_4)_2$ and 0.5 mM $(\text{NH}_4)_2\text{Fe}(\text{SO}_4)_2$ with a constant α KG concentration achieve similar turnover, while a constant $(\text{NH}_4)_2\text{Fe}(\text{SO}_4)_2$ concentration with different α KG concentrations achieve different results, with higher turnover in the presence of higher α KG concentration. Based on these results, for purified enzymes 5 mM α KG and 0.5 mM $(\text{NH}_4)_2\text{Fe}(\text{SO}_4)_2$ and only 10 μM enzyme are used.

In the group of Schofield, catalase is added to assays with NHI hydroxylases.^[376] In the literature, stabilizing effects of catalase towards hydroxylases were described.^[376–379] NHI enzymes are described to decouple electron consumption from product formation, especially when non-natural substrates are used.^[379] Catalases reduces H_2O_2 to O_2 and H_2O . The addition of catalase reduced a high background^[377] and increases enzyme activity^[378]. Since the catalytic

Results and Discussion

mechanism of NHI hydroxylases and halogenases is related, it would also be possible that α KG, H_2O and O_2 are converted to CO_2 , succinate and H_2O_2 within this reaction. However, the inhibition of catalase by DTT and ascorbic acid are literature known.^[380–382] Therefore these reducing agents were both tested again. In contrast to previous experiments, a new batch of ascorbic acid was purchased and opened. Figure 39 shows the results of comparison between reactions with and without catalase as well as with DTT in comparison to the new batch ascorbic acid in a time course of 1 h.

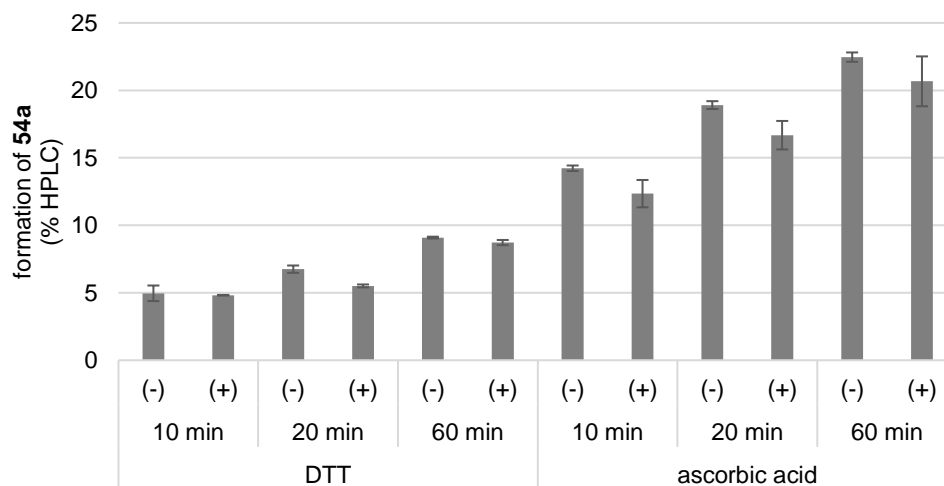


Figure 39. The reaction was performed in 2.0 mL reaction tubes with 0.2 mL volume in 50 mM HEPES, 10 mM NaCl and 10 μ M *Wi-5*. Final reaction conditions contained 5 mM α KG, 0.5 mM ascorbic acid or DTT, 0.5 mM $(NH_4)_2Fe(SO_4)_2$, 0.6 mg/mL catalase and 0.5 mM **54**.

Comparing DTT and the new batch of ascorbic acid, the latter one shows a clear activity improving effect. While <10 % **54a** is produced with DTT within 60 min, >20 % are produced in the presence of ascorbic acid. *Wi-5* and *Wi-8* the best variants found within the first three variant generations were again tested within 8 h reaction time.

Figure 40 shows that the product formation within the first minutes is fastest, more than 50% of the conversion happens within the first then minutes but an increase in product concentration can still be detected after 8 h.

Results and Discussion

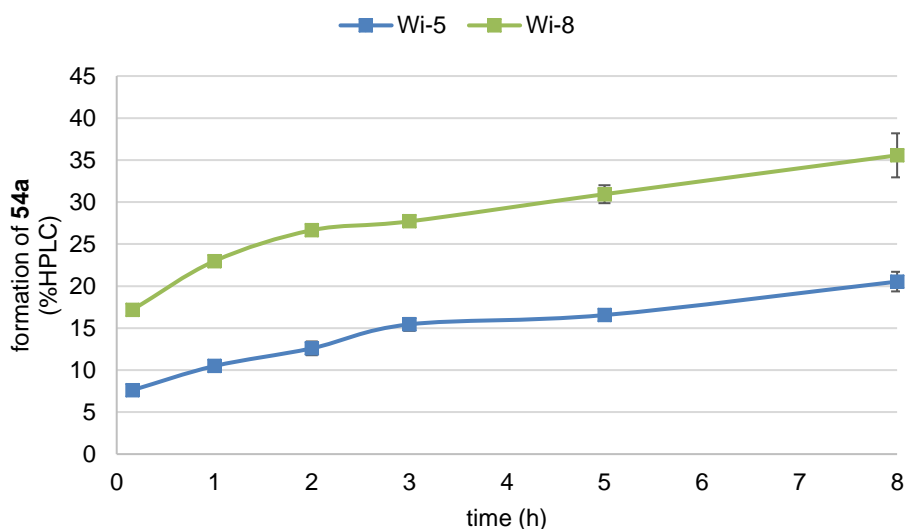


Figure 40. Formation of **54a**. The reactions were performed in 2.0 mL reaction tubes with 0.2 mL volume in 50 mM HEPES, 10 mM NaCl and 10 μ M *Wi-5* or *Wi-8*. Final reaction conditions contained 5 mM α KG, 0.5 mM ascorbic acid, 0.5 mM $(\text{NH}_4)_2\text{Fe}(\text{SO}_4)_2$ and 0.5 mM **54**.

During purification of the halogenase variants it was observed that the presence of 10% glycerol in HEPES buffer is necessary otherwise, the enzyme precipitates. Using glycerol is required to achieve enzyme concentrations up to 1.5 mM (50 mg/mL) without problems. To see if the additive and freezing of the enzyme also influences the activity, some reactions were performed with *Wi-5*.

While IMAC purification, a strong tailing can be observed. An increase of imidazole has no influence and a resin exchange to talon is not possible, because of a low binding affinity, a purification attempt was made at pH 6. Because Tris is not suitable to buffer a pH range of 6.0, phosphate buffer was used during this purification. The elution profile changed slightly, less tailing was present, but the peak broadened (figure 67, ch. 8.3.3). After eluting the enzyme from the IMAC resin, the enzyme is concentrated with the help of centrifugal filters. Then the enzyme solution is dialyzed against HEPES buffer (50 mM HEPES, 10 mM NaCl, 10% glycerol, pH 7.4). Therefore, the effect of purification at pH=6 and the presence of glycerol within the reaction was tested. Furthermore, within purification, the enzyme dialyses overnight. For longer storage, the enzyme is flash frozen in $\text{N}_2(\text{l})$ and stored at -80°C . It was tested if a difference is observable between freezing in $\text{N}_2(\text{l})$ followed by thawing on ice and storage overnight at 4°C . The reactions were performed with *Wi-5* that was stored overnight in the fridge (4°C) or flash frozen in N_2 after purification and stored overnight at -80°C in HEPES buffer pH 7.4 and with addition of 10% glycerol or without.

Results and Discussion

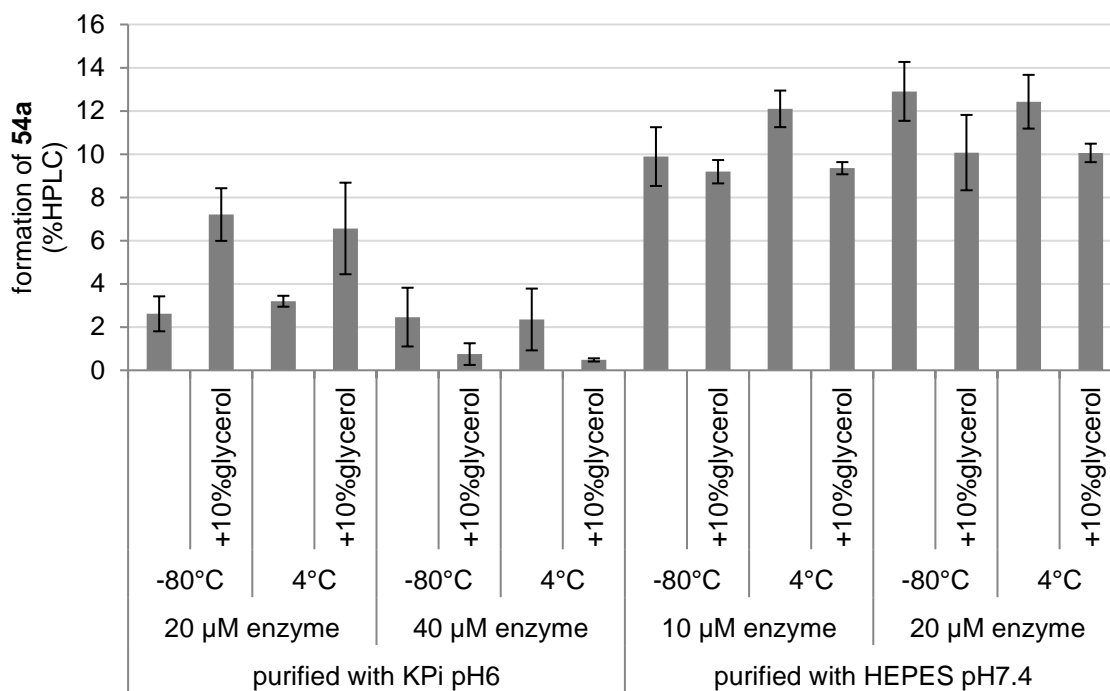


Figure 41. Formation of **54a**. The reactions were performed in 2.0 mL reaction tubes with 0.2 mL volume in 50 mM HEPES, 10 mM NaCl and *Wi-5*. Final reaction conditions contained 5 mM α KG, 0.5 mM DTT, 0.5 mM $(\text{NH}_4)_2\text{Fe}(\text{SO}_4)_2$ and 0.5 mM **54**. The tubes were incubated at 30 °C, 500 rpm in an Eppendorf Thermoshaker for 5 h. The reaction was stopped by extraction with ethyl acetate.

Figure 41 shows the formation of **54a** under tested conditions. It can clearly be seen, that purification at pH 6 with phosphate buffer results in a much lower activity than the purification with Tris buffer, even though the enzyme was dialyzed in both cases to HEPES buffer and all assays were performed in a HEPES buffer at pH 7.4. Fe^{III} -ions precipitate in the presence of phosphate as iron phosphate salts. However, through dialysis, phosphate should have been removed except it binds to the enzyme. Interestingly, the addition of glycerol to the enzyme that was purified at low pH leads to an increase in product formation, while the addition to the enzyme that was purified at pH 7.4 results in a decreased product formation. No difference can be observed between storage overnight at 4 °C or freezing and thawing which is important because it shows that the enzyme is not destabilized by the freezing and thawing process. It can be assumed that storage overnight during purification and the freezing and thawing process in general can be overcome without any activity loss. In this experiment, again, two enzyme concentrations were compared and in the presence of 5 mM α KG, 0.5 mM $(\text{NH}_4)_2\text{Fe}(\text{SO}_4)_2$ and 0.5 mM DTT, 10 μ M enzyme achieves almost comparable product concentrations as 20 μ M enzyme. Therefore 10 μ M enzyme was used as standard concentration.

3.5.5 Final Reaction Conditions

In the previous chapter, several conditions were tested and conditions that resulted in the highest turnover were HEPES buffer pH 7.4, 10 μ M enzyme with 5 mM α KG, 0.5 mM $(\text{NH}_4)_2\text{Fe}(\text{SO}_4)_2$, 0.5 mM ascorbic acid with reaction times of 8 h or longer. Some further reaction conditions were analyzed by N. Huwa within the scope of his master thesis.^[383] Several buffer systems including (MOPS, HEPES and Bis-Tris), pH (6.8, 7.2, 7.6, 8.0), NaCl concentrations (10, 50, 100, 250, 500 mM), ascorbic acid (0.5 and 2.5 mM) with different variants and β -damascone as substrate were tested.^[383] The results show that an increase of NaCl in the reaction from 10 to 100 mM results an increased product formation. Furthermore, an increase of ascorbic acid from 0.5 to 2.5 mM is beneficial. In table 9, product formation under different reaction conditions are compared. Even though the reaction with DTT was stopped after 5 h, it can be compared to the reaction that were run for 8 h, under the new and improved reaction conditions, because it is assumed that the enzyme was inactive after 5 h anyway, based on information described in the previous chapters.

Table 9. Formation of **54a** under different reaction conditions. For all reactions, a final volume of 200 μ L in a 2.2 mL 96-dw plate was used. All reactions contained 10 μ M halogenase, 50 mM HEPES buffer, 5 mM α KG, 0.5 mM $(\text{NH}_4)_2\text{Fe}(\text{SO}_4)_2$ 0.5 mM **54**, 1% EtOH and were stopped by extraction with ethyl acetate.

	formation of 54a (%HPLC)		
	10 mM NaCl, 0.5 mM DTT, 5 h*	10 mM NaCl, 0.5 mM asc. acid, 8 h**	100 mM NaCl, 2.5 mM asc. acid, 8h***
<i>Wi-0</i>	nc	nc	<1
<i>Wi-1</i>	4	11	27
<i>Wi-2</i>	2	3	9
<i>Wi-5</i>	13	37	68
<i>Wi-7</i>	6	12	23
<i>Wi-8</i>	18	44	74
<i>Wi-10</i>	2	8	17
<i>Hw-WelO15</i>	<1	1	11

As table 9 shows, the use of 0.5 mM ascorbic acid instead of 0.5 mM DTT triples the formation of **54a** from 13 to 37% (*Wi-5*). Another doubling is achieved if sodium chloride and ascorbic acid concentrations are increased. The quality of reducing agents is quite important since the performance of DTT and ascorbic acid was tested in the beginning and no difference could be observed, only after a fresh bottle of ascorbic acid was used, a significant improvement in product formation was detectable.

Important to notice is also that with first reaction conditions no activity of *Wi-0* and hardly detectable product formation of *Hw-WelO15* was observable. Under final reaction conditions,

Results and Discussion

Wi-0, still produces low amounts <1% of **54a** while the formation of **54a** with *Hw-WelO15* increased to 11%. This shows the difficulty of assigning a correct substrate scope for variants having minimal activity. These results underline the importance of properly analyzed reaction conditions. After finding a number of active variants, proper exploration of reaction conditions became possible and product formation was significantly improved, finally allowing for substrate scope exploration.

3.6 Substrate Scope

In the beginning of the project, an hapalindole C derivative (**53**) was synthesized to test the chlorination activity. Furthermore, another compound was synthesized, as target substrate for the directed evolution study, which contained a ketone instead of the isonitrile (**54**) (chapter 3.3). In parallel to the synthesis of **53** and **54** several commercially available isonitrile and isothiocyanate substrates were tested with *Hw*-WelO15 and *Wi*-0 (chapter 3.6.1). Since **54** was neither chlorinated nor hydroxylated by the two enzymes under our starting reaction conditions, mutagenesis of the halogenases were performed, looking for variants that chlorinate **54** (chapter 3.4). *Wi*-0 was chosen to be evolved, since it crystallized despite the late discovered higher activity of *Hw*-WelO15. After a number of variants was found that chlorinate **54**, several modified hapalindole-like ketones were tested with a panel of chlorinases. A number of substrates were chlorinated (ch. 3.6.2.1), and others were transformed into complex mixtures of products (ch. 3.6.2.2). Interestingly, one variant, *Wi*-4 is able to produce the chlorinated **54a** and the hydroxylated (**54b**) product (68% chemoselectivity for **54a**). Also, *Hw*-WelO15 has a low chemoselectivity of 70% towards chlorination of **54**. To obtain pure hydroxylation products, of **54**, hydroxylation with well-established oxygenase P450_{BM3} was pursued (ch. 3.6.4). Finally, also biotransformations with hapalindole-like isonitriles were performed (ch. 3.6.5).

3.6.1 Biotransformation with *Wi*-0 and *Hw*-WelO15 and Small Molecule Isonitriles

If cultures of cyanobacteria are analyzed for their secondary metabolites, all found chlorinated hapalindole-like alkaloids contain an isonitrile or isothiocyanate moiety in *beta* and *trans*-position to the chlorine within the six-membered ring. This suggests that the isonitrile group plays a major role in native substrate recognition. Biotransformation with purified *Hw*-WelO15 and *Wi*-0 were made with commercially available small molecules containing an isonitrile and isothiocyanate to test their ability to chlorinate non-natural compounds. The substrates are shown in figure 42.

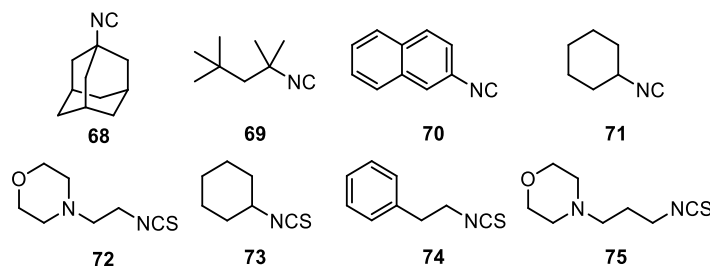
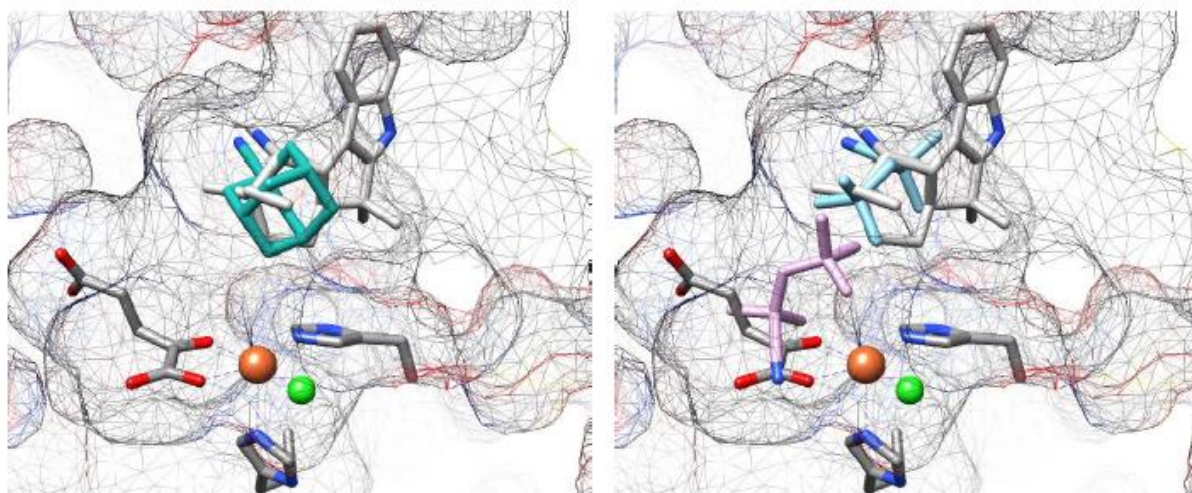


Figure 42. Tested isonitrile and isothiocyanate containing molecules.

When the reactions were performed, no positive control for the enzyme activity was available, because the synthesis of **53** was not finished yet. Therefore, the enzyme was used in a concentration of 0.1 mM in combination with 1 mM substrate in expectation that even a low activity would have been observed. Different reaction conditions were tested including different reducing agents (DTT, ascorbic acid or no additive). Also, different reaction times (3 h, 7 h 24 h) were used. Unfortunately, no conversion could be detected by GC-FID. Chromatograms of the starting material can be found in chapter 8.6.1.12. As a second strategy, a decoy molecule was used, which helps filling the active site, in case the enzyme needs allosteric activation or the lid of the enzyme only closes after recognition of a certain interaction.^[384] Since the indole moiety was missing in the commercial compounds, all assays were repeated with addition of indole. Product formation could not be observed.

To find an explanation, these substrates were docked with the help of SwissDock^[385] into the published crystal structure of WelO5 (PDB 5IQT) by H. Mueller. Since isonitrile groups are not applicable for the CHARMM force field, all isonitrile groups were substituted by nitrile groups. To check if this approach is working, first the nitriles of 12-*epi*-fischerindole U and 12-*epi*-hapalindole C, were docked into the active site. The crystal structure of WelO5 with soaked 12-*epi*-fischerindole U was used as reference. Both docked molecules were placed by the program as expected, confirming proper docking setup, with the terpene ring covering the soaked molecule, therefore it can be assumed that the results of the docking study are reliable for this system (figure 81, ch. 8.3.6.1).

Docking of the small molecule substrates **68-75** revealed that they predominantly bind to the binding site of the cofactor α KG. Only for adamantane-nitrile as substitute for **68** and 1,1,3,3 tetramethylbutyl nitrile (based on **69**) the docking showed a possible binding inside the substrate binding site, so that a conversion with the enzyme might be possible. In figure 43 the docking results of the two nitriles are shown.



Results and Discussion

Figure 43. Results of docking with SwissDock.^[385] a) The tested adamantane nitrile (turquoise) was docked into WelO5 and is overlaid with the soaked 12-*epi*-fischerindole U (gray). b) shows the docking results of 1,1,3,3 tetramethylbutyl nitrile (substrate shown in light blue and purple for two possible binding sites) and is overlaid with the soaked 12-*epi*-fischerindole U (gray). The iron is shown as orange ball and the chloride is shown as green ball. α KG is shown as grey sticks.

But also for 1,1,3,3 tetramethylbutyl nitrile, a binding inside the α KG binding site was also observable (possible binding mode shown in purple, figure 43), which would inhibit the activity of the enzyme since α KG is a necessary cofactor for the reaction.

Later, it could be seen that a concentration of 100 μ M enzyme has a low or even no activity in biotransformation if the cofactors are not available in greater excess (for details see chapter 3.5.4, especially figure 38). Therefore, it is likely that the inactivity of the enzyme under used conditions (50 mM HEPES, 10 mM NaCl, pH 7.4, 2 mM α KG, 0.5 mM $(\text{NH}_4)_2\text{Fe}(\text{SO}_4)_2$, 0.5 mM reducing agent and 1 mM substrate) was the reason why no product was formed and not the structure of the substrates or unfavorable binding. Under optimized reaction conditions (chapter 7.2.5), the transformation is probable, as it was shown that *Hw*-WelO15 produces hardly **54a** with initial reaction conditions, while optimized reaction conditions lead to a product formation of 11%. Parallel to this work on large compounds, H. Mueller and N. Huwa could show that a complementary set of *Wi*-0 variants is needed to accept smaller molecules.^[383,386]

3.6.2 Biotransformation with WelO15 variants and Hapalindole-like Ketones

After finding a number of variants that chlorinate **54**, more hapalindole-like ketones were synthesized. These substrates were first synthesized by L. Schmermund (**76-78**, **81-83**, **85**) in the scope of his master thesis^[317] and later resynthesized within this thesis. The synthesis of all compounds (figure 44) is based on the coupling of diversified indoles with different six-membered rings. Synthesis of **79** and **80** were performed by the group of R. Viswanathan. To synthesize **81** and **82**, the unsaturated ring was coupled, to first achieve **84** and **85** followed by a reduction with engineered ene-reductase *Ts*ER variants. Coupling of the reduced C=C bond rings (e.g *R*-dihydrocarvone, to form **87**) resulted in a mix of products, lowering the overall yield.

Under first reaction conditions (50 mM HEPES, 10 mM NaCl, 5 mM α KG, 0.5 mM DTT, 0.5 mM $(\text{NH}_4)_2\text{Fe}(\text{SO}_4)_2$, 10 μ M enzyme), substrates **54** and **76-78** with modification at the indole moiety were chlorinated. **79** was transformed by *Wi*-2 to two new products, one chlorinated and one that could not be identified so far. Substrates **80-87** were not converted. After changing the reaction buffer, also **80-83** were accepted however no chemoselectivity is achieved. **84-87** have not been tested under optimized conditions. An overview of all tested ketones is shown in figure 44 and detailed analysis is given in the next paragraphs.

Results and Discussion

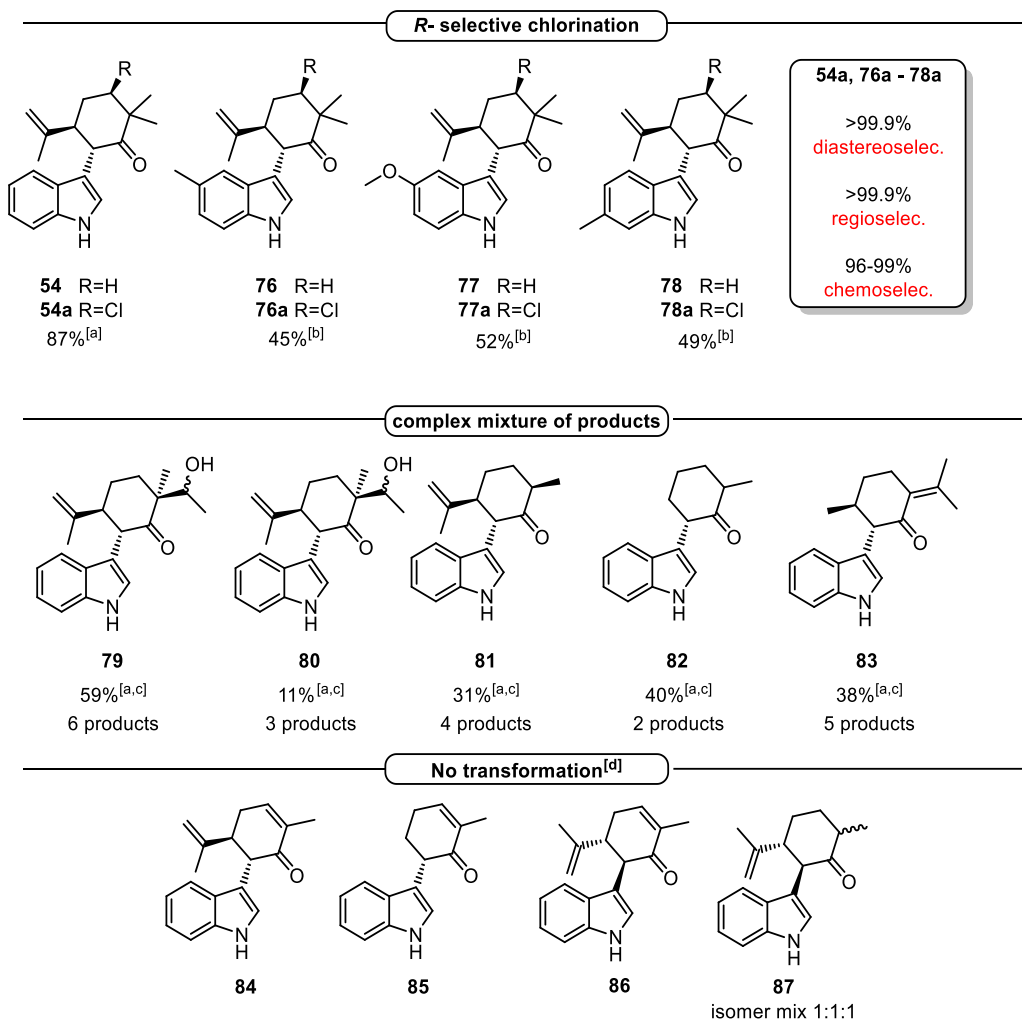


Figure 44. Tested hapalindole-like ketones and substrate scope of *Wi-WelO15* variants. Best product formation (% HPLC) is given for 8 h, 30 °C in 200 μ L 50 mM HEPES, 100 mM NaCl, pH 7.4 with 0.5 mM substrate with either [a] 2 mol% (10 μ M) purified enzyme or [b] cell lysate (prior to lysis normalized to OD₆₀₀=5.0). [c] total formation of all products. [d] no transformation with initial reaction conditions of 50 mM HEPES, 10 mM NaCl, pH 7.4 with 0.5 mM.

The results regarding substrate scope are divided into substrates with modification at the indole moiety **76-78** which are predominantly chlorinated. Modification at the terpene ring in **81-83** which mainly show complex mixtures of products. Mass analysis revealed only few chlorinated products. For first analyses 10 *Wi-WelO15* and three *Hw-WelO15* variants were selected and normalized to a cell density of OD₆₀₀=5.0. Therefore, heterologous expression was performed in a 2 L flask with 0.5 L culture as described in ch. 7.1.9.1. and aliquoted into a 2.2 mL 96-dw plate. The selected variants are shown in table 10. Well performing variants were isolated by purification and later analyses were performed with purified enzymes.

Results and Discussion

Table 10. Variants chosen for analysis with abbreviation and all mutations.

name	WelO15 variants
<i>Wi-0*</i>	<i>Wi-WelO15 V6I/D284N</i>
<i>Wi-1*</i>	<i>Wi-WelO15 V6I/A82L/D284N</i>
<i>Wi-2*</i>	<i>Wi-WelO15 V6I/N74R/D284N</i>
<i>Wi-3**</i>	<i>Wi-WelO15 V6I/V90P/D284N</i>
<i>Wi-4*</i>	<i>Wi-WelO15 V6I/A82V/I84H/D284N</i>
<i>Wi-5*</i>	<i>Wi-WelO15 V6I/A82L/V90P/D284N</i>
<i>Wi-6**</i>	<i>Wi-WelO15 V6I/A88V/V90P/D284N</i>
<i>Wi-7*</i>	<i>Wi-WelO15 V6I/V81T/A82M/A88V/V90P/D284N</i>
<i>Wi-8*</i>	<i>Wi-WelO15 V6I/N74R/V81T/A82M/A88V/V90P/D284N</i>
<i>Wi-9*</i>	<i>Wi-WelO15 V6I/M221L/M225I/D284N</i>
<i>Wi-10*</i>	<i>Wi-WelO15 V6I/A82L/V90P/M221L/M225I/D284N</i>
<i>Wi-11*</i>	<i>Wi-WelO15 V6I/N74R/V81T/A82M/A88V/V90P/S93L/S103A/D284N</i>
<i>Wi-12*</i>	<i>Wi-WelO15 V6I/N74R/A82L/V90P/S93D/D284N</i>
<i>Wi-13***</i>	<i>Wi-WelO15 V6I/N74R/A82L/V90P/S93H/S103A/A175N/D284N</i>
<i>Wi-5P3***</i>	<i>Wi-WelO15 V6I/A82L/V90P/S103A/Q123R/F230K/Q236N/S239W/S268R/Q282D/D284N</i>
<i>Hw-1**</i>	<i>Hw-WelO15 A82L</i>
<i>Hw-2**</i>	<i>Hw-WelO15 A82L/V90P</i>

*enzymes analyzed as lysate and purified catalyst, **enzymes analyzed only in cell lysate, *** enzymes analyzed only as purified catalyst

The expression level of the genes was analyzed by SDS-PAGE (figure 91). It can be seen that especially *Hw* variants as well as *Wi-9* show a lower soluble enzyme concentration in lysate, which could be explained by a lower expression level or low solubility. SDS-PAGE analysis of the whole cells (ch. 8.5.1, figure 90) shows, that the halogenase expression level is lower as well.

3.6.2.1 Modification at the Indole Moiety

The substrate scope was first tested with hapalindole-like ketones containing modifications at the indole moiety. The indole derivatives were coupled to the terpene ring **64** with similar yields as indole. In lysate-based biotransformations it was tested if methyl groups in position 5 or 6 or a methoxy group in position 5 have an influence on the acceptance of the chlorinase. The reaction procedure is described in ch. 7.2.5.1 and results are given in table 11.

Results and Discussion

Table 11: Total conversion of **54** and **76-78** and chemoselectivity obtained in lysate-based biotransformation with normalized cell mass. Final reaction conditions: 200 μ L volume in 2.2 mL 96 dw-plates sealed with a plastic lid, 50 mM HEPES, 100 mM NaCl, 2.5 mM α KG, 2.5 mM ascorbic acid, 0.5 mM $(\text{NH}_4)_2\text{Fe}(\text{SO}_4)_2$, 0.5 mM substrate, 8 h, 30 $^\circ\text{C}$, 200 rpm (Infors HT shaker). Area of starting material, chlorinated product and hydroxylated product (identified by LC-MS) were included. If relative conversion was below 5% no selectivity was determined. Highest product formation is highlighted in red.

enzymes	54	54a	76	76a	77	77a	78	78a
	conv. ^[a]	chemo-select.						
<i>Wi-0</i>	<1	nd	<1	nd	<1	nd	<1	nd
<i>Wi-1</i>	32	98	7	99	11	98	15	96
<i>Wi-2</i>	28	94	2	nd	4	nd	2	nd
<i>Wi-3</i>	3	nd	1	nd	1	nd	1	nd
<i>Wi-4</i>	43	68	34	80	36	82	23	75
<i>Wi-5</i>	59	98	33	99	48	98	42	97
<i>Wi-6</i>	22	81	17	90	18	92	2	nd
<i>Wi-7</i>	52	93	12	96	30	93	14	98
<i>Wi-8</i>	62	96	27	98	54	96	50	98
<i>Wi-9</i>	1	nd	2	nd	1	nd	<1	nd
<i>Wi-10</i>	30	95	18	96	45	96	30	96
<i>Wi-11</i>	69	96	25	97	44	96	38	91
<i>Wi-12</i>	63	92	14	47	10	72	18	94
<i>Hw-WelO15</i>	11	70	48	94	33	93	31	90
<i>Hw-1</i>	18	86	12	87	27	92	8	85
<i>Hw-2</i>	3	nd	2	nd	5	95	2	nd

[a] relative conversion (% HPLC), nd= not determined.

As shown in table 11, the chlorinated products can be produced with conversions of 33-69% and chemoselectivities of 96-99% by *Wi-WelO15* variants. *Wi-0* hardly (<1%) transforms the ketones **54**, **76-78**, whereas *Hw-WelO15* produces moderate amounts of chlorinated ketones **54a**, **76a-78a**, with **76** being the best substrate obtaining 45% **76a**. This indicates a change in substrate selectivity, since **76** is the substrate accepted worst by *Wi-WelO15* variants. The 4th generation variant *Wi-11* has the highest product formation for **54a** while modified substrates are converted best by variants found earlier in the evolution process which might be explained by an adaption to the screening substrate, not allowing larger residues within the structure.

NHI dependent halogenases are known to produce hydroxylated side products, especially if the substrate is modified from the natural substrate.^[159] Therefore it was gratifying to see that modification in the indole moiety did not change the chemoselectivity towards hydroxylation for most variants. *Hw-WelO15* as well as *Wi-4* however have a drastically reduced chemoselectivity for **54** with 68-70% selectivity for chlorination. Hydroxylation of **54** will be closer analyzed in chapter 3.6.4.

Results and Discussion

After preparative scale reaction (ch. 3.7), chlorinated products were analyzed by mass (ESI⁺) and NMR (¹H, ¹³C and NOESY). Products were found to be chlorinated on C13 with *R*-configuration, showing identical absolute stereochemistry as related 12-*epi*-hapalindole E. Based on this information, selected variants were purified, and the transformation repeated with purified enzyme (ch. 7.2.5.2). The results are shown in table 12.

Table 12: Total conversion of substrates **54** and **76-78** and chemoselectivity obtained in biotransformation with purified enzymes. Final reaction conditions: 200 μ L volume in 2.2 mL 96 dw-plates, 50 mM HEPES, 100 mM NaCl, 5 mM α KG, 2.5 mM ascorbic acid, 0.5 mM (NH₄)₂Fe(SO₄)₂, 0.5 mM substrate, 8 h reaction time, 30 °C, 200 rpm (Infors HT shaker). Area of starting material, chlorinated product and hydroxylated product (identified by LC-MS) were included. Selectivities for chlorinated products are given. If relative conversion was below 5% no selectivity was determined. Highest product formation is highlighted in red. Variant *Wi-5* and *Wi-5P3* are highlighted in orange to compare conversion of the template variant and a thermostabilized variant with 6 °C increased melting temperature based on 7 further mutations on the enzyme surface.

enzymes	54	54a	76	76a	77	77a	78	78a
	conv. ^[a]	chemo-select.						
<i>Wi-0</i>	<1	nd	<1	nd	<1	nd	<1	<1
<i>Wi-1</i>	28	96	2	nd	5	97	4	nd
<i>Wi-2</i>	9	95	<1	nd	<1	nd	<1	<1
<i>Wi-4</i>	3	nd	3	nd	7	80	3	nd
<i>Wi-5</i>	70	97	14	98	42	96	13	98
<i>Wi-7</i>	25	92	1	nd	8	91	2	nd
<i>Wi-8</i>	80	93	5	98	31	94	17	99
<i>Wi-9</i>	2	nd	2	nd	1	nd	<1	nd
<i>Wi-10</i>	18	93	5	94	23	92	5	95
<i>Wi-11</i>	90	96	8	98	41	94	26	99
<i>Wi-12</i>	91	96	9	98	21	93	16	98
<i>Wi-13</i>	69	96	6	99	26	96	21	98
<i>Wi-5P3</i> ^[b]	76	96	11	96	45	94	16	98
<i>Hw-WelO15</i>	11	73	33	91	28	95	9	78

[a] relative conversion (% HPLC), nd= not determined

[b] *Wi-WelO15* V6I/A82L/V90P/S103A/Q123R/F230K/Q236N/S239W/S268R/Q282D/D284N. This variant was created as stabilized variant, described in chapter 3.9.1.

SDS-PAGE analysis revealed that comparable amounts of halogenase are present in reactions that are performed in cell lysate or with purified enzymes(ch. 8.5.2), therefore the results can directly be compared.

The lead substrate **54** is chlorinated best under conditions with isolated enzymes (*Wi-11* purified: 86% versus lysate: 66%). The highest product formation for each compound is highlighted in red (table 12). The best variants *Wi-5*, *Wi-8*, *Wi-11* and *Wi-12* show higher **54a** formation in isolated form then in cell lysate. While formation of **76a-78a** with the same enzymes

worked better in cell lysate, indicating that the dependency of the reaction environment is dependent on the substrate, not the variant.

Introduction of a methyl group decreases product formation with purified enzymes to 14 and 26% for **76a** and **78a**, respectively. When cell lysate was used instead, product formation for **76a** and **78a** was twice as high (33% and 52%). Introducing the H-bond acceptor OMe at C5 the drop in product formation in comparison to **76a** (14%) could be recovered, giving 40% **77a** with purified enzymes and 52% with lysates.

Variant *Wi-4* with a medium conversion and decreased chemoselectivity in cell lysate lost its activity almost completely. While *Hw-WelO15* produces all chlorinated products in lysate and as isolated catalyst with decreased chemoselectivity.

Wi-5P3 (highlighted in orange) was produced as stabilized variant (see chapter 3.9) based on *Wi-5* and contains 7 further mutations on the enzyme surface which increased its melting temperature from 55 °C to 61 °C. The chlorinase has compared to *Wi-5* a higher conversion (except for **76**) but also a slight decrease in chemoselectivity. This indicates that a stabilization of the enzyme might result in a slight increase in activity.

In summary, the chlorinase panel allows late-stage chlorination and access to **54a**, **76a-78a** with regio- and diastereoselectivities >99.9%. Product formation differences between reactions with purified enzymes and cell lysate indicate that complex stabilizing effects must happen within the reaction which cannot easily be explained. Kinetic analysis was performed with selected variants to gain information about the binding affinity and reaction velocity (ch. 3.8).

3.6.2.2 Modification in the Terpene Ring

Substrates **79** and **80** were sent by R. Viswanathan as mix of epimers. The molecules are bigger than the screening substrate **54**, with an additional carbon and hydroxy group in position C12. The compound is an intermediate in the synthesis of 12-*epi*-hapalindole C. **79** and **80** were separated by preparative HPLC and tested individually even though no absolute assignment of the stereo conformation could be performed.

Under initial reaction conditions only **79** was converted into two new products, **79c** and **79d**. Using optimized reaction conditions, more products were formed starting from **79**. Also **80** was converted into several new products. Products of transformations with **79** and **80** could only be characterized with LC-MS due to a lack of further substrate. HPLC chromatograms of selected variants with **79** and **80** are shown in figure 45. A complete overview of selectivities with all variants is given in table 41, ch. 8.5.5.

Results and Discussion

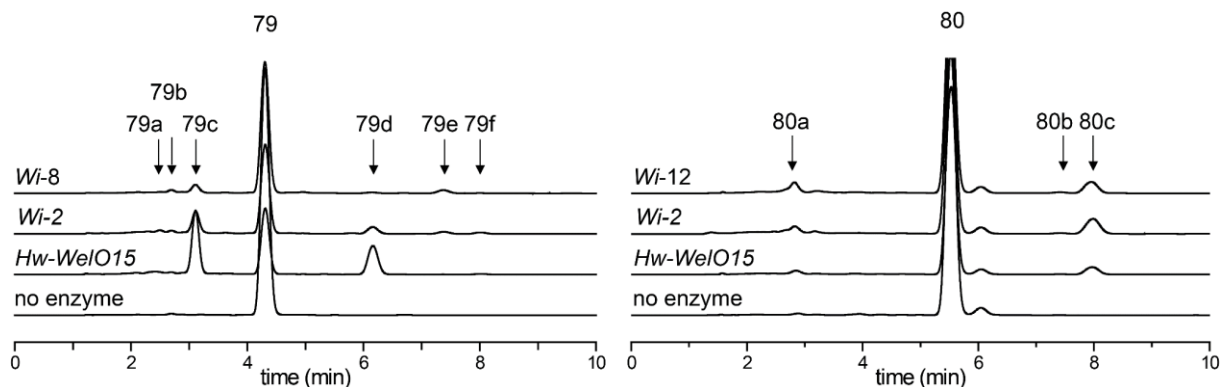
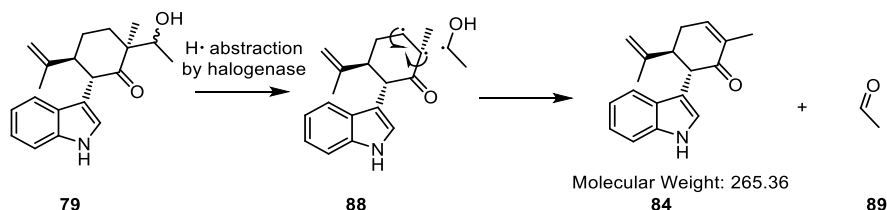


Figure 45. HPLC chromatograms of **79** and **80** after biotransformation with selected halogenase variants. Peaks that were not present in control reactions are highlighted with arrows. Final reaction conditions: 200 μ L volume in 2.2 mL 96 dw-plates, 10 μ M enzyme, 50 mM HEPES, 100 mM NaCl, 5 mM α -KG, 2.5 mM ascorbic acid, 0.5 mM $(\text{NH}_4)_2\text{Fe}(\text{SO}_4)_2$, 0.5 mM substrate, 8 h reaction time, 30 $^\circ\text{C}$, 200 rpm (Infors HT shaker).

While **79** is transformed best by *Hw-WelO15* and *Wi-1*, *Wi-2* and *Wi-12* have the highest conversion for **80**. LC-MS analysis revealed **79a** and **79b** to be hydroxylated products ($[\text{M}+\text{H}]^+$ $m/z = 328$). It was first assumed that **79c** is a hydroxylated product, however repeated LC-MS measurements assigned a mass of $[\text{M}+\text{H}]^+$ $m/z = 266$. The mass fit to a degradation product if acetaldehyde (**89**) is eliminated in α -position to the carbonyl group as shown in scheme 7.



Scheme 7. Possible radical elimination of acetaldehyde as degradation process from **79**.

However, the product of this elimination process (**84**) is in the scope of synthesized ketones and does not fit to the retention time in the HPLC measurement. For proper analysis and structure elucidation, more product is needed for NMR analysis. Remaining products were identified with the following masses: $[\text{M}+\text{H}]^+$ m/z (**79d**) = 266, m/z (**79e**) = 310, m/z (**79f**) = 266. **80** is also transformed into several new products with the following masses: $[\text{M}+\text{H}]^+$ m/z (**80a**) = 266, m/z (**80b**) = 268 and 310, m/z (**80c**) = 346.

In this way **80c** could be identified as chlorinated product and the typical isotopic peak could be observed. To elucidate at which position in the molecule, the halogenation did take place, NMR measurements are necessary. From the educt mass of 311 g/mol, products **79e** and **80b** show a mass that fit to desaturation, also masses **79f** and **80a** could be desaturated products from products **79c** and **80b**. What kind of transformation occurred from **79** to **79d**, with a mass difference of -46 g/mol is not known until now. Further, no assumptions can be made where these modifications happen. NHI enzymes are known to catalyse a broad spectrum of

different reactions. Hereby reactions like halogenation, demethylation, desaturation, O-cyclization, ring expansion and epimerization are catalyzed therefore it is hard to predict what happened, without further characterization of the products.^[162,167–177]

Small structural changes in the terpene ring of **81-83** proved to be as challenging for the enzymatic chlorination. Elimination of a methyl group at C12 (**81**) or sp² hybridization (**83**) in comparison to **54**, abolished detectable chlorination, proving that C12 position requires a quaternary carbon center for corrected substrate positioning prior to chlorination. Nevertheless, substrates **81-83** are transformed with moderate activity into several new products. All three compounds are converted best with variant *Wi-12*, a complete overview of conversion and selectivities is given in table 42, ch. 8.5.5. HPLC chromatograms are shown in figure 46.

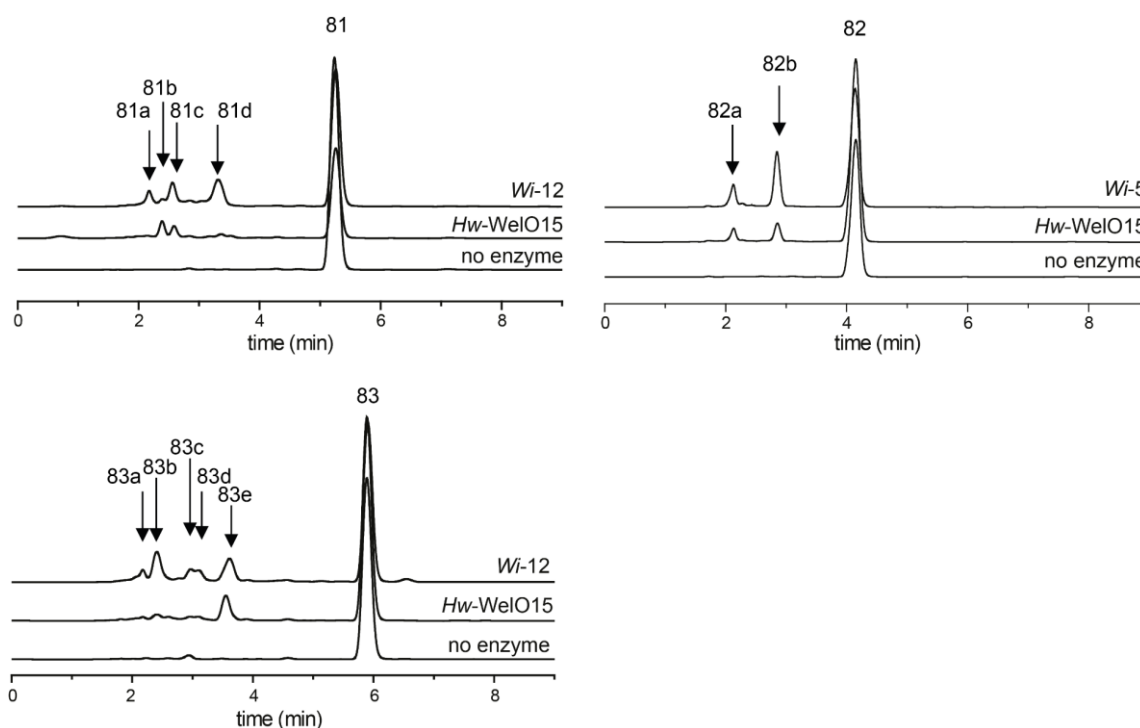


Figure 46. HPLC chromatograms of **81-83** after biotransformation with halogenase variants.

Preparative scale reactions (chapter 3.7) were performed with all three substrates however the resulting yields from **81** and **83** were not sufficient for NMR analysis (ch. 3.7.2). LC-MS analysis assigned different transformation to the products. Starting with **81** (267 g/mol), product **81a** with a retention time of 2.2 min has a mass of $[M+H]^+$ $m/z = 146$, **81b** and **81d** are hydroxylated $[M+H]^+$ $m/z = 284$, while **81c** has a mass of $[M+H]^+$ $m/z = 254$, which fits to a demethylated product.

Products of transformation with **83** (267 g/mol) are desaturated ($[M+H]^+$ m/z (**83c,d,e**)=266) and either methylated or hydroxylated combined with subsequent desaturation ($[M+H]^+$ m/z (**83b**)=282). **83a** has, as **81a**, both with identical retention times a mass of $[M+H]^+$ $m/z=146$.

Substrates **84-87** were only tested under non-optimized conditions and did not show any product formation. It could be assumed, that no modification of sp^2 -hybridized carbons is possible within this enzyme class. **87** has the needed sp^3 -configuration. Even though it has opposing stereocenters compared to **81**, a transformation with *Wi-1* is probable, based on results shown in chapter 3.6.3, however the starting material is already a mix of three isomers because *R*-dihydrocarvone was coupled to carvone. If this molecule should be analyzed, a new synthesis should be performed, first coupling *R*-carvone to indole followed by a reduction by the ene-reductase *TsER*.

3.6.3 Hapalindole-like Nitrile, Isothiocyanate and Isonitriles

Next to hapalindole-ketones also a nitrile, isothiocyanate and isonitriles with different stereo-information were available. While synthesizing **53**, **67** is received as major side product (chapter 3.3). Also, amine **65** is an intermediate in the synthesis of **53** and **67**. Hapalindole Q (**91**) is a natural product however with changed stereocenters and isothiocyanate group instead of the isonitrile which was synthesized by the group of R. Viswanathan. After finding a number of variants that transform hapalindole-like ketones, the panel of chlorinases was also tested with compounds shown in figure 48.

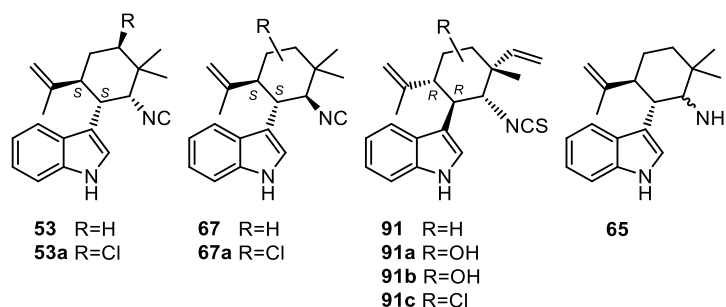


Figure 48. Hapalindole-like nitrile, isothiocyanate and isonitriles.

53 as close derivative to the naturally occurring 12-*epi*-hapaldindole C is chlorinated by the wild-type enzymes and also with the engineered *Wi-WelO15* variants, however, with reduced efficiency (table 13). Variants *Wi-1* and *Wi-2* with one mutation in the active site still have moderate activity of 67-73% conversion while an increased number of mutations in the active site results in conversions below 30%. Only *Wi-10*, which has the same mutations in the active site as *Wi-5* (A82L/V90P) showed again a higher formation with an increase in **53a** formation from 27% to 60%, revealing that for chlorination of **53** the two mutations M221L/M225I seem to be beneficial.

Results and Discussion

Table 13. Relative conversion of substrates **53**, **67**, **91** obtained in biotransformation with purified enzymes. Final reaction conditions: 200 μ L volume in 2.2 mL 96 dw-plates, 50 mM HEPES, 100 mM NaCl, 5 mM α KG, 2.5 mM ascorbic acid, 0.5 mM $(\text{NH}_4)_2\text{Fe}(\text{SO}_4)_2$, 0.5 mM substrate, 8 h reaction time, 30 $^\circ\text{C}$, 200 rpm (Infors HT shaker).

	relative conversion (%HPLC)		
	53	67*	91
<i>Hw</i> -WelO15	91	4	nc
<i>Wi</i> -0	93	nc	nc
<i>Wi</i> -1	67	88	86 (6% 91a , 2% 91b 77% 91c)
<i>Wi</i> -2	73	nc	nc
<i>Wi</i> -4	3	nc	nc
<i>Wi</i> -5	27	71	nc
<i>Wi</i> -7	15	5	nc
<i>Wi</i> -8	19	6	nc
<i>Wi</i> -9	93	nc	nc
<i>Wi</i> -10	60	57	nc
<i>Wi</i> -11	20	20	nc
<i>Wi</i> -12	26	55	nc

* aqueous phase measured after reaction. nc = no conversion,

Change of the stereocenter at C11, results in complete activity loss of product formation with *Wi*-0. Mutation of A82L in *Wi*-1, enables the conversion and chlorinated **67** best of all tested variants which supports the assumption that the position A82 is important for interaction with the isonitrile group. *Wi*-10 and *Wi*-12 also contain mutation A82L and have a moderate conversion whereas variants with V81T/A82M/A88V instead have a low product formation of $\leq 6\%$. After introduction of mutations S93L/S103A the formation of **67a** however increases to 20% (*Wi*-11).

Hapalindole Q is only accepted by *Wi*-1, which shows again the high versatility of *Wi*-1 for other stereo conformations. The main product **91c** is chlorinated (77% selectivity), while two side products **91a** and **91b** are hydroxylated.

Amine **65** is a mix of two epimers which could not be separated by flash column chromatography, therefore the mix was tested. No transformation could be observed by any variants under initial reaction conditions. Analysis of the educt and the reactions had to be performed in the presence of TFA, otherwise no distinct peaks could be identified but a broad signal. It could be possible that from a formed product, HCl or H₂O would eliminate in the presence of TFA. However, LC-MS analyses of all biotransformations were performed in the presence of TFA without observable decrease in product. More probable is the low activity based on the reaction conditions. The biotransformation should be repeated under optimized conditions.

In summary, the created chlorinase panel is able to transform a large scope of non-natural hapalindole-like compounds. Ketones **54** and **76-78** with modification at the indole moiety are chlorinated with excellent chemoselectivity of 96-99%. Achieving such a high selectivity is exceptional because non-natural substrates for Fe^{II}/ α KG dependent halogenases are dominantly reported to be hydroxylated.^[159,387] Isonitrile **67** and hapalindole Q (**91**) are chlorinated solely by one variant, *Wi-1*, revealing important information about further engineering processes with different stereo centers and perhaps leading to chlorination with different regio- or stereochemistry. To further examine this, the stereochemistry of the two products have to be analyzed. Modifications at the terpene moiety, present in substrates **79-83**, led to a loss of selectivity and abolished chlorination. Interestingly, albeit their low activity, *Hw-WelO15* wild type and *Wi-WelO15* variants carrying I84H start shifting chemoselectivity of substrates that are mainly chlorinated towards 30% hydroxylation of **54**, an indication that chemoselectivity can also be controlled solely by substrate binding site mutations. The hydroxylation of **54** is analyzed closer in chapter 3.6.4

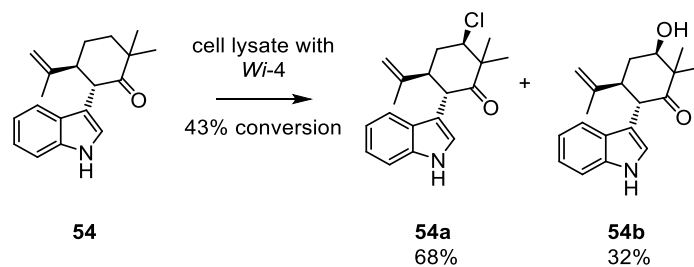
3.6.4 Hydroxylation of Screening Substrate **54**

3.6.4.1 Hydroxylation with *Wi-WelO15* Variants

Fe^{II} dependent halogenases are known to produce hydroxylated (side) products for non-native substrates.^[159] This ability is based on their close relationship with Fe^{II} dependent oxygenases. The difference is based on the active site, where the iron is coordinated to a His-Asp-His motif in the hydroxylases while in halogenases instead of an Asp, a small amino acid like Ala or Gly is incorporated whereby the binding of a chloride ion is enabled. It was shown that halogenase WelO5 G166D exclusively hydroxylates 12-*epi*-fischerindole U,^[160] while hydroxylase SadA D157G halogenates its substrate.^[181] Unfortunately, it is not as easy to interchange this residue to decide whether halogenation or hydroxylation should happen. Since mutation of Ala to Asp in halogenase SyrB2^[178] and Asp to Ala in hydroxylase TauD^[182] failed to convert enzyme activities. So far it is not exactly known but it is assumed that positioning of the substrate within the active site is very important.

In the screening process a number of variants were identified, carrying mutation I84H in combination with a bigger, unpolar amino acid in position A82 (L, V, I, T) that shifted their chemoselectivity from 98% chlorination to 32% hydroxylation. The highest formation of **54b** was observed with variant *Wi-WelO15* V6I/A82V/I84H/D284N (*Wi-4*). Also, *Hw-WelO15* shows a chemoselectivity of around 30% towards hydroxylation.

Results and Discussion



Scheme 8. Transformation of **54** with *Wi-4*. Final reaction conditions: 200 μL volume in 2.2 mL 96 dw-plates sealed with a plastic lid, 50 mM HEPES, 100 mM NaCl, 2.5 mM αKG , 2.5 mM ascorbic acid, 0.5 mM $(\text{NH}_4)_2\text{Fe}(\text{SO}_4)_2$, 0.5 mM substrate, 8 h, 30 $^\circ\text{C}$, 200 rpm (Infors HT shaker).

Under tested conditions, *Wi-4* seems to be only active in cell lysate. In an attempt to completely reverse chemoselectivity, mutation G166D was introduced into *Wi-0*, *Wi-1* and *Wi-4*. Expression levels of all *Wi*-variants producing **54b** as well as G166D variants were analyzed and transformation with **54** performed.

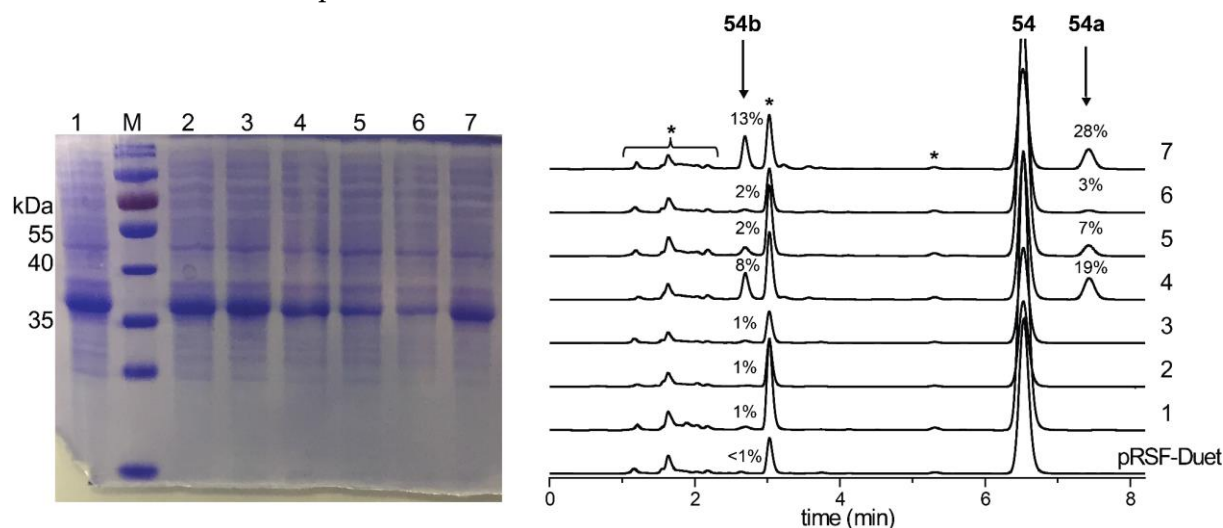


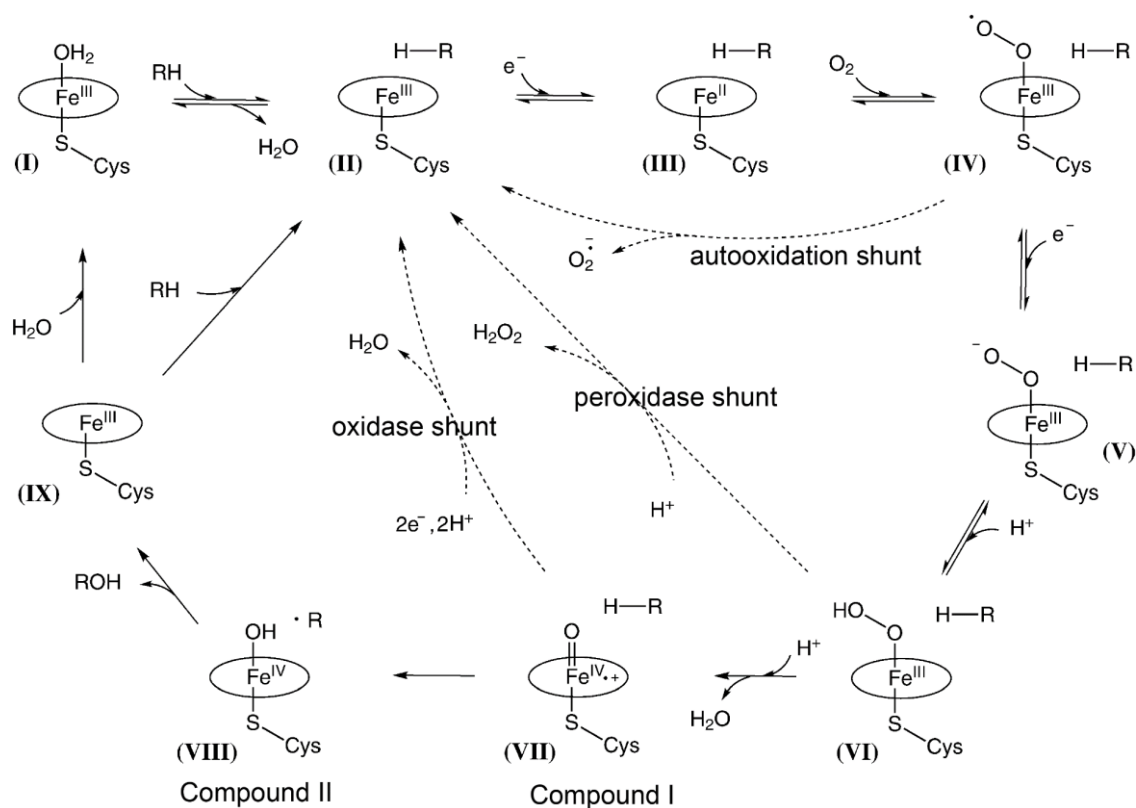
Figure 49. SDS-PAGE analysis of *Wi-WelO15* variant lysates, capable of hydroxylation. Recombinant expression was performed in 100 mL baffled flask as described in ch. 7.1.9.1. Cells were normalized to an optical density of 5.0. Reactions were performed in 2 mL reaction tubes as described in ch. 7.2.5.1. Lanes: 1= *Wi-WelO15 V6I/A82L/G166D/D284N*, M=Marker 26616 Thermo Fisher, 2= *Wi-WelO15 V6I/G166D/D284N*, 3= *Wi-WelO15 V6I/A82V/I84H/G166D/D284N*, 4= *Wi-WelO15 V6I/A82I/I84H/D284N*, 5= *Wi-WelO15 V6I/A82L/I84H/D284N*, 6= *Wi-WelO15 V6I/A82T/I84H/D284N* 7= *Wi-4*. Shown HPLC traces were measured with Agela Durashell C-18 column (150 mm \times 4.6 mm, 5 μm particle size + 10 mm precolumn), 71-29 ACN- H_2O , 1 mL/min. * Impurities from lysate.

While all G166D variants show comparable expression levels and solubility, decreased halogenase concentration was observed in lanes 5 and 6. Although chlorination was completely suppressed for G166D variants as expected, hydroxylation of **54** was equally affected and dropped below 1% (figure 49). In further studies, isonitrile **53** was tested with G166D variants and was not converted anymore, too. *WelO5* G166D was described to hydroxylate 12-*epi*-fischerindole U but no information is available if 12-*epi*-hapalindole C is transformed by the variant.

Since formation for **54b** remain low but hydroxylation is also an important handle for further functionalization, the enzyme class of cytochrome P450 was analyzed on its ability to hydroxylate **54**. P450_{BM3} is one P450 representative of *Bacillus megaterium* this enzyme is often used in research projects since it is well studied and already carries a reductase domain, so that only cofactors must be added to enable the reaction.

3.6.4.2 Hydroxylation with P450_{BM3}

Cytochrome P450 enzymes (P450s) are highly versatile monooxygenases that can be found throughout all domains of life and are believed to have been present in the last universal common ancestor.^[388] These enzymes catalyze a range of physiological functions and accept a diversity of substrates.^[388] Mechanistically, molecular oxygen is used as oxidant. While one oxygen atom is incorporated into the substrate, the other oxygen is reduced to water. A prosthetic heme group, bound to a cysteine, is the place where the oxidation process occurs. The catalytic mechanism is shown in scheme 9.



Scheme 9. Catalytic cycle of P450s modified by Krest *et al.*^[389] and Whitehouse *et al.*^[390].

The active iron center is present in its low-spin ferric form in the resting state of the enzyme (I). When the substrate is bound, the iron state changes to high-spin electron configuration and is subsequently reduced, using a nicotinamide cofactor, to its ferrous state (III). Molecular oxygen binds to the iron (IV) and undergoes reductive scission. The iron is again reduced (V) and after taking up two protons, the oxygen-oxygen bond is cleaved (VI). After releasing one

oxygen atom as water, the green ferryl-oxo intermediate (VII) compound I remains with the oxidized Fe^{IV} center.^[391] Compound II is formed, when a hydrogen is transferred from the substrate, which then transfers its hydroxyl group to the substrate radical in a rebound mechanism. The ferric iron state is regenerated (IX) when the product dissociates and the place is taken again by water, returning the enzyme to its resting state (I).^[389,390] It is also possible that the enzyme undergoes one of three shunt pathways which produces water, hydrogen peroxide or superoxide anion, using cofactor but no substrate transformation, which is also called leakage or uncoupling.^[389,390]

P450s have been classified by their electron shuttling mechanism.^[392] In the reduction step (II to III) a minority of P450s undergo a direct reduction by NADH (Class IX)^[393,394] while others catalyze isomerization reactions (Class X)^[395–397] or act as peroxygenase with a direct oxygenation of the heme without requirement of any redox partner.^[398–400] The majority however rely on one or more auxiliary redox partners.^[392] In some cases, the P450 and reductase domain are assembled on a single polypeptide chain (class VII and VIII) with CYP 102 being the best characterized family of enzymes. One member is the cytochrome P450_{BM3} (CYP102A1), originating from *Bacillus megaterium* which was isolated first by Miura and Fulco.^[401] The biocatalyst hydroxylates long-chain fatty acids at subterminal positions.^[402] It contains the required diflavin NADPH-P450 reductase and is therefore self-sufficient.^[403] P450_{BM3} has a size of 119 kDa^[404], is soluble, easily recombinant expressed in *Escherichia coli*, and highly active, with turnover rates in the thousands per minute for fatty acids.^[405,406]

As preparation for the hydroxylation of hapalindole-like ketone **54** with P450_{BM3}, the crystal structure of **54** (CCDC 1839575)^[158] and P450_{BM3} (PDB 1BU7)^[407] was used for docking with SwissDock.^[385] To enable binding of **54** in the active site, the enzyme pocket was enlarged in silico by mutating the following residues to Gly: V26, F87, A264, T268, A328, P329, E435, L439. In the next step, the poses received within the docking were opened together with an aligned wild-type structure to visualize where amino acids of the active site clash with the docked ligands. Visualization was made possible with Discovery Studio and 2D view of the binding modes. L75 as well as F87 were clashing in all poses. F87 is an important residue, for example in determining the regioselectivity of fatty acid hydroxylation.^[408] In table 14, all promising poses are analyzed and in figure 50 two examples of possible binding modes are shown.

Results and Discussion

Table 14. Results from docking of P450_{BM3} with **54** by SwissDock. The active site was enlarged before docking by mutating residues to glycine. Docking poses were analyzed with Chimera and Discovery Studio Visualizer.

close to heme	favorable interactions	clashing amino acids
indole	K69 A264 L437	L75, F87, A328
indole + C15	A74 A328 A264	L75, F87, L437
terpene ring	L437 A264	L75, F87, A328 T268
indole	A328 A264 I263, V78 L437	L75, F87, T268
C12	A264 A328 A74 L71 K69	L75, F87, L437
terpene ring		L75, F87, L437

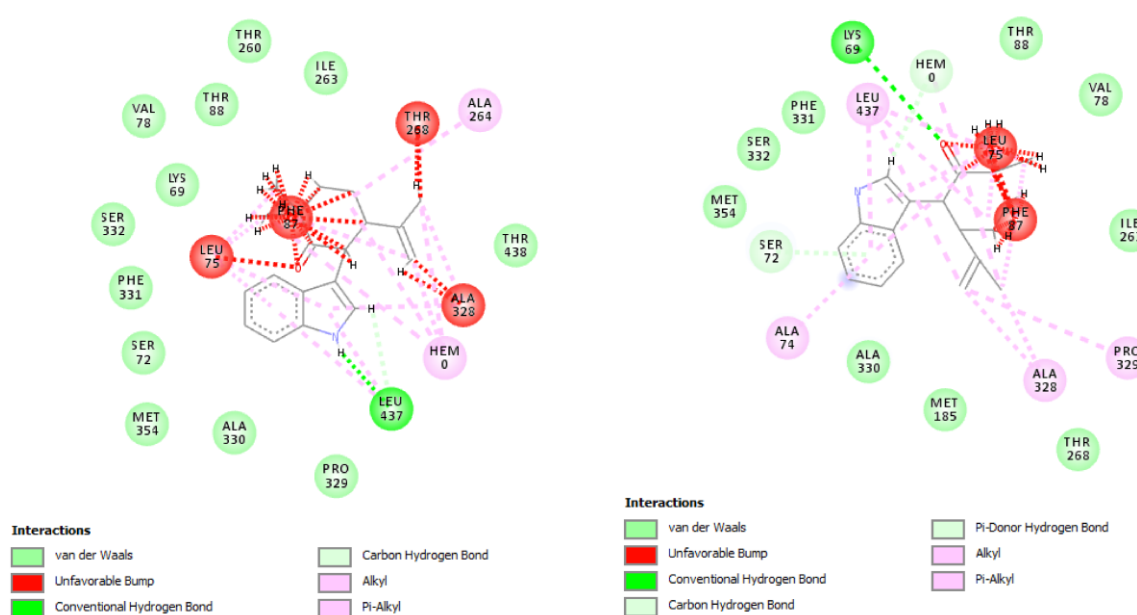


Figure 50. 2D view of docked **54** into the active site of P450_{BM3}. The active site was enlarged before docking by mutating residues to glycine. Resulting poses from docking were overlaid with the wild type to find clashing residues. Analysis was performed with 2D viewer of Discovery Studio Visualizer. Both poses show clashes with different residues. All poses are analyzed within table 14.

In table 14 and figure 50 it can be seen, that especially F87 and L75 are clashing with the substrate. Via the carbonyl group or indole N-H, hydrogen bonds can be formed with amino acids in the active site. Clashing amino acids are shown as well as amino acids that can form favorable interactions with the enzyme. Of the found binding modes, no preference can be derived, if preferential the terpene ring or the indole will be hydroxylated.

The groups of Hoebenreich, Reetz and Meggers already have performed a number of enzyme engineering studies with P450_{BM3}.^[307,409–415] Existing libraries of P450_{BM3} variants were checked if mutations were made in the identified positions, which should be mutated to enable binding of **54**. A test reaction with the wild-type enzyme and four variants, showed product formation for all five biocatalysts and proved that the reaction principally works. While in HPLC measurements of the wild-type reaction only one new peak appeared, two new signals with a shoulder each appeared in the reaction with P450_{BM3} R47Y/T49F/V78L, which suggest

Results and Discussion

the formation of four new products **54e** and **54f** (figure 97). After these positive results, in total, 10 plates of variants were selected and screened with **54**. Since the screening is the time limiting step, and 960 samples had to be analyzed, a short and isocratic method was used, in which the double peaks were not separated. In the reaction a NADP⁺, GDH recycling system was used to produce NADPH. Furthermore 5 mM EDTA, 5% glycerol was present to destabilize the cell walls (EDTA) and to stabilize the enzyme (glycerol). Biotransformations were performed in 400 μ L volume and a final concentration of 1 mM **54**. After 24 h the reaction was stopped by extraction and after transferring the organic phase to glass plates and drying the solvent, remaining dry samples were dissolved with acetonitrile and analyzed by HPLC. In table 15 an overview of found hit is given.

Table 15. Total conversion and selectivity of variants found to be active in the P450 library, screened with substrate **54**. The reaction was performed in 2.2 mL 96-dw-plates with 400 μ L final reaction volume. The cell pellet from heterologous expression was suspended in 196 μ L lysis buffer (0.1 M KPi pH 7.4 containing 1 mg/mL lysozyme). After incubation for 30 min at 37 °C, 200 rpm (Infors HT shaker), 200 μ L 2x reaction buffer (0.1 M KPi pH 7.4, 0.5 mM NADP⁺, 0.5 M glucose, 10% glycerol, 10 mM EDTA, 2 U/mL GDH) and 4 μ L **54a** (0.1 M in EtOH) was added and the plates incubated for 24 h at 30 °C, 200 rpm (Infors HT shaker).

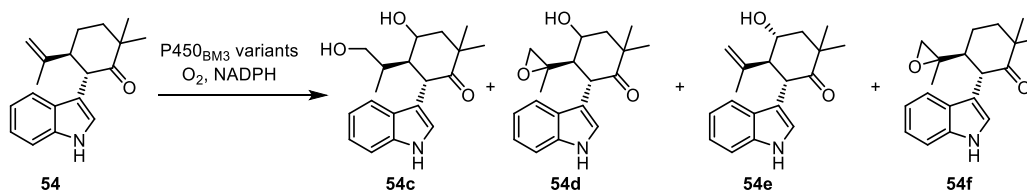
P450 _{BM3} variants	total conv. (%HPLC)	selectivity 54b	selectivity 54e	selectivity 54f
R47G/F87G	84	1	28	71
R47E/F87G	78	1	29	69
L181E/F87G	78	3	38	60
L181T/F87G	91	4	60	36
F87A/M185N/L188G	93	3	32	64

In the screening, the wild-type enzyme shows less than 1% total conversion and product **54b**, with hydroxy in position C13, was hardly formed. Instead the same the two double peaks were identified as in reactions with P450_{BM3} R47Y/T49F/V78L. Interestingly, variant L181T/F87G was the only variant producing **54e** with a selectivity >50%.

From collected information, it could be seen, that F87G or F87A was present in all variants and furthermore especially position R47 as well as L181, M185 and L188 were promising positions to be combined in a library. Therefore, five plasmids containing the P450_{BM3} gene with mutations R47G/F87G, R47V/F87G, R47H/F87G, R47E/F87G, R47V/F87G, were mixed in an equivalent stoichiometric ratio and used as template for a library including positions L181, M185 and L188. Mutagenesis should be performed via QuikChange PCR with all three positions coded on both, reverse and forward, primers. The library was planned with 675 possible variants and the following substituents L181 A, Q, E, L, K, M, P, T, V; M185 N, S, M; L188 G, A, V, L, N. Even though several PCR conditions were tested, it was not possible to achieve a good degeneration. While 1-2 bases of the triplets were mutated quite well, the third position, had mostly still its wild-type codon (ch. 8.5.6, figure 98). Therefore, the library was screened

Results and Discussion

as it was, with only the following amino acids: L181 Q, L, P; M185 I, M; L188 M, I, L, V. Two plates were screened, and some variants were found that had a good total conversion, however, no improvement in selectivity could be observed and two more new products were produced. The four products **54c-54f**, produced by P450_{BM3} variants are shown in scheme 10.



Scheme 10. Products formed by P450_{BM3} variants.

The variants with highest conversion were assayed again in triplicates (figure 51) and the sequence of active variants was analyzed. However, for two variants, the sequencing terminated early and gave incomplete results.

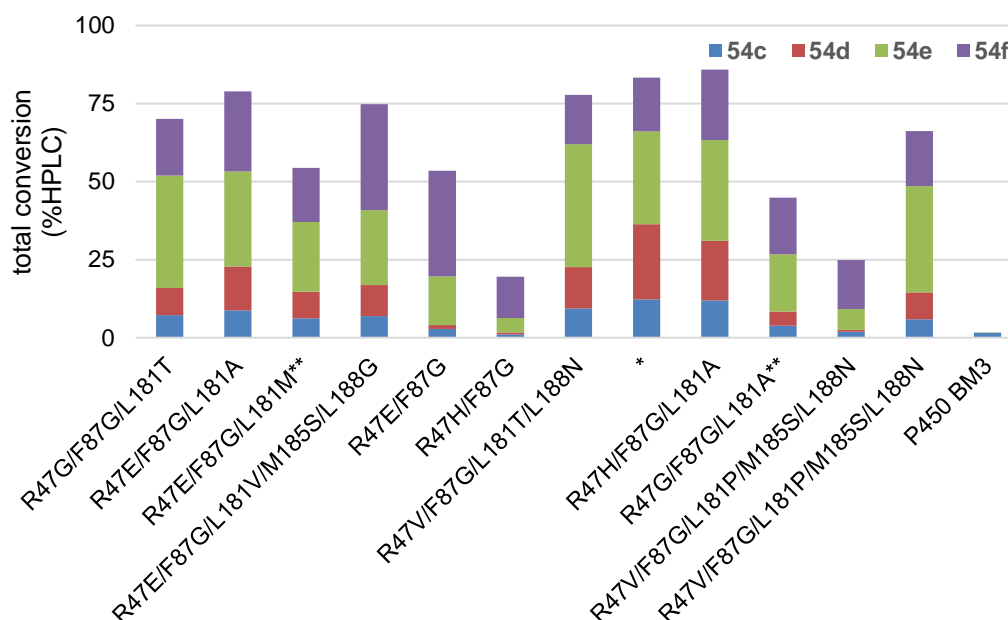


Figure 51. Total conversion of **54** and selectivities of P450_{BM3} variants. *sequencing failed, ** sequencing incomplete. The reaction was performed in 2.2 mL 96-dw-plates with 400 μ L final reaction volume. The cell pellet from heterologous expression was suspended in 196 μ L lysis buffer (0.1 M KPi pH 7.4 containing 1 mg/mL lysozyme). After incubation for 30 min at 37 $^{\circ}$ C, 200 rpm (Infors HT shaker), 200 μ L 2x reaction buffer (0.1 M KPi pH 7.4, 0.5 mM NADP⁺, 0.5 M glucose, 10% glycerol, 10 mM EDTA, 2 U/mL GDH) and 4 μ L **54a** (0.05 M in EtOH) was added and the plates incubated for 24 h at 30 $^{\circ}$ C, 200 rpm (Infors HT shaker).

Based on analysis of created and sequenced variants compared to the quick quality control, most mutations that were introduced should have not been present. The problems in creation of the library were first thought to be based on primers, because another project had similar problems, that single nucleotides are not degenerated while neighboring nucleotides are. Sequencing of the found variants, however, suggest that there might be some problems in the sequencing of the library mix and that the plasmid variety was bigger than first assumed.

Results and Discussion

Three variants: R47H/F87G/L181A, R47E/F87G/L181V/M185S/L188G and R47V/F87G/L181T/L188N were chosen based on their selectivity and total conversion. for biotransformations in preparative scale.

For reactions in mg-scale, first two hits found within the plates of the Reetz group were used, however, the product formation was not satisfying with total conversions <25%. Then the library was created to look for improved variants and three variants were chosen for further scale-up reactions. The results are summarized in table 16.

Table 16. Preparative reactions with P450 BM3 variants.

	subst. (mg) vol. (mL)	conv. (%HPLC)	sel. 54c	sel. 54d	sel. 54e	sel. 54f	yield ^[d]
R47G/F87G ^[a]	28 mg 100 mL	23%	na	na	65%	35%	
F87G/L181T ^[a]	28 mg 100 mL	18%	na	na	33%	67%	54c 0.9%
R47H/F87G/L181A ^[b]	46 mg 2x80 mL	60%	14	72	7	7	2 mg 54d 3.5%
R47V/F87G/L181T/L188N ^[b]	23 mg 82 mL	83%	16	66	14	4	8 mg 54e 3.5%
R47E/F87G/L181V/M185S/L188G ^[b]	27 mg 96 mL	65%	11	41	16	32	7.6 mg 54f 3.5%
R47E/F87G/L181V/M185S/L188G ^[c]	27 mg 96 mL	9%	na	na	46%	54%	7.5 mg
R47V/F87G/L181T/L188N ^[c]	23 mg 82 mL	14%	na	na	67%	33%	

[a] protocol 1, 21 h [b] protocol 2, 20 h [c] protocol 3, 2.5 h (ch. 7.3.2) [d] after preparative HPLC purification, for economic reasons the reaction mixtures were combined before purification. na not available

Additionally, to different variants, also the reaction conditions were adapted to a higher buffer concentration (100 mM previously to 200 mM potassium phosphate). Also, the glucose concentration was increased from 100 mM to 250 mM. EDTA was left out and the oxygenase concentration was determined by absorption measurement. During the second reaction, samples were taken after 2.5 h and 5 h to see the time resolved product formation. Since the HPLC samples had to dry before measurement, the results could only be seen the next day. Within the first 5 h mainly product **54e** and **54f** were produced but after 20 h product **54d** was present as main product. NMR analysis proved that both functionalities that were introduced individually into **54e** – hydroxylation at C14- and **54f** – epoxidation at C16 and C17- are both present in **54d**. This led to the conclusion that both products can act as substrate again and are two times oxidized if the enzyme is still active, which was presumably not the case in the screening.

Results and Discussion

Product **54c** with two hydroxy groups in position C14 and C17 was produced with all variants in quite low amounts of 11-16%. However, it is also possible that the epoxide **54d** is hydrolyzed to produce **54c**.

From the amino acids found to be clashing in the docking only F87G was finally present in active variants. Even though it already could be seen the wild type also can convert **54** with low activity. L75 which also seemed to be quite hindering was not present in screened libraries and it would further be interesting to analyze which effect it has on the reaction.

3.7 Preparative Scale Reactions with Halogenase *Wi-WelO15*

Preparative scale reactions are performed for different reasons. On the one hand, new produced products have to be characterized. Screening generally is performed in small volumes of 0.2-0.4 mL and low substrate concentrations of 0.5-1 mM. Depending on the conversion, after extraction often there is not even sufficient sample remaining for mass analysis. Therefore, reaction conditions have to be changed to gain sufficient material for full characterization with mass and NMR analysis. Next to chemical characterization, it is also interesting to analyze the bioactivity of products, therefore several mg are needed, too. On the other hand, also the properties of biocatalysts should be tested. After finding an enzyme, that performs the desired transformation in small scale, it must be tested if the catalyst is robust and if the scale can be increased since catalyst in applications will never be used in ng-scale as it is in the screening. The following chapters describe the optimization of conditions and testing of several halogenase variants within mg-scale.

3.7.1 Characterization of Chlorinated Products

None of the chlorinated hapalindole-like substrates have been described in the literature so far, therefore all products had to be fully characterized. Synthesis as well as preparative chlorination and characterization of both **53** and **53a** was made by L. Schmermund.^[317] To chlorinate **53**, purified *Hw-WelO15* was used. All further reactions were made with variants of *Wi-WelO15*.

The difficulty in the reactions with this enzyme family is based on the dependency on O₂ but at the same time the instability of Fe^{II} in presence of O₂ which often lead to a fast termination of the reaction. Furthermore, the substrates have a quite low solubility in water as well as partially in EtOH (**53** and **76** have a solubility of <100 mM in EtOH) and a tolerance of the enzymes against solvents is not present so far (ch. 3.9).

The reactions were made with cleared lysate. Cell pellets gained from heterologous expression were lysed by sonication and insoluble cell components were subsequently removed by centrifugation. The halogenase concentration cannot be determined from lysate except estimation by SDS-PAGE analysis which includes a high error.^[383] Therefore the enzyme concentration in the reactions were estimated based on a value of around 60-80 mg enzyme/L of cell culture. Based on a reproducible yield of around 60-65 mg enzyme /L of cell culture after IMAC for all purified variants.

Because the product formation was quite low in the beginning under initial reaction conditions, increased substrate loading of 1.5 mM was used to decrease the needed reaction volumes. This however did not increase the turnover but only yielded lower conversion. Within the project, the reaction conditions were improved for small scale reactions, which included an increase of NaCl from 10 to 100 mM and substitution of 0.5 mM DTT to 2.5 mM ascorbic

acid. Optimization for scale-up reactions were performed in analogy to the screening, including an increase of NaCl, ascorbic acid, α KG and $(\text{NH}_4)_2\text{Fe}(\text{SO}_4)_2$, as well as a decrease in substrate loading in comparison to first preparative reactions. All cofactors were finally used in doubled concentration compared to small scale. Since several conditions were tested, reactions shown in table 14 cannot easily be compared. A reaction volume of 50 mL was set as standard in combination with a 0.5 mL flat bottom flask, closed with a gas permeable foil, and incubation at 100 rpm and 30 °C in an Ecotron Infors shaker. If a 2x reaction buffer is prepared, the solution turns dark purple shortly after all components α KG, ascorbic acid and $(\text{NH}_4)_2\text{Fe}(\text{SO}_4)_2$ in 50 mM HEPES, 100 mM NaCl (N_2 flushed) were mixed. The enzyme, reconstituted with α KG and FeSO_4 , has a weak lilac colour (ch. 3.2, figure 14c), addition of the enzyme to the solution, does not change its colour probably based on its low concentration. Figure 52 shows the fast colour change in a preparative reaction performed with purified *Wi-1* and **67**.

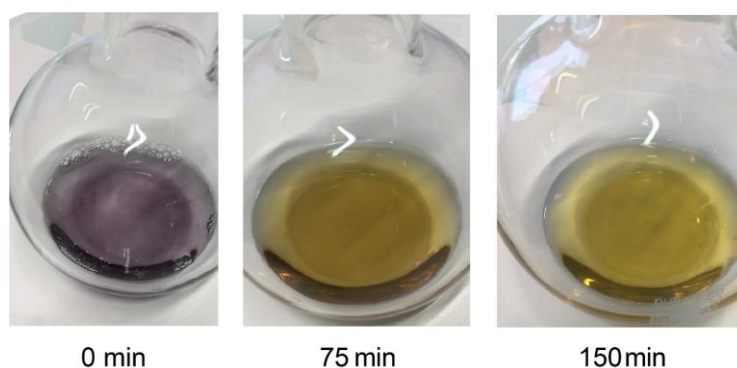


Figure 52. Preparative scale reaction with purified *Wi-1* and **67**. The change of color from dark purple to dark yellowish can be observed within 2.5 h. After that, no further change of color happens.

No further color change could be observed after 2.5 h. Time dependent measurement of a reaction performed with *Wi-5* lysate and **78** shows that the reaction runs up to 5 h, this however can individually be dependent on the variant and substrate. With the optimized and standardized reaction conditions, reproducible results as well as conversions matching the small-scale reactions could be achieved, even though the final conditions have an increased catalyst to substrate loading compared to small scale reactions.

Table 17 gives an overview of all performed scale-up reactions to chlorinate hapalindole-like ketones with different reaction conditions. The reactions were not yet repeated with optimized reaction conditions.

Results and Discussion

Table 17. Reactions with halogenase variants to chlorinate hapalindole-like ketones. Reaction conditions for scale-up reactions were optimized during the synthesis of chlorinated product. Individual reaction conditions and analysis of products are given in chapter 7.3.1. Conditions that worked best and are recommended to use are: 20-30 μ M enzyme*, 50 mM HEPES, 100 mM NaCl, pH 7.4, 10 mM α KG, 5 mM ascorbic acid, 1 mM $(\text{NH}_4)_2\text{Fe}(\text{SO}_4)_2$ and a substrate concentration of 0.75-1.5 mM, depending on solubility of substrate. *estimation of a chlorinase concentration of 60-80 mg/L expression culture, based on the fact that all variants reliably yield 60-65 mg/L after IMAC.

product	variant	scale (mL)	catalyst (mg)	substrate loading ^[a] (mg/L)	conv. (%HPLC)	yield ^[d]	
53a	<i>Hw</i> -WelO15	34	24 ^[b]	440	80% ^[e]	48%	8.0 mg
54a	<i>Wi</i> -5	142	48-64 ^[c]	423	20% ^[f]	13%	8.5 mg
54a	<i>Wi</i> -4	80	45-60 ^[c]	211	7% (71% 54a) ^[h]	42% (71% 54a)	20 mg 54a
&	<i>Wi</i> -4	3x50	135-180 ^[c]	141	35% (66% 54a) ^[h]		
54b	<i>Wi</i> -4	4x50	180-240 ^[c]	141	65% (77% 54a) ^[h]		
76a	<i>Wi</i> -5	120	28 ^[b]	375	2% ^[e]	1.2%	0.7 mg
	<i>Wi</i> -5	120	96-128 ^[c]	275	42% ^[h]	25%	8.1 mg
77a	<i>Wi</i> -5	129	48-64 ^[c]	470	13% ^[f]	7%	4.5 mg
78a	<i>Wi</i> -5	158	60-80 ^[c]	440	14% ^[g]	10%	7.0 mg
67a	<i>Wi</i> -1	50	35 ^[b]	220	86% ^[h]	<1%	

[a] 0.5 - 1.5 mM, [b] purified enzyme, [c] cleared lysate, [d] after preparative HPLC purification, [e] 50 mM HEPES, 10 mM NaCl, 5 mM α KG, 0.5 mM DTT, 0.5 mM $(\text{NH}_4)_2\text{Fe}(\text{SO}_4)_2$, experiment performed by L. Schmermund^[317] [f] 50 mM HEPES, 10 mM NaCl, 2.5 mM α KG, 0.5 mM DTT, 0.5 mM $(\text{NH}_4)_2\text{Fe}(\text{SO}_4)_2$, experiment performed by L. Schmermund^[317] [g] 50 mM HEPES, 50 mM NaCl, 2.5 mM ascorbic acid, [h] 50 mM HEPES, 100 mM NaCl, 10 mM α KG, 5 mM ascorbic acid, 1 mM $(\text{NH}_4)_2\text{Fe}(\text{SO}_4)_2$

From table 17 it can be seen, that conversions as well as yields were quite low when initial reaction conditions were used, both however could be increased for hapalindole-like ketones by using optimized reaction conditions. The yields, giving amounts of isolated product, however are still quite low in comparison to the conversion which is calculated from HPLC measurements without purification. Purification of products includes extraction with ethyl acetate. With lysate components as well as reaction cofactors, no phase separation is achieved after extraction. Separation of aqueous phase, organic phase and precipitated components was only achieved by centrifugation at 9000 rpm (40 min, Eppendorf 5810 R, rotor F-34-6-38). After transferring the organic phase to a new flask, ethyl acetate is removed under reduced pressure and the remaining sample dissolved in acetonitrile and filtered before applying it to preparative HPLC. All this results in a loss of 30-47% product (table 17), comparing conversion and yield. **67a** could not be isolated at all after the reaction. Even though extraction with ethyl acetate in small scale was possible, after purification with preparative HPLC, less than 1 mg compound was left over. Signals in analytical and preparative HPLC were quite low, indicating that the concentration of educt and product were low in the solution. For a repeated reaction, either a different solvent for extraction should be used or a solid phase extraction from the aqueous phase could also be tried instead.

3.7.2 Characterization of Unselective Reactions

After the reaction conditions were optimized, to 50 mL volume in a 0.5 L flat bottom flask with 50 mM HEPES, 100 mM NaCl, 10 mM α KG, 5 mM ascorbic acid and 1 mM $(\text{NH}_4)_2\text{Fe}(\text{SO}_4)_2$, also products of other transformations should be analyzed. Within the scope of the reactions, also the differences between lysate and purified enzyme as well as different substrate loadings were tested. In table 18, an overview of the reactions is given.

Table 18. Overview of mg-scale reactions. Reactions were performed in a total volume of 50 mL in a 0.5 L flat bottom flask with 50 mM HEPES, 100 mM NaCl, 10 mM α KG, 5 mM ascorbic acid, 1 mM $(\text{NH}_4)_2\text{Fe}(\text{SO}_4)_2$. Enzyme concentration was about 30 μM with an estimation of a chlorinase concentration of 60-80 mg/L expression culture, based on the fact that all variants reliably yield 60-65 mg/L after IMAC.

variant	substrate	scale (mL)	substrate loading (mM)	amount of catalyst	conv. (%HPLC)	yield ^[c]
<i>Wi-5</i>	82	50	0.75	51 ^[a]	58% (sel. 50% 82a)	10% 82a (5 mg)
<i>Wi-5</i>		2x50	0.75	90-120 ^[b]	43% (sel. 53% 82a)	
<i>Wi-5</i>		2x50	0.75	90-120 ^[b]	66% (sel. 64% 82a)	
<i>Wi-12</i>		50	0.75	45-60 ^[b]	55% (sel. 46% 82a)	
<i>Wi-5</i>	81	1x50	0.75	45-60 ^[b]	11%	<1 mg for individual products
<i>Wi-12</i>		3x50	0.75	135-180 ^[b]	28%	
<i>Wi-12</i>		2x50	0.50	90-120 ^[b]	37%	
<i>Wi-12</i>	83	2x50	0.50	90-120 ^[b]	19%	<1 mg for individual products

[a] purified enzyme, [b] cleared lysate, [c] reactions were combined before preparative HPLC purification

The reactions show that under optimized conditions, *Wi-5* has a comparable activity in cell lysate or as purified enzyme and *Wi-5* as well as *Wi-12* reach a higher conversion in the mg-scale reactions in comparison to the small-scale reactions with purified enzymes. This activity is important because it shows that the enzymes can tolerate higher reaction volumes, which is necessary if it should have an application. Also, the 4th generation variants were tested in these reactions and show that they can be used in mg-scale reactions. Another important aspect is substrate loading. Within small scale optimization, it could be seen, that *Wi-1* has a higher turnover with higher substrate loading (figure 36, ch. 3.5.3). *Wi-4* in mg-scale seems to not tolerate the increase from 0.5 to 0.75 mM (table 17) whereas *Wi-12* seem to work similar under both conditions with substrate **81** (table 18). Even though the conversion is lower, the estimated TON is 6 with 0.5 mM and 7 with 0.75 mM substrate. To analyze products from transformations with **81** and **83**, the activity and selectivity have to be increased combined with an

improved purification process. HPLC chromatograms showing reactions **81** and **83** after extraction are given in figure 95 and figure 96 in ch. 8.5.4.

3.8 Kinetic Analysis

Within the engineering process of halogenase *Wi-WelO15*, it was possible to increase the product formation of *Wi-0* (<1%) up to 87% with *Wi-12*. To get an idea about the kinetic properties, the variants were analyzed with **54**. *Wi-0* was also tested with **53**, however it must be noted that *Wi-0* is not the wild-type enzyme but variant *Wi-WelO15 V6I/D284N* and **53** is a non-natural hapalindole C derivative. No information was available how fast the wild type chlorinates its natural substrates. Still, *Wi-0* and **53** give a clue what characteristic lead to a high product formation of 93%. In table 19, enzyme substrate pairs and their kinetic parameters are listed.

Table 19. Overview of kinetic parameters of different *Wi-WelO15* variants with different substrates. Final reaction conditions: 200 μ L volume in 2.0 mL reaction tube, 50 mM HEPES, 10 mM NaCl, 5 mM α KG, 0.5 mM ascorbic acid, 0.5 mM $(\text{NH}_4)_2\text{Fe}(\text{SO}_4)_2$. Different substrate concentrations and reaction times were used as described in chapter 7.2.6.

variant	substrate	prod. form. ^[a]	K_m (μM)	K_i (μM)	k_{cat} (min^{-1})	k_{cat}/K_m ($\text{min}^{-1} \text{mM}^{-1}$)
<i>Wi-0</i>	53	93	22	-	1.60	71.5
<i>Wi-1</i>	54	27	158	-	0.12	0.7
<i>Wi-2</i>	54	9	99	2190	0.02	0.2
<i>Wi-5</i>	54	68	82	1106	0.43	5.3
<i>Wi-7</i>	54	23	64	-	0.06	0.9
<i>Wi-8</i>	54	74	158	-	0.42	2.6
<i>Wi-11</i>	54	86	68	-	0.64	9.4
<i>Wi-12</i>	54	87	20	-	0.37	18.5
<i>Wi-5</i>	76	14	43	-	0.24	5.6
<i>Wi-5</i>	77	40	127	-	0.18	1.4
<i>Wi-5</i>	78	13	85	-	0.11	1.3

[a] product formation calculated from relative conversion (%HPLC) based on areas of educt, hydroxylated and chlorinated products.

The effect of active site mutations on binding and turnover were analyzed by measurement of kinetics (table 19). Through directed evolution of the halogenase, catalytic rate and efficiency could be increased for chlorination of **54** and 4th generation variants have a 93-fold higher efficiency than *Wi-2*. From the best two variants, *Wi-11* is the fastest one, but a 3.4-fold higher K_m compared to *Wi-12* reduces the catalytic efficiency. *Wi-12* has a 2-fold lower k_{cat} than *Wi-11*, but the low K_m of 20 μM makes it the most efficient variant for transformation of **54**. In general, the k_{cat} is quite low with values $<1 \text{ min}^{-1}$, while an analysis of several thousand enzyme revealed an average enzyme to catalyze around 600 turnover per minute.^[416] The kinetic data

reveals that the *Wi-WelO15* variants are as efficient as the oxygenase TauD^[161,342] and the engineered flavin dependent halogenases PrnA^[417] and RebH^[418] with non-natural substrates. The engineered fluorinase *fah2114* shows a 20-fold higher $k_{\text{cat}}/K_{\text{M}}$ for conversion of 5'-CIDA into SAM while the $k_{\text{cat}}/K_{\text{M}}$ for the conversion of SAM into 5'-FDA still is 2.5.^[148]

Important to notice is that just as shown for flavin dependent halogenases and fluorinases also Fe^{II} dependent halogenases can be improved in their kinetic parameters. Which could be the key fact for using these enzymes as biocatalyst. If the reaction system of Fe^{II} and enzyme together with further reactants is not stable for a long time, the reaction velocity has to be increased in combination with a stabilization of the enzyme under used reaction conditions. In late stage functionalization, to create valuable and complex molecules, catalytic efficiency and turnover numbers are less important than in the synthesis of building blocks, where a high catalytic efficiency is needed.^[419]

It might also be interesting to analyze these kinetic parameters about binding and turnover frequency if a template for further mutation rounds is selected. If the activity for **54** should further be increased, *Wi-12* can be used, because it binds the substrate best. While a loose binding but higher velocity (*Wi-11*) might be beneficial if the enzyme should be adapted for other substrates. To analyze the catalytic properties, the total turnover number or total turnover/time is even more important. Since kinetics only describe the initial velocity, but if a fast catalyst is inactive after minutes, for reactions a slower catalyst that has a higher longtime stability might be more preferably. Therefore, the product formation which is measured in the screening to compare the variants is also a good indicator for the activity of the variants. In this study, variants that show highest product formation within 8 h also had the best $k_{\text{cat}}/K_{\text{M}}$.

To increase the efficiency and applicability of the reaction, the enzyme should further be evolved to higher turnovers but also adapted to higher substrate loadings which now limit to a total turnover to 50. Because enzymatic reactions are often performed in water and the substrate solubility therein often is a limiting step, the enzyme can be adapted to two phase systems with an organic solvent as substrate reservoir. Analysis of temperature and solvent stability is described in the next chapter.

3.9 Temperature and Solvent Stability of WelO15

The stability of biocatalysts is an important factor for their usage in synthetic applications. A high activity combined with long shelf-life and good stability against solvents could help to spread biocatalysis further into industrial applications.^[248]

The term protein stability is nowadays often used with different meanings, most frequently the reversible unfolding is meant, which is a measure of thermodynamic stability and can be represented by the melting temperature. Furthermore, kinetic stability can be determined which describes how long the protein remains active before it irreversible denatures.^[420] This is represented by the half-life of denaturation or the optimum operating temperature, the temperature at which the activity of the enzyme is reduced by half following incubation for a specific amount of time.^[420] In table 20 a summary is given, described by Polizzi *et al.*^[420], about various stability parameters.

Table 20. Definitions of various stability parameters by Polizzi *et al.*^[420]

measure	symbol	type of stability	definition
free energy of unfolding	ΔG_u	thermodynamic	change in Gibbs free energy going from the folded to unfolded state
melting temperature	T_m	thermodynamic	the temperature at which half of the protein is in the unfolded state
unfolding equilibrium constant	K_u	thermodynamic	the concentration of unfolded species divided by the concentration of folded species
half concentration	$C_{1/2}$	thermodynamic	the concentration of denaturant needed to unfold half of the protein
observed deactivation rate constant	k_d	kinetic	time required for residual activity to be reduced to half
half-life	$T_{1/2}$	kinetic	temperature of incubation to reduce residual activity by half during a defined time period
temperature of half-in-activation	T_{50}	kinetic	temperature of incubation to reduce residual activity by half during a defined time period
optimum temperature	T_{opt}	kinetic	temperature leading to the highest activity
total turnover number	TTN	kinetic	modes of product produced over the lifetime of the catalyst

Next to the thermal stability, which deals with the stability at elevated temperatures also the chemical stability is an important characteristic, which describes the stability in presence of organic solvents, salts or extreme pH ranges.^[420]

Two decades ago few mutagenesis strategies were available to target stability. To increase the stability of enzymes, chemical modifications, lyophilization and additives as well as immobilization was used, but the improvements were moderate and often insufficient for most chemical transformations.^[248] Nowadays, protein engineering is applied to increase the stability against temperature or reaction conditions, several successful engineering studies could be made^[421] by phylogenetic analysis^[422,423] or rational, structure based or computer design^[424–427]. In the next chapters, the temperature and solvent stability of halogenase *Wi-WelO15* is examined and the use of the PROSS Sever within this enzyme class.

3.9.1 Temperature Stability

One of the online available web applications, to predict solubility or stability increasing mutations, is PROSS^[428] (Protein Repair One-Stop Shop). In this application, problems like aggregation, short half-life and low melting temperatures are alleviated to increase the enzyme solubility.^[428] PROSS works with the fact that heterologous expression of proteins and their mutants often results in misfolding and aggregation. Large changes in stability will require large free energy changes in the folding–unfolding equilibrium. A molecular-level understanding of proteins enables the estimation of the strength of various interactions (ion pairs on the surface or entropic contributions of adding a proline residue), so that the needed changes to reach the goal can better be planned. Rarely, free energy-based measures are used to plan protein-engineering strategies today but converting case studies into engineering principles requires a quantitative approach. The design of variants with more favorable native-state energy results in higher yields of soluble and function protein obtained by heterologous overexpression.^[248,428]

PROSS aligns sequences of occurring homologues and scans the allowed sequence space. Frequently observed amino acids often increases stability (consensus effect) but instead of selecting these amino acids, the application foremost eliminates mutations that are rare or never seen. By applying Rosetta computational mutation scanning^[429], allowed mutations are modelled against the background of the wild-type structure and the energy difference between wild type and single-point mutant is calculated.^[428]

For the class of NHI dependent halogenases, only 5 halogenases are known and in total 12 sequences with an identity >77% (compared to *Wi-WelO15*, 20.07.2018) are available in the NCBI data base. This is a low number of homologous and a quite high identity which could negatively influence the outcome, because tools that work with the consensus effect mostly work best if many sequences are available.

If the closed structure of *WelO5* with soaked substrate (PDB 5IQT, chain B) is uploaded to the server, seven different designs are given as outcome. Within the designs the number of mutations increases, with 20 mutations as maximum. Figure 53 shows the structure of *WelO5* and all amino acids that are chosen by the PROSS server are highlighted in blue. No chosen

amino acid is located within the active site, but all are on the surface of the enzyme, most on loops.

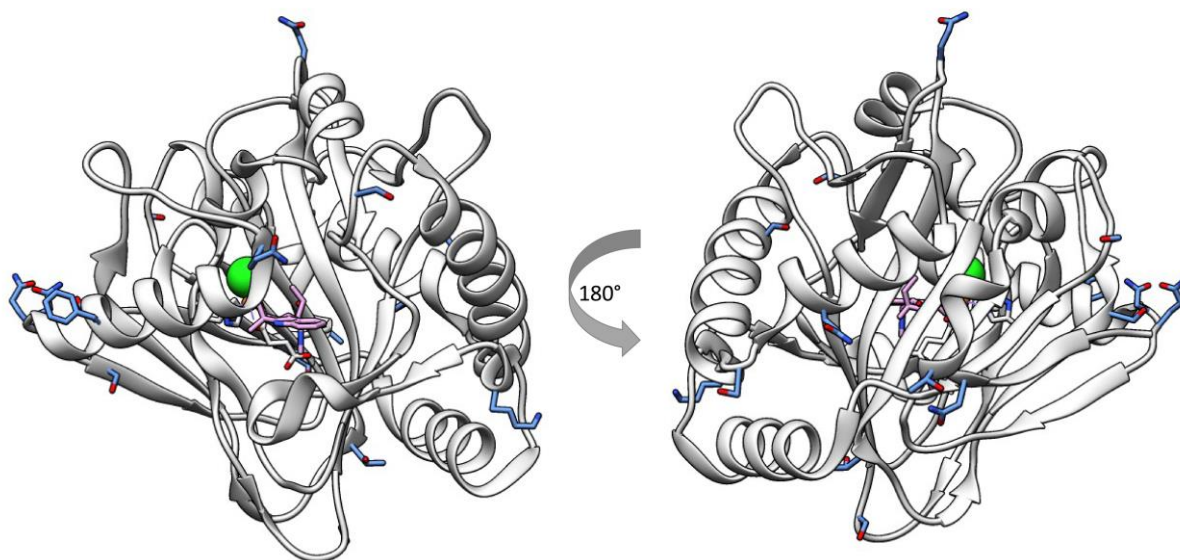


Figure 53. WelO5 (5IQT chain B) with highlighted amino acids that were chosen by the PROSS server to be mutated.^[428] 1) S103A; 2) S103A/Q123R/F230K; 3) S103A/Q123R/F230K/Q236N/S239W/S268R/Q282D; 4) S37K/S103A/Q123R/F230K/Q236N/S239W/S268R/Q282D; 5) S37K/S93D/S103A/S117N/Q123R/A175M/S207D/F230K/N235Q/Q236N/S239W/S268R/Q282D; 6) N18H/S37K/S93D/S103A/S117N/Q123R/A175M/T195S/S207D/Q220D/F230K/N235Q/Q236N/S239W/S268R/Q282D 7) N18H/T20S/S37K /K68S/S93D/S103A/T112E/S117N/Q123R/L171N/A175M/T195S/S207D/Q220D/F230K/N235Q/Q236N/S239W/S268R/Q282D

The easiest way to test the mentioned mutants would be ordering them by gene synthesis. Out of cost reasons, this was not possible therefore the first three mutants were created by mutagenic PCR on template *Wi-0*. The following variants result: *Wi-P1*: *Wi-WelO15* V6I/S103A/D284N, *Wi-P2*: *Wi-WelO15* V6I/S103A/Q123R/S230K/D284N, *Wi-P3*: *Wi-WelO15* V6I/S103A/Q123R/S230K/Q236N/S239W/S268R/Q282D/D284N. All variants could successfully be heterologous expressed and purified, followed by determining the melting temperature (T_m) by circular dichroism measurement. Also selected variants found during the engineering process were analyzed (table 21). First, the folding of the halogenase was measured and secondary structural elements determined but no meaningful information could be collected. High differences within the values lead to the assumption that this method is not applicable to determine the folding (table 38). This might be based on a high flexibility within the structure which can be seen from many different crystallization states within the $Fe^{II}/\alpha KG$ dependent enzymes. In some cases there were evidences showing that the overall structure of enzymes becomes more ordered when Fe^{II} and αKG is added,^[188,189] for WelO15 halogenases, no difference between apo and holo enzyme could be observed in the melting temperature. However, it was never determined, if the apo enzyme has cofactors incorporated, therefore it is just assumed to be the apo form after dialysis against EDTA. ICP-MS studies would be a possibility to measure remaining Fe content in the enzyme solution. To test if the stability increasing mutations

Results and Discussion

can be combined with activity increasing mutations, another variant was created combining PROSS variant 3 with A82L/V90P (*Wi-5P3*).

T_m of the variants were determined as well different conditions were tested to see the environmental influence on the enzyme. A triplicate measurement of the same variant resulted in an error of 0.3 °C. The T_m are given in table 21 and belonging curves can be found in ch. 8.3.5.2, figure 70 - figure 75.

Table 21. T_m of halogenase variants. The melting was observed with CD measurement. 25 μ M enzyme solution in 5 mM HEPES, 1 mM NaCl, were analyzed in the range of 20-80 °C with: $\lambda=220$ nm, data pitch 1 °C, a temperature slope of 2 °C/min, a response of 2 s and a bandwidth of 10 nm. The inflection point gives the melting temperature T_m .

enzyme	apo (°C)	+1eq α KG (°C)	+1eq α KG +1eq $(\text{NH}_4)_2\text{Fe}(\text{SO}_4)_2$ (°C)
<i>Hw-WelO15</i>	62.0	62.2	61.4
<i>Wi-0</i>	54.4	54.9	53.7
<i>Wi-2</i>	51.1	nd	51.7
<i>Wi-5</i>	55.3	54.1	55.6
<i>Wi-12</i>	55.0	nd	55.8
<i>Wi-8</i>	53.3	52.8	52.4
<i>Wi-11</i>	55.1	nd	54.4
<i>Wi-9</i>	55.8	nd	55.9
<i>Wi-10</i>	56.4	nd	56.9
<i>Wi-2</i> ^[a]		56.1 (high noise)	
<i>Wi-9</i> ^[b]		56.7	
<i>Wi-9</i> ^[c]		53.8	
<i>Wi-9</i> ^[d]		no melting observed	
<i>Wi-P1</i>	56.1	nd	55.6
<i>Wi-P2</i>	56.0	nd	56.2
<i>Wi-P3</i>	59.8	nd	59.7
<i>Wi-5P3</i>	61.3	nd	61.0

nd = not determined; [a] 5mM α KG + 0.5 mM $(\text{NH}_4)_2\text{Fe}(\text{SO}_4)_2$; [b] 1 eq α KG + 1eq NiCl_2 [c] 5 mM α KG+ 1eq NiCl_2 [d] 5 mM α KG+ 0.5 mM NiCl_2

The melting temperature of *Hw-WelO15* is about 8 °C higher than *Wi-0* with around 54 °C but also this T_m is already quite stable. Variant *Wi-9* was interesting to analyze because it is a scaffold sampling variant with L221/I225 transferred from *Hw-WelO15* to *Wi-0*, substituting M221/M225. Since the difference in melting temperatures between *Wi-0* and *Hw-WelO15* is already quite high, it would be interesting to know which substitutions cause the thermal stabilization. By transferring the two above mentioned residues, the melting temperature could be increased by 1.4 °C. Interestingly, most of the variants, which were created to have an increased activity to chlorinate **54** also have an increased melting temperature.

Results and Discussion

The PROSS variants show an increased stability against thermal unfolding. The mutation of S103 to Ala into *Wi-0* increases the T_m by ~ 2 °C, while additional incorporation of Q123R/F230K did not change the stability (*Wi-P2*). However further mutation of four amino acids to gain (*Wi-P3*), results in a melting temperature of 59.8 °C, which is an increase of about 5.5 °C in comparison to *Wi-0*. The turnover of purified PROSS variants 1-3 are comparable with *Wi-0* for isonitrile **53**, showing that no activity loss is caused by the mutations. The combination of stabilizing mutations of *Wi-P3* with mutations A82L/V90P (*Wi-5*) created the variant *Wi-5P3* which is able to chlorinate ketone **54**. The chimera enzyme that combines stability improvement and conversion of non-natural substrates shows an even increased stabilized structure with a melting temp of 61.3 °C and slightly increased activity to produce **54a** (70% *Wi-5* to 76% *Wi-5P3*, table 12).

Even though, the melting temperature is a measure for stability and a good way to compare enzymes, the temperature is increased quite rapidly (2 °C/min). To analyze the stability at constant temperatures for different times, *Wi-0* as well as *Wi-P1*, *Wi-P2*, *Wi-P3* and *Wi-5P3* were diluted to 50 μ M and incubated at different temperatures (30, 35, 40, 45 °C) for several hours (1 h, 2 h, 3 h and 4 h). Then the samples were centrifuged to remove precipitated enzyme and the remaining soluble enzyme was compared by SDS-PAGE analysis. After 1 h at 45 °C, an oligomerization of the wild type enzyme can be seen by the appearance of protein bands in the gel in the range above 70 kDa. After 3 h, few soluble proteins are left at 45 °C and the oligomerization is visible in the 40 °C sample. After 4 h, also the 40 °C sample contains almost no soluble protein anymore. PROSS variants 1 and 2 show already an increased stability since the oligomerization bands are less visible and no loss of soluble enzyme up to 40 °C and 4 h is detected. Figure 54 shows two gels of *Wi-0* and *Wi-P3*, all other gels can be seen in chapter 8.3.5.3.

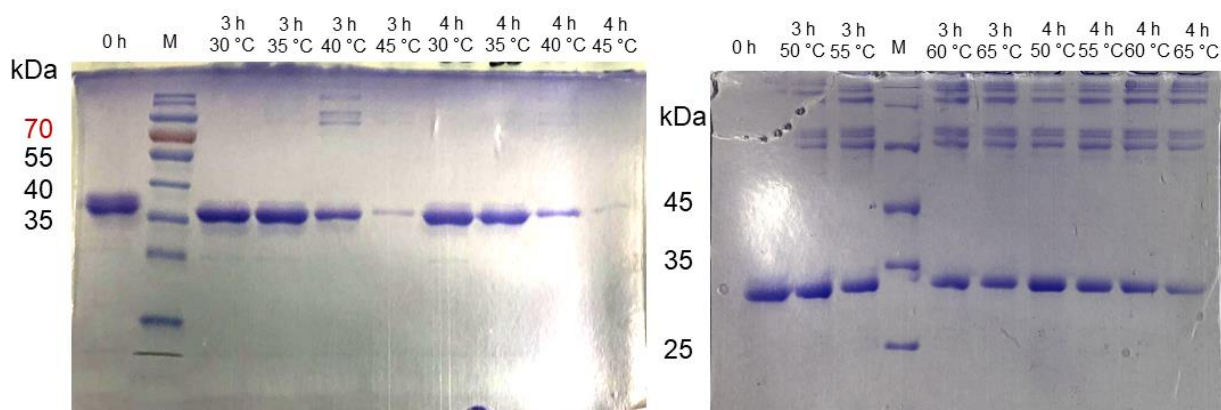


Figure 54. SDS-PAGE analysis of soluble fraction of *Wi-0* (left) and *Wi-P3* (right) after incubation at different temperatures.

For *Wi-P3* and *Wi-5P3* no oligomerization or decrease in soluble enzyme concentration is observed up to 45 °C within the analyzed time. Therefore *Wi-P3* samples were further incubated

in the range of 50-65 °C. Even though an oligomerization starts already after 1 h, after 4 h at 60-65 °C, some monomeric and oligomeric enzyme is still soluble (figure 54).

To see the effect of elevated reaction temperatures on the product formation, biotransformations were performed with the best variants *Wi-5*, *Wi-8*, *Wi-11*, *Wi-12* as well as the stabilized *Wi-5P3*. The reactions were incubated at different temperatures between 30 °C and 45 °C for 5 h. In figure 55, the enzymes are compared. The residual activity in comparison to the same variant at 30 °C (standard temperature) is given.

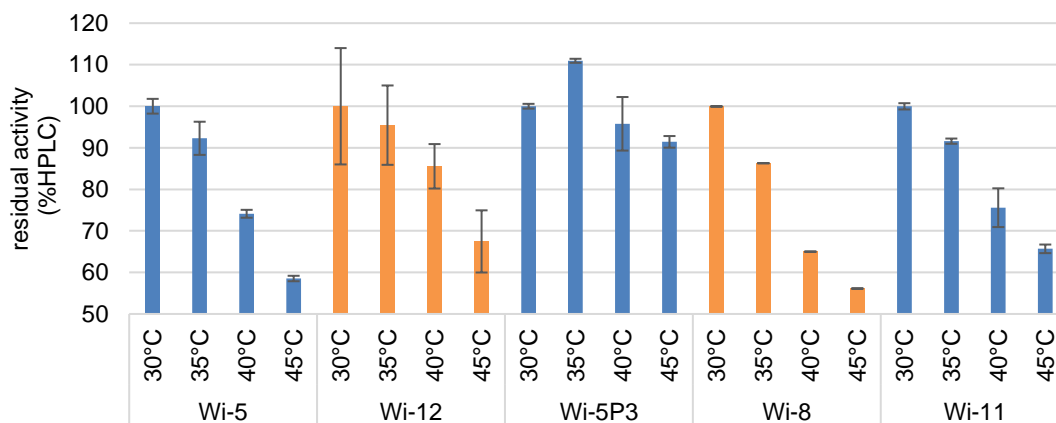


Figure 55. Temperature dependent formation of **54a**, normalized to the 30°C value and given as residual activity. Reaction conditions used: 10 μ M enzyme, 100 mM NaCl, 50 mM HEPES, 5 mM α KG, 2.5 mM ascorbic acid, 0.5 mM $(\text{NH}_4)_2\text{Fe}(\text{SO}_4)_2$, 0.5 mM **54**, 5 h reaction.

It can be seen that the activity of all tested variants decreases with increased temperature except *Wi-5P3* that shows a higher formation of **54a** at 35 °C. However, the residual activity at temperatures up to 45 °C is >50% which shows, that the overall stability and activity at increased temperatures is quite good. *Wi-5P3* even has a residual activity of 90% at a reaction temperature of 45 °C which is a great value compared to *Wi-5* with less than 60% residual activity at 45 °C. Interestingly variants *Wi-12* which is based on template *Wi-5*, and *Wi-11* which is based on template *Wi-8*, each have a higher residual activity in comparison to their template variants. Often it is believed that by introducing mutations into enzymes, the stability decreases, here the opposite seems to be the case. It is likely that under given screening conditions a generally improved variant also has a higher stability and is active for a longer time. The results from the PROSS server are promising and further analysis of other proposed mutations, not tested so far, should be followed.

It is questionable, if increased temperatures for this reaction are applicable because of the decreased solubility of O_2 in water. The O_2 concentration in water at 30 °C, 1 bar and 1.7 salinity (salt content of the used buffer is 17 g/L) is 234 μ M which shows, that for complete substrate conversion (500 μ M), oxygen has to diffuse into the buffer from the air. With increased tem-

peratures up to 45 °C, the solubility further decreases to 186 μM and with increased salt content, the solubility also decreases as well.^[430,431] However, heat purification of the enzyme would be of special because it simplifies purification. It could be seen, that incubation of purified *Wi*-P3 at 65 °C for 4 h leads partially to oligomerization but still monomeric, soluble enzyme is left. Heat purification of other enzymes was already achieved after incubation for 90 min at 70 °C,^[432] which is only 5 °C difference from tested conditions. Therefore, further analysis should be performed if an incubation at 70 °C is already applicable. Furthermore, it should be tested if the oligomerized enzyme still has activity.

In some cases, enzymes that have a higher temperature stability also have an increased solvent stability. Because of the low substrate solubility, it would be beneficial to add solvents to the reaction, therefore the same variants that were tested on their temperature stability also were checked on their solvent stability.

3.9.2 Solvent Stability

Next to thermal stability also chemical stability is a very important factor since low solubility of substrates often is a limiting factor in the reactions. By increasing the solvent concentration also an increased substrate loading would be made possible. In a first test with not optimized reaction conditions, the influence of 5% and 10% EtOH, acetone and acetonitrile was tested on variants *Wi*-5 and *Wi*-8 as shown in figure 56.

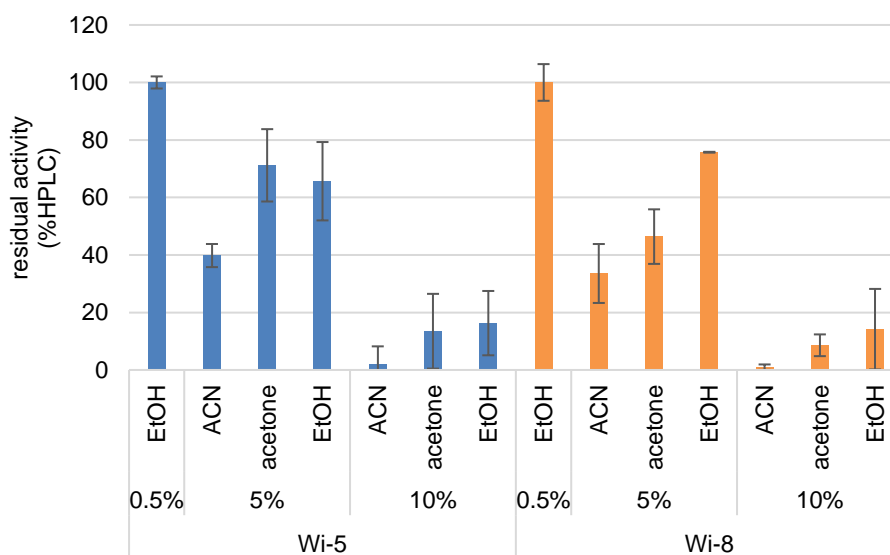


Figure 56. Formation of **54a** in presence of different solvents and concentrations, normalized to 0.5% EtOH and given as residual activity. Reaction conditions used: 10 μM enzyme, 10 mM NaCl, 50 mM HEPES, 5 mM αKG , 0.5 mM ascorbic acid, 0.5 mM $(\text{NH}_4)_2\text{Fe}(\text{SO}_4)_2$, 5 h reaction. Substrate added from 100 mM stock to solvent.

All tested solvents in concentrations of 5% or 10% decrease the formation of **54a** in comparison to 0.5% EtOH. It can be seen that the presence of acetonitrile results for all variants in the

lowest product formation while *Wi-5* seem to tolerate acetone and EtOH equally in both concentrations, *Wi-8* has the best formation of **54a** in presence of EtOH. After the reaction conditions were optimized and the last library screening was completed, again *Wi-5*, *Wi-8*, *Wi-11*, *Wi-12* as well as the stabilized *Wi-5P3* were tested with different EtOH and acetone concentrations in comparison to 1% EtOH (standard).

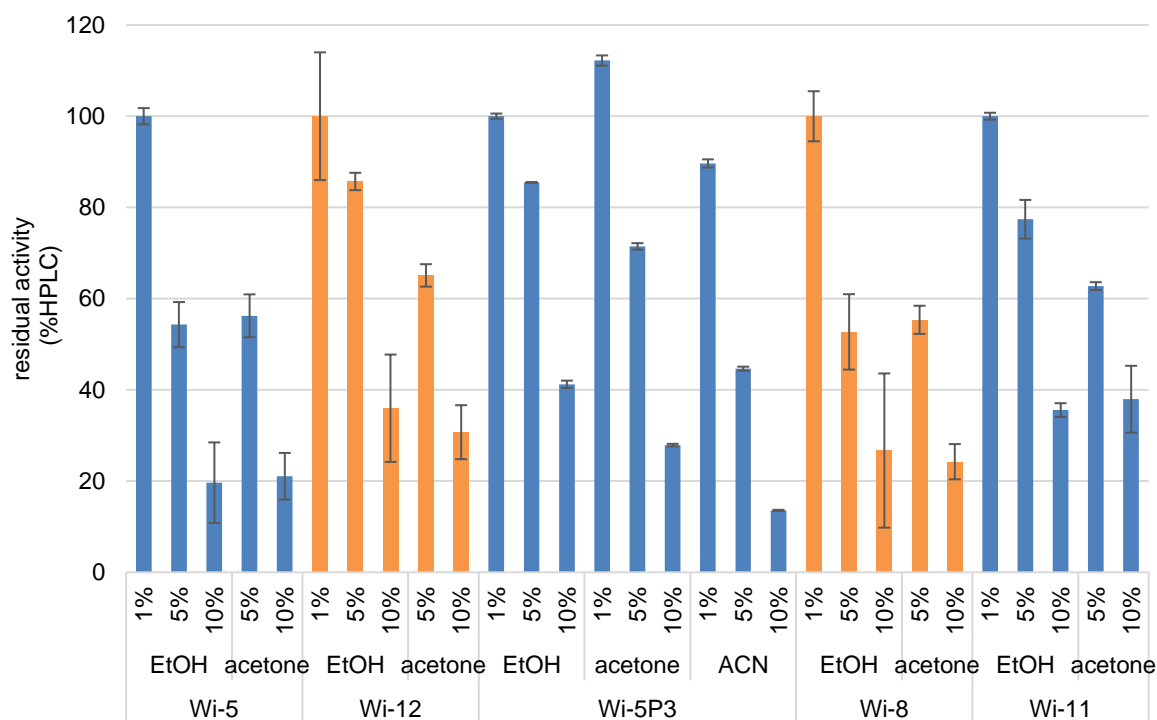


Figure 57. Formation of **54a** in presence of different solvents and concentrations, normalized to 1% EtOH and given as residual activity. Reaction conditions used: 10 μ M enzyme, 100 mM NaCl, 50 mM HEPES, 5 mM α KG, 2.5 mM ascorbic acid, 0.5 mM $(\text{NH}_4)_2\text{Fe}(\text{SO}_4)_2$, 5 h reaction. Substrate added from 50 mM stock to solvent.

As in the assays with increased temperature, it seems that the variants from the 4th generation library (*Wi-11*, *Wi-12*) have higher tolerance against an increased solvent concentration in comparison to their template variants *Wi-5* and *Wi-8*. Under optimized conditions, *Wi-5* as well as *Wi-8* seem to be equally stable against EtOH as well as acetone. While 5% EtOH results in a higher **54a** formation for *Wi-11* and *Wi-12* as well as *Wi-5P3* in comparison to 5% acetone. *Wi-5P3* was also tested with acetonitrile but confirms the result of the first experiment, that acetonitrile decreases product formation most. However, it seems that acetone instead of ethanol with 1% could be better or comparable, if the substrates have no sufficient solubility in ethanol. A residual activity of 85% with ethanol for *Wi-5P3* and *Wi-12* are already promising values that should further be tested in preparative scale reactions, especially if the reactions are performed with purified enzyme. If cell lysate should be used, further testing of different solvents with cleared lysate in bigger scale should be analyzed since denaturing *E. coli* enzymes based on an increased solvent level could have an impact on the reaction.

4. Summary and Conclusion

Direct and selective C-(sp³)-H chlorination is still a remaining challenge and an area of great interest in catalytic research. Until now, no selective transformation is known to chlorinate complex molecules under mild conditions. Therefore, enzymatic halogenation is an interesting alternative to synthetic methods and the discovery of a new class of aliphatic halogenases that is independent of acyl carrier proteins and which act on non-activated C-(sp³)-H bonds, opened the possibility to evolve this enzyme class towards a chlorination tool that can be added to today's synthesis toolbox.

Within this thesis, the halogenases *Wi-WelO15* from *Westiella intricata* HT-29-1 and *Hw-WelO15 Hapalosiphon welwitschii* IC-52-3 belonging to the class of Fe^{II}/αKG dependent halogenases, were analyzed on their evolvability towards new substrates and their potential for biocatalysis. The genes were successfully cloned into a high copy vector with restriction-free cloning.^[327] Efficient expression and purification protocols for the halogenase were established within this work. The optimized enzyme production yields around 60-65 mg purified enzyme per liter of cell culture which is three times the yield of the published protocol.^[155] Simple production with high yields are the basis to use these biocatalysts in synthesis.

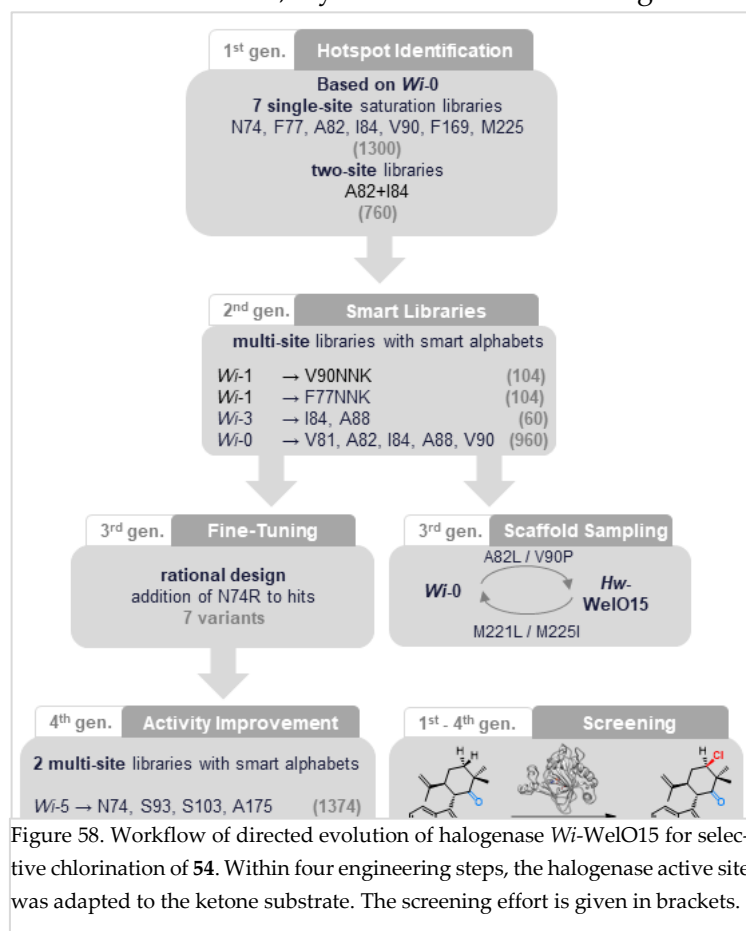
Based on primer design, the halogenase *Wi-0* (*Wi-WelO15* V6I/D284N) contained two surface mutations. While V6I is assumed to have a low impact on the activity, as the linker and His₆-tag should have, D284N was reversed and compared to *Wi-0* in biotransformations. It could be shown that this mutation has no influence on the activity. To test the activity of the halogenase, a simplified derivative of 12-*epi*-hapalindole C (**53**) was synthesized which was chlorinated by both *Wi-0* and *Hw-WelO15* with turnover frequencies (TOF) that are comparable to literature known values with 12-*epi*-hapalindole C (**39**) and *Hw-WelO15* as well as *WelO5*, a homologue that differs only in 2 amino acids to *Wi-WelO15*.^[157] The TOF of *Wi-0* is slower than the one of *Hw-WelO15* which confirms a lower product formation in cell lysate of *Wi-0* in comparison to *Hw-WelO15*. Analysis of the experiments however indicated a low stability of the isonitrile in cell lysate because low intensities of the substrate could be detected, in organic as well as aqueous phase after extraction. Purified, both enzymes achieved the same product formation within 8 h under optimized reaction conditions. The initially used reaction conditions yield comparable results to published results, optimized reaction conditions even improved the enzyme activity. Even though the enzymes have a high sequence similarity of 97%, a difference in TOF was observed, showing that the present differences in the structure influence the chlorination.

For the directed evolution process, a lead substrate was chosen that contains a ketone function instead of the naturally rare occurring isonitrile group. Synthesis of ketone **54** could be achieved in gram scale, in 3 steps and 32% yield, while isonitrile **53** needed 6 steps and could only be obtained with a yield of 4%. The substrate scope of the template halogenases *Wi-0* and

Hw-WelO15 was tested with **54** as well as with eight non-natural, commercially available isonitrile and isothiocyanate small molecules. No substrate conversion was detected. After analyzing the reaction conditions with a positive control, it is known that the non-natural small molecule isonitrile and isothiocyanates were screened under conditions at which the enzyme is likely to be inactive. Therefore, the substrates should be further tested under optimized conditions.

Since no structural information about the halogenases was available in the beginning of the project, random mutagenesis of *Hw*-WelO15 was performed by error prone PCR. Therefore, enzyme models were created with SwissModel, based on crystal structures of enzymes with a high amino acid sequence identity. Error prone PCR generally worked successfully for *Hw*-WelO15 although some variants are likely to be inactive due to frame shift mutations or early stop codons. 1750 colonies were screened with reaction conditions that should have yielded active halogenase, but no active variant towards **54** could be found until the halogenase structure of WelO5^[160] was available. Within epPCR, few mutations are introduced within a large part of the gene, therefore the probability of finding an active variant is low and structure guided semi-rational mutagenesis should always be preferable.

In the meantime, crystallization of both halogenases was pursued and the structure of *Wi*-0



could successfully be solved with molecular replacement based on the structure of WelO5^[160] in cooperation with the crystallization department of the Philipps-University Marburg. Structure guided directed evolution of *Wi*-0 was performed, following the engineering workflow shown in figure 58.

Halogenase *Wi*-0 was engineered from <1% product formation to 69% formation of **54a** in cell lysate and even 87% with purified enzymes. This also included optimization of reaction conditions which was made after finding the first variants producing **54a**. The engineering included four generations of improvement with several

semi-rational libraries and two rational design strategies. While single site libraries from 1st

Summary and Conclusion

generation yielded active variants for A82NNK, N74NNK and V90NNK, in two-site libraries several active variants were identified, with the best variant *Wi-1* containing mutation A82L in the active site. That one mutation already leads to an improvement of product formation in the range of 27% shows that few changes within the active site already have a high impact on substrate binding.

In the second generation, variants *Wi-1* and *Wi-3* from the first libraries were used as templates, furthermore a 5-site library based on *Wi-0* was created. The best variant of the second generation was *Wi-5* with mutations A82L/V90P in the active site. Even though variants resulting from a scaffold sampling strategy showed lower product formation than their template variants, the fine tuning of *Wi-7* by adding N74R, resulting in *Wi-8*, the variant with highest product formation within the first three generations.

After screening variants from generation 1-3, a selection of variants was first used to test a number of non-natural substrates in cell lysate and several variants were further purified and analyzed as isolated catalysts. The two best variants, *Wi-5* and *Wi-8* were used as templates for the 4th generation and together with *Wi-11* and *Wi-12*, they constitute a panel of promising chlorinases with highest product formation for ketone **54**. Formation of the chlorinated ketone (**54a**) **54**, was not detectable with the template variant *Wi-0* but engineering resulted in hit variant that show 87% product formation and a chemoselectivity of 96% as well as >99% dia- and regioselectivity. The possibility to find halogenase variants, able to chlorinate new, non-natural substrates proves the ability to evolve this enzyme class towards new substrate classes.

Within the project it was observed that the activity of the enzyme decreases quite fast with time and that most of the conversion happens within the first minutes. After finding several variants that produce **54a** and gathering knowledge about the system, several reaction conditions were tested. Exchanging 0.5 mM DTT with 2.5 mM ascorbic acid as well as increasing the NaCl concentration from 10 to 100 mM doubled to quadrupled the formation of **54a** for several variants (ch. 3.5 and results in ch. 3.5.5). Also, *Hw-WelO15* wild type which had under initial reaction conditions a product formation <1%, produced up to 8% **54a** under optimized reaction conditions. The increase in ascorbic acid concentration resulted in an elongated time in which product formation could be observed. This underlines the problem of fast Fe^{II} oxidation. Even though the reaction time was elongated, and product formation is still observable after 8 h, most of the product is formed within the first minutes. To overcome this problem, a balance has to be found between availability of O₂, present for the reaction but without an excess of the oxidant, to prevent oxidation of Fe^{II} to Fe^{III}, which abolishes the enzyme activity.

Under initial reaction conditions, substrates containing modifications within the indole moiety were chlorinated with low activity. Conversion could be improved by optimizing the reaction conditions. All tested hapalindole-like ketones with modifications in position 5 and 6 in the indole ring (**76-78**) were chlorinated, showing that this part of the substrate might have

Summary and Conclusion

a less important influence on substrate binding. *Wi*-11 and 12 show the highest formation of **54a** in isolated form, while modified substrates were converted better in cell lysate. **76a** and **77a** are produced best by *Wi*-5 and **78a** by *Wi*-11 (ch. 3.6.2.1).

Modification of the terpene ring lead to a complete loss of activity within initial reaction conditions. Already the removal of a methyl group at position C12 ketone **81** in comparison to **54** shows that the quaternary center in position C12 is important for the substrate binding. After using optimized reaction conditions, these substrates were also transformed best by *Wi*-5 and *Wi*-12, however, few to no chlorination could be observed. Instead complex mixtures of products were formed, which could not completely be analyzed. LC-MS measurements suggest mono- or dihydroxylation, desaturation or two modifications combined. After preparative HPLC purification, NMR analysis of two new products were performed, however the fractions revealed to contain more than one compound and no clear structure elucidation could be performed so far. The NMR of **82a** suggests that the terpene ring might be opened between positions C10 and C11 and a terminal carboxylate could have been formed (ch. 3.6.2.2). To further analyze this, more experiments need to be performed and purification of the single products need to be achieved followed by structure analysis by NMR, IR and crystallization.

These results highlight the importance of the reaction conditions for these enzymes. The substrate scope under optimized reaction conditions is much broader than initially thought. Since also the size and steric demand of naturally found hapalindole alkaloids varies within the different compounds. Fischerindole **42** as well as hapalindole **39** are both chlorinated by WelO5, which shows that the enzyme can accept a variety of different molecule shapes and the binding mode is far from being understood.

Further hapalindole-like alkaloids with isonitrile and isothiocyanate groups in position C11 but changed stereo conformation in comparison to 12-*epi*-hapalindole C were converted only (**91**) or best (**67**) by *Wi*-1 which shows the importance of position A82 (ch. 3.6.3). Considering only active site mutations, A82L is also the best single mutation variant that converts **54**. It would be very interesting to have a crystal structure of this variant, co-crystallized with the different substrates to explain the versatility of it, in comparison to the template variant *Wi*-0 which has a quite narrow substrate scope.

The conversion of all tested non-natural substrates, under optimized reaction conditions, shows that this enzyme class can be adapted towards new substrates and that the activity can be engineered by directed evolution as well as reaction conditions.

To analyze all new products, preparative scale reactions in mg-scale were performed. Initially, these reactions were tedious with low conversions and even lower yields. After optimizing the reaction conditions, the conversion and yield increased and several mg of the products could be isolated and analyzed. Unfortunately, still great amounts of catalyst need to be used. For a

Summary and Conclusion

50 mL reaction, a substrate to catalyst ratio of 25 : 1 are used, which correspond to 11 mg substrate (0.75 mM, 281 g/mol) and 45 mg catalyst (0.03 mM, MW 34450 g/mol). Therefore, the efficiency of the catalyst should be improved for further applications. Still the enzyme displays a great possibility to chlorinate unactivated C(sp³)-H which might be not accessible chemically.

No information about kinetic properties of *Wi-WelO15* with the natural substrate 12-*epi*-hapalindole C is available, published information of *WelO5* are turnover frequencies within the first two minutes. *Wi-0* in combination with non-natural isonitrile **53** achieves the highest catalytic efficiency of 71.5 min⁻¹mM⁻¹. Chlorination of ketone **54** is not possible with the template variant *Wi-0*. Through directed evolution of the enzyme, selective chlorination was enabled, and kinetic properties of the enzymes could be altered. The enzyme efficiency was improved 93-fold from the lowest measurable $k_{\text{cat}}/K_{\text{m}}$ of 0.2 (*Wi-2*) to 18.5 min⁻¹mM⁻¹ (*Wi-12*). Further analysis of *Wi-5* with **76-78** revealed that even though **77** is the substrate accepted best, the $k_{\text{cat}}/K_{\text{m}}$ for **76** is higher. All kinetic analysis was performed under non-optimized reaction conditions (10 mM NaCl, 0.5 mM ascorbic acid) and will likely improve, using 100 mM NaCl and 2.5 mM ascorbic acid. In comparison to an average enzyme (k_{cat} of 600 min⁻¹)^[416], the enzymes are still quite slow but within this thesis it was shown for the first time, that it is possible to evolve this enzyme class towards non-natural substrates and that kinetic properties can be improved. With these results, the class of enzyme displays a possibility for a selective chlorination and can be further evolved for further user defined needs.

When enzymes are evolved, stability can be important for two reasons, first, mutations introduced to alter activity, often reduce the enzyme stability which is not desired by the enzyme engineer, therefore the enzyme needs a high starting stability. The other option is, that the enzyme is engineered towards a higher stability. Higher stability can simplify the purification process if heat purification is enabled but also, it can increase the reaction rate at higher temperatures. If solvent stability is present, reactions in biphasic systems are preferred because these often result in higher conversions if the solubility of the substrates is low in water-based buffer.

To gain information about the stability of the halogenases, the melting temperature of several hit variants was determined by circular dichroism measurements. *Wi-0* has an 8 °C lower melting temperature as *Hw-WelO15* (54 °C and 62 °C) but both already display a medium to good stability. Interestingly, the stability of *Wi-0* variants did not decrease but mainly the melting temperature increased slightly, which suggests that the stability of the enzyme is a limiting factor in the screening assay and is optimized or kept constant within the new-found hits. To further improve the stability of *Wi-0*, the structure of *WelO5* was examined by the PROSS server^[428] and several proposed variants were created. All variants had an increased melting temperature in comparison to *Wi-0* with a maximal T_m of 61 °C for *Wi-5P3*, which is based on *Wi-5* in combination with mutations proposed for PROSS variant 3. Activity assays reveal that

Summary and Conclusion

Wi-5P3 is also able to chlorinate non-natural hapalindole-like ketones and has the highest tolerance against solvents and temperature increase within tested variants. A residual activity of 90% in assays performed at 45 °C and 85% residual activity in the presence of 5% ethanol could be observed. High temperatures during the reaction might be impractical because of a low O₂ saturation at increased temperatures but long-time storage and heat purification of the halogenase would simplify the handling and isolation process of the enzyme.

Incubation of stabilized variants in buffer at different temperatures with subsequent SDS-PAGE analysis showed that after incubation of *Wi-P3* at 65 °C for 4 h, still soluble enzyme is left, some in monomeric and some in oligomeric form, while *Wi-0* already completely precipitates if incubated at 45 °C for 3 h. Other enzymes such as the used thermostable ene-reductase *TsER* and glucose dehydrogenase *BsGDH*, could be isolated by heat purification by incubation for 90 min at 70 °C. The stabilized variant *Wi-P3* might already be suitable for purification by heat. However, no activity assay was performed with the incubated enzymes to see if oligomerization results in activity loss. It can be assumed that the low turnover number and a fast loss of activity is solely based on Fe^{II} oxidation. All in all, these results are promising for easy handling the halogenase within the lab as well as for further projects that will work on increasing the solvent and temperature stability of the halogenase.

In conclusion, *Wi-WeIO15* was evolved for mild, late-stage chlorination in water using NaCl as halogen source. This work demonstrates the power of directed evolution to improve catalytic efficiency for non-native substrate for the challenging class of Fe^{II}/ α KG dependent chlorinases. It was possible to exchange the isonitrile, present in natural substrates, to a common carbonyl group. Variants of the enzyme class are now able to functionalize non-activated, aliphatic C(sp³)-H bonds in the presence of more electron-rich functional groups of non-natural substrates.

5. Outlook

Chlorination of non-activated C(sp³)-H bonds is a remaining challenge in today's synthesis toolbox. Within this thesis it could be shown that a new class of halogenases is able to perform this transformation and that the limited substrate scope of the chlorinases can be evolved to new non-natural substrates.

While substitution of the isonitrile group to a ketone as well as modification of the indole ring is tolerated by the enzyme variants and chlorination is performed, modifications at the terpene ring are only conditionally tolerated. For these substrates, complex mixtures of several products are formed. For these substrates, existing libraries should be screened again, or mutagenesis performed to adapt the shape of the active site to the specific substrate, since the panel of tested chlorinases was chosen based on their chlorination activity for **54**. Screening of the 1st and 2nd generation libraries, created within this thesis could already contain suitable variants to increase selectivity.

Within the screening it was found, that mutation I84H, introduced in several variants as for example *Wi*-WelO15 V6I/A82V/D284N, reduces the chemoselectivity from 98% chlorination **54a** to 68%, with **54b** as hydroxylated side product. Also, *Hw*-WelO15 wild type which in contrast to *Wi*-WelO15 is able to produce around 8% **54a** has a decreased chlorination selectivity of 70%. This is a first indication that chemoselectivity can be controlled solely by substrate binding site mutations in *Wi*-WelO15, without modifying the 1st or 2nd ligand sphere of the active site Fe^{II} complex.

Motivated by the hydroxylation of the screening substrate, libraries of P450_{BM3} were screened with ketone **54**. Some hits were found which produced 2 new products. With the collected information, a new library was created with the goal to achieve a higher selectivity. While screening with **54**, in total 4 new products (**54c-f**) were formed. Preparative scale reactions followed by NMR analysis revealed the products to be dihydroxylated (**54c**), epoxidized and hydroxylated (**54d**), hydroxylated (**54e**) and epoxidized (**54f**). While the halogenase hydroxylated **54** in position C13 *R*-selective (**54b**), P450_{BM3} hydroxylates position C14, *R*-selective (**54e**). **54d** is produced from **54e** and **54f**, if the enzyme is still active, so the formation of it can be suppressed or triggered depending on different reaction conditions. Unfortunately, no enzyme with selectivity for either **54e** or **54f** could be found within the screened libraries.

No halogenase of P450_{BM3} variants could be found that selectively produces only one hydroxylated product. However, it could be seen that with several variants, different positions of the substrate are accessible. Further engineering needs to be performed to increase chemo- or regioselectivity.

The restriction-free cloning method was further successfully used to clone oxygenase genes *welO11-welO19* from *Westiella intricata* HT-29-1 and *welO11-welO17* *Hapalosiphon welwitschii* IC-

Outlook

52-3 into the pRSF-Duet vector. Except *Hw-welO14* which could not be isolated with primers 9 and 14 (table 26). Amplification of a gene was observable, sequencing revealed this gene however to be *welO13*. The fast and simple cloning of 18 genes by rf-cloning shows the power of ligase free cloning techniques, where low costs and time effort are needed. Initial protein production tests of oxygenases *Wi-WelO11-14* as well as *Hw-WelO16-17* and *Wi-WelO18* showed the production but indicate a low solubility (*WelO11-14*) and low stability *WelO16-18*, under used, non-optimized conditions. Optimization of protocols for heterologous expression of the latter oxygenases were not performed, since the focus was laid on halogenases *Wi-WelO15* and *Hw-WelO15*. Performed experiments however suggest that the enzyme production is possible. The same applies to *HpiI1*, *HpiI3* and *WelP1*. The enzymes seem to be accessible by heterologous expression in *E. coli*. Protocols for production and purification of the enzymes need further improvement and assays need to confirm their activity and in case of the oxygenase also the natural function needs to be explored. Since selective oxidation reactions are highly interesting reactions, too, further characterization of the enzymes may lead to interesting new biocatalysts.

A fast loss of activity within the first minutes could be observed. To overcome this problem, it could be examined if an engineering towards higher Fe^{II} affinity can be achieved. Different members of the non-heme iron enzyme family show that the iron is not bound equally well. The iron binding can for example be tested by addition of EDTA to the reaction. If the enzyme binds the metal ion tightly, higher EDTA concentration should be tolerated in the reaction in contrast to a loose binding affinity. A tightly bound Fe^{II} within the active site should prevent the oxidation. Another possibility to avoid iron oxidation, would be to run the reaction anaerobically and to flush the system with oxygen containing air, so that all oxygen is directly consumed and the reaction in total stays anaerobically. The anaerobic reaction set-up will probably be easier in large scale, for example run in a fermenter with oxygen sensor, but within a screening in 96 dw-format and small volumes as 0.2 mM this is almost impossible.

The substrates used within this project have a low solubility. If the substrate is added to the aqueous reaction mixture, local precipitation can be observed if the final concentration of substrate is 1 mM or higher. Even though the precipitated substrate in the tested concentration range up to 2 mM for **54** dissolves by mixing, the solubility problem will be present at higher substrate loadings that are needed to run efficient catalytic systems. To overcome a precipitation and aggregation of the molecules, it would be beneficial to run the reaction in a biphasic system. With some initial experiments, the solvent stability of some halogenase variants was tested and found to be quite promising. Residual activity for the best variants *Wi-12* and *Wi-5P3* were found to be >80% in the presence of 5% EtOH. A preparative reaction should be

Outlook

performed with 5% EtOH to see if the presence of EtOH has a beneficial effect on the transformation. Starting with these variants, further engineering can be performed to create variants that tolerate a higher solvent ratio. Especially the tolerance against water non-miscible solvents and their use in biphasic systems is of advantage because extraction of the products is much easier. Especially *Wi-P3* and *Wi-5P3* also possess a high tolerance against increased temperatures and tolerate incubation at temperatures up to 65 °C for several hours. In further studies, remaining PROSS variants should be created and analyzed on their temperature and solvent stability. Heat purification of the catalysts and a long shelf life simplify the use. Furthermore, the stabilized variants should be used as template for further directed evolution studies.

It is for sure that variants of this chlorinase are a great addition to the synthesis toolbox and halogenation of unactivated positions, that are not accessible so far, neither enzymatically nor chemically, can be addressed with these halogenases. More engineering will further increase the substrate scope and simplify the handling of the promising catalyst.

6. Material

6.1 Organisms and Genes

In table 22 all used vectors and plasmids are listed

Table 22. Used vectors and plasmids.

organism and vectors	resistance cassette	origin
<i>E. coli</i> BL21-Gold(DE3)	tetracycline	Novagen
<i>E. coli</i> DH5 α		Novagen
pET22	ampicillin	Novagen
pRSF-Duet	kanamycin	Novagen

In table 23 all cloned genes with corresponding vector and tag as well as original organism are listed.

Table 23. Cloned genes with vector and organism. gDNA of *Westiella intricata* UH HT-29-1 and *Hapalosiphon welwitschii* IC 52 were received as gift of Michelle Moffit.^[238]

gene	organism	vector (antibiotic resistance)	tag	origin
<i>tsER</i> C25D/I67T	<i>Thermus scotoductus</i> SA-01	pet22 (amp)	-	Hoebenreich group ^[315]
<i>welP1</i>	<i>Westiella intricata</i> UH HT-29-1	pJ-Express (kan)	C-His ₆	R. Viswanathan ^[238]
<i>hpI1</i>	<i>Fischerella</i> sp. ATCC 43239	pRSF-Duet (kan)	N-His ₆	Plasmids received of R. Viswanathan, cloned in pRSF dur- ing this research pro- ject
<i>hpI3</i>	<i>Fischerella</i> sp. ATCC 43239	pRSF-Duet (kan)	N-His ₆	
<i>welO11-18</i>	<i>Westiella intricata</i> UH HT-29-1	pRSF-Duet (kan)	N-His ₆	Cloned during this research project
<i>welO11-16</i>	<i>Hapalosiphon welwitschii</i> IC 52	pRSF-Duet (kan)	N-His ₆	

6.2 Media and Buffer

In this chapter all used media, antibiotics and buffers are listed. All buffers, used for chromatographic purification and antibiotics were sterile filtered (VWR, polyether sulfone 0.45 μm) before usage. Water was used in micropure grade (conductivity 0.055 $\mu\text{S}/\text{cm}$ MicroPure system of TKA) as solvent if not stated otherwise. The composition of used media and buffers are listed in table 24.

Table 24. Composition of different media and buffers. The pH was adjusted if a value is given.

media	composition
LB-medium	5 g/L NaCl, 10 g/L tryptone, 5 g/L yeast extract., pH 7.0
LB-agar	15 g agar in 1 L LB-medium.
TB-medium	900 mL (12 g/L tryptone, 24 g/L yeast extract, 4 mL/L glycerol) add 100 mL 10xphosphate buffer (125 g/L $\text{K}_2\text{HPO}_4 \cdot 3\text{-H}_2\text{O}$, 23 g/L KH_2PO_4).
SOC Medium	20 g/L tryptone, 5 g/L yeast extract, 10 g/L NaCl, pH 7.0 before use, add 10 mL 1 M MgCl_2 and 20 mL 1 M glucose
1 M KPi	160 g $\text{K}_2\text{HPO}_4 \cdot 3\text{-H}_2\text{O}$ und 40.6 g KH_2PO_4 in 1 L H_2O , pH=7.4.
KPi buffer	100 mM potassium phosphate, pH=7.4 (1-9 diluted from 1 M KPi)
Tris A	50 mM Tris, 500 mM NaCl, 0.1% Tween-20, 20 mM imidazole, 10 mM β -ME, pH=7.4
Tris B	50 mM Tris, 500 mM NaCl, 250 mM imidazole, 10 mM β -ME, pH=7.4
HEPES 1	50 mM HEPES, 10 mM EDTA, 10 mM NaCl, 10% glycerol, pH 7.4
HEPES 2	50 mM HEPES, 10 mM NaCl, 10% glycerol, pH 7.4
HEPES 3	50 mM HEPES, 10 mM NaCl, pH 7.4
HEPES 4	50 mM HEPES, 100 mM NaCl, pH 7.4
reaction buffer	50 mM HEPES, pH 7.4, 100 mM NaCl, 5 mM α KG, 2.5 mM ascorbic acid, 0.5 mM $(\text{NH}_4)_2\text{Fe}(\text{SO}_4)_2$
lysis buffer	1 mg/mL lysozyme in 50 mM HEPES, 100 mM NaCl, pH 7.4
TAE buffer	40 mM tris acetate, 1 mM EDTA, pH=8.0
10x SDS-PAGE buffer	10 g SDS, 144 g glycine, 30 g Tris in 1 L H_2O , pH adjusted to 8.3 with HCl
SDS-PAGE stain	0.25 (w/v) Coomassie Blue R250, 5% (v/v) acetic acid, 50% (v/v) ethanol filled up with H_2O
4x SDS-PAGE sample buffer	250 mM Tris-HCl (pH 6.8), 8% (w/v) SDS, 0.2% (w/v) bromo-phenol blue, 40% (v/v) glycerol, 20% (v/v) β -ME.
trace metal mix ^[433]	675.8 mg $\text{FeCl}_3 \cdot 6\text{H}_2\text{O}$ (50 mM), 111.0 mg CaCl_2 (20 mM), 84.5 mg $\text{MnSO}_4 \cdot \text{H}_2\text{O}$ (10 mM), 143.8 mg $\text{ZnSO}_4 \cdot 7 \text{H}_2\text{O}$ (10 mM), 23.8 mg CoCl_2 (2 mM), 17.1 mg CuCl_2 (2 mM), 23.77 mg $\text{NiCl}_2 \cdot 6 \text{H}_2\text{O}$ (2 mM), 24.19 mg $\text{Na}_2\text{MoO}_4 \cdot 2 \text{H}_2\text{O}$ (2 mM), 6.18 mg H_3BO_3 (2 mM), 312.5 μL conc. HCl, ad. 50 mL

Material

In table 25 all reagents necessary for heterologous expression are listed.

Table 25: All additives necessary for heterologous expression with stock solution concentration as well as working concentration and solvents. All stock solutions were filtered sterile (VWR, polyether sulfone 0.45 µm).

media additive	stock solution	working concentration	solvent	origin
kan ⁵⁰	50 mg/ml*	50 µg/ml	H ₂ O	AppliChem
amp ⁵⁰	100 mg/ml*	100 µg/ml	H ₂ O	AppliChem
IPTG	100 mM	10 µM (<i>TsER</i>) 20 µM (Halogenase)	H ₂ O	AppliChem
tet	10 mg/ml	10 µg/ml	EtOH	AppliChem
FeCl ₃	50 mM	50 µM	H ₂ O	
trace metal mix**	1000x	1x	H ₂ O	

*antibiotics were used as salts and counterion weight included, **composition in table 24.

6.3 Primer

In table 26 all used primers are listed with their sequence. The primers are subdivided by their use in sequencing, cloning or mutagenesis.

Table 26: All used primers are shown in this table. Lower case bases interact with the vector, upper case bases interact with the gene. Bases that are highlighted red are mutations and green highlighted bases are silent mutations

Primer for Sequencing		
1	pRSF_rev	gtgtgaccgtgtgcttc
2	T7minus1	aatacagactcactataggg
3	T7T	ctagtattgctcagcgg
4	BM3-2	cgagaacattcgctatc
5	BM3-3	ttaattgtaacggcgctc
6	BM3-4	ataccggcgtgtgaaatg
7	P450 _{BM3} seq primer	gtattccttcacntagcac
Primer for Cloning		
8	WelO11+12_fw	cagccaggatccgaattcgagctcgATGGTTAGCTATATTGAAAAGAGCG
9	WelO13+14_fw	CAGCCAGGATCCGAATTCGAGCTCGatggttagctatattgaaaacgacc
10	WelO15_Halogenase_fw	cagccaggatccgaattcgagctcgATGTCCAATAACACCATCTCTAC
11	Wi-WelO15_pRSF_rv	CAGCGGTGGCAGCAGCCTAGGTTAATcaactccagtaataaatcttat
12	WelO16_fw	cagccaggatccgaattcgagctcgATGTTCTCACAATTAAGCAACCAG
13	WelO17_fw	cagccaggatccgaattcgagctcgATGACTACTGCACACTACGATTTAATC
14	WelO18_fw	cagccaggatccgaattcgagctcgATGCGTAAGTTCTACTATTATTCAACC
15	WelO19_fw	cagccaggatccgaattcgagctcgATGGTTAATGTTGAAAAGAGCGTAG
16	Hw-WelO11_rv	cagcgggtggcagcagcctaggttaaTCATGGTATCGAAGATTGGTTTATC
17	Wi-WelO11_rv	cagcgggtggcagcagcctaggttaaTACTGTGCTTTAGCAACCCAAC
18	WelO12_rv	cagcgggtggcagcagcctaggttaaTACTGTGCCTTATTAACCCAAC
19	WelO13_rv	cagcgggtggcagcagcctaggttaaTTATTTGTTTGACTGTGCCTTATTAAC
20	WelO14_rv	cagcgggtggcagcagcctaggttaaTACTGTGCTTTATTAACCCAACCTTG
21	WelO15_Amb05_rv	cagcgggtggcagcagcctaggttaaTCAACTCCAGTAATAAATCTTATCACG
22	WelO16_rv	cagcgggtggcagcagcctaggttaaTCAAGAAATTAATGTGCGGTTGTC

Material

23	WelO17_rv	cagcggtaggcagcagcctagggttaaTTAA- GCCATACGTCCAATTAATG
24	WelO18_rv	cagcggtaggcagcagcctagggttaaCTAAGTTGTTTTACTT- GTAGACTGTG
25	WelO19_rv	cagcggtaggcagcagcctagggttaaTACTGTGCCTTATCAACCCAAT
26	Hw-WelO15_frameshiftrepair_fw	GTAATAAGATTATTACTGGAGTTAATTAACCTAGG
27	Hw-WelO15_frameshiftrepair_rv	CCAGTAATAAATCTTATTACGCTCTTTAGAG
28	WelO11_IC_rep_f	GTTCAATAAATGGGCAACTTATTGTTGG
29	WelO11_IC_rep_rv	GTTGCCCATTTATTGAACATAATTAACCTTGC
30	HpI1_pRSF_f	cagccaggatccgaattcagctcgATGATCAGCGAGAAAATCCTGC
31	HpI1_pRSF_rv	cagcggtaggcagcagcctagggttaaTTATGACTTGTGCGAAGGTGAC
32	HpI3_pRSF_f	cagccaggatccgaattcagctcgATGATGGTTAGCACGAGCGTAG
33	HpI3_pRSF_rv	cagcggtaggcagcagcctaggTTAATTACAGAATGTGCACACGCTGC
primer for mutagenesis		
34	WelO15_epPCR_1_f	GCGATACTATGGAGCAAGTAGCC
35	WelO15_epPCR_2_f	CTTTCTGAATTGCCAGTAGAAATTCCC
36	WelO15_epPCR_3_rv	TAGGTTTGCCCTTCTGGTCC
37	Wi-WelO15_A82_NNK_f	CAAAGTGNKCAAATATATGGTCATGCAATTGTCCG
38	Wi-WelO15_A82_NNK_r	GCATGACCATATATTTGMNNCACTTAGTACCAAATTC
39	Wi-WelO15_I84_NNK_f	GTGGCTCAANNKTATGGTCATGCAATTGTCCG
40	Wi-WelO15_I84_NNK_r	GGCATGACCATAMNNTTGAGCCACTTTGGTACC
41	Wi-WelO15_A82SAM_I84SAM_f	CCAAAGTGSAMCAASAMTATGGTCATGCAATTGTCCG
42	Wi-WelO15_A82SAM_I84SAM_r	GGCATGACCATAKTSITGKTSACTTTAGTACCAAATTC
43	Wi-WelO15_A82SAM_I84ANC_f	CCAAAGTGSAMCAAANCTATGGTCATGCAATTGTCCG
44	Wi-WelO15_A82SAM_I84ANC_r	GGCATGACCATAGNITTTGKTSACTTTAGTACCAAATTC
45	Wi-WelO15_A82DYG_I84SAM_f	CCAAAGTGDYGCASAMTATGGTCATGCAATTGTCCG
46	Wi-WelO15_A82DYG_I84SAM_r	GGCATGACCATAKTSITGCRHCACTTTAGTACCAAATTC
47	Wi-WelO15_A82DYG_I84ANC_f	CCAAAGTGDYGCAAANCTATGGTCATGCAATTGTCCG
48	Wi-WelO15_A82DYG_I84ANC_r	GGCATGACCATAGNITTTGCRHCACTTTAGTACCAAATTC
49	Wi-WelO15_A82AWC_I84SAM_f	CCAAAGTGAWCCASAMTATGGTCATGCAATTGTCCG
50	Wi-WelO15_A82AWC_I84SAM_r	GGCATGACCATAKTSITGWTCACTTTAGTACCAAATTC
51	Wi-WelO15_A82AWC_I84ANC_f	CCAAAGTGAWCCAAANCTATGGTCATGCAATTGTCCG
52	Wi-WelO15_A82AWC_I84ANC_r	GGCATGACCATAGNITTTGWTCACTTTAGTACCAAATTC
53	Wi-WelO15_A82TTC_I84SAM_f	CCAAAGTGTTCASAMTATGGTCATGCAATTGTCCG
54	Wi-WelO15_A82TTC_I84SAM_r	GGCATGACCATAKTSITGGAACACTTTAGTACCAAATTC
55	Wi-WelO15_A82TTC_I84ANC_f	CCAAAGTGTTCASAAANCTATGGTCATGCAATTGTCCG
56	Wi-WelO15_A82TTC_I84ANC_r	GGCATGACCATAGNITTTGGAACACTTTAGTACCAAATTC
57	Wi-WelO15_A82F_f	CAAAGTGTTCAAAATATATGGTCATGCAATTGTCCG
58	Wi-WelO15_A82F_r	GCATGACCATATATTTGGAACACTTTAGTACCAAATTC
59	Wi-WelO15_F77NNK_f	GAAGAAANNKGGTACCAAAGTG
60	Wi-WelO15_F77NNK_r	GGTACCMNNTTCTTATTCTTATTAAG
61	Wi-WelO15_V90NNK_f	GCCATTNNKGGTCAATCACCC
62	Wi-WelO15_V90NNK_r	GATTGACCMNNAATGGCATGACC
63	Wi-WelO15_N74NNK_f	CTTAATAAGNNKGAAGAATTTGGTACCAAAG
64	Wi-WelO15_N74NNK_rv	CAAATTCTTATTCTTNNNAAGAATGATTTCATAC
65	Wi-WelO15_F169NNK_f	GGCAATGANNKCTGTTAATGCCTGC

Material

66	Wi-WelO15_F169NNK_rv	GCATTAACAGGMNNTCATTGCCAACATGG
67	Wi-WelO15_M221NNK_f	GCAAATATGCTCAA NNK CAGGAATATATGGATG
68	Wi-WelO15_M221NNK_rv	ATTCTGCATTTGAG MNN ATTTGCTTGC
69	Wi-WelO15_M225NNK_f	CAGGAATAT NNK GATGATGTAGAGTCCAAG
70	Wi-WelO15_M225NNK_rv	CTCTACATCATC MNN ATATTCCTGCATTTG
71	Wi-WelO15_N74NNK_2_f	CAATTCCTAATAAG NNK GAAGAGTTTGGTAC- CAAAGTGGCTC
72	Wi-WelO15_N74NNK_2_rv	GTACCAAACCTTTC MNN CTTATTAAGAATTGAT- TTCATACCACCGTC
73	Wi-WelO15_F169NNK_2_f	GGCAATGAT NNK CTGTTAATGCCTGCGG
74	Wi-WelO15_F169NNK_2_rv	GGCATTAACAG MNN ATCATTGCCAACATGGAC
75	Wi-WelO15_I84ABC_A88ARC_V90RTG_f	CAA ABC TATGGTCAT ARC ATT RT - GGTCAATCACCCGATCTCAAAGACTAC
76	Wi-WelO15_V91BTT_A82GYG_I84ABC_r	ATGACCATAG V TTT GCRCAAV TTTGGTAC- CAAATTCTTCATTCTTATTAAG
77	Wi-WelO15_I84ABC_A88GYG_V90RTG_f	CAA ABC TATGGTCAT GYG ATT RT - GGTCAATCACCCGATCTCAAAGACTAC CAA ABC -
78	Wi-WelO15_I84ABC_A88ARC_V90CMG_f	TATGGTCAT ARC ATT CM GGTCAATCACCC GATCTCAAAGACTAC
79	Wi-WelO15_I84ABC_A88GYG_V90CMG_f	CAA ABC TATGGTCAT GYG AT- T CM GGTCAATCACCCGATCTCAAAGACTAC
80	Wi-WelO15_V91BTT_A82AWG_I84ABC_r	ATGACCATAG V TTT GCWTA AVTTTGGTAC- CAAATTCTTCATTCTTATTAAG
81	Wi-WelO15_V91AMC_A82AWG_I84ABC_r	ATGACCATAG V TTT GCWTGK TTTTGGTAC- CAAATTCTTCATTCTTATTAAG
82	Wi-WelO15_V91AMC_A82GYG_I84ABC_r	ATGACCATAG V TTT GCR CGKTTTTGGTAC- CAAATTCTTCATTCTTATTAAG
83	Wi-WelO15_N74R_rv	GGTACCAAA CT CTT CCG CTTATTAAGAATTGAT- TTCATACC
84	Wi-WelO15_I84A88V90P_fw	CAA ABC TATGGTCAT NN - KATT CCG GGTCAATCACCCGATCTCAAAGACTAC
85	Wi-WelO15_G166D_fw	GCGAAATCGCAGTCCATGTT GATA ATGAT- TTCTGTAAATGCC
86	Wi-WelO15_G166D_rv	GGCATTAACAG- GAAATCATT ATC AACATGGACTGCGATTTCGC
87	WelO15_V90P_fw	CAAATATATGGTCATGC A ATT CCG GGTCAATCACCC C
88	WelO15_A82L_rv	ATGACCATATATTT GCAA CACTTTGGTAC- CAAATTCTTCATTC
89	Wi-WelO15_M221L_M225I_rv	GGACTCTACATCATCT TAT ATATTCCT GTA ATTGAG- CATATTTGC
90	Wi-WelO15_N74ARC_fw	CTTAATAAG ARC GAAGAATTTGGTACCAAAG
91	Wi-WelO15_N74CRG_rv	CAAATTCTT CY GCTTATTAAGAATTGATTCATAC
92	Wi-WelO15_S103VAC_fw	CTTTGCTTCT VAC GCAATCTTCCGGCAGG
93	Wi-WelO15_S103KYG_fw	CTTTGCTTCT KY GGCAATCTTCCGGCAGG
94	Wi-WelO15_S93VAC_fw	GGTCAA VAC CCCGATCTCAAAGACTACTTTGC
95	Wi-WelO15_S93KYG_fw	GGTCAA KY GCCCGATCTCAAAGACTACTTTGC
96	Wi-WelO15_A175KYG_rv	CAGATGGTT CRM CGCAGGCATTAACAGG
97	Wi-WelO15_A175VAC_rv	CAGATGGTT GTB CGCAGGCATTAACAGG
98	Wi-WelO15_S103A_fw	CTTTGCTTCT GCG GCAATCTTCCGGCAGG
99	Wi-WelO15_Q123R_fw	GATTTTGAGGAA CGT GTAGAGTCAATATTTAC
100	Wi-WelO15_S230K_rv	GACTTAATCTT TTT CTCTACATCATCC

Material

101	Wi-WelO15_S230K-Q236N-S239W_fw	GATGATGTAGAGAAAAGAT- TAAGTCTAACAACTCTCAGTGGGTAGCTTATGC
102	Wi-WelO15_S268R_rv	CAATGGTTCGCCGTGGACGATTACCAATTA C
103	Wi-WelO15_Q282D_rv	CAGTAATAAATCTTATTACGATCTTTAGA- GAAGGCTAAAAATCC
104	Wi-WelO15_284D_rv	CAGTAATAAATCTTATCACGCTGTTTA GAGAAGG
105	P450BM3-L181-M185-L188-1_fw	GTCCGTGCAVHGGATGAAGCAAR- CAACAAGBCCAGCGAGCAAATCCAG
106	P450BM3-L181-M185-L188-2_fw	GTCCGTGCAVHGGATGAAGCAARCAACAAGAAC- CAGCGAGCAAATCCAG
107	P450BM3-L181-M185-L188-3_fw	GTCCGTGCAVHGGATGAAGCAARCAACAAGCTG- CAGCGAGCAAATCCAG
108	P450BM3-L181-M185-L188-4_rv	GCTCGCTGCAGCTTGTTCAATTGCTTCATCCDBTG- CACGGACCATACTTG
109	P450BM3-L181-M185-L188-5_rv	GCTCGCTGGTCTTGTTCAATTGCTTCATCCDBTG- CACGGACCATACTTG
110	P450BM3-L181-M185-L188-6_rv	GCTCGCTGVCCTTGTTCAATTGCTTCATCCDBTG- CACGGACCATACTTG

6.4 Programs and Online Tools

The following programs and online tools have been used:

Adobe Illustrator CC2015

ApE v2.0.47

BioEdit Version 7.2.5

ChemOffice 2015: ChemDraw Professional 15.1 and Chem3D 15.1

Chimera Version 1.11, 05.07.2016

Discover Studio Visualizer v17.2.0.16349

ExPASy ProtParam (<https://web.expasy.org/protparam/>)

ExPASy Translate Tool (<https://web.expasy.org/translate/>)

IDT Oligo Analyzer 3.1 (<https://eu.idtdna.com/calc/analyzer>)

Mestrenova Version 9.0.1-13254

Microsoft Office: Excel and Word 2010, Excel and Word 365

Origin Version 8.5 Pro

PROSS Server (<http://pross.weizmann.ac.il/bin/steps>)

PyMol Version 0.99rc6, 2006

SnapGeneViewer 3.2.1

SwissDock (<http://www.swissdock.ch/>)

SwissModel (<https://swissmodel.expasy.org/>)

6.5 Devices

Shaker for cell cultures:

- Infors HT Multitron shaker, 50 mm shaker throw, Modular equipped with angled holder for 96 dw-plates or for flasks
- Infors Ecotron shaker, 25 mm shaker throw

Liquid handling systems

- Mettler Toledo, Liquidator96 (96-channel pipette. Preparation of glycerol stocks and inoculation of cell cultures
- Tecan liquid handling system capable of pipetting water or organic solvents in 8- and 96- channels, for high throughput screening. Extraction of reactions and transfer of organic phase to 96-well glass plates

Sonicator: Bandelin Sonoplus HD 2070 with SGH 213G and TT13, 5x10cycles, 40% power

Centrifuges

- Thermo Sorvall RC 6 Plus, F21-8x50 at 16000 rpm, separate cell lysate components
- Thermo Sorvall RC 6 Plus, F10s-6x500y at 5000 rpm, harvest cells after heterologous expression in flasks
- Eppendorf 5810R at 4000 rpm, able to cool to 4 °C

UV-Vis Photometer: JASCO V650, (equipped with water bath Julabo, PAC-743 Peltier cell changer, temperature controller)

FPLC: Amersham Bioscience Äkta (Monitor UPC900 and pump P920, column: column body and material for Ni-NTA and Talon purification, GE Healthcare Hiload 26/60 Superdex)

GC: Agilent 7890B and 7820A GC-FID,

HPLC: Shimadzu Prominence LC-2030C capable for high throughput screening

LC-MS: Agilent 1200 HPLC coupled with Agilent 6120 Quadrupole MS system

Preparative HPLC: Gilson HPLC equipped with Macherey-Nagel Nucleodur C18 HTec 250/16, 5µm

6.6 Chemicals

All chemicals were purchased in the highest available purity. In table 27, some selected chemicals for biotransformation and synthesis are listed, all others can be found in the cataster of the Hoebenreich group.

Table 27. List of selected chemicals used for synthesis and

chemical	producer	purity
α -ketoglutarate disodium dihydrate	Alfa Aesar	99%
$(\text{NH}_4)_2\text{Fe}(\text{SO}_4)_2 \cdot 6\text{H}_2\text{O}$	Bernd Kraft	reinst
L(+) ascorbic acid	AppliChem	BioChemica
Dithioreithol	Carl Roth	$\geq 99\%$
Lysozym	AppliChem	BioChemica
NADP+ sodium	AppliChem	BioChemica
Glucose Dehydrogenase	self prepared	
HEPES	Carl Roth	$\geq 99.5\%$
NaCl	ChemSolute	$\geq 99\%$
dipotassiumhydrogenphosphate trihydrate	Merck	
potassiumdihydrogenphosphate	ChemSolute	$\geq 99.5\%$
LHMDS 1M in THF	Sigma Aldrich	
MeI	Alfa Aesar	99% stabilized with copper
(S)-Carvone	Sigma Aldrich	$\geq 96\%$

7. Methods

In this chapter, all methods are described. The chapter is subdivided in biological experiments (ch. 7.1), biotransformation (ch. 7.2), preparative scale biotransformation (ch. 7.3), chemical synthesis (ch. 7.4) and analytical methods (ch. 7.5).

7.1 Biological Experiments

Polymerase chain reactions (PCR) were performed in a Mastercycler Gradient of Eppendorf. Genes were sequenced using primer T7-1 and pRSF_rv (table 26) by GATC. For all experiments, water of micro pure grade (conductivity 0.055 $\mu\text{S}/\text{cm}$ MicroPure system of TKA) was used. To purify plasmid DNA, GeneElute Plasmid Miniprep kit (PLN350) purchased from Sigma Aldrich was used. To purify smaller fragments as genes or PCR products, GeneElute PCR purification kit (NA1020) purchased from Sigma Aldrich was used.

7.1.1 Cloning with Polymerase Chain Reaction

7.1.1.1 Polymerase Chain Reaction^[434]

Polymerase chain reaction describes the in vitro amplification of DNA with the help of purified DNA polymerase. Its discovery in 1968 was a milestone in establishing molecular biology research. All cloning and most mutagenic methods base on polymerase chain reaction.

7.1.1.2 Amplification of Genes

Amplification of genes was performed by mixing 80-100 ng template (2 μL genomic DNA, 50 ng/ μL) with 1 U KOD-polymerase (Novagen), 1xKOD-buffer, 1.5 mM MgSO_4 , 0.3 μM primer (forward and reverse), 0.2 mM dNTPs in a total volume of 50 μL . Hotstart PCR was performed by initial denaturation at 95 °C for 3 min, followed by 30 cycles of 95 °C for 25 s, 53 °C for 30 s and 72 °C for 90 s and final extension at 72 °C for 10 min.

Before usage in restriction-free cloning, the PCR product was purified by GeneElute PCR purification kit purchased from Sigma Aldrich (NA1020) following the given instructions except final elution with 35 μL H_2O instead of elution buffer. DNA concentration was measured by absorption (Eppendorf Biophotometer). A yield of 55-170 ng/ μL was obtained.

7.1.1.3 Restriction-Free Cloning^[327]

Restriction-free cloning (rf-cloning) was performed by using 100 ng gene (purified PCR product), 20 ng vector (pRSF-Duet), 1x HF buffer, 1 μL Phusion polymerase (self-produced without determination of U/ μL), 0.2 mM dNTPs in a total volume of 50 μL . The PCR reaction was started by initial heating to 98 °C for 30 s, followed by 18 cycles of 98 °C for 25s and 72 °C for 5.5 min. A final elongation time of 10 min was used. The PCR mix was digested with DpnI, dialyzed (ch. 7.1.4) and 50 μL electro competent *E. coli* BL21-Gold(DE3) cells were transformed

with 2 μL DNA and plated on LB-agar. To confirm the insertion of the gene, colony PCR was performed. In

table 36 all cloned genes with errors and silent mutations are given.

7.1.1.4 Colony PCR

For colony PCR, some cell material (taken off with 10 μL pipette tip) was suspended in 20 μL H_2O . 5 μL of the cell suspension were mixed with 0.2 mM dNTPs, 1x reaction buffer (Thermo-Pol or HF buffer), 2.5 U polymerase Taq or Phusion Polymerase, 0.3 μM primer flanking the inserted gene (reverse and forward), 1.5 mM MgSO_4 and water to a total volume of 50 μL . PCR was performed with an initial denaturation at 95 $^\circ\text{C}$ for 3 min, followed by 25 cycles of 95 $^\circ\text{C}$ for 25 s, 53 $^\circ\text{C}$ for 30 s and 72 $^\circ\text{C}$ for 90 s. A final elongation time of 10 min at 72 $^\circ\text{C}$ was used. The PCR was analyzed by agarose gel electrophoresis (1% agar in TAE buffer, stained with 3 $\mu\text{L}/100\text{ mL}$ midori green). If the gel confirmed gene incorporation, LB medium was inoculated with the remaining water-cell mixture and grown overnight. The preculture was used for plasmid preparation according to the manufacturer's instruction (GeneElute Plasmid Miniprep kit, Sigma Aldrich PLN350), using 70 μL H_2O for final elution and send for sequencing.

7.1.2 Mutagenesis with Polymerase Chain Reaction

Primers were created with SnapGene Viewer. Degeneration and tailor-made mixture of codons were designed using DC_Analyzer^[370] and purchased in desalted quality from Sigma Aldrich. Quick Quality Control (QQC)^[306] was performed to assess obtained degeneracy after PCR and transformation. If the degeneracy was not satisfying in the first attempt, a second round of PCR was performed using the plasmid pool resulting from the first PCR as template for the second PCR. For all experiments with *Wi-WelO15*, template *Wi-welO15* V6I/D284N (*Wi-0*) was used, containing two mutations from cloning.

7.1.2.1 QuikChange^[369]

For QuikChange PCR, two mutagenesis primer are designed which have a partially overlapping part. In the PCR, the whole plasmid is amplified, and the mutation introduced through the primer. The overlapping part can recombine homologue and *E. coli* BL21-Gold(DE3) are transformed with the plasmid (still with nicks). *E. coli* enzymes ligate the plasmid after transformation.

7.1.2.2 Repair of Frame Shift Mutation in *Hw-WelO15*

The reaction was performed by mixing 0.5 ng/ μL plasmid DNA, with 1 U KOD Hot-start polymerase, 1xKOD-buffer, 2 mM MgSO_4 , 0.3 μM primer 26 and 27, 0.2 mM dNTPs in a total volume of 25 μL . The reaction was initialized by a 2 min heating at 95 $^\circ\text{C}$, followed by 25 cycles of 95 $^\circ\text{C}$ for 20 s, 56 $^\circ\text{C}$ for 10 s and 70 $^\circ\text{C}$ for 5.50 min followed by a final elongation at 70 $^\circ\text{C}$ for 10 min. The PCR mixture was digested with DpnI by adding 1 μL of DpnI (20 U) into the

PCR mix. The mixture was incubated at 37 °C for 2 h, dialyzed against H₂O for 30 min at rt. 2 µL were transformed with 50 µL of electrocompetent cells and plated on LB-agar.

7.1.2.3 Error Prone PCR^[284,362,435,436]

The mutation was performed by two PCR steps. In the first PCR, the gene was mutated by error prone PCR (epPCR). The PCR product was digested with DpnI to remove the template gene, followed by PCR purification (Sigma Aldrich kit). In a second PCR, the mutated gene was used as megaprimer to amplify the remaining plasmid. The PCR conditions were adapted depending on the number of mutations that should be incorporated which is dependent on the length of the DNA strain. Therefore, different conditions were chosen for the two parts. In the following, mutation of both parts is described.

Error Prone PCR: Mutation of the Lid Region

This part of the gene is 297 bp long. To achieve an average of 2-3 mutations per gene, 15 rounds of amplification will be performed. To get sufficient DNA for further steps, in total 8 reactions were prepared as master mix and divided in 50 µL per vial. 20 pg/µL template DNA (pRSF-Duet containing *Hw-WelO15* (1 µL with 1 ng/µL) was mixed with 1x Thermopol buffer (NEB), 2 µM primer 34 (20 µM) and 2 µM primer 36 (20 µM), 0.5 mM MnCl₂ (25mM stock solution, self-prepared) and 7 mM MgSO₄ (25 mM stock solution, Novagen). 1 µL 10 mM dNTPs was added, for a final concentration of 0.2 mM dATP and dGTP. To reach a final concentration of 1 mM dCTP and dTTP, 1.6 µL of a 25 mM solution of each dCTP and dTTP (Carl Roth) was added. 18.3 µL H₂O and 0.05 U/µL Taq polymerase were added to reach the final volume of 50 µL. The reaction was performed by initial denaturation at 95 °C for 30 s followed by 15 cycles of 95 °C for 15 s, 57°C for 30 s and 68 °C for 25 s. A final elongation of 10 min at 68 °C was used.

To check if amplification occurred, an agarose gel (ch. 7.1.3) was run. Because of the low DNA concentration, 25 µL DNA sample were applied in one gel pocket. The template DNA was digested by adding 2 µL DpnI (NEB, 20 U/µL) to 375 µL PCR product, coming from 8 PCR and incubated for 2.5 h at 37°C. After that purification of the DNA fragment was performed (PCR purification kit from Sigma Aldrich). Elution with 35 µL H₂O yielded a DNA concentration of 16 ng/µL. The mutated gene was used in the following step as megaprimer.

Megaprimer PCR was prepared by mixing 1x HF buffer (NEB), 0.2 mM dNTPs each, either 0.5 mM betaine or 10% DMSO, 30 ng megaprimer (16 ng/µL), 1 ng/µL plasmid pRSF-Duet containing *Hw-WelO15*, 0.5 mM MgSO₄, 1 µL Phusion Polymerase and 8.1 µL H₂O to a final volume of 25 µL. Hotstart PCR was performed by initial denaturation at 98 °C for 30 s, followed by 25 cycles of 98°C for 25 s and 72 °C for 10 min. The reaction was finished by a final elongation of 10 min at 72 °C. The product was digested by DpnI, dialyzed and 50 µL *E. coli* BL21-Gold(DE3) were transformed with 3 µL DNA. After electroporation, cells were diluted with

1 mL LB-medium. After incubation for 1 h at 37°C, 300 µL medium with cells were plated on a big agar plate.

Error Prone PCR: Mutation of the Active Site Region

This part of the gene is 483 bp long. Originally only 2-3 bases should be mutated. Therefore only 8 amplification steps should have been used. Since no results were obtained by this trial, the amplification steps were increased to 13 which increases also the number of theoretical mutations. To get sufficient DNA for further steps, in total 10 reactions were prepared as master mix and divided in 50 µL per vial.

20 pg/µL template DNA (1 µL with 1 ng/µL) was mixed with 1x Thermopol buffer (NEB) and 2 µM primer 35 and 21 (table 26) (20 µM stock solution). 0.5 mM MnCl₂ (25 mM stock solution, self-prepared) and 7 mM MgSO₄ (25 mM stock solution from Novagen). 1 µL of a 10 mM dNTPs solution was added, for a final concentration of 0.2 mM dATP and dGTP. To reach a final concentration of 1 mM dCTP and dTTP, 1.6 µL of a 25 mM solution of each dCTP and dTTP (Carl Roth) were added. 18.3 µL H₂O were added and the initial denaturation was performed without polymerase for 2 min at 95 °C. Then 0.05 U/µL Taq polymerase (5 U/µL) was added and the reaction performed with 13 cycles of 95 °C for 20 s followed by 30 s at 53°C and 3 min at 68 °C. A final elongation of 10 min at 68 °C was used.

10x50 µL PCR product were combined and purified via PCR purification kit from Sigma Aldrich and eluted in the last purification step with 30 µL H₂O. The sample was digested by adding 4 µL CutSmart buffer (10x, NEB), 0.25 µL DpnI (20U/µL) and 5 µL H₂O. After digestion, it was purified again via purification kit, resulting in 33 µL with 31 ng/µL. The mutated gene was further used as megaprimer to amplify the complete plasmid.

Megaprimer PCR was prepared by mixing 1x HF buffer (NEB), 0.2 mM dNTPs each, either 0.5 mM betaine or 10% DMSO, 31 ng megaprimer (31 ng/µL), 1 ng/µL plasmid DNA, 0.5 mM MgSO₄, 1 µL Phusion Polymerase and 8.75 µL H₂O to a final volume of 25 µL. Hotstart PCR was performed by initial denaturation at 98 °C for 2 min, followed by 25 cycles of 98°C for 30 s and 72 °C for 12 min. The reaction was finished by a final elongation of 10 min at 72 °C. The product was digested by DpnI, dialyzed and 50 µL *E. coli* BL21-Gold(DE3) competent cells transformed with 3 µL. After electroporation, cells were diluted with 1 mL LB-medium. After incubation for 1 h at 37°C, 300 µL medium with cells were plated on a big agar plate. For further steps, the sample with betaine was used.

7.1.2.4 Structure Guided Mutagenesis

In the following the PCR conditions for each library are given. Codons in *italic* represent DNA bases, while single letter codes represent amino acids e.g. *V90NNK* (DNA bases) and *V90P* (amino acid). Sequencing results from quick quality control are shown in chapter 0.

For all PCRs a standard protocol was used, 95 °C, 2 min initial denaturation followed by 25 cycles 95 °C, 30 s; annealing time and temperature were individually chosen and are described in the following paragraphs, 9 min 70°C and a final elongation of 10 min at 70°C.

7.1.2.5 1st Generation: Hot Spot Identification

N74NNK: Primers 71 and 72 were used. An annealing time of 60 s was used in combination with $T_{\text{annealing}}=63.3$ °C and 0.5 M betaine. A second PCR round was performed using the resulting plasmid pool of the first PCR as template. Here an annealing time of 60 s was used in combination of $T_{\text{annealing}}=63.3$ °C and 0.25 M betaine.

F77NNK: Primers 59 and 60 were used. The best degeneration gave 1 M betaine with $T_{\text{annealing}}=47.8$ °C and an annealing time of 45 s.

A82NNK: Primers 37 and 38 were used. The first PCR was performed with 0.5 M betaine and 58.9 °C annealing temperature, 30 s annealing time. A second round of PCR was performed using the resulting plasmid pool of the first PCR. 0.25 M betaine with an annealing temperature of 58.9 °C (A82NNK-1) and 1 M betaine with an annealing temperature 60.5 °C (A82NNK-2) gave best results. Colonies from both libraries were screened.

I84NNK: Primers 39 and 40 were used. The first PCR was performed with 0.5 M betaine, 63.7 °C annealing temperature and 30 s annealing time. Since the degeneracy was not satisfying, a second round of PCR was performed using the resulting plasmid pool of the first PCR. The best results gave 0.25 M betaine in combination with $T_{\text{annealing}}=62.2$ °C.

V90NNK: Primers 61 and 62 were used. The best degeneration gave 0.5 M betaine with $T_{\text{annealing}}=54$ °C and an annealing time of 45 s was used.

F169NNK: Primers 73 and 74 and an annealing time of 45 s were used. The best degeneration gave 0.5 M betaine with $T_{\text{annealing}}=63.3$ °C.

M221NNK: Primers 67 and 68 with an annealing time of 45 s were used. Betaine concentration of 0.5 M were combined with 55.1 °C in a first PCR and in a second PCR a temperature range of 53.2-55.0 °C was tested with 0.25-1.0 M betaine. However, no degeneration could be achieved. If this library should be created, new primer should be designed.

M225NNK: Primers 69 and 70 and an annealing time of 45 s were used. The best degeneration gave 0.5 M betaine with $T_{\text{annealing}}=53.5$ °C. A second round of PCR was performed using the resulting plasmid pool of the first PCR. Here 0.5 M betaine, 55.1 °C annealing temperature and 45 s annealing time were used.

A82_/I84_: The following selected amino acids were chosen to be incorporated. For A82: D, Q, E, H, N, I, F, A, L, M, S, T, V. For I84: D, Q, E, H, N, I, S, T. To achieve this tailor-made set of

Methods

amino acids with minimal redundancy, the DC_Analyzer^[370] was used, resulting in codons AWC, DYG, SAM for position A82 and SAM, ANC for position I84. Mixing all primers and performing a single PCR resulted in poor degeneracy, leading to 8 separately optimized libraries as given below. Using an annealing time of 30 s, annealing temperature of 62.2 °C and 0.5 M betaine. A second round of PCR was prepared with individually chosen parameters.

A82AWC/I84SAM: Primers 49 and 50 were used. In the second PCR round, the annealing time was elongated to 60 s and an annealing temperature of 62.2 °C used.

A82AWC/I84ANC Primers 51 and 52 were used. In the second PCR round, a betaine concentration of 1 M and an annealing temperature of 61.5 °C was used.

A82DYG/I84SAM: Primers 45 and 46 were used. In the second PCR round, the annealing time was elongated to 60 s and an annealing temperature of 62.2 °C used.

A82DYG/I84ANC: Primers 47 and 48 were used. In the second PCR round, an annealing temperature of 61.5 °C and 0.25 M betaine were used.

A82SAM/I84SAM: Primers 41 and 42 were used. In the second PCR round, the annealing time was elongated to 60 s and an annealing temperature of 62.2 °C used.

A82SAM/I84ANC: With primers 43 and 44 the degeneration of I84ANC worked bad. Therefore, the plasmid pool from A82DYG/I84ANC was used as template where I84ANC was incorporated quite good. Based on this template, primer 29 and 30 were used for amplification in combination with 0.5 M betaine and annealing temperature of 62.1°C and an annealing time of 30 s.

A82F: Since the degeneration of A82F/I84ANC and A82F/I84SAM worked badly, A82F was created as single variant and the libraries were based on this template. For the creation of A82F, primers 57 and 58 were used with 0.5 M betaine, $T_{\text{annealing}}=61^{\circ}\text{C}$ and an annealing time of 30 s was used.

A82F/I84ANC: As template *Wi-welO15 V6I/A82F/D284N* in combination with primers 55 and 56 were used. A betaine concentration of 0.5 M, an annealing time of 30 s and an annealing temperature of 63.7 °C was used.

A82F/I84SAM: As template *Wi-welO15 V6I/A82F/D284N* in combination with primers 53 and 54 were used. A betaine concentration of 0.5 M, an annealing time of 30 s and an annealing temperature of 63.7 °C was used.

7.1.2.6 2nd Generation: Multi-Site Libraries

A82L/V90NNK: As template *Wi-welO15* V6I/A82L/D284N in combination with primer 61 and 62 were used. 0.5 M betaine was used with an annealing temperature of 56 °C and 30 s annealing time.

I84ABC/A88NNK/V90P: Mutagenesis with primers 21 and 84 was performed by Henrik Müller.^[386]

5-Residue-Site Library

To mutate positions V81, A82, I84, A88 and V90 at the same time, a QuikChange PCR strategy was chosen (figure 30). To incorporate all designed amino acids alphabets, 8 primers had to be bought. Amplification was tested by using only one set of primers, giving slight degenerations in desired positions (plasmid pool 1). Based on this template, a second and third round of PCR was set with the combination of all 8 primers, so that a complete absence of wild-type template was ensured. QQC revealed absence of thymine in the 1st base of position 81 in pool indicating that Phe will be missing in the library. Similarly, a very low presence of adenine and guanine in the 2nd base of A88 was observed. Therefore, a fourth round of PCR was set on plasmid pool 2 with primers especially encoding these missed bases, creating plasmid pool 4. Degeneration of all plasmid pools can be seen in figure 87.

Standard PCR conditions were used with the following changes: either *Wi-welO15* V6I/D284N in pRSF-Duet (PCR 1) or plasmid pools resulting from previous PCRs (PCR 2-4) were used as template, primers 75+76 were used for PCR 1, primers 75-82 for PCR 2 and 3 and primers 78+80 for PCR 4, betaine PCR1: 0.5 M, PCR 2+3: 0.6 M, PCR4: 0.8 M. Annealing time was 45 s and individually optimized annealing temperatures were PCR1: 57.3 °C, PCR 2+3: 53.0 °C PCR4: 51.6 °C. 100 µL *E. coli* DH5α competent cells were transformed with 2 µL PCR products and 1 mL plated on agar plates prior to QQC. *E. coli* BL21-Gold(DE3) competent cells were transformed with plasmid pools 2, 3 and 4 by mixing 1 µL DNA with 100 µL electro competent cells. After electro shock, the cell suspension was mixed with 2 mL prewarmed SOC medium. 150 µL cell suspension was plated on freshly prepared LB-kan⁵⁰ agar plate (15 g agar/L LB medium). Colonies for screening were picked from pools 2-4 in equal parts.

7.1.2.7 3rd Generation: Addition of N74R and Scaffold Sampling

N74R by Megaprimer PCR

To incorporate the N74R mutation, a PCR was prepared using the standard protocol and primer 10 and 83. Hotstart PCR was performed by initial denaturation at 95 °C for 2 min, followed by production of the megaprimer within 10 cycles of 95 °C for 30 s, 64.2 °C for 20 s and 68 °C for 15 s, followed by amplification of the whole plasmid by further 25 cycles of 95°C for 30 s and 68 °C for 6.5 min. The reaction was finished by a final elongation of 10 min at 68 °C.

M221L/M225I by Megaprimer PCR

The mutations M221L/M225I were introduced in *Wi-0* and *Wi-5* using primer 10 and 89. Megaprimer PCR was using the standard protocol with 0.5 M betain. Hotstart PCR was performed by initial denaturation at 95 °C for 2 min, followed by production of the megaprimer within 11 cycles of 95 °C for 30 s, 60.0 °C for 30 s and 68 °C for 45 s, followed by amplification of the whole plasmid by further 25 cycles of 95 °C for 30 s and 68 °C for 5.5 min. The reaction was finished by a final elongation of 10 min at 68 °C.

A82L/V90P by QuikChange PCR

These mutations were introduced into *Hw-WelO15*. PCR was performed by mixing 0.2 ng/μL plasmid DNA (pRSF-Duet with *Hw-welo15*), 0.3 μM each primers 87 and 88, 1x KOD buffer, 0.2 mM dNTPs each, 0.5 M betaine, 1.5 mM MgSO₄, 1 U KOD Polymerase and 18 μL H₂O to a total volume of 50 μL. Hotstart PCR was performed by initial denaturation at 95 °C for 2 min, followed by 25 cycles of 95 °C for 30 s, 62°C for 45 s and 68 °C for 5.5 min. The reaction was finished by a final elongation of 10 min at 68 °C. Successful incorporation of mutation was checked by sequencing. Hereby single mutants A82L, V90P and double mutant A82L/V90P were identified.

7.1.2.8 4th Generation: Multi-Site Libraries on *Wi-5* and *Wi-8*

N74(NSQR)/S93(NHDASVL)/S103(NHDASVL)/A175(NHDASVL) on template *Wi-WelO15 V6I/A82L/V90P/D284N (Wi-5)*

First the degeneration in position N74 was introduced by QuikChange PCR following standard protocol using primers 90 and 91 and 0.3 M betaine. The reaction was performed by incubation at 95 °C for 2 min, followed by 30 cycles of 95 °C for 30 s, 56.1 °C for 30 s and 68 °C for 6.5 min. The reaction was finished by a final elongation of 10 min at 68 °C. The product was digested by DpnI, dialyzed and transformed with *E. coli* BL21-Gold(DE3) cells. Successful incorporation of mutation was checked by QQC. Since degeneration was not satisfying, the same reaction was performed again but as template, the plasmid pool was used that was received in the first PCR. Positions S93, S103, A175 were mutated by megaprimer PCR. The PCR consisted of 10 ng template *Wi-WelO15 V6I/N74(NSQR)/A82L/V90P/D284N*, 0.3 μM reverse primer (primer 96 and 97, 0.15 μM each) and 0.3 μM forward primer (primer 92-95, 0.075 μM each), 1x KOD buffer, 0.3 M betaine, 1.5 mM MgSO₄, 0.2 mM dNTPs each and 1 U KOD hot start polymerase in a final volume of 50 μL. The mix was incubated for 2 min at 95 °C followed by 10 cycles of 95 °C for 30 s, 64.3 °C for 30 s and 68 °C for 30 s to produce the megaprimer. Followed by 25 cycles of 95 °C for 30 s and 68 °C for 6.5 min. The reaction was finished with a final elongation step for 10 min at 68 °C. The mix was digested with DpnI, dialyzed against H₂O and transformed into *E. coli* BL21-Gold(DE3) cells. Since degeneration was not satisfying, the same reaction was performed again but as template, the obtained plasmid pool from this PCR was used.

S93(NHDASVL)/S103(NHDASVL)/A175(NHDASVL) on template *Wi-WelO15* N74R/V81T/A82M/A88V/V90P (*Wi-8*)

Positions S93, S103, A175 were mutated by megaprimer PCR using the standard protocol with 0.3 μ M reverse primer 96 and 97 (0.15 μ M, each) and 0.3 μ M forward primer (primer 92-95, 0.075 μ M each), 0.3 M betaine. The mix was incubated for 2 min at 95 °C followed by 10 cycles of 95 °C for 30 s, 64.3 °C for 30 s and 68 °C for 30 s to produce the megaprimer. Followed by 25 cycles of 95 °C for 30 s and 68 °C for 6.5 min. The reaction was finished with a final elongation step for 10 min at 68 °C. QQC revealed bad degeneracy, so the PCR was repeated using the plasmid pool from the first mutagenesis PCR as template for the second round.

7.1.2.9 Single Mutants

G116D Mutants by Megaprimer PCR

To incorporate mutation G166D, the PCR was prepared by mixing 1x KOD buffer, 0.2 mM dNTPs each, 0.5 M betaine, 0.3 μ M primers 10 and 86, 0.2 ng/ μ L plasmid DNA, 1.5 mM MgSO₄, 1 U KOD Polymerase and 18 μ L H₂O. Hotstart PCR was performed by initial denaturation at 95 °C for 2 min, followed by production of the megaprimer within 11 cycles of 95 °C for 30 s, 64.2 °C for 20 s and 68 °C for 30 s, and amplification of the whole plasmid by further 25 cycles of 95°C for 30 s and 68 °C for 5.5 min. The reaction was finished by a final elongation of 10 min at 68 °C. The product was digested by DpnI, dialyzed and 50 μ L *E. coli* BL21-Gold(DE3) competent cells transformed with 2 μ L digested PCR product

284D by Megaprimer PCR

The PCR was prepared by mixing 1x KOD buffer, 0.2 mM dNTPs each, 0.5 M betaine, 0.3 μ M primers 10 and 104, 0.2 ng/ μ L plasmid DNA, 1.5 mM MgSO₄, 1 U KOD Polymerase and 18 μ L H₂O. Hotstart PCR was performed by initial denaturation at 95 °C for 2 min, followed by production of the megaprimer within 11 cycles of 95 °C for 30 s, 57.0 °C for 30 s and 68 °C for 60 s, followed by amplification of the whole plasmid by further 25 cycles of 95°C for 30 s and 68 °C for 6.5 min. The reaction was finished by a final elongation of 10 min at 68 °C. The product was digested by DpnI, dialyzed and 50 μ L *E. coli* BL21-Gold(DE3) competent cells transformed with 2 μ L digested PCR product.

S103A by Megaprimer PCR

The PCR was prepared by mixing 1x KOD buffer, 0.2 mM dNTPs each, 0.5 M betaine, 0.3 μ M primers 21 and 98, 0.2 ng/ μ L plasmid DNA, 1.5 mM MgSO₄, 1 U KOD Polymerase and 18 μ L H₂O. Hotstart PCR was performed by initial denaturation at 95 °C for 2 min, followed by production of the megaprimer within 11 cycles of 95 °C for 30 s, 66.0 °C for 30 s and 68 °C for 45 s, followed by amplification of the whole plasmid by further 25 cycles of 95°C for 30 s and 68 °C for 6.5 min. The reaction was finished by a final elongation of 10 min at 68 °C. The product

was digested by DpnI, dialyzed and 50 μ L *E. coli* BL21-Gold(DE3) competent cells transformed with 2 μ L digested PCR product.

S103A/Q123R/S230K by Megaprimer PCR

The PCR was prepared by mixing 1x KOD buffer, 0.2 mM dNTPs each, 0.5 M betaine, 0.3 μ M primers 99 and 100, 0.2 ng/ μ L plasmid DNA, 1.5 mM MgSO₄, 1 U KOD Polymerase and 18 μ L H₂O. Hotstart PCR was performed by initial denaturation at 95 °C for 2 min, followed by production of the megaprimer within 11 cycles of 95 °C for 30 s, 55.0 °C for 30 s and 68 °C for 30 s, followed by amplification of the whole plasmid by further 25 cycles of 95°C for 30 s and 68 °C for 6.5 min. The reaction was finished by a final elongation of 10 min at 68 °C. The product was digested by DpnI, dialyzed and transformed into *E. coli* BL21-Gold(DE3) cells.

S103A/Q123R/S230K/Q236N/S239W/S268R/Q282D by Megaprimer PCR

The PCR was prepared by mixing 1x KOD buffer, 0.2 mM dNTPs each, 0.5 M betaine, 0.3 μ M primer 101, 0.15 μ M primers 102 and 0.15 μ M 103, 0.2 ng/ μ L plasmid DNA, 1.5 mM MgSO₄, 1 U KOD Polymerase and 18 μ L H₂O. Hotstart PCR was performed by initial denaturation at 95 °C for 2 min, followed by production of the megaprimer within 11 cycles of 95 °C for 30 s, 61.0 °C for 30 s and 68 °C for 15 s, followed by amplification of the whole plasmid by further 25 cycles of 95°C for 30 s and 68 °C for 6.5 min. The reaction was finished by a final elongation of 10 min at 68 °C. The product was digested by DpnI, dialyzed and 50 μ L *E. coli* BL21-Gold(DE3) competent cells transformed with 2 μ L digested PCR product.

7.1.2.10 Mutagenesis of P450_{BM3}

The PCR was prepared by mixing 1x KOD buffer, 0.2 mM dNTPs each, 0.3 M betaine, 0.1 μ M primers 105-110, 0.2 ng/ μ L plasmid DNA, 1.5 mM MgSO₄, 1 U KOD Polymerase and 18 μ L H₂O. Hotstart PCR was performed by initial denaturation at 95 °C for 2 min, followed by 25 cycles of 95°C for 30 s, 68.0 °C for 30 s and 68 °C for 11 min. The reaction was finished by a final elongation of 10 min at 68 °C. The product was digested by DpnI, dialyzed and 50 μ L *E. coli* BL21-Gold(DE3) competent cells transformed with 2 μ L digested PCR product. The three variants used for bigger scale reactions were sequenced with primers 2 and 4-6 to cover the whole gene. When sequencing variant P450_{BM3} R47V/F87G/L181T/L188N, the sequence in the range between 1640-1720 bp was missing (between primer 2 and 3), therefore another sequencing primer 7 was created and used to sequence this part of the gene. It was confirmed, that the gene is complete and without any mutations in comparison to its wild type.

7.1.3 Agarose Gel Electrophoresis

DNA fragments were separated by agarose gel electrophoresis. For the set-up, 1% agarose in tris acetate EDTA (TAE) buffer were heated up in the microwave until all agarose was solved. After cooling to about 60 °C, 3 μ L/100 mL midori green was added which interacts with the

DNA and acts as dye. The agarose was poured into the form together with a comb to prepare pockets for the DNA sample.

The DNA samples were mixed with 6x DNA sample buffer (NEB), an appropriate amount of DNA (at least ~20 ng) were loaded to the gel. As size standard, a DNA ladder was added to one pocket of the gel. A voltage of 120 V was applied until the run is finished. Progress of separation was checked under UV light.

7.1.4 DpnI Digestion and Dialysis

To remove template DNA, a DpnI digestion was performed. DpnI from NEB (20U/ μ L) was used by preparation of a master mix, due to high DpnI concentration. To check performance of DpnI and avoid high background during mutagenesis, DpnI controls were always performed (one sample without polymerase in PCR). A master mix was prepared for digestion by mixing 5 μ L CutSmart buffer, 0.75 μ L H₂O and 0.25 μ L DpnI per sample. 5.75 μ L of the master mix was added to each probe and incubated for at least 2 h at 37 °C. For the following electroporation the DNA must be desalted. Therefore, dialysis membranes with a pore size of 0.05 μ m type VMWP (Merck Millipore) were used. H₂O was added into a petri dish and the membrane placed on top. The complete DNA sample was put on the membrane and dialyzed for 30 min at room temperature without lid. The DNA was taken into a new cup and electroporation performed.

7.1.5 Electrotransformation

By transformation, DNA such as plasmids can be inserted into cells. Since *E. coli* has no natural competence, the membrane has to be made permeable. Hereby electro transformation was used. For that it is necessary to use cells that are desalted (ch. 7.1.6).

The transformation was performed by thawing a 50 μ L aliquot of competent cells on ice and mixing it with 4 μ L of the digested, library PCR product or 1 μ L plasmid DNA (~100 ng). The mixture was transferred into a precooled electroporation cuvette with 2 mm gap (Peqlab). Then a MicroPulser electroporator (Bio-Rad) was used with the setting Ec2. The voltage duration is measured with an optimal value of about 5.8 ms. Afterwards 1 mL LB media was added, the cell suspension was put into 1.5 mL reaction tubes and the closed tube was incubated in a thermomixer at 700 rpm and 37 °C for one hour. Then the cells were centrifuged (1 min, 10000 rpm, Eppendorf centrifuge 5418) and resuspended in 100 μ L LB-medium. The suspension was plated on LB-agar-antibiotic plates and incubated overnight at 37 °C. For long time storage, the plates were kept at 4 °C.

To reuse electro cuvettes, the cuvettes were washed immediately after usage with water and 70% EtOH twice. Before reuse, the cuvettes were stored overnight in water. After drying the cuvettes in a heating oven (70°C), they were incubated with 0.1 M H₂SO₄ for 10 min, the cuvettes were washed again with water and 70% EtOH twice. After drying at 70°C, they were closed and stored in a box until further use.

7.1.6 Preparation of Electrocompetent Cells^[437]

5 mL LB preculture of *E. coli* BL21-Gold(DE3) with 10 μ M tetracycline were inoculated from a glycerol stock and incubated overnight at 37 °C, 200 rpm (Infors HT shaker). A 2 L baffled flask with 300 mL LB-Media was inoculated with 3 mL preculture and 10 μ M tetracycline. The flask was incubated in the shaker with 200 rpm, 37 °C. When OD₆₀₀ reached 0.4-0.6, the flask was cooled on ice for 30 min. Then the cell suspension was transferred into precooled 50 mL reaction tubes and centrifuged at 3500 rpm, 4 °C for 8 min. The supernatant was discarded, the pellets washed and resuspended in several steps, using 45, 25, 2 and 0.5 mL chilled 10 % glycerol. After every resuspension step, the cells were pelleted at 4 °C and 3500 rpm for 8 min. Finally, all cells were pooled together, centrifuged and resuspended in 1.7 mL 10% glycerol. The cells were aliquoted in 50 μ L, shock frozen in liquid nitrogen and kept frozen at -80 °C until further usage.

7.1.7 Plasmid Preparation

The isolation of plasmids was performed using the plasmid preparation kit of Sigma Aldrich. Either a 5 mL culture is prepared and at least incubated for 8 h at 37 °C and the cells pelleted, or to control the quality of libraries, the colonies, grown on an agar plate were resuspended in water and pelleted. The pellets were prepared as described in the manual. Before eluting, the column was additionally dried at room temperature for 5 min and incubated for 2 min with the eluent (H₂O), before centrifuging. The plasmid DNA from preculture is being eluted with 70 μ L water for pRSF-Duet vector, while the DNA prepared from plate only was eluted with 35 μ L. The procedure is checked by measuring concentration and absorption coefficients. A biophotometer of Eppendorf is used with cuvettes which are applicable in the UV range (Brand). A dilution of 70 μ L solvent with 5 μ L sample was prepared for concentration determination. First a blank measurement was performed for each cuvette with the 70 μ L solvent before adding DNA and measuring concentration.

7.1.8 Cultivation of Precultures and Preparation of Glycerol Stocks

Precultures, used for inoculation of heterologous expression, starting material for plasmid preparation etc. were prepared in test tubes. 5 mL LB medium with antibiotics were filled in a tube and either a colony from plate or some cell material from a glycerol stock was scratched off with a sterilized toothpick and put in the test tube. The culture was incubated at 37 °C with 200 rpm overnight (Infors HT shaker). For better oxygen transfer, tubes were attached in an inclined way if possible. Glycerol stocks were prepared by mixing 700 μ L preculture with 400 μ L 80% glycerol (aq) and stored at -80 °C.

For precultures in 2.2 mL squared 96 dw-plates (VWR), 900 μ L LB-kan⁵⁰ medium were provided in a plate. Single colonies from a LB-agar plate or material from glycerol stocks were picked with toothpicks, the plates sealed with a gas-permeable foil, attached in the shaker in an inclined way and cells grown overnight at 37 °C and 200 rpm (Infors HT shaker, equipped

with angled plate holders). Glycerol stocks of plates were prepared by mixing 50 μL 80% glycerol (aq) with 100 μL preculture in 96 dw-plates (Nunc). The plate was sealed with belonging plastic lid and stored at $-80\text{ }^{\circ}\text{C}$.

7.1.9 Heterologous Expression for Enzyme Production

7.1.9.1 WelO15 in Baffled Flasks

Halogenase production was performed in 2 L flasks with 0.5 L LB medium. For smaller scale the ratio of flask and volume was kept constant.

Heterologous expression was performed by inoculation of 0.5 L LB-kan⁵⁰ media containing 50 μM FeCl_3 (from a 0.05 M stock in H_2O) in a 2 L baffled flask with 5 mL of preculture. The culture was incubated at $37\text{ }^{\circ}\text{C}$, 200 rpm (Infors HT shaker) until an OD_{600} of 0.4 was reached. Then the temperature was shifted to $22\text{ }^{\circ}\text{C}$ and IPTG (0.1 M in H_2O) was added to a final concentration of 0.02 mM. Cells were grown overnight, harvested by centrifugation (5000 rpm, 15 min, $4\text{ }^{\circ}\text{C}$) and resuspended either in Tris A buffer (100 mM, $\text{pH}=7.4$) for purification or in HEPES 2 buffer for biotransformations. The cell suspension was transferred into 50 mL plastic tubes and stored at $-20\text{ }^{\circ}\text{C}$ until further use.

7.1.9.2 WelO15 Variants in 2.2 mL Squared Deep Well Plates

Heterologous expression was performed by adding 100 μL preculture to 700 μL LB-kan⁵⁰ with 20 μM IPTG and 50 μM FeCl_3 in a 2.2 mL dw-plate. The culture was grown at $37\text{ }^{\circ}\text{C}$, 200 rpm for 2 h followed by temperature reduction to $22\text{ }^{\circ}\text{C}$ and incubation for additional 16 h. The plates were centrifuged at 4000 rpm and $4\text{ }^{\circ}\text{C}$ (5810R Eppendorf centrifuge) for 10 min. The supernatant was discarded, the plates sealed with plastic lids and frozen at $-80\text{ }^{\circ}\text{C}$. For longer storage the plates were moved to a $-20\text{ }^{\circ}\text{C}$ freezer.

7.1.9.3 Heterologous Expression of WelP1, HpiI1 and HpiI3

Heterologous expression was performed by N. Braun in analogy to ene-reductase *TsER*. 315 mL TB-medium, 35 mL 10x phosphate buffer and 50 $\mu\text{g}/\text{mL}$ kanamycin were filled into a 2 L baffled flask. After adding 3.5 mL preculture the flask was incubated at $37\text{ }^{\circ}\text{C}$ and 200 rpm until OD_{600} of 0.4 - 0.6. Then 35 μL IPTG (0.1 M) were added and the culture incubated further incubated at $22\text{ }^{\circ}\text{C}$ and 200 rpm overnight. Next, harvest of the cells was accomplished by centrifugation at $4\text{ }^{\circ}\text{C}$ and 5000 rpm for 15 min. The cell pellets were resuspended in 5 mL KPi buffer (0.1 M, pH 7.4).

It must be noted that HpiI1 and HpiI3 are Fe^{II} dependent and probably the presence of high phosphate concentration is not suitable to produce these enzymes, if enzyme production should be repeated, LB medium should be tested in parallel.

7.1.9.4 Heterologous Expression of *Wi-WelO11-14*

Different expression conditions were tested in 100 mL flasks with 25 mL LB or TB medium. 250 μ L preculture was used to inoculate the medium, containing 50 μ M FeCl₃ and 50 μ g/mL kan. The culture was incubated at 37 °C, 200 rpm (Infors HT shaker) until an OD₆₀₀ of 0.4 was reached. Then the temperature was shifted to 30 °C or 23 °C and IPTG (0.1 M in H₂O) was added to a final concentration of 0.015, 0.05, 0.1 or 0.5 mM. Cells were grown overnight, and 1 mL harvested by centrifugation (14 000 rpm, 1 min, Eppendorf, 5418) and either resuspended with 4x SDS-PAGE sample buffer or lysed with HEPES 2 buffer containing 1 mg/mL lysozyme. The samples with lysis buffer were incubated for 37 °C for 30 min followed by centrifugation for 2 min at 14000 rpm, Eppendorf 5418 and the supernatant mixed with 4x SDS-PAGE sample buffer. The samples were further processed as described in chapter 7.1.11.

Wi-WelO11 should further be produced with 0.5 mM IPTG at 30 °C and LB medium. *Wi-WelO12* should further be produced with 0.05 mM IPTG at 30 °C and LB medium. The tests should be repeated for *Wi-WelO13* and 14 to get clear results.

7.1.9.5 Expression of *WelO16-WelO18*

Different expression conditions were tested in 250 mL flasks with 100 mL LB or TB medium. 1 mL preculture was used to inoculate the medium, containing 50 μ M FeCl₃ and 50 μ g/mL kan. The culture was incubated at 37 °C, 200 rpm (Infors HT shaker) until an OD₆₀₀ of 0.4-0.6 was reached. Then the temperature was shifted to 25 °C and IPTG (0.1 M in H₂O) was added to a final concentration of 0.025 or 0.25 mM. Cells were grown overnight, and 1 mL harvested by centrifugation (14 000 rpm, 1 min, Eppendorf, 5418) and either resuspended with 4x SDS-PAGE sample buffer or lysed with HEPES 2 buffer containing 1 mg/mL lysozyme. The samples with lysis buffer were incubated for 37 °C for 30 min followed by centrifugation for 2 min at 14000 rpm, Eppendorf 5418 and the supernatant mixed with 4x SDS-PAGE sample buffer. The samples were further processed as described in chapter 7.1.11.

WelO16 and 17 should further be produced in LB medium, for *WelO18* both media should be tested again. Also, the IPTG concentrations have to be tested again since no clear results were reported.

7.1.9.6 *TsER C25D/I67T*

Heterologous expression was performed by inoculation of 0.5 L TB-amp¹⁰⁰ in a 2 L baffled flask with 5 mL preculture. The culture was incubated at 37 °C, 200 rpm (Infors HT shaker) until an OD₆₀₀ of 0.4 was reached. Then the temperature was shifted to 22 °C and IPTG (0.1 M in H₂O) was added to a final concentration of 0.01 mM. Cells were grown overnight, harvested by centrifugation (5000 rpm, 15 min, 4 °C), resuspended in 5 mL potassium phosphate buffer (100 mM, pH=7.4), transferred into 50 mL plastic tubes and stored at -20 °C until further use.

7.1.9.7 P450_{BM3} Variants in 2.2 mL Squared Deep Well Plates

The protocol according to Kille was used.^[414] 800 μ L LB-kan⁵⁰ were provided in a 2.2 mL squared dw-plate. The medium was inoculated with existing glycerol stocks of the working group or with colonies picked from an agar plate. The dw plate was incubated overnight at 37 °C, 200 rpm (Infors HT shaker, attached in an inclined way). Expression was performed by providing 700 μ L LB-kan⁵⁰-IPTG (final concentration 0.1 mM) with addition of 10 mL/L power mix, 1 mM MgCl₂, 1 mL/L transition metal mix and 0.5% glucose. After inoculation with 100 μ L preculture, the plates were incubated for 8 h at 30 °C, centrifuged for 10 min at 4000 rpm, 4 °C (5810R Eppendorf centrifuge) and frozen at -80 °C.

7.1.9.8 P450 Variants in Baffled Flasks

A preculture was prepared, the day before by inoculation of 25 mL LB-kan⁵⁰ in a 100 mL baffled Erlenmeyer flask with *E. coli* cells from glycerol stock or from agar plates. The culture was grown overnight at 37 °C, 200 rpm (Infors HT shaker).

For expression, 1 L TB-medium was prepared with 40 μ g/mL kanamycin, 10 mL preculture and the following additives: 10 mL power mix, 1 mM MgCl₂, 1 mL transition metal mix and 0.5% glucose. The cells were grown at 37 °C, 200 rpm (Infors HT shaker) to an OD₆₀₀ of 0.8-1 and IPTG (0.1 M in H₂O) was added to a final concentration of 0.1 mM. The temperature was reduced to 25 °C and the culture incubated for 15 h. The cells were harvested by centrifugation (5000 rpm, 15 min, 4 °C), resuspended in 5 mL potassium phosphate buffer (100 mM, pH=7.4), transferred into 50 mL plastic tubes and stored at -20 °C until further use.

7.1.10 Purification of Enzymes and Determination of Concentration

7.1.10.1 WelO15

The frozen cell suspension was defrosted in cold water and cells were lysed by sonication for 6 min with 30 s pulses and 30 s rest. Because during sonification heat is generated, the suspension is put on ice water. The suspension was pelleted (16 000 rpm, 4 °C, 45 min) and the supernatant filtered by syringe filter (0.45 μ M pores, polyether sulfone, VWR).

Purification was performed at 4 °C, with a 6 mL column (1CV=6 mL) Ni-NTA agarose (article nr 30210) purchased from Qiagen. The cleared lysate was loaded on the column with a 10 mL loop and 100% buffer Tris A with a flow rate of 1 mL/min for the complete purification process. The loop was emptied with 25 mL Tris A buffer. If necessary, the process was repeated. Followed by a washing step of 12 CV with Tris A buffer. Then the protein was eluted by a gradient (0% to 100% buffer Tris B in 12 CV, delay 15 CV) and a final washing step of the column with 10 CV, 100% buffer B. The purity of proteins was checked by SDS-PAGE. The selected fractions were concentrated using 10 kDa concentrators of Merck Millipore. The protein solution was filled into the concentrators and centrifuged at 4 000 rpm for 6 min repeatedly with gentle mixing in between.

Methods

The protein solution was concentrated to about 30 mL and dialyzed overnight at 4°C against 2 L HEPES 1 buffer to remove imidazole, high sodium chloride concentration from Tris buffer as well as Ni²⁺ and Fe-ions which might be bound in the active site of the enzymes. Another dialyzing step of 4-5 h at 4 °C was performed against HEPES 2 buffer to remove EDTA. After concentrating the solution to about 10 mL, it was either aliquoted into 200 µL aliquots, shock frozen in N₂ (l) and stored at -80 °C or further purified by size exclusion chromatography.

The protein solution was concentrated to 1 mL and after preequilibrating the column with HEPES 2 buffer, the sample was loaded on a Superdex 26/60 (GE Healthcare) column from a 1 mL loop. The sample was loaded to the column with a flow rate of 1 mL/min, then the flow rate was increased to 1.5 mL/min. The WelO5 enzymes eluted at 227 mL which corresponds to a monomeric state in HEPES buffer. The fractions were analyzed again by SDS-PAGE. Selected fractions were combined and concentrated.

In the beginning, the enzyme concentration was measured by Nanodrop (Peylab). Molecular weights and extinction coefficients were calculated by ProtParam, Expasy (34.45 kDa and $\epsilon=30.37 \cdot 10^3$ for *Wi*-WelO15 and 34.37 kDa and $\epsilon=28.88 \cdot 10^3$ for *Hw*-WelO15). However, after comparing several defrosted enzymes via SDS-PAGE analysis, the band thickness was quite different, therefore later the concentration determination was made by Bradford assay.

7.1.10.2 Bradford Assay

The principle of concentration determination via Bradford assay is the interaction of Coomassie brilliant blue G-250 with basic amino acids of the protein. Because of this interaction the absorption maximum shifts from 465 nm to 595 nm.^[438] 5x Bradford solution from Bio-Rad was diluted to 1x and 1 mL mixed with different amounts of protein solution (1-20 µL), the mixture was incubated at room temperature for 5 min. It is important to work in a diluted range of concentration because of the limits of the Lambert-Beer-law. First, a calibration line was determined with bovine serum albumin. The same diluted 1x solution was made used to determine the concentration of several halogenases. The received equation for concentration determination is shown in equation (1).

Methods

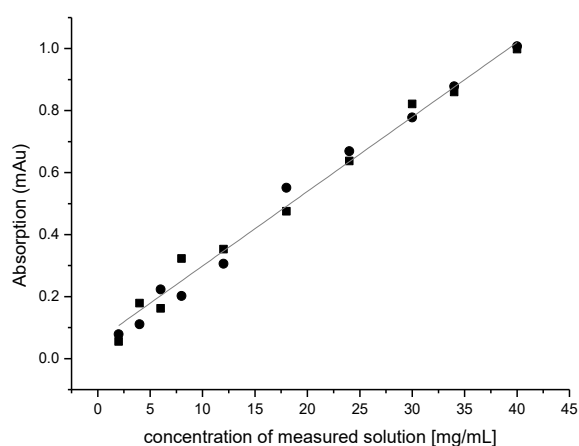


Figure 59. Calibration line of Bradford solution with BSA.

$$A = 0.024 \text{ mL/mg } c + 0.0586 \quad (1)$$

A=Absorption, c=concentration

The concentration determination was made with a fresh calibration curve each time. For further measurements, a calibration curve was made with *Wi-WelO15 V6I/A82L/D284N*.

7.1.10.3 *Ene-Reductase TsER C25D/I67T*

Cell pellets were thawed in cold water. Cells were lysed by sonication for 6 min with 30 s pulses and 30 s rest. After pelleting the suspension (16 000 rpm, 4 °C, 45 min), the cleared lysate was heat purified.

Since *TsER* is thermostable and does not have a His-tag, the enzyme was purified by incubating the cleared lysate in a 50 mL plastic tube at 70 °C for 90 min in a drying oven. Afterwards the suspension was stored at room temperature for 10 min to cool down. Followed by a centrifugation step (16 000 rpm, 4 °C, 45 min). FMN (0.1 M, aq) was added to the enzyme to a final concentration of 100 μM and dialyzed overnight against 5 L, 0.1 M potassium phosphate buffer. Concentration determination was performed by measuring absorption of the co-factor FMN in a wavelength region between 350-600 nm. The protein solution was shock frozen in N₂ (l) and stored at -80 °C. The measured absorption spectrum is shown in figure 60.

Methods

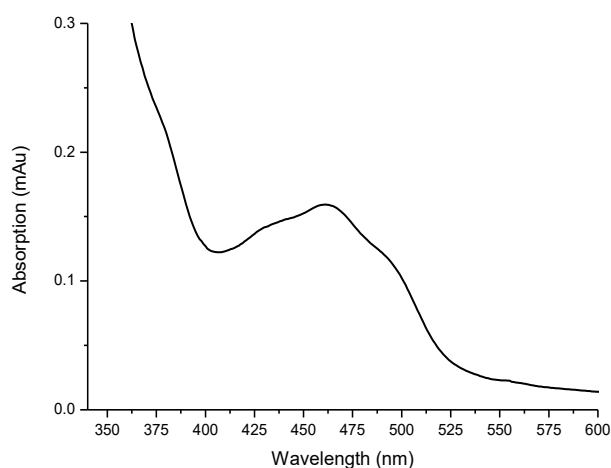


Figure 60. Absorption spectra of old yellow enzyme *TsER C25D/I67T* after heat purification.

The concentration of active enzyme can be calculated with the absorption maximum at about 450 nm, the extinction coefficient of $\epsilon=11600$ and equation 2.

$$c = \frac{A}{d \cdot \epsilon} = \frac{0.75}{1\text{cm} \cdot 11600\text{M}^{-1}\text{cm}^{-1}} = 65 \mu\text{M} \quad (2)$$

with

A = absorption (measured), d = length of cuvette (1 cm),

ϵ = extinction coefficient= $11600 \text{ M}^{-1}\text{cm}^{-1}$ ^[439]

7.1.11 Sodium Dodecyl Sulfate Polyacrylamide Gel Electrophoresis

To separate proteins by their molecular weight, sodium dodecyl sulfate polyacrylamide gel electrophoresis (SDS-PAGE) analysis can be performed.^[440] The sample preparation buffer contains SDS and β -mercaptoethanol. By heating the sample up to 95 °C the tertiary and secondary structures are denatured, so that the proteins are linearized, the disulphide bridges are split and the intrinsic charge of the proteins covered. In this way the linearized proteins are separated only depending on their length.

The preparation of the gel consists of a two-step procedure, first preparation of the separation gel followed by preparation of the stacking gel. The gels are prepared in a caster that can take up to 12 glass planes in which the gels are prepared. The gel is prepared by preparing an acrylamide containing buffer solution with radical starter (ammonium persulfate) and stabilator (tetramethylethylenediamine). Separation and stacking gel have different polymerization grades and different pH values.

12% acrylamide separation gel for proteins with a molecular weight of 30-40 kDa:

24 mL 40% acrylamide, 34.75 mL H₂O, 20 mL buffer (1.5 M Tris pH 8.8, 800 μ L SDS (10% in H₂O), 400 μ L APS (10% in H₂O), 40 μ L TEMED

Methods

5% acrylamide stacking gel:

4.4 mL 40% acrylamide, 21.26 mL H₂O, 8.75 mL buffer (1.5 M Tris pH 6.8, 350 µL SDS (10% in H₂O), 175 µL APS (10% in H₂O), 35 µL TEMED

The samples are prepared by mixing 3 volumes of sample with 1 volume of 4x sample buffer (100 mM tris/HCl, pH=6.8, 110 mM SDS, 2 mM β-mercaptoethanol, 40% (w/v) glycerol, 1 % (w/v) bromophenol blue) and denatured at 95 °C for 5 min, followed by centrifugation (14000 rpm, Eppendorf centrifuge 5418, 10 min).

The protein bands were stained with a staining solution of EtOH 50% (v/v), acetic acid 10% (v/v) and Coomassie brilliant blue G-250 250 mg/L. Excessive stain was removed by washing and boiling the SDS-PAGE gel three times for 5 min in water.

For good visualization, 3.3 µg purified protein should be applied. For cell or lysate samples, pellets normalized to OD₆₀₀=5.0 are resuspended in 100 µL water or lysis buffer. For lysis, the cells were suspended and incubated at 37 °C for 30 min. After centrifugation (14000 rpm, Eppendorf centrifuge 5418, 10 min), 30 µL supernatant were mixed with 10 µL 4x sample buffer. Whole cell samples were prepared by mixing 30 µL cell suspension with 10 µL 4x sample buffer. 6 µL of the sample are applied to the gel. As standard 10 µL of protein marker (page ruler 26610 by thermo scientific) were applied as well.

7.1.12 Determination of Intact Protein Mass (performed by Mass Department)

To analyze if a self-modification (oxidation or hydroxylation) occurs, 20 µL of a 5-50 µM solution with purified *Wi-WelO15 V6I/D284N* and *Hw-WelO15* were given to the mass department of the Philipps-University Marburg.

Depending on their concentration and the expected protein masses, 1-10 µL of the buffered protein solutions were desalted online using a Waters ACQUITY H-Class HPLC-system equipped with a monolithic 50/1 ProSwift RP-4H column (ThermoScientific). Desalted proteins were eluted into the ESI source of a Synapt G2Si mass spectrometer (Waters) by the following gradient of buffer A (water/0.05% formic acid) and buffer B (acetonitrile/0.045% formic acid) at a column temperature of 40 °C and a flow rate of 0.1 mL/min: Isocratic elution with 5% A for two minutes, followed by a linear gradient to 95% B within 8 min and holding 95% B for additional 4 min. Positive ions within the mass range of 500-5000 m/z were detected. Glu-Fibrinopeptide B was measured every 45 s for automatic mass drift correction. Averaged spectra were deconvoluted after baseline subtraction and eventually smoothing using MassLynx instrument software with MaxEnt1 extension.

7.1.13 Tryptic Digestion (performed by Mass department)

To determine masses of peptides from SDS-PAGE analysis, gel-bands were cut out of the gel and given to the mass department of the Philipps-University Marburg. After-destaining, samples were digested "in-gel" by the addition of sequencing grade modified trypsin (Promega) and incubated at 37 °C overnight.

The mass spectrometric analysis of the samples was performed using an Orbitrap Velos Pro mass spectrometer (ThermoScientific). An Ultimate nanoRSLC-HPLC system (Dionex), equipped with a custom 20 cm x 75 µm C18 RP column filled with 1.7 µm beads was connected online to the mass spectrometer through a Proxeon nanospray source. 1-15 µL of the tryptic digest (depending on sample concentration) were injected onto a C18 pre-concentration column. Automated trapping and desalting of the sample were performed at a flowrate of 6 µL/min using water/0.05% formic acid as solvent.

Separation of the tryptic peptides was achieved with the following gradient of water/0.05% formic acid (solvent A) and 80% acetonitrile/0.045% formic acid (solvent B) at a flow rate of 300 nL/min: holding 4% B for 5 min, followed by a linear gradient to 45%B within 30 minutes and linear increase to 95% solvent B in additional 5 min. The column was connected to a stainless steel nanoemitter (Proxeon, Denmark)) and the eluent was sprayed directly towards the heated capillary of the mass spectrometer using a potential of 2300 V. A survey scan with a resolution of 60000 within the Orbitrap mass analyzer was combined with at least three data-dependent MS/MS scans with dynamic exclusion for 30 s either using CID with the linear ion-trap or using HCD combined with orbitrap detection at a resolution of 7500.

Data analysis was performed using Proteome Discoverer (ThermoScientific) with SEQUEST and MASCOT (version 2.2; Matrix science) search engines using either SwissProt or NCBI databases.

7.1.14 Crystallization

The enzyme was purified as described in ch. 7.1.10 . The enzyme was not frozen before using it for crystallization. The purified enzyme was mixed with cofactors and 50 µL solution for each crystallization plate were given to the crystallization department MarXTal of the Philipps-University Marburg. Imaging was performed by automation in the beginning regularly, later after query. For an anaerobic crystallization trial, enzyme solution and plates were brought into an anaerobic chamber. There the solution was also pipetted by robot. The plates had to be checked manually with a microscope. Several crystallization trials were attempted using available commercial screens with 300 nL drop volume of enzyme solution with a Honeybee robot. The sitting drop vapor diffusion method was used for crystallization and crystals were obtained from 0.2 M KAc and 2.2 M AmSO₄ after storing the plates at 18°C The crystal structure was solved from the crystals that grew from an enzyme solution of 32.5 mg/mL *WiWelO15* in 50 mM HEPES, 10 mM NaCl, 10% glycerol, 0.5 mM DTT, 2 mM αKG and 1 mM

Methods

FeSO₄. Crystals were flash-frozen after a pre-treatment soak of the crystal in a solution consisting of the crystallization reservoir solution and a cryoprotectant, 20%(v/v) glycerol for data collection.

Diffraction data were collected at the European Synchrotron Radiation Facility (ESRF) microfocus beamline ID23-2. All data were processed using XDS^[441] in space group C121. Data reduction and scaling was done using the CCP4 suite of programs.^[442] Data collection and processing statistics are given in table 28. The structure was determined by molecular replacement with PHASER^[443] using the coordinates (PDB code: 5IQS) as a search model. After an initial rigid body refinement, the structure was further refined with rounds of simulated annealing, energy minimization, and individual *B*-factor refinement with a maximum likelihood target using Phenix.^[444] Difference Fourier maps were calculated with Phenix and used to locate electron density corresponding to bound Fe and α KG, and the structure was built using COOT.^[445] Structure validation was done with Molprobity^[446]. Final refinement statistics are given in table 28. All structural figures were generated with Chimera version 1.11.2.^[447] The coordinates and structure factors have been deposited in the Protein Data Bank (PDB 6GEM).

Table 28. Final refinement statistics of crystal structure of *Wi-WelO15 V6I/D284N*.

Wavelength (Å)	0.8726
Resolution range (Å)	49.48 - 3.46 (3.58-3.46)
Space group	C 1 2 1
Unit cell (Å, Å, Å °, °, °)	195.83 155.45 133.23 90.00 126.91 90.00
Total reflections	280951
Unique reflections	41091 (3643)
Multiplicity	6.8 (6.4)
Completeness (%)	98.2 (84.2)
Mean I/sigma (I)	8.0 (1.6)
R _{merge}	0.200 (1.284)
R _{factor}	0.1930
R _{free}	0.2418
Number of atoms	8836
Protein	8792
Ligands	44
RMS (bonds)	0.022
RMS (angles)	1.679
Ramachandran favored (%)	88.58
Ramachandran outliers (%)	1.81

In table 29 all crystallization projects are listed that were performed in cooperation with the MarXtal laboratory of the Philipps-University Marburg.

Methods

Table 29. List of all crystallization projects that were performed in cooperation with the MarXtal laboratory of the Philipps-University Marburg

Enzyme, Date Qiagen Plates	Drop1*	Drop2*
<i>Wi-0</i> 21.10.2015 JCSG I,II,III,IV, PACT, AmSO ₄ , Cryos, Classics, Morpheus, MBC II	32.5 mg/mL <i>Wi-0</i> + 2 mM αKG	32.5 mg/mL <i>Wi-0</i> +2mM αKG + 1mM FeSO ₄
<i>Hw-WelO15</i> JCSG III, IV, AmSO ₄ ,	32.5 mg/mL <i>Hw-WelO15</i> +2mM αKG	20 mg/mL <i>Hw-WelO15</i> ** +2 mM αKG + 1.5 mM hapalindole Q (8% EtOH)
<i>Wi-0</i> (aerobe) JCSG III, IV, Morpheus II, AmSO ₄ ,	33.8 mg/mL <i>Wi-0</i> +2mM αKG	35.0 mg/mL <i>Wi-0</i> +2mM αKG +1mM FeSO ₄
<i>Wi-0</i> (anaerobe) JCSG III, IV, Morpheus II, AmSO ₄ ,	35 mg/mL <i>Wi-0</i> +2mM αKG	35 mg/mL <i>Wi-0</i> +2mM αKG +1mM FeSO ₄

*The enzyme was prepared in 50 mM HEPES, 10 mM NaCl, 10% glycerol, 0.5 mM DTT pH 7.4 **an enzyme solution of 32.5 mg/mL was prepared, after addition of hapalindole Q in EtOH, precipitation was observable. After mixing, the solution was filtered, and the concentration was remeasured by Nanodrop to be only 20 mg/mL

Pictures of the crystals can be found in chapter 8.3.4, table 37. In addition, refinements were pipetted by hand. Hanging drop vapor diffusion method was used with 500 μL reservoir solution. Used conditions are shown in table 30. The final concentration of the well solution is given in row 1, pipetted volume in row 2 and enzyme to buffer ratio in row 3. One unit represents 1 μL, which means a ratio of 1 / 1 is 1 μL of each solution. After pipetting the drops on the cover slip, the wells were sealed with grease, so that no solution can evaporate. As salts, ammonium sulfate (AmSO₄), potassium acetate (KAc) and sodium acetate (NaAc) in bigrade were used. The enzyme solution was concentrated to 42 mg/mL and used with the following conditions: 50 mM HEPES, 10 mM NaCl, 10% glycerol, 42 mg/mL enzyme.

Methods

Table 30. Refinements for crystallization which was pipetted by hand. As salts, ammonium sulfate (AmSO_4), potassium acetate (KAc) and sodium acetate (NaAc) were used. Hanging drop vapor diffusion method was used with 500 μL reservoir solution. The final concentration of the well solution is given in row 1, pipetted volumes in row 2 and enzyme to buffer ratio in row 3. One unit represents 1 μL , which means a ratio of 1 / 1 is 1 μL of each solution. After pipetting the drops on the cover slip, the wells were sealed with grease, so that no solution can evaporate.

Plate 1						
final conc.	1.5 M	2 M	2.2 M	2.2 M	2.5 M	2.8 M
	AmSO_4	AmSO_4	AmSO_4	AmSO_4	AmSO_4	AmSO_4
	0.2 M KAc					
pipetted volume	187.5 μL	250 μL	275 μL	275 μL	312.5 μL	350 μL
	AmSO_4	AmSO_4	AmSO_4	AmSO_4	AmSO_4	AmSO_4
	20 μL KAc					
	292.5 μL	230 μL H_2O	205 μL H_2O	230 μL H_2O	167.5 μL	130 μL H_2O
	H_2O				H_2O	
ratio enzyme/buffer	1 / 1	1 / 1	1 / 1	2 / 1	1 / 1	1 / 1
Plate 2						
final conc.	1.5 M	2 M	2.2 M	2.2 M	2.5 M	2.8 M
	AmSO_4	AmSO_4	AmSO_4	AmSO_4	AmSO_4	AmSO_4
	0.2 M					
	NaAc	NaAc	NaAc	NaAc	NaAc	NaAc
pipetted volume	187.5 μL	250 μL	275 μL	275 μL	312.5 μL	350 μL
	AmSO_4	AmSO_4	AmSO_4	AmSO_4	AmSO_4	AmSO_4
	33.3 μL					
	NaAc	NaAc	NaAc	NaAc	NaAc	NaAc
	280 μL H_2O	217.5 μL	192.5 μL	155 μL H_2O	155 μL H_2O	117.5 μL
		H_2O	H_2O			H_2O
ratio enzyme/buffer	1 / 1	1 / 1	1 / 1	2 / 1	1 / 1	1 / 1

7.1.15 Circular Dichroism Spectroscopy

Selected variants were analyzed with circular dichroism spectroscopy (CD). Since high salt concentrations interfere with the measurement, a buffer concentration of 5 mM HEPES and 1 mM NaCl and an enzyme concentration of 25 μ M was used. The enzyme was assumed to be in apo state after purification without further analysis. In comparison, the addition of 1 eq α KG and the addition of 1 eq α KG and 1 eq $(\text{NH}_4)_2\text{Fe}(\text{SO}_4)_2$ (holo state) were compared. For measurements a Jasco J810 spectropolarimeter was used with a Jasco CDF 4265 Peltier element and Haake WKL26 water bath of Thermo. First a blank measurement with buffer was performed. Then the folding was analyzed by measuring the CD signal in the range of 190 nm-280 nm. The following settings were used: 20 $^{\circ}$ C, scanning mode continuous, 50 nm/s, 1 nm bandwidth, sensitivity: standard, data pitch: 0.2 nm, accumulations: 3.

Melting was analyzed in the range of 20-80 $^{\circ}$ C with conditions: λ =220 nm, data pitch 1 $^{\circ}$ C, a temperature slope of 2 $^{\circ}$ C/min, a response of 2 s and a bandwidth of 10 nm. The ellipticity (mdeg) was converted in molar ellipticity with equation (3)

$$[\theta](deg\ cm^2\ dmol^{-1}) = \frac{\theta}{c \cdot d \cdot 10} \quad (3)$$

$[\theta]$ = molar ellipticity, θ = ellipticity, c = enzyme concentration, d = length of cuvette (1 cm)

The data was analyzed with Origin 8.0. The molar ellipticity was plotted against the wavelength to show folding or the temperature to determine the melting temperature after fitting with the Boltzmann equation. The inflection point gives the melting temperature T_m . The melting curves are shown in figure 70-figure 75. An overview of all determined folding values is given in table 38.

7.1.16 Docking

7.1.16.1 Isonitrile and Isothiocyanate Molecules

The docking experiments were performed by Henrik Müller with SwissDock^[385] which is a web-based application that is able to predict molecular interactions between molecules and target proteins based on the EADock DSS docking software, whose algorithm consists of the following steps. First, many bindings modes of the molecule inside a predefined box are generated. At the same time, the CHARMM (Chemistry at Harvard Macromolecular Mechanics) energies of these are estimated. Based on that, the binding modes with the most favorable energies are *in silico* evaluated and clustered. These can be downloaded and manually evaluated in Chimera by eye. For that purpose, the small molecules were created in Chem3D and saved as a mol2-file. The crystal structure of WelO5 with substrate and closed lid was chosen as the target (PDB 5IQT). The docking box was defined based on the point with the coordinates X: -0.072, Y: 0.766, Z: -0.108 (Chain A) which is the center point of the box with a side length of 10 Å for each side. The apparently most favorable binding modes were chosen with due regard to the predicted energies.

7.1.16.2 Hapalindole-like Ketones

Rigid body docking was performed with Yasara STRUCTURE^[363] (Yet Another Scientific Artificial Reality Application) by Henrik Mueller. As ligand the crystal structure of **54** and as receptor, crystal structure chain D of *Wi-0* (PDB 6GEM) was used. The docking procedure requires a preparation of both structures. The preparation of the receptor was performed using the standard settings of Dock Prep tool from UCSF Chimera, Version 1.11.2. This program deletes the solvent, fixes incomplete side chains and adds hydrogens and charges to the protein and the bound ligands. In the prepared receptor-file, α KG had a charge of -2 and the Fe ion a charge of +2. A generously proportioned simulation cell was generated around the binding pocket of the protein with YASARA to cut down the calculation time and increase the accuracy of the docking. The docking process was performed by running YASARA's 'dock_run' macro. Here, the Amber99 force field was used. The results were visually analyzed using Chimeras ViewDock-tool.

7.2 Biotransformation

7.2.1 General Information

Biotransformations were conducted with lysate or purified enzymes (optimized reaction conditions are described in chapter 7.2.5). As buffer system 50 mM HEPES pH 7.4 was used, which was purged with N₂ gas for at least 0.5 h. As cofactor α -ketoglutarate was used as disodium salt. The salt was solved in buffer and frozen as 0.1 M stock solution at -20 °C. In lysate assays a final concentration of 2.5 mM was used since it was assumed that *E. coli* enzymes might recycle succinate or consume high α KG concentrations, while with purified enzymes 5 mM was used. It was found out that an increase of sodium chloride from originally 10 mM to later 100 mM leads to an increase of activity. As iron source (NH₄)₂Fe(SO₄)₂ · 6H₂O was used and freshly prepared each time before the reaction. A reducing agent was added to the reactions to recycle oxidized iron back to Fe^{II}. In the beginning DTT was used but later it was found out that ascorbic acid works better. Also, the reducing agent was freshly prepared each time before the reaction. It could be observed mixing the assumed apo enzyme with α KG and iron, the solution with *Wi*-WelO15 turned lilac while the reaction mixture with *Hw*-WelO15 stayed colorless. However, no further experiments were conducted to closer analyze if this behavior can be changed with different cofactor concentrations.

In the beginning, no positive control for the activity of the enzyme was available, a variety of different reaction conditions were tested. In the screening, variants able to chlorinate **54** were found. Variants *Wi*-1, *Wi*-5 and *Wi*-8 (ch. 8.2, p. 190) showed highest conversions and were further used to test different reaction conditions.

Extraction of Reactions in Vials

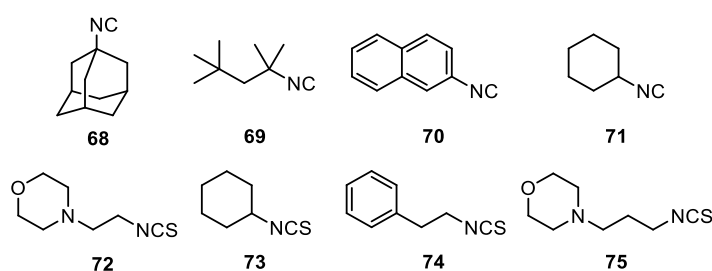
Reactions were stopped by extraction with 200 μ L ethyl acetate. Phase separation was performed by centrifugation. The organic phase was transferred in HPLC vials, placed at room

temperature in a clean fume-hood overnight, covered with a paper box, to evaporate all ethyl acetate but prevent dust to go in. Remaining dry samples were solved in 70 μL acetonitrile and analyzed via HPLC with detection at 280 nm.

7.2.2 Biotransformation and Analysis of Substrate Scope - *Hw*-WelO15 and *Wi*-0

The biotransformations were performed with *Hw*-WelO15 and *Wi*-WelO15 V6I/D284N (*Wi*-0) in various conditions. The following reactions were performed before any positive control was available. Conditions based on information from Hillwig *et al.*^[155] were used. Since a low turnover number for non-native substrates was expected, a higher enzyme concentration was used.

7.2.2.1 Assays with Isonitrile and Isothiocyanate Containing Molecules

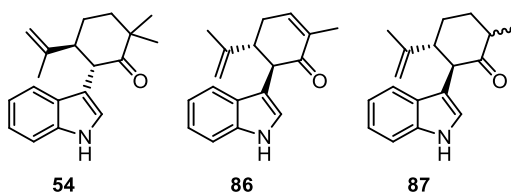


1) The reaction was performed in 1.5 mL reaction tubes and a total volume of 200 μL . The reaction was performed with 100 μM purified *Hw*-WelO15 or *Wi*-0, 2.5 mM αKG , 2 mM $(\text{NH}_4)_2\text{Fe}(\text{SO}_4)_2$ and 0.5 mM DTT. Finally, 2 μL of the substrate (100 mM stock solution in acetonitrile) was added. The reaction tubes were closed and incubated at 30 $^\circ\text{C}$ for 3 h. Then the reaction was extracted with 200 μL ethyl acetate and the organic layer analyzed by GC.

2) This assay was performed in a 2.2 mL dw-plate and a total volume of 200 μL . All reactions were performed in triplicates. Substrates **68-75** were tested in a combinatorial set-up, testing different reducing agents as well as the influence of indole as decoy molecule. A master mix of HEPES buffer (50 mM HEPES, 10 mM NaCl) containing 100 μM *Hw*-WelO15, 2 mM αKG and 0.5 mM $(\text{NH}_4)_2\text{Fe}(\text{SO}_4)_2$ was prepared. 194 μL reaction solution was pipetted into the plate. Stock solutions were prepared: 100 mM DTT in HEPES buffer, 100 mM ascorbic acid in HEPES buffer, 100 mM indole in acetonitrile, 100 mM **68-75** in acetonitrile. 2 μL of each of the needed additives was added by 8-channel pipette. The following 6 conditions were tested: DTT, DTT + indole, ascorbic acid, ascorbic acid + indole, no reducing agent, no reducing agent + indole. Resulting final concentrations were 1 mM DTT, 1 mM ascorbic acid, 1 mM indole, 1 mM substrate.

All reactions were performed in duplicates three times and stopped, after 3 h, 7 h and 24 h by extraction with 400 μL ethyl acetate. Phase separation was performed by centrifugation. The organic phase was transferred in microtiter plates with a Tecan robot equipped with a 96-tip head MCA (Multichannel Arm). The organic layer (ethyl acetate) was analyzed by GC.

7.2.2.2 Assays with Hapalindole-like Substrates



1) The reaction was performed in 1.5 mL reaction tubes and a total volume of 200 μ L. 1 mM α KG, 10 mM NaCl and 0.5 mM $(\text{NH}_4)_2\text{Fe}(\text{SO}_4)_2$ were mixed with either 60 μ M enzyme *Hw*-WelO15 or 60 μ M *Wi*-0 and HEPES 2 or KPi buffer. Substrate **86** or **87** was added by pipetting into the lid and it was mixed by inverting. After short centrifugation to collect the solution at the bottom of the tube, two holes were pricked into the lid of the reaction tube. The reaction was incubated at 1400 rpm, 30 $^\circ$ C in an Eppendorf Thermomixer. After 20 h the reaction was stopped by extraction with 200 μ L ethyl acetate. Phase separation was performed by centrifugation. The organic phase was handled as described above and analyzed by HPLC-UV/Vis.

2) The reaction was performed in 1.5 mL reaction tubes and a total volume of 200 μ L. Either 20 or 50 mM HEPES were combined with 0.0625 mM; 0.25 mM or 0.5 mM DTT or 50 or 100 mM potassium phosphate buffer were combined with 0.0625 mM; 0.25 mM or 0.5 mM DTT and individually tested. In all reactions 2 mM α KG, 10 mM NaCl and 0.5 mM $(\text{NH}_4)_2\text{Fe}(\text{SO}_4)_2$ and 44 μ M *Hw*-WelO15 were present. A master mix was prepared with a 10 mM NaCl solution N_2 purged. The master mix contained Fe, α KG and enzyme. HEPES and phosphate salts as well as DTT were prepared as 10x concentrated stock and added directly to the vials. Substrate **87** was added by pipetting 1 μ L into the lid and inverting. After short centrifugation to collect the solution at the bottom of the tube, two holes were pricked into the lid of the reaction tube.

3) No conversion could be detected, in the reaction described above, so the assay was repeated with purged buffers and overlaying the enzyme solution with N_2 after mixing everything. After 15 min the tubes were washed with pressed air by blowing to the top of the liquid. After 16 h the reaction was stopped by extraction with 200 μ L ethyl acetate. The organic phase was handled as described above and analyzed by HPLC-UV/Vis.

4) The reaction was performed in 2 mL reaction tubes and a total volume of 200 μ L. In the reaction set-up, 50 μ L *Hw*-WelO15 (250 μ M) was mixed with N_2 purged HEPES 2 (10 mM NaCl, 50 mM HEPES, 10 % glycerol) and cofactors, so that final concentrations of 62.5 μ M enzyme, 5 mM α KG (0.1 M in HEPES 2), 1 mM $(\text{NH}_4)_2\text{Fe}(\text{SO}_4)_2$, 1 mM DTT and a concentration of 2 mM substrate **54** (100 mM in EtOH) were present. After 16 h the reaction was stopped by extraction with 200 μ L ethyl acetate. The organic phase was handled as described above and analyzed by HPLC-UV/Vis.

7.2.3 Screening of Libraries in Cell Lysate

7.2.3.1 Pooling of Plates (Screening of Error Prone Variants)

For activity assays, enzyme production was performed in 2.2 mL dw-plates. After harvesting, the plates were frozen at -80°C . For reactions, cell pellets were thawed at room temperature and resuspended by vortexing with 200 μL HEPES 2 buffer and combined via liquidator. The plates were centrifuged (Eppendorf 5810R, 10 min, 4°C , 4000 rpm) and the supernatant discarded. The pellets were resuspended by vortexing with 100 μL N_2 purged HEPES 3 (50 mM HEPES, 10 mM NaCl, pH 7.4) buffer containing 1 mg/mL lysozyme. The plates were incubated at 37°C for 30 min. For the reaction buffer, N_2 purged HEPES 3 buffer was prepared and co-factors added to a concentration of 5 mM αKG , 1 mM $(\text{NH}_4)_2\text{Fe}(\text{SO}_4)_2$, 1 mM DTT in the 2x reaction buffer. While αKG was prepared as 0.1 mM stock solution, $(\text{NH}_4)_2\text{Fe}(\text{SO}_4)_2$ and DTT were weighed as solids and solved in 1 mL N_2 purged buffer just before usage. 100 μL of the 2x reaction buffer was added to the cell suspension. 2 μL of 0.1 M substrate solution in EtOH was added by 8-channel pipette*. The plate was closed with a plastic lid and incubated at 30°C , 200 rpm (Infors HT shaker, attached in an inclined way). After 24 hours, the reaction was stopped by extraction with 400 μL ethyl acetate. Phase separation was performed by centrifugation (Eppendorf 5810R, 10 min, 4°C , 4000 rpm). The organic phase was transferred in microtiter plates with a Tecan robot equipped with a 96-tip head MCA (Multichannel Arm). Plates were placed at room temperature in a clean fume-hood overnight, covered with a paper box to evaporate all ethyl acetate but prevent dust to get in. Remaining dry samples were solved in 100 μL acetonitrile and analyzed via HPLC-UV/Vis. For measurement in HPLC, the glass plates were put in a metal frame and closed with a white plastic septum.

*the addition with 8-channel pipette later was changed to Multipette since the solvent evaporated too fast from the container, needed to take up the substrate stock.

7.2.3.2 Screening of Libraries Generation 1-3

For activity assays, enzyme production was performed in 2.2 mL dw-plates (ch. 7.1.9.2). After harvesting, the plates were frozen at -80°C . The cell pellets were thawed at room temperature. For the reaction, first cells were resuspended by vortexing with 100 μL HEPES 3 buffer (50 mM HEPES, 10 mM NaCl, pH 7.4) containing 1 mg/mL lysozyme. To lyse the cells, the plates were incubated at 37°C for 30 min. In the meantime, 2xreaction buffer was prepared. For the reaction buffer, N_2 purged HEPES 3 buffer was used and mixed with freshly prepared reaction compounds so that a concentration of 5 mM αKG , 1 mM DTT and 1 mM $(\text{NH}_4)_2\text{Fe}(\text{SO}_4)_2$ were present in the 2x buffer. Fresh prepared $(\text{NH}_4)_2\text{Fe}(\text{SO}_4)_2$ solution has a turquoise color, fresh prepared reaction buffer has a dark reddish to brown color. If DTT is not added fresh to the reaction mix, the color of the reaction buffer is colorless. 100 μL of the reaction buffer were added to the cell suspension. 2 μL of the substrate prepared as stock solution in EtOH was first added by 8-channel pipette, later on with the Multipette, so that a final concentration of 1 mM

(library 1) or 0.5 mM (library 2 and 3) was present. The plates were closed with a plastic lid and incubated at 30°C, 200 rpm (Infors HT shaker, attached in an inclined way).

After 24 hours, the reaction was stopped by extraction with 400 µL ethyl acetate. Phase separation was performed by centrifugation (Eppendorf 5810R, 10 min, 4 °C, 4000 rpm). The organic phase was transferred in 96-well microtiter glass plates (Zinsser) with a Tecan robot equipped with a 96-tip head MCA. Plates were placed at room temperature in a clean fume-hood overnight, covered with a paper box to evaporate all ethyl acetate but prevent dust to get in. Remaining dry samples were solved in 100 µL acetonitrile and analyzed via HPLC-UV/Vis. For measurement in HPLC, the glass plates were put in a metal frame and closed with a white plastic septum.

7.2.3.3 Screening of Library Generation 4

The reaction was performed as described in chapter 7.2.3.2 above but using HEPES buffer with 50 mM HEPES, 50 mM NaCl, pH 7.4 and final cofactor concentrations of 2.5 mM α KG, 1.25 mM ascorbic acid, 1 mM $(\text{NH}_4)_2\text{Fe}(\text{SO}_4)_2$ and 0.5 mM substrate.

7.2.4 Analysis of Reaction Conditions with *Wi-WelO15* Variants

The following reactions were performed with substrate **54**, after the first activity was shown. If not mentioned otherwise, generally the reactions were performed in duplicates in a 2 mL reaction tube or in 2.2 mL squared 96 dw plate.

7.2.4.1 Concentration of Enzyme and Cofactors

1) The reactions were performed in a 2.2 mL squared 96 dw plate with a total volume of 300 µL and purified *Wi-1*. The reaction was performed in 50 mM HEPES, 10 mM NaCl which was purged with N_2 , before adding reaction components. 8 different master solutions with enzyme, $(\text{NH}_4)_2\text{Fe}(\text{SO}_4)_2$ and α KG were prepared. 50 µM or 100 µM enzyme were combined with 0.25 mM or 0.1 mM $(\text{NH}_4)_2\text{Fe}(\text{SO}_4)_2$, and 1.25 or 2.5 mM α KG. Different reducing agents were added to the plate directly with final concentrations of 0.5 mM DTT, 0.5 mM ascorbic acid or no reducing agent to see the influences on the reaction. Substrate **54** was used in a final concentration of 0.5 mM. The reaction was incubated for 4 h at 30 °C, 200 rpm (Infors HT shaker, attached in an inclined way) and stopped by extraction with 400 µL ethyl acetate. Phase separation was performed by centrifugation (Eppendorf 5810R, 10 min, 4 °C, 4000 rpm). The organic phase was transferred in microtiter plates with a Tecan robot equipped with a 96-tip head MCA. The plates were placed at room temperature in a clean fume-hood overnight to evaporate all ethyl acetate. Remaining dry samples were solved in acetonitrile and analyzed via HPLC-UV/Vis.

2) The above described reaction was repeated with 20, 50 and 100 µM enzyme in combination with 0.25 and 0.5 mM $(\text{NH}_4)_2\text{Fe}(\text{SO}_4)_2$ and again 1.25 and 2.5 mM α KG. All reactions were performed with 0.5 mM DTT and 0.5 mM **54**. The reaction was run for 24 h.

Methods

3) Different reducing agents in three different concentrations (0.25, 0.5 and 1 mM) were tested with cell lysate of *Wi-1*. The conversion in dependency to time was analyzed as well. A pellet from flask expression (0.5 L cell culture) was thawed in cold water and diluted to 47.5 mL with HEPES 3 buffer. 0.5 mL of the suspension was pipetted in each well of a 2.2 mL 96 dw plate. The cells were pelleted by centrifugation (4000 rpm, 4 °C, 5810R Eppendorf centrifuge) for 10 min and the supernatant discarded. The pellets were suspended in HEPES 3 buffer containing 1 mg/mL lysozyme and 100 µM FeCl₃ (which was forgotten during the enzyme production). After vortexing and incubation for 30 min at 37 °C (Infors HT shaker), 150 µL master mix consisting of N₂ purged HEPES 3 buffer with 1 mM (NH₄)₂Fe(SO₄)₂ and 5 mM αKG was added to the wells. Finally, the reducing agents and 3 µL substrate **54** (100 mM in EtOH) was added to each well by Multipette. After 1, 2, 4, 6, and 22 h, samples were taken out of the plate and extracted in 2 mL reaction tubes. The organic phase was handled as described above and analyzed by HPLC.

4) The reaction was performed in 2 mL reaction tubes and a total volume of 200 µL. Purified enzymes *Wi-5* and *Wi-8* were examined. The enzymes were diluted with N₂ purged HEPES 3 (50 mM HEPES, 10 mM NaCl, pH 7.4) to 20 µM. 100 µL of the enzyme solution was filled into the reaction tube. A 2x concentrated reaction buffer consisting of 10 mM αKG, 1 mM ascorbic acid, 1 mM (NH₄)₂Fe(SO₄)₂ was prepared and 100 µL added to the tube. Resulting in final concentrations of 10 µM enzyme, 5 mM αKG, 0.5 mM ascorbic acid, 0.5 mM (NH₄)₂Fe(SO₄)₂. 2 µL of **54** (50 mM in EtOH) was added to a final concentration of 0.5 mM. The reaction tubes were closed, incubated at 30 °C, 700 rpm and stopped by extraction with 200 µL ethyl acetate. The organic phase was handled as described above and analyzed by HPLC-UV/Vis.

7.2.4.2 Temperature Stability of *Wi-WelO15* Variants

The reaction was performed in 2 mL reaction tubes and a total volume of 200 µL. Variants *Wi-5*, *Wi-5P3*, *Wi-8*, *Wi-11* and *Wi-12* were analysed. The enzymes were diluted with N₂ purged HEPES 4 (50 mM HEPES, 100 mM NaCl, pH 7.4) to 20 µM. 100 µL of the enzyme solution was filled into the reaction tubes. A 2x concentrated reaction buffer consisting of 10 mM αKG, 5 mM ascorbic acid, 1 mM (NH₄)₂Fe(SO₄)₂ was prepared and 100 µL added to the tube. Resulting in final concentration of 10 µM enzyme, 5 mM αKG, 0.5 mM ascorbic acid, 0.5 mM (NH₄)₂Fe(SO₄)₂. 2 µL of **54** (50 mM in EtOH) was added to a final concentration of 0.5 mM. The reaction was incubated in an Eppendorf Thermomixer at 30 °C, 35 °C, 40 °C or 45 °C and 700 rpm. After 5 h, the reaction was stopped by extraction with 200 µL ethyl acetate. The organic phase was handled as described above and analyzed by HPLC-UV/Vis.

7.2.4.3 Solvent Stability of *Wi-WelO15* Variants

1) The reaction was performed in 2 mL reaction tubes and a total volume of 200 µL. Variants *Wi-5* and *Wi-8*, were analyzed. The enzymes were diluted with N₂ purged HEPES 3 (50 mM HEPES, 10 mM NaCl, pH 7.4) to 20 µM. The solvent (8 µL = 5% or 18 µL = 10%) was pipetted

into the vial together with 2 μL substrate **54** (50 mM in EtOH, ACN or acetone). N_2 purged HEPES 3 buffer was added to a volume of 50 μL . A 4x concentrated reaction buffer consisting of 20 mM αKG , 10 mM ascorbic acid, 2 mM $(\text{NH}_4)_2\text{Fe}(\text{SO}_4)_2$ was prepared and 50 μL added to the tube. 100 μL of the enzyme solution was filled into the reaction tube Resulting in final concentration of 10 μM enzyme, 5 mM αKG , 0.5 mM ascorbic acid, 0.5 mM $(\text{NH}_4)_2\text{Fe}(\text{SO}_4)_2$ and 0.5 mM **54**. The reaction was incubated in Eppendorf Thermomixer at 30 $^\circ\text{C}$, 700 rpm. After 5 h, the reaction was stopped by extraction with 200 μL ethyl acetate. The organic phase was handled as described above and analyzed by HPLC-UV/Vis.

2) The reaction was performed in 2 mL reaction tubes and a total volume of 200 μL . Variants *Wi-5*, *Wi-5P3*, *Wi-8*, *Wi-11* and *Wi-12* were analyzed. The enzymes were diluted with N_2 purged HEPES 4 (50 mM HEPES, 100 mM NaCl, pH 7.4) to 20 μM . EtOH or acetone (0 μL = 1%; 8 μL = 5% or 18 μL = 10%) was pipetted into the vial together with 2 μL substrate **54** (50 mM in EtOH, or acetone). N_2 purged HEPES 4 was added to a volume of 50 μL (48 μL = 1%; 40 μL = 5% or 30 μL = 20%). A 4x concentrated reaction buffer consisting of 20 mM αKG , 10 mM ascorbic acid, 2 mM $(\text{NH}_4)_2\text{Fe}(\text{SO}_4)_2$ was prepared and 50 μL added to the tube. 100 μL of the enzyme solution was filled into the reaction tube, resulting in final concentration of 10 μM enzyme, 5 mM αKG , 0.5 mM ascorbic acid, 0.5 mM $(\text{NH}_4)_2\text{Fe}(\text{SO}_4)_2$ and 0.5 mM substrate. The reaction was incubated in Eppendorf Thermomixer at 30 $^\circ\text{C}$, 700 rpm. After 5 h, the reaction was stopped by extraction with 200 μL ethyl acetate. The organic phase was handled as described above and analyzed by HPLC-UV/Vis.

7.2.4.4 Whole Cell Assay

To test if the biotransformation can take place in whole cells, the reaction was performed in 2.2 mL squared dw plates with 200 μL culture. 5 mL LB or TB medium containing 50 $\mu\text{g}/\text{mL}$ kan, 20 μM IPTG and 50 μM FeCl_3 was inoculated with either 1% preculture or other 10% preculture and distributed to the plate. The plate was incubated at 37 $^\circ\text{C}$, 200 rpm for 2 h or 4 h. Then substrate **54** (final conc. 0.5 mM) and αKG (final conc. 2.5 mM) were added to the culture and let grown for 4 h or 16 h at 30 $^\circ\text{C}$. After the according time, the samples were pipetted out of the plate and extracted in a 1.5 mL reaction tube with 200 μL ethyl acetate. The organic phase was handled as described above and analyzed by HPLC-UV/Vis.

7.2.5 Analysis of Substrate Scope with Optimized Reaction Conditions

7.2.5.1 Lysate-Based Biotransformation from Normalized Cell Mass

Expression was performed in flasks as described in ch. 7.1.9.1. To obtain equal cell mass in each reaction, the OD_{600} was determined and a volume of culture corresponding to an optical density of 5.0 was filled in plates or 2 mL reaction tubes and pelleted. The supernatant was discarded and the pellets frozen and stored at -20 $^\circ\text{C}$. The cell pellets were thawed at room temperature. For the reaction, cells were resuspended by vortexing with 100 μL HEPES 4

Methods

buffer (50 mM HEPES, 100 mM NaCl, pH 7.4) containing 1 mg/mL lysozyme. To lyse the cells, the plates were incubated at 37 °C for 30 min. In the meantime, 2x reaction buffer was prepared. For the reaction buffer, N₂ purged HEPES 4 buffer was used and mixed with freshly prepared reaction compounds so that a concentration of 5 mM α KG, 5 mM ascorbic acid and 1 mM (NH₄)₂Fe(SO₄)₂ were present in the 2x buffer. 100 μ L of the reaction buffer were added to the cell suspension. 2 μ L of the substrate prepared as stock solution in EtOH was added by Multipette, so that a final concentration of 0.5 mM was present. The plates were closed with a plastic lid and incubated at 30°C, 200 rpm (Infors HT shaker, attached in an inclined way).

After 8 hours, the reaction was stopped by extraction with 400 μ L ethyl acetate. Phase separation was performed by centrifugation. The organic phase was transferred in 96-well microtiter glass plates (Zinsser) with a Tecan robot equipped with a 96-tip head MCA. Plates were placed at room temperature in a clean fume-hood overnight, covered with a paper box to evaporate all ethyl acetate but prevent dust to get in. Remaining dry samples were solved in 100 μ L acetonitrile and analyzed via HPLC-UV/Vis. For measurement in HPLC, the glass plates were put in a metal frame and closed with a white plastic septum.

The expression levels were analyzed by SDS-PAGE analysis (see chapter 8.5.2): by resuspending the pellets in 100 μ L lysis buffer (50 mM HEPES, 100 mM NaCl, pH 7.4, 1 mg/mL lysozyme). After incubation 37 °C for 30 min for cell lysis, the suspension was centrifuged for 2 min at 14000 rpm. 15 μ L of the supernatant was mixed with 5 μ L 4x SDS-PAGE sample buffer and incubated at 95 °C for 10 min. The samples were centrifuged for 10 min at 14000 rpm and 6 μ L applied to the gel.

7.2.5.2 Analysis of Substrate Scope with Purified Enzyme

HEPES 4 buffer (50 mM HEPES, 100 mM NaCl, pH 7.4) was purged with N₂ for at least 0.5 h to remove oxygen. All reaction components were prepared in this buffer. α KG (as disodium α -ketoglutarate) was stored as 100 mM stock at -20°C, ascorbic acid and (NH₄)₂Fe(SO₄)₂ solutions were prepared each time fresh. The 2x reaction buffer consists of the N₂ purged HEPES 4 buffer containing 10 mM α KG, 5 mM ascorbic acid and 1 mM (NH₄)₂Fe(SO₄)₂. The reaction was performed in total a volume of 200 μ L. The purified enzymes were diluted with purged buffer to a concentration of 20 μ M. 100 μ L enzyme solution and 100 μ L of the 2x buffer were added in each well. 2 μ L (0.05 M in EtOH) substrate was added using a Multipette (Eppendorf) reaching a final concentration of 0.5 mM. After 8 hours incubation at 30°C and 200 rpm (Infors HT shaker), the reaction was stopped by extracting with 400 μ L ethyl acetate. Phase separation was performed by centrifugation. The organic phase was transferred in microtiter plates with a Tecan robot equipped with a 96-tip head MCA. Plates were placed at room temperature in a clean fume-hood overnight to evaporate all ethyl acetate. Remaining dry samples were solved in 100 μ L acetonitrile and analyzed via HPLC-UV/Vis.

7.2.6 Kinetic Analysis of Halogenase Variants

For kinetic analysis, enzyme and α KG were thawed on ice. HEPES 3 buffer (50 mM HEPES, 10 mM NaCl, pH 7.4) was purged with N_2 to remove oxygen. All reactions were made in duplicates or quadruplicates. Reaction buffer was prepared by mixing enzyme (final conc. 10 μ M), α KG (final conc. 5 mM), $(NH_4)_2Fe(SO_4)_2$ (final conc. 0.5 mM), ascorbic acid (final conc. 0.5 mM) in N_2 purged HEPES 3 buffer. Iron and ascorbic acid were solved with nitrogen purged buffer and added latest. The reaction mix was aliquoted as 200 μ L in 2 mL reaction tubes and incubated in an Eppendorf Thermomixer at 30 $^{\circ}$ C, 700 rpm at least for 2 min to reach the reaction temperature of 30 $^{\circ}$ C. The lid of all reaction tubes was left open during the reactions to allow O_2 diffusion into the reaction mixture. The reactions were stopped after different times to gain product formation versus time. For technical reasons, for short measurements (3, 6, 10 s), the vial was taken out of the Thermomixer. The substrate was added to one vial which was shaken by hand in the meantime and finally extracted by adding ethyl acetate and vortexing. For longer incubation times (20, 40 and 60 s) the vials were left in the Eppendorf Thermoshaker while 2 μ L substrate was added to the vials every 3 s. The tubes were taken out and the reaction stopped by adding ethyl acetate by Multipette (Eppendorf) and vortexing. Different substrate concentrations, 1.5, 1.0, 0.5, 0.25, 0.125, 0.0625 and 0.031 mM were used for enzymes with $K_m > 100$ μ M. Enzymes with lower K_m were further analyzed with substrate concentrations of 0.0156, 0.0078 and 0.0039 mM. A 150 mM stock solution of **54**, **77**, **78** was prepared in EtOH and diluted accordingly to create the lower concentrated stocks. However, **53** and **76** were only soluble in EtOH up to 75 mM. Lower stock solutions were prepared by diluting 1-1 with solvent. Resulting in stock solutions with 100-fold concentration so that a volume of 2 μ L was added to each reaction. The reaction was stopped by the addition of 200 μ L ethyl acetate. After phase separation by centrifugation, 140 μ L of the organic phase were transferred to an HPLC vial, ethyl acetate was evaporated, and remaining samples resuspended in 70 μ L acetonitrile. The samples were analyzed by HPLC and measured on a Shimadzu LC2030 HPLC. The injection volume varied depending on concentration. Extraction of **54** is linear in a concentration range of 0.0625-2.5 mM comparing HPLC-UV signal areas (figure 61). After the reaction, the obtained areas did not fit to the calibration curve anymore. Therefore, the conversion was calculated from relative areas. Based on the conversion, the product formation in μ M was calculated from the used substrate concentration. Product formation was plotted against time and initial velocity was determined. Initial velocity was plotted against substrate concentration. V_{max} and K_m were determined using GraphPad Prism 7 Michaelis Menten model (equation 4). *Wi-2* and *Wi-5* with substrate **54** showed substrate inhibition. Equation 5 was used for fitting curves with substrate inhibition.

$$[Y = V_{max} * X / (K_m + X)] \quad (4)$$

$$[Y = V_{max} * X / (K_m + X * (1 + X / K_i))] \quad (5)$$

Methods

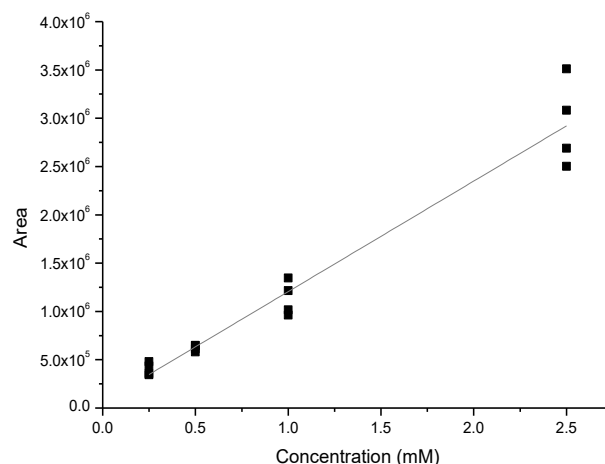


Figure 61. Comparing HPLC areas in dependency to concentration **54** after extraction out of 50 mM HEPES, 10 mM NaCl.

7.2.7 Screening of P450 Libraries

The reactions were performed in 2.2 mL dw 96-well plates. Protein production was performed as described in ch. 7.1.9.7. The cell pellets were stored at -80 °C. To start the reaction, the pellets were thawed in cold water and 196 μ L 1 mg/mL lysozyme in 0.1 M KPi buffer was added. The pellets were suspended by vortexing and the plate was incubated for 30 min at 200 rpm (Infors HT shaker). 2x reaction buffer was prepared, of which 200 μ L were added after the lysis, so that a final concentration of 0.25 mM NADP⁺, 0.25 M Glucose, 5% glycerol, 5 mM EDTA, 1 U GDH was present. 4 μ L of a 100 mM stock solution **54** in EtOH was added, so that a final concentration of 1 mM **54** was present in the reaction. The plates were incubated for 24 h at 30 °C then, the reaction was stopped by extraction with 400 μ L ethyl acetate. Phase separation was performed by centrifugation. The organic phase was transferred in microtiter plates with a Tecan robot equipped with a 96-tip head MCA. Plates were placed at room temperature in a clean fume-hood overnight to evaporate all ethyl acetate. Remaining dry samples were solved in acetonitrile and analyzed via HPLC-UV/Vis.

7.3 Preparative Scale Biotransformation

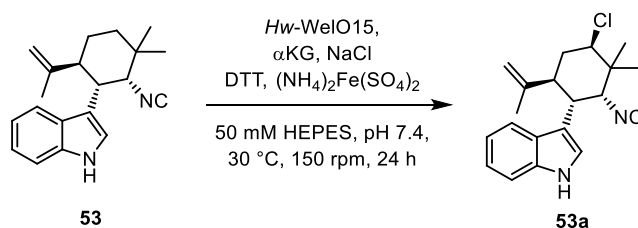
7.3.1 Halogenase

7.3.1.1 General Information

Within the different reaction set-ups, the conditions were optimized. Individual reaction conditions and analysis of products can be found below. Conditions that worked best and are recommended to use are: 20-30 μM enzyme*, 50 mM HEPES, 100 mM NaCl, pH 7.4, 10 mM αKG , 5 mM ascorbic acid, 1 mM $(\text{NH}_4)_2\text{Fe}(\text{SO}_4)_2$ and a substrate concentration of 0.5-0.75 mM. As standard, later, the reaction was performed in 0.5 L flat bottom round flasks with 50 mL volume. The flask was closed with a gas permeable foil and incubated at 30 $^\circ\text{C}$, 100 rpm in Infors Ecotron shaker.

*The enzyme concentration in lysate cannot be determined except by SDS-PAGE analysis which includes a high error.^[383] Therefore the chlorinase concentration was estimated to be 60-80 mg/L cell culture, based on the fact that all variants reliably yield 60-65 mg/L after IMAC purification.

7.3.1.2 Characterization of 53a



The reaction was performed by L. Schmermund^[317] in a total reaction volume of 34.2 mL with 1.00% (v/v) ethanol. The purified *Hw-WelO15* was diluted with nitrogen purged buffer (50 mM HEPES, 10 mM NaCl, pH 7.4) to a final concentration of 40 μM . Then 2x reaction buffer was added to the enzyme solution. For the reaction, reactants αKG , DTT and $(\text{NH}_4)_2\text{Fe}(\text{SO}_4)_2$ were solved in nitrogen purged buffer and added to the enzyme solution, to a final concentration of 5 mM αKG , 0.5 mM DTT, 0.5 mM $(\text{NH}_4)_2\text{Fe}(\text{SO}_4)_2$ and 20 μM *Hw-WelO15*. Then 15 mg (45.9 μmol , 1.0 eq, 1.35 mM) **53**, solved in 340 μL ethanol, were added to the reaction. The reaction was incubated at 30 $^\circ\text{C}$ and 150 rpm for 24 h. After 24 h the reaction was extracted with EtOAc (5 x 10 mL), the phases were separated by centrifugation (4000 rpm, 15 min, 4 $^\circ\text{C}$) and the solvent was removed under reduced pressure. The crude product was purified by preparative HPLC (isocratic ACN : water 60 : 40) and 8.0 mg (24.5 μmol , 48%) of **53a** were obtained as colorless solid.

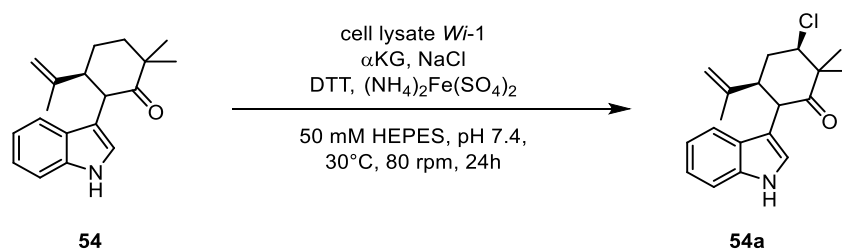
$^1\text{H-NMR}$ (500 MHz, CDCl_3), δ = 8.13 (s, 1H, NH), 7.45 (d, 1H, J = 7.85 Hz, H_4), 7.39 (d, 1H, J = 8.10 Hz, H_7), 7.23-7.20 (m, 1H, H_6), 7.39 (d, 1H, J = 2.30 Hz, H_2), 7.16-7.12 (m, 1H, H_5), 4.84 (s, 1H, $\text{H}_{17/\text{cis}}$), 4.72-4.71 (m, 1H, $\text{H}_{17/\text{trans}}$), 4.30 (dd, 1H, J = 12.5, 4.70 Hz, H_{13}), 3.81 (s, 1H, H_{11}), 3.62-

Methods

3.59 (m, 1H, H₁₀), 3.20 (td, 1H, $J = 12.3, 4.13$ Hz, H₁₅), 2.21-2.17 (m, 1H, H₁₄), 2.13-2.05 (m, 1H, H₁₄), 1.54 (s, 3H, H₁₈), 1.35 (s, 3H, H₁₉), 1.32 (s, 3H, H₂₀) ppm; ¹³C-NMR (125 MHz, CDCl₃), $\delta = 158.5$ (NC), 145.5 (C₁₆), 135.8 (C₈), 126.6 (C₉), 123.6 (C₂), 122.3 (C₆), 119.8 (C₅), 117.2 (C₄), 113.5 (C₁₇), 112.5 (C₃), 111.7 (C₇), 68.1 (C₁₁), 63.6 (C₁₃), 44.4 (C₁₅), 39.8 (C₁₂), 38.8 (C₁₄), 35.0 (C₁₀), 26.9 (C₂₀), 19.3 (C₁₉), 18.8 (C₁₈) ppm;

HRMS (ESI⁺): C₂₀H₂₃ClN₂H⁺ [M+H]⁺, m/z found: 327.1618; calc.: 327.1623.

7.3.1.3 Characterization of 54a



The reaction was performed in a total reaction volume of 100 mL with 1.9% (v/v) ethanol. The reaction was performed with cleared lysate of *Wi-1*. A pellet of *Wi-1* (0.8 L cell culture, ~48 mg enzyme) was suspended in 30 mL HEPES 3 buffer (50 mM HEPES, 10 mM NaCl, pH 7.4) and lysed by sonication. After centrifugation (45 min, 16 000 rpm, 4 °C), 25 mL cleared lysate were received. 75 mL of nitrogen purged HEPES 3 buffer was added and cofactors to a concentration of 7.5 mM α KG, 1 mM DTT, 2.5 mM (NH₄)₂Fe(SO₄)₂, 56 mg **54** were solved in 1.9 mL EtOH and added to the reaction (2 mM final concentration), which was recovered from plate reactions and therefore was impure with **54a**. The mixture was filled into a 500 mL Erlenmeyer flask and incubated at 30 °C and 80 rpm in Infors Ecotron shaker. After 24 h the reaction was stopped by extraction with ethyl acetate. First for separation and later sickness reasons the reaction mixture was left at room temperature for 2 weeks. Phase separation was achieved by centrifugation in an Eppendorf centrifuge (Eppendorf 5810 R, rotor F-34-6-38), 4000 rpm for 10 min and additional 5 min at 8000 rpm. The organic phase was concentrated in vacuo. Remaining samples were solved in 60 : 40 ACN : H₂O and filtered by a 0.45 μ m PTFE filter and purified via preparative HPLC. A total amount of 2.6 mL was injected via loop. An isocratic program with running time 60 min and 10 mL/min was used for purification. The product area increased to 15% in relative ratio to the educt, while the concentration of **54a** in the educt was not known. After purification, 2 mg pure **54a** (3.4%) were received. ¹H, ¹³C NMRs were successfully measured. The reaction was repeated by L. Schmermund to determine absolute stereo conformation of the chloride by NOESY NMR.^[317]

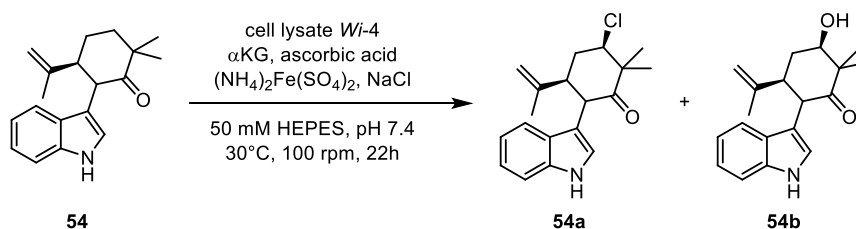
¹H-NMR (500 MHz, CDCl₃), $\delta = 8.05$ (s, 1H, NH), 7.33-7.31 (m, 1H, H₇), 7.30-7.29 (m, 1H, H₄), 7.17-7.14 (m, 1H, H₆), 7.08-7.05 (m, 1H, H₅), 6.92 (d, 1H, $J = 2.45$ Hz, H₂), 4.66 (s, 1H, H_{17/cis}), 4.63-4.62 (m, 1H, H_{17/trans}), 4.23 (d, 1H, $J = 12.8$ Hz, H₁₀), 4.12 (dd, 1H, $J = 12.4, 4.49$ Hz, H₁₃), 2.82 (td,

Methods

^1H , $J = 12.7, 3.60$ Hz, H_{15}), 2.55-2.47 (m, 1H, H_{14}), 2.34-2.30 (m, 1H, H_{14}), 1.59-1.58 (m, 3H, H_{18}), 1.46 (s, 3H, H_{19}), 1.30 (s, 3H, H_{20}) ppm; ^{13}C -NMR (125 MHz, CDCl_3), $\delta = 209.5$ (CO), 145.0 (C_{16}), 136.2 (C_8), 127.4 (C_9), 123.3 (C_2), 122.0 (C_6), 119.5 (C_5), 119.6 (C_4), 113.4 (C_{17}), 111.5 (C_7), 111.1 (C_3), 67.1 (C_{13}), 52.0 (C_{12}), 48.6 (C_{15}), 47.0 (C_{10}), 38.7 (C_{14}), 23.0 (C_{20}), 20.4 (C_{19}), 18.5 (C_{18}) ppm; HRMS (ESI⁺): $\text{C}_{19}\text{H}_{22}\text{ClNOH}^+$ [$\text{M}+\text{H}$]⁺, m/z found: 316.1467; calc.: 316.1463.

Optical rotation (in CHCl_3 , 22 °C, $\lambda = 589$ nm, cuvette 50 mm, 0.48 g/100mL) 27.776.

7.3.1.4 Characterization of 54b



Protocol 1:

The reaction was performed in a total reaction volume of 80 mL with 0.4% (v/v) ethanol. The reaction was performed with cleared lysate of *Wi-4*. Enzymes were produced as described in ch. 7.1.9.1. In total 1 L cell culture was cultivated and pelleted. The cell pellet was suspended with buffer (50 mM HEPES, 100 mM NaCl, pH 7.4) and frozen. The frozen cell suspension was thawed in cold water. Ascorbic acid was added to a final concentration of 1.5 mM and cells lysed by sonication (6 min with 30 s pulses and 30 s rest). During sonification the suspension is put on ice. Then the suspension was pelleted (16000 rpm, 4 °C, 45 min) and the supernatant used for the reaction. Reactants α -KG, ascorbic acid and $(\text{NH}_4)_2\text{Fe}(\text{SO}_4)_2$ were solved in N_2 purged buffer and added to the lysate, so that a final concentration of 10 mM α -KG, 5 mM ascorbic acid, 1 mM $(\text{NH}_4)_2\text{Fe}(\text{SO}_4)_2$ and roughly 20-30 μM *Wi-5* (based on average yield from purification of enzyme) was obtained. Then 17 mg **54** were solved in 0.3 mL ethanol and added to the reaction to achieve a final concentration of 0.75 mM substrate. The reactions were incubated at 30 °C, 100 rpm (Infors Ecotron shaker). After 24 h the reaction was stopped by extraction with ethyl acetate. 25 mL of the reaction solution were poured in a 50 mL falcon and extracted 2x with 25 mL ethyl acetate. Phase separation was achieved by centrifugation (9000 rpm, 45 min Eppendorf 5810 R, rotor F-34-6-38). The solvent was removed in vacuo. Conversion was analyzed by HPLC. A conversion of only 6.5% with 4.7% formation **54a** and 1.9% formation of **54b** could be achieved.

Protocol 2:

The reaction was performed in a total reaction volume of 11x50 mL with 1% (v/v) ethanol. The reaction was performed with cleared lysate of *Wi-4*. Enzymes were produced by heterologous expression as described in ch. 7.1.9.1. In total 8.25 L cell culture were prepared and pelleted (0.75 L/50 mL reaction). The cell pellets were resuspended with buffer (50 mM HEPES,

Methods

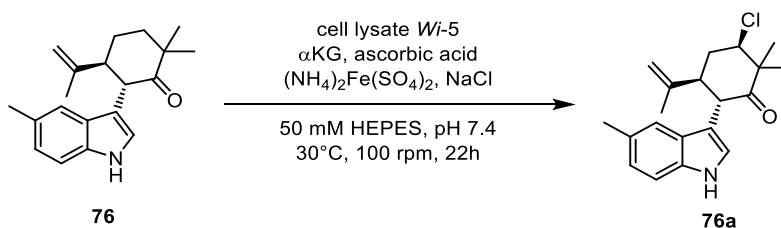
100 mM NaCl, pH 7.4) and frozen. The frozen cell suspension was defrosted in cold water and cells lysed by sonication (6 min with 30 s pulses and 30 s rest). During sonification the suspension is put on ice and was pelleted (16000 rpm, 4 °C, 45 min). The supernatant was used for the reaction. Reactants α KG, ascorbic acid and $(\text{NH}_4)_2\text{Fe}(\text{SO}_4)_2$ were solved in N_2 purged buffer and added to the lysate, so that a final concentration of 10 mM α KG, 5 mM ascorbic acid, 1 mM $(\text{NH}_4)_2\text{Fe}(\text{SO}_4)_2$ and roughly 20-30 μM *Wi-5* (based on average yield from purification of enzyme) was obtained. Then 77 mg **54** (7 mg/reaction, 0.5 mM final concentration) were solved in 3.5 mL ethanol, and 0.5 mL were added to the reaction to achieve a final concentration of 0.5 mM substrate. The reactions were incubated at 30 °C, 100 rpm (Infors Ecotron shaker). After 24 h the reaction was stopped by extraction with ethyl acetate. 25 mL of the reaction solution were poured in a 50 mL falcon and extracted 2x with 25 mL ethyl acetate. Phase separation was achieved by centrifugation (9000 rpm, 45 min, Eppendorf 5810 R, rotor F-34-6-38). The solvent was removed in vacuo. Conversion was analyzed by HPLC. A conversion of 35% with 23% formation **54a** and 12% formation of **54b** could be achieved.

Out of economical and time reasons, all samples from protocol 1 and 2 were combined before purification by preparative HPLC (ch. 7.5.4). In total 8 mg **54b** could be isolated and used for analysis

$^1\text{H-NMR}$ (500 MHz, DMSO), δ = 10.72 (s, 1H, NH), 7.27 (t, 2H, J = Hz), 7.00 (m, 2H), 6.88 (t, J =, 1H), 5.07 (d, 1H, J =, OH), 4.58 (s, 1H, H_{17}), 4.45 (s, 1H, H_{17}), 4.14 (d, 1H, J = Hz, H_{10}), 3.59 (dt, 1H, J = Hz, H_{13}), 2.79 (td, 1H, J = Hz, H_{15}), 2.08 (q, 1H, H_{14}), 1.82 (dt, 1H, H_{14}), 1.54 (s, 3H, H_{18}), 1.22 (s, 3H, H_{19}), 1.05 (s, 3H, H_{20}) ppm; $^{13}\text{C-NMR}$ (125 MHz, DMSO), δ = 211.74 (CO), 146.38, 136.02, 127.34, 124.13, 120.29, 118.88, 117.86, 111.85, 111.17, 110.67, 73.89, 81.17, 46.04, 45.01, 36.44, 22.01, 18.91, 18.01 ppm;

HRMS (ESI⁺): $\text{C}_{20}\text{H}_{24}\text{ClNO}_2\text{H}^+$ $[\text{M}+\text{H}]^+$, m/z found: 298.1804; calc.: 298.1802.

7.3.1.5 Characterization of 76a



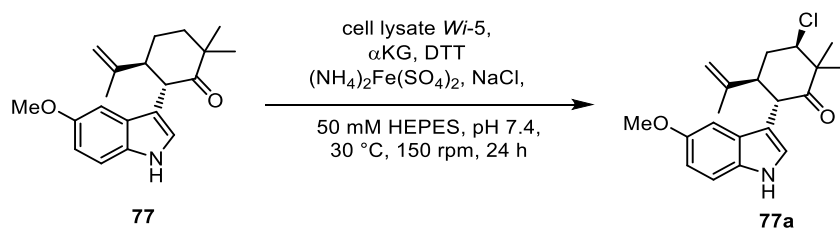
The reaction was performed in a total reaction volume of 120 mL with 1% (v/v) ethanol. *Wi-5* was produced as described in ch. 7.1.9.1. A pellet of 1.6 L cell culture was resuspended with buffer (50 mM HEPES, 100 mM NaCl, pH 7.4) and lysed by sonication. Solid components were removed by centrifugation (16000 rpm, 4 °C, 45 min). The supernatant was used for the reaction. Reactants α KG, ascorbic acid and $(\text{NH}_4)_2\text{Fe}(\text{SO}_4)_2$ were solved in N_2 purged buffer and added to the lysate, so that a final concentration of 10 mM α KG, 5 mM ascorbic acid, 1 mM $(\text{NH}_4)_2\text{Fe}(\text{SO}_4)_2$ and roughly 20-30 μM *Wi-5* (based on average yield from purification of enzyme) was obtained. 32 mg **76** solved in 1.2 mL ethanol, were added to the reaction (0.11 mmol, 0.92 mM). The reaction was incubated at 30 °C and 100 rpm (Infors Ecotron shaker). After 24 h, the reaction was extracted with 80 mL EtOAc, the phases were separated by centrifugation (9000 rpm, 45 min, 4 °C, Eppendorf 5810 R, rotor F-34-6-38) and the solvent was removed under reduced pressure. The crude product was purified by preparative HPLC (isocratic 60 : 40 ACN : water) and 8.1 mg (25.0 μmol , 25%) of product **76a** were obtained as colorless solid.

$^1\text{H-NMR}$ (500 MHz, CDCl_3), δ = 7.93 (s, 1H, NH), 7.22 (d, 1H, J = 8.20 Hz, H₇), 7.04 (d, 1H, J = 0.66 Hz, H₄), 7.00-6.96 (m, 1H, H₆), 6.89 (d, 1H, J = 2.37 Hz, H₂), 4.67 (s, 1H, H_{17/cis}), 4.64-4.63 (m, 1H, H_{17/trans}), 4.20 (d, 1H, J = 12.8 Hz, H₁₀), 4.13 (dd, 1H, J = 12.3, 4.55 Hz, H₁₃), 2.82 (td, 1H, J = 12.6, 3.89 Hz, H₁₅), 2.57-2.245 (m, 1H, H₁₄), 2.42 (s, 3H, H₂₁) 2.35-2.28 (m, 1H, H₁₄), 1.59 (s, 3H, H₁₈), 1.46 (s, 3H, H₁₉), 1.30 (s, 3H, H₂₀) ppm; $^{13}\text{C-NMR}$ (125 MHz, CDCl_3), δ = 209.5 (CO), 145.1 (C₁₆), 134.6 (C₈), 128.7 (C₅), 127.6 (C₉), 123.8 (C₆), 123.4 (C₂), 118.5 (C₄), 113.4 (C₁₇), 111.1 (C₇), 110.7 (C₃), 67.1 (C₁₃), 52.0 (C₁₂), 48.4 (C₁₅), 46.9 (C₁₀), 38.7 (C₁₄), 23.0 (C₂₀), 21.8 (C₂₁), 20.5 (C₁₉), 18.5 (C₁₈) ppm

HRMS (ESI+): $\text{C}_{20}\text{H}_{24}\text{ClN}_2\text{O}_2\text{Na}^+$ $[\text{M}+\text{Na}]^+$, m/z found: 352.1434; calc.: 352.1439.

Optical rotation (in CHCl_3 , 22 °C, λ =589 nm, cuvette 50 mm, 0.68 g/100mL) 7.814.

7.3.1.6 Characterization of 77a



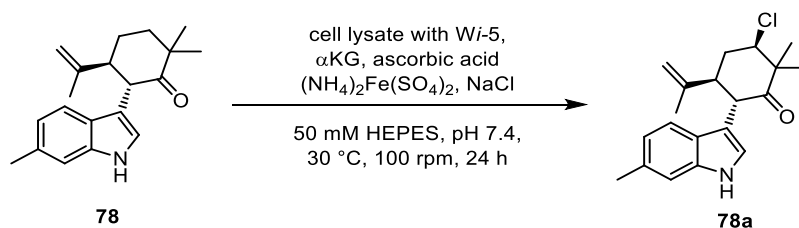
The reaction was performed by L. Schmermund^[317] in a total reaction volume of 129 mL with 1% (v/v) ethanol. *Wi-5* was produced as described in ch. 7.1.9.1. A pellet of 0.8 L cell culture was resuspended with buffer (50 mM HEPES, 10 mM NaCl, pH 7.4) and lysed by sonication. Solid components were removed by centrifugation (16000 rpm, 4 °C, 45 min). The supernatant was used for the reaction. Reactants α KG, DTT and $(\text{NH}_4)_2\text{Fe}(\text{SO}_4)_2$ were solved in N_2 purged buffer and added to the lysate, so that a final concentration of 2.5 mM α KG, 0.5 mM DTT, 0.5 mM $(\text{NH}_4)_2\text{Fe}(\text{SO}_4)_2$ and roughly 20-30 μM *Wi-5* (based on average yield from purification of enzyme) was obtained. 60 mg (0.19 mmol, 1.5 mM) ketone **77**, solved in 1.29 mL ethanol and added to the reaction. The reaction was incubated at 30 °C and 150 rpm for 24 h. After 24 h the reaction was extracted with EtOAc (4 x 10 mL), the phases were separated by centrifugation (4000 rpm, 15 min, 4 °C) and the solvent was removed under reduced pressure. The crude product was purified by preparative HPLC (isocratic 60 : 40 ACN : water) and 4.5 mg (13.0 μmol , 7%) of chlorinated product **77a** were obtained as colorless solid.

HPLC: Retention time 6.23 min (isocratic ACN/ H_2O 71:29); **$^1\text{H-NMR}$** (500 MHz, CDCl_3), δ = 7.95 (s, 1H, NH), 7.22 (d, 1H, J = 8.75 Hz, H₇), 6.90 (d, 1H, J = 2.45 Hz, H₄), 6.82 (dd, J = 8.75, 2.40 Hz, H₆), 6.72 (d, 1H, J = 2.41 Hz, H₂), 4.67 (s, 1H, H_{17/cis}), 4.64-4.63 (m, 1H, H_{17/trans}), 4.20 (d, 1H, J = 12.8 Hz, H₁₀), 4.11 (dd, 1H, J = 12.4, 4.53 Hz, H₁₃), 3.83 (s, 3H, H₂₁), 2.79 (td, 1H, J = 12.7, 3.65 Hz, H₁₅), 2.54-2.47 (m, 1H, H₁₄), 2.34-2.29 (m, 1H, H₁₄), 1.58-1.59 (m, 3H, H₁₈), 1.45 (s, 3H, H₁₉), 1.29 (s, 3H, H₂₀) ppm; **$^{13}\text{C-NMR}$** (125 MHz, CDCl_3), δ = 209.5 (CO), 154.0 (C₅), 144.9 (C₁₆), 131.5 (C₈), 127.9 (C₉), 124.2 (C₄), 113.4 (C₁₇), 112.0 (C₇), 111.5 (C₆), 110.7 (C₃), 101.6 (C₂), 67.1 (C₁₃), 56.1 (C₂₁), 52.0 (C₁₂), 48.4 (C₁₅), 46.9 (C₁₀), 38.6 (C₁₄), 23.0 (C₂₀), 20.4 (C₁₉), 18.5 (C₁₈) ppm;

HRMS (ESI⁺): $\text{C}_{20}\text{H}_{24}\text{ClNO}_2\text{H}^+$ [M+H]⁺, m/z found: 346.1570; calc.: 346.1568.

Optical rotation (in CHCl_3 , 22 °C, λ =589 nm, cuvette 50 mm, 0.65 g/100mL) 13.508.

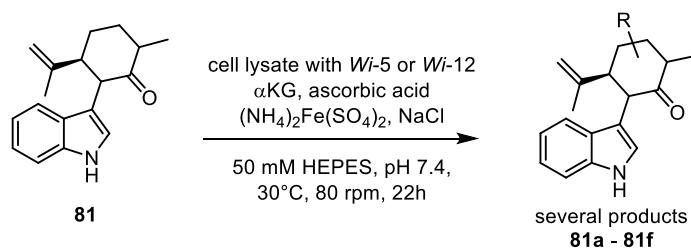
7.3.1.7 Characterization of 78a



The reaction was performed in a total reaction volume of 158 mL with 1% (v/v) ethanol. *Wi-5* was produced as described in ch. 7.1.9.1. A pellet originating from 1 L cell culture was resuspended with buffer (50 mM HEPES, 50 mM NaCl, pH 7.4) and lysed by sonication. Solid components were removed by centrifugation (16000 rpm, 4 °C, 45 min). The supernatant was used for the reaction. Reactants α KG, ascorbic acid and $(\text{NH}_4)_2\text{Fe}(\text{SO}_4)_2$ were solved in N_2 purged buffer and added to the lysate, so that a final concentration of 2.5 mM α KG, 1.25 mM ascorbic acid, 0.5 mM $(\text{NH}_4)_2\text{Fe}(\text{SO}_4)_2$ and roughly 20-30 μM *Wi-5* (based on average yield from purification of enzyme) was obtained. Then 70 mg (0.24 mmol, 1.5 mM) ketone **78**, solved in 1.58 mL ethanol, were added to the reaction. The reaction was incubated at 30 °C, 100 rpm (Infors Eco-tron shaker). The reaction was stopped by extraction after 24 h. The organic phase was dried in vacuo and purified via preparative HPLC. A conversion of 14% were achieved and after purification 7 mg pure **78a** (10% yield) were obtained.

$^1\text{H-NMR}$ (500 MHz, CDCl_3), δ = 7.90 (s, 1H, NH), 7.10 (d, 1H, J = 8.1 Hz, H_4), 7.12 (m, 1H, H_7), 6.90 (m, 1H, H_5), 6.85 (d, 1H, J = 2.30 Hz, H_2), 4.66 (m, 1H, $\text{H}_{17/\text{cis}}$), 4.62 (m, 1H, $\text{H}_{17/\text{trans}}$), 4.19 (d, 1H, J = 12.8 Hz, H_{10}), 4.12 (dd, 1H, J = 12.4, 4.5 Hz), 2.80 (dt, 1H, J = 12.7, 3.7 Hz, H_{15}), 2.54-2.46 (m, 1H, H_{14}), 2.43 (s, 3H, H_{21}), 2.33-2.29 (dt, 1H, J = 13.6, 4.1 H_{14}), 1.58-1.57 (m, 3H, H_{18}), 1.44 (s, 3H, H_{19}), 1.28 (s, 3H, H_{20}) ppm; **$^{13}\text{C-NMR}$** (125 MHz, CDCl_3), δ = 209.4 (CO), 142.0 (C_{16}), 136.7 (C_8), 131.8 (C_6), 125.2 (C_9), 122.6 (C_2), 121.4 (C_5), 118.6 (C_4), 113.4 (C_{17}), 111.4 (C_3), 111.0 (C_7), 67.1 (C_{13}), 52.0 (C_{12}), 48.5 (C_{15}), 47.0 (C_{10}), 38.7 (C_{14}), 23.0 (C_{20}), 21.8 (C_{21}), 20.4 (C_{19}), 18.5 (C_{18}) ppm; **HRMS** (ESI^+): $\text{C}_{20}\text{H}_{24}\text{ClNO}$ [$\text{M}+\text{H}$] $^+$, m/z found: 330.1614; calculated 330.1619.

Optical rotation (in CHCl_3 , 22 °C, λ = 589 nm, cuvette 50 mm, 0.49 g/100mL) 5.039.

7.3.1.8 Product Identification from Biotransformation with **81**

The reaction was performed in a total reaction volume of 6x50 mL with 1% (v/v) ethanol. The reaction was performed with cleared lysate (50 mL *Wi-5*, 5x50 mL *Wi-12*) to compare conversion. *Wi-5* and *Wi-12* were produced as described in ch. 7.1.9.1. The cell pellets of 0.75 L (*Wi-5*) and 3.75 L (*Wi-12*) cell culture were resuspended with buffer (50 mM HEPES, 100 mM NaCl, pH 7.4) and lysed by sonication. Solid components were removed by centrifugation (16000 rpm, 4 °C, 45 min). The supernatant was used for the reaction. Reactants α KG, ascorbic acid and $(\text{NH}_4)_2\text{Fe}(\text{SO}_4)_2$ were solved in N_2 purged buffer and added to the lysate, so that a final concentration of 10 mM α KG, 5 mM ascorbic acid, 1 mM $(\text{NH}_4)_2\text{Fe}(\text{SO}_4)_2$ and roughly 20-30 μM *Wi-5* and *Wi-12* (based on average yield from purification of enzyme) was obtained. Then 40 mg ketone **81** were solved in 2 mL ethanol (75 mM) and 13 mg **81** were solved in 1 mL ethanol (50 mM) so that 0.5 mL were added to the reaction to achieve a final concentration of 0.75 mM or 0.5 mM substrate. The reactions were incubated at 30 °C, 100 rpm (Infors Ecotron shaker). The reaction was stopped by extraction after 24 h. After extraction, a sample was taken to compare conversion of each reaction. At least 6 products were produced within the reactions. Total conversions of 11% (*Wi-5* lysate), 28% (*Wi-12* lysate, 0.75 mM **81**) and 37% (*Wi-12* lysate, 0.5 mM **81**) were obtained. The solvent was removed in vacuo and dry remaining samples solved again in acetonitrile. Out of economical and time reasons, the samples were combined before purification by preparative HPLC.

81a HPLC (71 : 29 ACN : H_2O): 2.2 min LC-MS (ESI⁺) (M+H)⁺: 146.100 g/mol

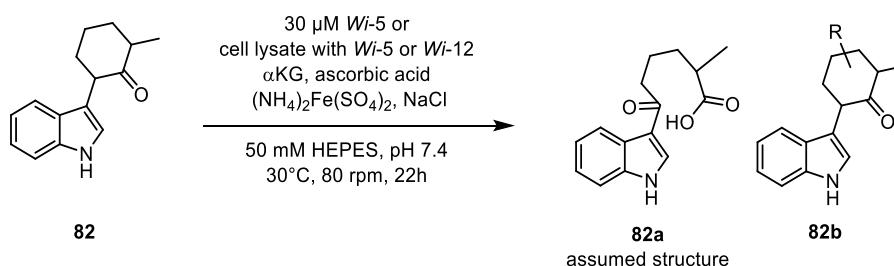
81b HPLC (71 : 29 ACN : H_2O): 2.6 min LC-MS (ESI⁺) (M+H)⁺: 284.100 g/mol

81c HPLC (71 : 29 ACN : H_2O): 3.0 min LC-MS (ESI⁺) (M+H)⁺: 254.200 g/mol

81d HPLC (71 : 29 ACN : H_2O): 3.2 min LC-MS (ESI⁺) (M+H)⁺: 284.100 g/mol

81e HPLC (71 : 29 ACN : H_2O): 3.4 min LC-MS (ESI⁺) (M+H)⁺: 282.100 g/mol

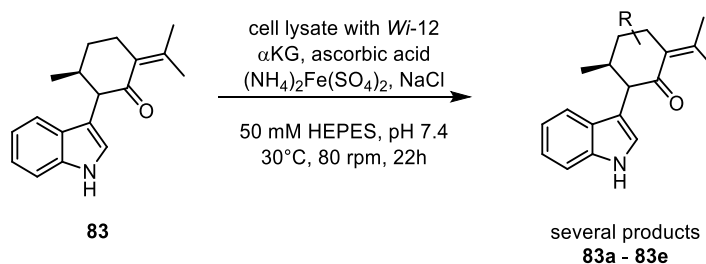
81f HPLC (71 : 29 ACN : H_2O): 4.5 min LC-MS (ESI⁺) (M+H)⁺: 310.100 g/mol and 266 g/mol

7.3.1.9 Product Identification from Biotransformation with **82**

The reaction was performed in a total reaction volume of 6x50 mL with 1% (v/v) ethanol. The reaction was performed with purified enzyme (1x50 mL *Wi-5*) and cleared lysate (4x50 mL *Wi-5*, 1x50 mL *Wi-12*) to compare conversion. *Wi-5* and *Wi-12* were produced as described above. The cell pellets of 3 L *Wi-5* and 0.75 L *Wi-12* cell culture were resuspended with buffer (50 mM HEPES, 100 mM NaCl, pH 7.4) and lysed by sonication. Solid components were removed by centrifugation (16 000 rpm, 4 °C, 45 min). The supernatant was used for the reaction. Reactants αKG , ascorbic acid and $(\text{NH}_4)_2\text{Fe}(\text{SO}_4)_2$ were solved in N_2 purged buffer and added to the lysate, so that a final concentration of 10 mM αKG , 5 mM ascorbic acid, 1 mM $(\text{NH}_4)_2\text{Fe}(\text{SO}_4)_2$ and roughly 20-30 μM *Wi-5* and *Wi-12* (based on average yield from purification of enzyme) was obtained. The reaction with purified enzyme was prepared with 30 μM *Wi-5*. Then 51 mg ketone **82** were solved in 3 mL ethanol, and 500 μL were added to the reaction to achieve a final concentration of 0.75 mM substrate. The reactions were incubated at 30 °C, 100 rpm (Infors Ecotron shaker). The reaction was stopped by extraction after 22 h. After extraction, a sample was taken to compare the conversion of each reaction. The solvent was removed in vacuo and dry remaining samples solved again in acetonitrile. Out of economical and time reasons, the samples were combined before purification by preparative HPLC. Two products were produced with all variants. Total conversions of 55% (*Wi-5* lysate), 58% (*Wi-5* purified enzyme) and 55% (*Wi-12* lysate) were achieved and after purification 5 mg **82a** and 5 mg **82b** were obtained.

82a HPLC (71-29 ACN/ H_2O): 2.0 min, HRMS (ESI⁺): $\text{C}_{15}\text{H}_{17}\text{NO}_3$ [$\text{M}+\text{Na}$]⁺, m/z found: 282.1098; calculated 282.1101. NMR analysis revealed **82a** to have an opened terpene ring and a carboxyl group, however no complete satisfying NMR analysis could be done since impurities were still remaining

82b HPLC (71-29 ACN/ H_2O): 2.8 min LC-MS: 226.100 g/mol. NMR analysis revealed **82b** to be a complex mix of at least two stereoisomers.

7.3.1.10 Product Identification from Biotransformation with **83**

The reaction was performed in a total reaction volume of 6x50 mL with 10% (v/v) ethanol. The reaction was performed with cleared lysate of *Wi-12*. Enzymes were produced by heterologous expression as described in ch.7.1.9.1. In total 4.5 L cell culture were prepared and pelleted (0.75 L/50 mL reaction). The cell pellets were resuspended with buffer (50 mM HEPES, 100 mM NaCl, pH 7.4) and frozen. The frozen cell suspension was defrosted in cold water and cells lysed by sonication (6 min with 30 s pulses and 30 s rest). During sonification the suspension is put on ice and was pelleted (16 000 rpm, 4 °C, 45 min). The supernatant was used for the reaction. Reactants α KG, ascorbic acid and $(\text{NH}_4)_2\text{Fe}(\text{SO}_4)_2$ were solved in nitrogen purged buffer and added to the lysate, so that a final concentration of 10 mM α KG, 5 mM ascorbic acid, 1 mM $(\text{NH}_4)_2\text{Fe}(\text{SO}_4)_2$ and roughly 20-30 μM *Wi-12* (based on average yield from purification of enzyme) was obtained. Then 41 mg ketone **83** (6.8 mg/reaction) were solved in 3.0 mL ethanol, and 0.5 mL were added to the reaction to achieve a final concentration of 0.5 mM substrate. The reactions were incubated at 30 °C, 100 rpm (Infors Ecotron shaker). The reaction was stopped by extraction after 22 h. After extraction, a sample was taken to compare conversion of each reaction. At least 5 products were produced within the reactions. The total conversions of 19% and 26% were obtained. The solvent was removed in vacuo and dry remaining samples solved again in acetonitrile. Out of economical and time reasons, the samples were combined before purification by preparative HPLC. Fractions were analyzed by LC-MS. Less than 1 mg of all products was obtained after purification process.

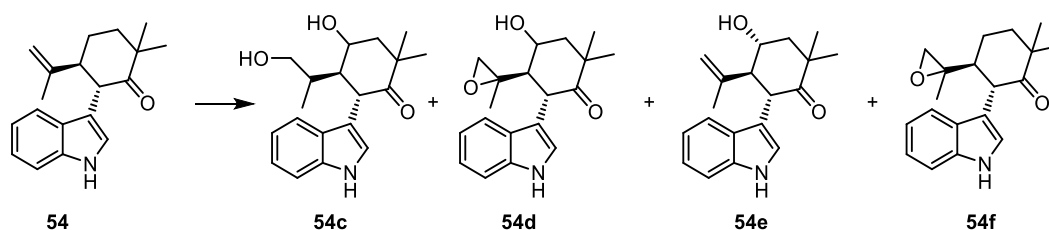
83a HPLC (71-29 ACN/H₂O): 2.2 min LC-MS (ESI⁺) (M+H)⁺: 146.100 g/mol

83b HPLC (71-29 ACN/H₂O): 2.4 min LC-MS (ESI⁺) (M+H)⁺: 282.100 g/mol

83c HPLC (71-29 ACN/H₂O): 3.0 min LC-MS (ESI⁺) (M+H)⁺: 266.200 g/mol

83d HPLC (71-29 ACN/H₂O): 3.6 min LC-MS (ESI⁺) (M+H)⁺: 266.100 g/mol

83e HPLC (71-29 ACN/H₂O): 4.3 min LC-MS (ESI⁺) (M+H)⁺: 282.100 g/mol

7.3.2 Oxygenase P450_{BM3}

Protocol 1:

Cell pellets from protein production P450_{BM3} variants R47G/F87G (1 L culture) and F87G/L181T (1 L culture) were thawed in cold water. The cell suspension was mixed with lysozyme to a final concentration of 2 mg/mL and 500 μ L DNase I (concentration unknown) in a 50 mL reaction tube. The tube was incubated at 80 rpm, 37 °C in an Infors Ecotron shaker. After 60 min, the probe was further lysed by sonication (6.5 min with 30 s pulses and 30 s pause). The cell suspension was cooled in a water/ice bath during sonication and subsequently pelleted (16000 rpm, 4 °C, 45 min). The supernatant was dark brown, indicating a high oxygenase concentration.

The reactions were performed in two 500 mL flat bottom flasks with each 100 mL reaction volume. 10 mL glucose (from 1 M stock solution), 10 mL EDTA (from 50 mM stock solution), 6.5 mL glycerol (80% in H₂O) were mixed with 22.5 mL 100 mM potassium phosphate buffer, pH 7.4 buffer and 50 mL lysate. Finally, 900 μ L substrate were added from a 0.115 M stock in acetonitrile to a final concentration of 1 mM. The flasks were incubated at 30 °C, 100 rpm in an Infors Ecotron incubator. The reactions were stopped by extraction after 21 h. 30 mL reaction volume were extracted with 2x20 mL ethyl acetate. The solvent was removed in vacuo. Variant F87G/L181T yielded a conversion of 23% with formation of two products (**54e** and **54f**) and 65% selectivity for **54e**. Variant R47G/F87G yielded a conversion of 18% with formation of two products (**54e** and **54f**) and 67% selectivity for **54f**.

Protocol 2:

Cell pellets from protein production P450_{BM3} variants R47H/F87G/L181A (0.53 L culture), R47V/F87G/L181T/L188N (0.58 L culture) and R47E/F87G/L181V/M185S/L188G (0.56 L culture) were thawed in cold water. The cell suspension was mixed with lysozyme to a final concentration of 1 mg/mL and a spatula tip of DNase I (concentration unknown) in a 50 mL reaction tube. The tube was incubated at 80 rpm, 37 °C in an Infors Ecotron shaker. After 20 min, the probe was further lysed by sonication (6.5 min with 30 s pulses and 30 s pause). The cell suspension was cooled in a water/ice bath during sonication and subsequently pelleted (16000 rpm, 4 °C, 45 min). The absorption of the supernatant was measured, and the concentration determined by Lambert-Beer law and $\epsilon_{417\text{nm}} = 121 \text{ mM}^{-1}\text{cm}^{-1}$.

Methods

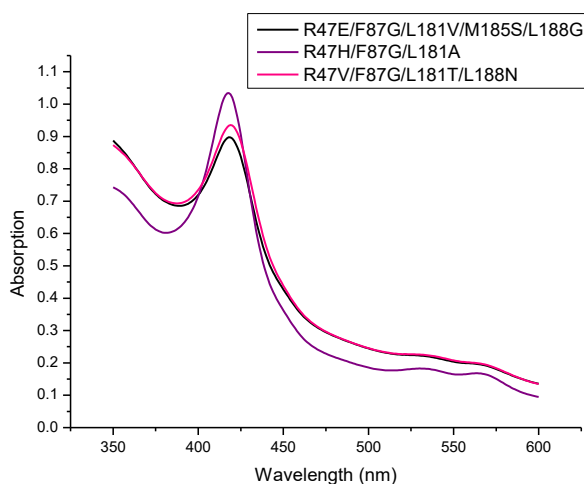


Figure 62. Absorption spectra of P450_{BM3} variants.

The reaction was prepared by mixing 250 eq glucose (250 mM), 0.25 eq NADP⁺ (0.25 mM), 2.2 U/ml glucose dehydrogenase, 5% glycerol and 5 μM enzyme in 100 mM potassium phosphate buffer pH 8.0. Finally, substrate was added from a 0.2 M stock in acetonitrile to a final concentration of 1 mM (1 eq). The flask was incubated at 30 °C, 80 rpm in an Infors Ecotron shaker. After 3.5 h the shaking speed was increased to 110 rpm and after 5 h, 6 mL lysate of each variant were added to the corresponding reactions. The reaction was stopped by extraction after 20 h. 30 mL reaction volume was extracted with 2x20 mL ethyl acetate. The solvent was removed in vacuo. Variant R47V/F87G/L181T/L188N yielded a conversion of 83%, R47E/F87G/L181V/M185S/L188G yielded a conversion of 65% and variant R47H/F87G/L181A 60%. All variants formed four products **54c**, **54d**, **54e** and **54f**. Selectivities are given in table 16, ch. 3.6.4.2.

Protocol 3:

Because only few **54e** and **54f** were produced in the above described reaction (protocol 2), the reaction was repeated with variants R47V/F87G/L181T/L188N and R47E/F87G/L181V/M185S/L188G. Lysate which was left over and frozen at -80 °C from protocol 2 was used. Reaction conditions were used as described in protocol 2 (without the second addition of lysate). The reaction was stopped after 2.5 h by extraction with ethyl acetate as described above.

Variant R47V/F87G/L181T/L188N yielded a conversion of 14% with formation of two products (**54e** and **54f**) and 67% selectivity for **54e**. Variant R47E/F87G/L181V/M185S/L188G yielded a conversion of 9% with formation of two products (**54e** and **54f**) and 46% selectivity for **54e**.

7.3.2.1 Characterization of 54c-54f

All products were combined and purified via prep HPLC in 2 runs. Fractions were analyzed by HPLC-UV/vis and the solvent removed in vacuo, followed by NMR analysis of the products. All products were analyzed by ^1H , ^{13}C and HMQC NMR. **54e** additionally by NOESY NMR. The spectra can be found in chapter 8.6.

54c

$^1\text{H-NMR}$ (500 MHz, DMSO- d_6) δ 10.69 (s, 1H, NH), 7.28 (d, J = 8.8 Hz, 2H), 7.01 – 6.97 (m, 1H), 6.93 (s, 1H), 6.89 – 6.85 (m, 1H), 5.01 (s, 1H, OH), 4.83 (s, 2H), 4.65 (t, J = 5.5 Hz, 1H), 4.19 (d, J = 12.3 Hz, 1H, H₁₀), 3.83 – 3.79 (m, 1H, H₁₄), 3.72 – 3.65 (m, 1H), 3.62 – 3.55 (m, 1H), 3.28 (dd, J = 12.4, 4.0 Hz, 1H, H₁₅), 2.39 – 2.33 (m, 1H, H₁₃), 2.07 (s, 2H, H₁₈), 1.84 (dt, J = 14.0, 3.9 Hz, 1H, H₁₃), 1.30 (s, 3H, H₁₉), 1.03 (s, 3H, H₂₀).

$^{13}\text{C-NMR}$ (126 MHz, DMSO) δ 212.61 (CO), 174.27, 151.94, 136.17, 129.66, 127.20, 123.96, 120.31, 119.42, 118.13, 117.74, 111.75, 111.20, 108.25, 76.06(C₁₄), 62.43, 49.56(C₁₂), 47.37(C₁₀), 41.49(C₁₅), 35.68(C₁₃), 24.87(C₁₉), 21.86(C₂₀), 1.19(C₁₈).

54d

$^1\text{H-NMR}$ (300 MHz, DMSO- d_6) δ 10.77 (s, 1H, NH), 7.33 (d, J = 8.1 Hz, 1H), 7.23 (d, J = 7.8 Hz, 1H), 7.15 (d, J = 2.4 Hz, 1H), 7.03 (ddd, J = 8.2, 6.9, 1.2 Hz, 1H), 6.89 (ddd, J = 8.0, 7.0, 1.1 Hz, 1H), 5.06 (d, J = 3.5 Hz, 1H, OH), 4.09 – 3.97 (m, 1H, H₁₀), 3.90 (t, J = 3.1 Hz, 1H, H₁₄), 2.35 (m, 2H, H₁₅, H₁₃), 1.95 (d, J = 5.2 Hz, 1H, H₁₇), 1.86 (m, 1H, H₁₃), 1.57 (d, J = 5.2 Hz, 1H, H₁₇), 1.28 (s, 3H, H₁₈), 1.23 (s, 3H, H₁₉), 1.06 (s, 3H, H₂₀) ppm.

$^{13}\text{C-NMR}$ (75 MHz, DMSO- d_6) δ 211.90 (CO), 136.40, 126.72, 124.13, 120.43, 119.54, 117.78, 111.35, 110.99, 75.67(C₁₄), 57.80(C₁₇), 54.68(C₁₆), 49.44(C₁₂), 46.32(C₁₀), 43.89(C₁₅), 29.70(C₁₃), 24.88(C₁₈), 21.76(C₂₀), 15.50(C₁₉) ppm.

HRMS (ESI⁺): C₁₉H₂₃NO₃ [M+H]⁺, m/z found: 314.1748; calculated 314.1751

54e

$^1\text{H-NMR}$ (300 MHz, DMSO- d_6) δ 10.69 (s, 1H, NH), δ 7.28 (d, J = 8.2 Hz, 2H), 7.03 – 6.96 (m, 2H), 6.92 – 6.83 (m, 1H), 5.03 (d, J = 3.4 Hz, 1H, OH), 4.50 (d, J = 2.4 Hz, 1H, H₁₇), 4.46 – 4.41 (m, 1H, H₁₇), 4.12 (d, J = 12.4 Hz, 1H, H₁₀), 3.84 (s, 1H, H₁₄), 3.41 (td, J = 12.5, 4.1 Hz, 1H, H₁₅), 2.36 (s, 1H, H₁₃), 1.75 (dt, J = 14.2, 4.0 Hz, 1H, H₁₃), 1.57 (s, 3H, H₁₈), 1.30 (s, 3H, H₁₉), 1.04 (s, 3H, H₂₀) ppm.

$^{13}\text{C-NMR}$ (75 MHz, DMSO) δ 212.36(CO), 146.79(C₁₆), 136.17, 127.10, 123.81, 120.23, 119.31, 117.67, 111.52, 111.39, 111.14(C₁₇), 76.03(C₁₄), 49.45(C₁₀), 46.69(C₁₂), 45.25(C₁₅), 34.22(C₁₃), 24.87, 21.76, 18.34(C₁₈) ppm.

HRMS (ESI⁺): C₁₉H₂₄NO₂ [M+H]⁺, m/z found: 298.1799; calculated 298.1802

54f

$^1\text{H-NMR}$ (300 MHz, DMSO- d_6) δ 10.82 (s, 1H, NH), 7.33 (d, J = 8.1 Hz, 1H), 7.25 (d, J = 7.6 Hz, 1H), 7.17 (d, J = 2.4 Hz, 1H), 7.03 (ddd, J = 8.2, 7.0, 1.2 Hz, 1H), 6.90 (ddd, J = 8.1, 7.0, 1.2 Hz,

Methods

1H), 4.11 – 4.05 (m, 1H, H₁₀), 2.18 (t, *J* = 7.3 Hz, 1H), 1.94 (d, 1H, , *J* = 5.1 Hz, H₁₇), 1.91-1.68 (m, 6H), 1.30 (s, 3H), 1.18 (s, 3H), 1.02 (s, 3H) ppm.

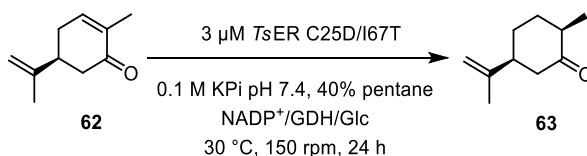
¹³C-NMR (75 MHz, DMSO) δ 212.02, 136.24, 136.24, 126.99, 124.42, 120.43, 119.16, 117.94, 111.37, 110.16, 58.67(C₁₆), 55.45(C₁₇), 50.96(C₁₅), 47.39(C₁₀), 44.97(C₁₂), 38.69(C_{13/14}), 26.30(C₁₈) 25.63(C₂₀), 23.48 (C_{13/14}) 15.99(C₁₉) ppm.

HRMS (ESI⁺): C₁₉H₂₃NO₂ [M+H]⁺, *m/z* found: 298.1799; calculated 298.1802

7.3.3 Reductase TsER

To synthesize substrates which further should be tested within the substrate scope of the halogenase, several reductions had to be performed. Therefore the reductase TsER of *Thermus scotoductus* SA-01 was used as variant TsER C25D/I67T as described by Nett *et al.*^[315,432]

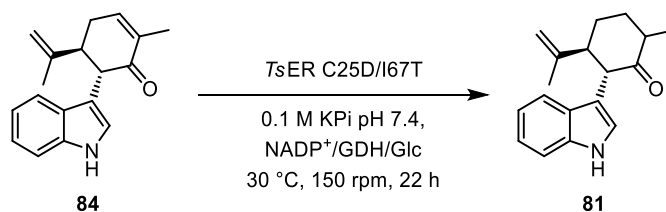
7.3.3.1 (2R,5S)-2-methyl-5-(prop-1-en-2-yl)cyclohexan-1-one (63)



The reaction was performed in a total reaction volume of 500 mL with 20% (v/v) n-pentane in analogy to Nett *et al.*^[315,432]. 9.91 g (50.0 mmol, 2.0 eq, 100 mM) glucose monohydrate, 1.25 mL of a 100 mM NADP⁺ disodium salt solution, 3 mL of a 222 U/mL BsGDH^[448] solution (2.2 U/mL), 250 μL of a 100 mM CoCl₂ (0.11 mM) and 14 mL of a 119 μM TsER C25DT/I67T solution were mixed with KPi-buffer (100 mM, pH 7.4) to a volume of 400 mL in a 500 mL Schott bottle. Then 5.4 mL (34.1 mmol, 67 mM) (S)-carvone **62** was solved in 100 mL n-pentane and added to the bottle. The reaction was incubated at 30 °C, 160 rpm for 24 h in an Infors HT Multitron shaker. Reaction progress was followed by GC. After 24 h no increase of conversion could be detected, and the reaction was extracted with diethyl ether (2 x 100 mL) with 98% conversion (%GC). The combined organic phases were washed with brine, dried over MgSO₄ and the solvent was removed under reduced pressure. 5.3 g (35.8 mmol) of product **63** was obtained as colorless oil. The diastereomeric ratio is 94:6 (*cis/trans*).

R_f = 0.90 (pentane/EtOAc 5:1); ¹H-NMR (500 MHz, CDCl₃), δ = 4.83 (s, 1H, H_{9/cis}), 4.69 (s, 1H, H_{9/trans}), 2.62-2.52 (m, 2H), 2.43-2.37 (m, 2H), 1.90-1.82 (m, 3H, 1/2 H₃, H₄), 1.73 (s, 3H, H₁₀), 1.65-1.56 (m, 1H, 1/2 H₃), 1.05 (d, 3H, *J* = 6.9 Hz, H₇) ppm; ¹³C-NMR (125 MHz, CDCl₃), δ = 214.0 (CO), 147.0 (C₈), 111.5 (C₉), 44.6 (C₆), 44.1 (C₅), 44.0 (C₂), 30.7 (C₃), 26.4 (C₄), 21.5 (C₁₀), 15.6 (C₇) ppm;

HRMS (EI⁺): C₁₀H₁₆O₁, *m/z* found: 152.12014, cal.: 152.12011.

7.3.3.1 2*S*,3*S*)-2-(1*H*-indol-3-yl)-6-methyl-3-(prop-1-en-2-yl)cyclohexan-1-one (81)

The reaction was performed in a total reaction volume of 625 mL with 20% (v/v) acetone. Based on synthesis instructions of Nett *et al.*^[315,432]. 11 g (55 mmol, 88 mM) glucose monohydrate, 0.24 mM NADP⁺ disodium salt, 2.2 U/mL engineered *BsGDH*^[448], 278 μ L of 100 mM aq. CoCl₂ (0.04 mM) and 16.0 μ M *TsER* C25DT/I67T variant were mixed with 407 mL KPi-buffer (200 mM, pH 7.4) in a 1 L Schott bottle. Then 1.122 g (4.24 mmol, 1.0 eq, 6.78 mM) ketone **84** was solved in 125 mL acetone and added to the reaction. The reaction was incubated at 30 °C, 160 rpm for 24 h in an Infors HT shaker. After 24 h the reaction was extracted with EtOAc. HPLC analysis showed 73% conversion. The solvent was removed in vacuo and the crude product was purified by flash column chromatography (pentane : EtOAc 4:1) to give 635 mg (2.34 mmol, 55%) of product **81** as a brown solid. Further 240 mg product/educt mix (83% educt, 17% product) were collected as impure fractions after column chromatography.

HPLC: Retention time 7.05 min (isocratic ACN/H₂O 65:35); **¹H-NMR** (500 MHz, CDCl₃), δ = 8.09 (s, 1H, NH), 7.53 (d, 1H, *J* = 7.68 Hz, H₇), 7.32 (d, 1H, *J* = 7.93, H₄), 7.18-7.15 (m, 1H, H₆), 7.10-7.07 (m, 1H, H₅), 7.01 (d, 1H, *J* = 1.68 Hz, H₂), 4.75-4.74 (m, 2H, H₁₇), 4.15 (dd, 1H, *J* = 8.05, 0.50 Hz, H₁₀), 3.08-3.04 (m, 1H, H₁₅), 2.78-2.71 (m, 1H, H₁₂), 2.05-2.00 (m, 3H, H_{13/14}), 1.80-1.74 (m, 1H, H₁₃), 1.69 (s, 3H, H₁₈), 1.20 (d, 3H, *J* = 6.90, H₁₉) ppm; **¹³C-NMR** (125 MHz, CDCl₃), δ = 213.8 (CO), 146.8 (C₁₆), 136.2 (C₈), 127.2 (C₉), 122.2 (C₂), 122.2 (C₆), 119.6 (C₅), 119.6 (C₄), 113.1 (C₃), 112.4 (C₁₇), 111.3 (C₇), 50.0 (C₁₅), 49.7 (C₁₀), 43.1 (C₁₂), 31.3 (C₁₃), 25.9 (C₁₄), 20.7 (C₁₈), 16.2 (C₁₉) ppm;

HRMS (ESI⁺): C₁₈H₂₁NONa⁺ [M+Na]⁺, *m/z* found: 290.1511; calc.: 290.1515.

7.3.3.2 2-(1H-indol-3-yl)6-methylcyclohexan-a-one (**82**)

The reaction was performed in a total reaction volume of 625 mL with 20% (v/v) acetone. Based on synthesis instructions of Nett *et al.*^[315,432]. 11 g (55 mmol, 88 mM) glucose monohydrate, 0.24 mM NADP⁺ disodium salt, 2.2 U/mL engineered BsGDH^[448], 278 μL of 100 mM aq. CoCl₂ (0.04 mM) and 16.2 μM TsER C25DT/I67T variant were mixed with 407 mL KPi-buffer (200 mM, pH 7.4) in a 1 L Schott bottle. Then 1.25 g (5.5 mmol, 1.0 eq, 8.88 mM) ketone **21** was solved in 125 mL acetone and added to the reaction. The reaction was incubated at 30 °C, 160 rpm for 24 h in an Infors HT shaker. After 24 h the reaction was extracted with EtOAc. The solvent was removed in vacuo and the crude product was purified by flash column chromatography (pentane : EtOAc 4:1) to give 424.4 mg (1.86 mmol, 34%) of product **82** as a brown solid. The diastereomeric ratio is 50:50 and was determined by HPLC-UV/Vis. The diastereomers were not separated.

$R_f = 0.42$ (pentane : EtOAc 5:1); ¹H-NMR (500 MHz, CDCl₃), $\delta = 8.07$ (s, 1H, NH), 7.45 (d, 1H, $J = 7.95$ Hz, H₄), 7.38 (d, 1H, $J = 8.75$, H₇), 7.23 (s, 1H, H₂), 7.22-7.18 (m, 1H, H₆), 7.14-7.09 (m, 1H, H₅), 4.00-3.96 (m, 1H, H₁₀), 2.73-2.68 (m, 1H, H₁₂), 2.51-2.47 (m, 1H, H₁₅), 2.29-2.24 (m, 1H, H₁₅), 2.02-1.98 (m, 2H, H₁₄), 1.61-1.55 (m, 2H, H₁₃), 1.13 (d, 3H, $J = 6.56$ Hz, H₁₆) ppm; ¹³C-NMR (75 MHz, CDCl₃), $\delta = 199.5, 146.2, 136.5, 135.8, 127.4, 122.8, 119.6, 119.5, 113.2, 113.0, 111.5, 49.4, 48.6, 31.1, 19.7, 16.5$ ppm;

HRMS (ESI⁺): C₁₅H₁₇NOH⁺ [M+H]⁺, m/z found: 228.1380; calc.: 228.1383.

7.4 Chemical Synthesis

7.4.1 General Information

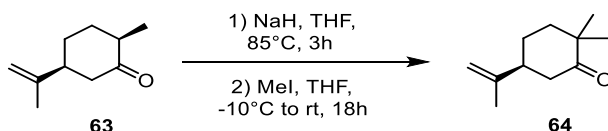
Commercially available chemicals were ordered in highest available purity and used without further purification. Analytical grade solvents for reactions and HPLC were purchased from VWR, if necessary dried using standard protocols.^[449] Solvents for chromatography were used from the institute's supply after distillation. Compressed air, liquid and gaseous nitrogen were used from the institutes supply without further purification. High-purity water was generated by further purifying the deionized water from the institute with a TKA Micropure purification system.

Chemical syntheses were performed under inert nitrogen gas atmosphere unless otherwise specified, using Schlenk technique and flasks dried by repeated heating and flushing with inert gas. Transfer of solvents and liquid compounds was achieved using syringes and septa.

For analysis by thin layer chromatography (TLC), commercially available silica gel sheets were used (TLC Silica 60 F₂₅₄ from Merck). Detection of the substances was performed under UV light at wavelengths of 254 or by staining with a potassium permanganate dip. Purification by flash column chromatography was carried out using silica gel 60 (particle size of 40-60 μm, from Merck), and under increased pressure from the house air supply.

Synthesis of **53**, **67** and **77** were performed solely by L. Schmermund instructions can be found in his master thesis,^[317] synthesis of substrates **76**, **78**, **82** and **83** were first made by L. Schmermund but later resynthesized within this thesis. Synthesis of **79** and **80** was made in the group of R. Viswanathan (unpublished results) and can be compared to a synthesis route to hapalindole Q by Baran and Richter.^[350] Analytical data to the latter compounds can be found in chapter 8.6. NMR spectra as well as HPLC chromatograms for all compounds can also be found in chapter 8.6.

7.4.2 (S)-2,2-dimethyl-5-(prop-1-en-2-yl)cyclohexan-1-one (**64**)



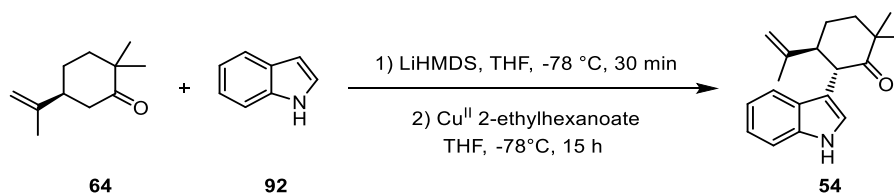
In analogy to instructions of Laplace *et al.*^[450] under nitrogen atmosphere NaH (1.45 g, 36.3 mmol, 1.0 eq) was suspended in abs. THF (111 mL). After adding (5S)-dihydrocarvone (**63**) (5.516 mg, 36.3 mmol, 1.0 eq), the suspension was heated to reflux (85°C) for 3 h. The resulting orange solution was cooled down to -10°C (acetone/ice bath) and MeI (4.52 mL, 72.6 mmol, 2.0 eq) was added dropwise within 10 min. The reaction was warmed up to rt (~22°C) and stirred for 18 h. Brine (100 mL) was added to the reaction mixture and it was stirred for 30 min. The suspension was extracted with Et₂O (3 x 150 mL), the combined organic phases were dried over MgSO₄ and the solvent was removed under reduced pressure. The crude product was purified by column chromatography (pentane : EtOAc 50:1) and 4.19 g (25.23 mmol, 70%) of **64** were obtained as colorless oil.

R_f = 0.43 (pentane : EtOAc 25:1); **¹H-NMR** (500 MHz, CDCl₃), δ = 4.77 (s, 1H, H₁₀), 4.72 (s, 1H, H₁₀), 2.57-2.47 (m, 1H, 1/2 H₆), 2.37-2.34 (m, 1H, 1/2 H₆), 2.33-2.30 (m, 1H, H₅), 1.82-1.78 (m, 1H, 1/2 H₄), 1.77-1.76 (m, 2H, 1/2 H₄, 1/2 H₃), 1.73 (s, 3H, H₁₁), 1.60-1.55 (m, 1H, 1/2 H₃), 1.16 (s, 3H, H₇), 1.07 (s, 3H, H₈) ppm; **¹³C-NMR** (125 MHz, CDCl₃), δ = 215.7 (CO), 147.8 (C₉), 110.0 (C₁₀), 46.5 (C₅), 44.7 (C₂), 43.2 (C₆), 39.7 (C₃), 26.6 (C₄), 25.3 (C₇), 25.3 (C₈), 20.8 (C₁₁) ppm;

HRMS (EI⁺): C₁₁H₁₈O₁, m/z found: 166.13497, cal.: 166.13576.

7.4.3 (5*S*,6*S*)-6-(1*H*-indol-3-yl)-2,2-dimethyl-5-(prop-1-en-2-yl)cyclohexan-1-one

(54)



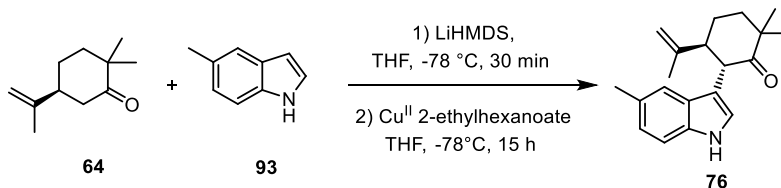
In analogy to instructions of Maimone *et al.*^[352] 1.65 g (8.3 mmol, 1.0 eq) **64** and 1.95 g (16.6 mmol, 2.0 eq) **92** were solved in 50 mL abs. THF under nitrogen atmosphere. The solution was cooled to -78°C (acetone/dry ice) and 25.0 mL 1.0 M LiHMDS in THF (25.0 mmol, 3.0 eq) were added dropwise within 10 min. After stirring for 30 min, 4.35 g (12.45 mmol, 1.5 eq) copper(II) 2-ethylhexanoate were added rapidly and stirring was continued for 15 h, while the dry ice/acetone bath was slowly warmed to room temperature. The solution was poured into 1 M HCl (100 mL) and EtOAc (90 mL). Subsequently the aqueous phase was extracted with EtOAc (3 x 90 mL). The combined organic phase was washed with 1 M HCl (100 mL), 1 M NaOH (100 mL), then brine (100 mL) and was dried over MgSO_4 . The solvent was removed under reduced pressure and the crude product was purified by flash column chromatography (pentane : EtOAc gradient from 6:1 to 3:1) to give 730 mg (2.6 mmol, 31%) of the coupled product **54** as a light brown solid.

$R_f = 0.35$ (pentane : EtOAc 4:1); $^1\text{H-NMR}$ (500 MHz, CDCl_3), $\delta = 8.04$ (s, 1H, NH), 7.34 (d, 1H, $J = 7.90$ Hz, H_7), 7.28 (td, 1H, $J = 8.08, 0.83$ Hz, H_4), 7.14-7.11 (m, 1H, H_6), 7.06-7.03 (m, 1H, H_5), 6.87 (d, 1H, $J = 2.25$ Hz, H_2), 4.62-4.61 (m, 1H, $\text{H}_{17/\text{cis}}$), 4.56-4.55 (m, 1H, $\text{H}_{17/\text{trans}}$), 4.20 (d, 1H, $J = 12.5$ Hz, H_{10}), 2.90 (dt, 1H, $J = 12.2, 3.70$ Hz, H_{15}), 2.22-2.13 (m, 1H, H_{14}), 1.95-1.90 (m, 1H, H_{13}), 1.85-1.78 (m, 2H, $\text{H}_{13/14}$), 1.58-1.57 (m, 3H, H_{18}), 1.41 (s, 3H, H_{19}), 1.14 (s, 3H, H_{20}) ppm; $^{13}\text{C-NMR}$ (125 MHz, CDCl_3), $\delta = 213.7$ (CO), 147.0 (C_{16}), 136.2 (C_8), 127.6 (C_9), 123.3 (C_2), 121.7 (C_6), 119.3 (C_5), 119.1 (C_7), 112.1 (C_3), 112.0 (C_{17}), 111.3 (C_4), 53.3 (C_{15}), 47.8 (C_{10}), 45.3 (C_{12}), 40.3 (C_{13}), 28.2 (C_{14}), 26.0 (C_{20}), 25.5 (C_{19}), 18.7 (C_{18}) ppm;

HRMS (ESI⁺): $\text{C}_{19}\text{H}_{23}\text{NOH}^+$ [M+H]⁺, m/z found: 282.1852; calc.: 282.1854.

Optical rotation (in CHCl_3 , 22°C , $\lambda = 589$ nm, cuvette 50 mm, 0.44 g/100 mL) -77.849

7.4.4 (5*S*,6*S*)-2,2-dimethyl-6-(5-methyl-1*H*-indol-3-yl)-5-(prop-1-en-2-yl)cyclohexan-1-one (**76**)



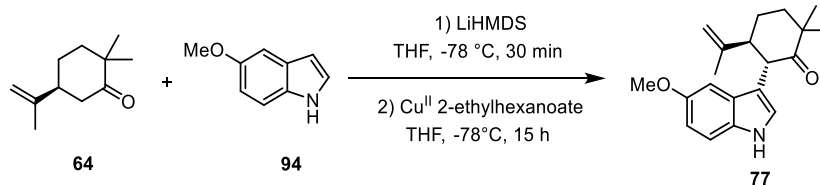
The synthesis was performed by M. Nikisch within the OC-FPR (practical training within the bachelor study). In analogy to instructions of Maimone *et al.*^[352] 1.34 g (8.1 mmol, 1.0 eq) **64** and 2.3 g (17.6 mmol, 2.5 eq) **93** were solved in 42 mL dry THF under nitrogen atmosphere. Then the solution was cooled to -78 °C and 25.0 mL 1.0 M LiHMDS in THF (25.0 mmol, 3.5 eq) were added dropwise within 10 min. After stirring for 30 min, 3.74 g (10.7 mmol, 1.5 eq) copper(II) 2-ethylhexanoate were added rapidly and stirring was continued for 15 h at -78 °C. Afterwards the reaction was warmed to rt and was poured into 1 M HCl (120 mL) and EtOAc (120 mL). Subsequently the aqueous phase was extracted with EtOAc (3 x 120 mL). The combined organic phase was washed with 1 M HCl (75 mL), 1 M NaOH (150 mL), then brine (75 mL) and was dried over MgSO₄. The solvent was removed under reduced pressure and the crude product was purified by flash column chromatography (pentane : EtOAc gradient from 6:1 to 5:1) to give 290 mg (0.98 mmol, 12%) of the coupled product **76** as a brown solid.

R_f = 0.29 (pentane : EtOAc 4:1); ¹H-NMR (500 MHz, CDCl₃), δ = 7.93 (s, 1H, NH), 7.18 (d, 1H, J = 8.25 Hz, H₇), 7.09-7.08 (m, 1H, H₄), 6.95 (dd, 1H, J = 8.25, 1.40 Hz, H₆), 6.84 (d, 1H, J = 2.30 Hz, H₂), 4.63-4.62 (m, 1H, H_{17/cis}), 4.57-4.56 (m, 1H, H_{17/trans}), 4.17 (d, 1H, J = 12.5 Hz, H₁₀), 2.89 (dt, 1H, J = 12.3, 3.70 Hz, H₁₅), 2.42 (s, 3H, H₂₁), 2.22-2.13 (m, 1H, H₁₄), 1.94-1.90 (m, 1H, H₁₃), 1.85-1.78 (m, 2H, H_{13/14}), 1.59-1.58 (m, 3H, H₁₈), 1.42 (s, 3H, H₁₉), 1.15 (s, 3H, H₂₀) ppm; ¹³C-NMR (125 MHz, CDCl₃), δ = 213.7 (CO), 147.1 (C₁₆), 134.6 (C₈), 128.4 (C₅), 127.9 (C₉), 123.4 (C₆), 123.4 (C₂), 118.7 (C₄), 112.0 (C₁₇), 111.6 (C₃), 111.0 (C₇), 53.1 (C₁₅), 47.7 (C₁₀), 45.3 (C₁₂), 40.3 (C₁₃), 28.3 (C₁₄), 26.0 (C₂₀), 25.5 (C₁₉), 21.8 (C₂₁), 18.7 (C₁₈) ppm;

HRMS (ESI⁺): C₂₀H₂₅NONa⁺ [M+Na]⁺, m/z found: 318.1829; calc.: 318.1828.

Optical rotation (in CHCl₃, 22 °C, λ =589 nm, cuvette 50 mm, 0.58 g/100mL) -86.156.

7.4.5 (5*S*,6*S*)-6-(5-methoxy-1*H*-indol-3-yl)-2,2-dimethyl-5-(prop-1-en-2-yl)cyclohexan-1-one (77)



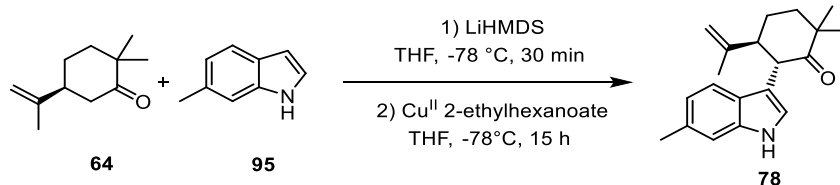
The synthesis was performed by L. Schermund.^[317] In analogy to instructions of Maimone *et al.*^[352] 400 mg (2.41 mmol, 1.0 eq) **64** and 1.24 g (8.42 mmol, 3.5 eq) **94** were solved in 14 mL dry THF under nitrogen atmosphere. The solution was cooled to -78 °C and 8.18 mL 1.0 M LiHMDS in THF (8.18 mmol, 3.4 eq) were added dropwise within 5 min. After stirring for 30 min, 1.26 g (3.61 mmol, 1.5 eq) copper(II) 2-ethylhexanoate were added rapidly and stirring was continued for 15 h at -78 °C. The reaction was warmed to rt and poured into 1 M HCl (40 mL) and EtOAc (20 mL). Subsequently the aqueous phase was extracted with EtOAc (3 x 30 mL). The combined organic phase was washed with 1 M HCl (40 mL), 1 M NaOH (40 mL), then brine (30 mL) and was dried over MgSO₄. The solvent was removed under reduced pressure and the crude product was purified by flash column chromatography (pentane : EtOAc gradient from 7:1 to 3:1) to give 318 mg (1.02 mmol, 42%) of the coupled product **77** as a pale pink solid.

R_f = 0.32 (pentane : EtOAc 4:1); **¹H-NMR** (500 MHz, CDCl₃), δ = 7.93 (s, 1H, NH), 7.18 (dd, 1H, *J* = 8.70, 0.50 Hz, H₇), 6.88 (d, 1H, H₂), 6.80 (dd, 1H, *J* = 8.77, 2.52 Hz, H₆), 6.77 (d, 1H, *J* = 2.35 Hz, H₄), 4.63-4.62 (m, 1H, H_{17/cis}), 4.57-4.56 (m, 1H, H_{17/trans}), 4.14 (d, 1H, *J* = 12.4 Hz, H₁₀), 3.83 (s, 3H, H₂₁), 2.86 (dt, 1H, *J* = 12.4, 3.74 Hz, H₁₅), 2.21-2.12 (m, 1H, H₁₄), 1.94-1.90 (m, 1H, H₁₃), 1.84-1.77 (m, 2H, H_{13/14}), 1.59-1.58 (m, 3H, H₁₈), 1.41 (s, 3H, H₁₉), 1.14 (s, 3H, H₂₀) ppm; **¹³C-NMR** (125 MHz, CDCl₃), δ = 213.6 (CO), 153.9 (C₅), 147.0 (C₁₆), 131.6 (C₈), 128.2 (C₉), 124.2 (C₂), 112.0 (C₁₇), 111.8 (C₇), 111.8 (C₃), 111.3 (C₆), 101.9 (C₄), 56.2 (C₂₁), 53.2 (C₁₅), 47.8 (C₁₀), 45.3 (C₁₂), 40.3 (C₁₃), 28.2 (C₁₄), 26.0 (C₂₀), 25.5 (C₁₉), 18.7 (C₁₈) ppm;

HRMS (ESI⁺): C₂₀H₂₅NO₂H⁺ [M+H]⁺, *m/z* found: 312.1958; calc.: 312.1958.

Optical rotation (in CHCl₃, 22 °C, λ=589 nm, cuvette 50 mm, 0.61 g/100mL) -55.674.

7.4.6 (5*S*,6*S*)-2,2-dimethyl-6-(6-methyl-1*H*-indol-3-yl)-5-(prop-1-en-2-yl)cyclohexan-1-one (78)

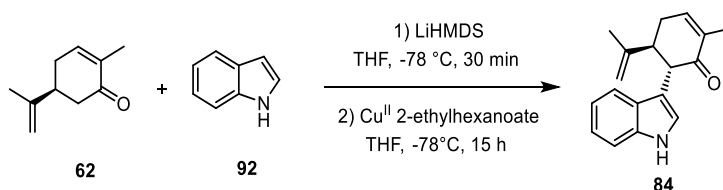


The synthesis was performed by Tobias Itzenhäuser within the OC-FPR (practical training within the bachelor study). In analogy to instructions of Maimone *et al.*^[352] 793 mg (4.78 mmol, 1.0 eq) **64** and 2.2 g (16.8 mmol, 3.5 eq) **95** were solved in 37 mL dry THF under nitrogen atmosphere. The solution was cooled to -78 °C and 17.0 mL 1.0 M LiHMDS in THF (17.0 mmol, 3.5 eq) were added dropwise within 5 min. After stirring for 30 min, 2.52 g (7.2 mmol, 1.5 eq) copper(II) 2-ethylhexanoate were added rapidly and stirring was continued for 15 h, while the dry ice/acetone bath was slowly warmed to room temperature. The solution was poured into 1 M HCl (40 mL) and EtOAc (25 mL). Subsequently the aqueous phase was extracted with EtOAc (3 x 30 mL). The combined organic phase was washed with 1 M HCl (30 mL), 1 M NaOH (35 mL), then brine (30 mL) and was dried over MgSO₄. The solvent was removed under reduced pressure and the crude product was purified by flash column chromatography (pentane : EtOAc gradient from 6:1 to 3:1) to give 320 mg (1.08 mmol, 23%) of the coupled product **78** as a colorless solid.

R_f = 0.36 (pentane : EtOAc 4:1); ¹H-NMR (500 MHz, CDCl₃), δ = 7.91 (s, 1H, NH), 7.21 (d, 1H, J = 8.05 Hz, H₄), 7.07-7.06 (m, 1H, H₇), 6.87 (dd, 1H, J = 8.10, 1.00 Hz, H₅), 6.81 (d, 1H, J = 2.30 Hz, H₂), 4.62-4.61 (m, 1H, H_{17/cis}), 4.56-4.55 (m, 1H, H_{17/trans}), 4.17 (d, 1H, J = 12.4 Hz, H₁₀), 2.88 (dt, 1H, J = 12.3, 3.74 Hz, H₁₅), 2.42 (s, 3H, H₂₁), 2.21-2.12 (m, 1H, H₁₄), 1.94-1.89 (m, 1H, H₁₃), 1.84-1.77 (m, 2H, H_{13/14}), 1.58-1.57 (m, 3H, H₁₈), 1.40 (s, 3H, H₁₉), 1.14 (s, 3H, H₂₀) ppm; ¹³C-NMR (125 MHz, CDCl₃), δ = 213.6 (CO), 147.0 (C₁₆), 136.7 (C₈), 131.4 (C₆), 125.5 (C₉), 122.6 (C₂), 121.1 (C₅), 118.7 (C₄), 112.0 (C₃), 111.9 (C₁₇), 111.3 (C₇), 53.2 (C₁₅), 47.8 (C₁₀), 45.3 (C₁₂), 40.3 (C₁₃), 28.2 (C₁₄), 26.0 (C₂₀), 25.4 (C₁₉), 21.8 (C₂₁), 18.7 (C₁₈) ppm;

HRMS (ESI⁺): C₂₀H₂₅NONa⁺ [M+Na]⁺, m/z found: 318.1828; calc.: 318.1828.

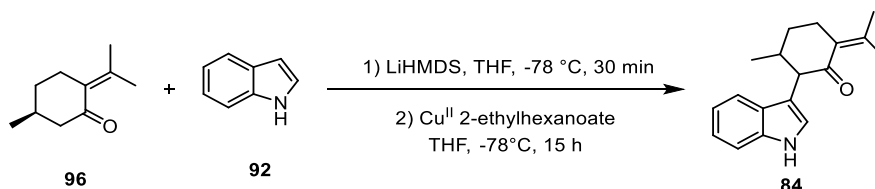
Optical rotation (in CHCl₃, 22 °C, λ =589 nm, cuvette 50 mm, 0.48 g/100mL) -45.886.

7.4.7 (5*S*,6*S*)-6-(1*H*-indol-3-yl)-2-methyl-5-(prop-1-en-2-yl)cyclohex-2-en-1-one (84)

The synthesis was performed in analogy to instructions of Maimone *et al.*^[352] 1.32 mL (8.3 mmol, 1.0 eq) (*S*)-carvone **62** and 1.95 g (16.6 mmol, 2.0 eq) indole **92** were solved in 50.0 mL THF. Then the solution was cooled to $-78\text{ }^{\circ}\text{C}$ and 25.0 mL 1.0 M LiHMDS in THF (25.0 mmol, 3.0 eq) were added dropwise within 5 min. After stirring for 30 min, 4.35 g (12.5 mmol, 1.5 eq) copper(II) 2-ethylhexanoate were added rapidly and stirring was continued for 16 h at $-78\text{ }^{\circ}\text{C}$. Afterwards the reaction was warmed to rt and was poured into 1 M HCl (100 mL) and EtOAc (100 mL). Subsequently the aqueous phase was extracted with EtOAc (3 x 100 mL). The combined organic phase was washed with 1 M HCl (100 mL), 1 M NaOH (100 mL), then brine (100 mL) and was dried over MgSO_4 . The solvent was removed under reduced pressure and the crude product was purified by flash column chromatography (pentane : EtOAc gradient from 5:1 to 3:1) to give 1.12 g (3.96 mmol, 47.6%) of product **84** as a brown solid.

$R_f = 0.28$ (pentane : EtOAc 4:1); $^1\text{H-NMR}$ (500 MHz, CDCl_3), $\delta = 8.01$ (s, 1H, NH), 7.45 (d, 1H, $J = 7.59$ Hz, H₇), 7.32 (d, 1H, $J = 8.02$, H₄), 7.18-7.13 (m, 1H, H₅), 7.09-7.04 (m, 1H, H₆), 6.90 (d, 1H, $J = 2.19$ Hz, H₂), 6.81-6.78 (m, 1H, H₁₃), 4.68-4.66 (m, 1H, H_{17/cis}), 4.65-4.64 (m, 1H, H_{17/trans}), 3.92 (d, 1H, $J = 10.7$ Hz, H₁₀), 3.31-3.23 (m, 1H, H₁₅), 2.63-2.41 (m, 2H, H₁₄), 1.87-1.86 (m, 1H, H₁₉), 1.63 (s, 3H, H₁₈) ppm; $^{13}\text{C-NMR}$ (125 MHz, CDCl_3), $\delta = 199.4$ (CO), 146.1 (C₁₆), 143.6 (C₁₃), 136.4 (C₈), 135.7 (C₁₂), 127.3 (C₉), 122.7 (C₂), 122.0 (C₅), 119.5 (C₆), 119.4 (C₇), 113.1 (C₃), 112.9 (C₁₇), 111.4 (C₄), 49.2 (C₁₀), 48.5 (C₁₅), 31.0 (C₁₄), 19.6 (C₁₈), 16.4 (C₁₉) ppm;

HRMS (ESI⁺): $\text{C}_{18}\text{H}_{19}\text{NONa}^+$ $[\text{M}+\text{Na}]^+$, m/z found: 288.1359; calc.: 288.1359.

7.4.8 (*S*)-2-(1*H*-indol-3-yl)-3-methyl-6-(propan-2-ylidene)cyclohexan-1-one (8)

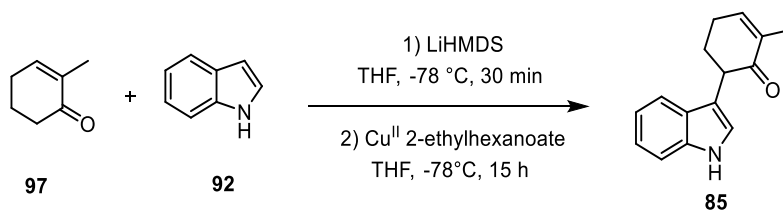
In analogy to instructions of Maimone *et al.*^[352] 1.28 g (8.4 mmol, 1.0 eq) (*R*)-pulegone **96** and 1.95 g (16.6 mmol, 2.0 eq) indole **92** were dissolved in 45 mL THF. Then the solution was cooled to $-78\text{ }^{\circ}\text{C}$ (dry ice/acetone) and 25.0 mL 1.0 M LiHMDS in THF (25.0 mmol, 3.5 eq) were added dropwise within 5 min. After stirring for 30 min, 4.35 g (12.6 mmol, 1.5 eq) copper(II) 2-ethylhexanoate were added rapidly and stirring was continued for 15 h, while the dry ice/acetone bath was slowly warmed to room temperature. Afterwards the reaction was warmed to

Methods

rt and poured into 1 M HCl (100 mL) and EtOAc (60 mL). Subsequently the aqueous phase was extracted with EtOAc (3 x 35 mL). The combined organic phase was washed with 1 M HCl (100 mL), 1 M NaOH (100 mL), then brine (50 mL) and was dried over MgSO₄. The solvent was removed under reduced pressure and the crude product was purified by flash column chromatography (pentane : EtOAc gradient from 6:1 to 4:1) to give 300 mg product **84** which was only 70% pure based on HPLC analysis. After a second flash column chromatography, 110 mg (90% pure) product **84** could be obtained.

R_f = 0.33 (pentane : EtOAc 5:1); **¹H-NMR** (500 MHz, CDCl₃), δ = 8.11 (s, 1H, NH), 7.46 (d, 1H, *J* = 7.95 Hz, H₄), 7.32 (d, 1H, *J* = 8.15, H₇), 7.17-7.14 (m, 1H, H₆), 7.07-7.04 (m, 1H, H₅), 6.97 (d, 1H, *J* = 12.4 Hz, H₂), 3.40 (d, 1H, *J* = 10.2 Hz, H₁₀), 2.82-2.79 (m, 1H, H₁₃), 2.59-2.52 (m, 1H, H₁₃), 2.35-2.27 (m, 1H, H₁₅), 2.05-1.99 (m, 1H, H₁₄), 1.88 (m, 3H, H₁₉), 1.84 (s, 3H, H₁₈), 1.58-1.50 (m, 1H, H₁₄), 0.93 (d, 3H, *J* = 6.55 Hz, H₁₆) ppm; **¹³C-NMR** (125 MHz, CDCl₃), δ = 204.7 (CO), 141.6 (C₁₇), 136.7 (C₈), 132.7 (C₁₂), 126.9 (C₉), 123.0 (C₂), 122.0 (C₆), 119.7 (C₄), 119.4 (C₅), 114.2 (C₃), 111.4 (C₇), 57.4 (C₁₀), 37.5 (C₁₅), 32.3 (C₁₄), 28.8 (C₁₃), 22.9 (C₁₉), 22.1 (C₁₈), 21.4 (C₁₆) ppm; **HRMS** (ESI⁺): C₁₈H₂₁NONa⁺ [M+Na]⁺, *m/z* found: 290.1516; calc.: 290.1515.

7.4.9 6-(1H-indol-3-yl)-2-methylcyclohex-2-en-1-one (**85**)



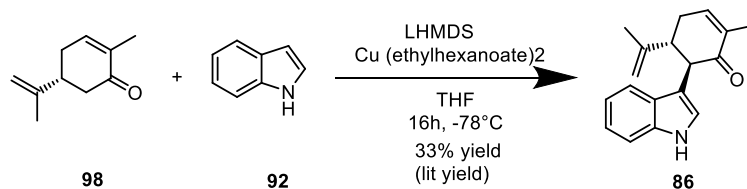
In analogy to instructions of Maimone *et al.*^[352] 1.04 mL (9.14 mmol, 1.0 eq) 2-methylcyclohex-2-en-1-one **97** and 2.69 g (24.2 mmol, 2.6 eq) indole **92** were solved in 50 mL dry THF under nitrogen atmosphere. The solution was cooled to -78 °C and 32.0 mL 1.0 M LiHMDS in THF (32.0 mmol, 3.5 eq) were added dropwise within 10 min. After stirring for 30 min, 5.58 g (16.0 mmol, 1.75 eq) copper(II) 2-ethylhexanoate were added rapidly and stirring was continued for 15 h at -78 °C. Afterwards the reaction was warmed to rt and poured into 1 M HCl (120 mL) and EtOAc (80 mL). Subsequently the aqueous phase was extracted with EtOAc (3 x 90 mL). The combined organic phase was washed with 1 M HCl (90 mL), 1 M NaOH (90 mL), then brine (90 mL) and was dried over Na₂SO₄. The solvent was removed under reduced pressure and the crude product was purified by flash column chromatography (pentane : EtOAc gradient from 6:1 to 3:1) to give 1.25 g (5.5 mmol, 60.1 %) of product **85** as brown solid.

R_f = 0.38 (pentane : EtOAc 5:1); **¹H-NMR** (500 MHz, CDCl₃), δ = 8.09 (s, 1H, NH), 7.53 (d, 1H, *J* = 8.05 Hz, H₇), 7.33 (td, 1H, *J* = 8.11, 0.89 Hz, H₄), 7.19-7.16 (m, 1H, H₅), 7.12-7.08 (m, 1H, H₆), 6.94 (d, 1H, *J* = 2.35, 0.50 Hz, H₂), 6.82-6.79 (m, 1H, H₁₃), 3.97-3.94 (m, 1H, H₁₀), 2.46-2.40 (m, 2H, H₁₄), 2.40-2.33 (m, 2H, H₁₅), 1.89-1.88 (m, 3H, H₁₆) ppm; **¹³C-NMR** (125 MHz, CDCl₃), δ = 200.0

(CO), 145.1 (C₁₃), 136.4 (C₈), 135.9 (C₁₂), 127.2 (C₉), 122.1 (C₅), 121.7 (C₂), 119.5 (C₆), 119.4 (C₇), 114.2 (C₃), 111.4 (C₄), 45.1 (C₁₀), 30.4 (C₁₅), 25.3 (C₁₄), 16.5 (C₁₆) ppm;

HRMS (ESI⁺): C₁₅H₁₅NONa⁺ [M+Na]⁺, m/z found: 248.1046; calc.: 248.1046.

7.4.1 6-(1H-indol-3-yl)-2-methyl-5-(prop-1-en-2-yl)cyclohex-2-en-1-one (86)

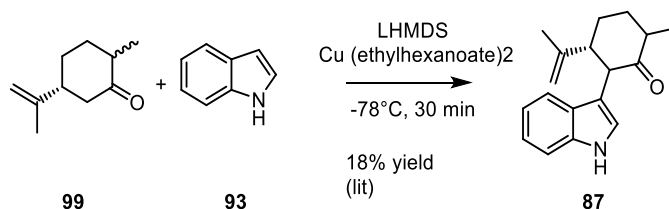


In analogy to instructions of Baran *et al.*^[350], 1.06 mL (6.6 mmol, 1.0 eq) (*R*)-carvone **98** and 1.55 g (13.2 mmol, 2 eq) indole **92** were solved in 1.00 mL dry THF. The solution was cooled down to -78°C. 19.8 mL (19.8 mmol, 3 eq) 1 M LHMDS and 20 mL dry THF was added. After stirring for 30 min, 3.46 g (9.89 mmol, 1.5 eq) Cu(II)ethylhexanoate were added. The solution was stirred for 16 h at -78°C and then was warmed up to rt. The reaction was quenched with 100 mL 1 M HCl. After extraction with 100 mL EA, the organic phase was washed with 100 mL 1 M HCl, 1 M NaOH, 100 mL H₂O and 100 mL brine. The organic phase was dried with MgSO₄ and concentrated in vacuo. The obtained product was purified via flash chromatography (n-hexane : EtOAc 5:1 gradient 2:1). 0.59 g (2.23 mmol, 33%) of the product was obtained as brown foam.

¹H-NMR (300MHz, CDCl₃) δ= 7.46-7.43 (m, 1H, indole-H_{arom}), 7.32 (dt, 3J = 8.0 Hz, 1H, indole-H_{arom}), 7.18-7.12 (m, 1H, indole-H_{arom}), 7.09-7.04 (m, 1H, indole-H_{arom}), 6.89 (d, 3J = 8.0 Hz, 1H, H₆), 6.80 (sept, 1H, indole-H_{arom}), 4.67 (quint, 1H, H₉), 4.64 (quint, 1H, H₉), 3.91 (d, 3J = 10.7 Hz, 1H, H₅), 3.31-3.23 (m, 1H, H₃), 2.63-2.47 (m, 2H, H₄), 1.88-1.86 (m, 3H, H₇), 1.66 (m, 3H, H₁₀) ppm
¹³C-NMR: 75 MHz, CDCl₃; d = 199.3, 146.1, 143.6, 135.7, 127.3, 122.6, 122.0, 119.5, 119.4, 113.3, 112.9, 111.4, 49.3, 48.5, 31.1, 19.6, 16.4 ppm.

HRMS (ESI⁺): C₁₈H₁₉NO (M+H)⁺ calculated: 266.1539, found: 266.1542.

7.4.1 (1H-indol-3-yl)-6-methyl-3-(prop-1-en-2-yl)cyclohexan-1-one (87)



0.28 mL (1.71 mmol, 1.0 eq) (*5R*)-dihydrocarvone **99** (mixture of isomers with 96% purity) and 0.39 g (3.33 mmol, 2.0 eq) indole **92** were solved in 2.00 mL dry THF. The solution was cooled down to -78 °C. 5.00 mL (5.00 mmol, 3.0 eq) 1 M LHMDS and 20 mL THF were added. After stirring for 30 min, 0.87 g (2.49 mmol, 1.5 eq) Cu(II)ethylhexanoate was added. The solution was stirred for 14.5 h at -78 °C and then was warmed to rt. The reaction was quenched with

Methods

20 mL 1 M HCl solution. After extraction with 50 mL EtOAc, the organic phase was washed with 20 mL 1 M HCl solution, 20 mL 1 M NaOH solution, 20 mL H₂O and 20 mL saturated brine. The organic phase was dried with MgSO₄ and concentrated in vacuo. The obtained product was purified via flash chromatography (n-hexane : EtOAc gradient 5:1 to 2:1). 80.2 mg (0.30 mmol, 18%) of the product was obtained as brown colored oil.

¹H-NMR: 300 MHz, CDCl₃; d = 7.53 (d, 3J = 8.0 Hz, 1H, indole-Harom), 7.47 (d, 3J = 7.8 Hz, 1H, indole-Harom), 7.40-7.03 (m, indole-Harom), 6.94 (d, 3J = 2.4 Hz, 1H, indole-Harom), 4.88, 4.83 (m, 2H, H10) 4.60, 4.54 (m, 2H, H10), 4.14 (d, 3J = 7.5 Hz, 1H, H2), 3.93 (d, 3J = 12.1 Hz, 1H, H2), 3.09-3.03 (m, 1H, H3), 2.90 (dt, 3J = 12.0 Hz, 4.0 Hz, 1H, H3), 2.78-2.66 (m, 2H, H6), 2.53-2.46 (m, 1H, H5), 2.28-2.19 (m, 1H, H5), 2.03-1.93 (m, 5H, H4), 1.80 (bs, 3H, 10), 1.57 (m, 3H, H10), 1.20 (d, 3J = 6.9 Hz, 3H, H7), 1.10 (d, 3J = 6.5 Hz, 3H, H7) ppm. **¹³C-NMR:** 75 MHz, CDCl₃; d = 146.8, 123.2, 122.3, 122.2, 121.8, 119.7, 119.7, 119.6, 119.4, 19.3, 112.4, 112.1, 111.3, 111.2, 54.1, 52.5, 50.0, 49.8, 45.5, 43.4, 43.0, 35.8, 32.4, 31.3, 25.9, 25.8, 20.7, 18.7, 16.1, 14.9 ppm.

7.5 Analytical Methods

7.5.1 GC Measurements

GC analysis was performed at different temperatures and gradients, using a Agilent GC7820A system with FID-detector (Heater 300 °C, H₂-Flow 30 mL/min, Air-Flow 400 mL/min, Makeup Flow 25 mL/min; Date Rate/ Min Peak width 50 Hz/0.004 min) with a 30 m HP-5 column with 0.25 µm inner diameter with a flow of 6.5 mL/min. 1 µL of a diluted sample was injected with a split of 40-1 with 250 mL/min. Heater was at 250 °C, 1 bar, gas saver 20 mL/min after 2 min. In table 31 all used GC programs are listed with retention time of compounds.

Table 31: Temperature programs for GC runs. Measurements were performed on a HP-5 column.

substrate	program	retention time
adamanthanisonitril 68	120°C to 132°C with 4°C/min, hold 3 min, 10°C/min to 200°C	2.1 min
tetramethylbutylisocyanide 69	56°C to 66°C with 2°C/min hold 3 min 10°C/min to 120°C	2.3 min
2-naphtylisocyanide 70	120°C to 140°C with 4°C/min, hold 3 min, 10°C/min to 190°C	2.5 min
cyclohexylisonitril 71	82°C to 96°C with 4°C/min, hold 3 min, go to 160°C with 10°C/min	1.0 min
2(4-morpholinyl)ethylisocyanid 72	120°C to 144°C with 4°C/min, hold 3 min, 10°C/min to 190°C	3.0 min
cyclohexylisothiocyanat 73	102°C to 120°C with 4°C/min, hold 3 min, 10°C/min to 180°C	2.1 min
3-morpholinopropylisothiocyanat 74	120°C to 144°C with 4°C/min, hold 3 min, 10°C/min to 190°C	4.2 min
phenethylisothiocyanat 75	120°C to 140°C with 4°C/min, hold for 3 min	3.0 min
(S)-carvone 62	92°C, 4min	3.6 min
(2S,5S)-dihydrocarvone 63	92°C, 4min	2.9 min
2,2 dimethyl-(5S)-dihydrocarvone 64	92°C, 4min	3.3 min

7.5.2 HPLC Measurements

For HPLC measurements, either a Shimadzu LC2030 or a Shimadzu LC2010C HT category number 228-41501-38, serial number C2154103183LP was used.

The samples were prepared in acetonitrile. The measurements were performed on a Shimadzu Prominence-i LC2030. As solvents, acetonitrile and water were used. The mixtures were analyzed with an Agilent Zorbax Eclipse C-18 (150 mmx4.6 mm, 5.4 µm particle size) or Durashell C-18 column (150 mmx4.6 mm, 5.4 µm particle size). An isocratic solvent mixture of 71:29 ACN : H₂O was used for a length of 9.0 min. The time was elongated for measurement of

Methods

hapalindole Q to 30 min. The injection volume (1-10 μ L) was adapted to absorption of substrate, so that an average absorption of about 150 mV for the starting material was present. In table 32, the retention time and solvent composition of HPLC measurements is given.

Table 32: Retention time of chemicals in Shimadzu HPLC system with Agela Durashell C-18 column. 1mL/min flow rate.

substrate	retention time (min)	solvent
53	8.41	73 : 27 ACN/H ₂ O
53a	9.18	
54	6.66	71 : 29 ACN/H ₂ O
54a	7.48	
54b	2.69	
54c	2.09	
54d	2.37	
54e	2.99	
54f	3.79	
65	6.07 6.31	30 : 70 to 80 : 20 ACN : H ₂ O+0.1%TFA in 20 min
67	9.37	68 : 31 ACN : H ₂ O
67a	9.95	
76	7.77	71 : 29 ACN/H ₂ O
76a	8.89	
77	5.48	
77a	6.30	
78	8.12	
78a	9.35	
79	4.39	60 : 40 ACN/H ₂ O
80	5.63	
81	5.30	71 : 29 ACN : H ₂ O
81a	2.16	
81b	2.58	
81c	3.0	
81d	3.2	
81e	3.4	
81f	4.5	
82	4.16	
82a	2.01	
82b	2.86	
83	5.96	
83a	2.16	
83b	2.4	
83c	3.0	
83d	3.6	
83e	4.3	
84	4.67	
85	5.5	60 : 40
86	11 min	63 : 37
87	14.40 15.14 16.35	55 : 45
91	7.81	80 : 20 ACN/H ₂ O
91a	2.93	
91b	3.22	
91c	6.63	

7.5.3 LC-MS

LC-MS was performed at an Agilent 1260 Infinity II HPLC-System using a D₂ lamp coupled to Mass Infinity Lab G6 125 B, equipped with a 1 cm precolumn and 150x4.6 mm, 5 μ m Agela DuraShell column.

7.5.4 Preparative HPLC Purification

Preparative reverse-phase HPLC was performed at a Gilson HPLC equipped with Macherey-Nagel Nucleodur C18 HTec 250/16, 5 μ m (762556-160). To analyze new occurring peaks during biocatalytic transformation, the reactions were scaled up and the extracted compounds purified via preparative HPLC.

Remaining samples from dried organic phase were resolved in 60%-40% ACN-H₂O and centrifuged for 5 min at 14000 rpm. The supernatant was filtered (0.45 μ m PTFE-filter, VWR) and the flow through applied on the pre-equilibrated column by loop injection (loop volume 4.5 mL). An isocratic eluent (60%-40% ACN-H₂O) was used and run for 60 min. For reactions with substrate **54**, the last peak eluted at about 38 min. Collected fractions were rechecked on analytical HPLC. Pure peaks were concentrated in vacuo and analyzed by mass and NMR.

7.5.5 Mass Analysis

Samples were given to the mass department of Philipps University Marburg.

HR-ESI-spectra: HR-ESI mass spectra were acquired with a LTQ-FT Ultra mass spectrometer (Thermo Fischer Scientific). The resolution was set to 100.000.

HR-EI-spectra: HR-EI mass spectra were acquired with a AccuTOF GCv 4G (JEOL) Time of Flight (TOF) mass spectrometer. An internal or external standard was used for drift time correction.

Enzyme Characterization from SDS-PAGE Gel: Samples from SDS-PAGES were destained and were digested "in-gel" by the addition of Sequencing Grade Modified Trypsin (PROMEGA) and incubated at 37 °C overnight.

The mass spectrometric analysis of the samples was performed using an Orbitrap Velos Pro mass spectrometer (Thermo Scientific). An Ultimate nanoRSLC-HPLC system (Dionex), equipped with a custom 20cm x 75 μ m C18 RP column filled with 1.7 μ m beads was connected online to the mass spectrometer through a Proxeon nanospray source. 1-15 μ L of the tryptic digest (depending on sample concentration) were injected onto a C18 pre-concentration column. Automated trapping and desalting of the sample was performed at a flowrate of 6 μ L/min using water/0.05% formic acid as solvent.

Separation of the tryptic peptides was achieved with the following gradient of water/0.05% formic acid (solvent A) and 80% acetonitrile/0.045% formic acid (solvent B) at a flow rate of 300 nL/min: holding 4% B for five minutes, followed by a linear gradient to 45%B within 30 minutes and linear increase to 95% solvent B in additional 5 minutes. The column was connected to a stainless steel nanoemitter (Proxeon, Denmark) and the eluent was sprayed directly towards the heated capillary of the mass spectrometer using a potential of 2300 V. A survey scan with a resolution of 60000 within the Orbitrap mass analyzer was combined with at least three data-dependent MS/MS scans with dynamic exclusion for 30 s either using CID with the linear ion-trap or using HCD combined with orbitrap detection at a resolution of 7500.

Methods

Data analysis was performed using Proteome Discoverer (Thermo Scientific) with Sequest and Mascot (version 2.2; Matrix science) search engines using either SwissProt or NCBI databases.

8. Appendix

8.1 List of Abbreviations

Abbreviations of proteinogenic amino acids are listed in table 33, general abbreviations are given in table 34.

Table 33. Abbreviation of proteinogenic amino acids in one and three letter code.

amino acid	3 letter code	1 letter code
alanine	Ala	A
arginine	Arg	R
asparagine	Asn	N
aspartic acid	Asp	D
cysteine	Cys	C
glutamine	Gln	Q
glutamic acid	Glu	E
glycine	Gly	G
histidine	His	H
isoleucine	Ile	I
leucine	Leu	L
lysine	Lys	K
methionine	Met	M
phenylalanine	Phe	F
proline	Pro	P
serine	Ser	S
threonine	Thr	T
tryptophan	Trp	W
tyrosine	Tyr	Y
valine	Val	V

General Abbreviations

Table 34. General abbreviations used in this document.

2OG	2-oxoglutarate
aa	amino acid
ac	acetate
ACN	acetonitrile
ACP	acyl carrier protein
<i>ad.</i> (lat)	bring to volume
α KG	α -ketoglutarate
amp	ampicillin
amp ¹⁰⁰	100 μ g/mL ampicillin
AmSO ₄	(NH ₄) ₂ SO ₄ – ammonium sulfate
anh.	anhydrous
asc. acid	ascorbic acid
aq.	aqueous
β -ME	beta-mercaptoethanol
bp	base pairs
CD	circular dichroism
ch.	chapter
CPO	chloroperoxidase
conc.	concentration
conv.	conversion
Da	Dalton
DCM	dichloromethane
ddH ₂ O	deionized water
dep.	dependent
DTT	dithioreithol
dw	deep-well
EtOAc	ethyl acetate
EDTA	ethylenediaminetetraacetic acid
e.g.	exempli gratia (for example)
epPCR	error prone PCR
etc.	et cetera
EtOH	ethanol
eq	equivalent
FeCl ₃ ⁵⁰	50 μ M FeCl ₃
ff	following
fl.	flavin
FMN	flavin mononucleotide
form.	formation
gDNA	genomic DNA
HEPES	4-(2-hydroxyethyl)-1-piperazineethanesulfonic acid

HPLC	high performance liquid chromatography
IMAC	immobilized metal-ion affinity chromatography
IPTG	Isopropyl β -D-1-thiogalactopyranoside
kan	kanamycin
kan ⁵⁰	50 μ g/mL kanamycin
K _m	Michaelis Menten constant
LB	lysogeny broth
MCA	multi-channel arm
ms	milliseconds
na	not available
nd	not determined
nc	no conversion
NHI	non-heme iron
PAGE	polyacrylamide gel electrophoresis
PCR	polymerase chain reaction
Pi	phosphates
PROSS	Protein Repair One Stop Shop
rf-cloning	restriction free cloning
rt	room temperature
SDS	sodium dodecyl sulfate
TB	terrific broth
tet	tetracycline
T _m	melting temperature
T _r	retention time
Tris	2-amino-2-(hydroxymethyl)propan-1,3-diol
TOF	turnover frequency
TON	turnover number
UV	ultra violet
VCPO	vanadium chloroperoxidase
Vis	visible
V _{max}	maximal initial velocity
wt	wild type

8.2 Names of Enzyme Variants

Table 35. Abbreviation of selected WelO15 variants.

name	WelO15 variant
<i>Wi-0</i>	<i>Wi-WelO15 V6I/D284N</i>
<i>Wi-1</i>	<i>Wi-WelO15 V6I/A82L/D284N</i>
<i>Wi-2</i>	<i>Wi-WelO15 V6I/N74R/D284N</i>
<i>Wi-3</i>	<i>Wi-WelO15 V6I/V90P/D284N</i>
<i>Wi-4</i>	<i>Wi-WelO15 V6I/A82V/I84H/D284N</i>
<i>Wi-5</i>	<i>Wi-WelO15 V6I/A82L/V90P/D284N</i>
<i>Wi-6</i>	<i>Wi-WelO15 V6I/A88V/V90P/D284N</i>
<i>Wi-7</i>	<i>Wi-WelO15 V6I/V81T/A82M/A88V/V90P/D284N</i>
<i>Wi-8</i>	<i>Wi-WelO15 V6I/N74R/V81T/A82M/A88V/V90P/D284N</i>
<i>Wi-9</i>	<i>Wi-WelO15 V6I/M221L/M225I/D284N</i>
<i>Wi-10</i>	<i>Wi-WelO15 V6I/A82L/V90P/M221L/M225I/D284N</i>
<i>Wi-11</i>	<i>Wi-WelO15 V6I/N74R/V81T/A82M/A88V/V90P/ S93L/S103A/D284N</i>
<i>Wi-12</i>	<i>Wi-WelO15 V6I/N74R/A82L/V90P/S93D/D284N</i>
<i>Wi-13</i>	<i>Wi-WelO15 V6I/N74R/A82L/V90P/S93H/S103A/A175N/D284N</i>
<i>Wi-P1</i>	<i>Wi-WelO15 V6I/S103A/D284N</i>
<i>Wi-P2</i>	<i>Wi-WelO15 V6I/S103A/Q123R/S230K//D284N</i>
<i>Wi-P3</i>	<i>Wi-WelO15 V6I/S103A/Q123R/S230K/Q236N/S239W/S268R/Q282D/D284N</i>
<i>Wi-5P3</i>	<i>Wi-WelO15 V6I/A82L/V90P/ S103A/Q123R/S230K/Q236N/S239W/S268R/Q282D/D284N</i>
<i>Hw-1</i>	<i>Hw-WelO15 A82L</i>
<i>Hw-2</i>	<i>Hw-WelO15 A82L/V90P</i>

8.3 Biological Part

8.3.1 Cloning Information

In figure 63, a part of the multiple cloning site of the pRSF-Duet vector is given. In the first and last row, the two primer (shown in purple) are given that overlap with the vector when restriction free cloning into this vector was used. In figure 64, a vector map of the pRSF-Duet vector carrying *welO* genes is given. All oxygenase genes were cloned at identical positions.



Figure 63. DNA sequence of the multiple cloning site of the pRSF-Duet vector. In the first and the last row, the overlap with the vector is shown as primer which was used in restriction free cloning. The bases between the primers is exchanged by the restriction free cloning against the gene that should be inserted. The sequence is shown with SnapGene Viewer version 2.8.3.

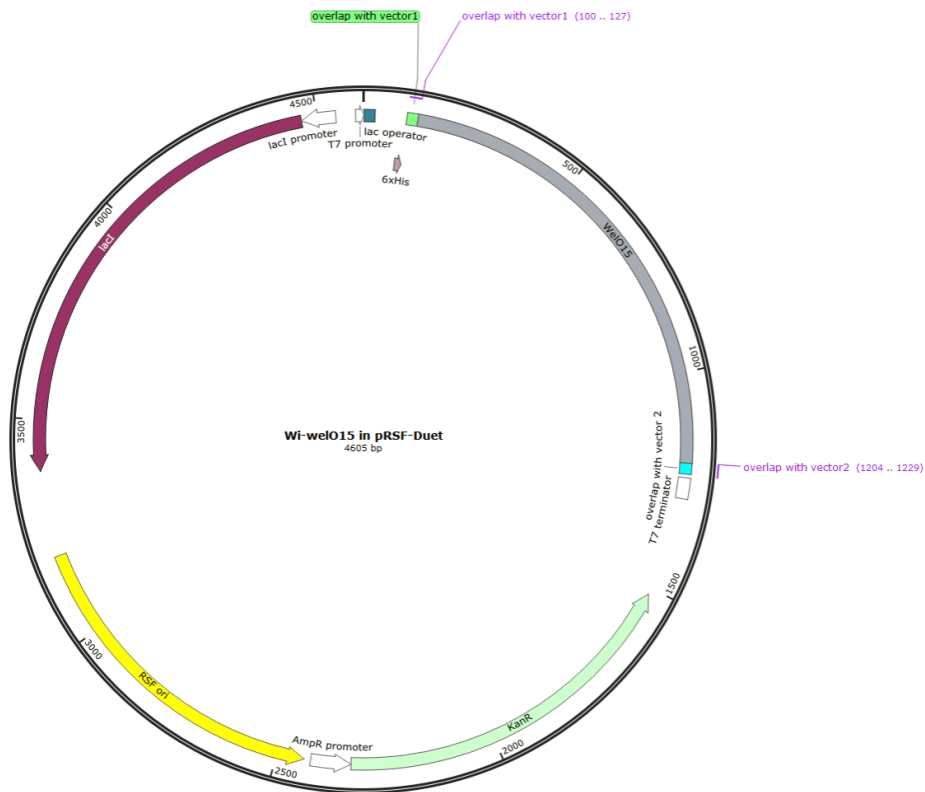


Figure 64. Vector map of pRSF-Duet vector carrying *WelO* genes. DNA sequences were modified and edited with Ape and SnapGene Viewer version 2.8.3. With green and cyan, the sequences are shown that are line the incorporated genes.

Appendix

In table 36 an overview of all cloned genes is given. Furthermore, errors and silent mutations that were seen by sequencing after the cloning, are listed.

Table 36. Overview of all genes that were cloned within this project. For some genes, errors or silent mutations in comparison to published sequences (NCBI databank, date of retrieving 08/2015) were seen and are listed here.

enzyme	aa*	bp*	MW (Da)	errors and silent mutations
<i>Wi-WelO11</i>	359	1077	40699	silent mutation in stop codon (taa instead of tga)
<i>Hw-WelO11</i>	328	984	37179	
<i>Wi-WelO12</i>	357	1071	40652	I5V (primer att instead of gtt position 13) silent mutation: act instead of acc (421-423)
<i>Hw-WelO12</i>	357	1071	40682	
<i>Wi-WelO13</i>	362	1086	41202	3 silent mutations: 217-219 cac instead of cat; 394-396 tat instead of tac; 469-471 aac instead of aat
<i>Hw-WelO13</i>	362	1086	41282	
<i>Wi-WelO14</i>	359	1077	40877	
<i>Hw-WelO14</i>	359	1077	40868	
<i>Wi-WelO15</i>	290	870	32450	I6V (16-18 atc instead of gtc); D284N (aat instead of gat 850-852)
<i>Hw-WelO15</i>	290	870	32406	
<i>Wi-WelO16</i>	382	1146	43660	ttc instead of ttt position 4-6; aaa instead of aag posi- tion 16-18
<i>Hw-WelO16</i>	382	1146	43693	ttc instead of ttt position 4-6; aaa instead of aag posi- tion 16-18
<i>Wi-WelO17</i>	518	1554	58110	G515E (gga instead of gaa position 1543-1545)
<i>Hw-WelO17</i>	518	1554	58137	att instead of ttt (I436F, 1306-1308); Silent: agg instead of aga (silent, 1303-1305); att in- stead of atc silent 1309-1311
<i>Wi-WelO18</i>	482	1446	55682	
<i>Wi-WelO19</i>	358	1074	40673	

*without His₆-tag

Appendix

8.3.2 Genes

The following genes are depicted as they were sequenced after cloning in pRSF-Duet vector if not noted otherwise. In the cloning process, a His₆-tag with linker is incorporated within the open reading frame with the following sequence:

atgggcagcagccatcacatcatcaccacagccaggatccgaattcgagctcg

welO11 KJ767018.1 | *Westiella intricata* UH HT-29-1 wel gene cluster, partial sequence

atggtagctatattgaaaagagcgtaaatctagtcacaagaaccagaaactcaaattaagcagtcctgaatctggcagcaagttggatatattgcatgcaatcggtgg
aactaggcaaaaaaccaatagcaattgagctatttggcgcgccttagttgcatggcgagacaaagaccgaaagcagtaattatggaacgcttctgttccatgctcgg
tgcacttttagctataggtgaagtcgtagatgggttcattcaatgtcctttcatcactggcgctatgatagttctgggtgatgctgcatataccaaaagtggaactctc
acacagaccacattccatctacagcacgtcaaaaaacctatgtcactgaagaagataatggttaccatttgggttggatggtactgcaactccttgttgaattacctgg
gtttgatgagcagaaagcaacaagcataaataatgccttatcgtcttctttagtaaaaaactagtgctgacgggtagtggaacgcaattgatcaccaccattt
gttaccagtacacaatgtgctgtagctgattcaattgaactaactctagttaatcacaaggatacagaactgagcgaactaccgatgcaaaagaagcctggttggaa
ctgtaattgaggcccgaattaaaactttagctgggttgggtgctcgatcgtaagtttttagggtaaatattgaaactcaaaagaaccgagtagatgcttggcctactg
gatacataaataatattagctgacggcagcagaggggtaaagtactcttgggttaccatctctaaaaacgaacaagattgcaagtttaattatgttcaata
aaatgggcaactattgttgatctgttttctacattgttttgaagcaattcaaaagcaacggattgctgataaaccaatattcgataccatgagtagacagatacaacg
ggcggggcatttattagctgatcagccattgtgaaatttagacagtttatcaagttgggttctaagcacagtga

welO12 KJ767018.1 | *Westiella intricata* UH HT-29-1 wel gene cluster, partial sequence

atggtagctatgttgaagagcgaatctagtcacaagaaccagaaactcaaattaagcagtcctgaatctggcagcaagttggatatattgcatgcaatcagtg
aactagacaaaaaccaatagcaattgagctatttggcgcgccttagttgcatggcgagacaaagaccgaaagcagtgattatggaacgcttctgttccatgctcgg
tgcacttttagctataggtgaagttgtagatgggttcattcaatgtcctttcatcactggcgctatgatagttctgggtgatgctgcatataccaaaagtggaactctc
acacagaccacattccatctacagcacgtcaaaaaacctatgtcaccgaagaagataatggttaccatttgggttggatggtactgcaacccttgttgaattacctgg
gtttgatgagcagaaagcaacaagcataaataatgccttatcgtcttcttccaaactgaaactagtgctgacgggcaattgaaatggattgaccaccatcatttt
gtttcagtagctgttaccagtaattgatcaaatgaaatgacttgcctgatgagaaagatgagaatattagcgaactaacttgcaaaagaagcctggattggaag
caaactcgatgctgaattaaaaatttattggggtaggtgctgctgaagtttttaggattaaatgttgaactatatacagcacgaatagatgcttggcctagtgagg
tttaagtacaataaaataaaacagcaaaagatgaagctattttagtgttactccaatctctgaaaccaacaataattgcaatattgatcatgataaa caaaactg
gtaactatggctaaacttctacattgttttgggtggcaaaacaaagctagtgcttggaggacacaaaaatcttgacactatgagtgagatacaggcaaaag
catttatcaaatccgaccagccagattgaaatttagcaattttatcaagttgggttaataaggcacagtaa

welO13 KJ767018.1 | *Westiella intricata* UH HT-29-1 wel gene cluster, partial sequence

atggtagctatattgaaaacgacctacagccaaaactcacaatacagaagctcaaattgagagtaaggggataaatctggcagcaggttggatatattgcatggaa
tccaaagaattaggcaaaaagccactagcaattgagctatttggcgcgccttagttgcatggcgagacaaagaccgaaagcagtaattatggaacgcttctgttcc
atgctggtgcatcttttagctataggtgaagttgtagatgggttcattcaatgtcctttcatcactggcgctatgatagttctgggtgatgctgcatataccaaaagtgga
actcctcacagaccacattccatctacagcacgtcaaaaaacctatgtcaccgaagaagatacgggttaccatttgggttggatggtactgcaacccttgttggacc
taccgaaattcgatgccgagaagcaataagcataaataatgccttatcgtcttccataatggttcaacaatgtacgacggatcattgaaaactcatgtgatc
atcatcttgcacaatacatgatgatgaagcaatgattcagtaaaatgacgggtgcttggatgagaaggtatgcaattgaaactaccgatcgcaaaagaagctg
gatgggattcatagtcgaagcccggattaagacttttctggtgtacgccaatcaaaagctttaggggttaaatgttgaacaatgtcaaccgagcagatcttggcc
cagtggaactcctagccactacaaagctgacggacaagaagactttagtactggaactgtcactccatctctgaaacagacaaaattggaagtttggatcatgg
ttaataaaactggaactgtttttagctgcttctacatagttttggctggcaaggtcgagccaatggatttccgataaatacttttgataatagtgctgggata
caggtcgagcatttataatgtgaccagccagattgaaatttggcaatttatcaagttgggttaataaggcacagtcaacaataa

welO14 KJ767018.1 | *Westiella intricata* UH HT-29-1 wel gene cluster, partial sequence

atggtagctatattgaaaacgacctacagccaaaactcacaatacagaagctcaaattgagagcaagggataaatctggcagcaggttggatatattgcatggaa

Appendix

tccaaagaattaggcaaaaagccactagcaattgagctattggctcgccttagttgcatggcgagacaaagaccgcaagcagtaattatggaacgtttctgttcac
atgtcgggtgcatctttagctataggtgaagttgtagatgggtgcatcaatgtccttttcatcactggcgctatgatagttctggtgatgctgcatataccaaaagtgga
actcctcacagaccacattcctctacagcagcgtcaaaaaacatgtcaccgaagaagatacgggttacattgggtttggtatggtactgcaactcctttgtttgacc
taccgaaattcgatgccgagaagcaataagcatcgctatatacctatcgtttcttccacggctaatactagcgtgacgagttatfgaaaatattttgatcatcat
cacctcgttctgtacatgatagcaggtaaatgatttaactaacctcacctcgttggatgagaaggatgtcgaattgagtgaaactaccgatcacgaaagaagcctgggtt
ggatgcaaaatagaagccaacatgaaagcctttctgggtgacgtggaattgctaagtttttagggtaaatgtcgaagttctgctggctcggatagatgcttggcctact
ggatacataaatacactcaagttgacggaaaacagaagtttaactactcattgggtattactcctttctctgagaataaaaacaagatggaacgttttggctcatgctgaata
aaactgtaacttggctggacatacttcttcttcttggcaagcaaggcgaagcttctcgggtgtagataaaatctttcgtatagcatgagtcagacacaggg
caaggcatttgcagctgaccaaccagtctgaagtttagacagtttatcaagttgggttaataaagcacagtaa

welO15 KJ767018.1 | *Westiella intricata* UH HT-29-1 wel gene cluster, partial sequence

atgggagcagccatcacatcacaccagccaggatccgaattcgagctgatgccaataacacctctctacaaagcctgtttgcatttttatagatcaatgca
acagaggtaaaaaataatcccactgctattcaagacataattatcaaccgtagcttcgatgggatgatcattcgcggatattcctcgcgatactatggagcaagtagc
ccgttcttggaaagggaaatgacggtggatgaaatcaattcttaataagaatgaagaatttgggtacaaagtggtcctaaatataatggatgcatcattgtcggatcaat
caccgatctcaaagactacttcttctcagcaatctccggcaggcttctgctactatgtttcaaggaaagtcggattttgaggaacaagtagagtaaatcttactct
cttttgaattgccagtagaaatcccacaggaccagaaggcacaacctataccccagctactatccggctattactcggggctcgcaaatcgcagtcattgttggca
atgatttctgttaatgctcggcctaaccatctgaaaaatttcttgaattatctgatcagcttagttacttctcccccttactgttctgaagctgggtgtagctggtagt
ctatagtttggaaatggaaatccacaagaagcaagcaaatatgctcaaatgaggaataatgagtagtagagccaagatgaagtaaccaatctcagagtgtagct
tatgcaccaggccctggagatagctgctgttcaatgggtgctgatactaccatcagtagtaggaatggtaattctccacggcaaccattgggtgatttttagcc
ttctctaaacagcgttaataagattttactggagttaa

welO16 KJ767018.1 | *Westiella intricata* UH HT-29-1 wel gene cluster, partial sequence

atgtttcacaattaaaaaacaccagtaattgataatttagacgctatcaagctgatttgaacgaggtttttaccgaaagaagatccactgaaagattaccagatcaatt
tgaaatcatagaaaaattgtcaaaaactgtctcacttttaattacaggtcaatacagacatgtaattgataaagtacaatttctgataatttccaattagaactcaac
ggcaaatcaagcgtgcatcttctctatgtcaacttttggtaatgcatatgtatgggggtggagagatacctgcaacagtaattccacattcgtcggccataaccgttgttaa
gctcgaacataactgtatgcccccaatagttgcgttcagttcgatgggttggataactggagaagaatcgataaaaactcaaccaattgaatagataatgtctcc
actccagctttccttggcggaaatgatgaatattggttttacgcaacgcaatcgaatgaagcaaaaggagcgcctgctgatacgtttagaagcacaataat
tgtcaacctgataaactgactagtgatgcaattgcaaaaaattgttgcggttattgctagaatgcaggcgatattfaaagaaactaacaataatgtaccatac
atttttatcatcgtgtgctcaatttggcagctggcaagaaccgggtgtaattatcagggagtcagcgatactccacaatgltttaggaggaagtgcagcaca
aagttcgtctccagtcttggatgcaagtttaggaatcaaacacgaccgagaaaaacgcaatcatttgcggcagatacgtgtgtatagccgtagcgcacgc
cgatttctgaagcgttggagatgggaccatcaattcgagaattgtactcaacaatcaagaaaattatccgggttgcgtcaacattacaacgaatgtgtcagggcat
cgagcattttagaaagcagcatatggaaattgcggtccattacataccaagcaggcaccaccagcataaacaaggtacaggtagtaacaacttggccatttctaaga
aaagttaaacaacagacaaccgcacatttaatttctga

welO17 KJ767018.1 | *Westiella intricata* UH HT-29-1 wel gene cluster, partial sequence

atgactactgcactacgattfaatcattattggtactggggcgggtggtgtagcctggcttataaactgctccactgtaagaaaattcgttttagaacgtggtt
ctttttacctcgtgagaaagctaactgggataccgtggaagtagtacagaaagaccgttatcataccaatgaagtttggtagcaccaaaaggaacgactattatccc
ggtacaggttactttgggtggttaactaaagtattggtggagcgtgttctggtggcgagaacaagattttaatcaggtgattcacaaggtggtatttcccga
atggccttgaagtagcgcgatttgaaccttactacaccaagcagaaaaactgtacgaagttcatggttaaacggggttagatccgactgaaccagttgcaactgaa
gattatcctatctcgtcgaatcgcagcaaccagctattcaagaaatcagactcttattagacgaaggttatcaccgttttactcctcttctatcaagttaatgagg
tgaatcggcgtttgagtagttgattctgttaacttctgtagtgggttcttctgtagtgatgcaaaagcggatgctgatgtaactgtgtgctccagccgagcaaat
gataatgttactcgtgactgaagctaaaggttaacatactagctactagggcgagaagttactaatgtagaagtcgaaatgatagagaatcattttttt
tctagtgataattgtagtgggttcttggggcaataatcagctgcttattgttacgttctgctaagcagcaccctaatgtaggcaatagttctgactggtggg
acgaaactaatgaagcatcaaaatggagcgtgattggggtaagttgaaatcaatttaccgcttcaaaaaactttagcaatcaacgattttactggggtgatg
cagattttagattcaatgggtcagctgattgggttaaagtgatgagatgattgctcaagagctccatcgggttttaggattatcatttaagaaagaatac

Appendix

tttgaagcgatgccactcactcagtagactgggtggtgactgcggaagattgccagacccaataatcgctcactcttagaggtgattctatccaattgcattacact
gagaacaacacccaagcctacaatcgtcttgcaatcgtggacacaggattgaaaaaattgggtggtgaaaggattatccccctcttctatttccgtaaaaaa
ctaccactgcaagggtggcgcatcagtgcggtacttgccttggggaagattctaaaacgctgctattggatcaattgctgtactcatgacgtgataattgtatgt
agtagatggtagttcttccgttccagtgctgctgtaatccaacctcacaattattgctaattcttacgggtaggcgaacfttaattggacgtatggcttaa

welO18 KJ767018.1 | *Westiella intricata* UH HT-29-1 wel gene cluster, partial sequence

atgctgaagtctactatttcaacctattgtaagacagcttctgctactaaatcaaatgcaacaaccaatccactaaaagctccctcttattcaatcactcagttta
ttctaatccagtaggattttggaaaaagtcacagcagatcctgataatttctactgctaaaattttggtttacgggtatcccagttgtagttgtacagcatcctcaagc
aattcaagaaatattaaccaatgatagaaaaagttttagtccaggtcatgcaacaaaattttgcaaccctttaggtaagcattctttaaattggtatcaggagaa
cagcacaacgctcagcgtcaacttggatgcctctgttcataaagagcggatgcaatcctatgggcaacttattgtaactgactgaaaaagtcagtgactgtgctg
cttaatacaagatttctcagctttagtgcagcagaaatttcttacaagttattttacaggtgctgtttggcttatacgaagggcaaagatacgaaaaaactaaagcatt
actaccattgatgtgggtcttttagatccccactgtacaatagtttctatttttcttctacaaaaagattttggagcagtgagcttggggaagattgtacgattc
gccagcagatagatgaattgtatcagctgagattgctgaacgctgtacaaccaatcagatcgtattgatcctctcattatgtggaagcaacagatgaagaa
ggcaaccaatgacagataaggagttgctgcatgagttgatgactatgttgggtgggatttgacagtacgcaatgcaatggctgggaattatattggactcatc
atttaccagaagttggtaaaaaactcgtcaagaactggataactgggtaattcaaaaaatcaatggatattttcggctgccttattgagtgctgtttgtaataaact
ttgctatttctctgtaggagtaatggcgaatgttagattgtgcaagaacctgtcgaactactggggtatcacttagagcctggtagggcagtgattcctgtatctatc
gactcatcatcgaaggattatatacaaaagccaagcagtttctccagaacgcttgtacaacgtaataatacctcagaattcctgccgtttgggtgggtgctcgt
cgttgattggcagctttagctatgttgaatgaagtttagcttggcaactatcctgtcacactataaactagcactggcagatcatcaaccagtaacactcaacggc
aaattatgttgggtggcctggaaatggaatcaagatgggtatgacaggacgactacgcctttagattccacagtctacaagtaaaacaacttag

welO19 KJ767018.1 | *Westiella intricata* UH HT-29-1 wel gene cluster, partial sequence

atggtaattgtgaaaagagcgtagtagcaaaaaaacaaaattgaaactcaattgaaaataaagtaattggatctggcagctagttggtatattgccatgcaatcga
aggaactaggtaaaaagccacaagcaatccagttatttggtagacctttagttgcatggcgagacaaaactggcaaacagctgattatggagcgtttctctcacaat
gggtgcatcttagcaatcgtcagatcatagatgggtgattcaatgctcttctactggcgtagatagttccggtgtgtgtggtgataaccaaggtagcaac
accgacaacagatgtaattccgtcaacagcgcataacatactatgtgaccaagaaaaatggttacatttgggtctggtatggttccgtaaacctttgttcccttg
cccaagttgatcctgccgaagcgaacagcataactatattgcttaccgttctttagcaaaaactaaaactactgtgttaccgggtactgtgaaatcattgatcatcca
tgttgttgaacacataatctaccgtaataatcaaaftaaacagacctccttaataaagaagataaaaaattagtaactatcgaattgcaaaagaagcctgggttgg
aacagtaattggaagctcagataaaaagttatgctgggtgtaggtgcgactgctaaagttttagggftaaatgttgaacttgaagaccgactggatgcttggcggagt
ggcagcttaggcacaacgagcttfaatggacaacagaaaaaagactctctggcatcactccaatttctgaaaaccagacaacatggcactgtgttcatgatcaaa
aaaaactggtaactgtgctgtagtacttctcattgttttggctggcaaacgaagtgtctgtatcggcagatgtagtcatctggatccatgatgagcgaaaaa
agggcaagcattatcaagcctgaccagccagattaaaaattagacaattttacaaaattgggtgataaggcacagtaa

welO11 KJ767017.1 *Hapalosiphon welwitschii* UH IC-52-3 wel gene cluster,

atgggcagcagccatcaccatcatcaccacagccagatccgaattcgaactcagctgtagctatattgaaaagagcgtaaatcagtaaaagaaccagaaactcaa
attaagcagtcattgaatctagcagcaagttggtatattgccatgcaatcgggtggaactaggcaaaaaaccaatagcaattgagctatttggctgcgccttagttgcatg
gcgagacaaagaccgaaagcagtgattatggaacgttctgttcacacgtcggtgcatcttttagctataggtgaagttgtagatggttcattcaatgtccatttcatca
ctggcgctatgatagttctgggtatgctgcatataccaaaagtggaactcctcacagaccacattcattcagcacgtcaaaaaacctatgttaccgaagaaa
gatatggttacatctgggttggatggtactgcaactccttgttgaactctgggtttagtcagcagaaagcaacaacagcataaataatgcttattcgtctctt
tcttagtaaaaactagtgctgcagcgggtagtggaaacgatttgcaccacattcgttacagtagcaaatgtacctgtagctgattcaattgacctaacctagtttaa
tcaaaaggatacagaactgagcgaactaccgatcgaagaagcgttgggttgaactgtaattgaggcccgaattaaanctttagctggtgtggtgctgcgactcgt
aagtttttagggftaaatattgaaactcaaaagaaccgagtagatgcttggcctactggatataaaatatttagctgcagcggacagcagagggttaagttactctt
tgggttaccctaatctcaaaaacgaacaagattgcaagtttaattatgttcaataaaatgggcaactntnggtgggatcngtttncctacattgttttgcagca
attcaaaagccaagcagattgta

Appendix

welO12 KJ767017.1 *Hapalosiphon welwitschii* UH IC-52-3 wel gene cluster,

atggtagctatattgaaaagagcgcgcaaatctagtagcaagaaccagaaactcaaaattaagcagtcctgaatctggcagcaagttggatatattgcatgcaatcgggtgg
aactagacaaaaaaccaatagcaattgagctatttggcgcgccttagttgcatggcgagacaaagaccgcaagcagtgattatggaacgtttctgttccatgctgg
tgcatctttagctataggtgaagttgtagatgggttcattcaatgtccatttcatcactggcgctatgatagttctgggtgatgctgcatataccaaaagtggaactcctc
acacagaccacattccatctacagcacgtcaaaaaacctatgttaccgaagaagatatggttacatttgggttggatggactgcaactccttggttgaattacctgg
gtttgatgacgagaaagcaacaagcataaataatgcttcttcttccaaactgaaactagtgctgacgggcaattgaaaatggattgaccaccatcattt
gttcagtagatggtttaccagtaattgatcaaatgaaatgacctgtcctgatgagaaagatgcagaatttagcgaactaacttgcaaaagaagcctggattggaag
caaacctgatgctcgaattaaatatttggggtaggtgctgactaactgatttaggattaaatgtgaaactatacagcacgaaatagatcctggcctagtgagggt
ttaagtacaatcaattataaacagcaaaagatgaagctattttagtgttactccaatctctgaaanccaacaatattgcaatattgatcatgataacaaaactg
gtaacttatggctaaatctacttctacatnttttnggtggcaaaaanaagctag

welO13 KJ767017.1 *Hapalosiphon welwitschii* UH IC-52-3 wel gene cluster,

atggtagctatattgaaaacgacctacagccaaaactcaciaaatcagaagttcaaatgagagtaaggaataaatctggcagcaagttggatatattgcatgcaat
cagtggaactagacaaaaaaccaatagcaattgagctatttggcgcgccttagttgcatggcgagacaaagaccgcaagcagtgattatggaacgtttctgttccaca
gtcgggtgcatctttagctataggtgaagtcgtagatgggttcattcaatgtccatttcatcactggcgctatgatcattctgggtgatgctgcatataccaaaagtgga
actcctcacagaccacattccatctacagcacgtcaaaaaacctatgtcactgaagaagatatggttacatttgggttggatggactgcaactccttggttgacct
accgaaatcgatgctcagaaagcaacaagcataaataatgcttctcctcataatggttcaacaaatgtacgacggatcattgaaaactcatgtgatc
atcatcttgcacaatacatgatgatgaagtgatgattcagtaaaatgacgggtcttgatgagaaggatgtcgaattgagtgaaactaccgatcgcgaaagaagcttg
gatgggattcatagtcgaagcccggattaagacttcttgggtgacgctgactaactaaagctttagggftaaatgtgaaacaatgtcaaccgagcagatcttggc
ccagtggaaatcttagccaccacaaagcttgacggacaagaagactgttagtactggatactgtcactccatctctgaaaaccagacaaatggcaagttttagatcatg
gtaataaaactggtaactgtttctag

welO14 KJ767017.1 *Hapalosiphon welwitschii* UH IC-52-3 wel gene cluster,

atggtagctatattgaaaacgacctacagccaaaactcaciaaatcagaagttcaaatgagagtaaggaataaatctggcagcaagttggatatattgcatgcaat
cagtggaactagacaaaaaaccaatagcaattgagctatttggcgcgccttagttgcatggcgagacaaagaccgcaagcagtgattatggaacgtttctgttccaca
gtcgggtgcatctttagctataggtgaagtcgtagatgggttcattcaatgtccatttcatcactggcgctatgatcattctgggtgatgctgcatataccaaaagtgga
actcctcacagaccacattccatctacagcacgtcaaaaaacctatgtcactgaagaagatatggttacatttgggttggatggactgcaactccttggttgacct
accgaaatcgatgctcagaaagcaacaagcataaataatgcttctcctcataatggttcaacaaatgtacgacggatcattgaaaactcatgtgatc
atcatcttgcacaatacatgatgatgaagtgatgattcagtaaaatgacgggtcttgatgagaaggatgtcgaattgagtgaaactaccgatcgcgaaagaagcttg
gatgggattcatagtcgaagcccggattaagacttcttgggtgacgctgactaactaaagctttagggftaaatgtgaaacaatgtcaaccgagcagatcttggc
ccagtggaaatcttagccaccacaaagcttgacggacaagaagactgttagtactggatactgtcactccatctctgaaaaccagacaaatggcaagttttagatcatg
gtaataaa

welO15 >gi|669033326|gb|KJ767017.1| *Hapalosiphon welwitschii* UH IC-52-3 wel gene cluster,

atgtccaataacacctctcaaaagcctgttgcanttttagatatcaatgcaacagaggtaaaaaataatcccactgctattcaagacataattcaaccgtagctt
cgatgggatgatcattcgcggagtattccctcgcgatactatggagcaagtgccggttcttggaaaggggaaatgacgggtgatgaaatcaatttctaataagaa
tgaagaatttggtagcaaaagtgctcaaatatggtcatgccattgtcggtaacacccgatctcaagactacttcttctcagcaatctccggcaggcttgcgta
ctatgtttcaaggaagtcggattttaggaacaagtagagtaaatcttctcttctgattgccagtagaaatcccacagaccagaaagggcaaacctataccc
cagctactatccggcttactcagaggtcgcgaatcgagtcctatgtggcaatgatttctgttaatgctcctcgggtaaacctctgaaaacttctgttattctgat
cagcttagttacttcatcccccttactgttctgaagctgggtgagctgtagctataatctcgaatggaaccctcaagaagtagacaaatctgctgatttacaaaat
acatagatgaggtcaggtctaagttcaagtcaaccaatcagagtgtagcttatgaccaggctctggagatgctgctgttcaatgggtgctgatactaccatcga
gttagtgaagtaattggaattctccacggcgaaccattgggtgattttagccttctaaagagcgttaataagatttactggagttaa

welO16 KJ767017.1 *Hapalosiphon welwitschii* UH IC-52-3 wel gene cluster,

Appendix

atgttctcacaattaaagcaaccagtaattgataattagaagcctatcaagtagatttgaacgaggTTTTaccgaaagaagatccacttgaaagattaccagatcaat
ttgaaatcatagaaaattgtctcaaaactgtctgcactttaaatacagtgcaatcacagatgtaattgataaagtaaatctctgatatttccaattagactgaac
ggcaaatcaagcgtgacttctctcatgtcaatctttggtaatgcatatgtatgggggtggagagatacctgcaacagtaattccacattcgctggccataccgttgtaa
gctcgaacataactgtatgcccgaatagttgctgctcagttcagttcagttggtgataactggagaagaatcgataaaactcaaccaattgaatagataatgtctc
actccagcttttcttggcgggaattgatgaatattggtttacgcaacgcaatcgtaattgaagcgaaggagcgcctgctctgatactgtgacaagcacaataatt
gtcaacctgataaactgcaactagtgagatgctttgcaaaaaattgtgctggttattgctagaatgaggcgatattaaagaataactaacaatgtgacctafac
atTTTTatcatcgtgtacttccattgttggcagctggcaagaaccgggtgtaattatgaggagtcagcgatactccacaatgtttgtagggaggaagtgcagcaca
angttcgtctcctcagcttggatgcaggttaggaatcaaacacgaccgagaaaancacgaatcatatttgcggcagatagctgtgtatagccgtagcgcacgc
cgatttctga

welO17 KJ767017.1 *Hapalosiphon welwitschii* UH IC-52-3 wel gene cluster

atgactactgcactacgatttaatacatttggactggggcggtggtgtagctggcttataaactgctccactggtagaataattctgattttagaacgtggtt
cttttttagctcgtgagaagtaactgggatacctgggaagtagtacagaaagaccgttatcataccaatgaagtttggtagcaccaaaaggacaagctattcatcc
cgttacaggttacttgggggtgtaacactaaagttatggcggagcgtgttctgtggcagagaacaagtttaacaggtgattcacaagggtgatttccgccg
aatggccttgaagtaccgcatttgaaacttactacaccaagcagaaaaactgtacgaagtcatggtaaacggggttagatccgactgaaccagttgcaactga
agattatccttactcgtcattcgtcacgaaccagctattcaagaaattcatgactcttatttagacgaaggttatcatccgttttactcctctgctatcaagttaatgag
gtgaatcggcgtttagtagtattgattcgttgaataactgtgatggtttccttctagttgagatgcaaaagccgatgctgatgtaactgtgtgctccagccgagcaat
atgataatgttactcgtgatgactgaagctaaaggttaaaacgggtatatactagctactggcagagaagttactagtgtagaagtcgaaattgatagagaaattctttt
tttctagtgatattgtagtgggtgcttgggagcaattaactcagctcttattgttactgtctaatgagcagcatcctaattgattagccaatagttctgactggtgg
gacgaaacttaataagcatcagaatggagcgtgatgggggtgagttgaaatccaatttgcagcattcaaaaaactttagcaatcaacgattttactgggggtgat
gcagatttga

welP1 – Orf2-1-related aromatic prenyltransferase [*Westiella intricata* UH HT-29-1]

Sequence ID: AIH14803.1 codon optimized^[238] in pJ express vector

atgaacgacgtcaaccgcattagaaccgacatcgtcaaccgtagcaaccactttggtgctgagtatagcgagaaggttctggatgaagtgtccaagttttggtgaac
agtttccgacaacagcttcatgatccgtaccagcaataaacaaccggataaactgggttacttccgctaccaggaagatgagagccatctgggtctggcgtg
ggatattgctgctaaagcggctgctgctccgatcaagccgctccggtcgtatcaactgattccggagatttgcgaaacttccgatcatggcggatggcgtgacttt
gatgtgaaacacggcctggcgaagatcgtgagcagccatcaaaagcgtggttccggctcaagatgcttcaagctgtccctgccaccgtctgtaattcccacgaggac
ttctgaagaatcatcacctggacgctgtatgctgctgctgactatcaccacagcagcgtgaacctgtacttgcacacttaccacccgaagcatcatacagcga
atactacgagaacctgctgcaagacctgagttcagccactgagatgaggtcctggagctgttggtaacaatggcgagatcgcgctgacttcaacttgcgaagc
ccgctattgaacgtttgtcttttactgcccgttctgaatcgtgaggttccgcagaatttgtgacgctgctgaagaaatacattaatgaagcaccggccttgg
tggacaatccgggtttctcttgggctggagctttggtccgaggggtgtaaaaggtacgtatacacaagttgatgtggactaccacggtcgcaggttccgctgttact
aaggtcattctcagcctcgcgaagcagcggacttgcactggcgaagcttggccccatcatcatcatcattga

hpI1 tryptophan isonitrile synthase [*Fischerella* sp. ATCC 43239] Sequence ID: AIJ28525.1 codon optimized^[238]

atgatcagcgagaaaactctgcgccacattttccagatcgtcgtctgctgatacggagccgtgtgcaaaagaacctgctcatttgcctggcccctcatctgccg
aagattcagagctttatcgaanaaatgagccgatccacttatttaccggcgttccggcaaaagagcccgaaccgcagaaagtactgggtccaatcgcgataggg
gcaacgtgttgccttcaatttctgcaaaaactgtgcaacaaatctccgagatttacgctagcgggtgcaaaaatcacatttgttctgacggtcgcgtgttactgatct
ggtcgcgatcacggacgagaatgttcttctgatacgggcatccagcgcctgctgaacgaaatcaatgcggatgccattgataccttctgctggagaacgtgttta
ccggtatgagcttaccagatgctgtaaaacctggttaagcaatcgcacagccgattgaaagcattcaagagcgtgaaatagcaggataaacaccgtcagttt
tcaagggcatttaccctgttctgacgactactggtctgtaccggacaagagccgtgaacaaatcgaagtggagtgcaaccttctgctgctacgaagtattca
cgcttcaatgcttgaccacgctggttggcagcatttcccagagcctccgtttagatcctcctcaagattatcacagcaaaaaatcggtatccacatgattaa

Appendix

gaccagcgaccagtggggcacccgtggcacaatgcaccgatgtcaatggcaaagaatttctgctgatgaagcgtaacatattgaggacattggtgagcagcctgg
tctggcataatgatcaccgagccactacatctctgagcgagcaagtttagccaagcactggtcaccttcgacaacaagcataa

hpI3 tryptophan isonitrile synthase [*Fischerella* sp. ATCC 43239] Sequence ID: AIJ28523.1
codon optimized^[238]

atgatggttagcacgagcgtagaacaaagcaccatatttagcgttaaatcttaactccgtttggcgcgctgttgaagcgaccgagatcacagcgacatccagcag
ctgagcattgaacaactgtgccagttgacctgggaacaccgtctgattgtgctgcgcggtttctctctgctggagcgcgaggaactgagcatctattgccagcgttggg
gtgaattgctggtctggaatttcggtacggctctggtatgattgtaccagaaccggagaactacctttaccaacggcaatgtgccgttccattgggacgggtgcat
tcgccgaagcgggttcgggtttctgttctcaatgtctgaagcaccggaagctggcagcgggtggcgagctctgttttgtgatacggctccgtacctgcagaacgtc
agcccgaacagcgtgagatctggcaaaagaccgagatctgtacaaaaccgagaagtggtcattatggtggcgagatcacgaagtcctgtggtgattaaacacc
cgatcaccggtctgagcagctgcgttttgagagccattgaacgatgcgagcgttacctgaatccgctgtatgttaggtgtgcaatctccgaccgaagaacaga
atagcttcaatgaactgattgagaacctgtacttccgcaaanctgttttgcgatgagtggaagggcgacttctgattgccgacaatcatgctgcttccac
ggtcgaatctttctgtccaacagccagcgcctatgcagcgtgtgacattctgtaa

tser AM902709.1 | *Thermus scotoductus* chrR gene for chromate reductase, strain SA-01

ttcaattgggtaacgcccgggtttccagtcgagcgtcagaacgacggctaagctctcagagatccatccccgaagaggaggcttccacgtagcgaagg
cagcccgagatcggagccttccccgaccgaagccggggttcaaaagaccagctatccccaaaaagagcgcggggaaaccggccccacgggactgtttcctt
acgtttcttcaagaccctcacaatggaggtatggccttcttccccctggaactcggcgctccggctgaaaaaccgctgccaatgtccccatgtgcc
agtactccgccacttggaggagaggttaaccgactggcactctcactaccacgcgggcttggggcgctggggctcattctggtggaggccaccgctg
gaaccttgggctgatcagcccctatgacctgggcatctggtcggaggatcaccttccgggctgaaggagctcggcgaggatccgggaagctggagcgggtgc
cggggatccagctggcccacgcccggcgcaaggcggggaccgccagccctgggaagggggaaagcccctgggctgcggggtggtggggccaagcccattc
cctttgacgagggctaccggtaccgaaccctggacgaagcagggatggagcgcacctccaggccttctggaaggagccagacgtgcccttagggcaggctt
tcaggatcagagctccacatggccatggtactcttcttcttcttcccccttccaaccagcgcaccgacgcctacgggggaagcctggaaaaccgcatgc
gctttcccctcagggtggcccagcagtgccggaggtggtgccagggagcttcccccttctgctcgggtctccgccagcactggggggaagggagatggagcct
cgaggacacctggccttccggaggcctaaggagctgggggtggaccttggactgctctcggcggggtggtgctcagggtgctgattccccctggccccg
ggcttccaggtgcccttccgacgcccgtgcgaaggggtggcctgcaaacgggagccgtgggctcatcaaccccccagcagcgggaaccctctgcag
gcgggaagcgcgatctggtgcttctggcgggttctctcagggaccctacttccccctacgggctgccaagccttggcgctggccccggaggatccccccag
taccaaaggggttttagcaccatccaacctggcaggaaccaggttggagggcaccggccaggttctc

P450_{BM3}

atggcaataaagaatgctcagccaaaacgtttggagagctfaaaattaccgttataaacacagataaacgggtcaagctttagataaaattgcggatgaatt
aggagaaatcttaaatcagggcgctgctgtgtaacgcctactatcaagtcagcgttcaataaagaagcagcagatgaatcacgctttagataaaaaactaagtc
aagcgttaaatgttacgtgattttgaggagacgggtatttacaagctggacgcatgaaaaaattggaaaaagcgcataatcttactccaagctttagtcag
caggcaatgaaaggctatcatgcatgatggtgatgatccgtgagcgttgcataaagtgaggagcgttaaatgcagatgagcatattgaagtaccggaagacat
gacaggttaacgcttgatacaattggtcttgcggcttactatcgcttaacagctttaccgagatcagcctcatcatttatacaagatggtccgtgactggtgatga
agcaatgaacaagctgagcagcaaatccagacgaccagcttatgatgaaaacaagcgcagtttcaagaagatataaggtgatgaacgacttagataaaa
attattgcagatcgaagcaagcgggtgaacaagcagatatttataacgcatatgctaaacggaaaagatccagaaacgggtgagccgctttagtcagagaacat
tcgctatcaaatattacatttattgctgggacacgaacaacaagtggtctttatcatttgcgctgatttcttagtgaataatccaatgatttcaaaaagcagcag
aagaagcagcagagtttagtagatctgttcaagctacaacaagcaaacgcttaaatatgctggcatggtcttaaacgaagcgtcgccttaggccaactgc
tctgctgtttccctatatgcaaaaagaalacgggtgcttggaggagaatctttagaaaaagcgacgaactaatggttctgattcctcagcttaccggtgataaaac
aatttggggagacagatgtggaagagttccgtccagagcgttttgaatccaagtcgactccgagcagcgtttaaaccgcttggaaaccggtcagcgtgctgtatc
ggtcagcagttcgtcttcatgaagcaacgctggtacttggatgatgctaaaactttagcttgaagatcatataaaactcagagctggatataaagaaacttcaacg
ttaaaccctgaaggcttgggtgtaaaagcaaaatcgaaaaaatccgcttggcggtatcttccactagcactgaacagctgctaaaaaagtagcaaaaaggcag
aaaacgctcataatcgcgctgcttctgtctatcaggttcaataatgggaacagctgaaggaacggcgctgatttagcagatattgcaatgagcaaaagatttcac
cgcaggtcgaacgcttattcacacgcccgaatctccgcggaaggagctgtataatgtaacggcgtctataacggtcatccgctgataacgcaaaagcaattt

Appendix

gtcgactggtagaccaagcgtctgctgatgaagtaaaaggcgttcgctactccgtatttggatgcggcgataaaaactgggctactacgtatcaaaaagtcctgcttt
tatcgatgaaacgcttgcgctaaggggcagaaaacatcgtgaccgcggtgaagcagatgcaagcgacgacttgaaggcacatatgaagaatggcgtgaacat
atgtggagtgcgtagcagcctactttaacctgacattgaaaacagtgaagataataatctactcttcaatttgcgacagcgccgagatgccgctgcg
aaaatgcacggcgtttcaacgaacgtcgtagcaagcaaaactcaacagccaggcagtcacgaagcacgacatcttgaattgaactccaaaagaagc
ttcttatcaagaaggagatcattaggtgttattcctcgcaactatgaaggaatagtaaaccgtgtaacagcaaggctcggcctagatgcatcacagcaaatccgtctgg
aagcagaagaagaaaaatagctcattgcccactcgtfaaaacagatccgtagaagagcttctgcaatacgtggagcttcaagatcctgttacgacgacgacgcttcg
cgcaatggctgctaaaacggtctgcccgcgataaagtagagcttgaagccttgcctgaaaagcaagcctacaaaagaacaagtgctggcaaaacgfttaacaatgct
tgaactgctgaaaaataccggcgtgtgaaatgaattcagcgaattatcgcccttctgccaagcatacggcgcgctattactcgatttctcatcacctcgtctgat
gaaaaacaagcaagcatcacggtcagcgttctcaggagaagcgtggagcgatggagaatataaaggaaatgctcgaactatctgccgagctgcaagaa
ggagatacattacgtctttattccacaccgagtcagaattacgctgcaaaagaccctgaaacgcccgttatcatggtcggaccgggaacaggcgtcgcgct
ttagaggcttctgtagcgcgcaaacagcctaaaagaacaaggacagtcacttggagaagcatttatacttggctgccgttacctcatgagactatctgtatcaa
gaagagcttgaaaacgccaagcgaaggcatattacgcttataccgcttttctcgcgcatgcaaaatcagccgaaaacatacgttcagcacgtaataaacaagac
ggcaagaaatgattgaacttctgatcaaggagcgcacttctataattgcgagacggaagccaaatggcacctgcccgttgaagcaacgcttatgaaaagtatgctga
cgttaccaagtgaagcagacgctcgttatggctgcagcagctagaagaaaaaggccgatacgaaaagacgtgtgggctgggtaa

8.3.3 Fast Protein Liquid Chromatography

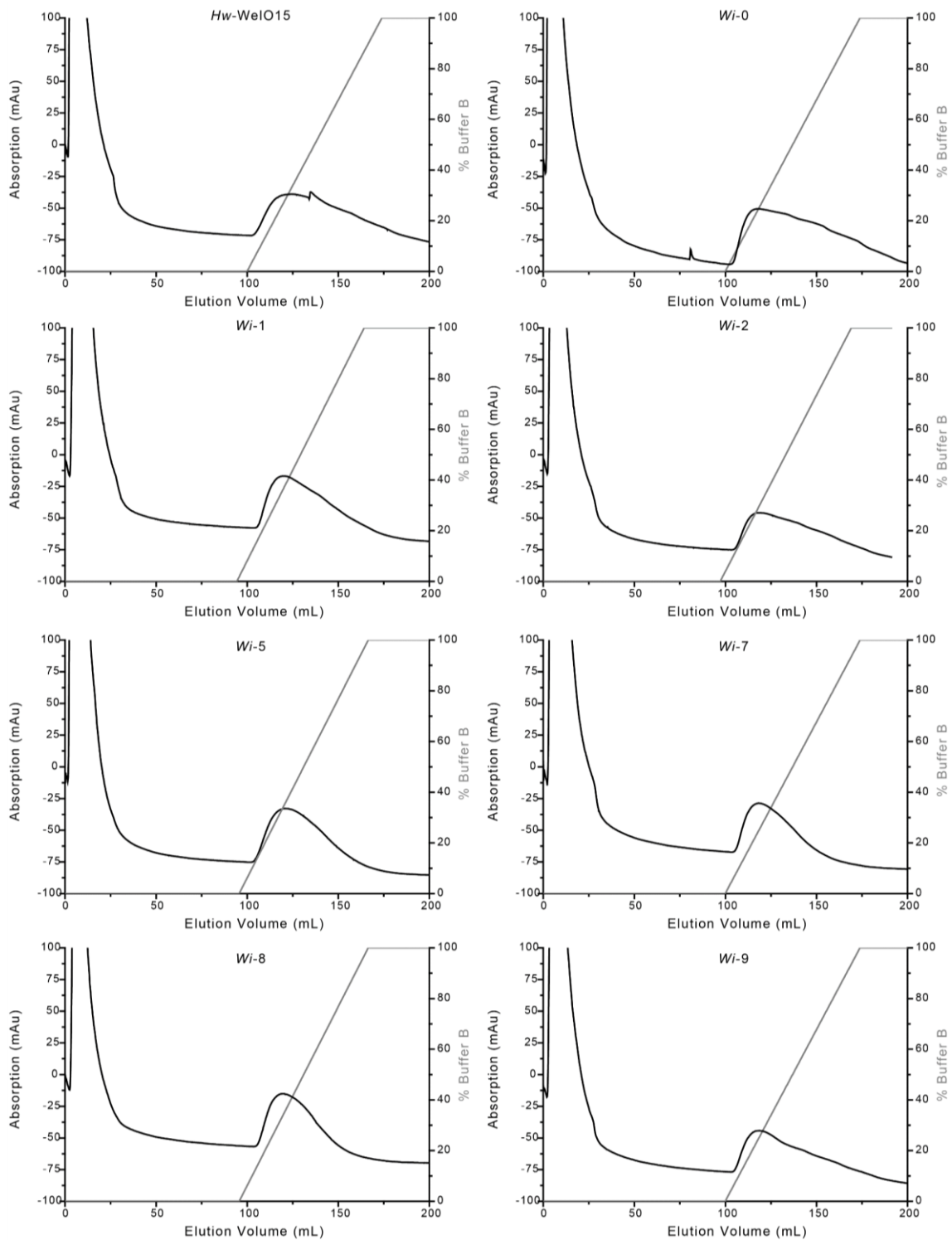


Figure 65. Ni-NTA IMAC elution profile of *Wi*-WelO15 and *Hw*-WelO15 variants. Elution buffer (buffer B) is increased in a linear gradient from 20 mM imidazole (0% buffer B) to 250 mM imidazole (100% buffer B) in 12 CV. Tailing was also observed with steeper gradients (up to 0.5 M imidazole/12CV).

Appendix

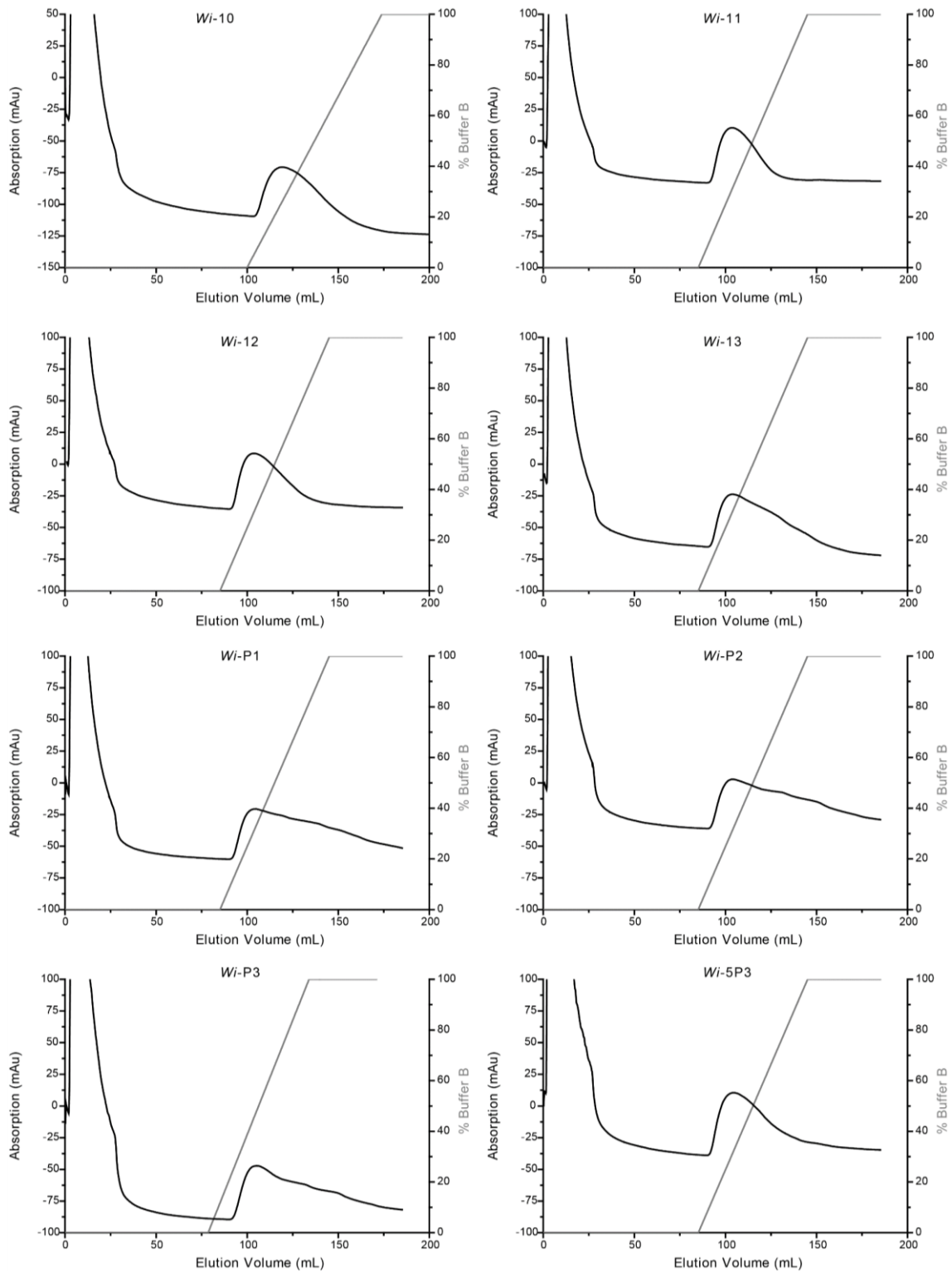


Figure 66. Ni-NTA IMAC elution profile of *Wi*-WelO15 and *Hw*-WelO15 variants. Elution buffer (buffer B) is increased in a linear gradient from 20 mM imidazole (0% buffer B) to 250 mM imidazole (100% buffer B) in 12 CV. Tailing was also observed with steeper gradients (up to 0.5 M imidazole/12CV).

Appendix

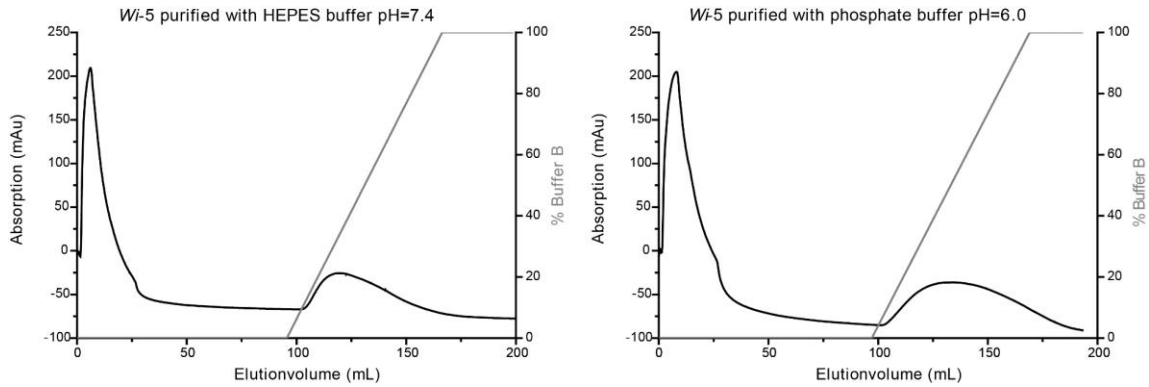


Figure 67. Ni-NTA IMAC elution profile of *Wi-5* in comparison with two different buffer systems.

Calibration of Superdex 26/60 Column

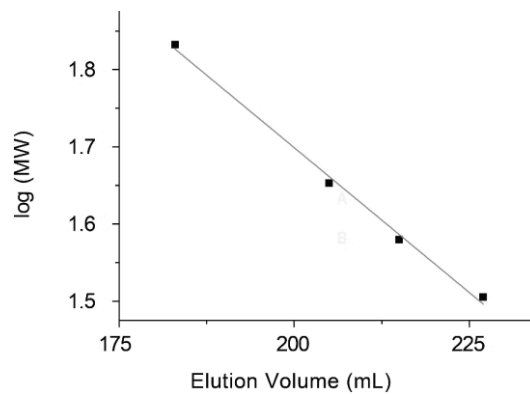


Figure 68. Calibration of size exclusion column by measuring different enzymes. Measured samples are bovine serum albumin (68 kDa, 183 mL elution volume), lysozyme (trimer 45 kDa, 205 mL elution volume), TsER (38 kDa, 215 mL elution volume), *Wi-WeIO15 V6I/D284N* (35 kDa, 227 mL elution volume). Linear regression : $MW(kDa)=3.06-0.0007 \cdot \text{elution volume (mL)}$.

Mass spectrum of isolated, denatured *Hw-WeIO15*

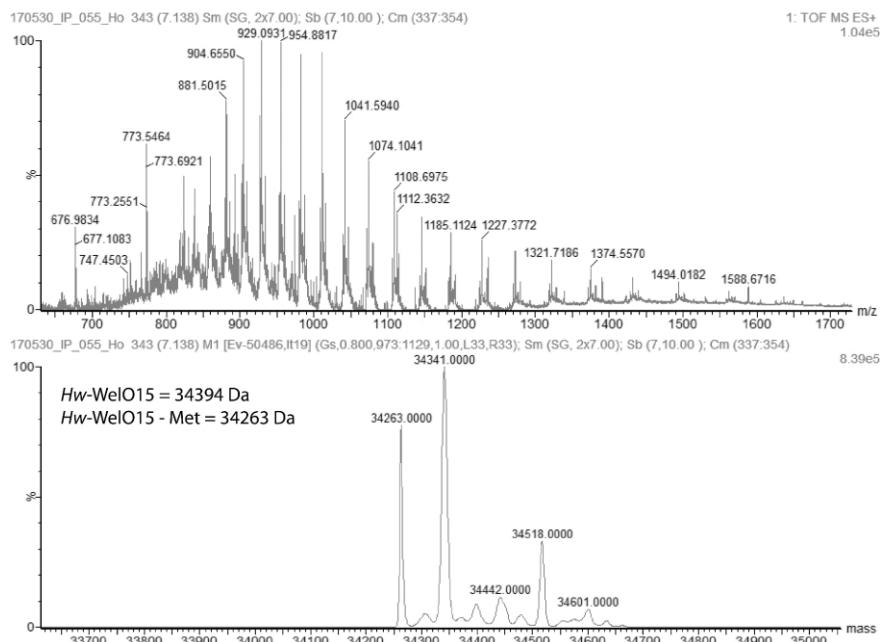
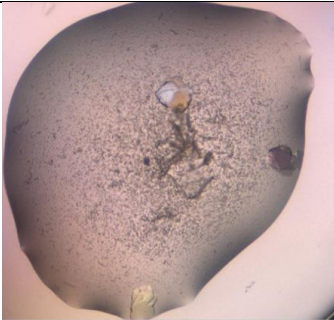
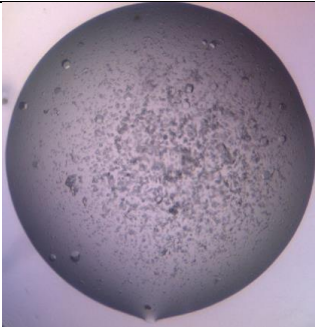
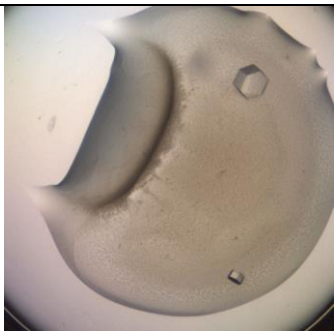
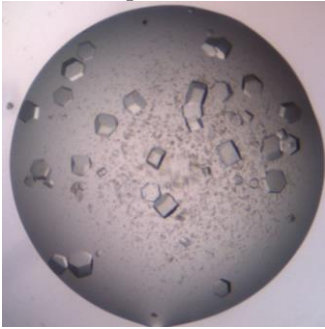


Figure 69. Mass spectra of *Hw-WeIO15*. The denatured enzymes were measured via HPLC by the mass department of Philipps-University Marburg. The theoretical, with ExPASy ProtParam calculated, mass of *Hw-WeIO15* is 34394 Da.

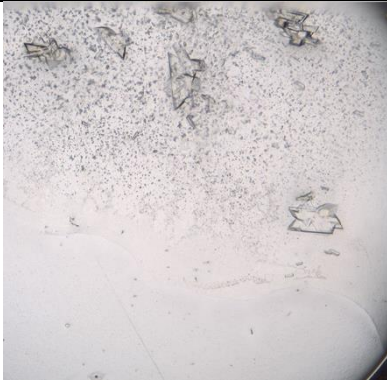
8.3.4 Crystallization

Table 37. Pictures of all crystals that were obtained from WelO15 enzymes.

crystallization set up (<i>Wi-0</i>) 20.10.2015, pictures taken 27.10.2015	
	
AmSO ₄ plate well B10 drop2 0.2 M KOAc, 2.2 M AmSO ₄	JCSG IV plate well A12 drop1 0.1 M Bicine pH9, 2.4 M AmSO ₄
crystallization set up (<i>Wi-0</i>) 20.10.2015, pictures taken 15.01.2016	
	
AmSO ₄ plate well D6 drop1: 0.2 M Na ₂ HPO ₄ , 2.2 M AmSO ₄	AmSO ₄ F5 drop1: 0.1 M Tris pH8, 0.8 M AmSO ₄
	
AmSO ₄ plate well F6 drop1: 0.1 M Bicine pH9, 0.8 M AmSO ₄	JCSG III plate well B10 drop1: 0.1 M Tris pH8.5, 2.4 M AmSO ₄
	
JCSG IV plate well A12 drop1: 0.1 M Bicine pH9, 2.4 M AmSO ₄	

Appendix

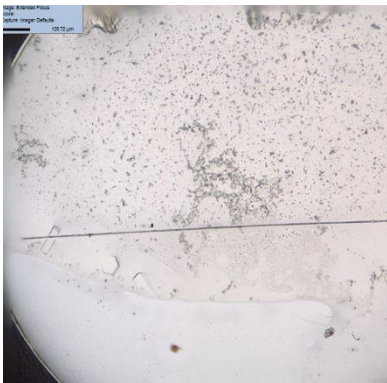
aerobic crystallization set up (Wi-0) 14.7.2016, pictures taken 16.03.2017



AmSO₄ plate well E12 drop1:
0.1 M Bicine pH9, 1.6 M AmSO₄

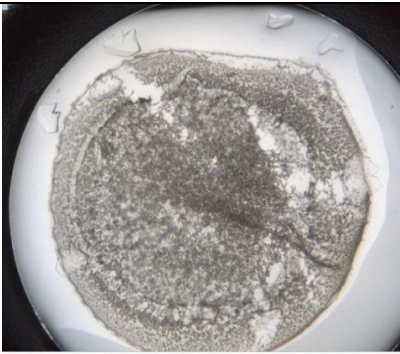


AmSO₄ plate well G10 drop1
0.2 M NaCl, 0.1 M HEPES sodium salt
pH 7.5, 1.6 M AmSO₄



AmSO₄ plate well G12 drop1
0.1 M MES sodium salt pH 6.5
1.6 M AmSO₄ in 5%(w/v) PWG 400

anaerobic crystallization set up (Wi-0) 14.7.2016, pictures taken 29.03.2017



SG Core III E3 drop2:
0.1 M MES pH 6.5, 1.6 M AmSO₄

8.3.5 Circular Dichroism and Stability

8.3.5.1 Folding

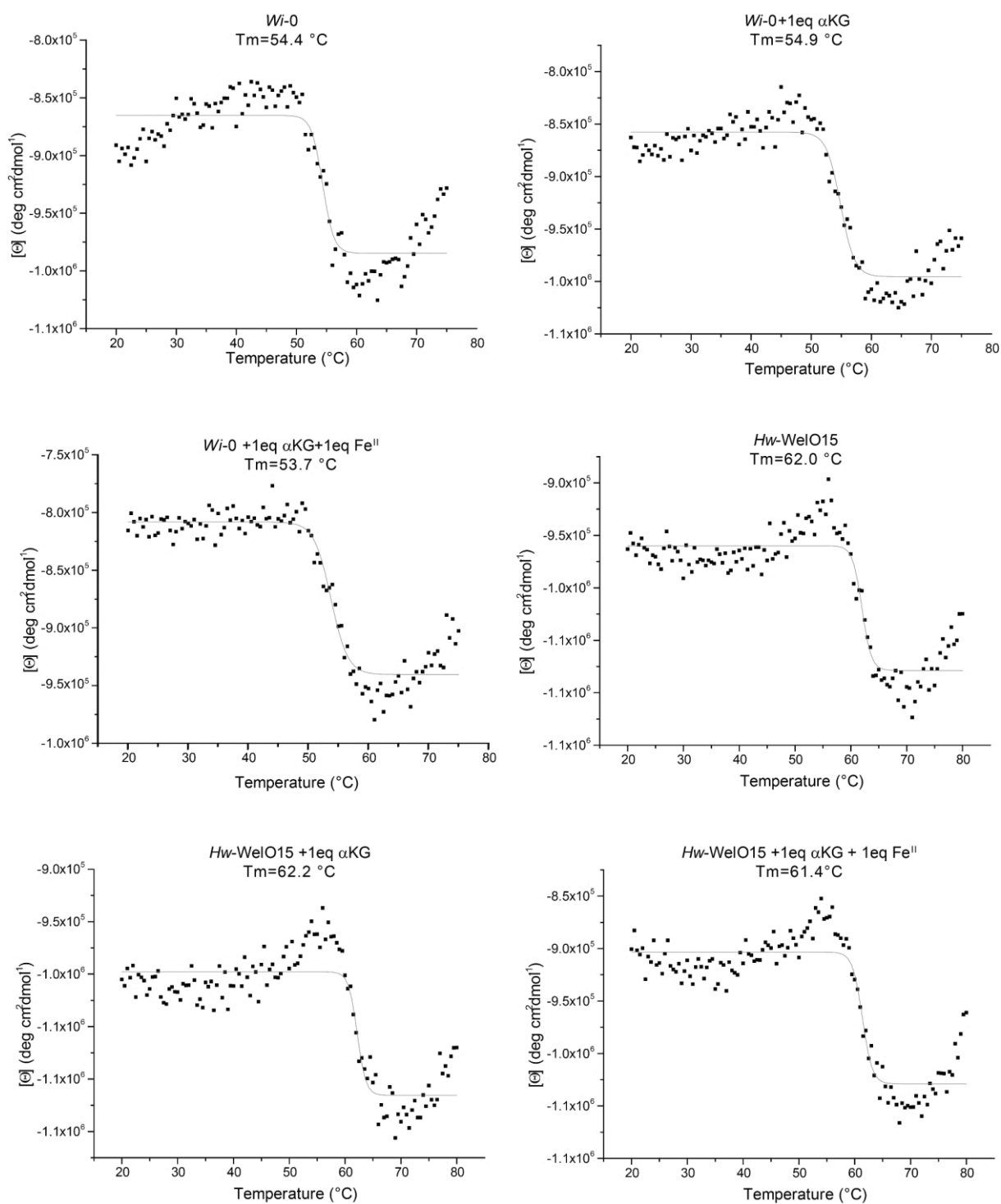
Table 38: Folding properties of WelO15 variants in presence of 5 mM HEPES, 1 mM NaCl, pH 7.4 and given cofactors.

		<i>Wi-0</i>	<i>Hw-WelO15</i>	<i>Wi-5</i>	<i>Wi-8</i>	<i>Wi-2</i>	<i>Wi-9</i>
apo enzyme	α -helices	30	16	18	23	19	21
	β -sheet	24	36	32	32	33	13
	turn	16	18	19	27	24	26
	random	24	30	31	19	24	41
1eq α KG	α -helices	16	22	24	20	25	18
	β -sheet	49	23	0	41	23	24
	turn	25	23	34	19	32	25
	random	21	32	42	20	21	34
1eq α KG + 1eq Fe ^{II}	α -helices	17	22	27	14	32 ^[a]	17 ^[b]
	β -sheet	55	29	20	42	0 ^[a]	35 ^[b]
	turn	10	18	30	16	38 ^[a]	22 ^[b]
	random	18	30	24	28	30 ^[a]	27 ^[b]

[a] 5 mM α KG+0.5 mM (NH₄)₂Fe(SO₄)₂ [b] 1 eq α KG+1 eq NiCl₂

The error of measured melting temperature was determined by measuring 5 times the melting temperature of apo enzyme *Wi-13* and calculate standard deviation which was 0.3°C.

8.3.5.2 Melting Curves

Figure 70. Melting curve of *Hw-WelO15* and *Wi-WelO15* in combination with different cofactors.

Appendix

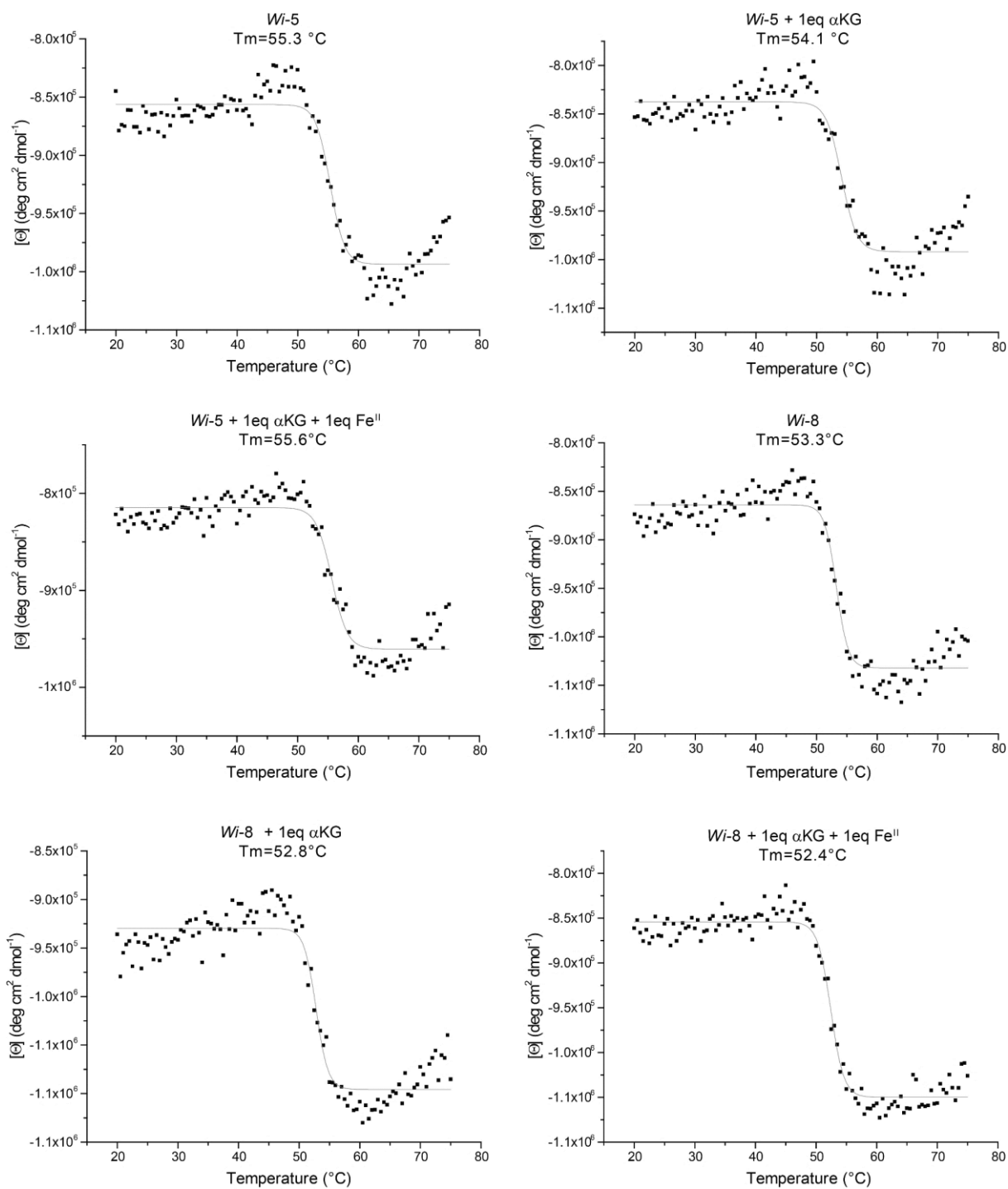


Figure 71. Melting curves of *Wi-5* and *Wi-8* in combination with different cofactors.

Appendix

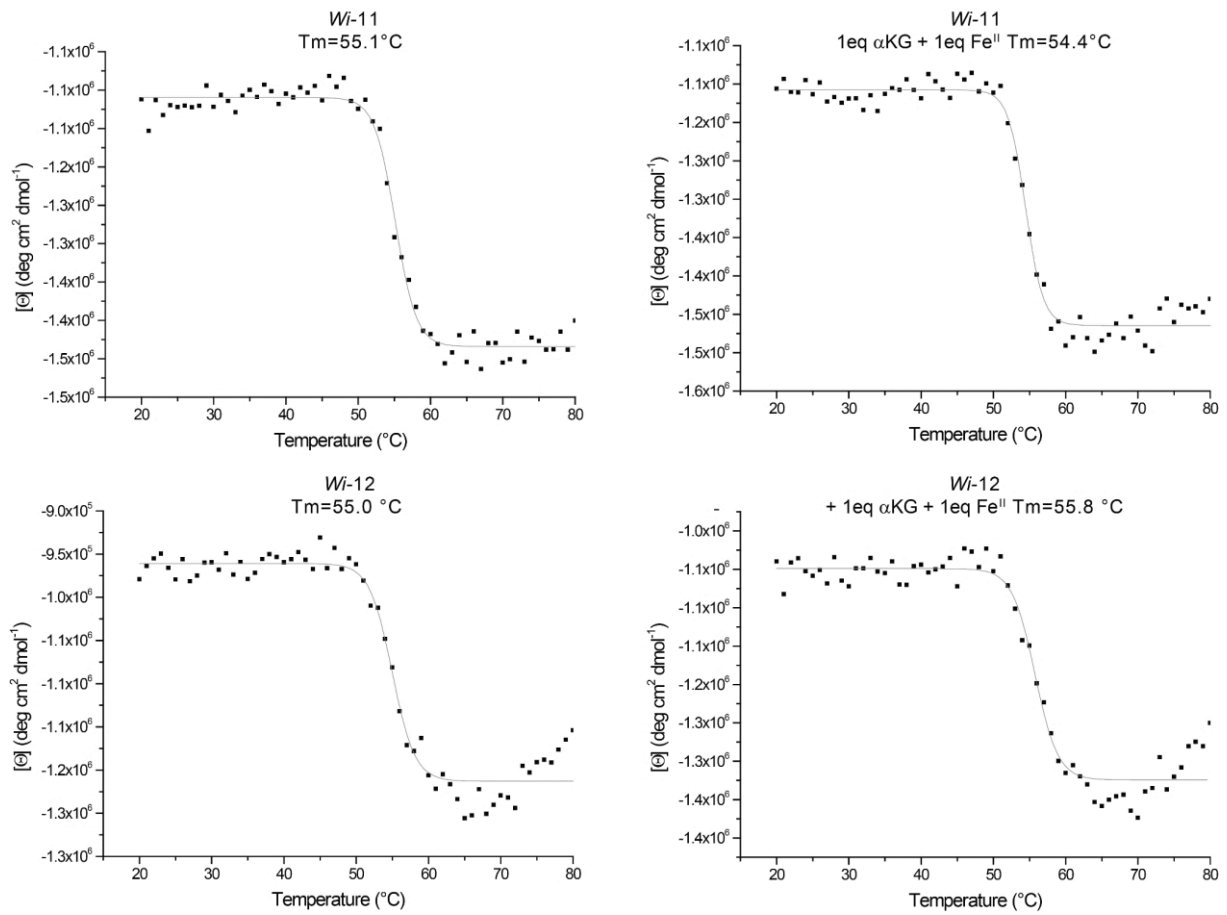


Figure 72. Melting curves of *Wi-11* and *Wi-12* in combination with different cofactors.

Appendix

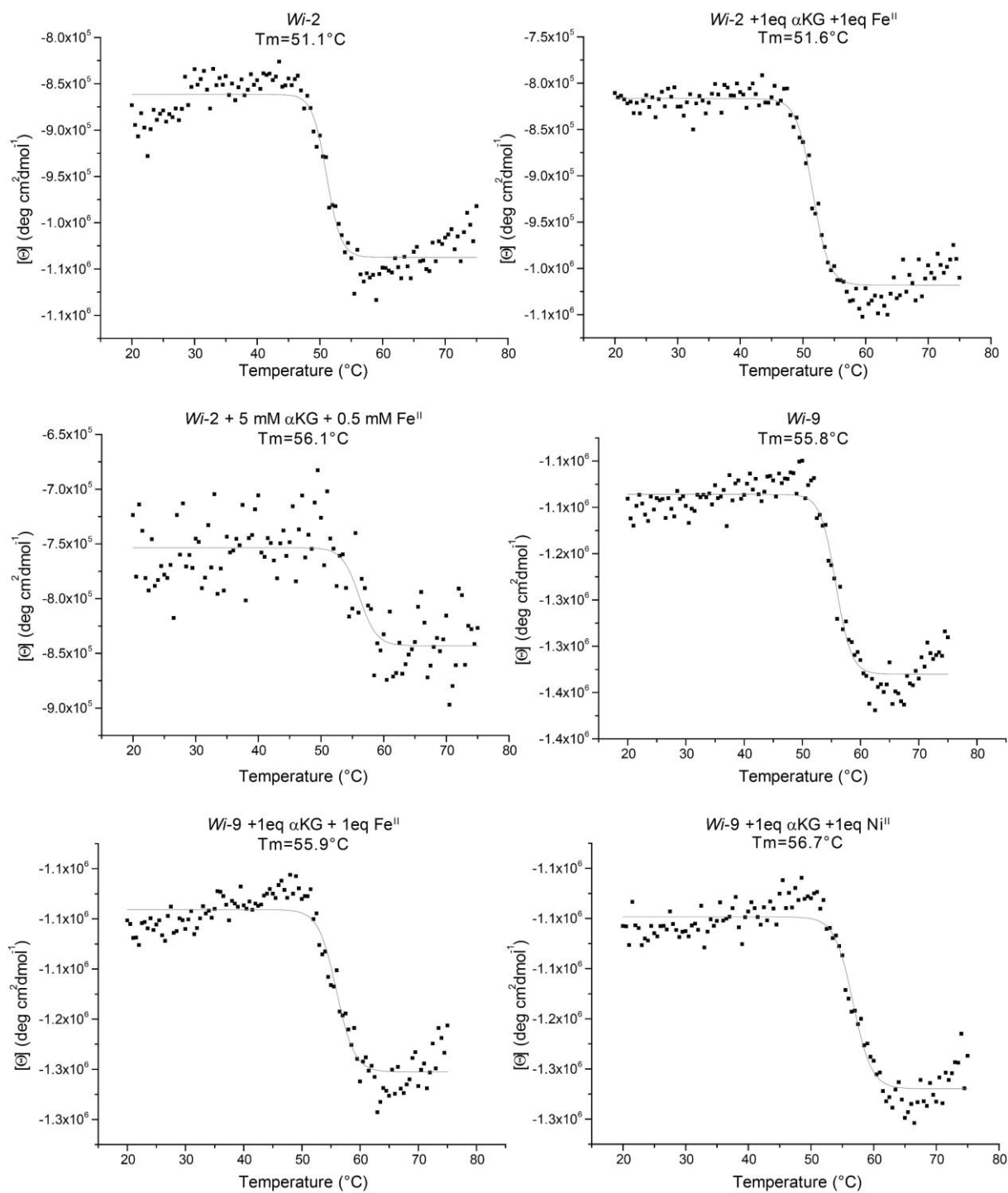


Figure 73. Melting curves of *Wi-2* and *Wi-9* in combination with different cofactors.

Appendix

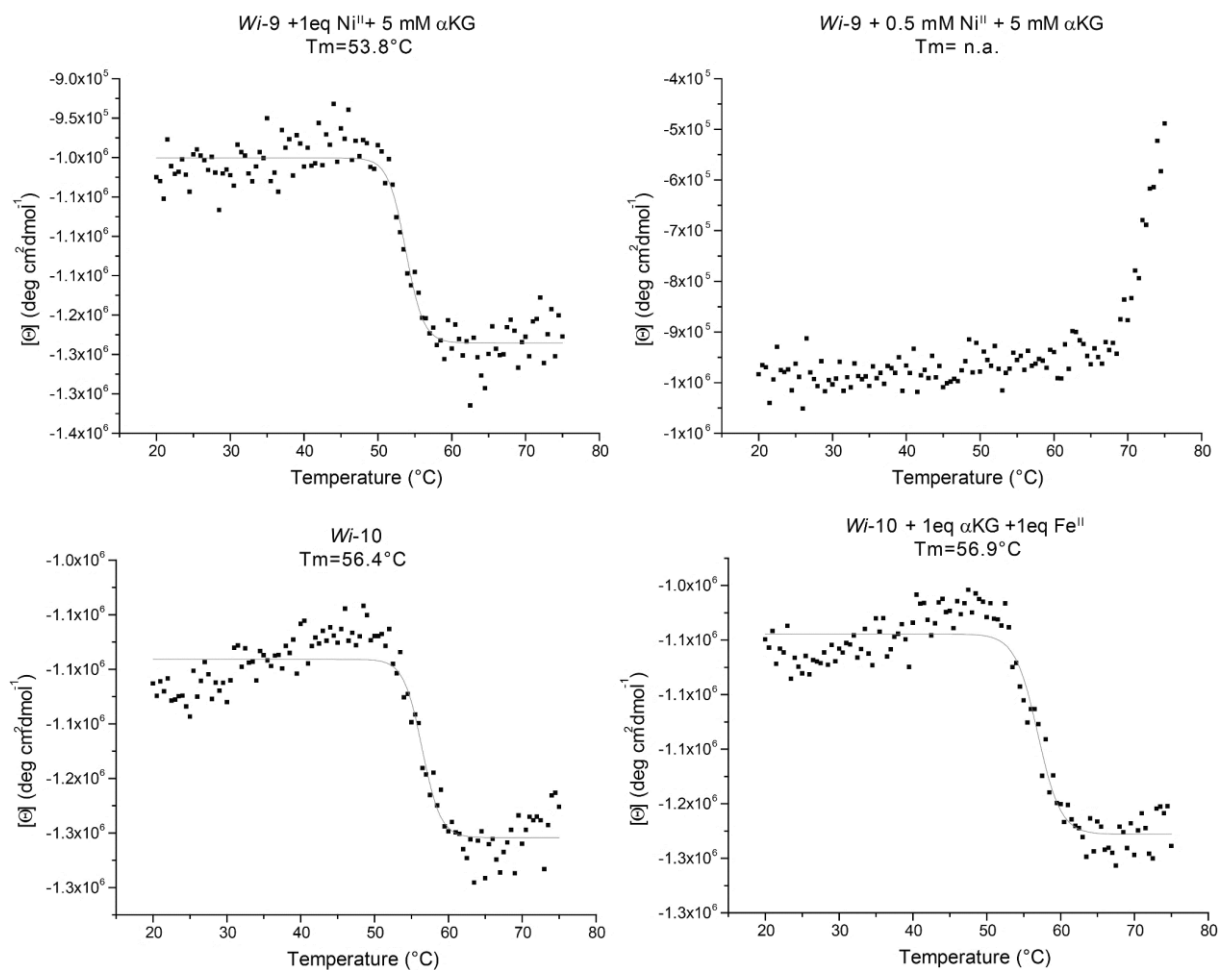
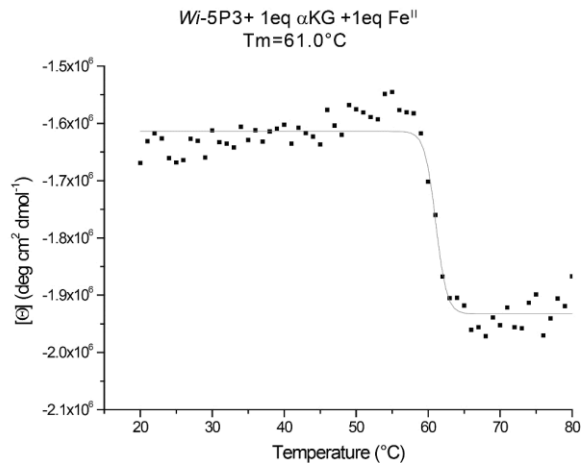
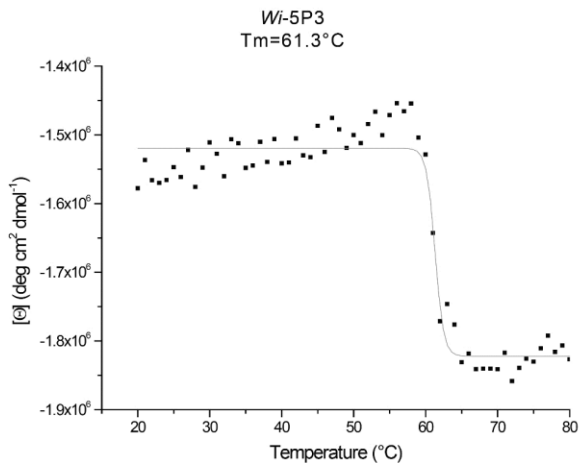
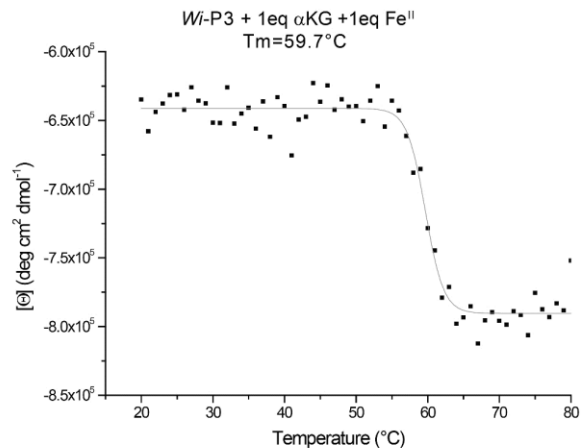
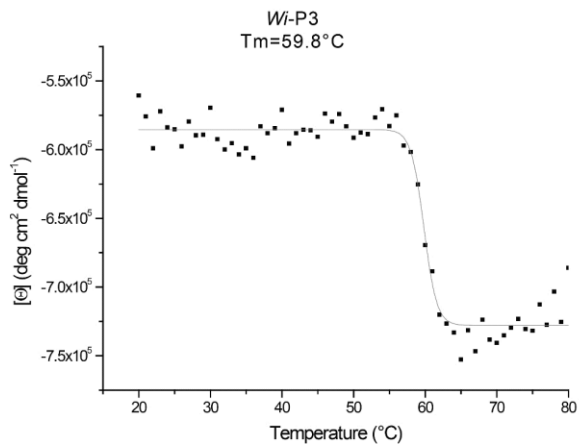
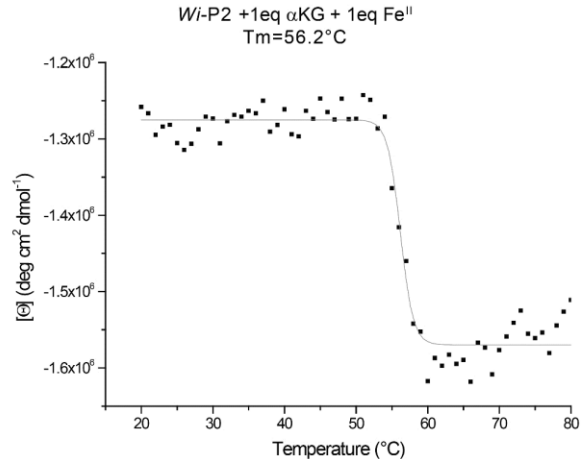
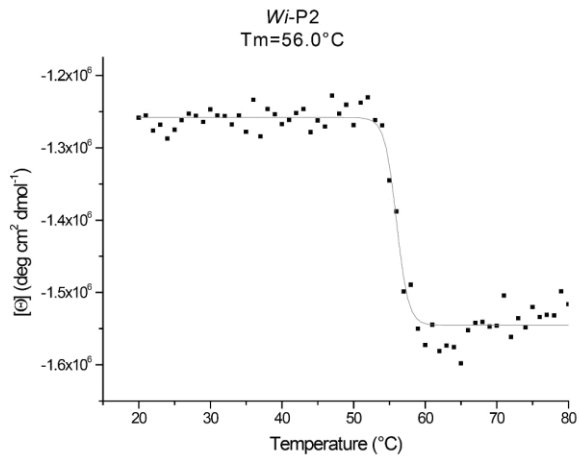
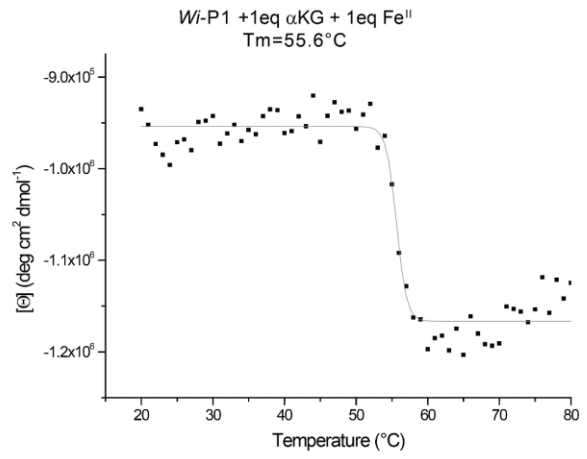
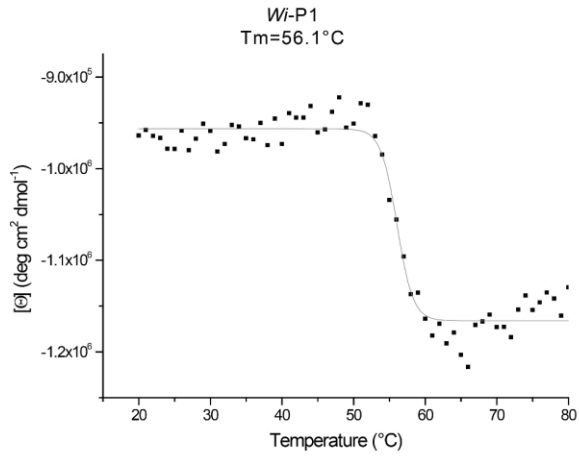


Figure 74. Melting curves of *Wi-9* and *Wi-10* in combination with different cofactors.

Appendix



Appendix

Figure 75. Melting curves of *Wi*-P1, *Wi*-P2, *Wi*-P3 and *Wi*-5P3 in combination with different cofactors.

8.3.5.3 SDS-PAGE Analysis of Stabilized Variants

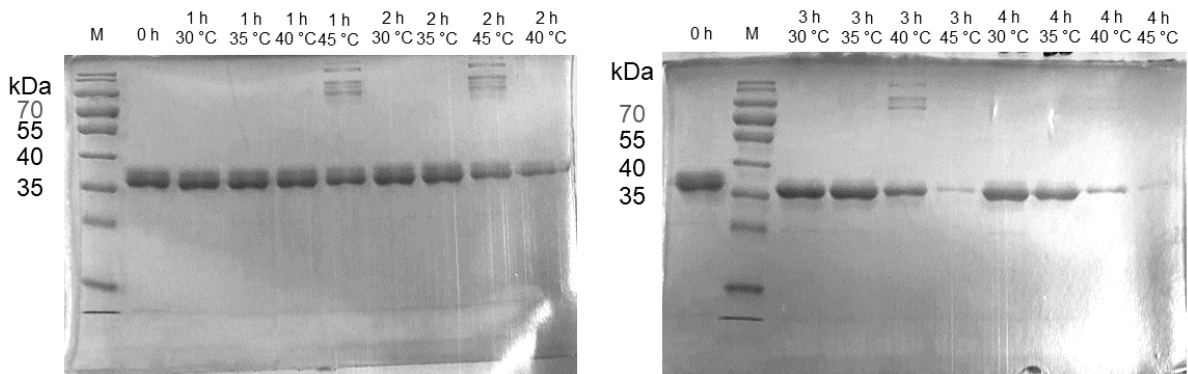


Figure 76. SDS-PAGE analysis of soluble fraction of *Wi*-0 after incubation at different temperatures.

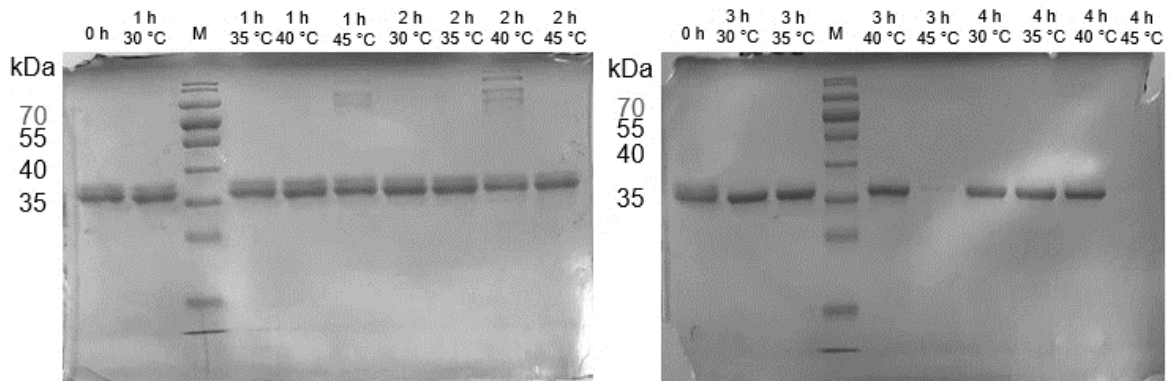


Figure 77. SDS-PAGE analysis of soluble fraction of *Wi*-P1 after incubation at different temperatures.

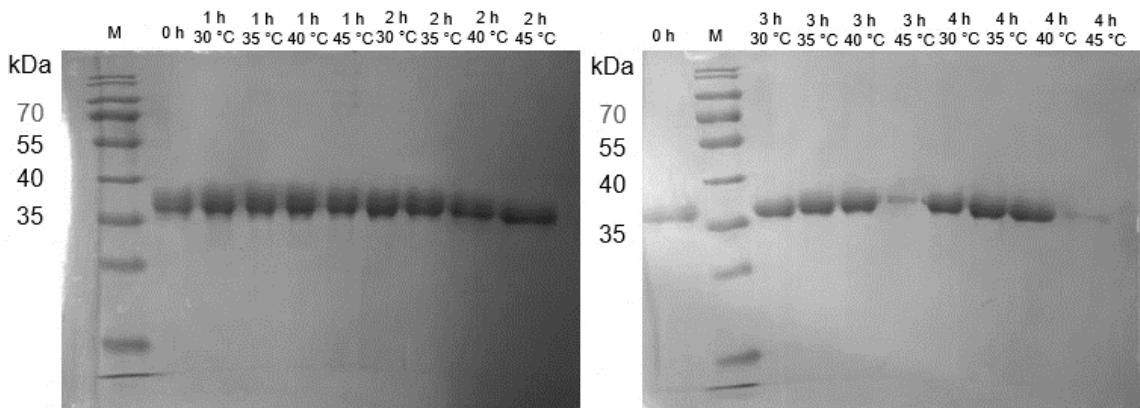


Figure 78. SDS-PAGE analysis of soluble fraction of *Wi*-P2 after incubation at different temperatures.

Appendix

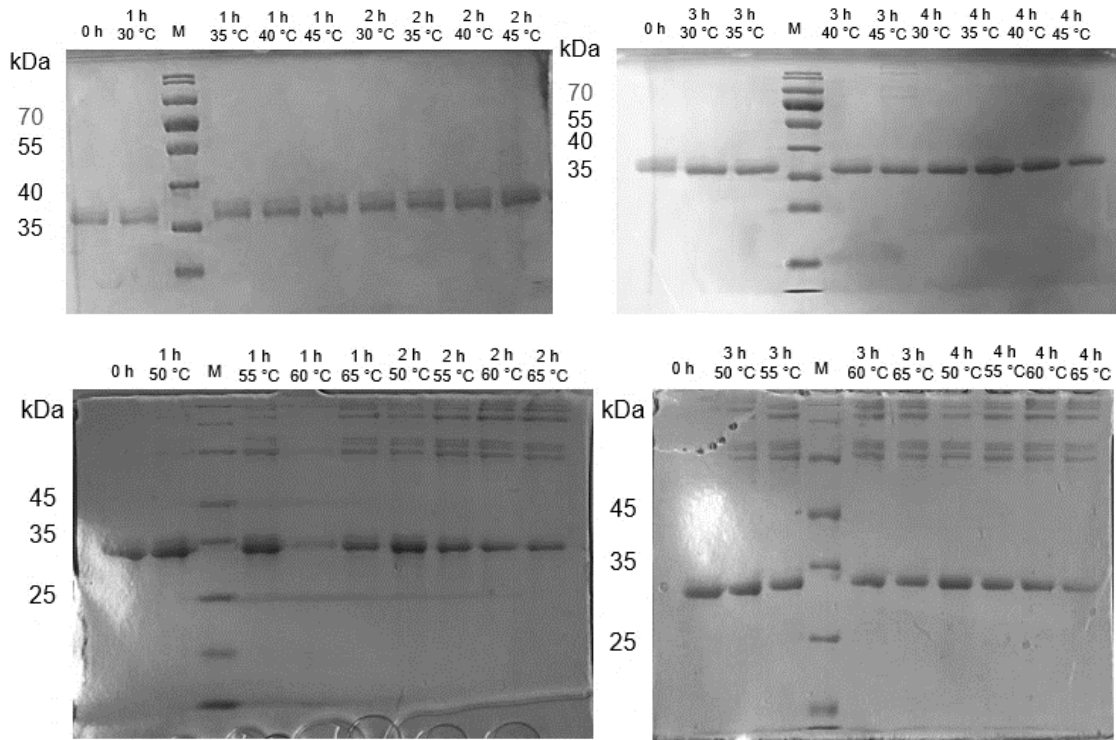


Figure 79. SDS-PAGE analysis of soluble fraction of *Wi-P3* after incubation at different temperatures.

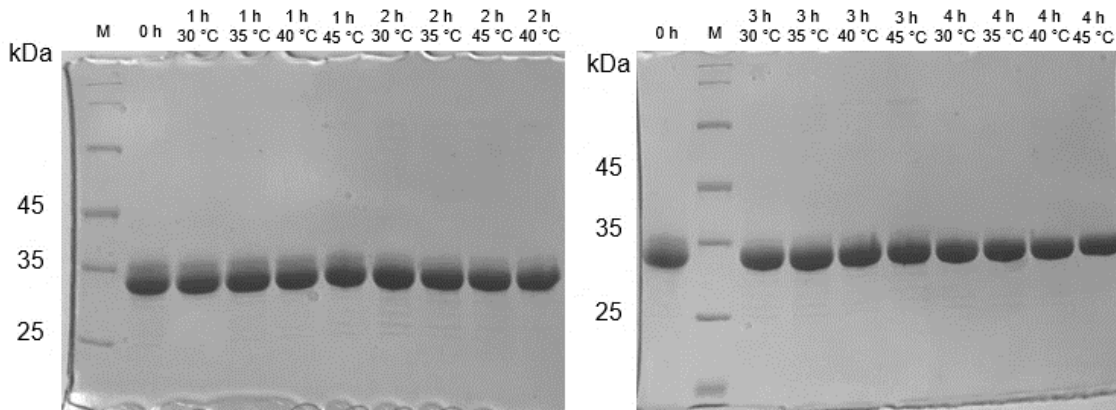


Figure 80. SDS-PAGE analysis of soluble fraction of *Wi-5P3* after incubation at different temperatures.

8.3.6 Docking

8.3.6.1 Isonitrile and Isothiocyanate Molecules

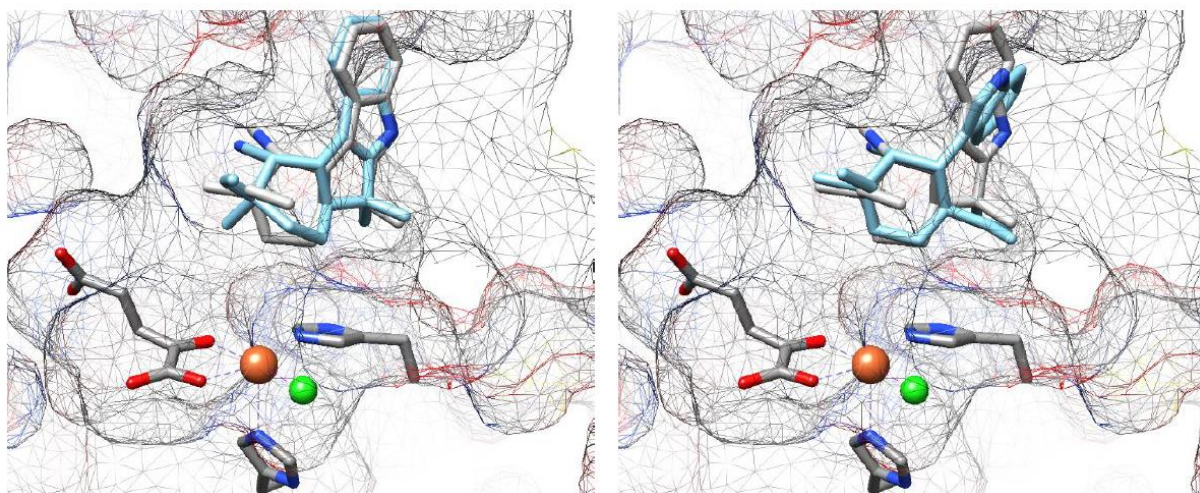


Figure 81. On the left, the docking results of 12-*epi*-fischerindole U (light blue) is shown, overlaid with the soaked 12-*epi*-fischerindole U (gray). On the right, the docking results of 12-*epi*-hapalindole C (light blue) is shown, overlaid with the soaked 12-*epi*-fischerindole U (gray).

8.3.6.2 Hapalindole-like ketones

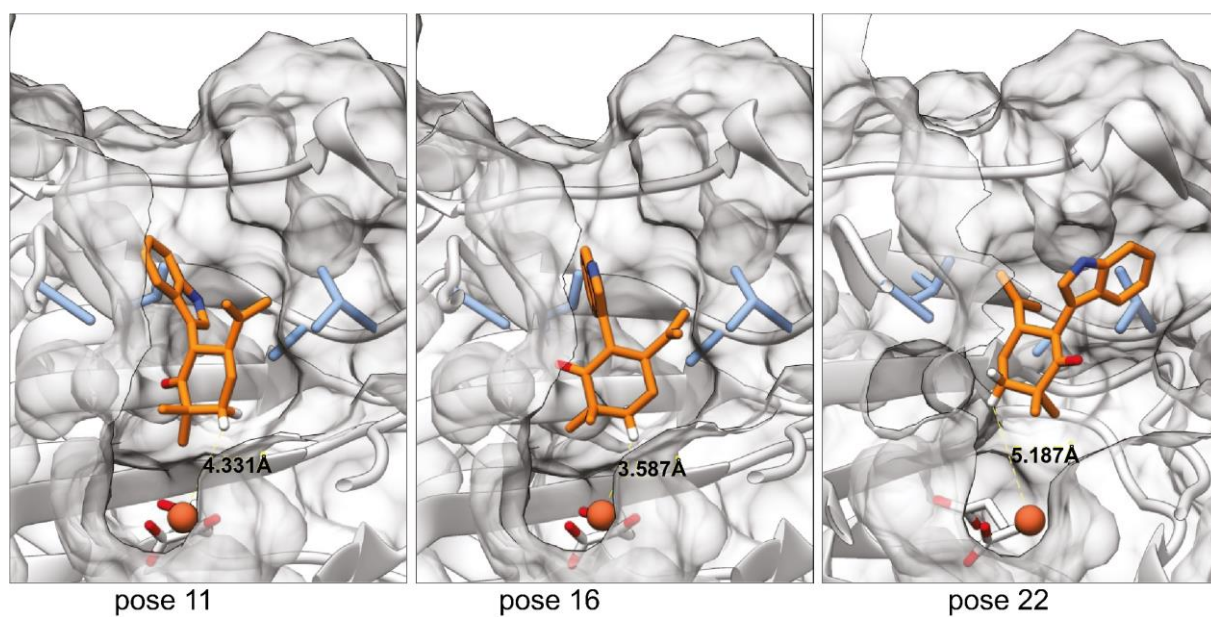


Figure 82. Docking poses after docking with YASARA docking tool. Shown are proposed poses 11, 16 and 22.

Appendix

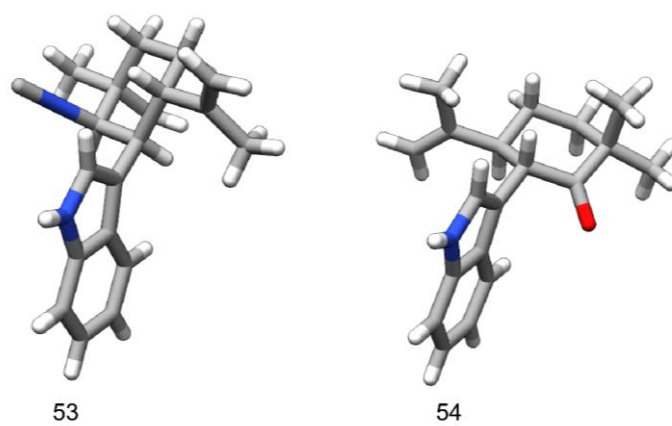


Figure 83. Crystal structures of **53** (left) and **54** (right). It can be seen that the isonitrile and ketone functionality points in opposite directions based on the indole ring.

8.4 Mutagenesis

8.4.1 Mutations in Sequenced Clones after Error Prone PCR

In table 39 all mutations, found in the sequenced clones after error prone are listed.

Table 39: Mutations incorporated with error prone PCR. Out of 6 variants that were sequenced for each library, 3 variants without frameshift were identified. Two sequenced mutants were wild type and one mutant had a frameshift. m= mutations, silent = silent mutation, fs = frameshift, aa= amino acid

	number of mutations(m)	mutations
active site region	2m +1silent	Y190F, P244P, R256Q
	4m +1silent	V196V, V228D, F232L, S262G
	5m + 1silent	A104A, T180A, T195P, D220V, F252I, F279V,
	3m + 1 silent + 1fs	fs (additional A at 756), S234S, V264E, K285R
	2 sequenced genes still had the template sequence	
lid region	7m	M67K, S69T, I70V, L71I, K73M, E75V, K80I
	3m	K73R, G78S, K80N
	2m	M113V, Q123H
	1 variant with frameshift	
	1 variant with stop codon after 52 aa	
	1 sequenced gene still had the template sequence	

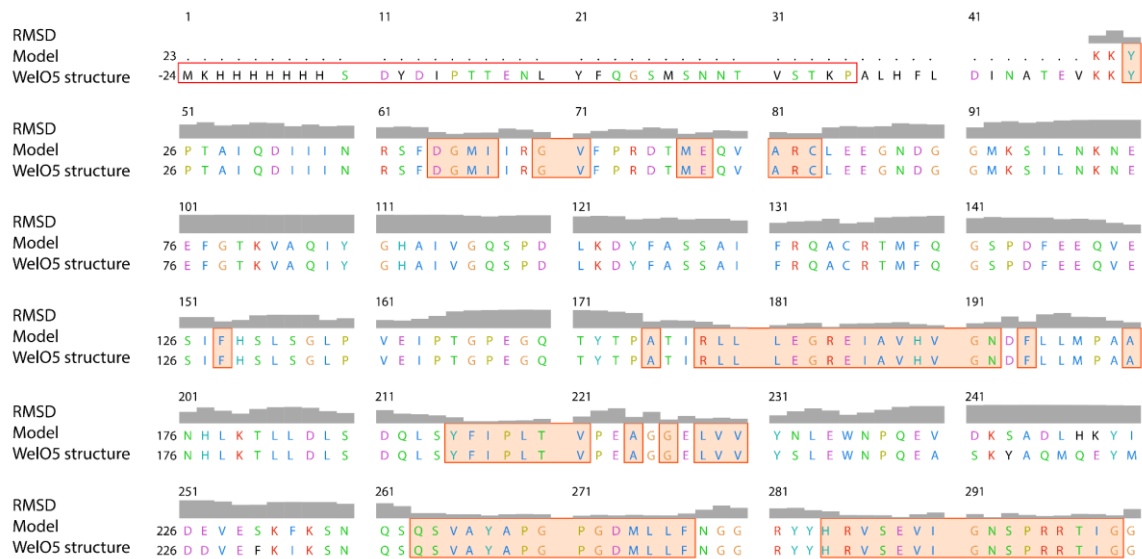


Figure 84. Amino acid sequence alignment of the *Hw*-WelO15 sequence, used to create the model and the sequence of WelO5. Red boxes indicate a low RMSD and highlight the amino acids that were used to calculate the RMSD from 74 pruned atom pairs.

8.4.2 Quick Quality Control after Semi-Rational Mutagenesis

8.4.1.1 1st Generation

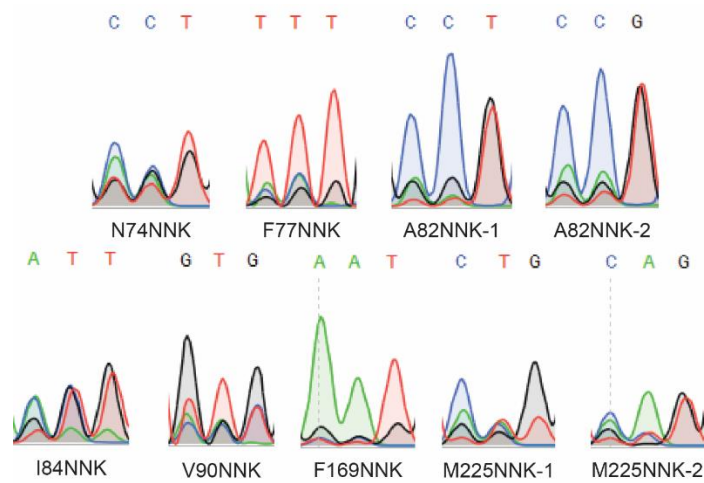


Figure 85. Sequencing chromatogram: Height of the signal correlates with the concentration of the base. Every color represents one base (adenine=green, thymine=red, cytosine=blue, guanine=black). Degeneration of mutated positions from library generation 1.

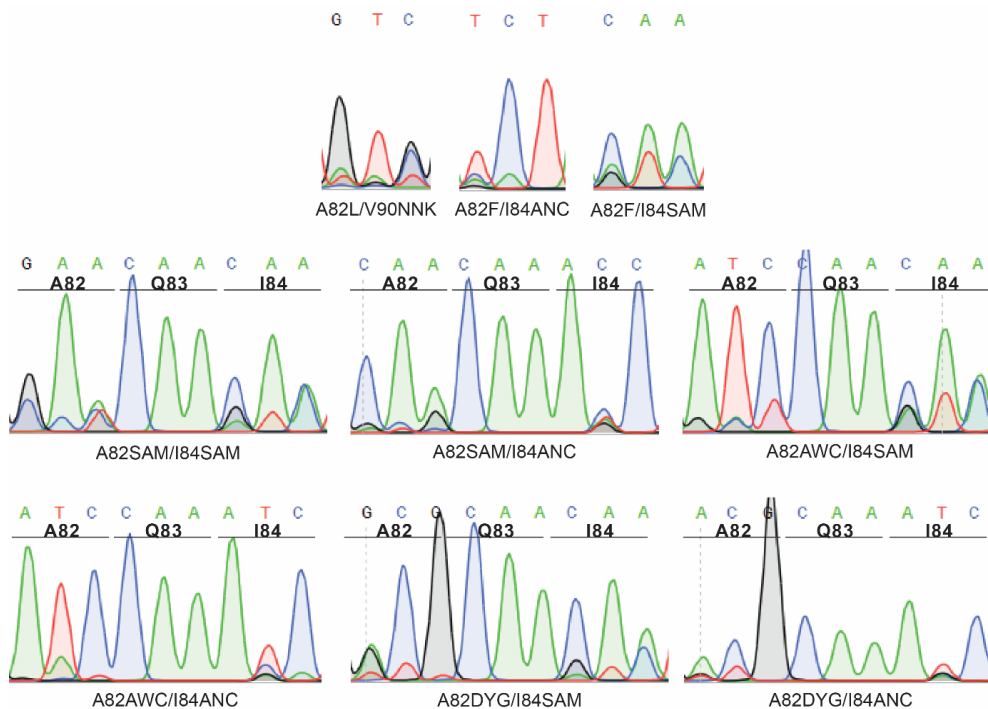


Figure 86. Sequencing chromatogram: Height of the signal correlates with the concentration of the base. Every color represents one base (adenine=green, thymine=red, cytosine=blue, guanine=black). Degeneration of mutated positions from two site libraries in generation 2.

8.4.1.2 2nd Generation

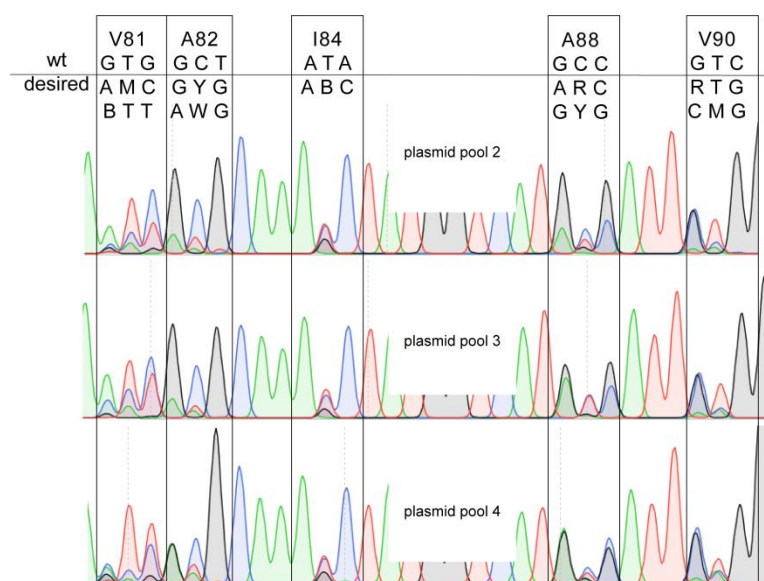


Figure 87. Sequencing chromatogram: Height of the signal correlates with the concentration of the base. Every color represents one base (adenine=green, thymine=red, cytosine=blue, guanine=black). Degeneration of mutated positions from 5-site library in generation 2. The amino acid position is given with the wild-type codon (1st row) and selected DNA codons which should be introduced are shown.

8.4.1.3 4th Generation Library

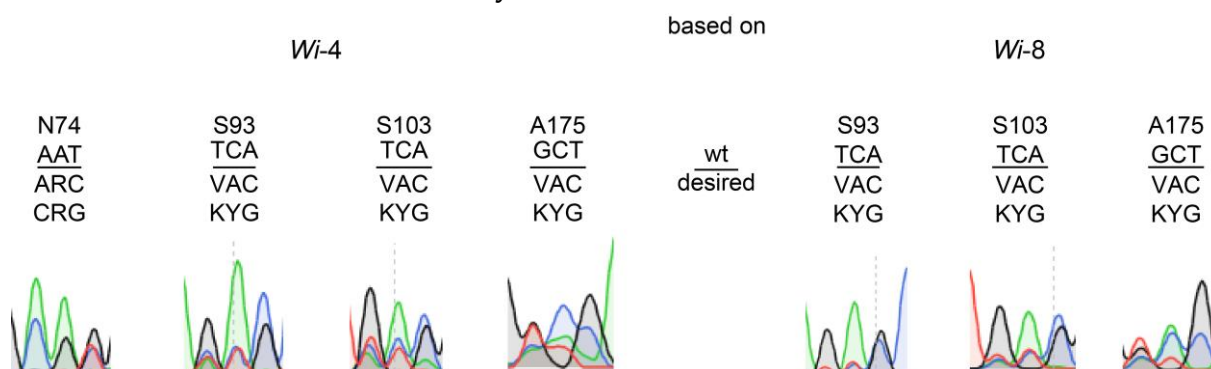


Figure 88. Sequencing chromatogram: Height of the signal correlates with the concentration of the base. Every color represents one base (adenine=green, thymine=red, cytosine=blue, guanine=black). Degeneration of mutated positions from library generation 4. The amino acid position is given with the wild-type codon (1st row) and selected DNA codons which should be introduced are shown.

In table 40, all sequenced variants from the 4th generation library are shown.

Table 40. Found variants in the 4th generation library, sorted by their template DNA. Given letters represent positions S93, S103 and A175. Letters shown in grey are still the wild-type amino acid.

V6I/N74Q/A82L/	V6I/N74R/A82L/	V6I/A82L/V90P/	V6I/N74R/V81T/A82M/
V90P/D284N	V90P/D284N	D284N	A88V/V90P/D284N
SAA	DSA	NSH	DSA
DAH	DSN	DSA	NAS
DSV	AAN	DSN	NSS
LAN	ASV	DSH	VSL
DSL	LSN	DSS	DAA

Appendix

HAS	HSH	HAS	LAA
ASA	HAN	LSN	
		HSH	
		SSN	
		SSS	

Appendix

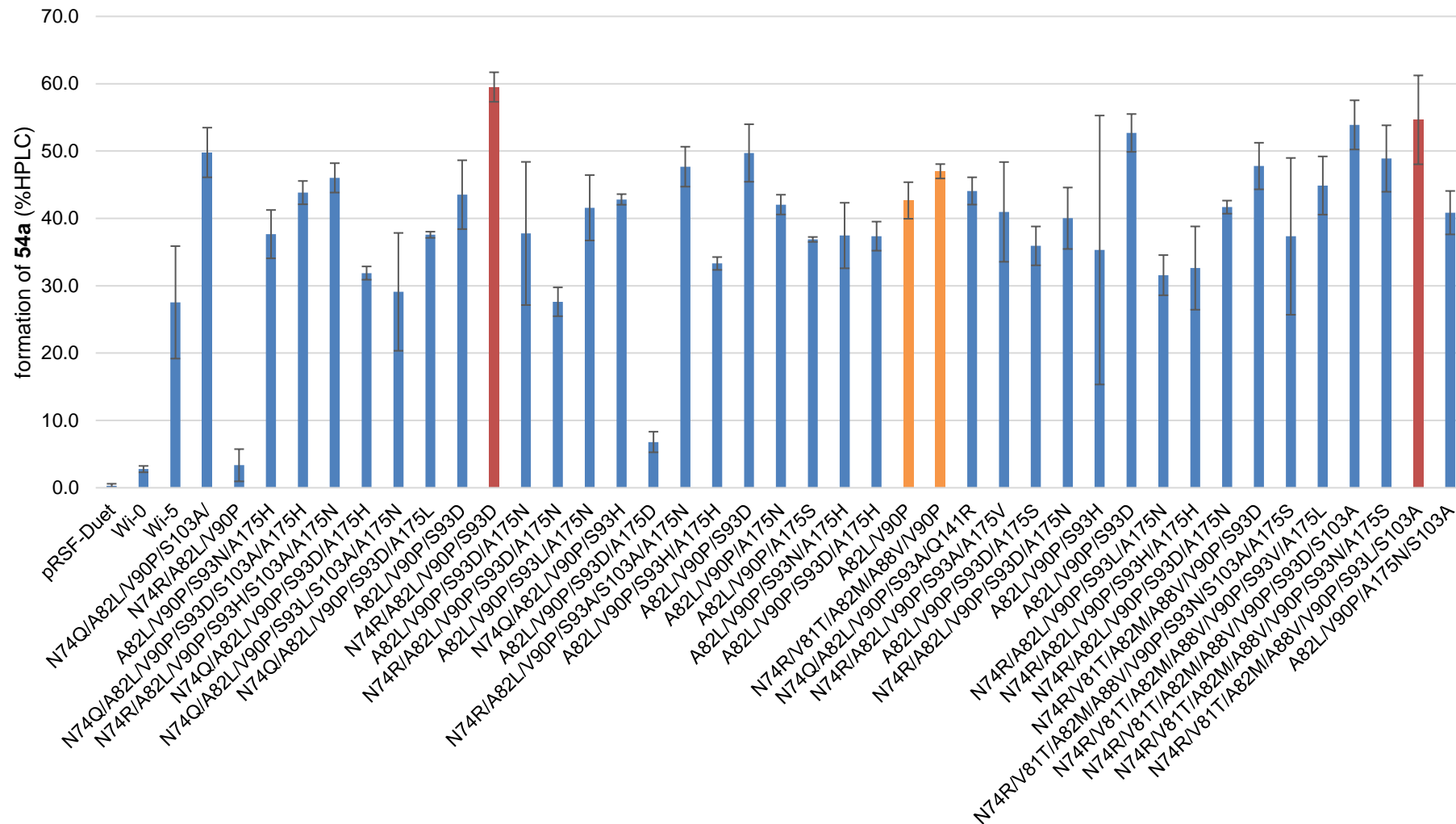


Figure 89. Triplicate measurement of found hits from library generation 4. All variants are based on Wi-0.

8.5 Biotransformation

8.5.1 SDS-PAGE Analysis of Whole Cells

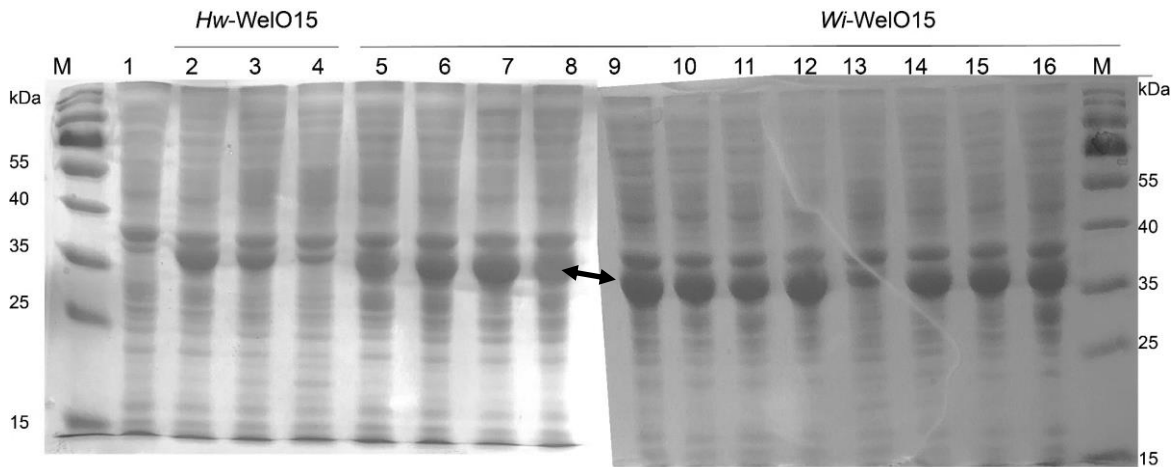


Figure 90. SDS-PAGE analysis of OD₆₀₀ normalized *E. coli* BL21-Gold(DE3) cells induced with IPTG. The cell pellet was suspended in water and mixed with SDS-PAGE sample buffer. After heating for 10 min at 95 °C, insoluble components were removed by centrifugation and supernatant was applied to a gel (12% separation gel, 5% stacking gel). 1) pRSF-Duet 2) *Hw*-WeiO15 3) *Hw*-1 4) *Hw*-2 5) *Wi*-0 6) *Wi*-3 7) *Wi*-2 8) *Wi*-1 9) *Wi*-7 10) *Wi*-8 11) *Wi*-5 12) *Wi*-6 13) *Wi*-9 14) *Wi*-10 15) *Wi*-13 16) *Wi*-4

8.5.2 SDS-PAGE Analysis of OD₆₀₀ normalized Cell Lysate

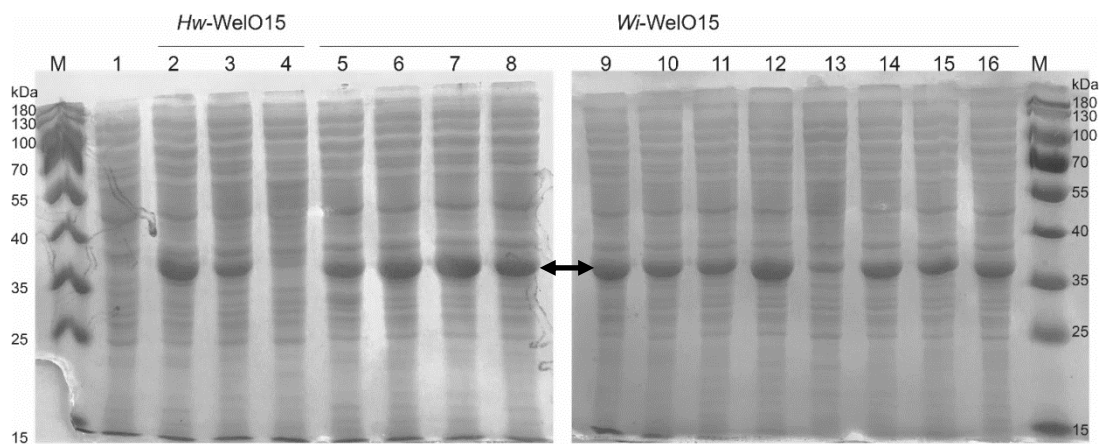


Figure 91. SDS-PAGE analysis of OD₆₀₀ normalized *E. coli* BL21-Gold(DE3) cells induced with IPTG after lysis with lysozyme. After removing insoluble cell debris, the cleared lysate was with SDS-PAGE sample buffer. After heating for 10 min at 95 °C, the sample was centrifuged for 10 min at 14000 rpm and the supernatant applied to a gel (12% separation gel, 5% stacking gel). 1) pRSF-Duet 2) *Hw*-WeiO15 3) *Hw*-1 4) *Hw*-2 5) *Wi*-0 6) *Wi*-3 7) *Wi*-2 8) *Wi*-1 9) *Wi*-7 10) *Wi*-8 11) *Wi*-5 12) *Wi*-6 13) *Wi*-9 14) *Wi*-10 15) *Wi*-13 16) *Wi*-4

SDS-PAGE analysis shows that in assays with lysate approximately the same amount of catalyst is present as with purified enzymes. In both gels (figure 91 and figure 92), the thickness of the bands is comparable. The following calculation shows how the concentration was calculated.

- 1) lysate: Cell pellet was suspended in 100 μ L lysis buffer, lysed and centrifuged to remove insoluble cell debris. 50 μ L of the supernatant was mixed with 17.5 μ L 4x SDS-

Appendix

PAGE sample buffer. 6 μL of the mix was applied to the gel, resulting in 4.4% of the total enzyme amount within one reaction.

- 2) Purified enzyme: 100 μL of 20 μM enzyme was prepared (total enzyme amount of assay, which is performed with 200 μL but 10 μM) and mixed with 33 μL 4x SDS-PAGE sample buffer. 6 μL of this solution was applied to the gel, resulting in 4.5% of the total enzyme amount.

8.5.3 SDS-PAGE Analysis of Purified Enzymes

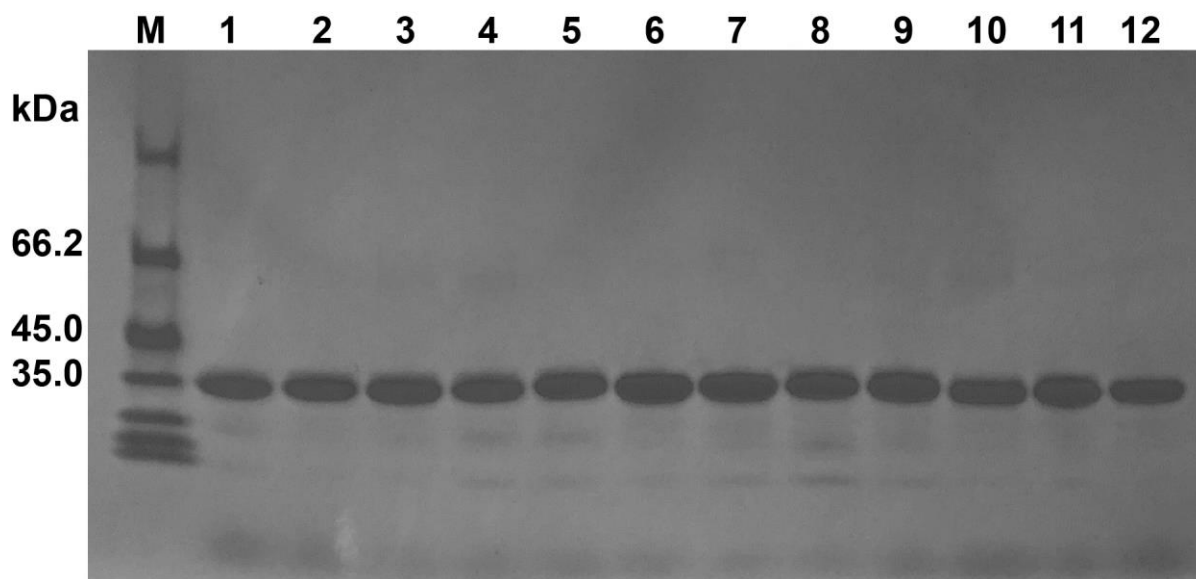


Figure 92. The SDS-PAGE analysis shows purified halogenase variants. Enzyme stock solutions were diluted to 20 μM before starting assays. 3.1 μg enzyme was applied to the gel, which represents 4.5% of the enzyme present in the assay (gradient gel 4-15% BioRad). M=Marker, 1) *Wi-0* 2) *Wi-2* 3) *Wi-1* 4) *Wi-5* 5) *Wi-12* 6) *Wi-9* 7) *Wi-10* 8) *Wi-7* 9) *Wi-8* 10) *Wi-11* 11) *Wi-4* 12) *Hw-WelO15*.

8.5.4 HPLC Chromatograms of Biotransformation

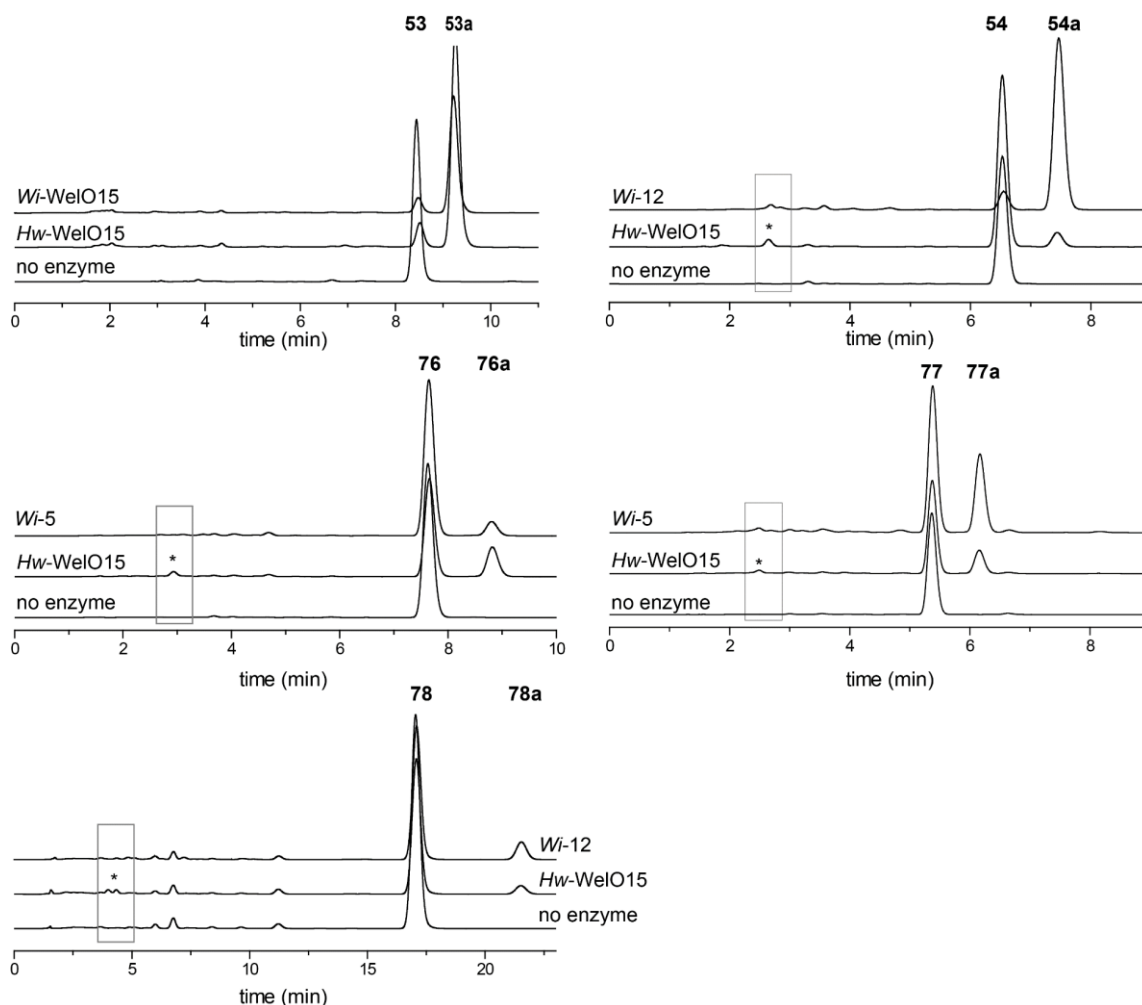


Figure 93. HPLC chromatograms of hapalindole-like ketones in 200 μ L scale and purified enzymes.

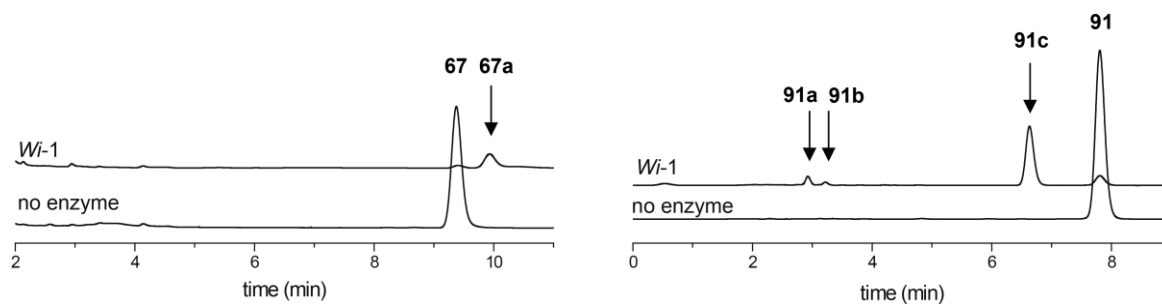


Figure 94. HPLC chromatograms of biotransformation with *Wi-1* and **67** or **91** in 200 μ L scale and purified enzymes.

Appendix

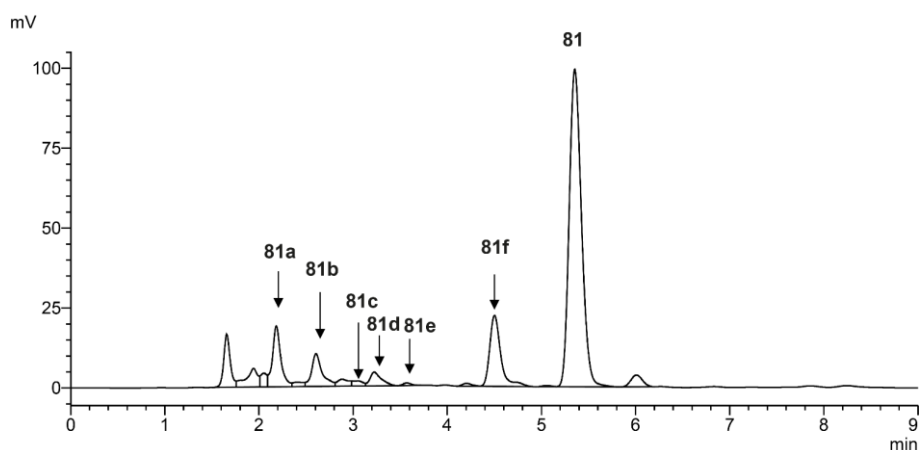


Figure 95. HPLC chromatograms of biotransformation with cell lysate containing *Wi-12* and **81** in 50 mL scale.

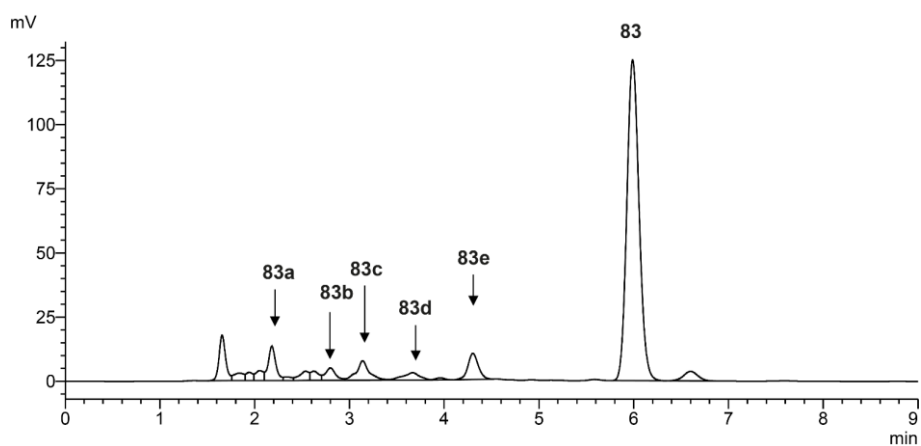


Figure 96. HPLC chromatograms of biotransformation with cell lysate containing *Wi-12* and **83** in 50 mL scale.

T_R (**79a**) = 2.5 min with $[M+H]^+$ m/z = 328

T_R (**80a**) = 2.8 min with $[M+H]^+$ m/z = 266

T_R (**79b**) = 2.7 min with $[M+H]^+$ m/z = 328

T_R (**80b**) = 7.4 min with $[M+H]^+$ m/z = 268

T_R (**79c**) = 3.1 min with $[M+H]^+$ m/z = 266

T_R (**80c**) = 7.9 min with $[M+H]^+$ m/z = 346

T_R (**79d**) = 6.1 min with $[M+H]^+$ m/z = 266

T_R (**79e**) = 7.4 min with $[M+H]^+$ m/z = 310

T_R (**79f**) = 8.0 min with $[M+H]^+$ m/z = 266

Retention times and masses of products **81a-81d**, **82a** and **82b** as well as **83a-83e** are further described in chapter 7.3.1.8 - 7.3.1.10.

Appendix

8.5.5 Selectivities of Hapalindole-like Ketones

Table 41. Overview of selectivities and conversion of variants transforming **79** and **80**. Final reaction conditions: 200 μ L volume in 2.2 mL 96 dw-plates, 50 mM HEPES, 100 mM NaCl, 5 mM α KG, 2.5 mM ascorbic acid, 0.5 mM $(\text{NH}_4)_2\text{Fe}(\text{SO}_4)_2$, 0.5 mM substrate, 8 h reaction time, 30 $^\circ\text{C}$, 200 rpm (Infors HT shaker). Area of starting material and new produced products (new peak in HPLC in comparison to control reaction without halogenase) were included. If relative conversion was below 5% no selectivity was determined.

	79							80			
	conv. (%HPLC)	sel. 79a	sel. 79b	sel. 79c	sel. 79d	sel. 79e	sel. 79f	conv. (%HPLC)	sel. 80a	sel. 80b	sel. 80c
<i>Wi-0</i>	3	nd	nd	nd	nd	nd	nd	1	nd	nd	nd
<i>Wi-2</i>	28	5	3	55	23	8	5	11	24	3	73
<i>Wi-1</i>	50	3	74	2	17	4	0	9	34	4	62
<i>Wi-4</i>	11	<1	24	66	5	2	2	2	nd	nd	nd
<i>Wi-5</i>	45	3	2	83	9	2	1	8	41	4	55
<i>Wi-7</i>	6	4	12	36	4	31	13	1	nd	nd	nd
<i>Wi-8</i>	12	<1	7	45	10	36	2	1	nd	nd	nd
<i>Wi-11</i>	10	<1	13	49	8	28	2	1	nd	nd	nd
<i>Wi-12</i>	45	3	2	77	14	3	0	11	36	3	61
<i>Wi-9</i>	6	1	18	38	27	14	1	1	nd	nd	nd
<i>Wi-10</i>	31	4	4	77	10	3	2	2	nd	nd	nd
<i>Hw-WelO15</i>	59	3	1	59	37	0	1	6	22	0	78

Table 42. Overview of selectivities and conversion of variants transforming **81** and **82**. Final reaction conditions: 200 μ L volume in 2.2 mL 96 dw-plates, 50 mM HEPES, 100 mM NaCl, 5 mM α KG, 2.5 mM ascorbic acid, 0.5 mM $(\text{NH}_4)_2\text{Fe}(\text{SO}_4)_2$, 0.5 mM substrate, 8 h reaction time, 30 $^\circ\text{C}$, 200 rpm (Infors HT shaker). Area of starting material and new produced products (new peak in HPLC in comparison to control reaction without halogenase) were included. If relative conversion was below 5% no selectivity was determined.

	81					82			83					
	conv. %HPLC	sel. 81a	sel. 81b	sel. 81c	sel. 81d	conv. %HPLC	sel. 82a	sel. 82b	conv. %HPLC	sel. 83a	sel. 83b	sel. 83c	sel. 83d	sel. 83e
<i>Wi-0</i>	7	8	23	20	49	14	46	54	26	3	20	19	0	55
<i>Wi-2</i>	2	nd	nd	nd	nd	15	51	49	17	5	15	30	0	46
<i>Wi-1</i>	3	nd	nd	nd	nd	27	31	69	6	13	23	18	6	34
<i>Wi-4</i>	<1	nd	nd	nd	nd	3	nd	nd	1	nd	nd	nd	nd	nd
<i>Wi-5</i>	10	21	8	22	49	31	28	72	15	9	30	28	0	29
<i>Wi-12</i>	31	19	7	29	46	40	29	71	38	14	32	11	10	28
<i>Wi-7</i>	3	nd	nd	nd	nd	12	23	77	11	5	31	35	0	24
<i>Wi-8</i>	3	nd	nd	nd	nd	15	21	79	26	12	39	27	0	20
<i>Wi-11</i>	7	12	13	19	57	14	20	80	30	12	36	27	0	21
<i>Wi-9</i>	3	nd	nd	nd	nd	18	50	50	6	6	16	28	0	41
<i>Wi-10</i>	4	nd	nd	nd	nd	29	30	70	9	5	30	29	0	31
<i>Hw-WelO15</i>	20	8	45	33	13	10	41	59	16	8	14	9	8	57

8.5.6 Hydroxylation with P450_{BM3}

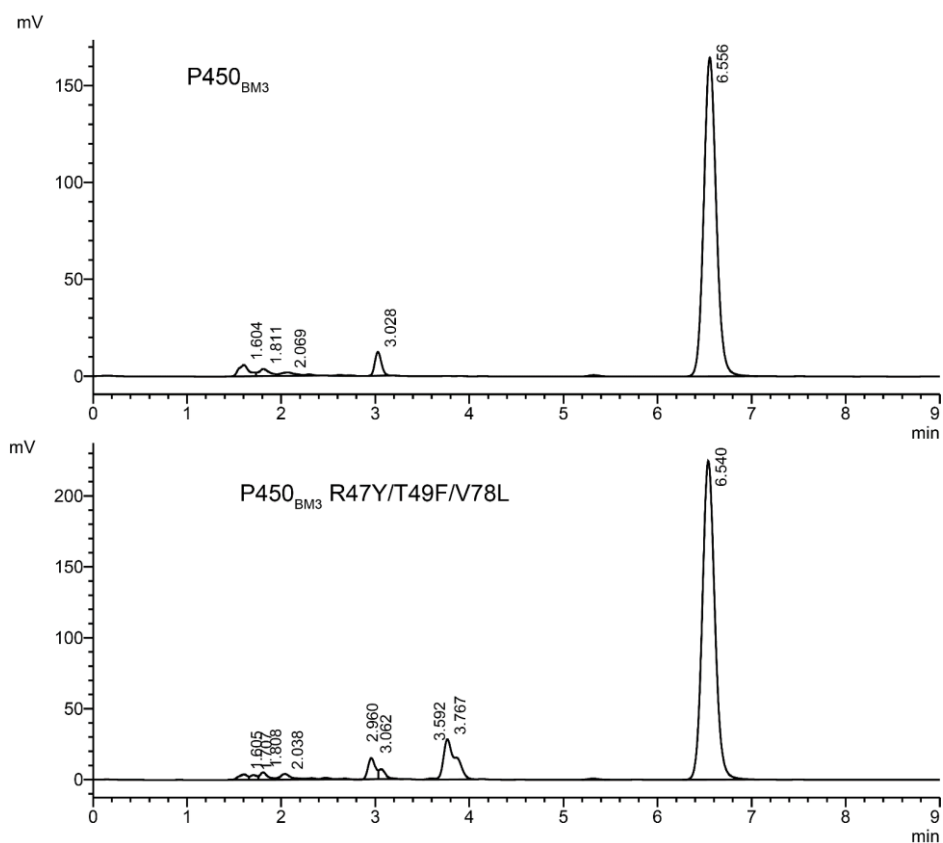


Figure 97. HPLC chromatograms of P450_{BM3} with ketone 54.

Quick Quality Control of P450_{BM3} Library

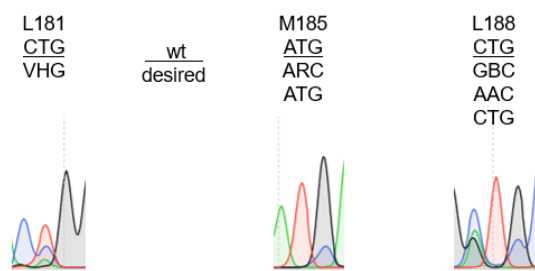


Figure 98. Quick quality control of P450_{BM3} library.

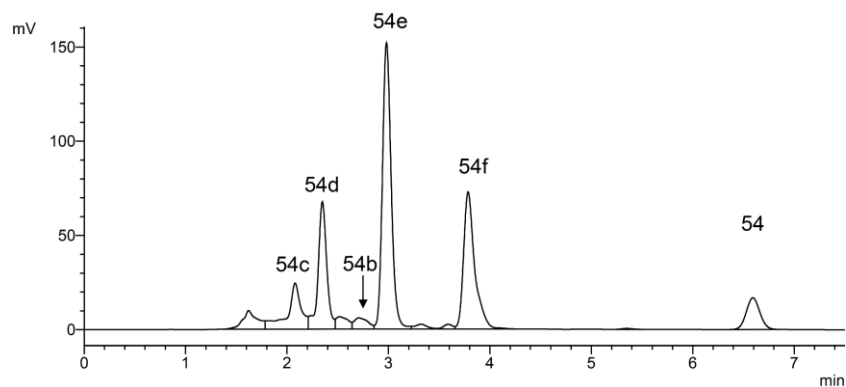


Figure 99. HPLC chromatogram of biotransformation with P450_{BM3} variant. New arising peaks are assigned to products which have to be characterized in the next steps.

8.5.7 Kinetics

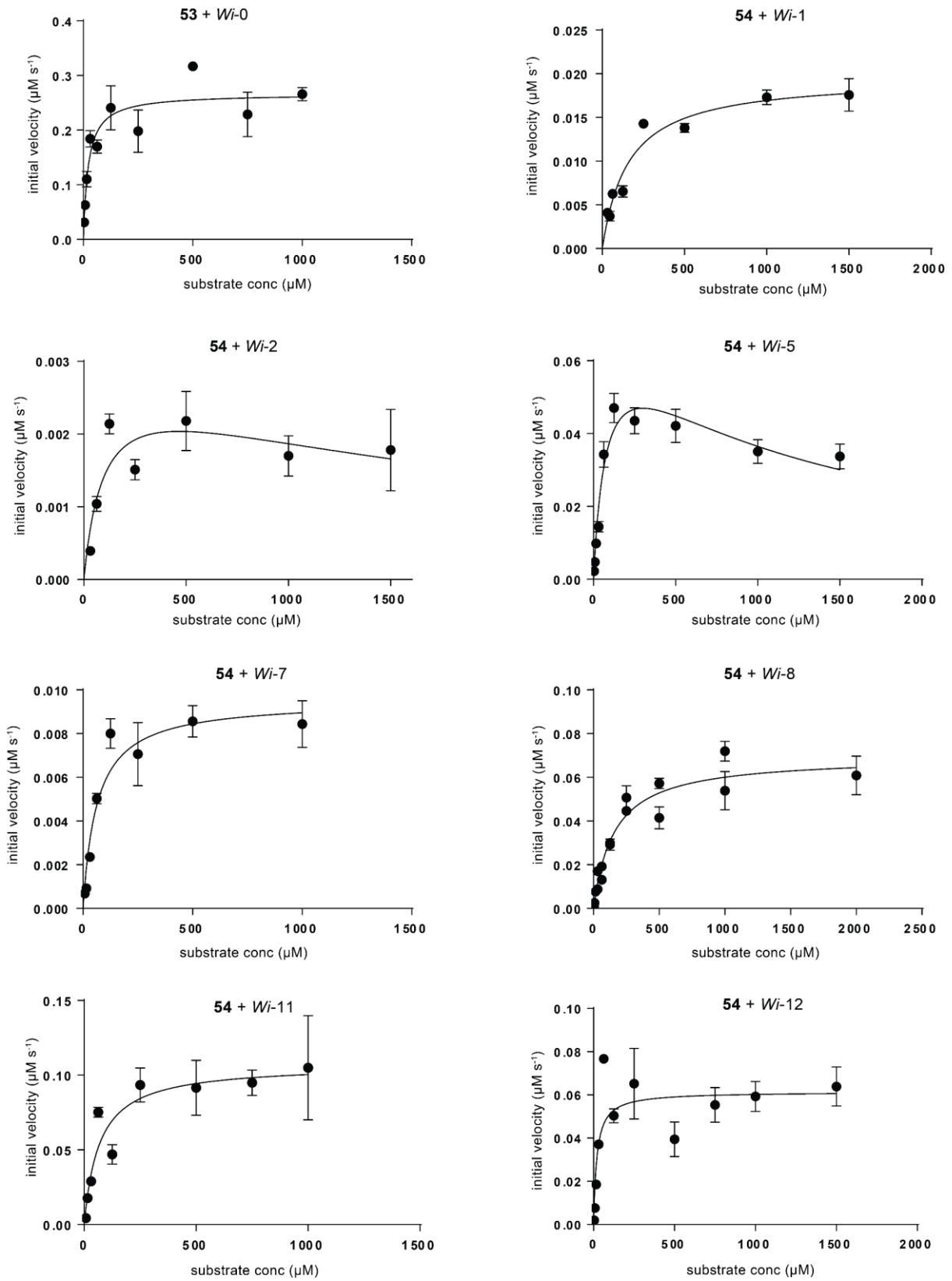


Figure 100. Kinetic assays of *Wi-0* and *53* and *Wi-WelO15* variants and *54*.

Appendix

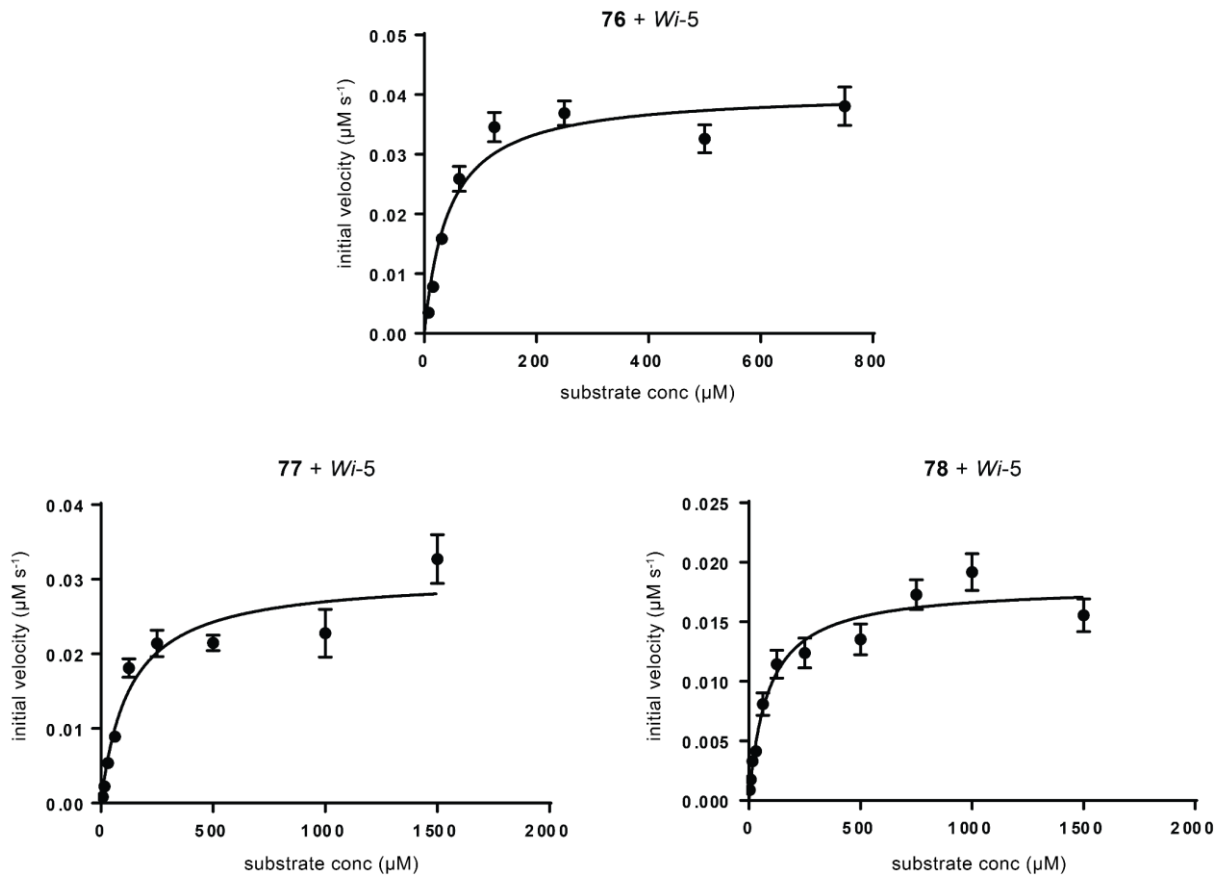


Figure 101. Kinetic assays of *Wi-5* and 76, 77, and 78.

8.6 Analytic of Compound Characterization

8.6.1 NMR and HPLC/GC Chromatograms of Compounds 53-87

8.6.1.1 Analytic of 53 and 67

Synthesis was performed by L. Schmermund within his Master Thesis^[317]

53 Minor diastereomer: $R_f = 0.73$ (pentane:EtOAc 4:1); $^1\text{H-NMR}$ (500 MHz, CDCl_3), $\delta = 8.09$ (s, 1H, NH), 7.46 (d, 1H, $J = 8.15$ Hz, H_4), 7.37 (td, 1H, $J = 8.10, 0.85$ Hz, H_7), 7.21-7.18 (m, 2H, H_6, H_2), 7.14-7.11 (m, 1H, H_5), 4.81-4.80 (m, 1H, $\text{H}_{17/\text{cis}}$), 4.66-4.65 (m, 1H, $\text{H}_{17/\text{trans}}$), 3.61-3.60 (m, 1H, H_{11}), 3.54-3.50 (m, 1H, H_{10}), 2.84 (dt, 1H, $J = 11.9, 4.30$ Hz, H_{15}), 1.89-1.82 (m, 1H, H_{14}), 1.80-1.72 (m, 1H, H_{13}), 1.71-1.66 (m, 2H, H_{13}), 1.53-1.52 (m, 3H, H_{18}), 1.46-1.42 (m, 1H, H_{14}), 1.28 (s, 3H, H_{19}), 1.15 (s, 3H, H_{20}) ppm; $^{13}\text{C-NMR}$ (125 MHz, CDCl_3), $\delta = 156.4$ (NC), 147.7 (C_{16}), 135.8 (C_8), 126.8 (C_9), 123.7 (C_2), 122.0 (C_5), 119.5 (C_6), 117.3 (C_4), 114.0 (C_3), 112.3 (C_{17}), 111.6 (C_7), 67.5 (C_{11}), 43.6 (C_{15}), 35.4 (C_{10}), 34.2 (C_{12}), 32.8 (C_{14}), 29.6 (C_{20}), 28.6 (C_{13}), 24.0 (C_{19}), 19.0 (C_{18}) ppm;

HRMS (ESI⁺): $\text{C}_{20}\text{H}_{24}\text{N}_2\text{Na}^+$ [$\text{M}+\text{Na}$]⁺, m/z found: 315.1835; calc.: 315.1832.

Optical rotation (in CHCl_3 , 22 °C, $\lambda = 589$ nm, cuvette 50 mm, 0.43 g/100mL) 38.742

67 Major diastereomer: $R_f = 0.61$ (pentane:EtOAc 4:1); $^1\text{H-NMR}$ (500 MHz, CDCl_3), $\delta = 8.12$ (s, 1H, NH), 7.50 (d, 1H, $J = 8.16$ Hz, H_4), 7.40 (d, 1H, $J = 8.10$, H_7), 7.24-7.21 (m, 2H, H_6, H_2), 7.17-7.14 (m, 1H, H_5), 4.84-4.83 (m, 1H, $\text{H}_{17/\text{cis}}$), 4.69-4.68 (m, 1H, $\text{H}_{17/\text{trans}}$), 3.63-3.63 (m, 1H, H_{11}), 3.57-3.55 (m, 1H, H_{10}), 2.86 (dt, 1H, $J = 11.9, 4.36$ Hz, H_{15}), 1.91-1.78 (m, 1H, H_{14}), 1.77-1.70 (m, 2H, H_{13}), 1.55-1.54 (m, 3H, H_{18}), 1.49-1.45 (m, 1H, H_{14}), 1.30 (s, 3H, H_{19}), 1.17 (s, 3H, H_{20}) ppm; $^{13}\text{C-NMR}$ (125 MHz, CDCl_3), $\delta = 156.5$ (NC), 147.8 (C_{16}), 135.9 (C_8), 126.9 (C_9), 123.8 (C_2), 122.2 (C_5), 119.6 (C_6), 117.4 (C_4), 114.2 (C_3), 112.4 (C_{17}), 111.7 (C_7), 67.5 (C_{11}), 43.7 (C_{15}), 35.5 (C_{10}), 34.4 (C_{12}), 32.9 (C_{14}), 29.8 (C_{20}), 28.7 (C_{13}), 24.1 (C_{19}), 19.1 (C_{18}) ppm;

HRMS (ESI⁺): $\text{C}_{20}\text{H}_{24}\text{N}_2\text{Na}^+$ [$\text{M}+\text{Na}$]⁺, m/z found: 315.1833; calc.: 315.1832.

Optical rotation (in CHCl_3 , 22 °C, $\lambda = 589$ nm, cuvette 50 mm, 0.46 g/100mL) 78.336.

Appendix

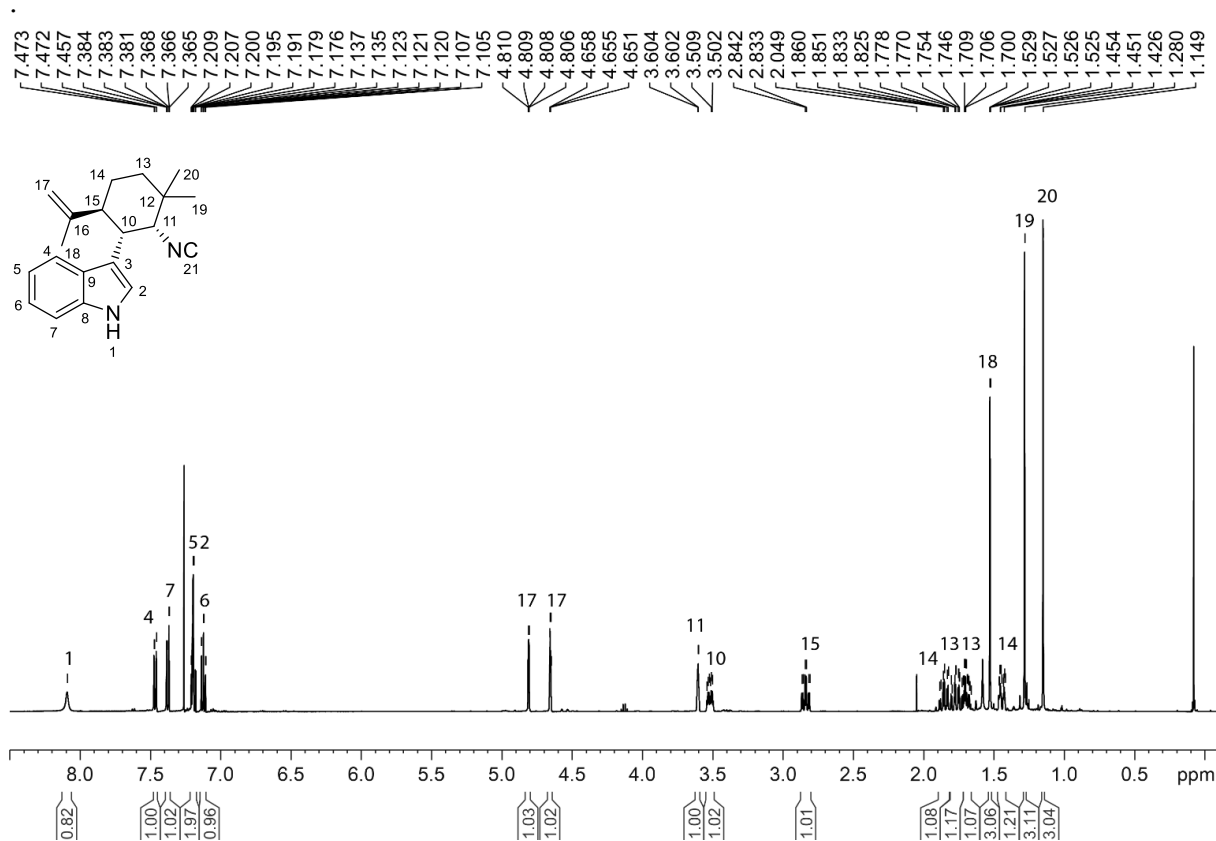


Figure 102. ¹H-NMR of 53 measured in CDCl₃.

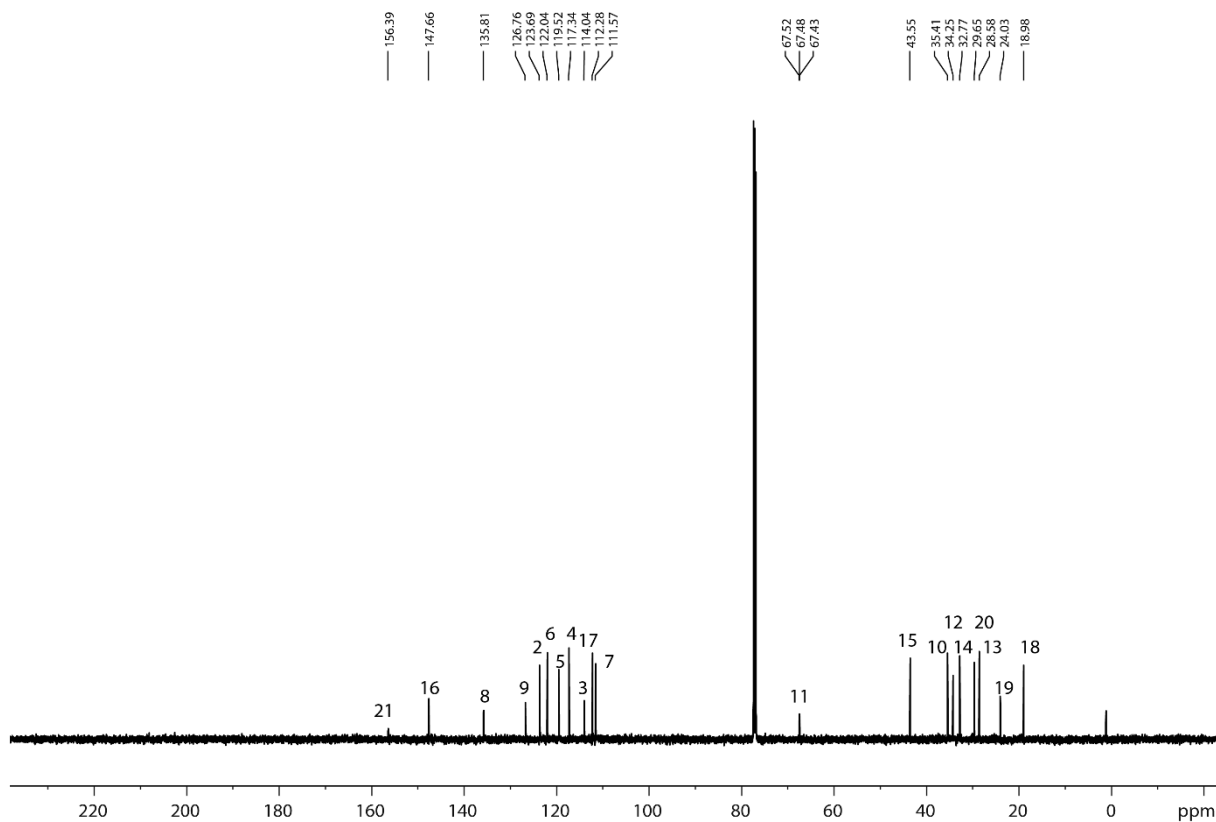


Figure 103. ¹³C-NMR of 53 measured in CDCl₃.

Appendix

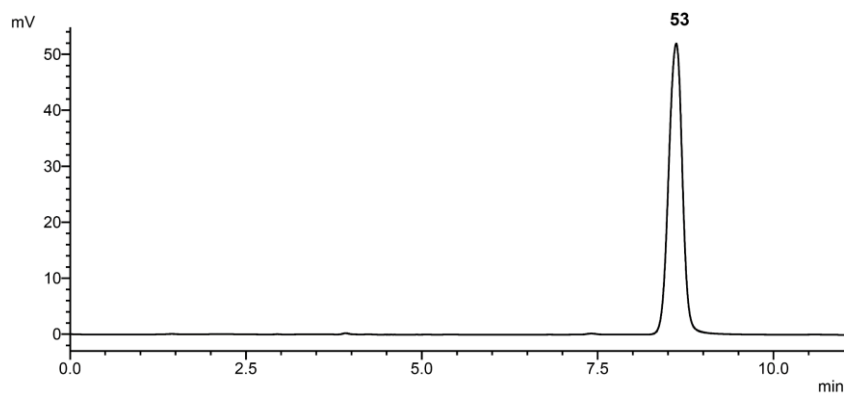


Figure 104. HPLC chromatogram of **53**. The sample was measured on Agela Durashell C-18 column (150 mm x 4.6 mm, 5 μ m particle size + 10 mm precolumn). The analysis was performed with 1 mL/min and an isocratic flow 73 : 27 ACN-H₂O for 11 min. The retention time is 8.41 min.

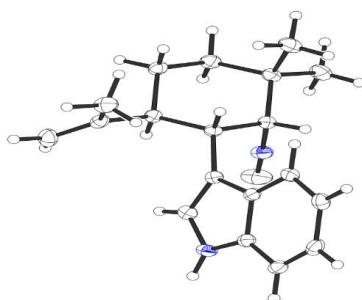


Figure 105. Crystal structure of isonitrile **53** with the (*R*)-configuration of the isonitrile group. The nitrogen atoms are shown in blue, the carbon atoms as large white spheres with black stripes and the hydrogen atoms as small white spheres. Crystals were obtained, storing a 50 mM solution of **53** in EtOH at -20°C. CCDC 1839577

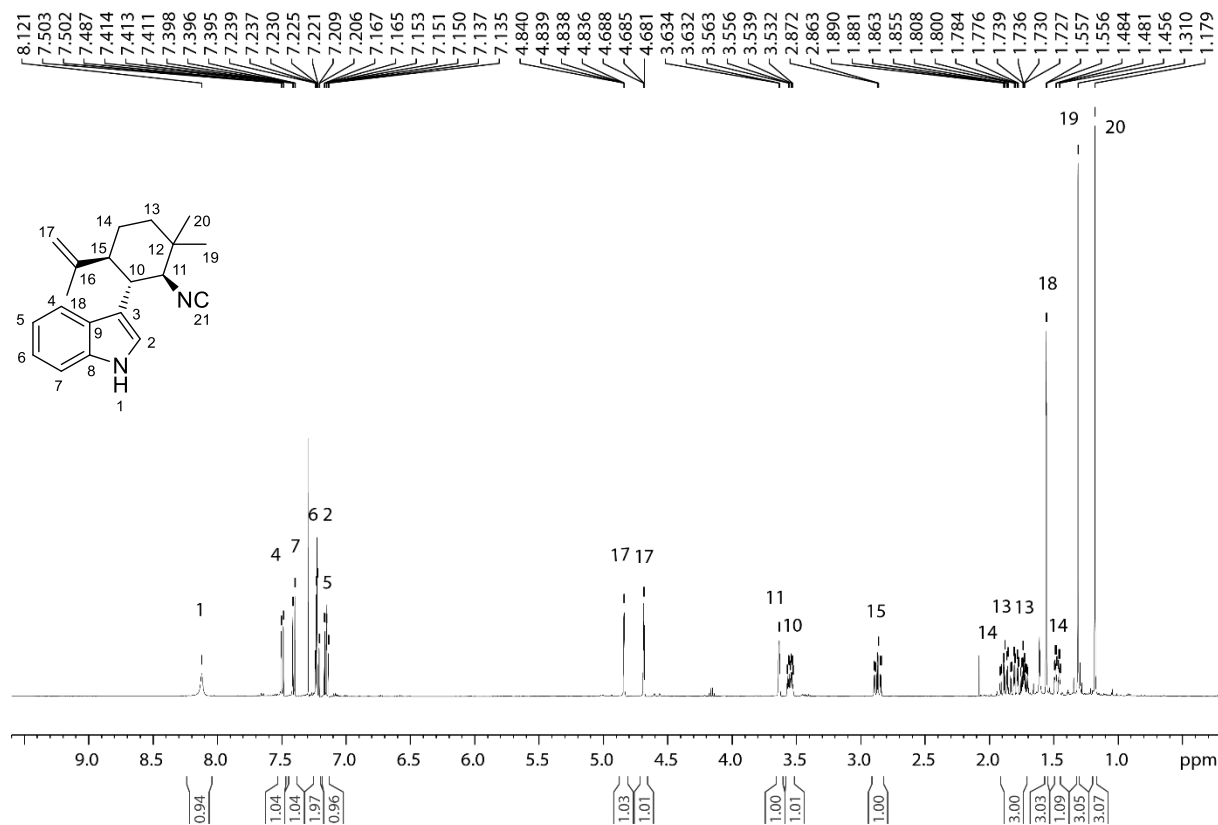


Figure 106. ¹H-NMR of isonitrile **67** measured in CDCl₃.

Appendix

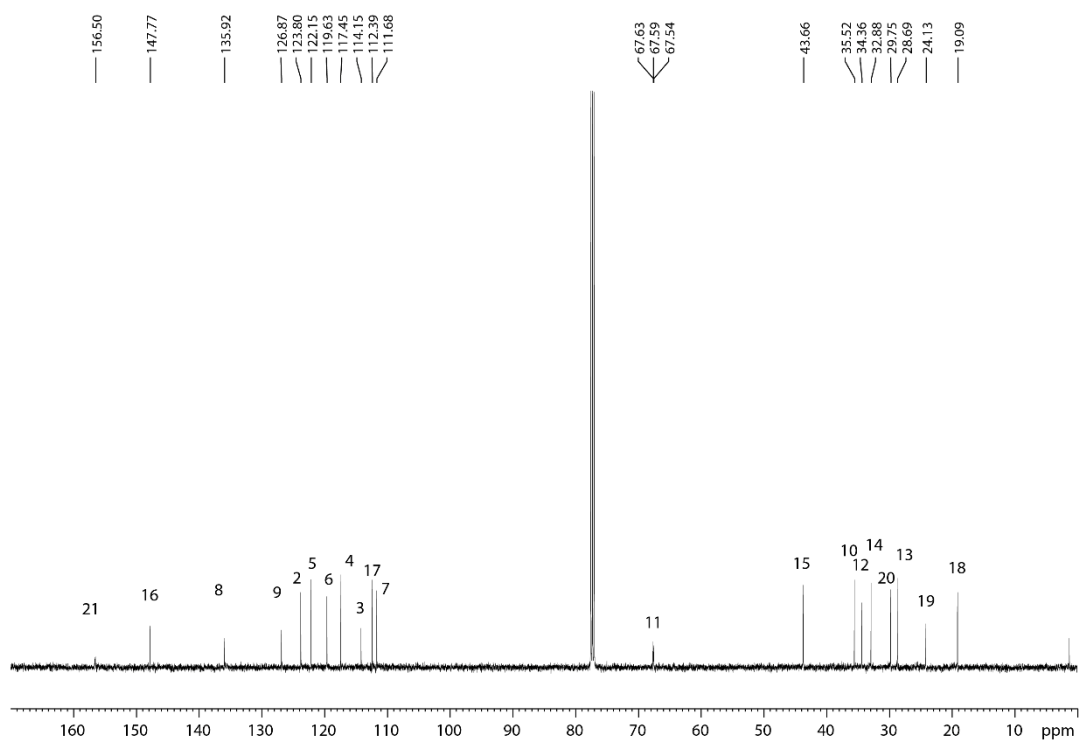


Figure 107. ^{13}C -NMR of isonitrile **67** measured in CDCl_3 .

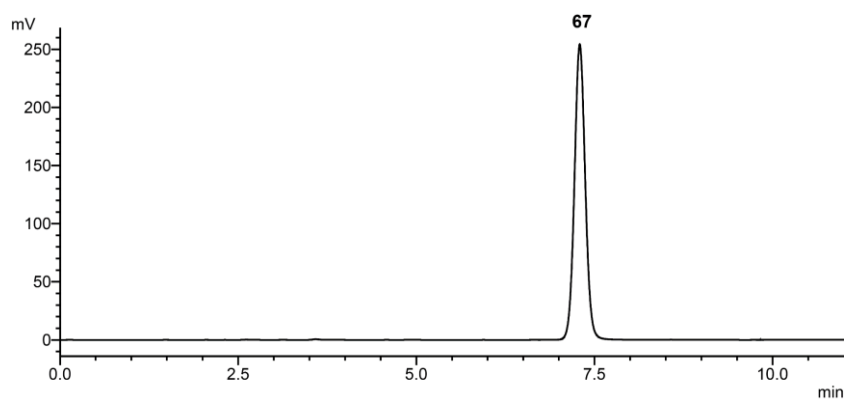
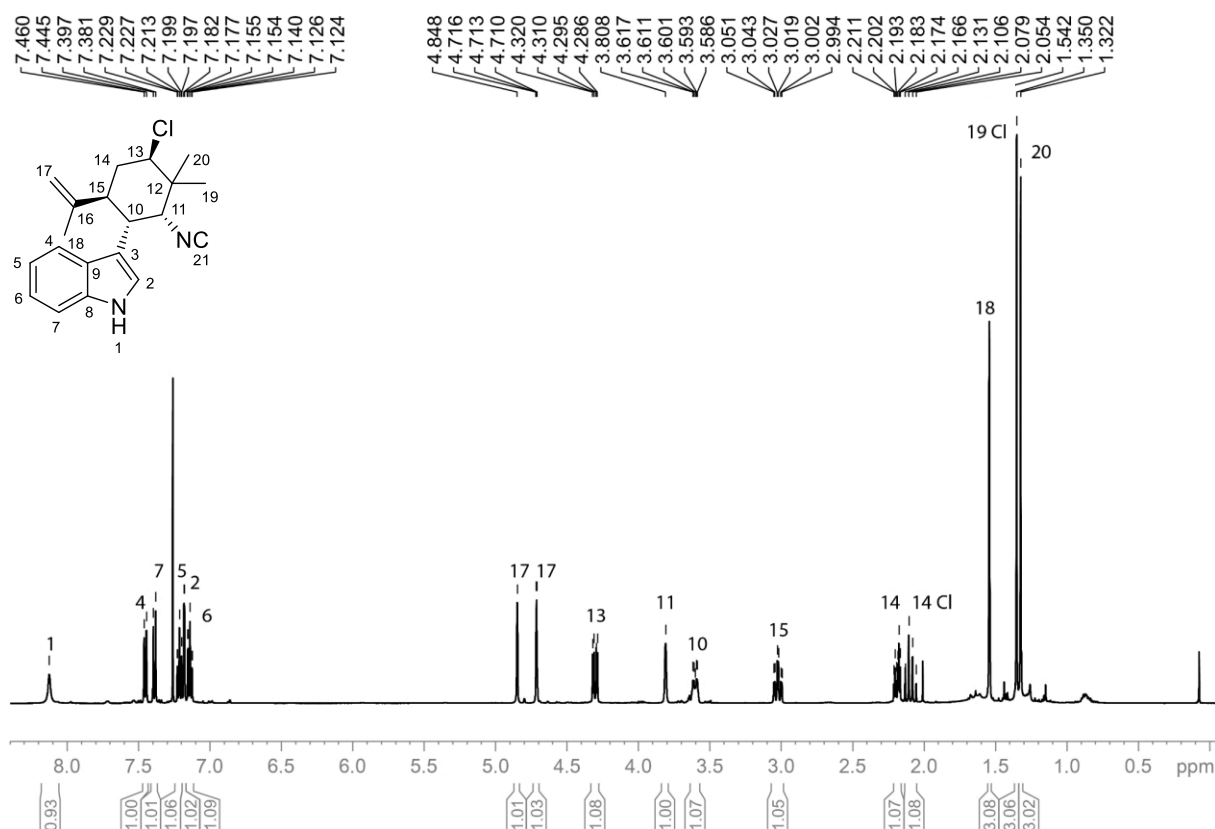
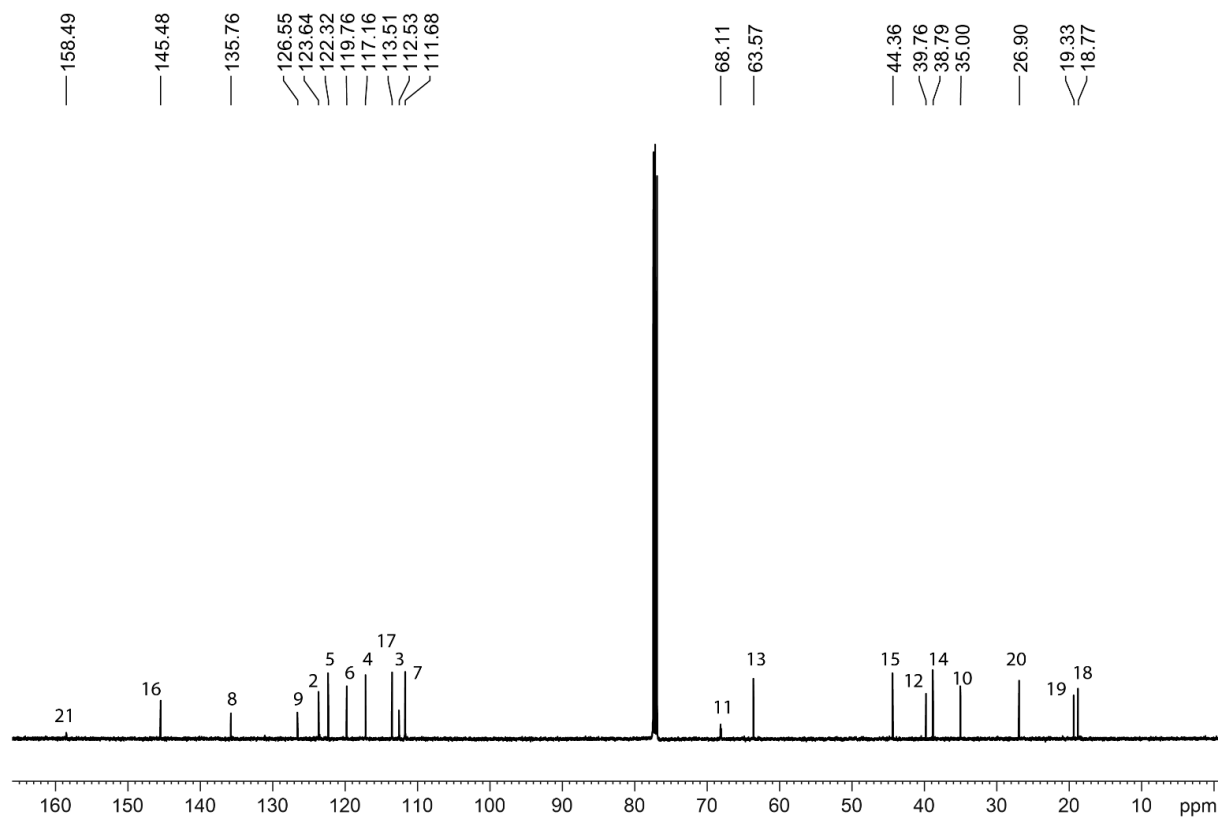


Figure 108. HPLC chromatogram of **67**. The sample was measured on Agela Durashell C-18 column (150 mm \times 4.6 mm, 5 μm particle size + 10 mm precolumn). The analysis was performed with 1 mL/min and an isocratic flow 73 : 27 ACN- H_2O for 11 min. The retention time is 7.29 min.

8.6.1.2 Analytic of 53a

Figure 109. ¹H-NMR of 53a measured in CDCl₃.Figure 110. ¹³C-NMR of 53a measured in CDCl₃.

Appendix

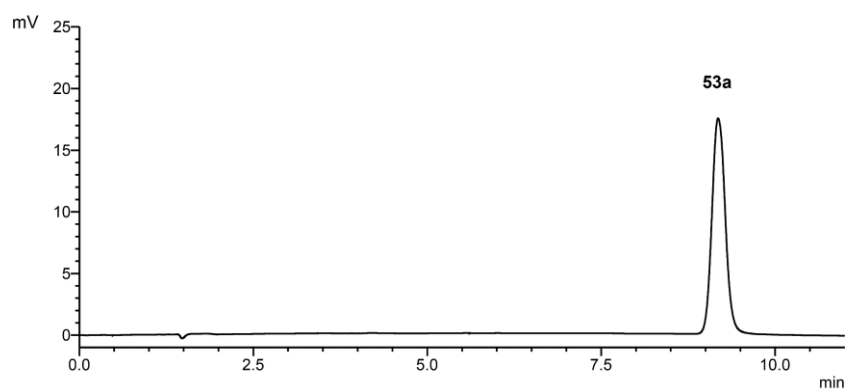


Figure 111. HPLC chromatogram of **53a**. The sample was measured on Agela Durashell C-18 column (150 mm × 4.6 mm, 5 μm particle size + 10 mm precolumn). The analysis was performed with 1 mL/min and an isocratic flow 73 : 27 ACN-H₂O for 11 min. The retention time is 9.18 min.

8.6.1.3 Analytic of 54

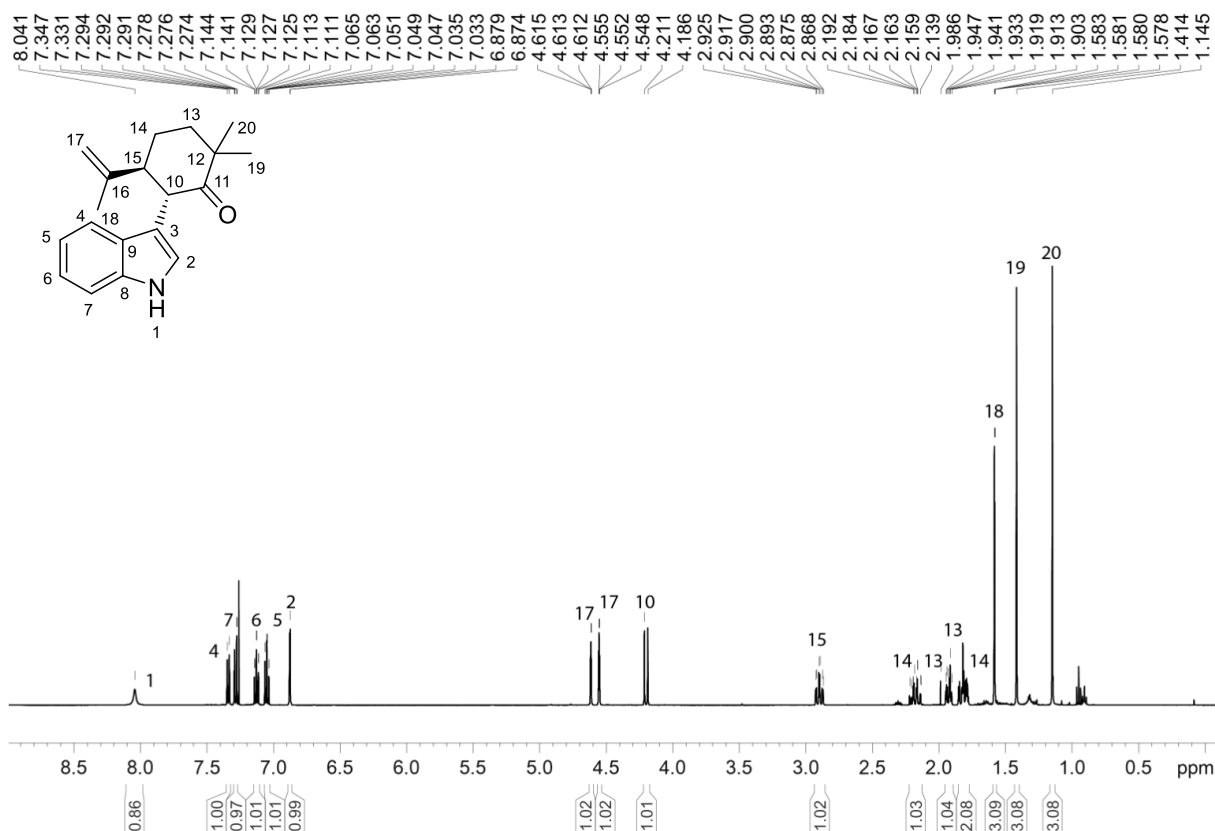


Figure 112. ¹H-NMR of **54** measured in CDCl₃.

Appendix

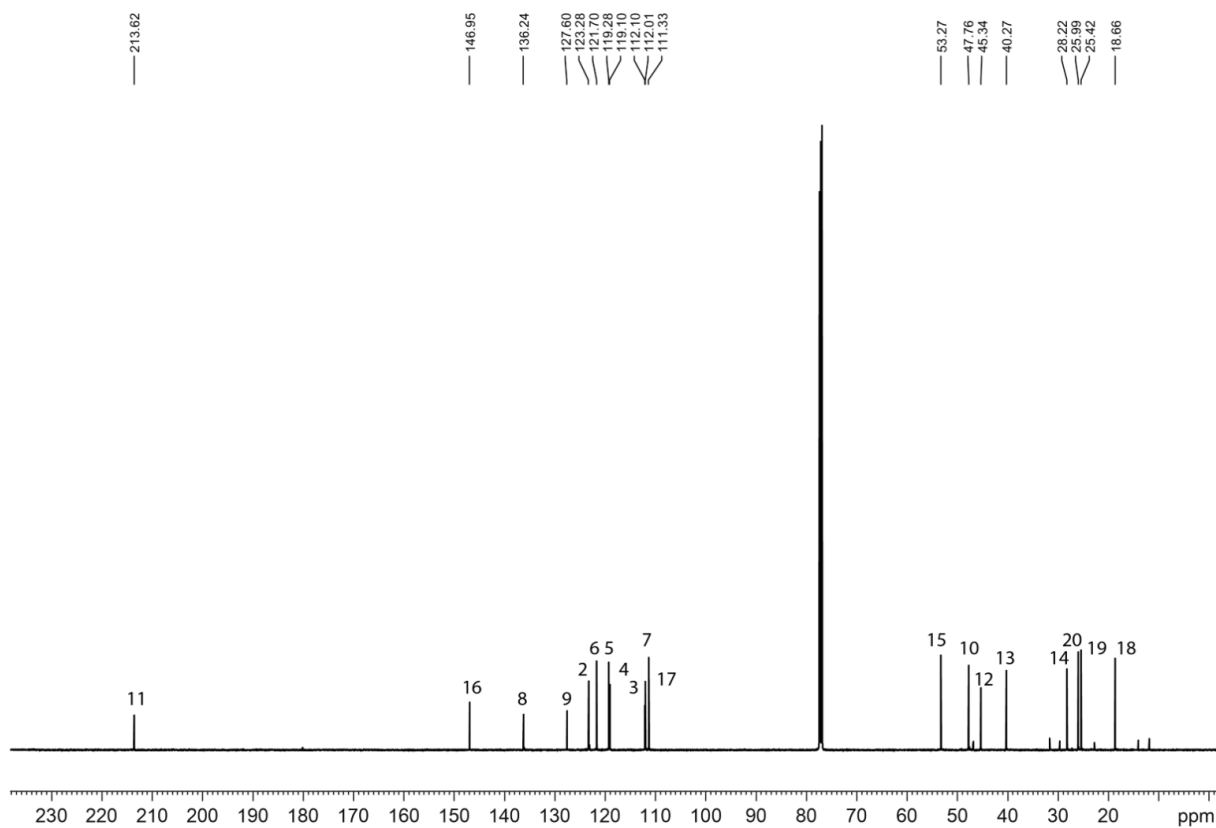


Figure 113. ^{13}C -NMR of **54** measured in CDCl_3 .

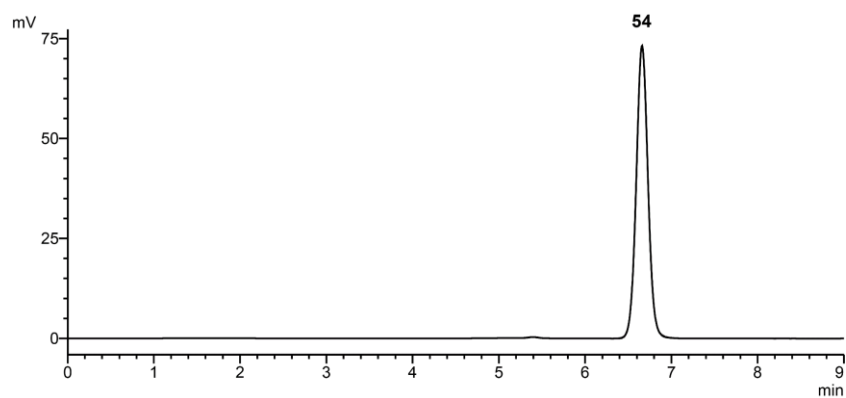


Figure 114. HPLC chromatogram of **54**. The sample was measured on Agela Durashell C-18 column (150 mm \times 4.6 mm, 5 μm particle size + 10 mm precolumn). The analysis was performed with 1 mL/min and an isocratic flow 71 : 29 ACN- H_2O for 9 min. The retention time is 6.66 min.

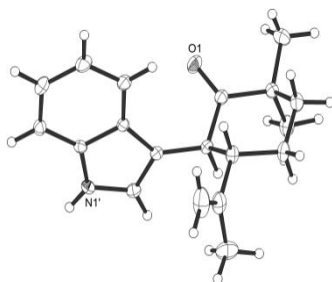
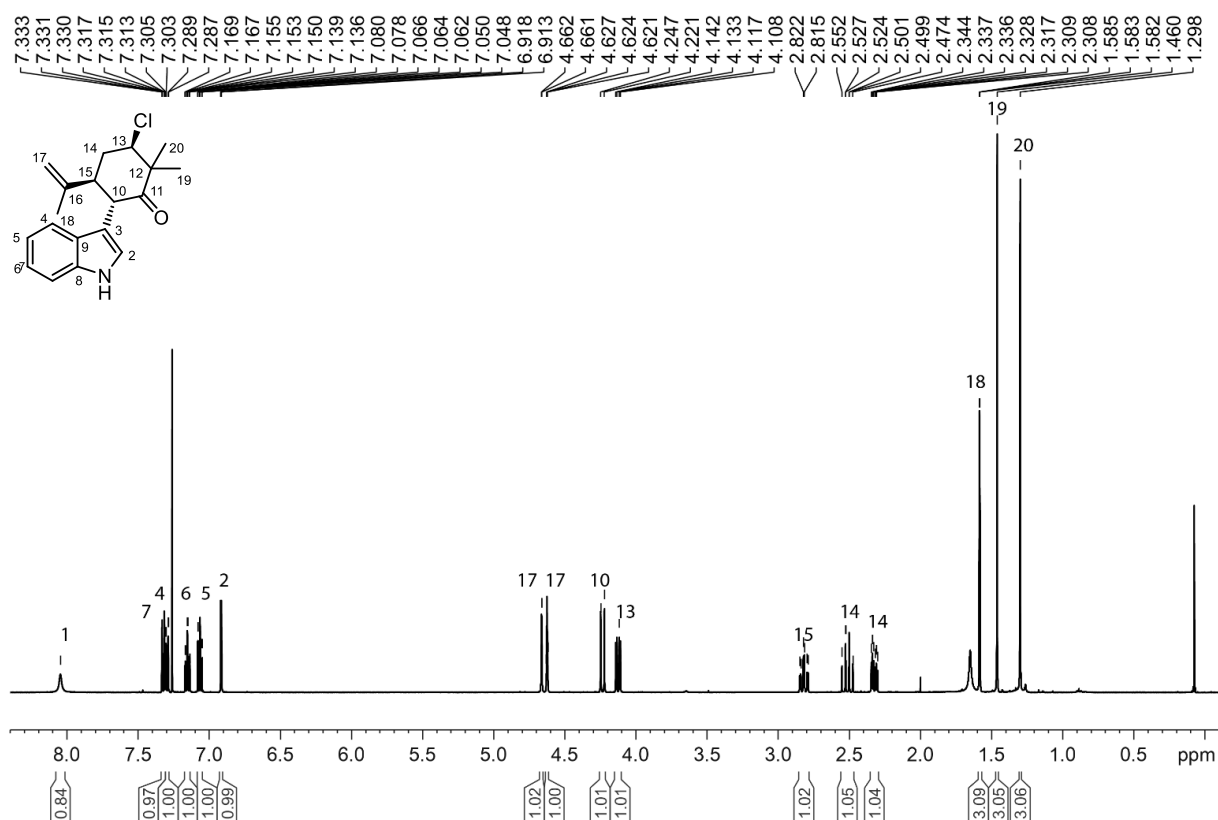
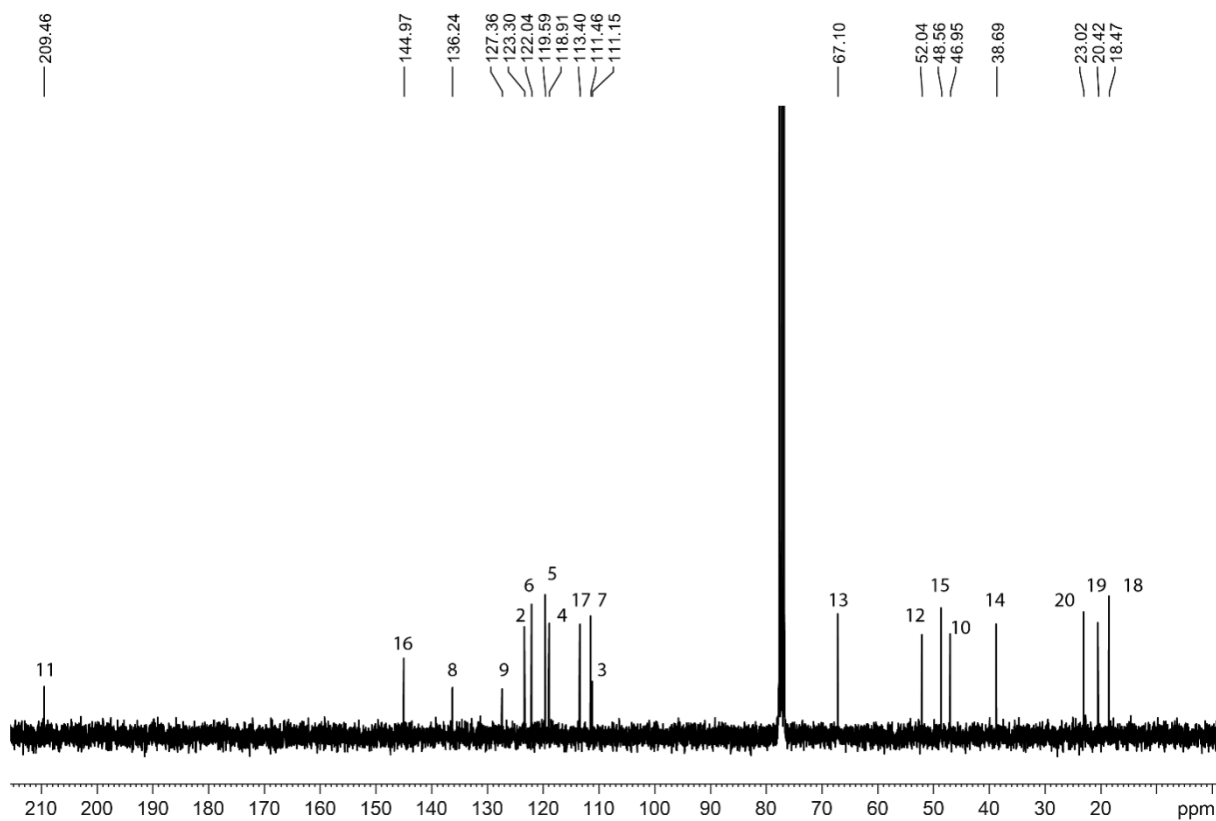


Figure 115. Crystal structure of **54**. The carbon atoms as large white spheres with black stripes and the hydrogen atoms as small white spheres. Crystals were obtained after storing a saturated solution of **54** in EtOH at $-20\text{ }^\circ\text{C}$. CCDC 1839575.

8.6.1.4 Analytic of 54a

Figure 116. ¹H-NMR of 54a measured in CDCl₃.Figure 117. ¹³C-NMR of 54a measured in CDCl₃.

Appendix

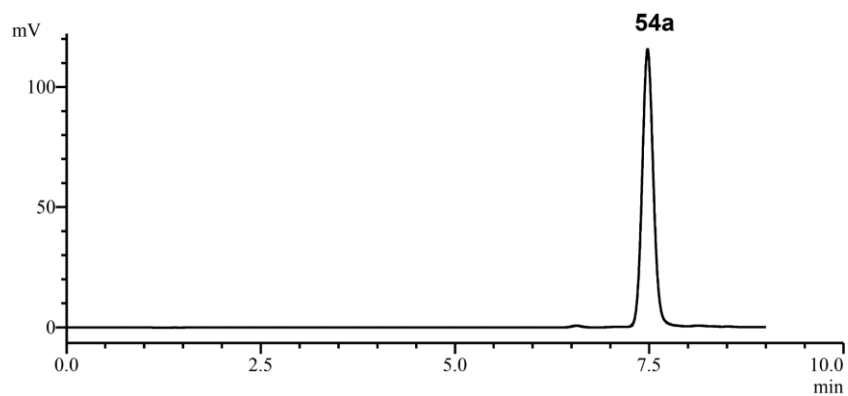


Figure 118. HPLC chromatogram of **54a**. The sample was measured on Agela Durashell C-18 column (150 mm x 4.6 mm, 5 μ m particle size + 10 mm precolumn). The analysis was performed with 1 mL/min and an isocratic flow 71 : 29 ACN-H₂O for 11 min. The retention time is 7.48 min.

8.6.1.5 Analytic of **54b**

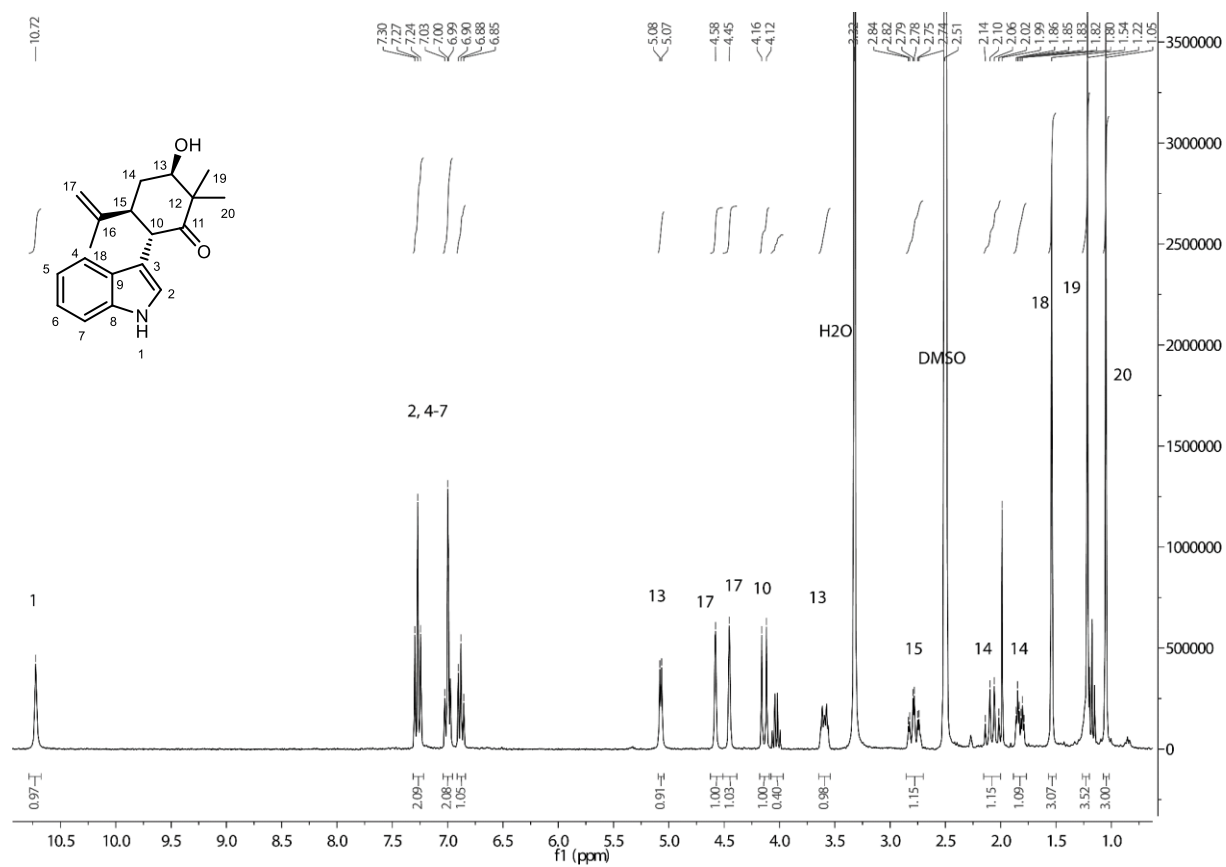


Figure 119. ¹H-NMR of **54b** measured in d₆-DMSO.

Appendix

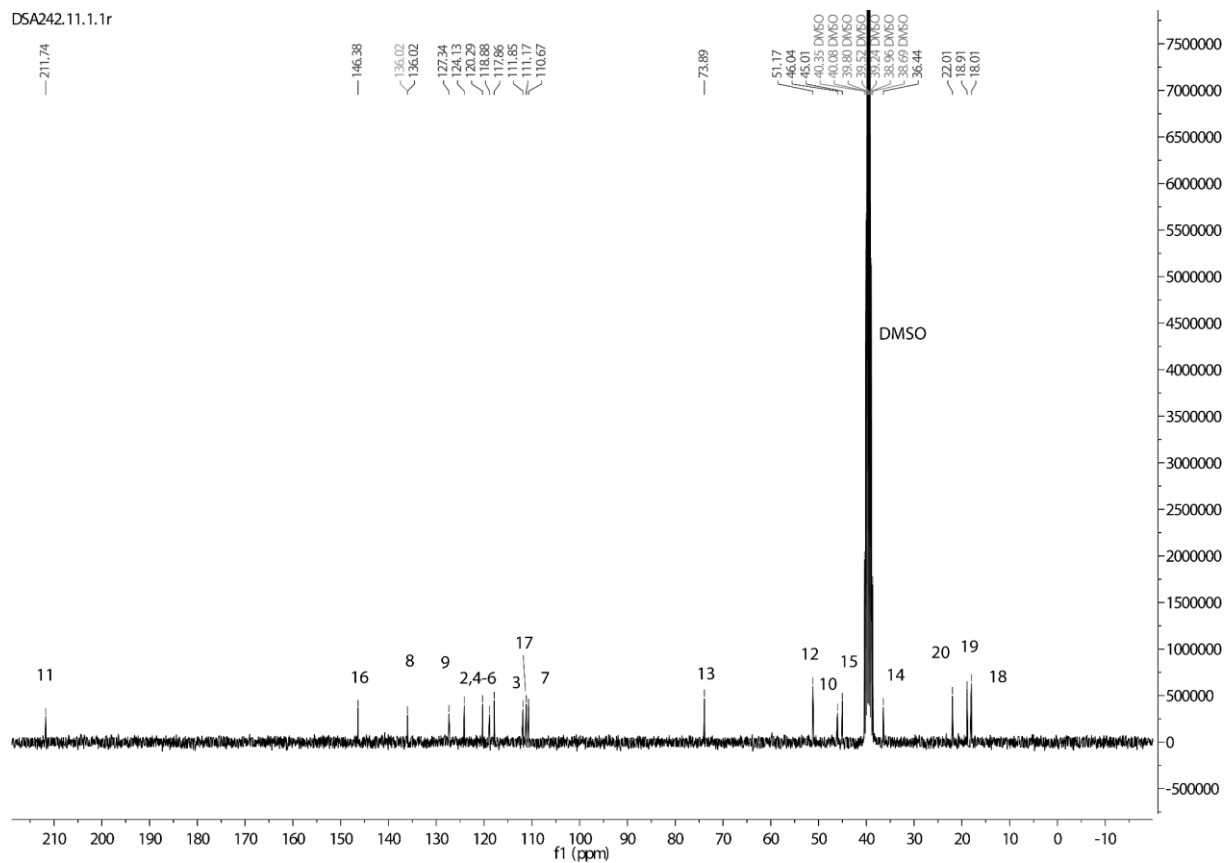


Figure 120. ^{13}C -NMR of **54b** measured in d_6 -DMSO.

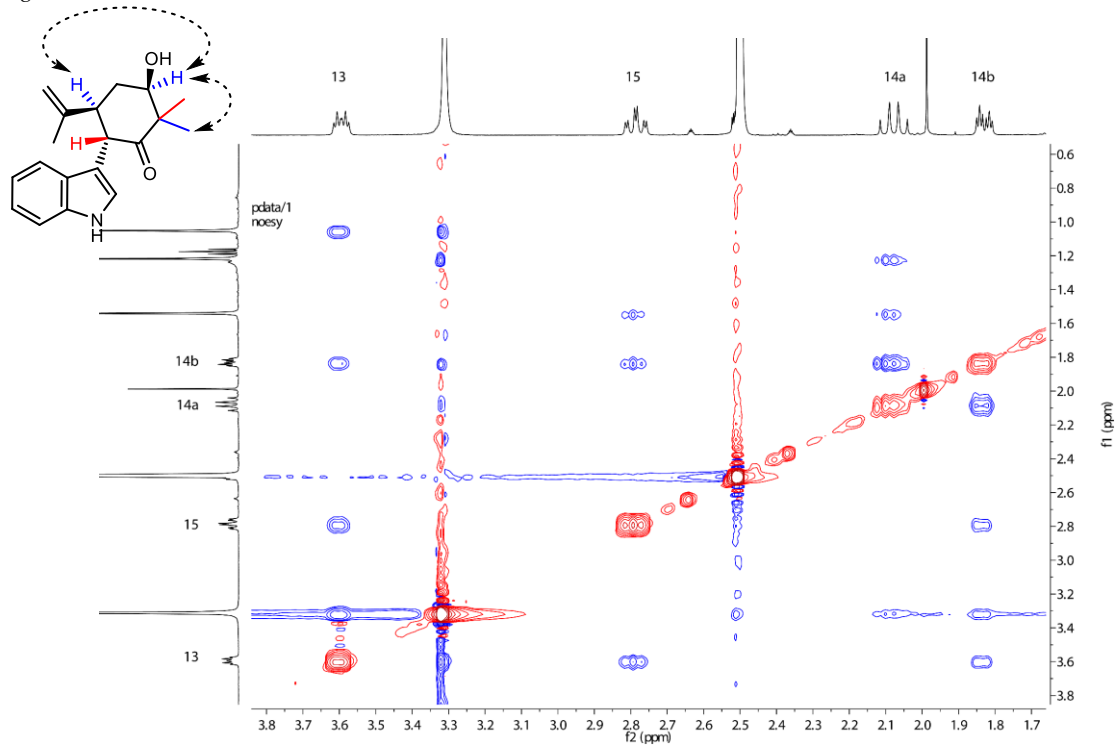


Figure 121. NOESY-NMR of **54b** measured in d_6 -DMSO.

Appendix

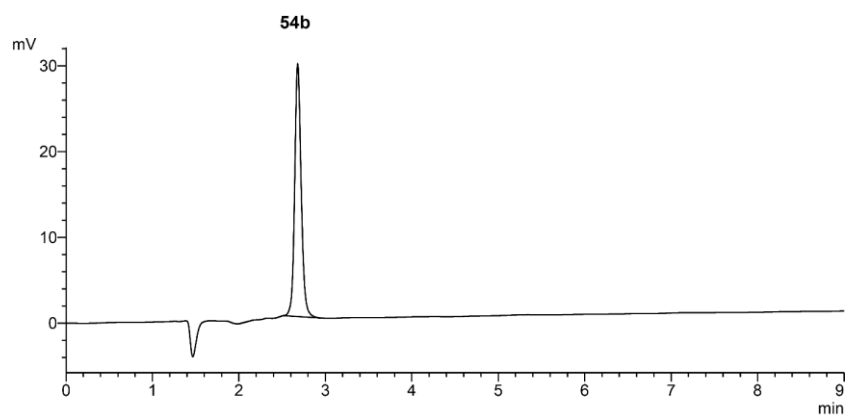


Figure 122. HPLC chromatogram of **54b**. The sample was measured on Agela Durashell C-18 column (150 mm x 4.6 mm, 5 μ m particle size + 10 mm precolumn). The analysis was performed with 1 mL/min and an isocratic flow 71 : 29 ACN-H₂O for 11 min. The retention time is 2.69 min.

8.6.1.6 Analytic of 54c

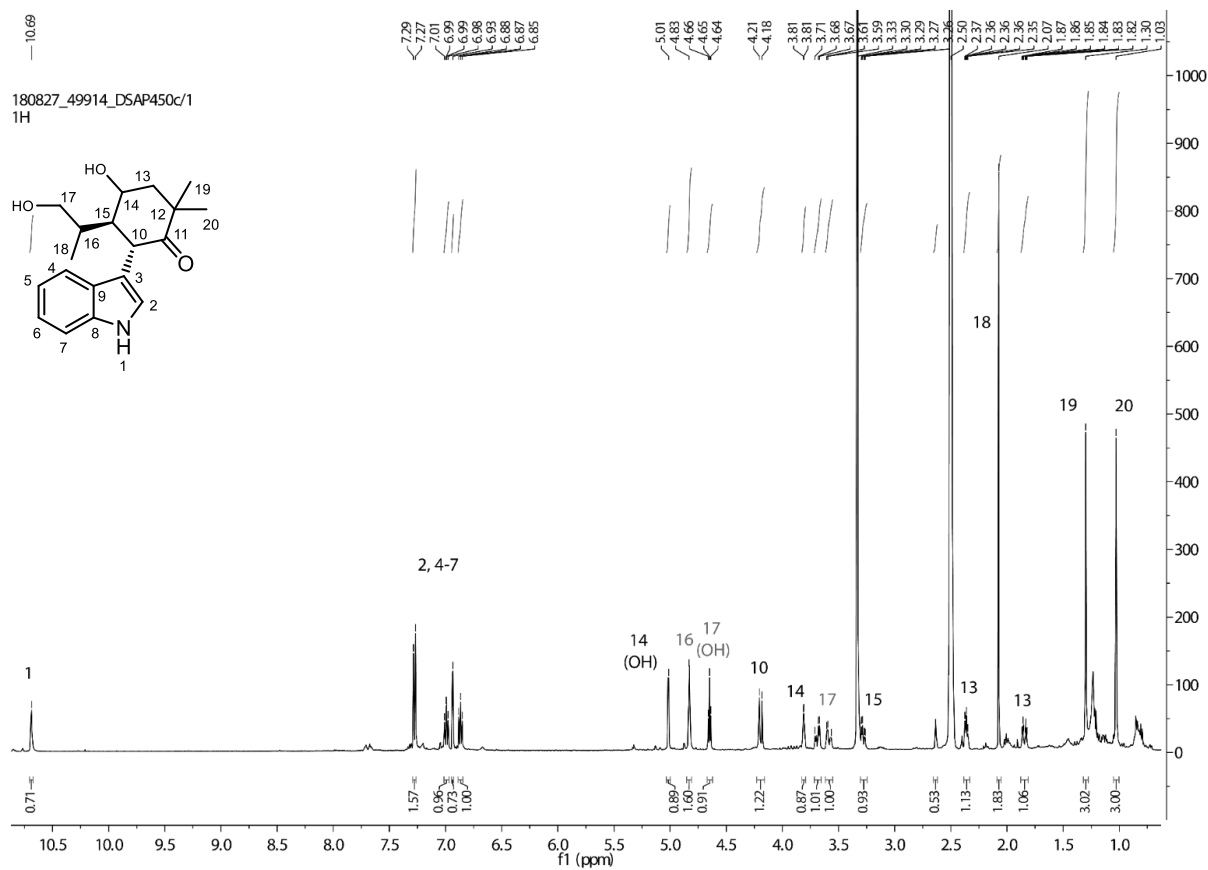


Figure 123. ¹H-NMR of **54c** measured in d₆-DMSO. Protons from carbon 16 and 17 cannot clearly be assigned.

Appendix

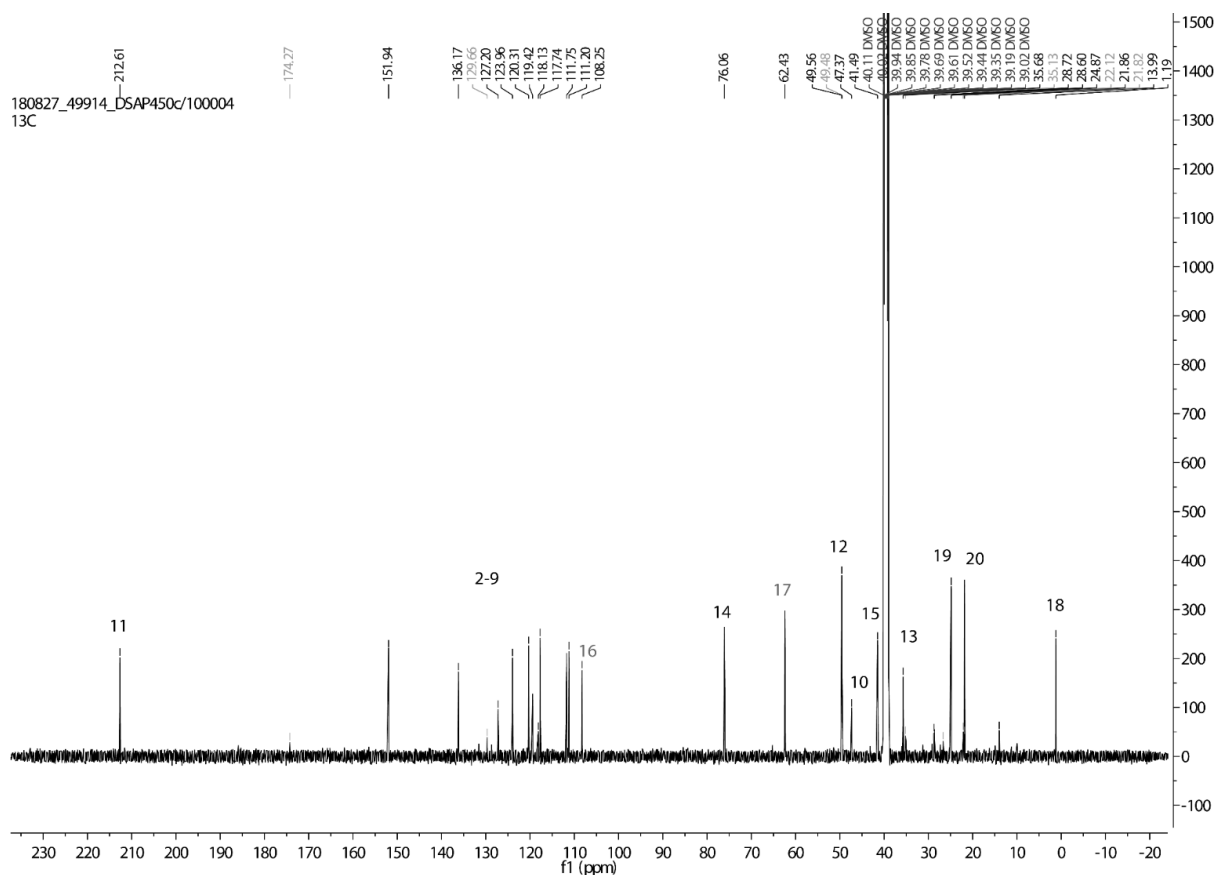


Figure 124. ^{13}C -NMR of **54c** measured in d_6 -DMSO. Carbons 16 and 17 cannot clearly be assigned.

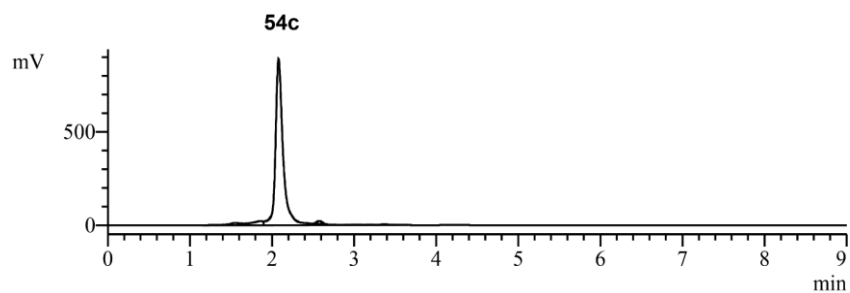
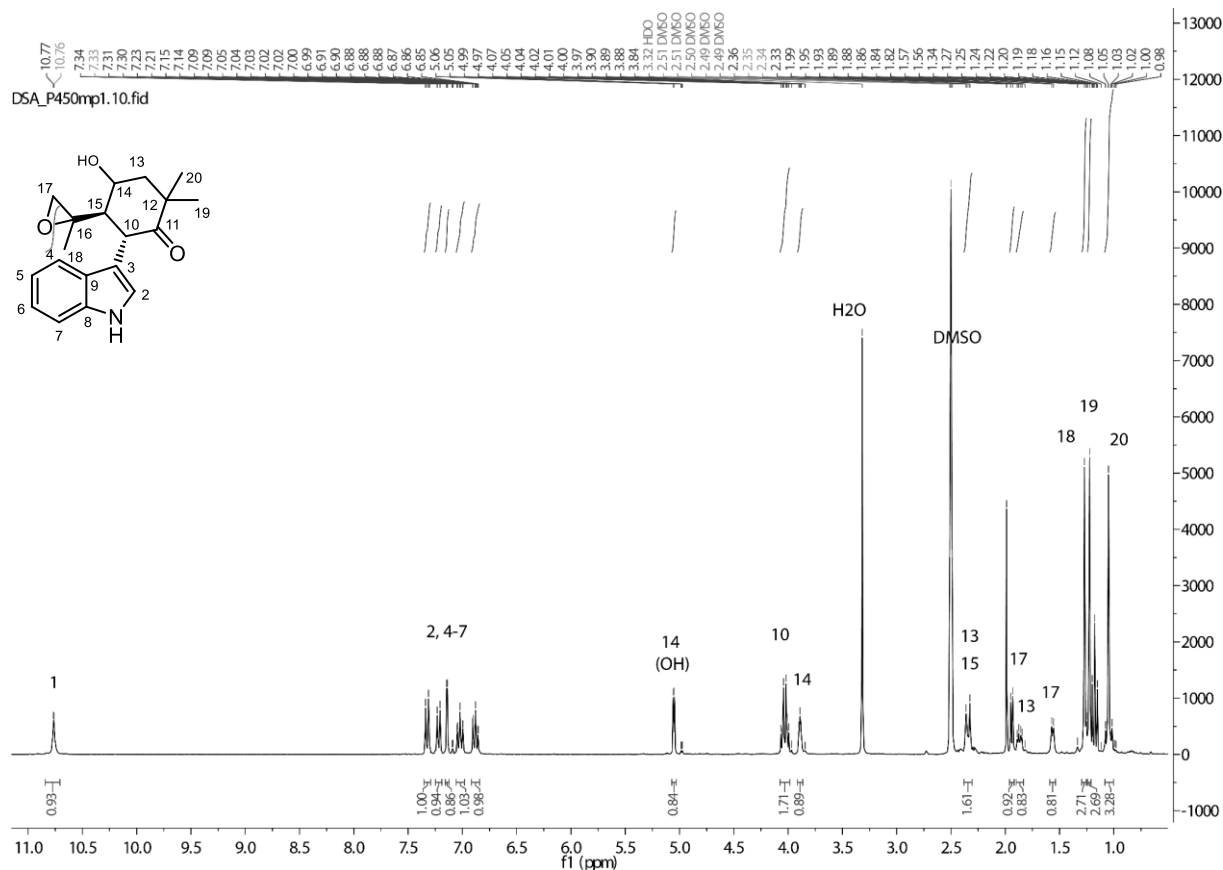
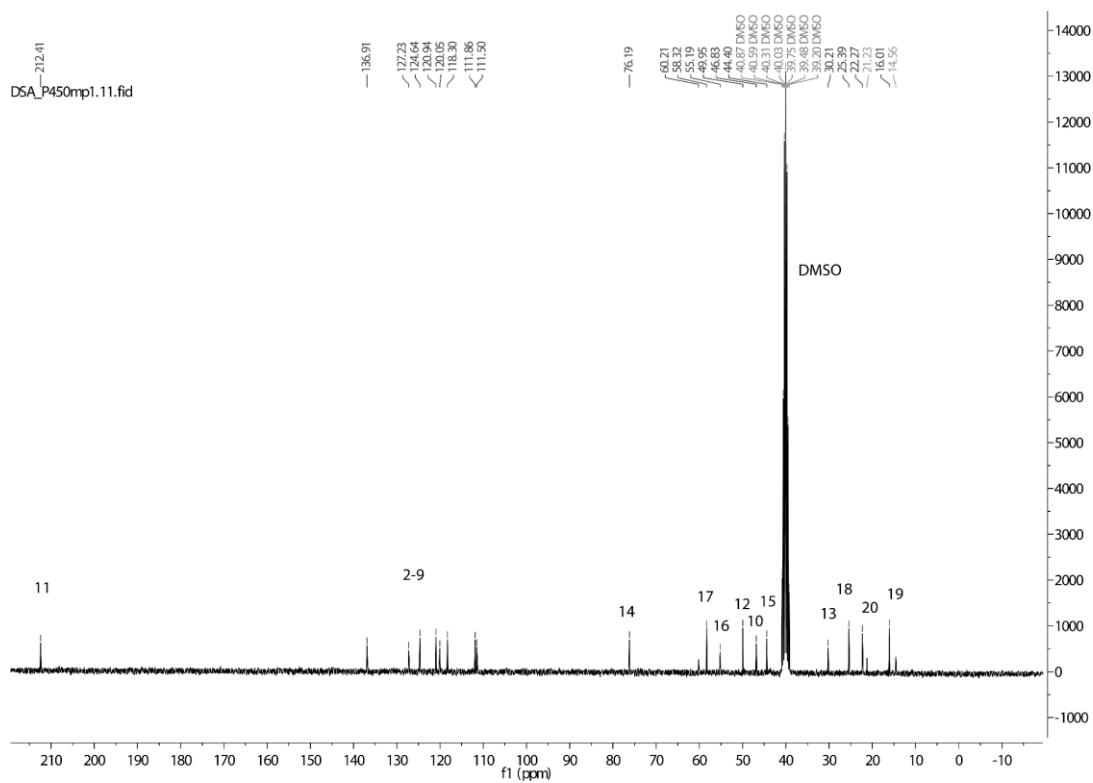


Figure 125. HPLC chromatogram of **54c**. The sample was measured on Agela Durashell C-18 column (150 mm \times 4.6 mm, 5 μm particle size + 10 mm precolumn). The analysis was performed with 1 mL/min and an isocratic flow 71 : 29 ACN- H_2O for 11 min. The retention time is 2.08 min.

8.6.1.7 Analytic of 54d

Figure 126. ¹H-NMR of 54d measured in d₆-DMSO.Figure 127. ¹³C-NMR of 54d measured in d₆-DMSO.

8.6.1.8 Analytic of 54e

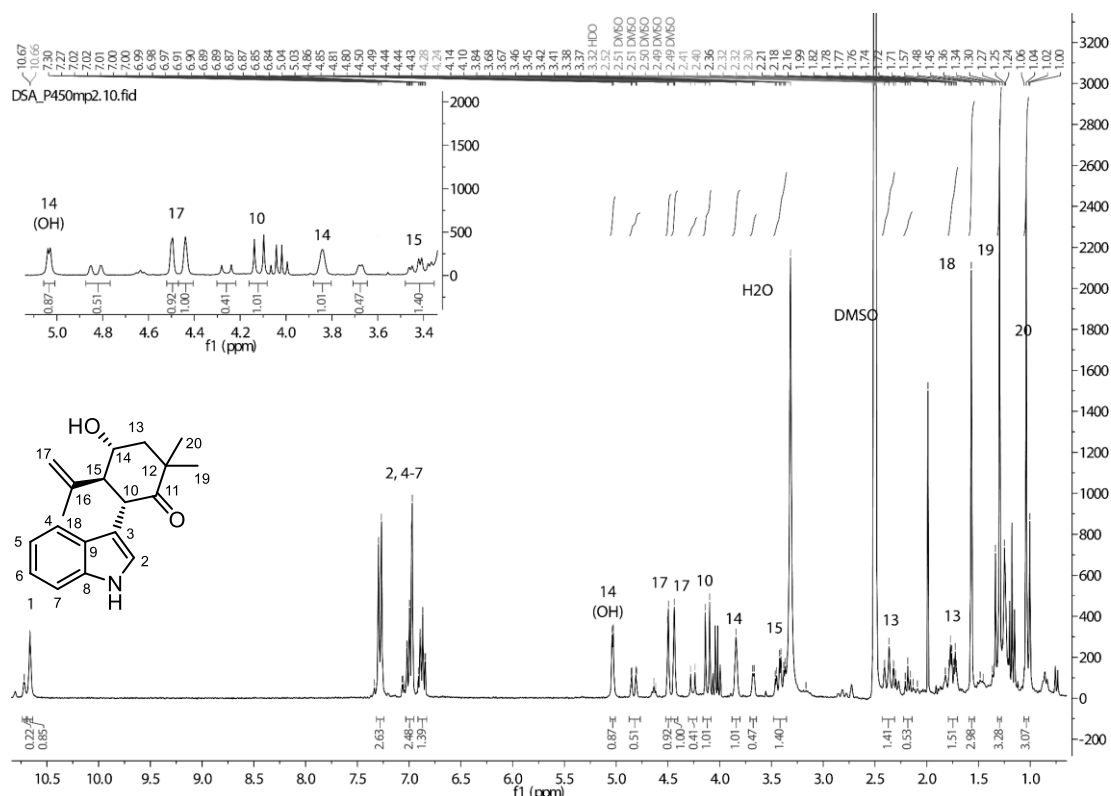


Figure 128: $^1\text{H-NMR}$ of **54e** measured in $d_6\text{-DMSO}$. In the area between 5.0 and 3.4 it can be seen that a second product is present in the sample because a double set of signals is present for peaks of C-H 14, 10 and 17 with an integral of 0.5. Also, the signals of C-H 13 have an integral of 1.5 instead of 1. From HPLC measurements it could be seen, that the peak is quite broad. These results indicate that a mix of two diastereomers is produced.

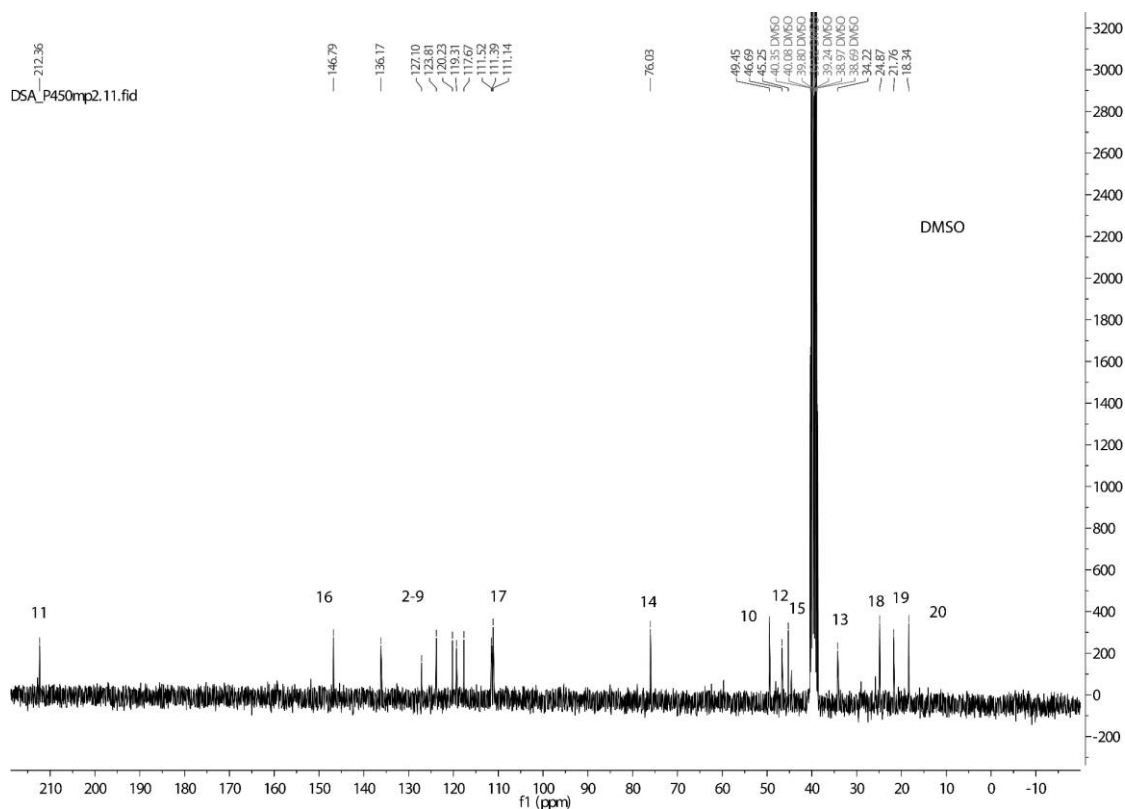


Figure 129: $^{13}\text{C-NMR}$ of **54e** measured in $d_6\text{-DMSO}$.

Appendix

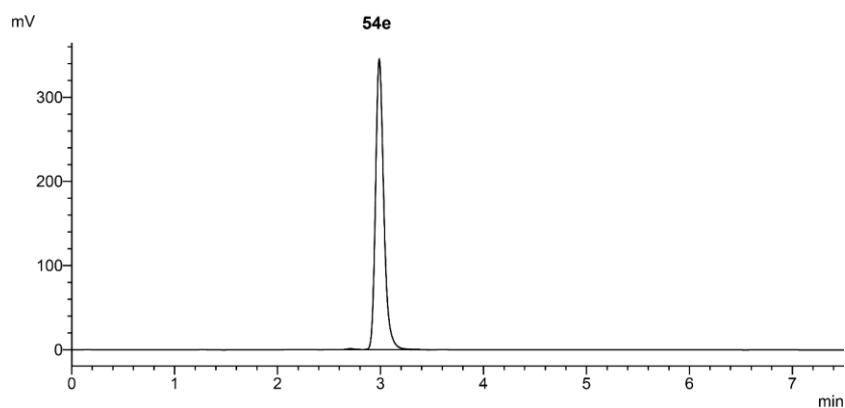


Figure 130. HPLC chromatogram of **54e**. The sample was measured on Agela Durashell C-18 column (150 mm x 4.6 mm, 5 μ m particle size + 10 mm precolumn). The analysis was performed with 1 mL/min and an isocratic flow 71 : 29 ACN-H₂O for 11 min. The retention time is 2.99 min.

8.6.1.9 Analytic of **54f**

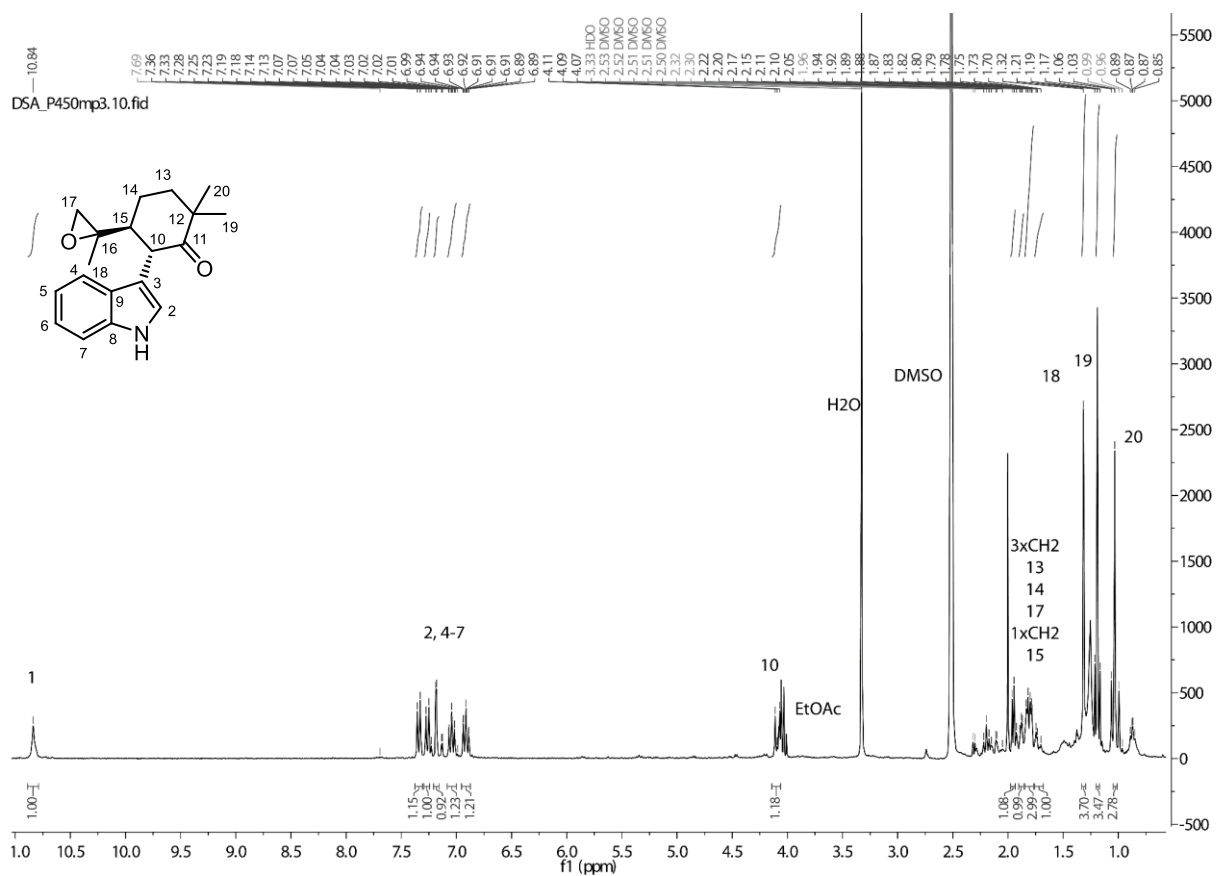


Figure 131. ¹H-NMR of **54f** measured in d₆-DMSO.

Appendix

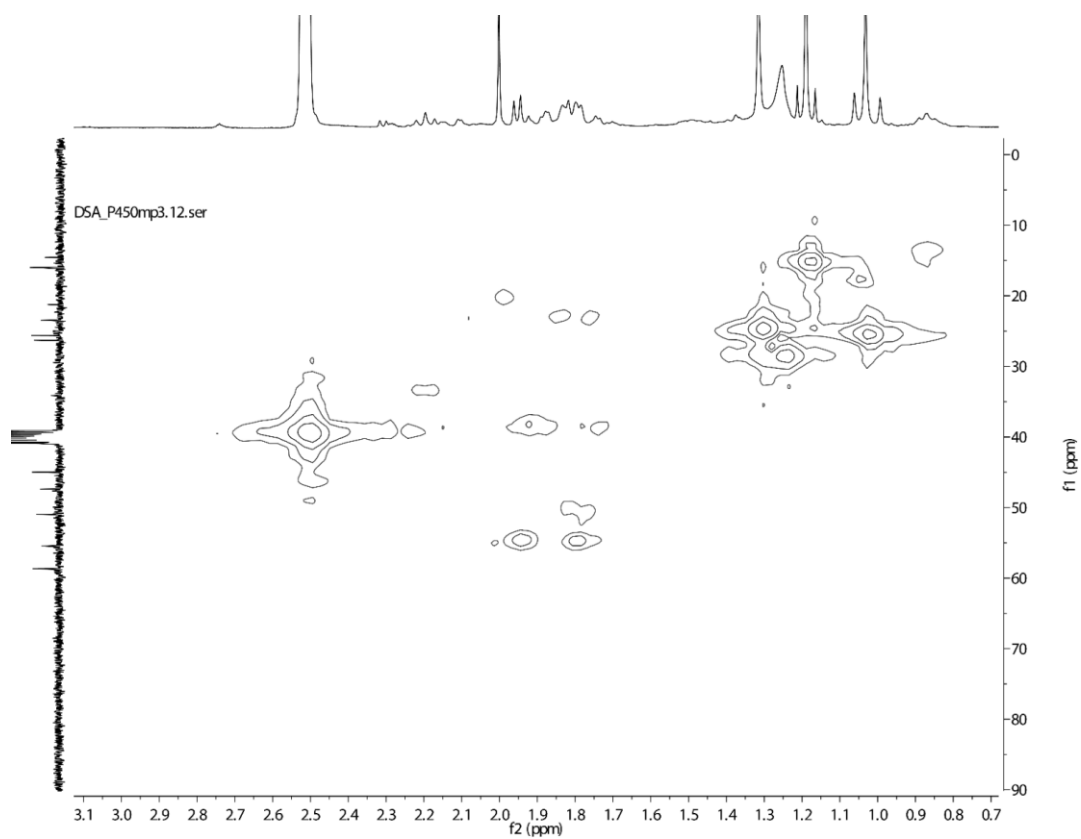


Figure 132. HMQC NMR of **54f** measured in d_6 -DMSO.

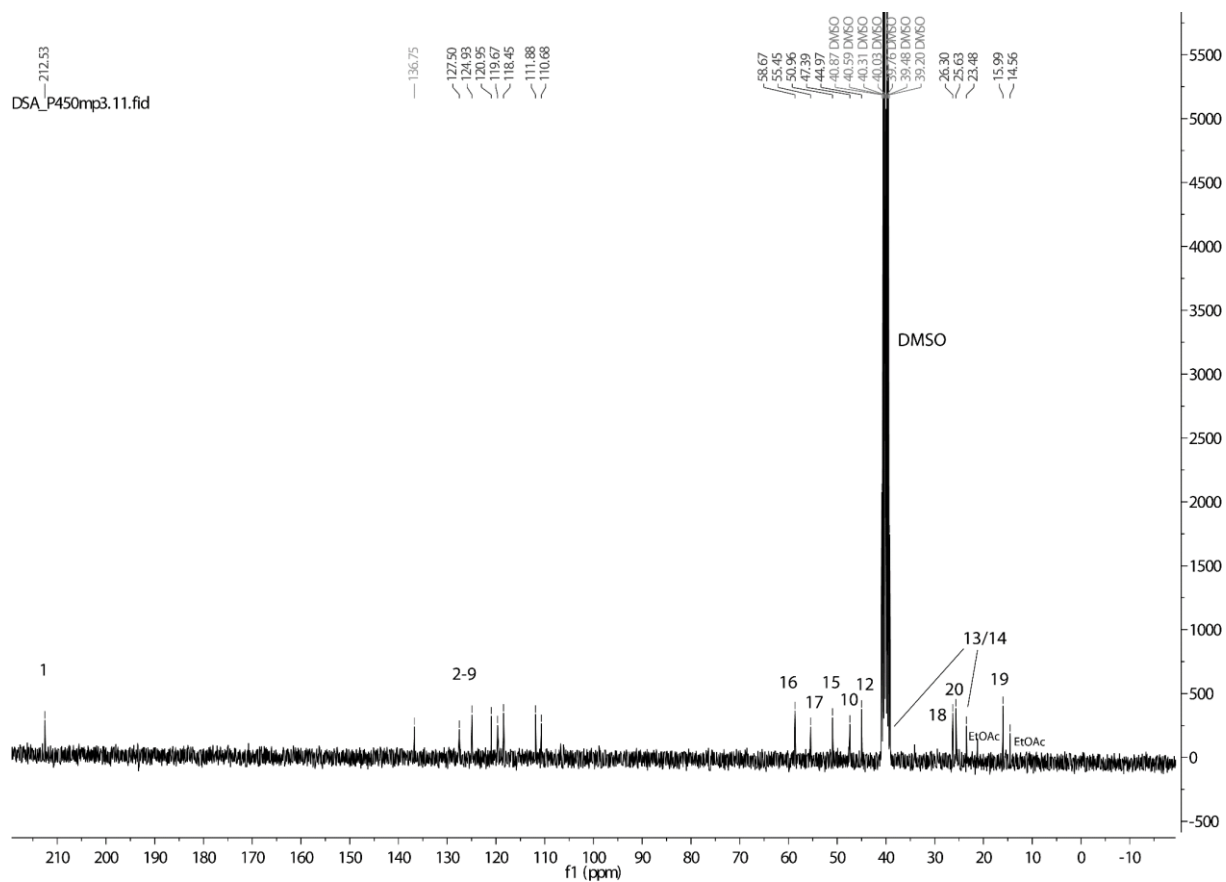


Figure 133. ^{13}C -NMR of **54f** measured in d_6 -DMSO.

Appendix

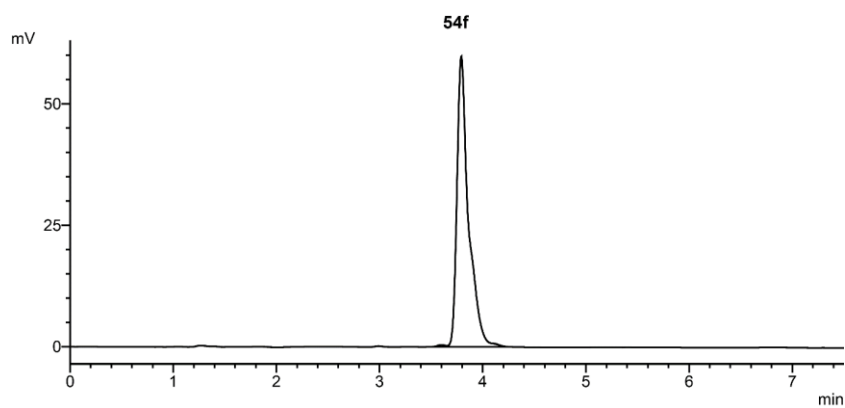


Figure 134. HPLC chromatogram of **54f**. The sample was measured on Agela Durashell C-18 column (150 mm × 4.6 mm, 5 μm particle size + 10 mm precolumn). The analysis was performed with 1 mL/min and an isocratic flow 71 : 29 ACN-H₂O for 11 min. The retention time is 3.79 min.

8.6.1.10 Analytic of **63**

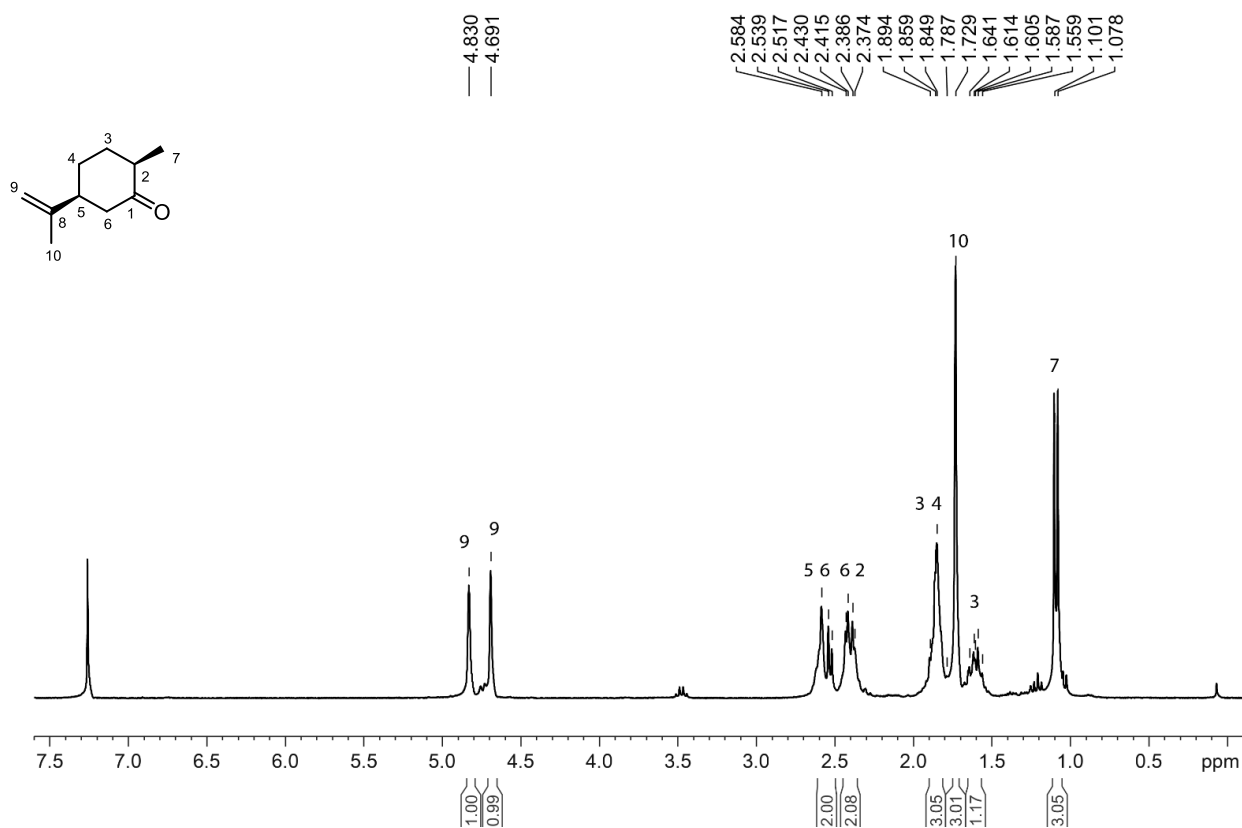
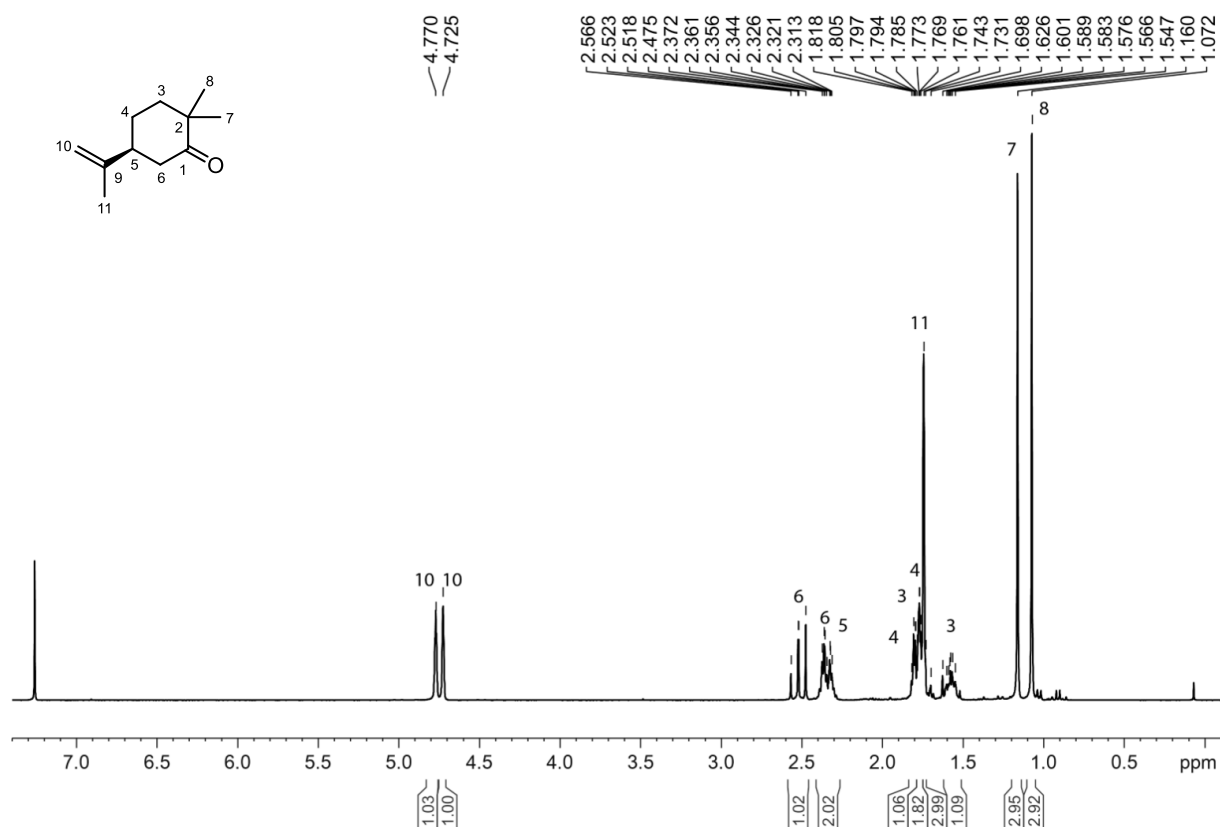
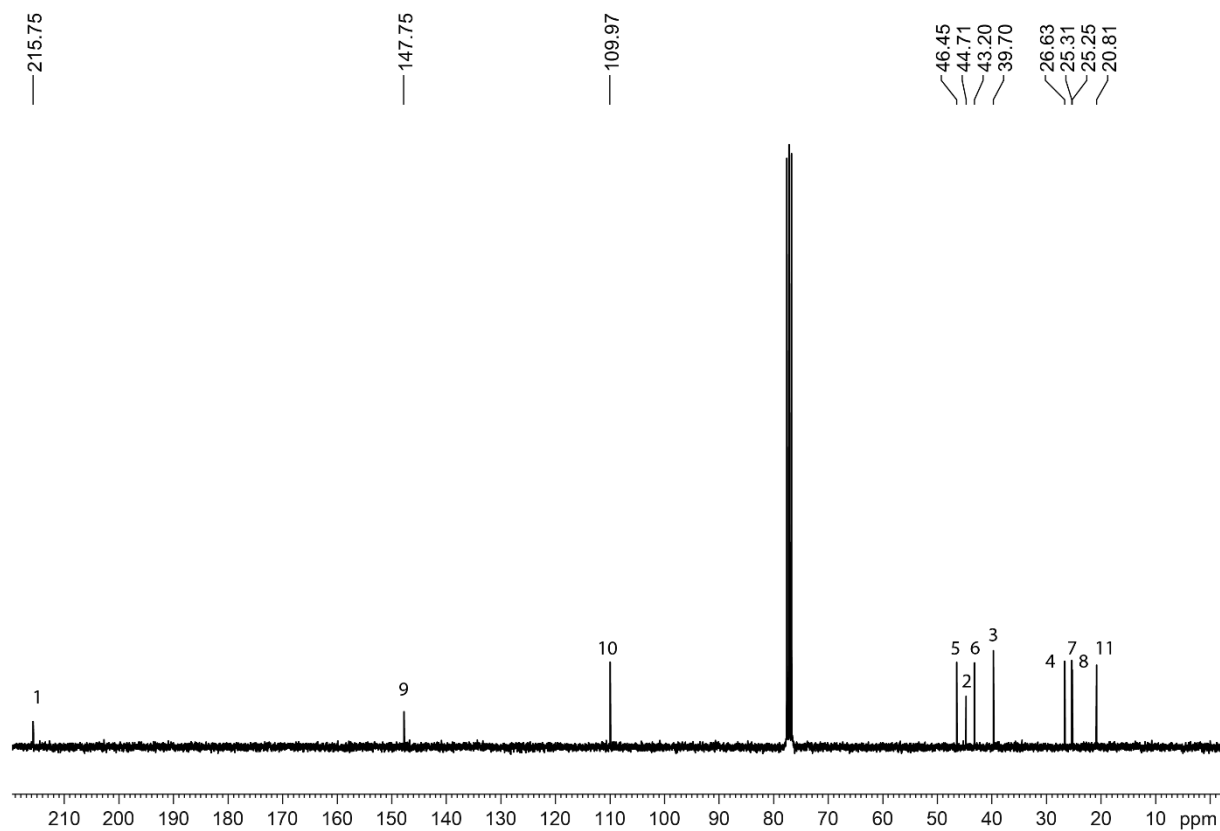


Figure 135. ¹H-NMR of **63** measured in CDCl₃.

8.6.1.11 Analytic of 64

Figure 138. $^1\text{H-NMR}$ of 64 measured in CDCl_3 .Figure 139. $^{13}\text{C-NMR}$ of 64 measured in CDCl_3 .

Appendix

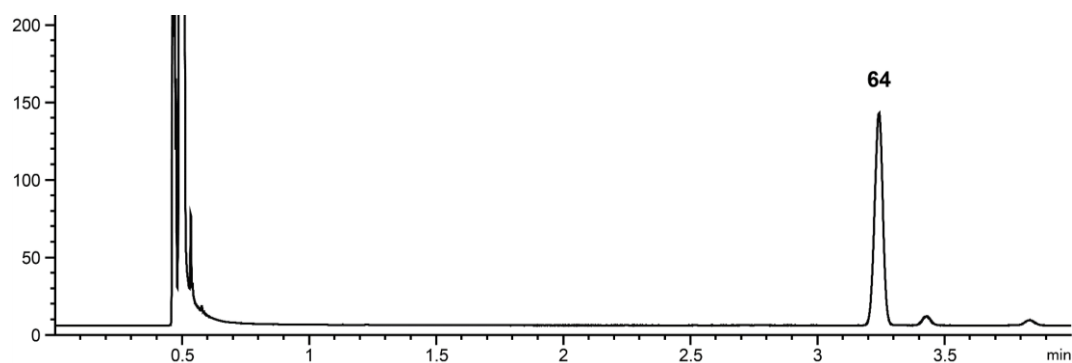


Figure 140. GC chromatogram of **64**. Analysis was performed for 4 min at 92 °C, using a Agilent GC7820A system with FID-detector (Heater 300 °C, H₂-Flow 30 mL/min, Air-Flow 400 mL/min, Makeup Flow 25 mL/min; Date Rate/ Min Peak width 50 Hz/0.004 min) with a 30 m HP-5 column with 0.25 µm inner diameter with a flow of 6.5 mL/min. 1 µL sample was injected with a split of 40-1 with 250 mL/min. Heater was at 250 °C, 1 bar, gas saver 20 mL/min after 2 min.

8.6.1.12 GC chromatograms of 68-75

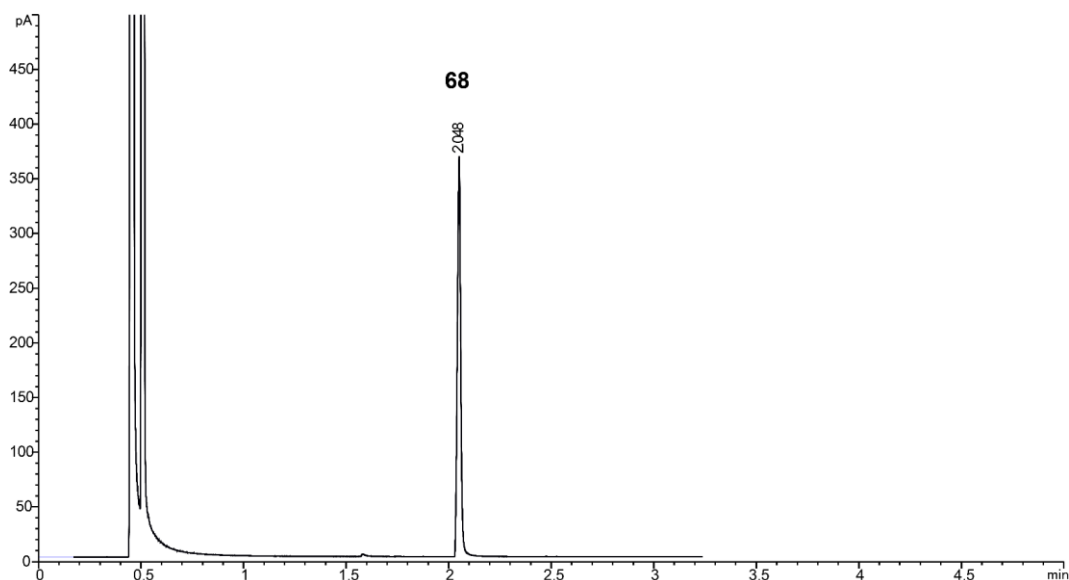


Figure 141. Adamantanisonitril (**68**) was measured 120°C to 132°C with 4°C/min, hold 3 min, 10°C/min to 200°C

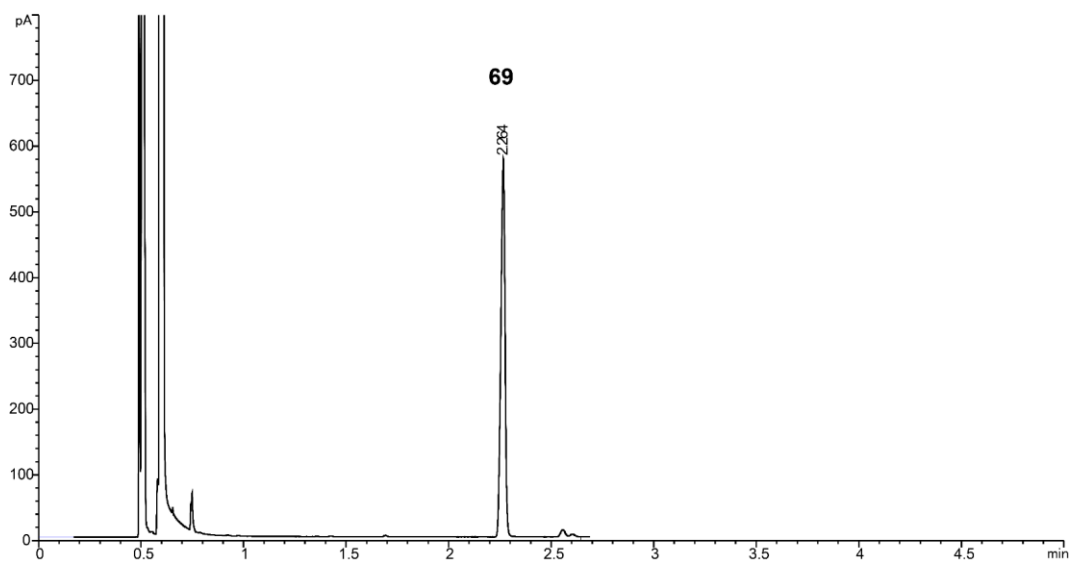


Figure 142. Tetramethylbutylisocyanide (**69**) 56°C to 66°C with 2°C/min hold 3 min 10°C/min to 120°C.

Appendix

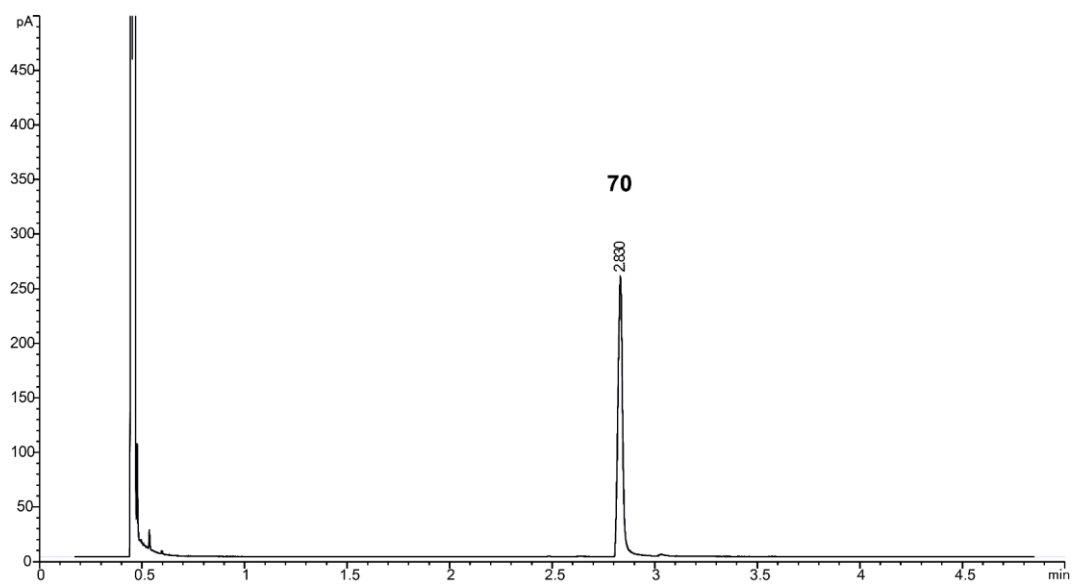


Figure 143. 2-naphtylisocyanide (70) 120°C to 140°C with 4°C/min, hold 3 min, 10°C/min to 190°C.

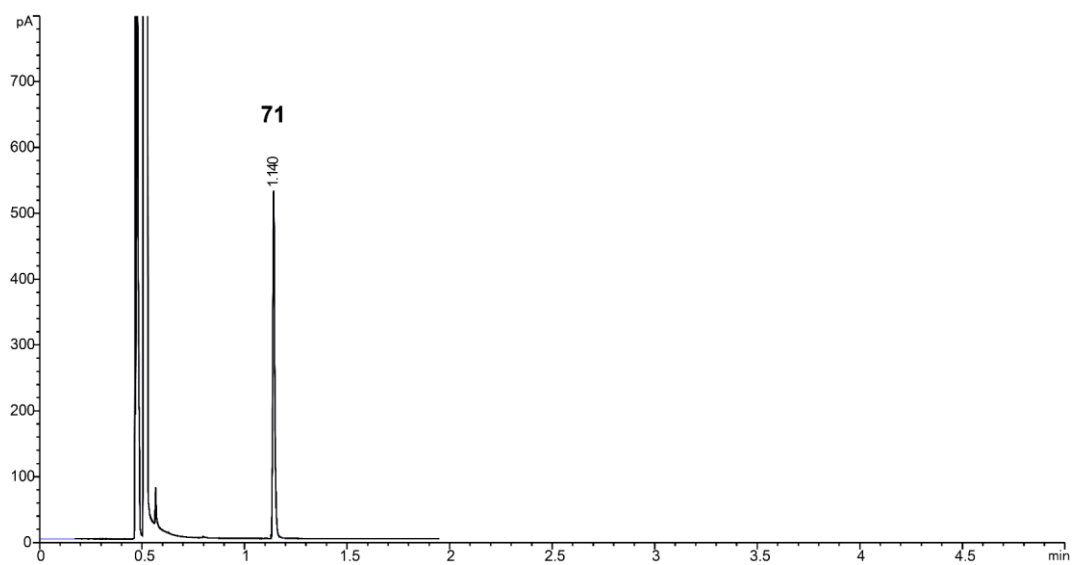


Figure 144. Cyclohexylisocyanitrile (71) 82°C to 96°C with 4°C/min, hold 3 min, go to 160°C with 10°C/min

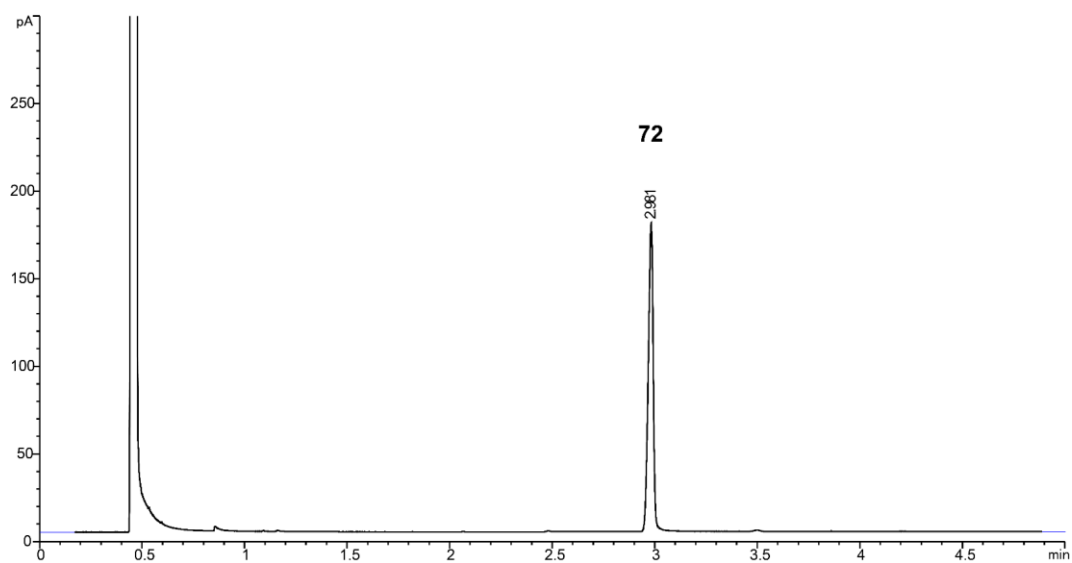


Figure 145. 2(4-morpholinyl)ethylisocyanid (72) 120°C to 144°C with 4°C/min, hold 3 min, 10°C/min to 190°C

Appendix

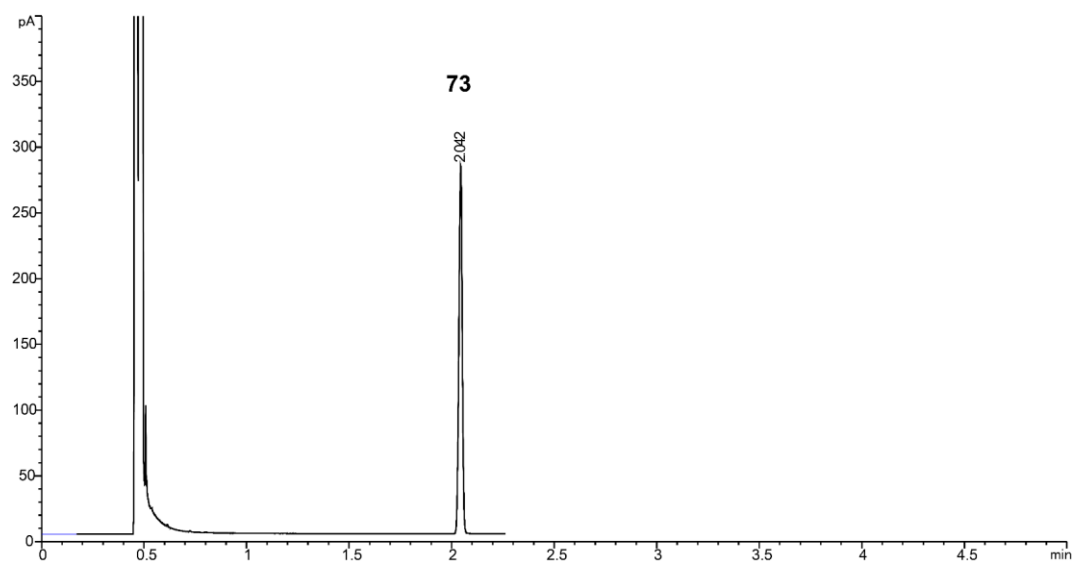


Figure 146. Cyclohexylisothiocyanat (**73**) 102°C to 120°C with 4°C/min, hold 3 min, 10°C/min to 180°C

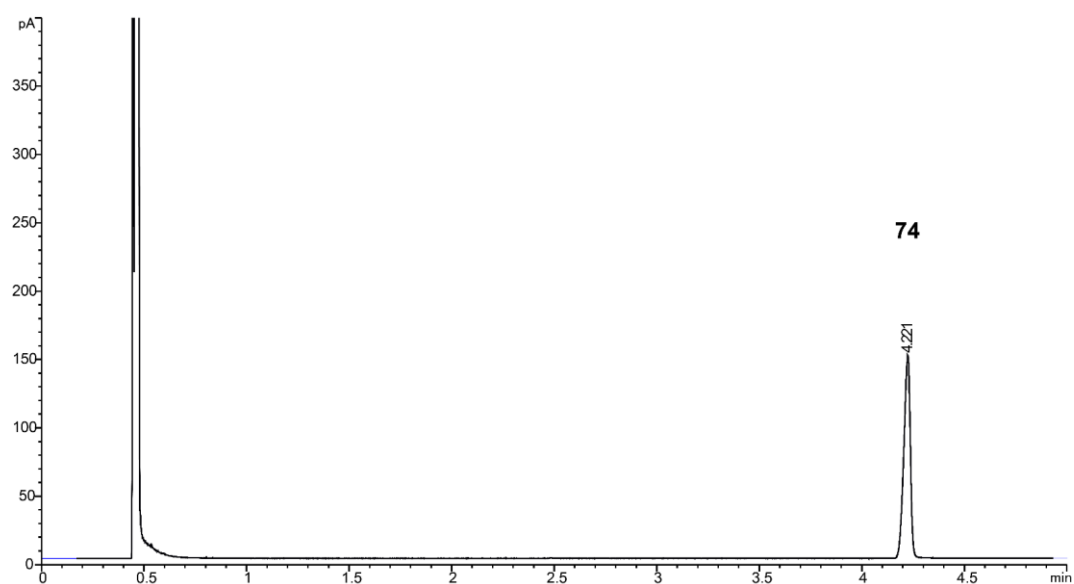


Figure 147. 3-Morpholinopropylisothiocyanat(**74**) 120°C to 144°C with 4°C/min, hold 3 min, 10°C/min to 190°C

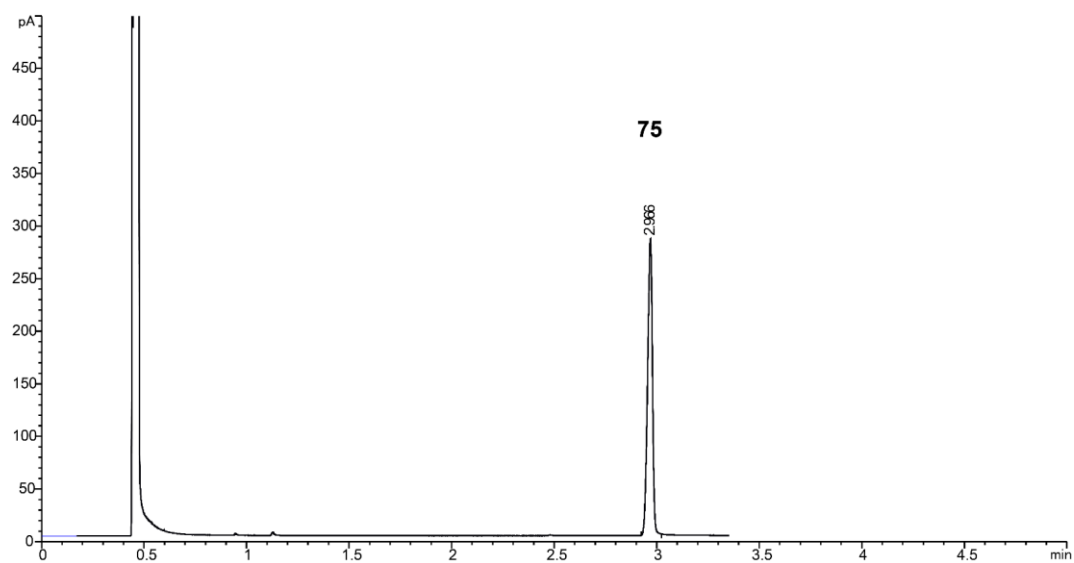


Figure 148. Phenethylisothiocyanat (**75**) 120°C to 140°C with 4°C/min, hold for 3 min

Appendix

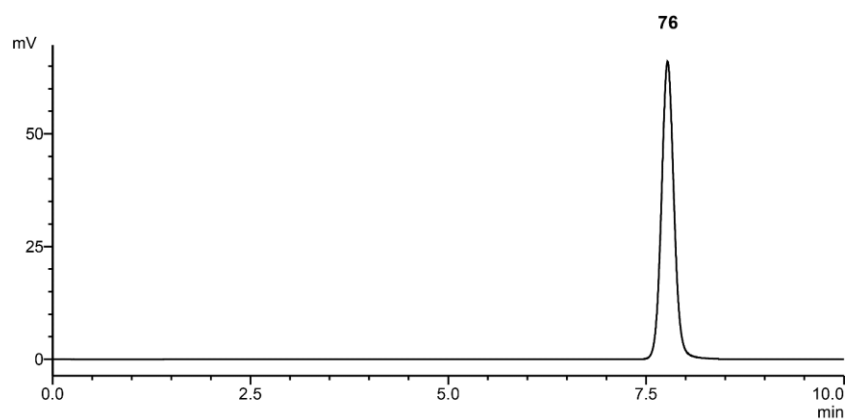


Figure 151. HPLC chromatogram of **76**. The sample was measured on Agela Durashell C-18 column (150 mm \times 4.6 mm, 5 μ m particle size + 10 mm precolumn). The analysis was performed with 1 mL/min and an isocratic flow 71 : 29 ACN-H₂O for 10 min. UV detection was set to 280 nm. The retention time is 7.77 min.

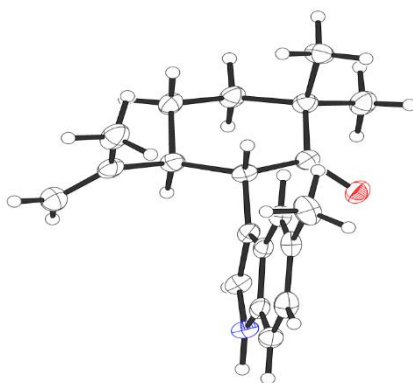
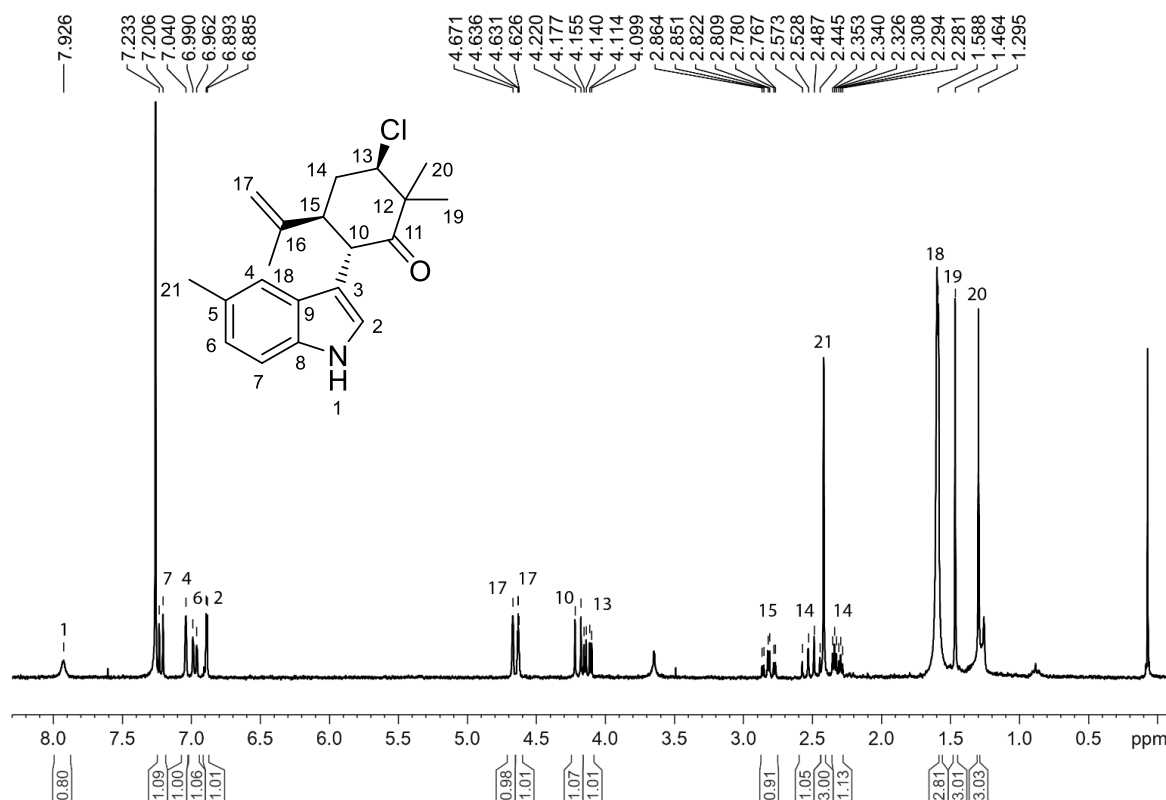
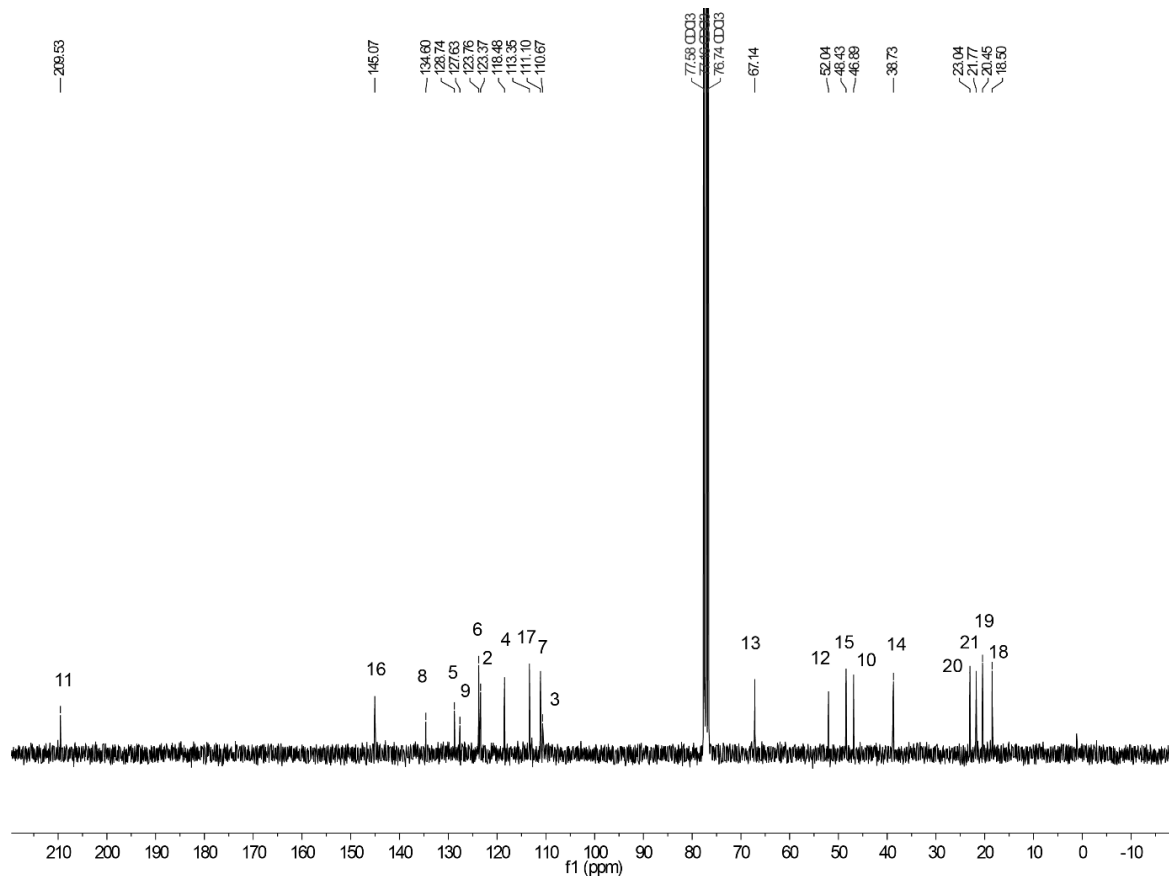


Figure 152. Crystal structure of **76** with a methyl group at the C5 of the indole ring. The nitrogen atom is shown in blue, the oxygen atom in red, the carbon atoms as large white spheres with black stripes and the hydrogen atoms as small white spheres. CCDC 1839576

8.6.1.14 Analytic of 76a

Figure 153. ¹H-NMR of 76a. Measurement in CDCl₃.Figure 154. ¹³C-NMR of 76a. Measurement in CDCl₃.

Appendix

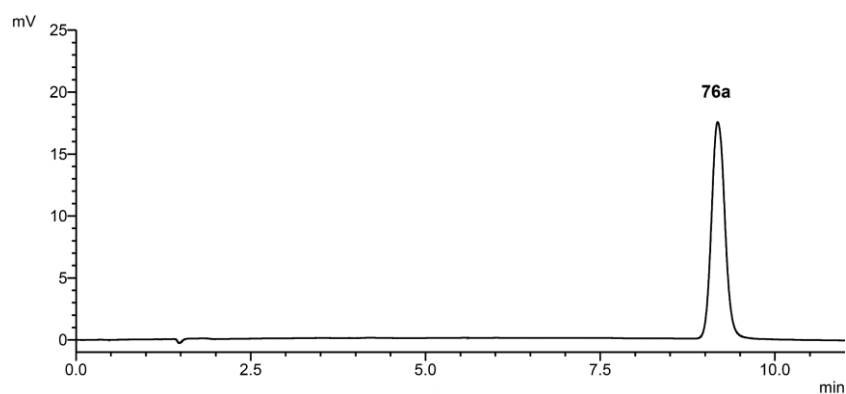


Figure 155. HPLC chromatogram of **76a**. The sample was measured on Agela Durashell C-18 column (150 mm x 4.6 mm, 5 μ m particle size + 10 mm precolumn). The analysis was performed with 1 mL/min and an isocratic flow 71 : 29 ACN-H₂O for 11 min. The retention time is 8.89 min.

8.6.1.15 Analytic of **77**

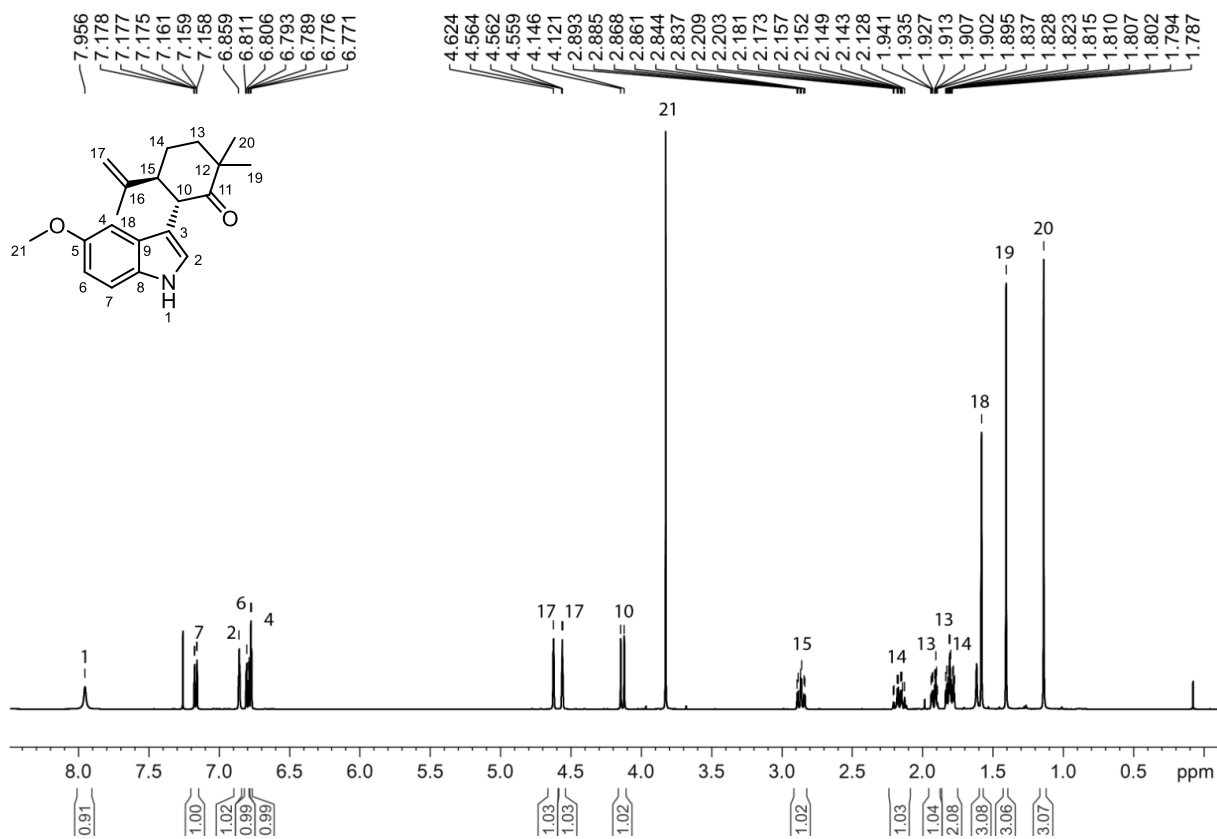


Figure 156. ¹H-NMR of **77** measured in CDCl₃.

Appendix

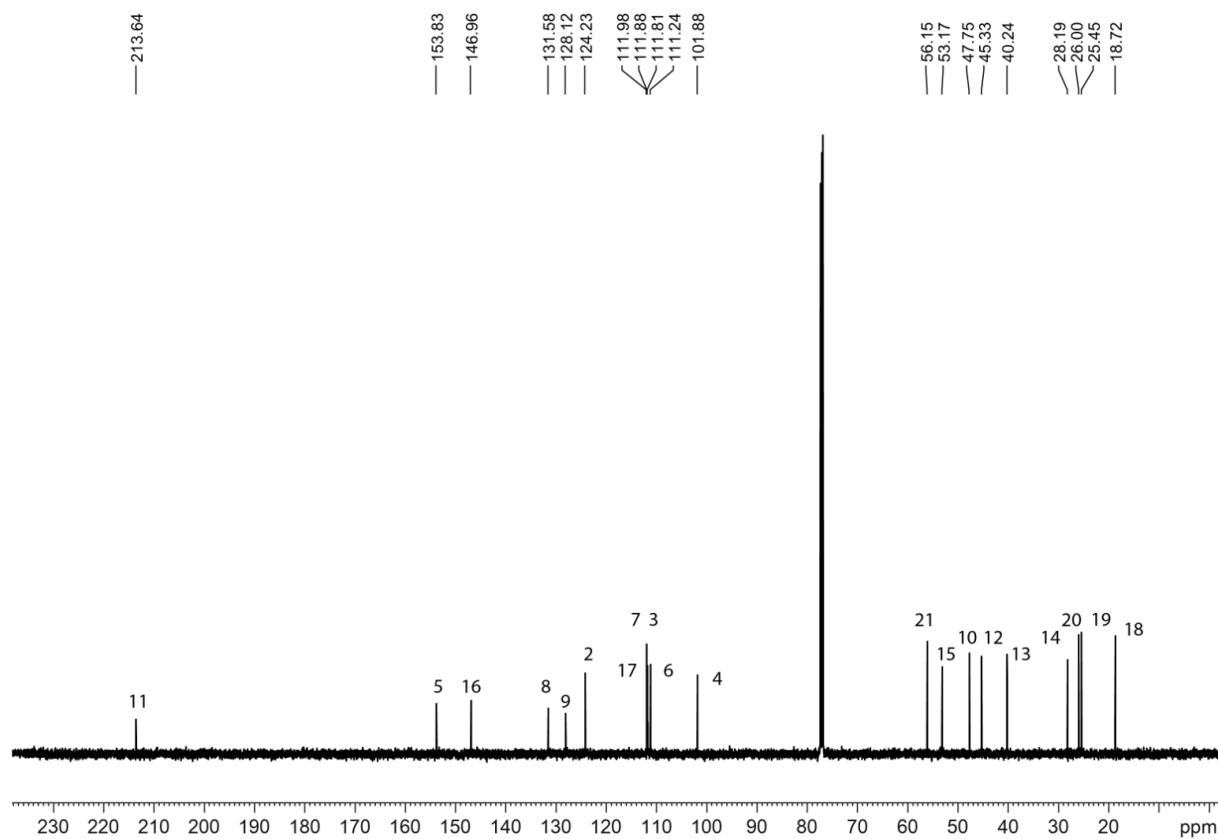


Figure 157. ^{13}C -NMR of 77 measured in CDCl_3 .

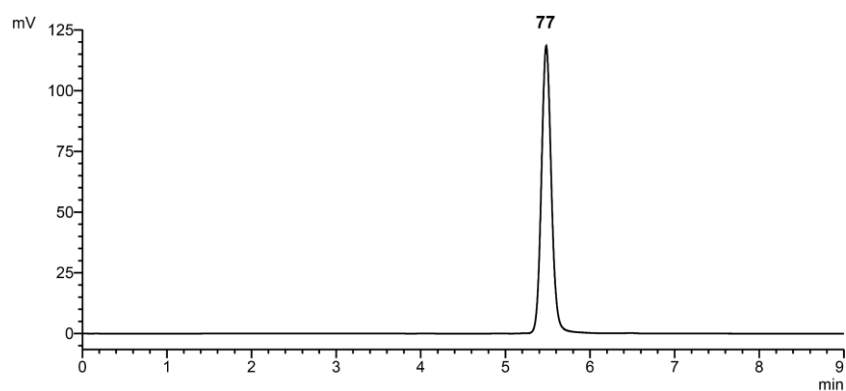


Figure 158. HPLC chromatogram of 77. The sample was measured on Agela Durashell C-18 column (150 mm \times 4.6 mm, 5 μm particle size + 10 mm precolumn). The analysis was performed with 1 mL/min and an isocratic flow 71 : 29 ACN- H_2O for 9 min. The retention time is 5.48 min.

Appendix

8.6.1.16 Analytic of 77a

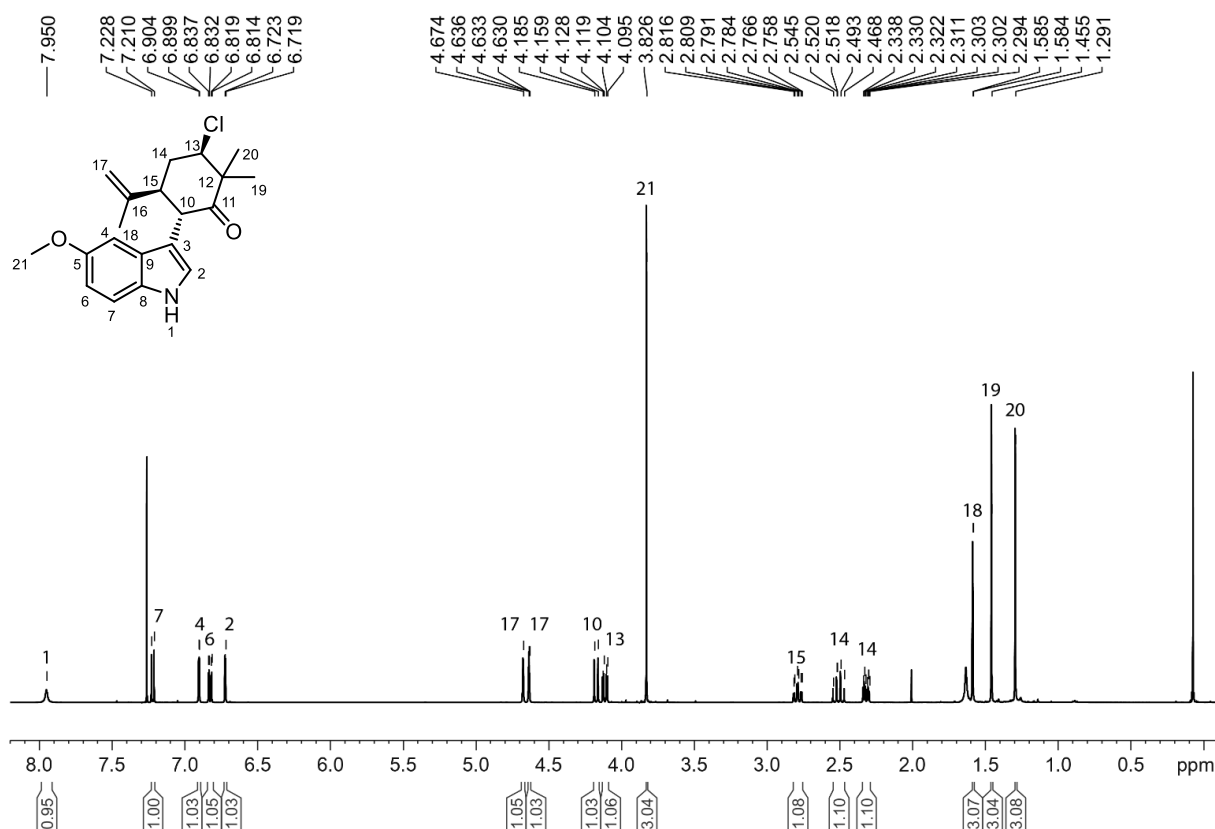


Figure 159. ¹H-NMR of 77a measured in CDCl₃.

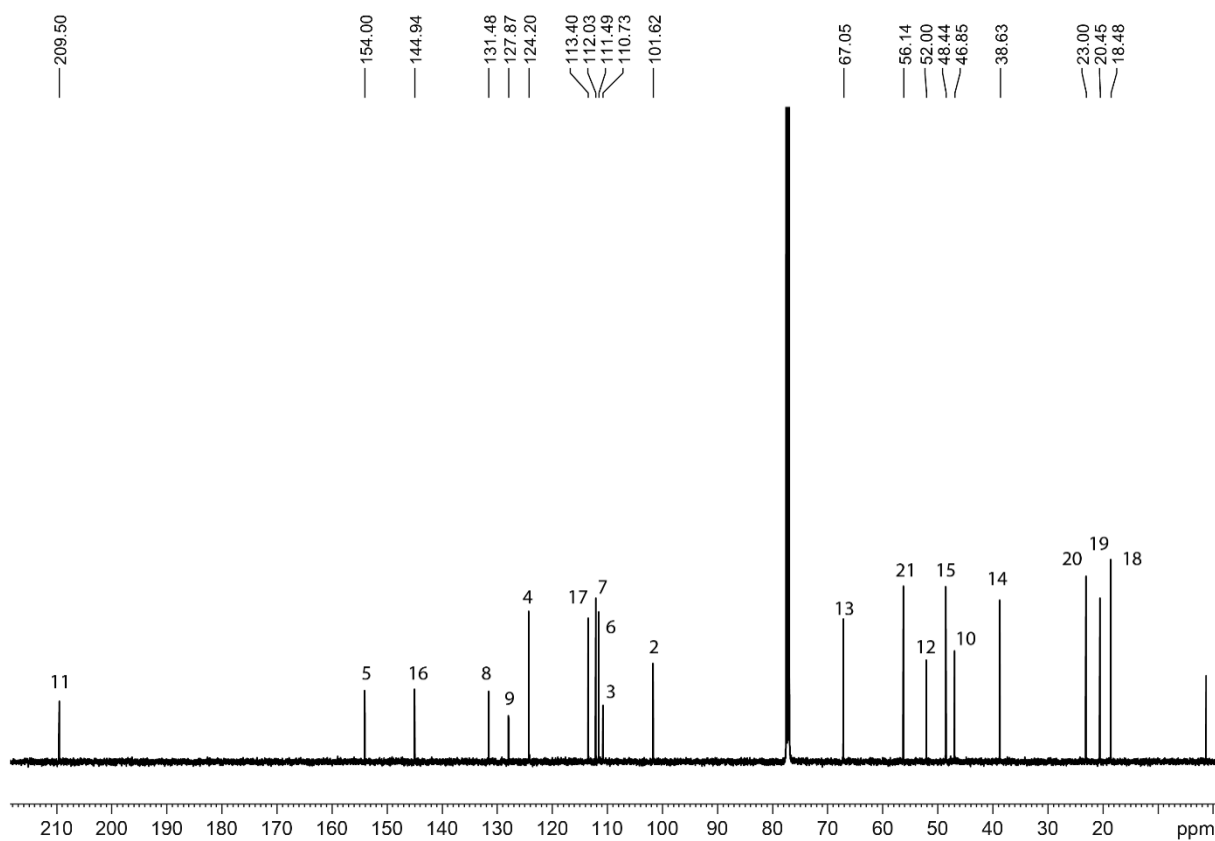


Figure 160. ¹³C-NMR of 77a measured in CDCl₃.

Appendix

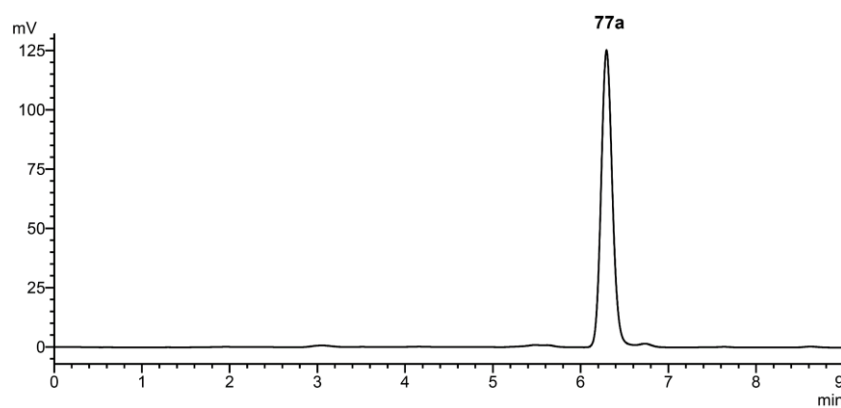


Figure 161. HPLC chromatogram of **77a**. The sample was measured on Agela Durashell C-18 column (150 mm x 4.6 mm, 5 μ m particle size + 10 mm precolumn). The analysis was performed with 1 mL/min and an isocratic flow 71 : 29 ACN-H₂O for 9 min. The retention time is 6.30 min.

8.6.1.17 Analytic of **78**

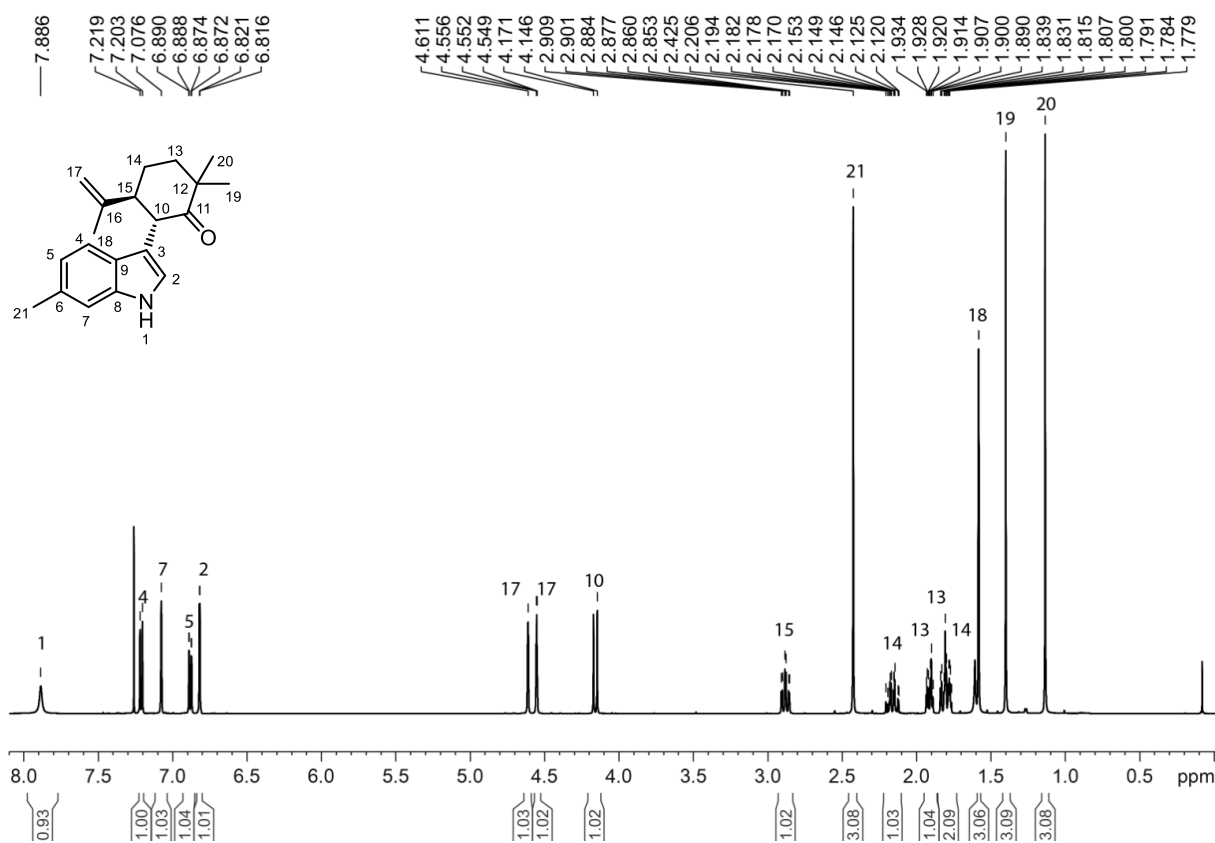


Figure 162. ¹H-NMR of **78** measured in CDCl₃.

Appendix

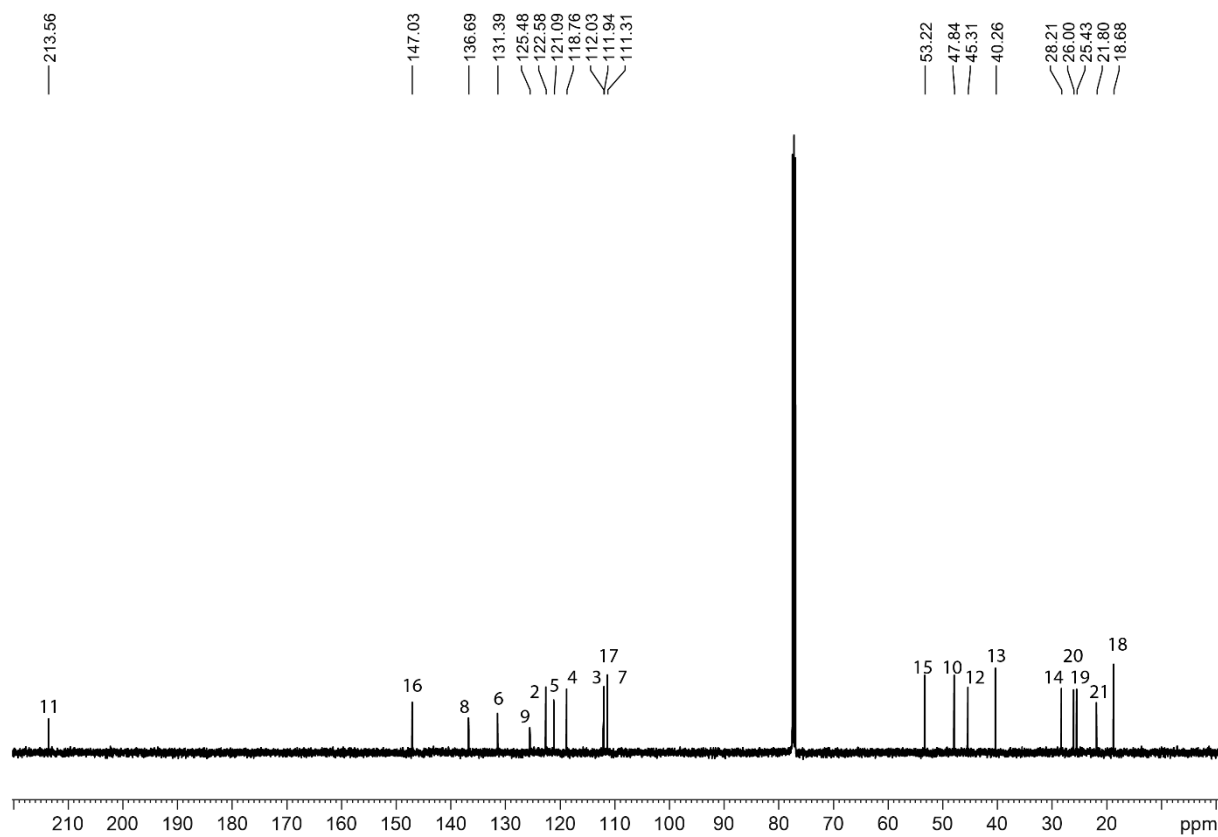


Figure 163. ^{13}C -NMR of **78** measured in CDCl_3 .

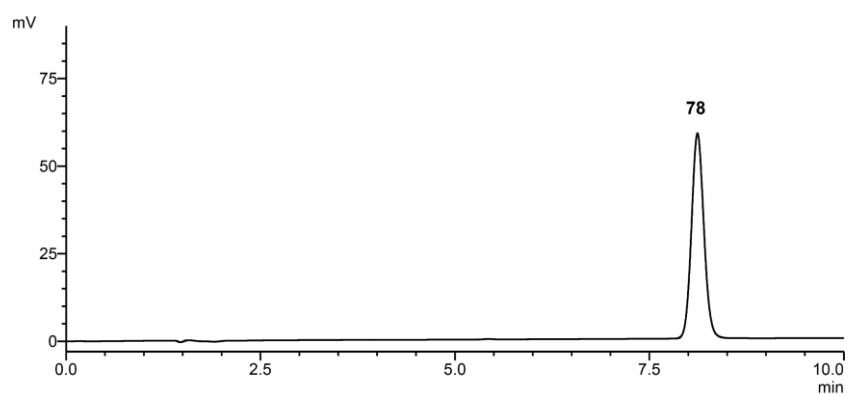
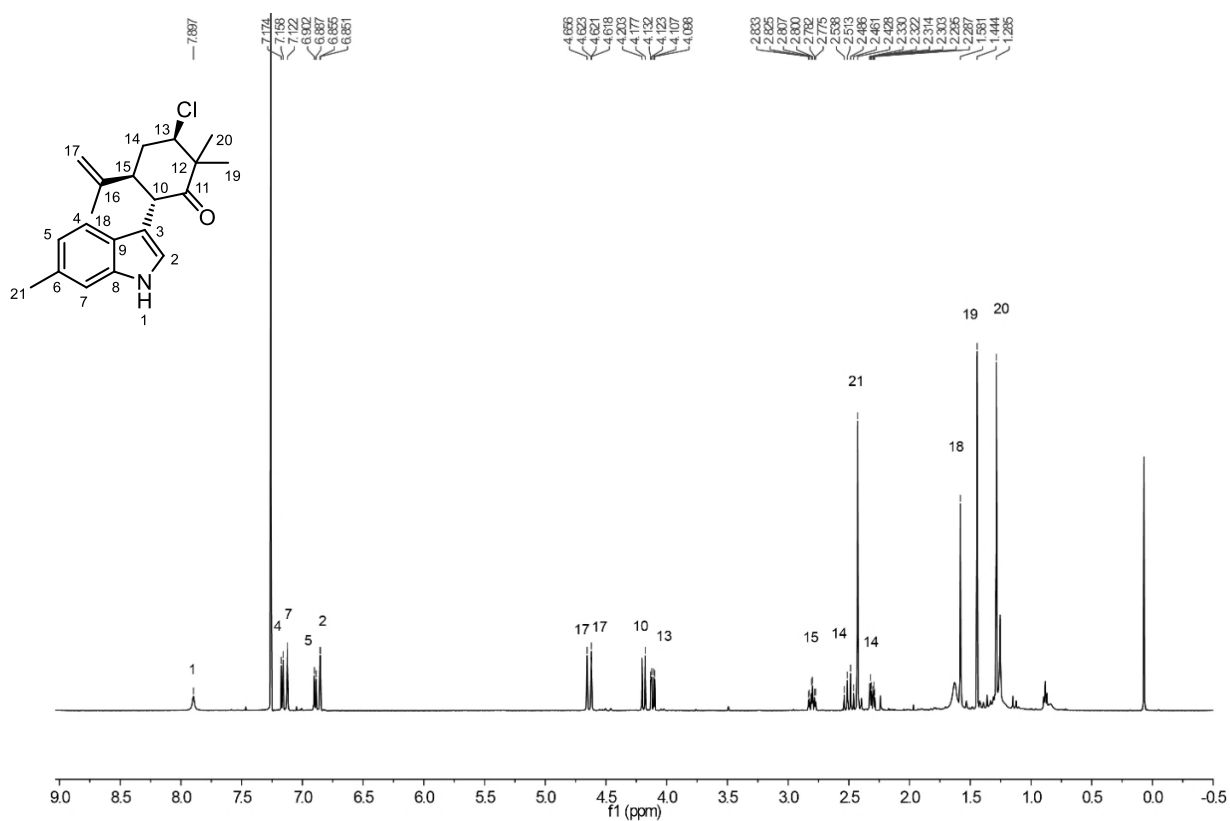
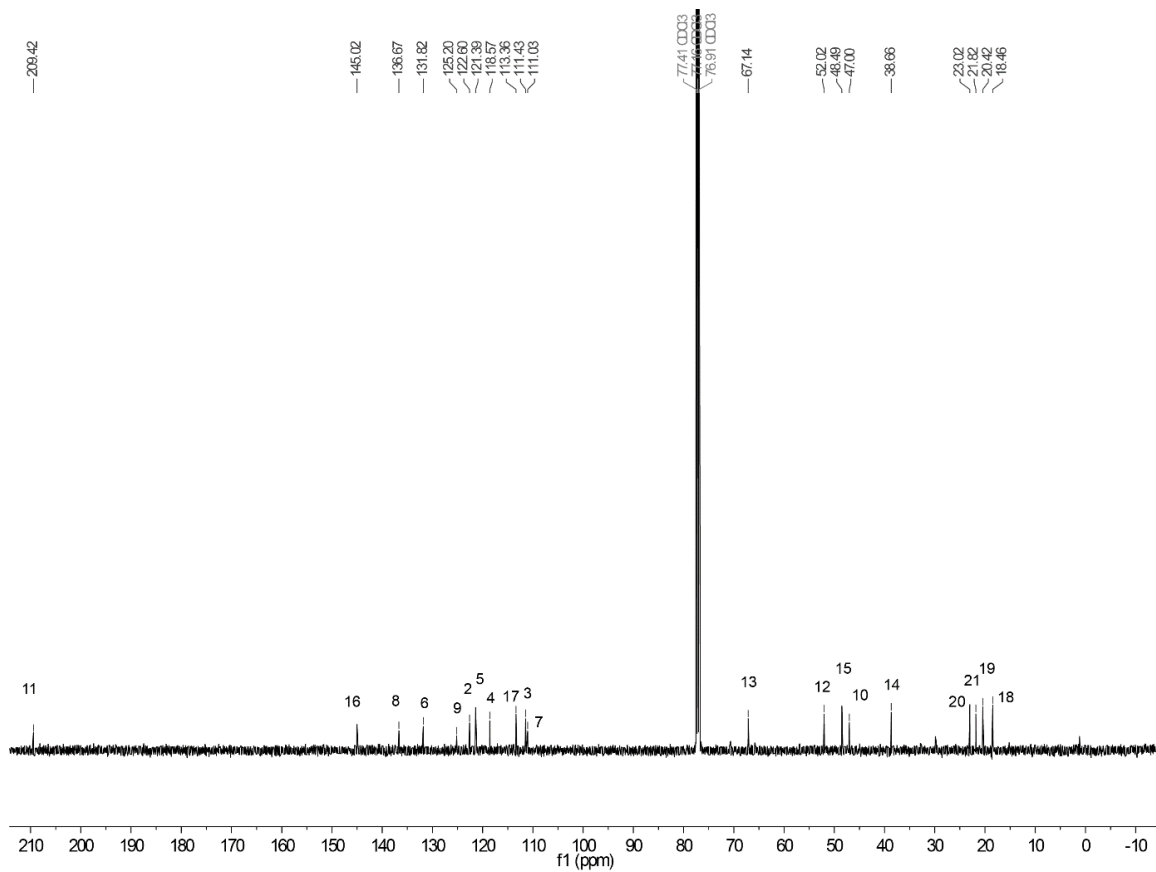


Figure 164. HPLC chromatogram of **78**. The sample was measured on Agela Durashell C-18 column (150 mm \times 4.6 mm, 5 μm particle size + 10 mm precolumn). The analysis was performed with 1 mL/min and an isocratic flow 71 : 29 ACN- H_2O for 10 min. The retention time is 8.12 min.

8.6.1.18 Analytic of 78a

Figure 165. ¹H-NMR of 78a measured in CDCl₃.Figure 166. ¹³C-NMR of 78a measured in CDCl₃.

Appendix

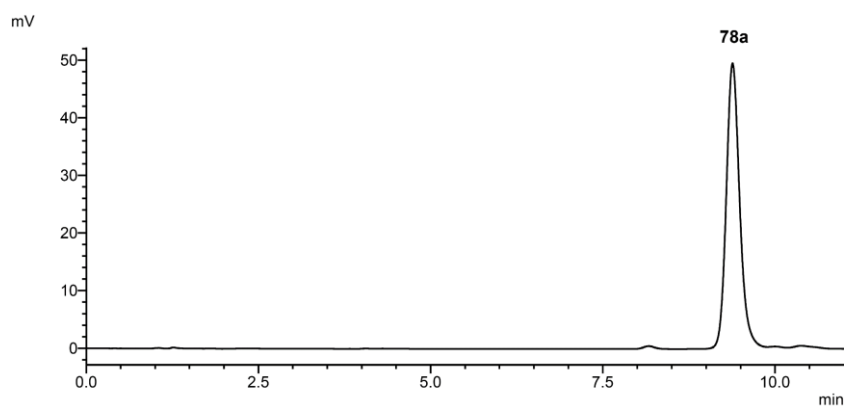


Figure 167. HPLC chromatogram of **78a**. The sample was measured on Agela Durashell C-18 column (150 mm × 4.6 mm, 5 μm particle size + 10 mm precolumn). The analysis was performed with 1 mL/min and an isocratic flow 71 : 29 ACN-H₂O for 11 min. The retention time is 9.35 min.

8.6.1.19 Analytic of 79 and 80

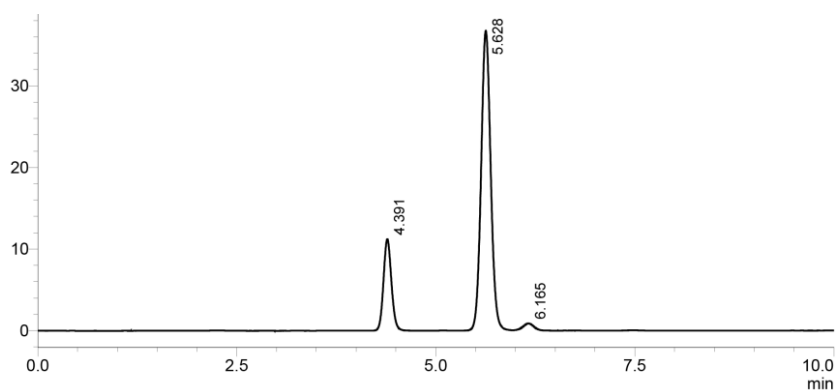


Figure 168. HPLC chromatogram of diastereomer mix of **79** (4.39 min) and **80** (5.63 min). Measurement was performed with Shimadzu LC2030 and C18 Durashell column by Agela and an isocratic flow of 60 : 40 ACN : H₂O and 1 mL/min. Detection by UV/Vis at 280 nm.

Appendix

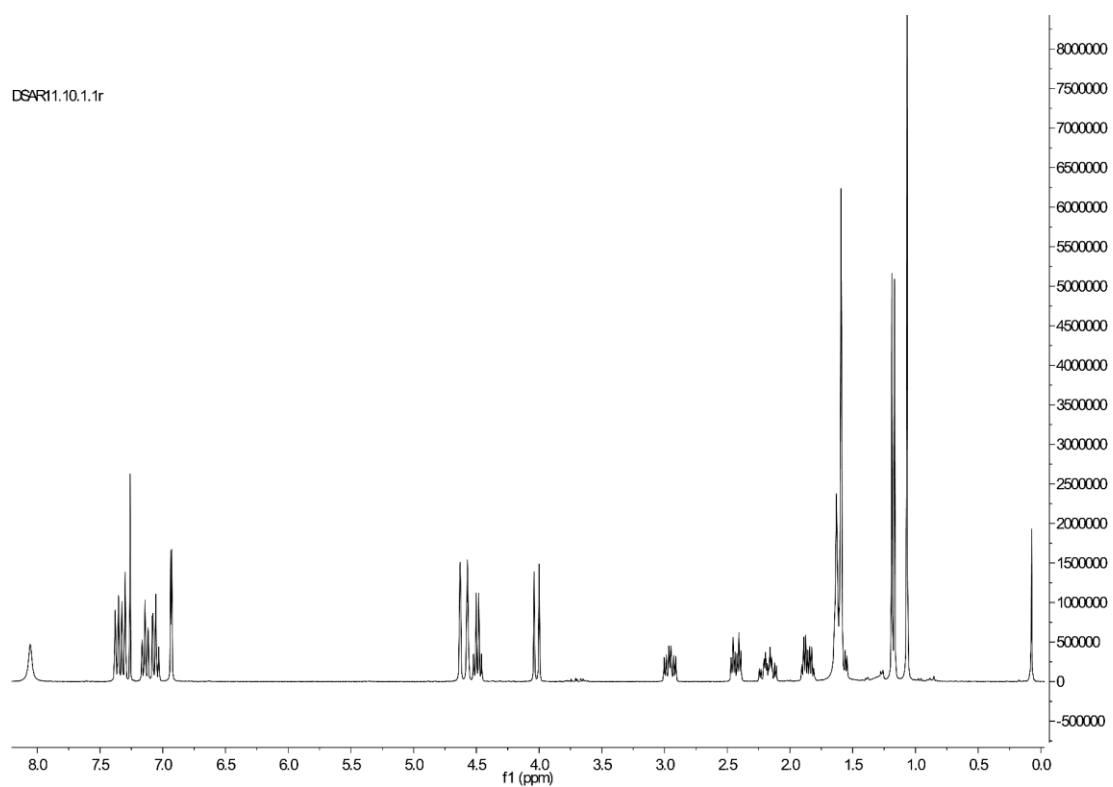


Figure 169. $^1\text{H-NMR}$ of **79** measured in CDCl_3 .

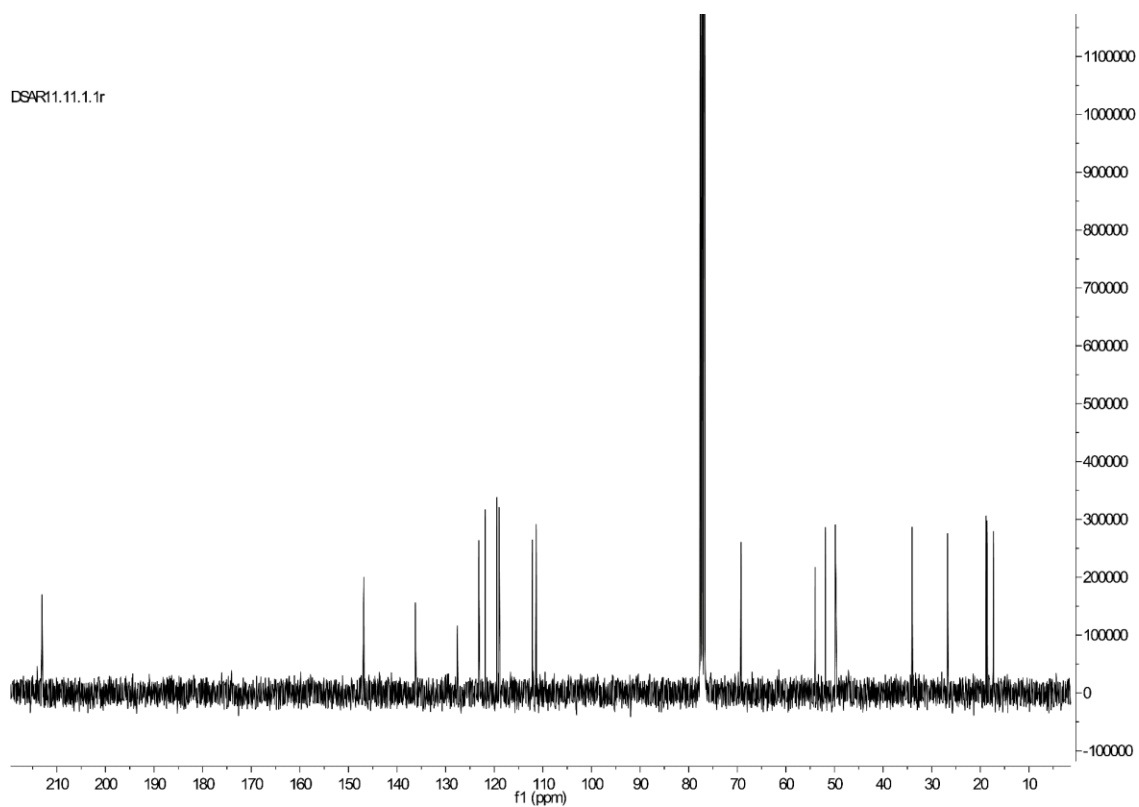


Figure 170. $^{13}\text{C-NMR}$ of **79** measured in CDCl_3 .

Appendix

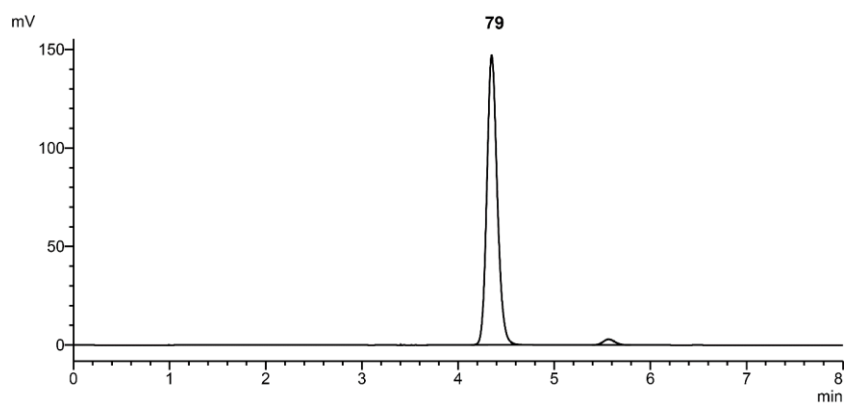


Figure 171. HPLC chromatogram of **79**. The sample was measured on Agela Durashell C-18 column (150 mm × 4.6 mm, 5 μm particle size + 10 mm precolumn). The analysis was performed with 1 mL/min and an isocratic flow 60 : 40 ACN-H₂O for 8 min. The retention time is 4.39 min.

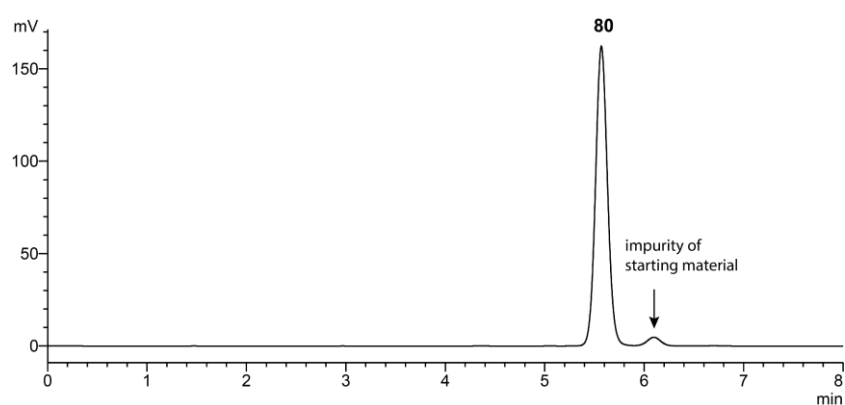


Figure 172. HPLC chromatogram of **80**. The sample was measured on Agela Durashell C-18 column (150 mm × 4.6 mm, 5 μm particle size + 10 mm precolumn). The analysis was performed with 1 mL/min and an isocratic flow 60 : 40 ACN-H₂O for 8 min. The retention time is 5.63 min.

Appendix

8.6.1.20 Analytic of 81

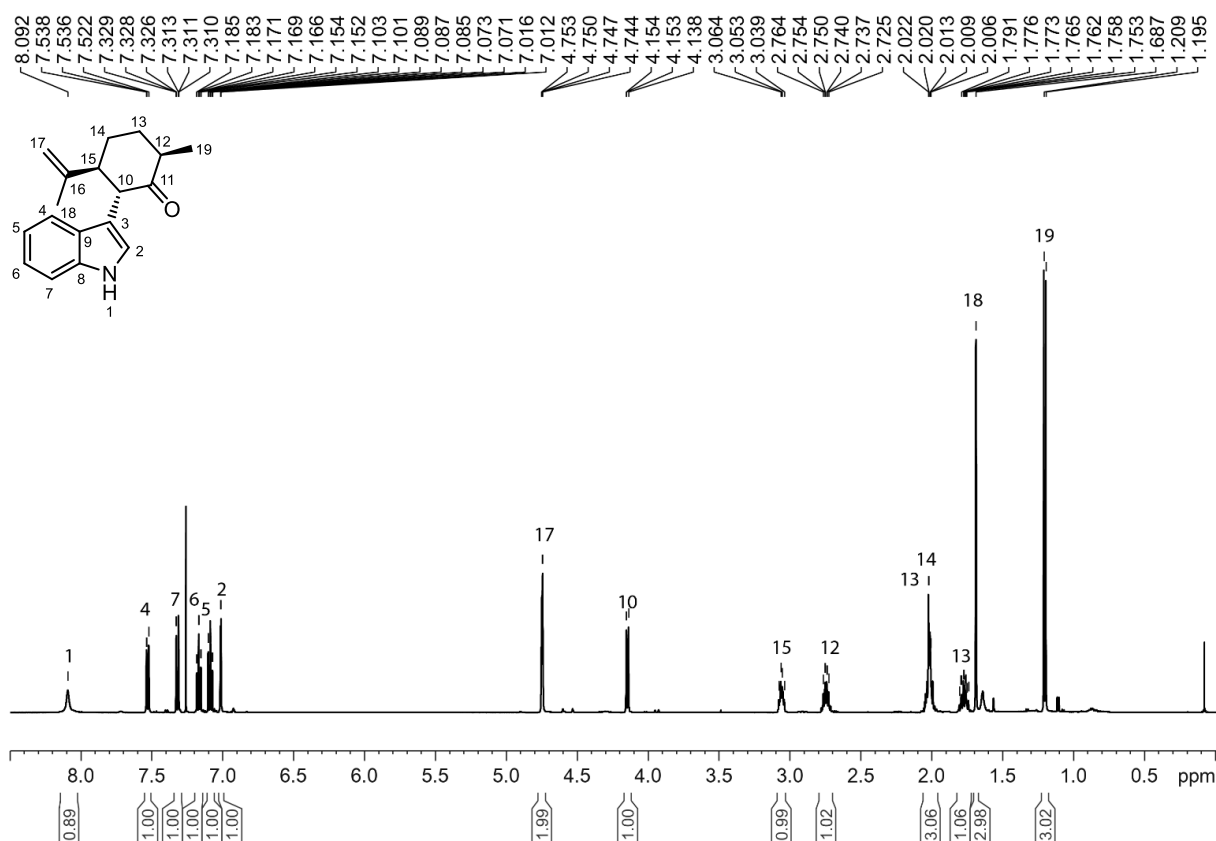


Figure 173. ¹H-NMR of 81 measured in CDCl₃.

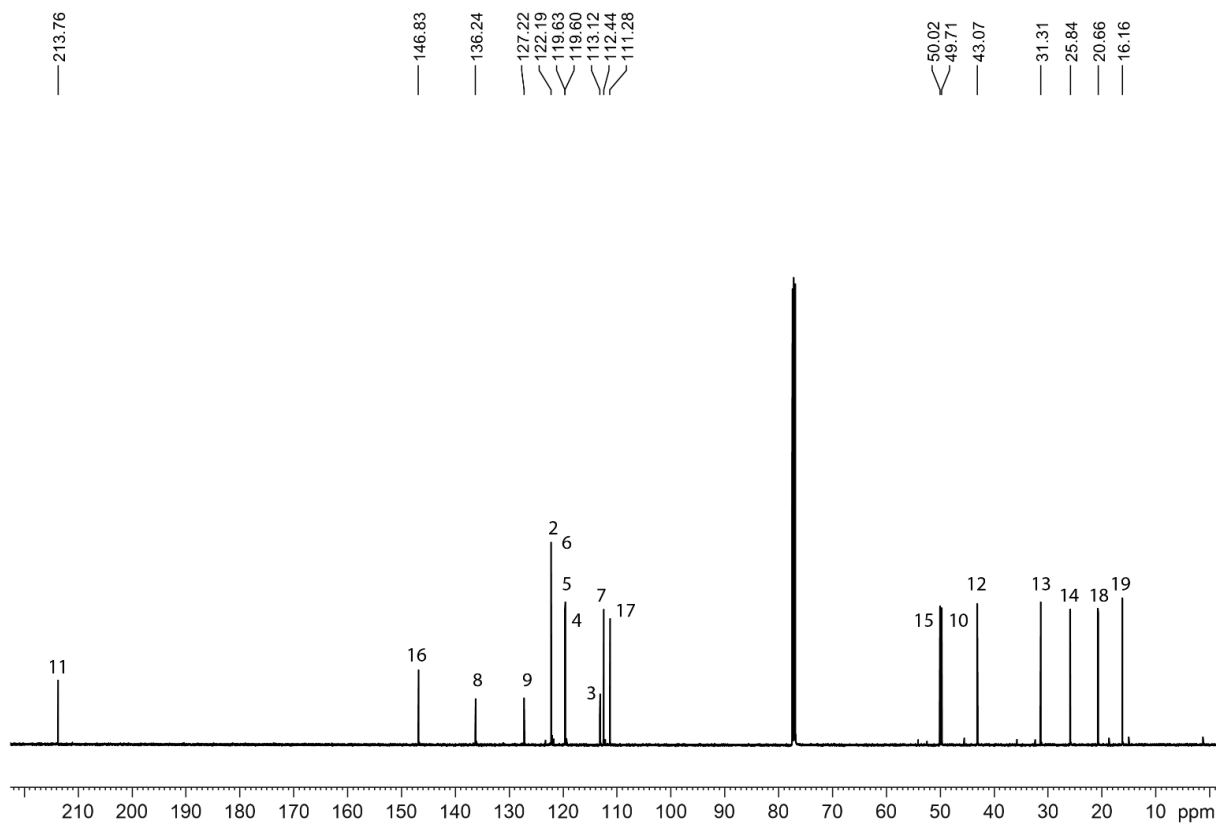


Figure 174. ¹³C-NMR of 81 measured in CDCl₃.

Appendix

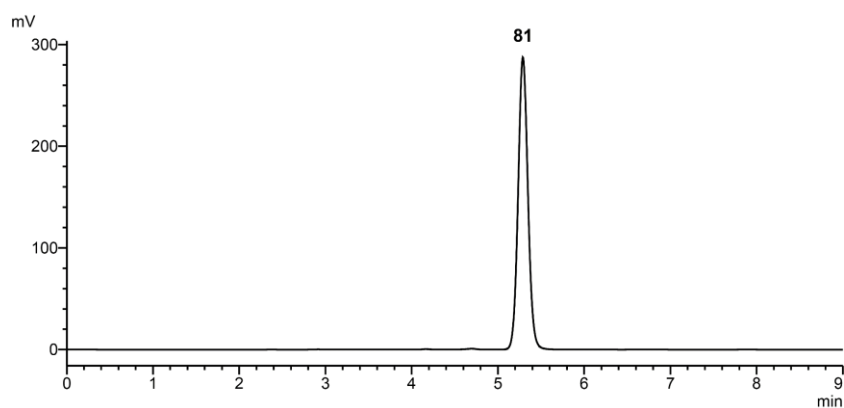


Figure 175. HPLC chromatogram of **81**. The sample was measured on Agela Durashell C-18 column (150 mm x 4.6 mm, 5 μ m particle size + 10 mm precolumn). The analysis was performed with 1 mL/min and an isocratic flow 71 : 29 ACN-H₂O for 9 min. The retention time is 5.30 min.

8.6.1.21 Analytic of **82**

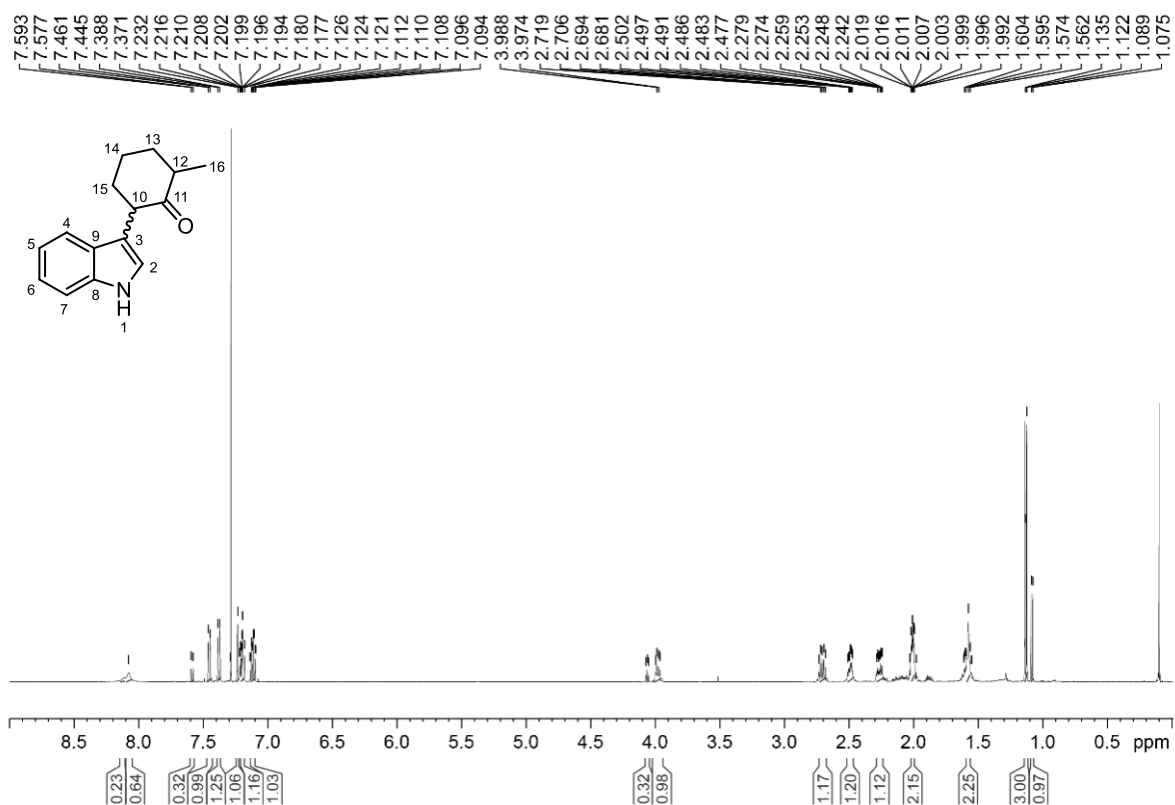


Figure 176. ¹H-NMR of **82** measured in CDCl₃.

Appendix

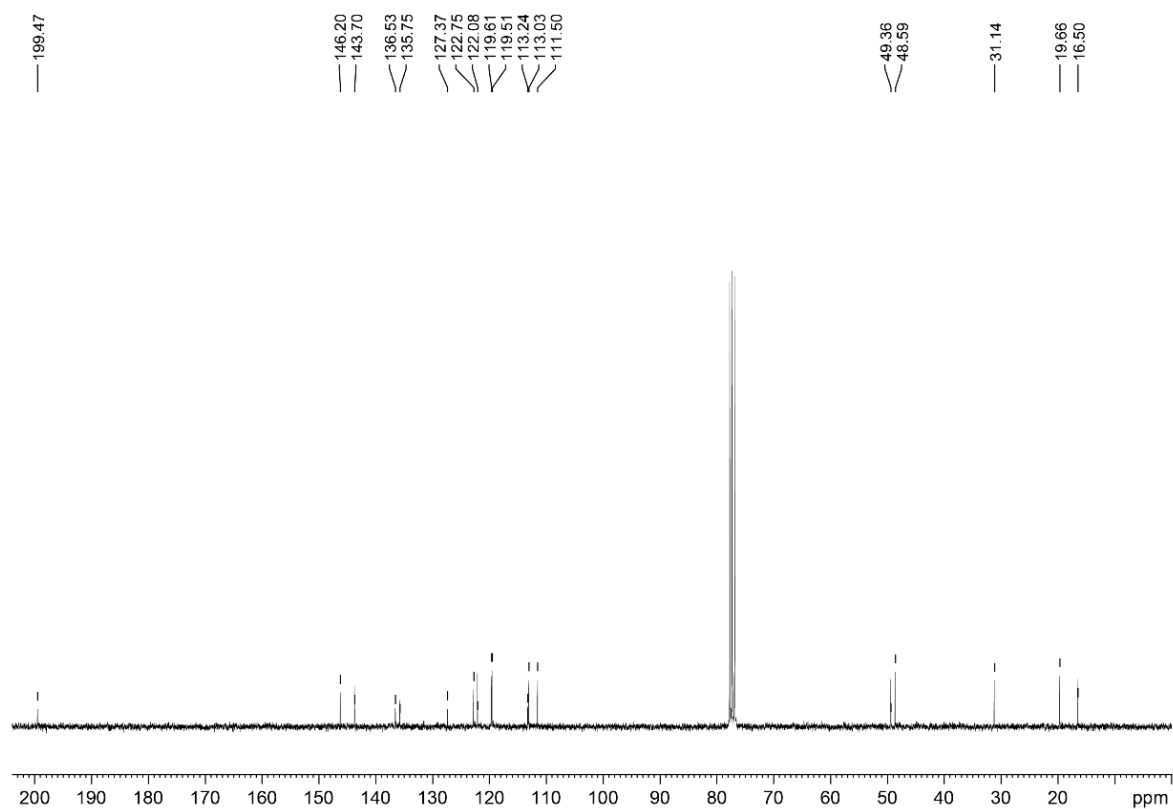


Figure 177. ^{13}C -NMR of **82** measured in CDCl_3 .

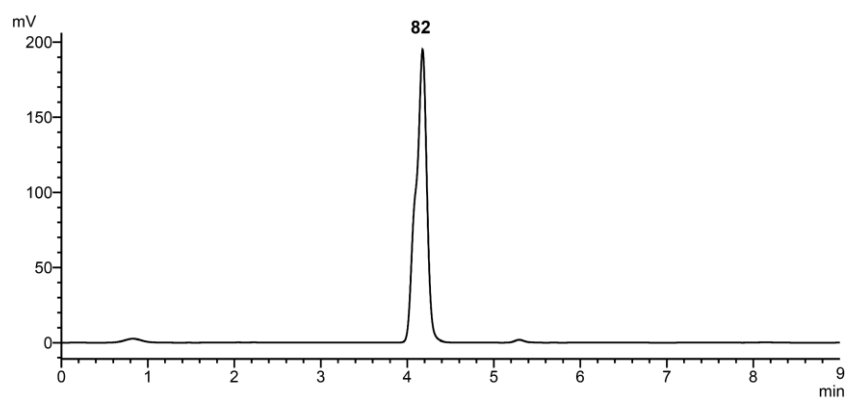
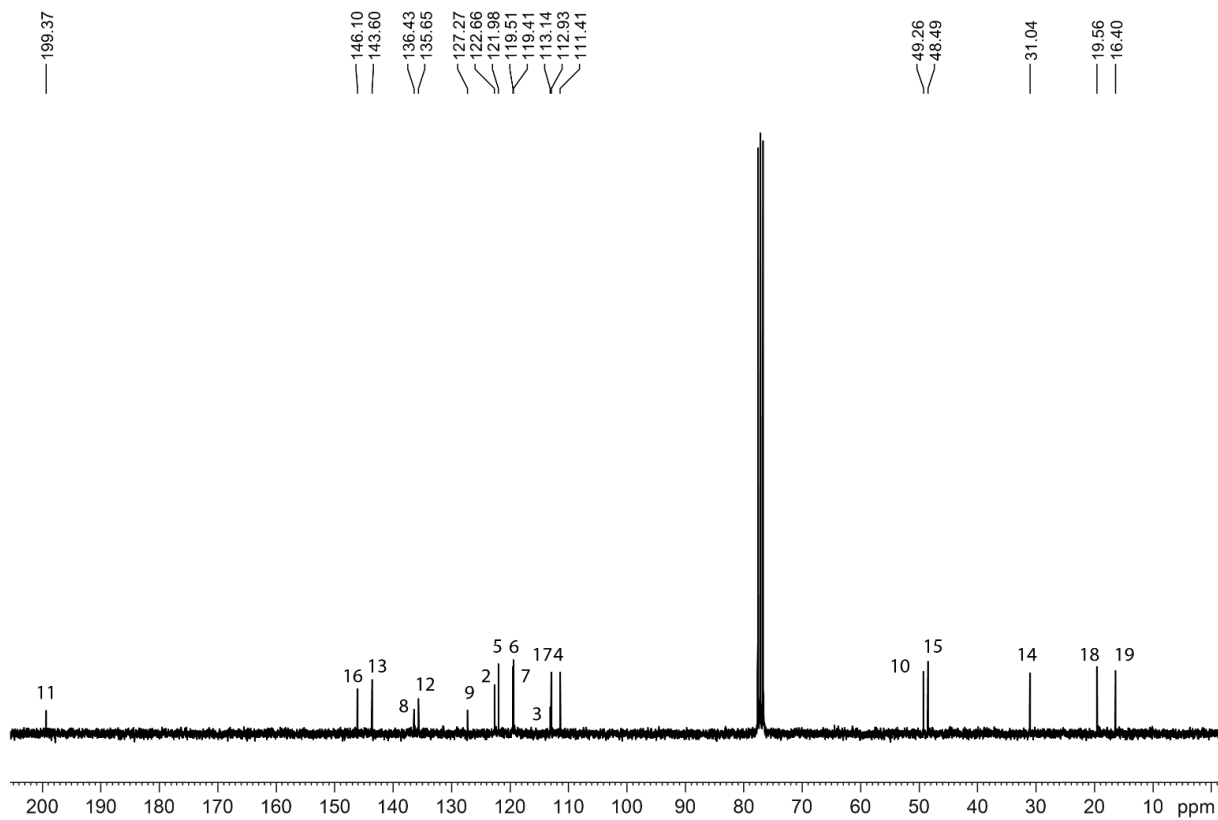
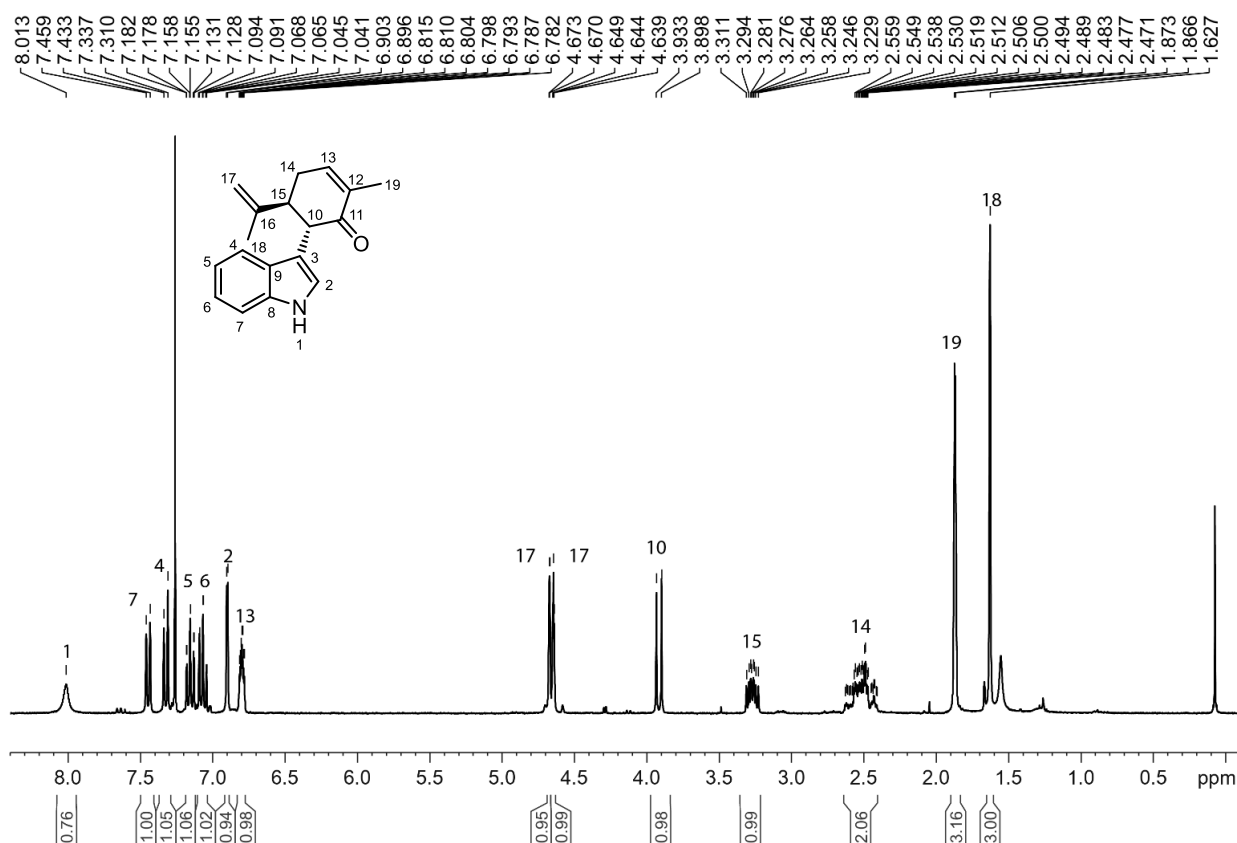


Figure 178. HPLC chromatogram of **82**. The sample was measured on Agela Durashell C-18 column (150 mm \times 4.6 mm, 5 μm particle size + 10 mm precolumn). The analysis was performed with 1 mL/min and an isocratic flow 71 : 29 ACN- H_2O for 9 min. The retention time is 4.16 min.

8.6.1.22 Analytic of 84



Appendix

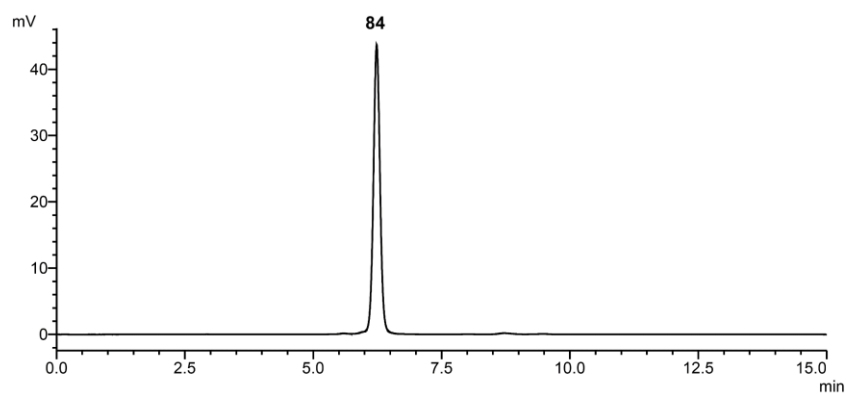


Figure 181. HPLC chromatogram of **84**. The sample was measured with an Agela Durashell C-18 column (150 mm x 4.6 mm, 5 μ m particle size + 10 mm precolumn) with an isocratic program of 65 : 35 ACN/H₂O and a flow rate of 1 mL/min. The retention time is 6.24 min.

8.6.1.23 Analytic of **85**

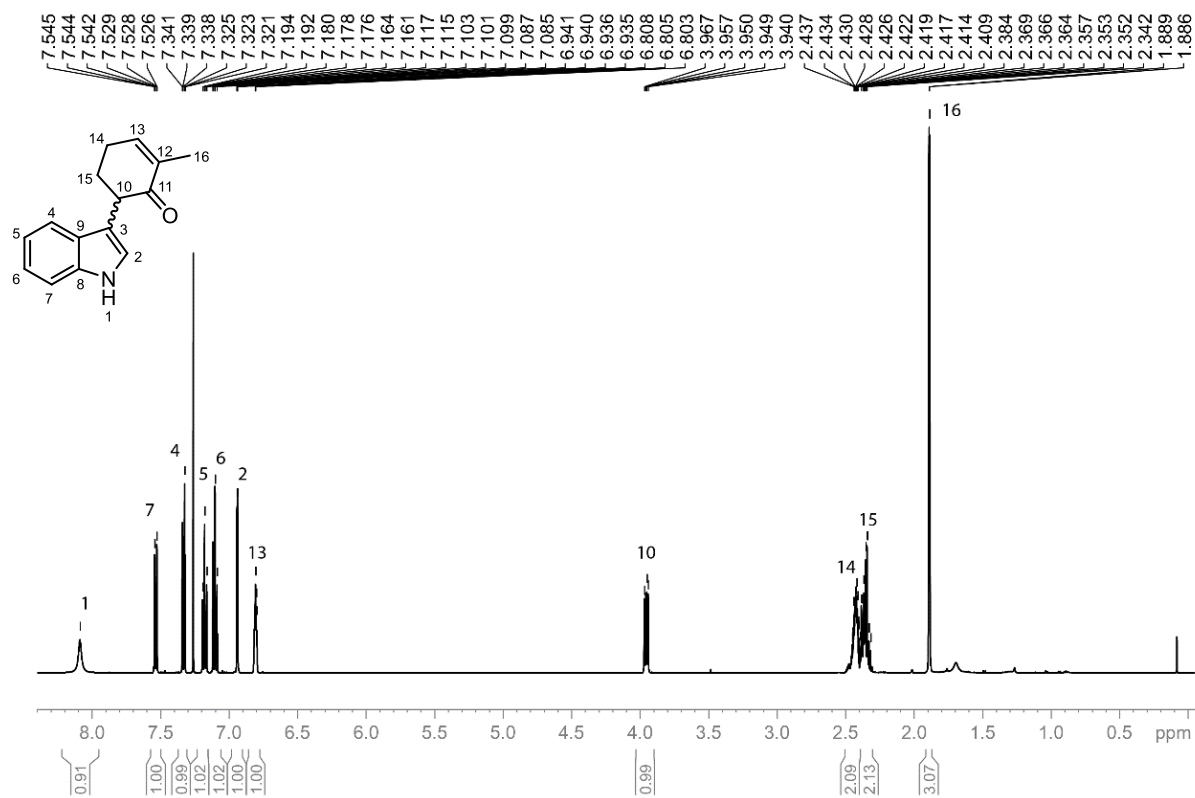


Figure 182. ¹H-NMR of **85** measured in CDCl₃.

Appendix

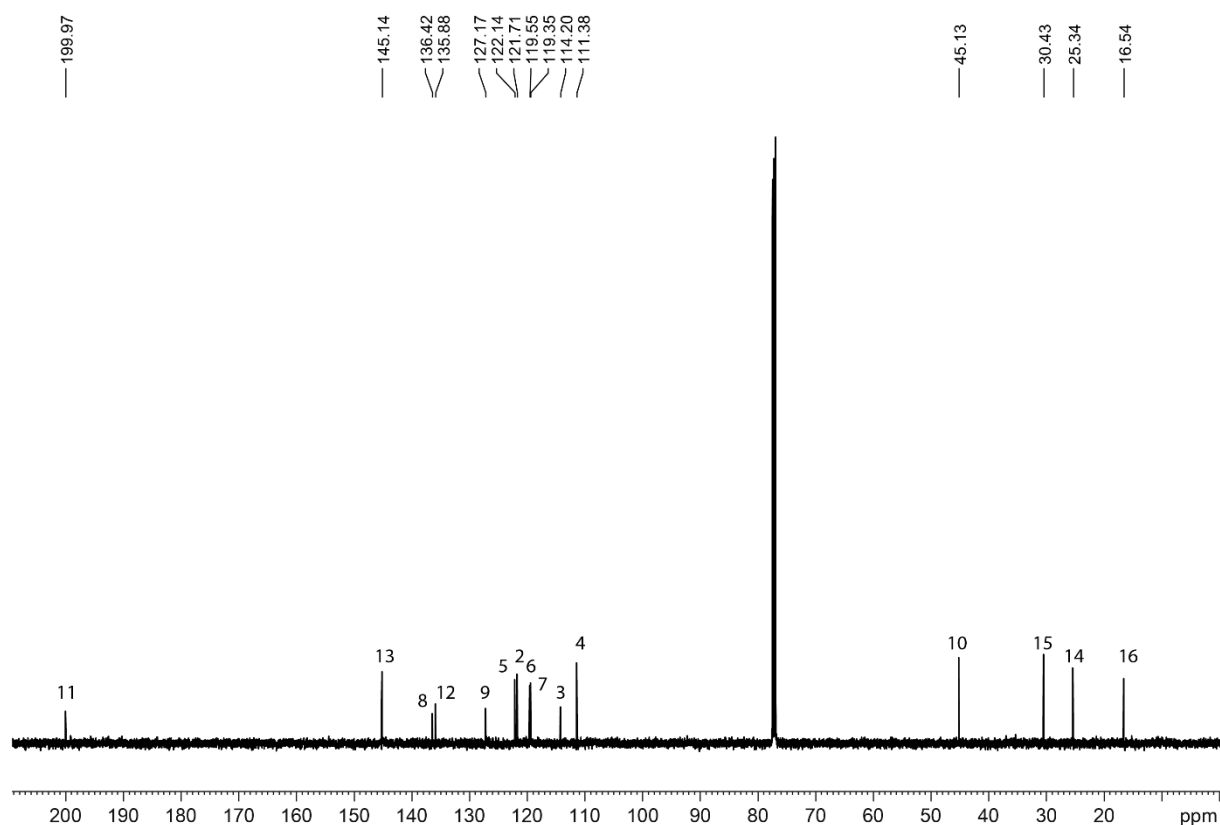


Figure 183. ^{13}C -NMR of **85** measured in CDCl_3 .

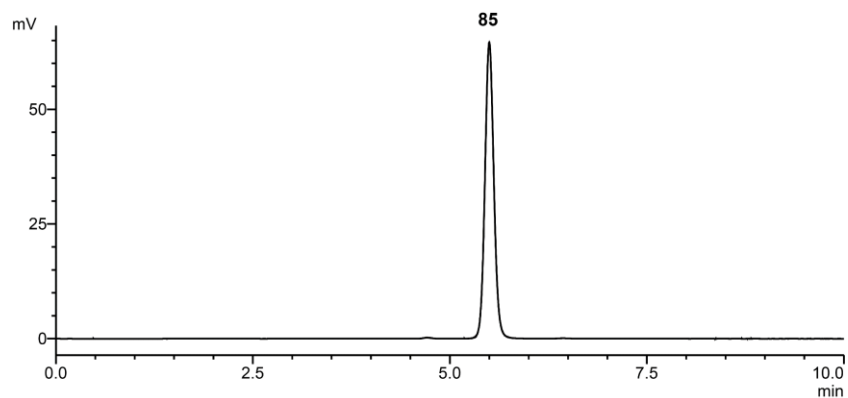


Figure 184. HPLC chromatogram of **85**. The sample was measured with an Agela Durashell C-18 column (150 mm \times 4.6 mm, 5 μm particle size + 10 mm precolumn) with an isocratic program of 60 : 40 ACN/ H_2O and a flow rate of 1 mL/min. The retention time is 5.5 min.

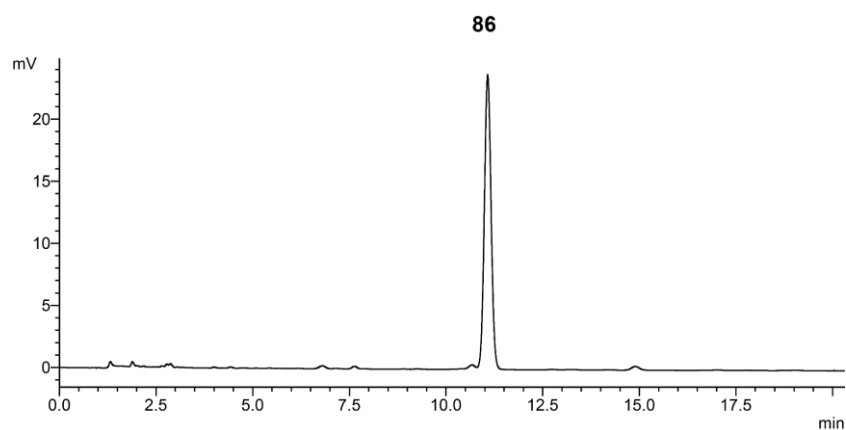
8.6.1.24 Analytic of 86

Figure 185. HPLC chromatogram of **86**. The sample was measured with Zorbax Eclipse C-18 column (150 mm x 4.6 mm, 5 μ m particle size) with an isocratic program of 63 : 37 ACN/H₂O and a flow rate of 1 mL/min. The retention time is 11 min. Detection was made at 254 nm.

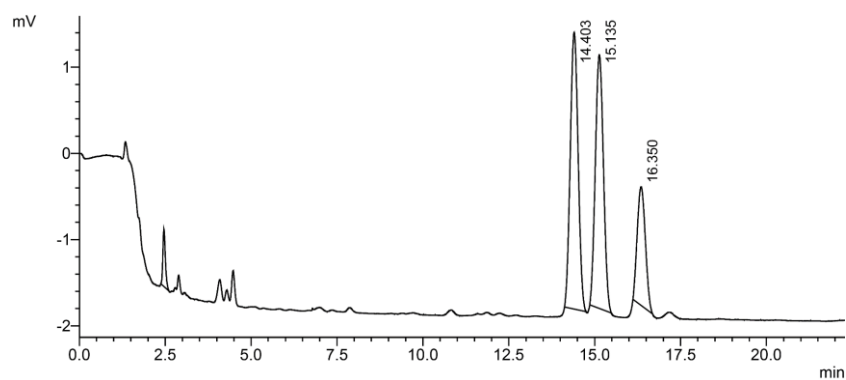
8.6.1.25 Analytic of 87

Figure 186. HPLC chromatogram of **87**. The sample was measured with Zorbax Eclipse C-18 column (150 mm x 4.6 mm, 5 μ m particle size) with an isocratic program of 55 : 45 ACN/H₂O and a flow rate of 1 mL/min. The retention time is 11 min. Detection was made at 254 nm.

9. Literature

- [1] G. W. Gribble, *Biological Activity of Recently Discovered Halogenated Marine Natural Products*, *Mar. Drugs* **2015**, 13(7), 4044–4136, DOI: 10.3390/md13074044.
- [2] G. W. Gribble, *Natural Organohalogens: A New Frontier for Medicinal Agents?*, *J. Chem. Educ.* **2004**, 81(10), 1441, DOI: 10.1021/ed081p1441.
- [3] L. N. Herrera-Rodriguez, F. Khan, K. T. Robins, H.-P. Meyer, *Perspectives on biotechnological halogenation*, *Chim. Oggi* **2011**(29).
- [4] T. L. Simmons, E. Andrianasolo, K. McPhail, P. Flatt, W. H. Gerwick, *Marine natural products as anticancer drugs*, *Mol. Cancer Ther.* **2005**(4), 333–342.
- [5] M. Hernandez, S. M. Cavalcanti, D. R. Moreira, W. de Azevedo Junior, A. C. Leite, *Halogen Atoms in the Modern Medicinal Chemistry*, *Curr. Drug Targets* **2010**, 11(3), 303–314, DOI: 10.2174/138945010790711996.
- [6] P. Jeschke, *The unique role of halogen substituents in the design of modern agrochemicals*, *Pest Manage. Sci.* **2010**, 66(1), 10–27, DOI: 10.1002/ps.1829.
- [7] G. W. Gribble, *A recent survey of naturally occurring organohalogen compounds*, *Environ. Chem. Lett.* **2015**, 12(4), 396, DOI: 10.1071/EN15002.
- [8] G. W. Gribble, *Naturally occurring organohalogen compounds: A comprehensive update*; Springer-Verlag; SpringerWienNewYork, Wien, New York, **2010**.
- [9] P. D. Nightingale, G. Malin, P. S. Liss, *Production of chloroform and other low molecular-weight halocarbons by some species of macroalgae*, *Limnol. Oceanogr.* **1995**, 40(4), 680–689, DOI: 10.4319/lo.1995.40.4.0680.
- [10] M. T. Cabrita, C. Vale, A. P. Rauter, *Halogenated compounds from marine algae*, *Mar. Drugs* **2010**, 8(8), 2301–2317, DOI: 10.3390/md8082301.
- [11] M. H. McCormick, J. M. McGuire, G. E. Pittenger, Pittenger R. C, W. M. Stark, *Vancomycin, a new antibiotic. I. Chemical and biologic properties*, *Antibiotics annual* **1955**, 3, 606–611.
- [12] L. T. Wright, *Aureomycin*, *J. Am. Med. Assoc.* **1948**, 138(6), 408, DOI: 10.1001/jama.1948.02900060012006.
- [13] J. Ehrlich, Q. R. Bartz, R. M. Smith, D. A. Joslyn, P. R. Burkholder, *Chloromycetin, a New Antibiotic From a Soil Actinomycete*, *Science* **1947**, 106(2757), 417, DOI: 10.1126/science.106.2757.417.
- [14] N. T. Doan, R. W. Rickards, J. M. Rothschild, G. D. Smith, *Allelopathic actions of the alkaloid 12-epi-hapalindole E isonitrile and calothrixin A from cyanobacteria of the genera Fischerella and Calothrix*, *J. Appl. Phycol.* **2000**, 12(3), 409–416, DOI: 10.1023/A:1008170007044.
- [15] C. Malochet-Grivois, C. Roussakis, N. Robillard, J. F. Biard, D. Riou, C. Débitus, J. F. Verbist, *Effects in vitro of two marine substances, chlorolissoclimide and dichlorolissoclimide, on a non-small-cell bronchopulmonary carcinoma line (NSCLC-N6)*, *Anti-cancer drug design* **1992**, 7(6), 493–502.

- [16] D. J. Edwards, B. L. Marquez, L. M. Nogle, K. McPhail, D. E. Goeger, M. A. Roberts, W. H. Gerwick, *Structure and biosynthesis of the jamaicamides, new mixed polyketide-peptide neurotoxins from the marine cyanobacterium Lyngbya majuscula*, *Chem. Biol.* **2004**, *11*(6), 817–833, DOI: 10.1016/j.chembiol.2004.03.030.
- [17] C. M. Harris, R. Kannan, H. Kopecka, Harris T. M, *The role of the chlorine substituents in the antibiotic vancomycin: preparation and characterization of mono- and didechlorovancomycin*, *J. Am. Chem. Soc.* **1985**(23), 6652–6658, DOI: 10.1021/ja00309a038.
- [18] L. A. Hardegger, B. Kuhn, B. Spinnler, L. Anselm, R. Ecabert, M. Stihle, B. Gsell, R. Thoma, J. Diez, J. Benz, J.-M. Plancher, G. Hartmann, D. W. Banner, W. Haap, F. Diederich, *Systematic investigation of halogen bonding in protein-ligand interactions*, *Angew. Chem. Int. Ed.* **2011**, *50*(1), 314–318, DOI: 10.1002/anie.201006781.
- [19] Z. Xu, Z. Yang, Y. Liu, Y. Lu, K. Chen, W. Zhu, *Halogen bond*, *J. Chem. Inf. Model.* **2014**, *54*(1), 69–78, DOI: 10.1021/ci400539q.
- [20] Y. Lu, T. Shi, Y. Wang, H. Yang, X. Yan, X. Luo, H. Jiang, W. Zhu, *Halogen bonding—a novel interaction for rational drug design?*, *J. Med. Chem.* **2009**, *52*(9), 2854–2862, DOI: 10.1021/jm9000133.
- [21] Z. Xu, Z. Liu, T. Chen, T. Chen, Z. Wang, G. Tian, J. Shi, X. Wang, Y. Lu, X. Yan, G. Wang, H. Jiang, K. Chen, S. Wang, Y. Xu, J. Shen, W. Zhu, *Utilization of halogen bond in lead optimization*, *J. Med. Chem.* **2011**, *54*(15), 5607–5611, DOI: 10.1021/jm200644r.
- [22] R. Wilcken, M. O. Zimmermann, A. Lange, A. C. Joerger, F. M. Boeckler, *Principles and applications of halogen bonding in medicinal chemistry and chemical biology*, *J. Med. Chem.* **2013**, *56*(4), 1363–1388, DOI: 10.1021/jm3012068.
- [23] J. F. Hartwig, *Evolution of C-H Bond Functionalization from Methane to Methodology*, *J. Am. Chem. Soc.* **2016**, *138*(1), 2–24, DOI: 10.1021/jacs.5b08707.
- [24] P. Ruiz-Castillo, S. L. Buchwald, *Applications of Palladium-Catalyzed C-N Cross-Coupling Reactions*, *Chem. Rev.* **2016**, *116*(19), 12564–12649, DOI: 10.1021/acs.chemrev.6b00512.
- [25] F.-S. Han, *Transition-metal-catalyzed Suzuki-Miyaura cross-coupling reactions*, *Chem. Soc. Rev.* **2013**, *42*(12), 5270–5298, DOI: 10.1039/c3cs35521g.
- [26] K. C. Nicolaou, P. G. Bulger, D. Sarlah, *Palladium-catalyzed cross-coupling reactions in total synthesis*, *Angew. Chem. Int. Ed.* **2005**, *44*(29), 4442–4489, DOI: 10.1002/anie.200500368.
- [27] J. F. Hartwig, *Carbon-heteroatom bond formation catalysed by organometallic complexes*, *Nature* **2008**, *455*(7211), 314–322, DOI: 10.1038/nature07369.
- [28] S. Z. Tasker, E. A. Standley, T. F. Jamison, *Recent advances in homogeneous nickel catalysis*, *Nature* **2014**, *509*(7500), 299–309, DOI: 10.1038/nature13274.
- [29] T. Kuranaga, Y. Sesoko, M. Inoue, *Cu-mediated enamide formation in the total synthesis of complex peptide natural products*, *Nat. Prod. Rep.* **2014**, *31*(4), 514–532, DOI: 10.1039/c3np70103d.

- [30] F. Monnier, M. Taillefer, *Catalytic C-C, C-N, and C-O Ullmann-type coupling reactions*, *Angew. Chem. Int. Ed.* **2009**, 48(38), 6954–6971, DOI: 10.1002/anie.200804497.
- [31] V. F. Slagt, A. H. M. de Vries, J. G. de Vries, R. M. Kellogg, *Practical Aspects of Carbon–Carbon Cross-Coupling Reactions Using Heteroarenes*, *Org. Process Res. Dev.* **2010**, 14(1), 30–47, DOI: 10.1021/op900221v.
- [32] H. M. L. Davies, D. Morton, *Guiding principles for site selective and stereoselective intermolecular C-H functionalization by donor/acceptor rhodium carbenes*, *Chem. Soc. Rev.* **2011**, 40(4), 1857–1869, DOI: 10.1039/c0cs00217h.
- [33] A. Raveh, S. Carmeli, *Antimicrobial ambiguines from the cyanobacterium Fischerella sp. collected in Israel*, *J. Nat. Prod.* **2007**, 70(2), 196–201, DOI: 10.1021/np060495r.
- [34] N.-Y. Ji, X.-M. Li, K. Li, B.-G. Wang, *Halogenated Sesquiterpenes from the Marine Red Alga Laurencia saitoi (Rhodomelaceae)*, *HCA* **2009**, 92(9), 1873–1879, DOI: 10.1002/hlca.200900073.
- [35] E. T. McBee, H. B. Hass, and Earl. Pierson, *Chlorinolysis of Chloropentanes*, *Ind. Eng. Chem.* **1941**(2), 181–185.
- [36] E. T. McBee, H. B. Hass, C. M. Neher, and H. Strickland, *Chlorination of Methane*, *Ind. Eng. Chem.* **1942**(3), 296–300.
- [37] P. S. Skell, H. N. Baxter, *Multiple substitutions in radical-chain chlorinations. A new cage effect*, *J. Am. Chem. Soc.* **1985**(9), 2823–2824, DOI: 10.1021/ja00295a054.
- [38] Russell G. A, Brown H. C, *The Liquid Phase Photochlorination and Sulfuryl Chloride Chlorination of Branchedchain Hydrocarbons; the Effect of Structure on the Relative Reactivities of Tertiary Hydrogen in Free Radical Chlorinations*, *J. Am. Chem. Soc.* **1955**(15), 4031–4035, DOI: 10.1021/ja01620a021.
- [39] C. Djerassi, *Brominations with N-Bromosuccinimide and Related Compounds. The Wohl-Ziegler Reaction*, *Chem. Rev.* **1948**(2), 271–317, DOI: 10.1021/cr60135a004.
- [40] F. Minisci, R. Galli, A. Galli, R. Bernardi, *A new, highly selective type of radical chlorination*, *Tetrahedron Lett.* **1967**(23), 2207–2209, DOI: 10.1016/S0040-4039(00)90798-6.
- [41] R. K. Quinn, Z. A. Konst, S. E. Michalak, Y. Schmidt, A. R. Szklarski, A. R. Flores, S. Nam, D. A. Horne, C. D. Vanderwal, E. J. Alexanian, *Site-Selective Aliphatic C-H Chlorination Using N-Chloroamides Enables a Synthesis of Chlorolissoclimide*, *J. Am. Chem. Soc.* **2016**, 138(2), 696–702, DOI: 10.1021/jacs.5b12308.
- [42] V. A. Schmidt, R. K. Quinn, A. T. Brusoe, E. J. Alexanian, *Site-selective aliphatic C-H bromination using N-bromoamides and visible light*, *J. Am. Chem. Soc.* **2014**, 136(41), 14389–14392, DOI: 10.1021/ja508469u.
- [43] P. A. Delaney, R. A.W. Johnstone, Entwistle Ian D, *Ring opening and Dimerization of Cyclic Ethers by Titanium Halides*, *J. Chem. Soc. Perkin Trans.* **1986**(0), 1855–1860, DOI: 10.1039/P19860001855.

- [44] M. Koreeda, R. Gopaldaswamy, *Regio- and Stereocontrolled Synthesis of the Bay-Region anti-Diol Epoxide Metabolites of the Potent Carcinogens Benzo[a]pyrene and 7,12-Dimethylbenz[a]anthracene*, *J. Am. Chem. Soc.* **1995**, *117*(42), 10595–10596, DOI: 10.1021/ja00147a031.
- [45] D. L. J. Clive, M. Sannigrahi, S. Hisaindee, *Synthesis of (±)-Puraquinonic Acid*, *J. Org. Chem.* **2001**, *66*(3), 954–961, DOI: 10.1021/jo001523s.
- [46] K. E. MaloneyHuss, P. S. Portoghese, *Synthesis of novel 6.beta,14-epoxy-bridged opiates*, *J. Org. Chem.* **1990**(9), 2957–2959, DOI: 10.1021/jo00296a074.
- [47] N. A. Weires, E. D. Styduhar, E. L. Baker, N. K. Garg, *Total synthesis of (-)-N-methylwelwitindolinone B isothiocyanate via a chlorinative oxabicyclic ring-opening strategy*, *J. Am. Chem. Soc.* **2014**, *136*(42), 14710–14713, DOI: 10.1021/ja5087672.
- [48] L. Hunter, D. O'Hagan, A. M. Z. Slawin, *Enantioselective synthesis of an all-syn four vicinal fluorine motif*, *J. Am. Chem. Soc.* **2006**, *128*(51), 16422–16423, DOI: 10.1021/ja066188p.
- [49] N. Halland, A. Braunton, S. Bachmann, M. Marigo, K. A. Jørgensen, *Direct organocatalytic asymmetric alpha-chlorination of aldehydes*, *J. Am. Chem. Soc.* **2004**, *126*(15), 4790–4791, DOI: 10.1021/ja049231m.
- [50] M. D. Dowle, D. I. Davies, *Synthesis and synthetic utility of halolactones*, *Chem. Soc. Rev.* **1979**(8), 171–197, DOI: 10.1039/CS9790800171.
- [51] S. Hu, S. Jayaraman, A. C. Oehlschlager, *Diastereoselective Chloroallylboration of α -Chiral Aldehydes*, *J. Org. Chem.* **1998**, *63*(24), 8843–8849, DOI: 10.1021/jo980977a.
- [52] L. Hintermann, A. Togni, *Catalytic Enantioselective Fluorination of β -Ketoesters*, *Angew. Chem. Int. Ed.* **2000**, *39*(23), 4359–4362, DOI: 10.1002/1521-3773(20001201)39:23<4359:AID-ANIE4359>3.0.CO;2-P.
- [53] A. M. Hafez, A. E. Taggi, H. Wack, J. Esterbrook, T. Lectka, *Reactive Ketenes through a Carbonate/Amine Shuttle Deprotonation Strategy*, *Org. Lett.* **2001**, *3*(13), 2049–2051, DOI: 10.1021/ol0160147.
- [54] H. Wack, A. E. Taggi, A. M. Hafez, W. J. Drury, T. Lectka, *Catalytic, Asymmetric α -Halogenation*, *J. Am. Chem. Soc.* **2001**, *123*(7), 1531–1532, DOI: 10.1021/ja005791j.
- [55] M. P. Brochu, S. P. Brown, D. W. C. MacMillan, *Direct and enantioselective organocatalytic alpha-chlorination of aldehydes*, *J. Am. Chem. Soc.* **2004**, *126*(13), 4108–4109, DOI: 10.1021/ja049562z.
- [56] E. C. Lee, K. M. McCauley, G. C. Fu, *Catalytic asymmetric synthesis of tertiary alkyl chlorides*, *Angew. Chem. Int. Ed.* **2007**, *46*(6), 977–979, DOI: 10.1002/anie.200604312.
- [57] M. Oestreich, *Strategies for catalytic asymmetric electrophilic alpha halogenation of carbonyl compounds*, *Angew. Chem. Int. Ed.* **2005**, *44*(16), 2324–2327, DOI: 10.1002/anie.200500478.
- [58] M. Ueda, T. Kano, K. Maruoka, *Organocatalyzed direct asymmetric alpha-halogenation of carbonyl compounds*, *Org. Biomol. Chem.* **2009**, *7*(10), 2005–2012, DOI: 10.1039/b901449g.
- [59] A. Castellanos, S. P. Fletcher, *Current methods for asymmetric halogenation of olefins*, *Chem. Eur. J.* **2011**, *17*(21), 5766–5776, DOI: 10.1002/chem.201100105.

- [60] J. Rodriguez, J.-P. Dulcère, *Cohalogenation in Organic Synthesis*, *Synthesis* **1993**(12), 1177–1205, DOI: 10.1055/s-1993-26022.
- [61] M. J. R. Bougault, *Acad. Sci.* **1904**(139), 864.
- [62] A. N. French, S. Bissmire, T. Wirth, *Iodine electrophiles in stereoselective reactions*, *Chem. Soc. Rev.* **2004**, 33(6), 354–362, DOI: 10.1039/b310389g.
- [63] H. Ibrahim, A. Togni, *Enantioselective halogenation reactions*, *Chem. Commun.* **2004**(10), 1147, DOI: 10.1039/b317004g.
- [64] G. Guillena, D. J. Ramón, *Enantioselective α -heterofunctionalisation of carbonyl compounds*, *Tetrahedron: Asymmetry* **2006**, 17(10), 1465–1492, DOI: 10.1016/j.tetasy.2006.05.020.
- [65] H. Tu, S. Zhu, F.-L. Qing, L. Chu, *Visible-light-induced Halogenation of Aliphatic C-H Bonds*, *Tetrahedron Lett.* **2017**, DOI: 10.1016/j.tetlet.2017.12.023.
- [66] T. Yoshimitsu, N. Fukumoto, T. Tanaka, *Enantiocontrolled synthesis of polychlorinated hydrocarbon motifs*, *J. Org. Chem.* **2009**, 74(2), 696–702, DOI: 10.1021/jo802093d.
- [67] C. Nilewski, R. W. Geisser, E. M. Carreira, *Total synthesis of a chlorosulpholipid cytotoxin associated with seafood poisoning*, *Nature* **2009**, 457(7229), 573–576, DOI: 10.1038/nature07734.
- [68] G. M. Shibuya, J. S. Kanady, C. D. Vanderwal, *Stereoselective dichlorination of allylic alcohol derivatives to access key stereochemical arrays of the chlorosulfolipids*, *J. Am. Chem. Soc.* **2008**, 130(37), 12514–12518, DOI: 10.1021/ja804167v.
- [69] D. A. Evans, J. A. Ellman, R. L. Dorow, *Asymmetric halogenation of chiral imide enolates*, *Tetrahedron Lett.* **1987**(11), 1123–1126, DOI: 10.1016/S0040-4039(00)95305-X.
- [70] D. A. Evans, E. B. Sjogren, A. E. Weber, R. E. Conn, *Asymmetric synthesis of anti-beta-hydroxy-alpha amino acids*, *Tetrahedron Lett.* **1987**(1), 39–42, DOI: 10.1016/S0040-4039(00)95643-0.
- [71] S. Hu, S. Jayaraman, A. C. Oehlschlager, *Diastereo- and Enantioselective Synthesis of syn - α -Vinylchlorohydrins and cis -Vinylepoxides*, *J. Org. Chem.* **1996**, 61(21), 7513–7520, DOI: 10.1021/jo960875p.
- [72] S. Jayaraman, S. Hu, A. C. Oehlschlager, *New access to chiral syn- α -Chlorohydrins and cis-vinyloxiranes through chloroallylboration*, *Tetrahedron Lett.* **1995**, 36(27), 4765–4768, DOI: 10.1016/0040-4039(95)00928-6.
- [73] M. Shen, C. Li, *Asymmetric iodolactamization induced by chiral oxazolidine auxiliary*, *J. Org. Chem.* **2004**, 69(23), 7906–7909, DOI: 10.1021/jo0488006.
- [74] D. P. Galonić, E. W. Barr, C. T. Walsh, J. M. Bollinger, C. Krebs, *Two interconverting Fe(IV) intermediates in aliphatic chlorination by the halogenase CytC3*, *Nat. Chem. Biol.* **2007**, 3(2), 113–116, DOI: 10.1038/nchembio856.
- [75] C. S. Neumann, D. G. Fujimori, C. T. Walsh, *Halogenation strategies in natural product biosynthesis*, *Chem. Biol.* **2008**, 15(2), 99–109, DOI: 10.1016/j.chembiol.2008.01.006.

Literature

- [76] I. Grgurina, Barca, A, Cervigni, S, M. Gallo, Scaloni, A.: Pucci, P, *Relevance of chlorine-substituent for the antifungal activity of syringomycin and syringotoxin, metabolites of the phytopathogenic bacterium Pseudomonas syringae*, *Experientia* **1994**(50), 130–133.
- [77] F. H. Vaillancourt, E. Yeh, D. A. Vosburg, S. Garneau-Tsodikova, C. T. Walsh, *Nature's inventory of halogenation catalysts: oxidative strategies predominate*, *Chem. Rev.* **2006**, 106(8), 3364–3378, DOI: 10.1021/cr050313i.
- [78] J. F. Hartwig, M. A. Larsen, *Undirected, Homogeneous C-H Bond Functionalization*, *ACS Cent. Sci.* **2016**, 2(5), 281–292, DOI: 10.1021/acscentsci.6b00032.
- [79] J. R. Reyes, J. Xu, K. Kobayashi, V. Bhat, V. H. Rawal, *Total Synthesis of (-)- N -Methylwelwitindolinone B Isothiocyanate*, *Angew. Chem.* **2017**, 116, 9935, DOI: 10.1002/ange.201705322.
- [80] D. Y.-K. Chen, S. W. Youn, *C-H activation*, *Chem. Eur. J.* **2012**, 18(31), 9452–9474, DOI: 10.1002/chem.201201329.
- [81] M. C. White, *Chemistry. Adding aliphatic C-H bond oxidations to synthesis*, *Science* **2012**, 335(6070), 807–809, DOI: 10.1126/science.1207661.
- [82] T. Cernak, K. D. Dykstra, S. Tyagarajan, P. Vachal, S. W. Krska, *The medicinal chemist's toolbox for late stage functionalization of drug-like molecules*, *Chem. Soc. Rev.* **2016**, 45(3), 546–576, DOI: 10.1039/C5CS00628G.
- [83] W. Liu, J. T. Groves, *Manganese porphyrins catalyze selective C-H bond halogenations*, *J. Am. Chem. Soc.* **2010**, 132(37), 12847–12849, DOI: 10.1021/ja105548x.
- [84] W. Liu, J. T. Groves, *Manganese Catalyzed C-H Halogenation*, *Acc. Chem. Res.* **2015**, 48(6), 1727–1735, DOI: 10.1021/acs.accounts.5b00062.
- [85] M. Puri, A. N. Biswas, R. Fan, Y. Guo, L. Que, JR, *Modeling Non-Heme Iron Halogenases: High-Spin Oxoiron(IV)-Halide Complexes That Halogenate C-H Bonds*, *J. Am. Chem. Soc.* **2016**, 138(8), 2484–2487, DOI: 10.1021/jacs.5b11511.
- [86] A. Butler, M. Sandy, *Mechanistic considerations of halogenating enzymes*, *Nature* **2009**, 460(7257), 848–854, DOI: 10.1038/nature08303.
- [87] P. D. Shaw, L. P. Hager, *Biological Chlorination*, *J. Biol. Chem.* **1959**(10), 2565–2569.
- [88] L. C. Blasiak, C. L. Drennan, *Structural perspective on enzymatic halogenation*, *Acc. Chem. Res.* **2009**, 42(1), 147–155, DOI: 10.1021/ar800088r.
- [89] L. Hager, D. R. Morris, F. S. Brown, H. Eberwein, *Chloroperoxidase*, *J. Biol. Chem.* **1966**(8), 1769–1977.
- [90] A. Frank, C. J. Seel, M. Groll, T. Gulder, *Characterization of a Cyanobacterial Haloperoxidase and Evaluation of its Biocatalytic Halogenation Potential*, *ChemBioChem* **2016**, 17(21), 2028–2032, DOI: 10.1002/cbic.201600417.
- [91] C. Wagner, M. El Omari, G. M. König, *Biohalogenation: nature's way to synthesize halogenated metabolites*, *J. Nat. Prod.* **2009**, 72(3), 540–553, DOI: 10.1021/np800651m.

- [92] K.-H. van Pée, E. P. Patallo, *Flavin-dependent halogenases involved in secondary metabolism in bacteria*, *Appl Microbiol Biotechnol* **2006**, 70(6), 631–641, DOI: 10.1007/s00253-005-0232-2.
- [93] P. Bernhardt, T. Okino, J. M. Winter, A. Miyanaga, B. S. Moore, *A stereoselective vanadium-dependent chloroperoxidase in bacterial antibiotic biosynthesis*, *J. Am. Chem. Soc.* **2011**, 133(12), 4268–4270, DOI: 10.1021/ja201088k.
- [94] J. M. Winter, B. S. Moore, *Exploring the chemistry and biology of vanadium-dependent haloperoxidases*, *J. Biol. Chem.* **2009**, 284(28), 18577–18581, DOI: 10.1074/jbc.R109.001602.
- [95] L. Kaysser, P. Bernhardt, S.-J. Nam, S. Loesgen, J. G. Ruby, P. Skewes-Cox, P. R. Jensen, W. Fenical, B. S. Moore, *Merochlorins A-D, cyclic meroterpenoid antibiotics biosynthesized in divergent pathways with vanadium-dependent chloroperoxidases*, *J. Am. Chem. Soc.* **2012**, 134(29), 11988–11991, DOI: 10.1021/ja305665f.
- [96] J. N. Carter-Franklin, A. Butler, *Vanadium bromoperoxidase-catalyzed biosynthesis of halogenated marine natural products*, *J. Am. Chem. Soc.* **2004**, 126(46), 15060–15066, DOI: 10.1021/ja047925p.
- [97] H. B. ten Brink, H. E. Schoemaker, R. Wever, *Sulfoxidation mechanism of vanadium bromoperoxidase from *Ascophyllum nodosum**, *Eur J Biochem* **2001**, 268(1), 132–138, DOI: 10.1046/j.1432-1327.2001.01856.x.
- [98] F. H. Vaillancourt, D. A. Vosburg, C. T. Walsh, *Dichlorination and bromination of a threonyl-S-carrier protein by the non-heme Fe(II) halogenase SyrB2*, *ChemBioChem* **2006**, 7(5), 748–752, DOI: 10.1002/cbic.200500480.
- [99] Q. Zhu, M. L. Hillwig, Y. Doi, X. Liu, *Aliphatic Halogenase Enables Late-Stage C-H Functionalization*, *ChemBioChem* **2016**, 17(6), 466–470, DOI: 10.1002/cbic.201500674.
- [100] A. P. Doerschuk, J. R. D. McCormick, J. J. Goodman, S. A. Szumski, J. A. Growich, P. A. Miller, B. A. Bitler, E. R. Jensen, M. Matrishin, M. A. Petty, A. S. Phelps, *Biosynthesis of Tetracyclines. I. The Halide Metabolism of *Streptomyces aureofaciens* Mutants. The Preparation and Characterization of Tetracycline, 7-Chloro 36 -tetracycline and 7-Bromotetracycline*, *J. Am. Chem. Soc.* **1959**, 81(12), 3069–3075, DOI: 10.1021/ja01521a040.
- [101] D. S. Gkotsi, J. Dhaliwal, M. M. McLachlan, K. R. Mulholand, R. J. M. Goss, *Halogenases*, *Curr. Opin. Chem. Biol.* **2018**, 43, 119–126, DOI: 10.1016/j.cbpa.2018.01.002.
- [102] L. de Matteis, R. Germani, M. V. Mancini, F. Di Renzo, N. Spreti, *Encapsulation of chloroperoxidase in novel hybrid polysaccharide-silica biocomposites*, *Appl. Catal, A* **2015**, 492, 23–30, DOI: 10.1016/j.apcata.2014.12.016.
- [103] S. Aoun, C. Chebli, M. Babouléne, *Noncovalent immobilization of chloroperoxidase onto talc: Catalytic properties of a new biocatalyst*, *Enzyme Microb. Technol.* **1998**(23), 380–385, DOI: 10.1016/S0141-0229(98)00061-1.
- [104] E. Terrés, M. Montiel, S. Le Borgne, E. Torres, *Immobilization of chloroperoxidase on mesoporous materials for the oxidation of 4,6-dimethyldibenzothiophene, a recalcitrant organic sulfur*

Literature

- compound present in petroleum fractions*, *Biotechnology letters* **2008**, 30(1), 173–179, DOI: 10.1007/s10529-007-9512-5.
- [105] C. Montiel, E. Terrés, J.-M. Domínguez, J. Aburto, *Immobilization of chloroperoxidase on silica-based materials for 4,6-dimethyl dibenzothiophene oxidation*, *J. Mol. Catal. B: Enzym.* **2007**, 48(3-4), 90–98, DOI: 10.1016/j.molcatb.2007.06.012.
- [106] J. Aburto, M. Ayala, I. Bustos-Jaimes, C. Montiel, E. Terrés, J. M. Domínguez, E. Torres, *Stability and catalytic properties of chloroperoxidase immobilized on SBA-16 mesoporous materials*, *Microporous and Mesoporous Materials* **2005**, 83(1-3), 193–200, DOI: 10.1016/j.micromeso.2005.04.008.
- [107] S. Hudson, J. Cooney, B. K. Hodnett, E. Magner, *Chloroperoxidase on Periodic Mesoporous Organosilanes*, *Chem. Mater.* **2007**, 19(8), 2049–2055, DOI: 10.1021/cm070180c.
- [108] M. Hartmann, C. Streb, *Selective oxidation of indole by chloroperoxidase immobilized on the mesoporous molecular sieve SBA-15*, *J Porous Mater* **2006**, 13(3-4), 347–352, DOI: 10.1007/s10934-006-8029-y.
- [109] M. Pešić, C. López, G. Álvaro, J. López-Santín, *A novel immobilized chloroperoxidase biocatalyst with improved stability for the oxidation of amino alcohols to amino aldehydes*, *J. Mol. Catal. B: Enzym.* **2012**, 84, 144–151, DOI: 10.1016/j.molcatb.2012.04.010.
- [110] D. Jung, C. Streb, M. Hartmann, *Covalent anchoring of chloroperoxidase and glucose oxidase on the mesoporous molecular sieve SBA-15*, *International journal of molecular sciences* **2010**, 11(2), 762–778, DOI: 10.3390/ijms11020762.
- [111] E. Guerrero, P. Aburto, E. Terrés, O. Villegas, E. González, T. Zayas, F. Hernández, E. Torres, *Improvement of catalytic efficiency of chloroperoxidase by its covalent immobilization on SBA-15 for azo dye oxidation*, *J Porous Mater* **2013**, 20(2), 387–396, DOI: 10.1007/s10934-012-9608-8.
- [112] G. Bayramoglu, B. Altintas, M. Yilmaz, M. Y. Arica, *Immobilization of chloroperoxidase onto highly hydrophilic polyethylene chains via bio-conjugation*, *Bioresour. Technol.* **2011**, 102(2), 475–482, DOI: 10.1016/j.biortech.2010.08.056.
- [113] L.-H. Zhang, C.-H. Bai, Y.-S. Wang, Y.-C. Jiang, M.-C. Hu, S.-N. Li, Q.-G. Zhai, *Improvement of chloroperoxidase stability by covalent immobilization on chitosan membranes*, *Biotechnology letters* **2009**, 31(8), 1269–1272, DOI: 10.1007/s10529-009-0009-2.
- [114] G. Bayramoğlu, S. Kiralp, M. Yilmaz, L. Toppare, M. Y. Arica, *Covalent immobilization of chloroperoxidase onto magnetic beads*, *Biochemical Engineering Journal* **2008**, 38(2), 180–188, DOI: 10.1016/j.bej.2007.06.018.
- [115] T. A. Kadima, M. A. Pickard, *Immobilization of chloroperoxidase on aminopropyl-glass*, *Appl. Environ. Microbiol.* **1990**, 56(11), 3473–3477.

Literature

- [116] J. Zhang, C. Roberge, J. Reddy, N. Connors, M. Chartrain, B. Buckland, R. Greasham, *Bioconversion of indene to trans-2S,1S-bromoindanol and 1S,2R-indene oxide by a bromoperoxidase/dehydrogenase preparation from Curvularia protuberata MF5400*, *Enzyme Microb. Technol.* **1999**, 24(1-2), 86–95, DOI: 10.1016/S0141-0229(98)00111-2.
- [117] C. Dong, S. Flecks, S. Unversucht, C. Haupt, K.-H. van Pée, J. H. Naismith, *Tryptophan 7-halogenase (PrnA) structure suggests a mechanism for regioselective chlorination*, *Science* **2005**, 309(5744), 2216–2219, DOI: 10.1126/science.1116510.
- [118] M. L. Mascotti, M. Juri Ayub, N. Furnham, J. M. Thornton, R. A. Laskowski, *Chopping and Changing*, *J. Mol. Biol.* **2016**, 428(15), 3131–3146, DOI: 10.1016/j.jmb.2016.07.003.
- [119] S. Keller, T. Wage, K. Hohaus, M. Hölzer, E. Eichhorn, K.-H. van Pée, *Purification and Partial Characterization of Tryptophan 7-Halogenase (PrnA) from Pseudomonas fluorescens*, *Angew. Chem. Int. Ed.* **2000**, 39(13), 2300–2302, DOI: 10.1002/1521-3773(20000703)39:13<2300:AID-ANIE2300>3.0.CO;2-I.
- [120] J. Latham, E. Brandenburger, S. A. Shepherd, Menon, Binuraj R. K, J. Micklefield, *Development of Halogenase Enzymes for Use in Synthesis*, *Chem. Rev.* **2017**, DOI: 10.1021/acs.chemrev.7b00032.
- [121] E. Yeh, L. C. Blasiak, A. Koglin, C. L. Drennan, C. T. Walsh, *Chlorination by a long-lived intermediate in the mechanism of flavin-dependent halogenases*, *Biochemistry* **2007**, 46(5), 1284–1292, DOI: 10.1021/bi0621213.
- [122] R. M. Williams, E. M. Stocking, J. F. Sanz-Cervera in *Biosynthesis: Aromatic Polyketides, Isoprenoids, Alkaloids*; (Eds. F. J. Leeper, J. C. Vederas), Springer Berlin Heidelberg, Berlin, Heidelberg, **2000**, 97–173, DOI: 10.1007/3-540-48146-X_3.
- [123] K. Podzelinska, R. Latimer, A. Bhattacharya, L. C. Vining, D. L. Zechel, Z. Jia, *Chloramphenicol biosynthesis*, *J. Mol. Biol.* **2010**, 397(1), 316–331, DOI: 10.1016/j.jmb.2010.01.020.
- [124] W. S. Glenn, E. Nims, S. E. O'Connor, *Reengineering a tryptophan halogenase to preferentially chlorinate a direct alkaloid precursor*, *J. Am. Chem. Soc.* **2011**, 133(48), 19346–19349, DOI: 10.1021/ja2089348.
- [125] J. T. Payne, M. C. Andorfer, J. C. Lewis, *Regioselective arene halogenation using the FAD-dependent halogenase RebH*, *Angew. Chem. Int. Ed.* **2013**, 52(20), 5271–5274, DOI: 10.1002/anie.201300762.
- [126] C. B. Poor, M. C. Andorfer, J. C. Lewis, *Improving the stability and catalyst lifetime of the halogenase RebH by directed evolution*, *ChemBioChem* **2014**, 15(9), 1286–1289, DOI: 10.1002/cbic.201300780.
- [127] Menon, Binuraj R. K, J. Latham, M. S. Dunstan, E. Brandenburger, U. Klemstein, D. Leys, C. Karthikeyan, M. F. Greaney, S. A. Shepherd, J. Micklefield, *Structure and biocatalytic scope of thermophilic flavin-dependent halogenase and flavin reductase enzymes*, *Org. Biomol. Chem.* **2016**, 14(39), 9354–9361, DOI: 10.1039/c6ob01861k.

- [128] M. Frese, N. Sewald, *Enzymatic halogenation of tryptophan on a gram scale*, *Angew. Chem. Int. Ed.* **2015**, 54(1), 298–301, DOI: 10.1002/anie.201408561.
- [129] A. Deb Roy, S. Grüşchow, N. Cairns, R. J. M. Goss, *Gene expression enabling synthetic diversification of natural products: chemogenetic generation of pacidamycin analogs*, *J. Am. Chem. Soc.* **2010**, 132(35), 12243–12245, DOI: 10.1021/ja1060406.
- [130] W. Runguphan, S. E. O'Connor, *Diversification of monoterpene indole alkaloid analogs through cross-coupling*, *Org. Lett.* **2013**, 15(11), 2850–2853, DOI: 10.1021/ol401179k.
- [131] M. Frese, C. Schnepel, H. Minges, H. Voß, R. Feiner, N. Sewald, *Modular Combination of Enzymatic Halogenation of Tryptophan with Suzuki-Miyaura Cross-Coupling Reactions*, *ChemCatChem* **2016**, 8(10), 1799–1803, DOI: 10.1002/cctc.201600317.
- [132] L. J. Durak, J. T. Payne, J. C. Lewis, *Late-Stage Diversification of Biologically Active Molecules via Chemoenzymatic C–H Functionalization*, *ACS Catal.* **2016**, 6(3), 1451–1454, DOI: 10.1021/acscatal.5b02558.
- [133] A. D. Roy, R. J. M. Goss, G. K. Wagner, M. Winn, *Development of fluorescent aryltryptophans by Pd mediated cross-coupling of unprotected halotryptophans in water*, *Chem. Commun.* **2008**(39), 4831–4833, DOI: 10.1039/b807512c.
- [134] W. Baricos, R. Chambers, W. Cohen, *Considerations on the use of cofactor-requiring enzymes in enzyme engineering*, *Enzyme Technol. Dig.* **1975**(2), 39–53, DOI: 10.1016/S0076-6879(76)44025-9.
- [135] S. S. Wang, C.-K. King, *The use of coenzymes in biochemical reactors*, *Adv. Biochem. Eng.* **1979**(12), 119–146, DOI: 10.1007/3540092625_8.
- [136] P. B. OELRICHS, T. McEWAN, *Isolation of the toxic principle in Acacia georginae*, *Nature* **1961**, 190, 808–809.
- [137] C. Dong, F. Huang, H. Deng, C. Schaffrath, J. B. Spencer, D. O'Hagan, J. H. Naismith, *Crystal structure and mechanism of a bacterial fluorinating enzyme*, *Nature* **2004**, 427(6974), 561–565, DOI: 10.1038/nature02280.
- [138] H. Deng, S. L. Cobb, A. R. McEwan, R. P. McGlinchey, J. H. Naismith, D. O'Hagan, D. A. Robinson, J. B. Spencer, *The fluorinase from Streptomyces cattleya is also a chlorinase*, *Angew. Chem. Int. Ed.* **2006**, 45(5), 759–762, DOI: 10.1002/anie.200503582.
- [139] A. S. Eustáquio, F. Pojer, J. P. Noel, B. S. Moore, *Discovery and characterization of a marine bacterial SAM-dependent chlorinase*, *Nat. Chem. Biol.* **2008**, 4(1), 69–74, DOI: 10.1038/nchembio.2007.56.
- [140] H. Deng, L. Ma, N. Bandaranayaka, Z. Qin, G. Mann, K. Kyeremeh, Y. Yu, T. Shepherd, J. H. Naismith, D. O'Hagan, *Identification of Fluorinases from Streptomyces sp MA37, Norcardia brasiliensis, and Actinoplanes sp N902-109 by Genome Mining*, *ChemBioChem* **2014**(3), 364–368, DOI: 10.1002/cbic.201300732.

Literature

- [141] Y. Wang, Z. Deng, X. Qu, *Characterization of a SAM-dependent fluorinase from a latent biosynthetic pathway for fluoroacetate and 4-fluorothreonine formation in Nocardia brasiliensis*, F1000Research **2014**, 3, 61, DOI: 10.12688/f1000research.3-61.v1.
- [142] S. Huang, L. Ma, M. H. Tong, Y. Yu, D. O'Hagan, H. Deng, *Fluoroacetate biosynthesis from the marine-derived bacterium Streptomyces xinghaiensis NRRL B-24674*, Org. Biomol. Chem. **2014**, 12(27), 4828–4831, DOI: 10.1039/c4ob00970c.
- [143] S. Dall'Angelo, N. Bandaranayaka, A. D. Windhorst, D. J. Vugts, D. van der Born, M. Onega, L. F. Schweiger, M. Zanda, D. O'Hagan, *Tumour imaging by Positron Emission Tomography using fluorinase generated 5-¹⁸Ffluoro-5-deoxyribose as a novel tracer*, Nuclear medicine and biology **2013**, 40(4), 464–470, DOI: 10.1016/j.nucmedbio.2013.02.006.
- [144] S. Thompson, Q. Zhang, M. Onega, S. McMahon, I. Fleming, S. Ashworth, J. H. Naismith, J. Passchier, D. O'Hagan, *A localized tolerance in the substrate specificity of the fluorinase enzyme enables "last-step" 18F fluorination of a RGD peptide under ambient aqueous conditions*, Angew. Chem. Int. Ed. **2014**, 53(34), 8913–8918, DOI: 10.1002/anie.201403345.
- [145] S. Thompson, M. Onega, S. Ashworth, I. N. Fleming, J. Passchier, D. O'Hagan, *A two-step fluorinase enzyme mediated (18)F labelling of an RGD peptide for positron emission tomography*, Chem. Commun. **2015**, 51(70), 13542–13545, DOI: 10.1039/c5cc05013h.
- [146] M. Thomsen, S. B. Vogensen, J. Buchardt, M. D. Burkart, R. P. Clausen, *Chemoenzymatic synthesis and in situ application of S-adenosyl-L-methionine analogs*, Org. Biomol. Chem. **2013**, 11(43), 7606–7610, DOI: 10.1039/c3ob41702f.
- [147] M. E. Sergeev, F. Morgia, M. Lazari, C. Wang, R. M. van Dam, *Titanium-catalyzed radiofluorination of tosylated precursors in highly aqueous medium*, J. Am. Chem. Soc. **2015**, 137(17), 5686–5694, DOI: 10.1021/jacs.5b02659.
- [148] H. Sun, W. L. Yeo, Y. H. Lim, X. Chew, D. J. Smith, B. Xue, K. P. Chan, R. C. Robinson, E. G. Robins, H. Zhao, E. L. Ang, *Directed Evolution of a Fluorinase for Improved Fluorination Efficiency with a Non-native Substrate*, Angew. Chem. Int. Ed. **2016**, 55(46), 14277–14280, DOI: 10.1002/anie.201606722.
- [149] F. H. Vaillancourt, J. Yin, C. T. Walsh, *SyrB2 in syringomycin E biosynthesis is a nonheme FeII alpha-ketoglutarate- and O₂-dependent halogenase*, Proc. Natl. Acad. Sci. U.S.A. **2005**, 102(29), 10111–10116, DOI: 10.1073/pnas.0504412102.
- [150] A. Busche, D. Gottstein, C. Hein, N. Ripin, I. Pader, P. Tufar, E. B. Eisman, L. Gu, C. T. Walsh, D. H. Sherman, F. Löhr, P. Güntert, V. Dötsch, *Characterization of molecular interactions between ACP and halogenase domains in the Curacin A polyketide synthase*, ACS Chem. Biol. **2012**, 7(2), 378–386, DOI: 10.1021/cb200352q.
- [151] F. H. Vaillancourt, E. Yeh, D. A. Vosburg, S. E. O'Connor, C. T. Walsh, *Cryptic chlorination by a non-haem iron enzyme during cyclopropyl amino acid biosynthesis*, Nature **2005**, 436(7054), 1191–1194, DOI: 10.1038/nature03797.

- [152] D. P. Galonić, F. H. Vaillancourt, C. T. Walsh, *Halogenation of Unactivated Carbon Centers in Natural Product Biosynthesis: Trichlorination of Leucine during Barbamide Biosynthesis*, *J. Am. Chem. Soc.* **2006**, 128(12), 3900–3901, DOI: 10.1021/ja060151n.
- [153] M. Ueki, D. P. Galonić, F. H. Vaillancourt, S. Garneau-Tsodikova, E. Yeh, D. A. Vosburg, F. C. Schroeder, H. Osada, C. T. Walsh, *Enzymatic generation of the antimetabolite gamma,gamma-dichloroaminobutyrate by NRPS and mononuclear iron halogenase action in a streptomycete*, *Chem. Biol.* **2006**, 13(11), 1183–1191, DOI: 10.1016/j.chembiol.2006.09.012.
- [154] S. M. Pratter, K. M. Light, E. I. Solomon, G. D. Straganz, *The role of chloride in the mechanism of O(2) activation at the mononuclear nonheme Fe(II) center of the halogenase HctB*, *J. Am. Chem. Soc.* **2014**, 136(26), 9385–9395, DOI: 10.1021/ja503179m.
- [155] M. L. Hillwig, X. Liu, *A new family of iron-dependent halogenases acts on freestanding substrates*, *Nat. Chem. Biol.* **2014**, 10(11), 921–923, DOI: 10.1038/nchembio.1625.
- [156] M. L. Hillwig, Q. Zhu, K. Ittiamornkul, X. Liu, *Discovery of a Promiscuous Non-Heme Iron Halogenase in Ambiguine Alkaloid Biogenesis*, *Angew. Chem. Int. Ed.* **2016**, 55(19), 5780–5784, DOI: 10.1002/anie.201601447.
- [157] Q. Zhu, X. Liu, *Characterization of non-heme iron aliphatic halogenase WelO5* from Hapalosiphon welwitschii IC-52-3*, *Beilstein J. Org. Chem.* **2017**, 13, 1168–1173, DOI: 10.3762/bjoc.13.115.
- [158] S. Duewel, L. Schermund, T. Faber, K. Harms, V. Srinivasan, Hoebenreich S, *Directed Evolution of an FeII-Dependent Halogenase for Asymmetric C(sp³)-H Chlorination* **submitted 2018**.
- [159] M. L. Matthews, C. S. Neumann, L. A. Miles, T. L. Grove, S. J. Booker, C. Krebs, C. T. Walsh, J. M. Bollinger, *Substrate positioning controls the partition between halogenation and hydroxylation in the aliphatic halogenase, SyrB2*, *Proc. Natl. Acad. Sci. U.S.A.* **2009**, 106(42), 17723–17728, DOI: 10.1073/pnas.0909649106.
- [160] A. J. Mitchell, Q. Zhu, A. O. Maggiolo, N. R. Ananth, M. L. Hillwig, X. Liu, A. K. Boal, *Structural basis for halogenation by iron- and 2-oxo-glutarate-dependent enzyme WelO5*, *Nat. Chem. Biol.* **2016**, DOI: 10.1038/nchembio.2112.
- [161] D. Wetzl, J. Bolsinger, B. M. Nestl, B. Hauer, *α -Hydroxylation of Carboxylic Acids Catalyzed by Taurine Dioxygenase*, *ChemCatChem* **2016**(8), 1361–1366, DOI: 10.1002/cctc.201501244.
- [162] E. Eichhorn, van der Ploeg, J. R. M. A. Kertesz, T. Leisinger, *Characterization of -Ketoglutarate-dependent Taurine Dioxygenase from Escherichia coli*, *J. Biol. Chem.* **1997**, 272(37), 23031–23036, DOI: 10.1074/jbc.272.37.23031.
- [163] J. M. Elkins, M. J. Ryle, I. J. Clifton, Dunning Hotopp, Julie C, J. S. Lloyd, N. I. Burzlaff, J. E. Baldwin, R. P. Hausinger, P. L. Roach, *X-ray Crystal Structure of Escherichia coli Taurine/ α -Ketoglutarate Dioxygenase Complexed to Ferrous Iron and Substrates †,‡*, *Biochemistry* **2002**, 41(16), 5185–5192, DOI: 10.1021/bi016014e.

- [164] J. C. Price, E. W. Barr, B. Tirupati, J. M. Bollinger, C. Krebs, *The first direct characterization of a high-valent iron intermediate in the reaction of an alpha-ketoglutarate-dependent dioxygenase: a high-spin FeIV complex in taurine/alpha-ketoglutarate dioxygenase (TauD) from Escherichia coli*, *Biochemistry* **2003**, 42(24), 7497–7508, DOI: 10.1021/bi030011f.
- [165] K. P. McCusker, J. P. Klinman, *Modular behavior of tauD provides insight into the origin of specificity in alpha-ketoglutarate-dependent nonheme iron oxygenases*, *Proc. Natl. Acad. Sci. U.S.A.* **2009**, 106(47), 19791–19795, DOI: 10.1073/pnas.0910660106.
- [166] J. R. O'Brien, D. J. Schuller, V. S. Yang, B. D. Dillard, W. N. Lanzilotta, *Substrate-Induced Conformational Changes in Escherichia coli Taurine/alpha-Ketoglutarate Dioxygenase and Insight into the Oligomeric Structure ‡*, *Biochemistry* **2003**, 42(19), 5547–5554, DOI: 10.1021/bi0341096.
- [167] R. P. Hausinger, *FeII/alpha-ketoglutarate-dependent hydroxylases and related enzymes*, *Crit. Rev. Biochem. Mol. Biol.* **2004**, 39(1), 21–68, DOI: 10.1080/10409230490440541.
- [168] V. Purpero, G. R. Moran, *The diverse and pervasive chemistries of the alpha-keto acid dependent enzymes*, *J. Biol. Inorg. Chem.* **2007**, 12(5), 587–601, DOI: 10.1007/s00775-007-0231-0.
- [169] C. Loenarz, C. J. Schofield, *Physiological and biochemical aspects of hydroxylations and demethylations catalyzed by human 2-oxoglutarate oxygenases*, *Trends Biochem. Sci.* **2011**, 36(1), 7–18, DOI: 10.1016/j.tibs.2010.07.002.
- [170] C. Q. Herr, R. P. Hausinger, *Amazing Diversity in Biochemical Roles of Fe(II)/2-Oxoglutarate Oxygenases*, *Trends Biochem. Sci.* **2018**, DOI: 10.1016/j.tibs.2018.04.002.
- [171] R. P. Hausinger, C. J. Schofield, Eds, *2-Oxoglutarate-Dependent Oxygenases*; Royal Society of Chemistry, Cambridge, **2015**.
- [172] A. G. Prescott, *A Dilemma of Dioxygenases (or Where Biochemistry and Molecular Biology Fail to Meet)*, *J. Exp. Bot.* **1993**(262), 849–861, DOI: 10.1093/jxb/44.5.849.
- [173] A. G. Prescott, M. D. Lloyd, *The iron(II) and 2-oxoacid-dependent dioxygenases and their role in metabolism (1967 to 1999)*, *Nat. Prod. Rep.* **2000**, 17(4), 367–383, DOI: 10.1039/a902197c.
- [174] E. Flashman, C. J. Schofield, *The most versatile of all reactive intermediates?*, *Nat. Chem. Biol.* **2007**, 3(2), 86–87, DOI: 10.1038/nchembio0207-86.
- [175] C. Loenarz, C. J. Schofield, *Expanding chemical biology of 2-oxoglutarate oxygenases*, *Nat. Chem. Biol.* **2008**, 4(3), 152–156, DOI: 10.1038/nchembio0308-152.
- [176] S. Martinez, R. P. Hausinger, *Catalytic Mechanisms of Fe(II)- and 2-Oxoglutarate-Dependent Oxygenases*, *J. Biol. Chem.* **2015**, DOI: 10.1074/jbc.R115.648691.
- [177] L.-F. Wu, S. Meng, G.-L. Tang, *Ferrous iron and alpha-ketoglutarate-dependent dioxygenases in the biosynthesis of microbial natural products*, *Biochim. Biophys. Acta* **2016**, DOI: 10.1016/j.bbapap.2016.01.012.

Literature

- [178] L. C. Blasiak, F. H. Vaillancourt, C. T. Walsh, C. L. Drennan, *Crystal structure of the non-haem iron halogenase SyrB2 in syringomycin biosynthesis*, *Nature* **2006**, 440(7082), 368–371, DOI: 10.1038/nature04544.
- [179] C. Wong, D. G. Fujimori, C. T. Walsh, C. L. Drennan, *Structural analysis of an open active site conformation of nonheme iron halogenase CytC3*, *J. Am. Chem. Soc.* **2009**, 131(13), 4872–4879, DOI: 10.1021/ja8097355.
- [180] E. L. Hegg, L. Q. Jr, *The 2-His-1-Carboxylate Facial Triad - An Emerging Structural Motif in Mononuclear Non-Heme Iron(II) Enzymes*, *Eur J Biochem* **1997**, 250(3), 625–629, DOI: 10.1111/j.1432-1033.1997.t01-1-00625.x.
- [181] A. J. Mitchell, N. P. Dunham, J. A. Bergman, B. Wang, Q. Zhu, W.-C. Chang, X. Liu, A. K. Boal, *Structure-guided reprogramming of a hydroxylase to halogenate its small molecule substrate*, *Biochemistry* **2016**, DOI: 10.1021/acs.biochem.6b01173.
- [182] P. K. Grzyska, T. A. Müller, M. G. Campbell, R. P. Hausinger, *Metal ligand substitution and evidence for quinone formation in taurine/alpha-ketoglutarate dioxygenase*, *J. Inorg. Biochem.* **2007**, 101(5), 797–808, DOI: 10.1016/j.jinorgbio.2007.01.011.
- [183] D. Khare, B. Wang, L. Gu, J. Razelun, D. H. Sherman, W. H. Gerwick, K. Håkansson, J. L. Smith, *Conformational switch triggered by alpha-ketoglutarate in a halogenase of curacin A biosynthesis*, *Proc. Natl. Acad. Sci. U.S.A.* **2010**, 107(32), 14099–14104, DOI: 10.1073/pnas.1006738107.
- [184] I. Müller, A. Kahnert, T. Pape, G. M. Sheldrick, W. Meyer-Klaucke, T. Dierks, M. Kertesz, I. Usón, *Crystal structure of the alkylsulfatase AtsK: insights into the catalytic mechanism of the Fe(II) alpha-ketoglutarate-dependent dioxygenase superfamily*, *Biochemistry* **2004**, 43(11), 3075–3088, DOI: 10.1021/bi035752v.
- [185] I. J. Clifton, L.-C. Hsueh, J. E. Baldwin, K. Harlos, C. J. Schofield, *Structure of proline 3-hydroxylase*, *Eur J Biochem* **2001**, 268(24), 6625–6636, DOI: 10.1046/j.0014-2956.2001.02617.x.
- [186] K. Valegard, A. C. van Scheltinga, M. D. Lloyd, T. Hara, S. Ramaswamy, A. Perrakis, A. Thompson, H. J. Lee, J. E. Baldwin, C. J. Schofield, J. Hajdu, I. Andersson, *Structure of a cephalosporin synthase*, *Nature* **1998**, 394(6695), 805–809, DOI: 10.1038/29575.
- [187] Z. Zhang, J. Ren, D. K. Stammers, J. E. Baldwin, K. Harlos, C. J. Schofield, *Structural origins of the selectivity of the trifunctional oxygenase clavaminic acid synthase*, *Nature structural biology* **2000**, 7(2), 127–133, DOI: 10.1038/72398.
- [188] B. Bleijlevens, T. Shivarattan, E. Flashman, Y. Yang, P. J. Simpson, P. Koivisto, B. Sedgwick, C. J. Schofield, S. J. Matthews, *Dynamic states of the DNA repair enzyme AlkB regulate product release*, *EMBO Rep* **2008**, 9(9), 872–877, DOI: 10.1038/embor.2008.120.

Literature

- [189] C. J. Stubbs, C. Loenarz, J. Mecinović, K. K. Yeoh, N. Hindley, B. M. Liénard, F. Sobott, C. J. Schofield, E. Flashman, *Application of a proteolysis/mass spectrometry method for investigating the effects of inhibitors on hydroxylase structure*, *J. Med. Chem.* **2009**, 52(9), 2799–2805, DOI: 10.1021/jm900285r.
- [190] G. M. Montero-Morán, M. Li, E. Rendón-Huerta, F. Jourdan, D. J. Lowe, A. W. Stumpff-Kane, M. Feig, C. Scazzocchio, R. P. Hausinger, *Purification and characterization of the FeII- and alpha-ketoglutarate-dependent xanthine hydroxylase from Aspergillus nidulans*, *Biochemistry* **2007**, 46(18), 5293–5304, DOI: 10.1021/bi700065h.
- [191] E. G. Pavel, J. Zhou, R. W. Busby, M. Gunsior, C. A. Townsend, E. I. Solomon, *Circular Dichroism and Magnetic Circular Dichroism Spectroscopic Studies of the Non-Heme Ferrous Active Site in Clavaminate Synthase and Its Interaction with α -Ketoglutarate Cosubstrate*, *J. Am. Chem. Soc.* **1998**, 120(4), 743–753, DOI: 10.1021/ja972408a.
- [192] E. L. Hegg, A. K. Whiting, R. E. Saari, J. McCracken, R. P. Hausinger, L. Que, *Herbicide-Degrading α -Keto Acid-Dependent Enzyme TfdA*, *Biochemistry* **1999**, 38(50), 16714–16726, DOI: 10.1021/bi991796l.
- [193] M. J. Ryle, R. Padmakumar, R. P. Hausinger, *Stopped-Flow Kinetic Analysis of Escherichia coli Taurine/ α -Ketoglutarate Dioxygenase*, *Biochemistry* **1999**, 38(46), 15278–15286, DOI: 10.1021/bi9912746.
- [194] S. C. Trewick, T. F. Henshaw, R. P. Hausinger, T. Lindahl, B. Sedgwick, *Oxidative demethylation by Escherichia coli AlkB directly reverts DNA base damage*, *Nature* **2002**, 419(6903), 174–178, DOI: 10.1038/nature00908.
- [195] D. A. Proshlyakov, R. P. Hausinger in *Iron-Containing Enzymes*; (Eds. de Visser, Sam P, D. Kumar), Royal Society of Chemistry, Cambridge, **2011**, 67–87, DOI: 10.1039/9781849732987-00067.
- [196] M. J. Ryle, A. Liu, R. B. Muthukumar, R. Y. N. Ho, K. D. Koehntop, J. McCracken, Que,, Lawrence, R. P. Hausinger, *O₂ - and α -Ketoglutarate-Dependent Tyrosyl Radical Formation in TauD, an α -Keto Acid-Dependent Non-Heme Iron Dioxygenase †*, *Biochemistry* **2003**, 42(7), 1854–1862, DOI: 10.1021/bi026832m.
- [197] M. Mantri, Z. Zhang, M. A. McDonough, C. J. Schofield, *Autocatalysed oxidative modifications to 2-oxoglutarate dependent oxygenases*, *FEBS J.* **2012**, 279(9), 1563–1575, DOI: 10.1111/j.1742-4658.2012.08496.x.
- [198] A. Liu, R. Y. N. Ho, L. Que, M. J. Ryle, B. S. Phinney, R. P. Hausinger, *Alternative Reactivity of an α -Ketoglutarate-Dependent Iron(II) Oxygenase*, *J. Am. Chem. Soc.* **2001**, 123(21), 5126–5127, DOI: 10.1021/ja005879x.
- [199] P. F. Fitzpatrick, *Mechanism of Aromatic Amino Acid Hydroxylation*, *Biochemistry* **2003**(42), 14083–14091, DOI: 10.1021/bi035656u.

Literature

- [200] M. Costas, M. P. Mehn, M. P. Jensen, L. Que, *Dioxygen activation at mononuclear non-heme iron active sites: enzymes, models, and intermediates*, Chem. Rev. **2004**, 104(2), 939–986, DOI: 10.1021/cr020628n.
- [201] A. M. Rocklin, D. L. Tierney, V. Kofman, N. M. W. Brunhuber, B. M. Hoffman, R. E. Christoffersen, N. O. Reich, J. D. Lipscomb, L. Que, *Role of the nonheme Fe(II) center in the biosynthesis of the plant hormone ethylene*, Proc. Natl. Acad. Sci. U.S.A. **1999**, 96(14), 7905–7909, DOI: 10.1073/pnas.96.14.7905.
- [202] J. E. Baldwin, M. Bradley, *Isopenicillin N synthase*, Chem. Rev. **1990**, 90(7), 1079–1088, DOI: 10.1021/cr00105a001.
- [203] M. L. Neidig, A. Decker, O. W. Choroba, F. Huang, M. Kavana, G. R. Moran, J. B. Spencer, E. I. Solomon, *Spectroscopic and electronic structure studies of aromatic electrophilic attack and hydrogen-atom abstraction by non-heme iron enzymes*, Proc. Natl. Acad. Sci. U.S.A. **2006**, 103(35), 12966–12973, DOI: 10.1073/pnas.0605067103.
- [204] E. I. Solomon, T. C. Brunold, M. I. Davis, J. N. Kemsley, S.-K. Lee, N. Lehnert, F. Neese, A. J. Skulan, Y.-S. Yang, J. Zhou, *Geometric and Electronic Structure/Function Correlations in Non-Heme Iron Enzymes*, Chem. Rev. **2000**, 100(1), 235–350, DOI: 10.1021/cr9900275.
- [205] E. I. Solomon, S. Goudarzi, K. D. Sutherlin, *O₂ Activation by Non-Heme Fe Enzymes*, Biochemistry **2016**, DOI: 10.1021/acs.biochem.6b00635.
- [206] H. M. Hanauske-Abel, A. M. Popowicz, *The HAG mechanism: A molecular rationale for the therapeutic application of iron chelators in human diseases involving the 2-oxoacid utilizing dioxygenases*, Curr. Med. Chem. **2003**, 10(12), 1005–1019.
- [207] H. M. Hanauske-Abel, V. Günzler, *A Stereochemical Concept for the Catalytic Mechanism of Prolylhydroxylase*, J. theor. Biol. **1982**(94), 421–455, DOI: 10.1016/0022-5193(82)90320-4.
- [208] J. M. Bollinger, J. C. Price, L. M. Hoffart, E. W. Barr, C. Krebs, *Mechanism of Taurine*, Eur. J. Inorg. Chem. **2005**, 2005(21), 4245–4254, DOI: 10.1002/ejic.200500476.
- [209] P. K. Grzyska, E. H. Appelman, R. P. Hausinger, D. A. Proshlyakov, *Insight into the mechanism of an iron dioxygenase by resolution of steps following the FeIV=HO species*, Proc. Natl. Acad. Sci. U.S.A. **2010**, 107(9), 3982–3987, DOI: 10.1073/pnas.0911565107.
- [210] H. J. Kulik, C. L. Drennan, *Substrate placement influences reactivity in non-heme Fe(II) halogenases and hydroxylases*, J. Biol. Chem. **2013**, 288(16), 11233–11241, DOI: 10.1074/jbc.M112.415570.
- [211] H. J. Kulik, L. C. Blasiak, N. Marzari, C. L. Drennan, *First-principles study of non-heme Fe(II) halogenase SyrB2 reactivity*, J. Am. Chem. Soc. **2009**, 131(40), 14426–14433, DOI: 10.1021/ja905206k.
- [212] D. G. Fujimori, E. W. Barr, M. L. Matthews, G. M. Koch, J. R. Yonce, C. T. Walsh, J. M. Bollinger, C. Krebs, P. J. Riggs-Gelasco, *Spectroscopic evidence for a high-spin Br-Fe(IV)-oxo intermediate in the alpha-ketoglutarate-dependent halogenase CytC3 from Streptomyces*, J. Am. Chem. Soc. **2007**, 129(44), 13408–13409, DOI: 10.1021/ja076454e.

- [213] C. Krebs, D. Galonic Fujimori, C. T. Walsh, J. M. Bollinger, JR, *Non-heme Fe(IV)-oxo intermediates*, *Acc. Chem. Res.* **2007**, *40*(7), 484–492, DOI: 10.1021/ar700066p.
- [214] J.-U. Rohde, J.-H. In, M. H. Lim, W. W. Brennessel, M. R. Bukowski, A. Stubna, E. Münck, W. Nam, L. Que, *Crystallographic and Spectroscopic Characterization of a Nonheme Fe(IV)=O complex*, *Science* **2003**(299), 1037–1039, DOI: 10.1126/science.299.5609.1037.
- [215] M. H. Lim, J.-U. Rohde, A. Stubna, M. R. Bukowski, M. Costas, R. Y. N. Ho, E. Munck, W. Nam, L. Que, *An FeIV=O complex of a tetradentate tripodal nonheme ligand*, *Proc. Natl. Acad. Sci. U.S.A.* **2003**, *100*(7), 3665–3670, DOI: 10.1073/pnas.0636830100.
- [216] F. Tiago de Olivera, A. Chanda, D. Banerjee, X. Shan, S. pmadal, L. Que, *Chemical and Spectroscopic Evidence for an FeIV-Oxo Complex*, *Science* **2007**(315), 835–838, DOI: 10.1126/science.1133417.
- [217] O. Pestovsky, S. Stoian, E. L. Bominaar, X. Shan, E. Münck, L. Que, A. Bakac, *Aqueous FeIV=O*, *Angew. Chem. Int. Ed.* **2005**, *44*(42), 6871–6874, DOI: 10.1002/anie.200502686.
- [218] S. Pandian, M. A. Vincent, I. H. Hillier, N. A. Burton, *Why does the enzyme SyrB2 chlorinate, but does not hydroxylate, saturated hydrocarbons? A density functional theory (DFT) study*, *Dalton Trans.* **2009**(31), 6201–6207, DOI: 10.1039/b906866j.
- [219] de Visser, Sam P, R. Latifi, *Carbon dioxide: a waste product in the catalytic cycle of alpha-ketoglutarate dependent halogenases prevents the formation of hydroxylated by-products*, *J. Phys. Chem. B* **2009**, *113*(1), 12–14, DOI: 10.1021/jp8097632.
- [220] T. Borowski, H. Noack, M. Radon, K. Zych, P. E. M. Siegbahn, *Mechanism of selective halogenation by SyrB2: a computational study*, *J. Am. Chem. Soc.* **2010**, *132*(37), 12887–12898, DOI: 10.1021/ja101877a.
- [221] D. Usharani, D. Janardanan, S. Shaik, *Does the TauD enzyme always hydroxylate alkanes, while an analogous synthetic non-heme reagent always desaturates them?*, *J. Am. Chem. Soc.* **2011**, *133*(2), 176–179, DOI: 10.1021/ja107339h.
- [222] J. Huang, C. Li, B. Wang, D. A. Sharon, W. Wu, S. Shaik, *Selective Chlorination of Substrates by the Halogenase SyrB2 Is Controlled by the Protein According to a Combined Quantum Mechanics/Molecular Mechanics and Molecular Dynamics Study*, *ACS Catal.* **2016**, *6*(4), 2694–2704, DOI: 10.1021/acscatal.5b02825.
- [223] S. D. Wong, M. Srnc, M. L. Matthews, L. V. Liu, Y. Kwak, K. Park, C. B. Bell, E. E. Alp, J. Zhao, Y. Yoda, S. Kitao, M. Seto, C. Krebs, J. M. Bollinger, E. I. Solomon, *Elucidation of the Fe(IV)=O intermediate in the catalytic cycle of the halogenase SyrB2*, *Nature* **2013**, *499*(7458), 320–323, DOI: 10.1038/nature12304.
- [224] R. Y. N. Ho, M. P. Mehn, E. L. Hegg, A. Liu, M. J. Ryle, R. P. Hausinger, L. Que, *Resonance Raman Studies of the Iron(II)- α -Keto Acid Chromophore in Model and Enzyme Complexes*, *J. Am. Chem. Soc.* **2001**, *123*(21), 5022–5029, DOI: 10.1021/ja0041775.

- [225] J. C. Price, E. W. Barr, B. Tirupati, Bollinger, J. Martin, C. Krebs, *The First Direct Characterization of a High-Valent Iron Intermediate in the Reaction of an α -Ketoglutarate-Dependent Dioxygenase*, *Biochemistry* **2003**, 42(24), 7497–7508, DOI: 10.1021/bi030011f.
- [226] J. C. Price, E. W. Barr, L. M. Hoffart, C. Krebs, J. M. Bollinger, *Kinetic Dissection of the Catalytic Mechanism of Taurine*, *Biochemistry* **2005**, 44(22), 8138–8147, DOI: 10.1021/bi050227c.
- [227] M. L. Matthews, C. M. Krest, E. W. Barr, F. H. Vaillancourt, C. T. Walsh, M. T. Green, C. Krebs, J. M. Bollinger, *Substrate-triggered formation and remarkable stability of the C-H bond-cleaving chloroferryl intermediate in the aliphatic halogenase, SyrB2*, *Biochemistry* **2009**, 48(20), 4331–4343, DOI: 10.1021/bi900109z.
- [228] J. C. Price, E. W. Barr, T. E. Glass, C. Krebs, J. M. Bollinger, *Evidence for hydrogen abstraction from C1 of taurine by the high-spin Fe(IV) intermediate detected during oxygen activation by taurine:alpha-ketoglutarate dioxygenase (TauD)*, *J. Am. Chem. Soc.* **2003**, 125(43), 13008–13009, DOI: 10.1021/ja037400h.
- [229] J. M. Bollinger, C. Krebs, *Stalking intermediates in oxygen activation by iron enzymes: motivation and method*, *J. Inorg. Biochem.* **2006**, 100(4), 586–605, DOI: 10.1016/j.jinorg-bio.2006.01.022.
- [230] L. M. Hoffart, E. W. Barr, R. B. Guyer, J. M. Bollinger, C. Krebs, *Direct spectroscopic detection of a C-H-cleaving high-spin Fe(IV) complex in a prolyl-4-hydroxylase*, *Proc. Natl. Acad. Sci. U.S.A.* **2006**, 103(40), 14738–14743, DOI: 10.1073/pnas.0604005103.
- [231] G. Rugg, H. M. Senn, *Formation and structure of the ferryl Fe double bond, length as $m\text{-}O$ intermediate in the non-haem iron halogenase SyrB2*, *Phys. Chem. Chem. Phys.* **2017**, 19(44), 30107–30119, DOI: 10.1039/c7cp05937j.
- [232] M. Srncic, E. I. Solomon, *Frontier Molecular Orbital Contributions to Chlorination versus Hydroxylation Selectivity in the Non-Heme Iron Halogenase SyrB2*, *J. Am. Chem. Soc.* **2017**, 139(6), 2396–2407, DOI: 10.1021/jacs.6b11995.
- [233] T. Kojima, R. A. Leising, S. Yan, L. Que, *Alkane functionalization at nonheme iron centers. Stoichiometric transfer of metal-bound ligands to alkane*, *J. Am. Chem. Soc.* **1993**, 115(24), 11328–11335, DOI: 10.1021/ja00077a035.
- [234] X. Huang, J. T. Groves, *Beyond ferryl-mediated hydroxylation*, *J. Biol. Inorg. Chem.* **2017**, 22(2-3), 185–207, DOI: 10.1007/s00775-016-1414-3.
- [235] R. J. Martinie, J. Livada, W.-C. Chang, M. T. Green, C. Krebs, J. M. Bollinger, A. Silakov, *Experimental Correlation of Substrate Position with Reaction Outcome in the Aliphatic Halogenase, SyrB2*, *J. Am. Chem. Soc.* **2015**, 137(21), 6912–6919, DOI: 10.1021/jacs.5b03370.
- [236] M. L. Micallef, D. Sharma, B. M. Bunn, L. Gerwick, R. Viswanathan, M. C. Moffitt, *Comparative analysis of hapalindole, ambiguine and welwitindolinone gene clusters and reconstitution of indole-isonitrile biosynthesis from cyanobacteria*, *BMC Microbiology* **2014**, 14, 213, DOI: 10.1186/s12866-014-0213-7.

- [237] R. Rippka, J. Deruelles, J. B. Waterbury, M. Herdman, R. Stanier, *Generic Assignments, Strain Histories and Properties of Pure Cultures of Cyanobacteria*, *Journal of General Microbiology* **1979**(111), 1–61, DOI: 10.1099/00221287-111-1-1.
- [238] M. L. Micallef, P. M. D'Agostino, B. Al-Sinawi, B. A. Neilan, M. C. Moffitt, *Exploring cyanobacterial genomes for natural product biosynthesis pathways*, *Marine genomics* **2014**, DOI: 10.1016/j.margen.2014.11.009.
- [239] V. Bhat, A. Dave, J. A. MacKay, V. H. Rawal in *Chemistry and Biology, The Alkaloids: Chemistry and Biology*, Elsevier, **2014**, 65–160, DOI: 10.1016/B978-0-12-411565-1.00002-0.
- [240] R. E. Moore, C. Cheuk, G. M. L. Patterson, *Hapalindoles*, *J. Am. Chem. Soc.* **1984**, 106(21), 6456–6457, DOI: 10.1021/ja00333a079.
- [241] M. L. Hillwig, Q. Zhu, X. Liu, *Biosynthesis of ambiguine indole alkaloids in cyanobacterium Fischerella ambigua*, *ACS Chem. Biol.* **2014**, 9(2), 372–377, DOI: 10.1021/cb400681n.
- [242] M. L. Hillwig, H. A. Fuhrman, K. Ittiamornkul, T. J. Sevco, D. H. Kwak, X. Liu, *Identification and characterization of a welwitindolinone alkaloid biosynthetic gene cluster in the stigonematalean Cyanobacterium Hapalosiphon welwitschii*, *ChemBioChem* **2014**, 15(5), 665–669, DOI: 10.1002/cbic.201300794.
- [243] S. Li, A. N. Lowell, F. Yu, A. Raveh, S. A. Newmister, N. Bair, J. M. Schaub, R. M. Williams, D. H. Sherman, *Hapalindole/Ambiguine Biogenesis Is Mediated by a Cope Rearrangement, C-C Bond-Forming Cascade*, *J. Am. Chem. Soc.* **2015**, DOI: 10.1021/jacs.5b10136.
- [244] S. Li, A. N. Lowell, S. A. Newmister, F. Yu, R. M. Williams, D. H. Sherman, *Decoding cyclase-dependent assembly of hapalindole and fischerindole alkaloids*, *Nat. Chem. Biol.* **2017**, DOI: 10.1038/nchembio.2327.
- [245] T. Awakawa, T. Mori, Y. Nakashima, R. Zhai, C. P. Wong, M. L. Hillwig, X. Liu, I. Abe, *Molecular Insight into the Mg²⁺-Dependent Allosteric Control of Indole Prenylation by Aromatic Prenyltransferase AmbP1*, *Angew. Chem. Int. Ed.* **2018**, 57(23), 6810–6813, DOI: 10.1002/anie.201800855.
- [246] X. Liu, M. L. Hillwig, L. M. I. Koharudin, A. M. Gronenborn, *Unified biogenesis of ambiguine, fischerindole, hapalindole and welwitindolinone: identification of a monogeranylated indolenine as a cryptic common biosynthetic intermediate by an unusual magnesium-dependent aromatic prenyltransferase*, *Chem. Commun.* **2016**, 52(8), 1737–1740, DOI: 10.1039/c5cc10060g.
- [247] K. Ittiamornkul, Q. Zhu, D. S. Gkotsi, D. R. M. Smith, M. L. Hillwig, N. Nightingale, R. J. M. Goss, X. Liu, *Promiscuous indolyl vinyl isonitrile synthases in the biogenesis and diversification of hapalindole-type alkaloids*, *Chem. Sci.* **2015**, 6(12), 6836–6840, DOI: 10.1039/C5SC02919H.
- [248] U. T. Bornscheuer, G. W. Huisman, R. J. Kazlauskas, S. Lutz, J. C. Moore, K. Robins, *Engineering the third wave of biocatalysis*, *Nature* **2012**, 485(7397), 185–194, DOI: 10.1038/nature11117.

- [249] M. Wang, T. Si, H. Zhao, *Biocatalyst development by directed evolution*, *Bioresour. Technol.* **2012**, *115*, 117–125, DOI: 10.1016/j.biortech.2012.01.054.
- [250] T. J. Collins, *McEncyGCEntry*, *Green Chem.* **1997**, 691–697.
- [251] P. T. Anastas, *Introduction*, *Chem. Rev.* **2007**, *107*(6), 2167–2168, DOI: 10.1021/cr0783784.
- [252] P. Anastas, N. Eghbali, *Green chemistry*, *Chem. Soc. Rev.* **2010**, *39*(1), 301–312, DOI: 10.1039/b918763b.
- [253] P. T. Anastas, J. C. Warner, *Green chemistry: Theory and practice*; Oxford University Press, Oxford, **1998**.
- [254] S. Brown, S. E. O'Connor, *Halogenase Engineering for the Generation of New Natural Product Analogues*, *ChemBioChem* **2015**, DOI: 10.1002/cbic.201500338.
- [255] S. H. Combe, A. Hosseini, A. Parra, P. R. Schreiner, *Mild Aliphatic and Benzylic Hydrocarbon C-H Bond Chlorination Using Trichloroisocyanuric Acid*, *J. Org. Chem.* **2017**, *82*(5), 2407–2413, DOI: 10.1021/acs.joc.6b02829.
- [256] M. Eissen, M. Strudthoff, S. Backhaus, C. Eismann, G. Oetken, S. Kaling, D. Lenoir, *Oxidation Numbers, Oxidants, and Redox Reactions*, *J. Chem. Educ.* **2011**, *88*(3), 284–291, DOI: 10.1021/ed101055j.
- [257] M. Eissen, D. Lenoir, *Electrophilic bromination of alkenes*, *Chem. Eur. J.* **2008**, *14*(32), 9830–9841, DOI: 10.1002/chem.200800462.
- [258] P. Domínguez de María, F. Hollmann, *On the (Un)greenness of Biocatalysis: Some Challenging Figures and Some Promising Options*, *Frontiers in microbiology* **2015**, *6*, 1257, DOI: 10.3389/fmicb.2015.01257.
- [259] P. Tufvesson, J. Lima-Ramos, N. A. Haque, K. V. Gernaey, J. M. Woodley, *Advances in the Process Development of Biocatalytic Processes*, *Org. Process Res. Dev.* **2013**, *17*(10), 1233–1238, DOI: 10.1021/op4001675.
- [260] J. C. Lewis, P. S. Coelho, F. H. Arnold, *Enzymatic functionalization of carbon-hydrogen bonds*, *Chem. Soc. Rev.* **2011**, *40*(4), 2003–2021, DOI: 10.1039/c0cs00067a.
- [261] C. K. Savile, J. M. Janey, E. C. Mundorff, J. C. Moore, S. Tam, W. R. Jarvis, J. C. Colbeck, A. Krebber, F. J. Fleitz, J. Brands, P. N. Devine, G. W. Huisman, G. J. Hughes, *Biocatalytic asymmetric synthesis of chiral amines from ketones applied to sitagliptin manufacture*, *Science* **2010**, *329*(5989), 305–309, DOI: 10.1126/science.1188934.
- [262] S. K. Ma, J. Gruber, C. Davis, L. Newman, D. Gray, A. Wang, J. Grate, G. W. Huisman, R. A. Sheldon, *A green-by-design biocatalytic process for atorvastatin intermediate*, *Green Chem.* **2010**, *12*(1), 81–86, DOI: 10.1039/B919115C.
- [263] G. A. Strohmeier, H. Pichler, O. May, M. Gruber-Khadjawi, *Application of designed enzymes in organic synthesis*, *Chem. Rev.* **2011**, *111*(7), 4141–4164, DOI: 10.1021/cr100386u.
- [264] R. J. Kazlauskas, U. T. Bornscheuer, *Finding better protein engineering strategies*, *Nat. Chem. Biol.* **2009**, *5*(8), 526–529, DOI: 10.1038/nchembio0809-526.

- [265] H. M. Dudek, M. J. Fink, A. V. Shivange, A. Dennig, M. D. Mihovilovic, U. Schwaneberg, M. W. Fraaije, *Extending the substrate scope of a Baeyer-Villiger monooxygenase by multiple-site mutagenesis*, *Appl. Microbiol. Biotechnol.* **2014**, 98(9), 4009–4020, DOI: 10.1007/s00253-013-5364-1.
- [266] D. J. Bougioukou, S. Kille, A. Taglieber, M. T. Reetz, *Directed Evolution of an Enantioselective Enoate-Reductase*, *Adv. Synth. Catal.* **2009**, 351(18), 3287–3305, DOI: 10.1002/adsc.200900644.
- [267] K. Engström, J. Nyhlén, A. G. Sandström, J.-E. Bäckvall, *Directed evolution of an enantioselective lipase with broad substrate scope for hydrolysis of alpha-substituted esters*, *J. Am. Chem. Soc.* **2010**, 132(20), 7038–7042, DOI: 10.1021/ja100593j.
- [268] C. A. Denard, H. Ren, H. Zhao, *Improving and repurposing biocatalysts via directed evolution*, *Curr. Opin. Chem. Biol.* **2015**, 25, 55–64, DOI: 10.1016/j.cbpa.2014.12.036.
- [269] M. T. Reetz, P. Soni, L. Fernández, Y. Gumulya, J. D. Carballeira, *Increasing the stability of an enzyme toward hostile organic solvents by directed evolution based on iterative saturation mutagenesis using the B-FIT method*, *Chem. Commun.* **2010**, 46(45), 8657–8658, DOI: 10.1039/c0cc02657c.
- [270] V. Stepankova, S. Bidmanova, T. Koudelakova, Z. Prokop, R. Chaloupkova, J. Damborsky, *Strategies for Stabilization of Enzymes in Organic Solvents*, *ACS Catal.* **2013**, 3(12), 2823–2836, DOI: 10.1021/cs400684x.
- [271] R. Yamada, T. Higo, C. Yoshikawa, H. China, H. Ogino, *Improvement of the stability and activity of the BPO-A1 haloperoxidase from Streptomyces aureofaciens by directed evolution*, *J. Biotechnol.* **2014**, 192 Pt A, 248–254, DOI: 10.1016/j.jbiotec.2014.10.030.
- [272] R. Yamada, T. Higo, C. Yoshikawa, H. China, M. Yasuda, H. Ogino, *Random mutagenesis and selection of organic solvent-stable haloperoxidase from Streptomyces aureofaciens*, *Biotechnol. Prog.* **2015**, 31(4), 917–924, DOI: 10.1002/btpr.2117.
- [273] Rosenthaler L, *Durch Enzyme bewirkte asymmetrische Synthese*, *Biochem. Z.* **1908**(14), 238–253.
- [274] L. Sedlaczek, *Biotransformations of steroids*, *Critical reviews in biotechnology* **1988**, 7(3), 187–236, DOI: 10.3109/07388558809146602.
- [275] J. C. Francis, P. E. Hansche, *Directed evolution of metabolic pathways in microbial populations I. Modification of the acid phosphatase pH optimum in S. cerevisiae*, *Genetics* **1972**(70), 59–73.
- [276] J. C. Kendrew, G. Codo, H. M. Dinitzis, R. G. Parrish, H. Wyckoff, D. C. Phillips, *A Three-Dimensional Model of the Myoglobin Molecule Obtained by X-Ray Analysis*, *Nature* **1958**(181), 662–666, DOI: 10.1038/181662a0.
- [277] M. Perutz, M. G. Rossmann, A. F. Cullis, H. Muirhead, G. Will, A. C. T. North, *Structure of Haemoglobin*, *Nature* **1960**(183), 416–411, DOI: 10.1038/185416a0.

- [278] H. Griengl, H. Schwab, M. Fechter, *The synthesis of chiral cyanohydrins by oxynitrilases*, Trends in Biotechnology **2000**, 18(6), 252–256, DOI: 10.1016/S0167-7799(00)01452-9.
- [279] T. Nagasawa, T. Nakamura, H. Yamada, *Production of acrylic acid and methacrylic acid using Rhodococcus rhodochrous J1 nitrilase*, Appl. Microbiol. Biotechnol. **1990**(34), 322–324, DOI: 10.1007/BF00170051.
- [280] M. T. Reetz, A. Zonta, K. Schimossek, K.-E. Jaeger, K. Liebeton, *Creation of Enantioselective Biocatalysts for Organic Chemistry by In Vitro Evolution*, Angew. Chem. Int. Ed. **1997**, 36(24), 2830–2832, DOI: 10.1002/anie.199728301.
- [281] W. P. C. Stemmer, *Rapid evolution of a protein in vitro by DNA shuffling*, Nature **1994**(370), 389–391, DOI: 10.1038/370389a0.
- [282] F. H. Arnold, *Directed Evolution: Creating Biocatalysts for the Future*, Chem. Eng. Sci. **1996**(23), 5091–5102, DOI: 10.1016/S0009-2509(96)00288-6.
- [283] D. W. Leung, E. Chen, D. V. Goeddel, *A method for random mutagenesis of a defined DNA segment using a modified polymerase chain reaction*, Technique **1989**, 1, 11–15.
- [284] C. R. Cadwell, G. F. Joyce, *Randomization of Genes by PCR Mutagenesis*, Cold Spring Harbor Laboratory **1992**(2), 28–33, DOI: 10.1101/gr.2.1.28.
- [285] K. A. Powell, S. W. Ramer, S. B. del Cardayré, W. P. C. Stemmer, M. B. Tobin, P. F. Longchamp, G. W. Huisman, *Directed Evolution and Biocatalysis*, Angew. Chem. Int. Ed. **2001**(40), 3948–3959.
- [286] M. T. Reetz, *What are the Limitations of Enzymes in Synthetic Organic Chemistry?*, Chemical record (New York, N.Y.) **2016**, 16(6), 2449–2459, DOI: 10.1002/tcr.201600040.
- [287] M. Goldsmith, D. S. Tawfik, *Directed enzyme evolution: beyond the low-hanging fruit*, Curr. Opin. Struct. Biol. **2012**, 22(4), 406–412, DOI: 10.1016/j.sbi.2012.03.010.
- [288] S. Lutz, *Beyond directed evolution – semi-rational protein engineering and design*, Curr. Opin. Biotechnol. **2010**, 21(6), 734–743, DOI: 10.1016/j.copbio.2010.08.011.
- [289] A. Currin, N. Swainston, P. J. Day, D. B. Kell, *Synthetic biology for the directed evolution of protein biocatalysts*, Chem. Soc. Rev. **2015**, 44(5), 1172–1239, DOI: 10.1039/c4cs00351a.
- [290] W. M. Patrick, A. E. Firth, J. M. Blackburn, *User-friendly algorithms for estimating completeness and diversity in randomized protein-encoding libraries*, Protein Eng. Des. Sel. **2003**, 16(6), 451–457, DOI: 10.1093/protein/gzg057.
- [291] W. M. Patrick, A. E. Firth, *Strategies and computational tools for improving randomized protein libraries*, Biomol. Eng. **2005**, 22(4), 105–112, DOI: 10.1016/j.bioeng.2005.06.001.
- [292] A. D. Bosley, M. Ostermeier, *Mathematical expressions useful in the construction, description and evaluation of protein libraries*, Biomol. Eng. **2005**, 22(1-3), 57–61, DOI: 10.1016/j.bioeng.2004.11.002.
- [293] J. Damborsky, J. Brezovsky, *Computational tools for designing and engineering enzymes*, Curr. Opin. Chem. Biol. **2014**, 19, 8–16, DOI: 10.1016/j.cbpa.2013.12.003.

Literature

- [294] M. C. Ebert, J. N. Pelletier, *Computational tools for enzyme improvement: why everyone can - and should - use them*, *Curr. Opin. Chem. Biol.* **2017**, *37*, 89–96, DOI: 10.1016/j.cbpa.2017.01.021.
- [295] R. J. Fox, S. C. Davis, E. C. Mundorff, L. M. Newman, V. Gavrilovic, S. K. Ma, L. M. Chung, C. Ching, S. Tam, S. Muley, J. Grate, J. Gruber, J. C. Whitman, R. A. Sheldon, G. W. Huisman, *Improving catalytic function by ProSAR-driven enzyme evolution*, *Nat. Biotechnol.* **2007**, *25*(3), 338–344, DOI: 10.1038/nbt1286.
- [296] L. Jiang, E. A. Althoff, F. R. Clemente, L. Doyle, D. Röthlisberger, A. Zanghellini, J. L. Gallaher, J. L. Betker, F. Tanaka, C. F. Barbas, D. Hilvert, K. N. Houk, B. L. Stoddard, D. Baker, *De novo computational design of retro-aldol enzymes*, *Science* **2008**, *319*(5868), 1387–1391, DOI: 10.1126/science.1152692.
- [297] M. T. Reetz, M. Bocola, J. D. Carballeira, D. Zha, A. Vogel, *Expanding the range of substrate acceptance of enzymes*, *Angew. Chem. Int. Ed.* **2005**, *44*(27), 4192–4196, DOI: 10.1002/anie.200500767.
- [298] M. T. Reetz, J. D. Carballeira, *Iterative saturation mutagenesis (ISM) for rapid directed evolution of functional enzymes*, *Nature protocols* **2007**, *2*(4), 891–903, DOI: 10.1038/nprot.2007.72.
- [299] J. A. Wells, *Additivity of mutational effects in proteins*, *Biochemistry* **1990**, *29*(37), 8509–8517, DOI: 10.1021/bi00489a001.
- [300] D. M. Weinreich, N. F. Delaney, M. A. DePristo, D. L. Hartl, *Darwinian Evolution Can Follow Only Very Few Mutational Paths to Fitter Proteins*, *Science* **2006**, *312*(5770), 11–114, DOI: 10.1126/science.1123539.
- [301] M. T. Reetz, J. Sanchis, *Constructing and analyzing the fitness landscape of an experimental evolutionary process*, *ChemBioChem* **2008**, *9*(14), 2260–2267, DOI: 10.1002/cbic.200800371.
- [302] M. T. Reetz, *The Importance of Additive and Non-Additive Mutational Effects in Protein Engineering*, *Angew. Chem. Int. Ed.* **2013**, *52*(10), 2658–2666, DOI: 10.1002/anie.201207842.
- [303] Z. Sun, Y. Wikmark, J.-E. Bäckvall, M. T. Reetz, *New Concepts for Increasing the Efficiency in Directed Evolution of Stereoselective Enzymes*, *Chem. Eur. J.* **2016**, *22*(15), 5046–5054, DOI: 10.1002/chem.201504406.
- [304] Z. Sun, R. Lonsdale, G. Li, M. T. Reetz, *Comparing Different Strategies in Directed Evolution of Enzyme Stereoselectivity*, *ChemBioChem* **2016**, *17*(19), 1865–1872, DOI: 10.1002/cbic.201600296.
- [305] M. T. Reetz, D. Kahakeaw, R. Lohmer, *Addressing the numbers problem in directed evolution*, *ChemBioChem* **2008**, *9*(11), 1797–1804, DOI: 10.1002/cbic.200800298.
- [306] S. Kille, C. G. Acevedo-Rocha, L. P. Parra, Z.-G. Zhang, D. J. Opperman, M. T. Reetz, J. P. Acevedo, *Reducing codon redundancy and screening effort of combinatorial protein libraries created by saturation mutagenesis*, *ACS Synth. Biol.* **2013**, *2*(2), 83–92, DOI: 10.1021/sb300037w.

- [307] S. Hoebenreich, F. E. Zilly, C. G. Acevedo-Rocha, M. Zilly, M. T. Reetz, *Speeding up directed evolution*, ACS Synth. Biol. **2015**, 4(3), 317–331, DOI: 10.1021/sb5002399.
- [308] Y. Nov, *When second best is good enough: another probabilistic look at saturation mutagenesis*, Appl. Environ. Microbiol. **2012**, 78(1), 258–262, DOI: 10.1128/AEM.06265-11.
- [309] S. C. Hammer, A. M. Knight, F. H. Arnold, *Design and evolution of enzymes for non-natural chemistry*, Curr Opin Green Sustain Chem **2017**, 7, 23–30, DOI: 10.1016/j.cogsc.2017.06.002.
- [310] H. Renata, Z. J. Wang, F. H. Arnold, *Expanding the enzyme universe: accessing non-natural reactions by mechanism-guided directed evolution*, Angew. Chem. Int. Ed. **2015**, 54(11), 3351–3367, DOI: 10.1002/anie.201409470.
- [311] S. B. J. Kan, R. D. Lewis, K. Chen, F. H. Arnold, *Directed evolution of cytochrome c for carbon-silicon bond formation*, Science **2016**, 354(6315), 1048–1051, DOI: 10.1126/science.aah6219.
- [312] S. B. J. Kan, X. Huang, Y. Gumulya, K. Chen, F. H. Arnold, *Genetically programmed chiral organoborane synthesis*, Nature **2017**, 552(7683), 132–136, DOI: 10.1038/nature24996.
- [313] T. Davids, M. Schmidt, D. Böttcher, U. T. Bornscheuer, *Strategies for the discovery and engineering of enzymes for biocatalysis*, Curr. Opin. Chem. Biol. **2013**, 17(2), 215–220, DOI: 10.1016/j.cbpa.2013.02.022.
- [314] F. Cheng, L. Zhu, U. Schwaneberg, *Directed evolution 2.0*, Chem. Commun. **2015**, 51(48), 9760–9772, DOI: 10.1039/C5CC01594D.
- [315] N. Nett, S. Duewel, A. A. Richter, S. Hoebenreich, *Revealing Additional Stereocomplementary Pairs of Old Yellow Enzymes by Rational Transfer of Engineered Residues*, ChemBioChem **2017**, 18(7), 685–691, DOI: 10.1002/cbic.201600688.
- [316] G. Li, J.-B. Wang, M. T. Reetz, *Biocatalysts for the pharmaceutical industry created by structure-guided directed evolution of stereoselective enzymes*, Bioorg. Med. Chem. **2018**, 26(7), 1241–1251, DOI: 10.1016/j.bmc.2017.05.021.
- [317] L. L. Schmermund, Master Thesis, Philipps-Universität Marburg, **2017**.
- [318] C. D. Smith, J. T. Zilfou, K. Stratmann, G. M. Patterson, R. E. Moore, *Welwitindolinone analogues that reverse P-glycoprotein-mediated multiple drug resistance*, Mol. Pharmacol. **1995**, 47(2), 241–247.
- [319] X. Zhang, C. D. Smith, *Microtubule effects of welwistatin, a cyanobacterial indolinone that circumvents multiple drug resistance*, Mol. Pharmacol. **1996**, 49(2), 288–294.
- [320] S. Mo, A. Kronic, B. D. Santarsiero, S. G. Franzblau, J. Orjala, *Hapalindole-related alkaloids from the cultured cyanobacterium Fischerella ambigua*, Phytochemistry **2010**, 71(17-18), 2116–2123, DOI: 10.1016/j.phytochem.2010.09.004.
- [321] S. Mo, A. Kronic, G. Chlipala, J. Orjala, *Antimicrobial ambiguine isonitriles from the cyanobacterium Fischerella ambigua*, J. Nat. Prod. **2009**, 72(5), 894–899, DOI: 10.1021/np800751j.

Literature

- [322] H. Kim, D. Lantvit, C. H. Hwang, D. J. Kroll, S. M. Swanson, S. G. Franzblau, J. Orjala, *Indole alkaloids from two cultured cyanobacteria, Westiellopsis sp. and Fischerella muscicola*, *Bioorg. Med. Chem.* **2012**, 20(17), 5290–5295, DOI: 10.1016/j.bmc.2012.06.030.
- [323] Q. Zhu, X. Liu, *Molecular and genetic basis for early stage structural diversifications in hapalindole-type alkaloid biogenesis*, *Chem. Commun.* **2017**, DOI: 10.1039/C7CC00782E.
- [324] K. Kleigrew, L. Gerwick, D. H. Sherman, W. H. Gerwick, *Unique marine derived cyanobacterial biosynthetic genes for chemical diversity*, *Nat. Prod. Rep.* **2016**, 33(2), 348–364, DOI: 10.1039/c5np00097a.
- [325] Q. Zhu, X. Liu, *Discovery of a Calcium-Dependent Enzymatic Cascade for the Selective Assembly of Hapalindole-Type Alkaloids*, *Angew. Chem. Int. Ed.* **2017**, 56(31), 9062–9066, DOI: 10.1002/anie.201703932.
- [326] M. R. Wilkins, E. Gasteiger, A. Bairoch, J.-C. Sanchez, K. L. Williams, R. D. Appel, D. F. Hochstrasser in *2-D Proteome Analysis Protocols*; (Ed. A. J. Link), Humana Press, New Jersey, **1998**, 531–552, DOI: 10.1385/1-59259-584-7:531.
- [327] T. Unger, Y. Jacobovitch, A. Dantes, R. Bernheim, Y. Peleg, *Applications of the Restriction Free (RF) cloning procedure for molecular manipulations and protein expression*, *J. Struct. Biol.* **2010**, 172(1), 34–44, DOI: 10.1016/j.jsb.2010.06.016.
- [328] “National Center for Biotechnology Information”.
- [329] M. Marigo, K. A. Jørgensen, *Organocatalytic direct asymmetric alpha-heteroatom functionalization of aldehydes and ketones*, *Chem. Commun.* **2006**(19), 2001–2011, DOI: 10.1039/b517090g.
- [330] D. A. Petrone, J. Ye, M. Lautens, *Modern Transition-Metal-Catalyzed Carbon-Halogen Bond Formation*, *Chem. Rev.* **2016**, 116(14), 8003–8104, DOI: 10.1021/acs.chemrev.6b00089.
- [331] S. Chatterjee, T. K. Paine, *Hydroxylation versus Halogenation of Aliphatic C-H Bonds by a Dioxxygen-Derived Iron-Oxygen Oxidant*, *Angew. Chem. Int. Ed.* **2016**, 55(27), 7717–7722, DOI: 10.1002/anie.201509914.
- [332] Y. He, C. Goldsmith, *The Halogenation of Aliphatic C-H Bonds with Peracetic Acid and Halide Salts*, *Synlett* **2010**, 2010(09), 1377–1380, DOI: 10.1055/s-0029-1219832.
- [333] V. Agarwal, Z. D. Miles, J. M. Winter, A. S. Eustaquio, A. A. El Gamal, B. S. Moore, *Enzymatic Halogenation and Dehalogenation Reactions: Pervasive and Mechanistically Diverse*, *Chem. Rev.* **2017**, DOI: 10.1021/acs.chemrev.6b00571.
- [334] V. Weichold, D. Milbredt, K.-H. van Pee, *Specific Enzymatic Halogenation-From the Discovery of Halogenated Enzymes to Their Applications In Vitro and In Vivo*, *Angew. Chem. Int. Ed.* **2016**, 55(22), 6374–6389, DOI: 10.1002/anie.201509573.
- [335] C. Schnepel, N. Sewald, *Enzymatic Halogenation*, *Chem. Eur. J.* **2017**, DOI: 10.1002/chem.201701209.
- [336] A. E. Fraley, M. Garcia-Borràs, A. Tripathi, D. Khare, E. V. Mercado-Marin, H. Tran, Q. Dan, G. P. Webb, K. R. Watts, P. Crews, R. Sarpong, R. M. Williams, J. L. Smith, K. N.

- Houk, D. H. Sherman, *Function and Structure of MalA/MalA', Iterative Halogenases for Late-Stage C-H Functionalization of Indole Alkaloids*, *J. Am. Chem. Soc.* **2017**, 139(34), 12060–12068, DOI: 10.1021/jacs.7b06773.
- [337] G. Chen, S. Ma, *Enantioselective halocyclization reactions for the synthesis of chiral cyclic compounds*, *Angew. Chem. Int. Ed.* **2010**, 49(45), 8306–8308, DOI: 10.1002/anie.201003114.
- [338] C. Tan, L. Zhou, Y.-Y. Yeung, *Organocatalytic Enantioselective Halolactonizations*, *Synlett* **2011**, 2011(10), 1335–1339, DOI: 10.1055/s-0030-1260578.
- [339] P. Stothard, *The sequence manipulation suite*, *BioTechniques* **2000**, 28(6), 1102, 1104, DOI: 10.2144/00286ir01.
- [340] E. Kalliri, P. K. Grzyska, R. P. Hausinger, *Kinetic and spectroscopic investigation of CoII, NiII, and N-oxalylglycine inhibition of the FeII/alpha-ketoglutarate dioxygenase, TauD*, *Biochem. Biophys. Res. Commun.* **2005**, 338(1), 191–197, DOI: 10.1016/j.bbrc.2005.08.223.
- [341] M. Biermeier, Philipps-Universität Marburg, **2016**.
- [342] P. K. Grzyska, M. J. Ryle, G. R. Monterosso, J. Liu, D. P. Ballou, R. P. Hausinger, *Steady-state and transient kinetic analyses of taurine/alpha-ketoglutarate dioxygenase: effects of oxygen concentration, alternative sulfonates, and active-site variants on the FeIV-oxo intermediate*, *Biochemistry* **2005**, 44(10), 3845–3855, DOI: 10.1021/bi048746n.
- [343] O. Sundheim, C. B. Vågbø, M. Bjørås, M. M. L. Sousa, V. Talstad, P. A. Aas, F. Drabløs, H. E. Krokan, J. A. Tainer, G. Slupphaug, *Human ABH3 structure and key residues for oxidative demethylation to reverse DNA/RNA damage*, *The EMBO journal* **2006**, 25(14), 3389–3397, DOI: 10.1038/sj.emboj.7601219.
- [344] K. D. Koehntop, S. Marimanikkuppam, M. J. Ryle, R. P. Hausinger, L. Que, *Self-hydroxylation of taurine/alpha-ketoglutarate dioxygenase*, *J. Biol. Inorg. Chem.* **2006**, 11(1), 63–72, DOI: 10.1007/s00775-005-0059-4.
- [345] T. F. Henshaw, M. Feig, R. P. Hausinger, *Aberrant activity of the DNA repair enzyme AlkB*, *J. Inorg. Biochem.* **2004**, 98(5), 856–861, DOI: 10.1016/j.jinorgbio.2003.10.021.
- [346] B. Nölting, *Methods in modern biophysics*; Springer, Heidelberg, New York, **2009**.
- [347] D. H.A. Corrêa, C. H.I. Ramos, *The use of circular dichroism spectroscopy to study protein folding, form and function*, *Afr. J. Biochem. Res.* **2009**(3), 164–173, DOI: 10.5897/AJBR/15798EB10962.
- [348] E. O. Gallimore, M. A. McDonough, Clifton I.J, C. J. Schofield, “WelO5 Small Molecule Halogenase with Ni(II) and 2-Oxoglutarate, PDB ID: 5J4R”, DOI: , **2017**.
- [349] S. Doehring, Philipps-Universität Marburg, **2017**.
- [350] P. S. Baran, J. M. Richter, *Direct coupling of indoles with carbonyl compounds: short, enantioselective, gram-scale synthetic entry into the hapalindole and fischerindole alkaloid families*, *J. Am. Chem. Soc.* **2004**, 126(24), 7450–7451, DOI: 10.1021/ja047874w.
- [351] J. M. Richter, Y. Ishihara, T. Masuda, B. W. Whitefield, T. Llamas, A. Pohjakallio, P. S. Baran, *Enantiospecific total synthesis of the hapalindoles, fischerindoles, and welwitindolinones*

Literature

- via a redox economic approach*, *J. Am. Chem. Soc.* **2008**, *130*(52), 17938–17954,
DOI: 10.1021/ja806981k.
- [352] T. J. Maimone, Y. Ishihara, P. S. Baran, *Scalable Total Syntheses of (-)-Hapalindole U and (+)-Ambiguine H*, *Tetrahedron* **2015**, *71*(22), 3652–3665, DOI: 10.1016/j.tet.2014.11.010.
- [353] P. S. Baran, J. M. Richter, *Enantioselective Total Syntheses of Welwitindolinone A and Fischerindoles I and G*, *J. Am. Chem. Soc.* **2005**, *127*(44), 15394–15396, DOI: 10.1021/ja056171r.
- [354] R. Myllylä, E.-R. Kuutti-Savolainen, K. I. Kivirikko, *The Role of Ascorbate in the Prolyl Hydroxylase Reaction*, *Biochem. Biophys. Res. Commun.* **1978**(2), 441–448,
DOI: 10.1016/0006-291X(78)91010-0.
- [355] B. Tadolini, *Iron Autoxidation in Mops and Hepes Buffers*, *Free Radical Res. Commun.* **2009**, *4*(3), 149–160, DOI: 10.3109/10715768709088100.
- [356] G. A. Behrens, A. Hummel, S. K. Padhi, S. Schätzle, U. T. Bornscheuer, *Discovery and Protein Engineering of Biocatalysts for Organic Synthesis*, *Adv. Synth. Catal.* **2011**, *353*(13), 2191–2215, DOI: 10.1002/adsc.201100446.
- [357] M. Bertoni, F. Kiefer, M. Biasini, L. Bordoli, T. Schwede, *Modeling protein quaternary structure of homo- and hetero-oligomers beyond binary interactions by homology*, *Sci. Rep.* **2017**, *7*(1), 10480, DOI: 10.1038/s41598-017-09654-8.
- [358] A. Waterhouse, M. Bertoni, S. Bienert, G. Studer, G. Tauriello, R. Gumienny, F. T. Heer, T. A. P. de Beer, C. Rempfer, L. Bordoli, R. Lepore, T. Schwede, *SWISS-MODEL*, *Nucleic Acids Res.* **2018**, DOI: 10.1093/nar/gky427.
- [359] P. Benkert, M. Biasini, T. Schwede, *Toward the estimation of the absolute quality of individual protein structure models*, *Bioinformatics* **2011**, *27*(3), 343–350, DOI: 10.1093/bioinformatics/btq662.
- [360] S. Bienert, A. Waterhouse, T. A. P. de Beer, G. Tauriello, G. Studer, L. Bordoli, T. Schwede, *The SWISS-MODEL Repository-new features and functionality*, *Nucleic Acids Res.* **2017**, *45*(D1), D313–D319, DOI: 10.1093/nar/gkw1132.
- [361] N. Guex, M. C. Peitsch, T. Schwede, *Automated comparative protein structure modeling with SWISS-MODEL and Swiss-PdbViewer*, *Electrophoresis* **2009**, *30 Suppl 1*, S162–73,
DOI: 10.1002/elps.200900140.
- [362] F. M. Ausubel, R. Brent, R. E. Kingston, D. D. Moore, J. G. Seidman, J. A. Smith, K. Struhl, *Current Protocols in Molecular Biology*; John Wiley & Sons, Inc, Hoboken, NJ, USA, **2001**.
- [363] E. Krieger, G. Vriend, *Models@Home*, *Bioinformatics* **2002**, *18*(2), 315–318.
- [364] C. G. Acevedo-Rocha, S. Hoebenreich, M. T. Reetz, *Iterative saturation mutagenesis: a powerful approach to engineer proteins by systematically simulating Darwinian evolution*, *Methods Mol. Biol.* **2014**, *1179*, 103–128, DOI: 10.1007/978-1-4939-1053-3_7.
- [365] A. E. Firth, W. M. Patrick, *Statistics of protein library construction*, *Bioinformatics* **2005**, *21*(15), 3314–3315, DOI: 10.1093/bioinformatics/bti516.

Literature

- [366] A. E. Firth, W. M. Patrick, *GLUE-IT and PEDEL-AA*, *Nucleic Acids Res.* **2008**, 36(Web Server issue), W281-5, DOI: 10.1093/nar/gkn226.
- [367] R. D. Kirsch, E. Joly, *An improved PCR-mutagenesis strategy for two-site mutagenesis or sequence swapping between related genes*, *Nucleic Acids Res.* **1998**, 26(7), 1848–1850, DOI: 10.1093/nar/26.7.1848.
- [368] L. Zheng, U. Baumann, J.-L. Reymond, *An efficient one-step site-directed and site-saturation mutagenesis protocol*, *Nucleic Acids Res.* **2004**, 32(14), e115, DOI: 10.1093/nar/gnh110.
- [369] Y. Xia, W. Chu, Q. Qi, L. Xun, *New insights into the QuikChange™ process guide the use of Phusion DNA polymerase for site-directed mutagenesis*, *Nucleic Acids Res.* **2015**, 43(2), e12, DOI: 10.1093/nar/gku1189.
- [370] L. Tang, H. Gao, X. Zhu, X. Wang, M. Zhou, R. Jiang, *Construction of “small-intelligent” focused mutagenesis libraries using well-designed combinatorial degenerate primers*, *BioTechniques* **2012**, 52(3), 149–158, DOI: 10.2144/000113820.
- [371] C. G. Acevedo-Rocha, M. T. Reetz, Y. Nov, *Economical analysis of saturation mutagenesis experiments*, *Sci. Rep.* **2015**, 5, DOI: 10.1038/srep10654.
- [372] V. Siitonen, B. Selvaraj, L. Niiranen, Y. Lindqvist, G. Schneider, M. Metsa-Ketela, *Divergent non-heme iron enzymes in the nogalamycin biosynthetic pathway*, *Proc. Natl. Acad. Sci. U.S.A.* **2016**, 113(19), 5251–5256, DOI: 10.1073/pnas.1525034113.
- [373] A. Rahim, P. Saha, K. K. Jha, N. Sukumar, B. K. Sarma, *Reciprocal carbonyl-carbonyl interactions in small molecules and proteins*, *Nat Comms* **2017**, 8(1), 78, DOI: 10.1038/s41467-017-00081-x.
- [374] R. N. V. K. Deepak, R. Sankararamakrishnan, *Unconventional N-H...N Hydrogen Bonds Involving Proline Backbone Nitrogen in Protein Structures*, *Biophys. J.* **2016**, 110(9), 1967–1979, DOI: 10.1016/j.bpj.2016.03.034.
- [375] M. R. Dunn, C. Otto, K. E. Fenton, J. C. Chaput, *Improving Polymerase Activity with Unnatural Substrates by Sampling Mutations in Homologous Protein Architectures*, *ACS Chem. Biol.* **2016**, 11(5), 1210–1219, DOI: 10.1021/acscchembio.5b00949.
- [376] L. A. McNeill, L. Bethge, K. S. Hewitson, C. J. Schofield, *A fluorescence-based assay for 2-oxoglutarate-dependent oxygenases*, *Anal. Biochem.* **2005**, 336(1), 125–131, DOI: 10.1016/j.ab.2004.09.019.
- [377] E. de Carolis, F. Chan, J. Balsevich, V. de Luca, *Isolation and Characterization of a 2-Oxoglutarate Dependent Dioxygenase Involved in the Second-to-Last Step in Vindoline Biosynthesis*, *Plant Physiol.* **1990**, 94(3), 1323–1329, DOI: 10.1104/pp.94.3.1323.
- [378] Z. Zhang, C. J. Schofield, J. E. Baldwin, P. Thomas, P. John, *Expression, purification and characterization of 1-aminocyclopropane-1-carboxylate oxidase from tomato in Escherichia coli*, *Biochem. J.* **1995**, 307(Pt 1), 77–85.
- [379] A. Thalhammer, Z. Bencokova, R. Poole, C. Loenarz, J. Adam, L. O’Flaherty, J. Schoedel, D. Mole, K. Giaslakiotis, C. J. Schofield, E. M. Hammond, P. J. Ratcliffe, P. J. Pollard,

Literature

- Human AlkB homologue 5 is a nuclear 2-oxoglutarate dependent oxygenase and a direct target of hypoxia-inducible factor 1alpha (HIF-1alpha)*, PloS one **2011**, 6(1), e16210, DOI: 10.1371/journal.pone.0016210.
- [380] C. W. M. Orr, *Studies on Ascorbic Acid. I. Factors Influencing the Ascorbate-Mediated Inhibition of Catalase **, Biochemistry **1967**, 6(10), 2995–3000, DOI: 10.1021/bi00862a004.
- [381] C. W. M. Orr, *Studies on Ascorbic Acid. II. Physical Changes in Catalase Following Incubation with Ascorbate or Ascorbate and Copper(II) **, Biochemistry **1967**, 6(10), 3000–3006, DOI: 10.1021/bi00862a005.
- [382] J. M. Chandlee, A. S. Tsaftaris, J. G. Scandalios, *Purification and partial characterization of three genetically defined catalases of maize*, Plant Sci. Lett. **1983**, 29(2-3), 117–131, DOI: 10.1016/0304-4211(83)90136-0.
- [383] N. Huwa, Master Thesis, Philipps-Universität Marburg, **2018**.
- [384] O. Shoji, T. Fujishiro, H. Nakajima, M. Kim, S. Nagano, Y. Shiro, Y. Watanabe, *Hydrogen peroxide dependent monooxygenations by tricking the substrate recognition of cytochrome P450BSbeta*, Angew. Chem. Int. Ed. **2007**, 46(20), 3656–3659, DOI: 10.1002/anie.200700068.
- [385] A. Grosdidier, V. Zoete, O. Michielin, *SwissDock, a protein-small molecule docking web service based on EADock DSS*, Nucleic Acids Res. **2011**, 39(Web Server issue), W270-7, DOI: 10.1093/nar/gkr366.
- [386] H. Mueller, Master Thesis, Philipps-Universität Marburg, **2017**.
- [387] M. Schmittel, M. Lal, R. Lal, M. Röck, A. Langels, Z. Rappoport, A. Basheer, J. Schlirf, H.-J. Deiseroth, U. Flörke, G. Gescheidt, *A comprehensive picture of the one-electron oxidation chemistry of enols, enolates and α -carbonyl radicals*, Tetrahedron **2009**, 65(52), 10842–10855, DOI: 10.1016/j.tet.2009.10.039.
- [388] K. L. Harris, R. E. S. Thomson, S. J. Strohmaier, Y. Gumulya, E. M. J. Gillam, *Determinants of thermostability in the cytochrome P450 fold*, Biochim. Biophys. Acta **2018**, 1866(1), 97–115, DOI: 10.1016/j.bbapap.2017.08.003.
- [389] C. M. Krest, E. L. Onderko, T. H. Yosca, J. C. Calixto, R. F. Karp, J. Livada, J. Rittle, M. T. Green, *Reactive intermediates in cytochrome p450 catalysis*, J. Biol. Chem. **2013**, 288(24), 17074–17081, DOI: 10.1074/jbc.R113.473108.
- [390] C. J. C. Whitehouse, S. G. Bell, L.-L. Wong, *P450(BM3) (CYP102A1)*, Chem. Soc. Rev. **2012**, 41(3), 1218–1260, DOI: 10.1039/c1cs15192d.
- [391] J. Rittle, M. T. Green, *Cytochrome P450 compound I*, Science **2010**, 330(6006), 933–937, DOI: 10.1126/science.1193478.
- [392] F. Hannemann, A. Bichet, K. M. Ewen, R. Bernhardt, *Cytochrome P450 systems—biological variations of electron transport chains*, Biochim. Biophys. Acta **2007**, 1770(3), 330–344, DOI: 10.1016/j.bbagen.2006.07.017.

Literature

- [393] R. Oshima, S. Fushinobu, F. Su, L. Zhang, N. Takaya, H. Shoun, *Structural evidence for direct hydride transfer from NADH to cytochrome P450_{nor}*, *J. Mol. Biol.* **2004**, 342(1), 207–217, DOI: 10.1016/j.jmb.2004.07.009.
- [394] A. Daiber, H. Shoun, V. Ullrich, *Nitric oxide reductase (P450_{nor}) from *Fusarium oxysporum**, *J. Inorg. Biochem.* **2005**, 99(1), 185–193, DOI: 10.1016/j.jinorgbio.2004.09.018.
- [395] L.-H. Wang, R. J. Kulmacz, *Thromboxane synthase*, *Prostaglandins Other Lipid Mediators* **2002**, 68-69, 409–422, DOI: 10.1016/S0090-6980(02)00045-X.
- [396] A. N. Grechkin, *Hydroperoxide lyase and divinyl ether synthase*, *Prostaglandins Other Lipid Mediators* **2002**, 68-69, 457–470, DOI: 10.1016/S0090-6980(02)00048-5.
- [397] N. Tijet, A. R. Brash, *Allene oxide synthases and allene oxides*, *Prostaglandins Other Lipid Mediators* **2002**, 68-69, 423–431, DOI: 10.1016/S0090-6980(02)00046-1.
- [398] I. Matsunaga, A. Ueda, N. Fujiwara, T. Sumimoto, K. Ichihara, *Characterization of the ybdT gene product of *Bacillus subtilis**, *Lipids* **1999**, 34(8), 841–846, DOI: 10.1007/s11745-999-0431-3.
- [399] I. Matsunaga, E. Kusunose, I. Yano, K. Ichihara, *Separation and partial characterization of soluble fatty acid alpha-hydroxylase from *Sphingomonas paucimobilis**, *Biochem. Biophys. Res. Commun.* **1994**, 201(3), 1554–1560, DOI: 10.1006/bbrc.1994.1881.
- [400] M. Girhard, S. Schuster, M. Dietrich, P. Dürre, V. B. Urlacher, *Cytochrome P450 monooxygenase from *Clostridium acetobutylicum**, *Biochem. Biophys. Res. Commun.* **2007**, 362(1), 114–119, DOI: 10.1016/j.bbrc.2007.07.155.
- [401] Y. Miura, A. J. Fulco, *(Omega -2) hydroxylation of fatty acids by a soluble system from *Bacillus megaterium**, *J. Biol. Chem.* **1974**, 249(6), 1880–1888.
- [402] P. C. Cirino, F. H. Arnold, *Protein engineering of oxygenases for biocatalysis*, *Curr. Opin. Chem. Biol.* **2002**, 6(2), 130–135, DOI: 10.1016/S1367-5931(02)00305-8.
- [403] R. T. Ruettinger, L.-P. Wen, A. J. Fulco, *Coding Nucleotide, 5' Regulatory, and Deduced Amino Acid Sequences of P-450_{BM-3}, a Single Peptide Cytochrome P-450:NADPH-P-450 Reductase from *Bacillus megaterium**, *J. Biol. Chem.* **1989**, 264(19), 10987–10995.
- [404] L. O. Narhi, A. J. Fulco, *Characterization of a catalytically self-sufficient 119,000-dalton cytochrome P-450 monooxygenase induced by barbiturates in *Bacillus megaterium**, *J. Biol. Chem.* **1986**, 261(16), 7160–7169.
- [405] S. S. Boddupalli, R. W. Estabrook, J. A. Peterson, *Fatty Acid Monooxygenation by Cytochrome P-450_{BM-3}*, *J. Biol. Chem.* **1990**, 265(8), 4233–4239.
- [406] J. H. Capdevila, S. Wei, C. Helvig, J. R. Falck, Y. Belosludtsev, G. Truan, S. E. Graham-Lorence, J. A. Peterson, *The Highly Stereoselective Oxidation of Polyunsaturated Fatty Acids by Cytochrome P450_{BM-3}*, *J. Biol. Chem.* **1996**, 271(37), 22663–22671, DOI: 10.1074/jbc.271.37.22663.

Literature

- [407] I. F. Sevrioukova, H. Li, H. Zhang, J. A. Peterson, T. L. Poulos, *Structure of a cytochrome P450-redox partner electron-transfer complex*, Proc. Natl. Acad. Sci. U.S.A. **1999**, 96(5), 1863–1868.
- [408] C. F. Oliver, S. Modi, M. J. Sutcliffe, W. U. Primrose, L. Y. Lian, G. C. Roberts, *A single mutation in cytochrome P450 BM3 changes substrate orientation in a catalytic intermediate and the regiospecificity of hydroxylation*, Biochemistry **1997**, 36(7), 1567–1572, DOI: 10.1021/bi962826c.
- [409] M. Spinck, Master Thesis, Philipps-Universität Marburg, **2016**.
- [410] C. Ritter, N. Nett, C. G. Acevedo-Rocha, R. Lonsdale, K. Kräling, F. Dempwolff, S. Hoebenreich, P. L. Graumann, M. T. Reetz, E. Meggers, *Bioorthogonal Enzymatic Activation of Caged Compounds*, Angew. Chem. Int. Ed. **2015**, 54(45), 13440–13443, DOI: 10.1002/anie.201506739.
- [411] R. Agudo, G.-D. Roiban, M. T. Reetz, *Achieving regio- and enantioselectivity of P450-catalyzed oxidative CH activation of small functionalized molecules by structure-guided directed evolution*, ChemBioChem **2012**, 13(10), 1465–1473, DOI: 10.1002/cbic.201200244.
- [412] G.-D. Roiban, R. Agudo, A. Ilie, R. Lonsdale, M. T. Reetz, *CH-activating oxidative hydroxylation of 1-tetralones and related compounds with high regio- and stereoselectivity*, Chem. Commun. **2014**, 50(92), 14310–14313, DOI: 10.1039/C4CC04925J.
- [413] R. Agudo, G.-D. Roiban, R. Lonsdale, A. Ilie, M. T. Reetz, *Biocatalytic route to chiral acyloins*, J. Org. Chem. **2015**, 80(2), 950–956, DOI: 10.1021/jo502397s.
- [414] S. Kille, *Flavoproteins in directed evolution : iterative CASTing to evolve YqjM and P450BM3*.
- [415] S. Kille, F. E. Zilly, J. P. Acevedo, M. T. Reetz, *Regio- and stereoselectivity of P450-catalysed hydroxylation of steroids controlled by laboratory evolution*, Nature chemistry **2011**, 3(9), 738–743, DOI: 10.1038/nchem.1113.
- [416] A. Bar-Even, E. Noor, Y. Savir, W. Liebermeister, D. Davidi, D. S. Tawfik, R. Milo, *The moderately efficient enzyme: evolutionary and physicochemical trends shaping enzyme parameters*, Biochemistry **2011**, 50(21), 4402–4410, DOI: 10.1021/bi2002289.
- [417] S. A. Shepherd, C. Karthikeyan, J. Latham, A.-W. Struck, M. L. Thompson, Menon, Binuraj R. K, M. Q. Styles, C. Levy, D. Leys, J. Micklefield, *Extending the biocatalytic scope of regiocomplementary flavin-dependent halogenase enzymes*, Chem. Sci. **2015**, 6(6), 3454–3460, DOI: 10.1039/C5SC00913H.
- [418] J. T. Payne, C. B. Poor, J. C. Lewis, *Directed Evolution of RebH for Site-Selective Halogenation of Large Biologically Active Molecules*, Angew. Chem. Int. Ed. **2015**, DOI: 10.1002/anie.201411901.
- [419] F. Li, X. Zhang, H. Renata, *Enzymatic CH functionalizations for natural product synthesis*, Curr. Opin. Chem. Biol. **2018**, 49, 25–32, DOI: 10.1016/j.cbpa.2018.09.004.

- [420] K. M. Polizzi, A. S. Bommarius, J. M. Broering, J. F. Chaparro-Riggers, *Stability of biocatalysts*, *Curr. Opin. Chem. Biol.* **2007**, *11*(2), 220–225, DOI: 10.1016/j.cbpa.2007.01.685.
- [421] T. J. Magliery, *Protein stability*, *Curr. Opin. Struct. Biol.* **2015**, *33*, 161–168, DOI: 10.1016/j.sbi.2015.09.002.
- [422] M. Lehmann, L. Pasamontes, S. F. Lassen, M. Wyss, *The consensus concept for thermostability engineering of proteins*, *Biochim. Biophys. Acta* **2000**, *1543*(2), 408–415, DOI: 10.1016/S0167-4838(00)00238-7.
- [423] B. Steipe, B. Schiller, A. Plückthun, S. Steinbacher, *Sequence statistics reliably predict stabilizing mutations in a protein domain*, *J. Mol. Biol.* **1994**, *240*(3), 188–192, DOI: 10.1006/jmbi.1994.1434.
- [424] B. Borgo, J. J. Havranek, *Automated selection of stabilizing mutations in designed and natural proteins*, *Proc. Natl. Acad. Sci. U.S.A.* **2012**, *109*(5), 1494–1499, DOI: 10.1073/pnas.1115172109.
- [425] R. Jacak, A. Leaver-Fay, B. Kuhlman, *Computational protein design with explicit consideration of surface hydrophobic patches*, *Proteins* **2012**, *80*(3), 825–838, DOI: 10.1002/prot.23241.
- [426] A. Korkegian, M. E. Black, D. Baker, B. L. Stoddard, *Computational thermostabilization of an enzyme*, *Science* **2005**, *308*(5723), 857–860, DOI: 10.1126/science.1107387.
- [427] M. S. Lawrence, K. J. Phillips, D. R. Liu, *Supercharging proteins can impart unusual resilience*, *J. Am. Chem. Soc.* **2007**, *129*(33), 10110–10112, DOI: 10.1021/ja071641y.
- [428] A. Goldenzweig, M. Goldsmith, S. E. Hill, O. Gertman, P. Laurino, Y. Ashani, O. Dym, T. Unger, S. Albeck, J. Prilusky, R. L. Lieberman, A. Aharoni, I. Silman, J. L. Sussman, D. S. Tawfik, S. J. Fleishman, *Automated Structure- and Sequence-Based Design of Proteins for High Bacterial Expression and Stability*, *Molecular cell* **2016**, *63*(2), 337–346, DOI: 10.1016/j.molcel.2016.06.012.
- [429] T. A. Whitehead, A. Chevalier, Y. Song, C. Dreyfus, S. J. Fleishman, C. de Mattos, C. A. Myers, H. Kamisetty, P. Blair, I. A. Wilson, D. Baker, *Optimization of affinity, specificity and function of designed influenza inhibitors using deep sequencing*, *Nat. Biotechnol.* **2012**, *30*(6), 543–548, DOI: 10.1038/nbt.2214.
- [430] colby.edu, “Solubility of Oxygen in Water”, DOI: , **2018**.
- [431] Engineering ToolBox, “Oxygen - Solubility in Fresh Water and Sea Water”, DOI: , **2005**.
- [432] N. Nett, Dissertation, Philipps-Universität Marburg, **2017**.
- [433] F. William Studier, *Non-inducing media*.
- [434] K. Mullis, F. Faloona, S. Scharf, R. Saiki, G. Horn, H. Erlich, *Specific Enzymatic Amplification of DNA In Vitro*, *Cold Spring Harb Symp Quant Biol* **1986**(51), 263–273.
- [435] A. Keefe, D. Wilson, *Random Mutagenesis by PCR*.
- [436] L. Pritchard, D. Corne, D. Kell, J. Rowland, M. Winson, *A general model of error-prone PCR*, *J. theor. Biol* **2005**, *234*(4), 497–509, DOI: 10.1016/j.jtbi.2004.12.005.

- [437] Sambrook J. Russel D.W, *The Condensed Protocols from Molecular Cloning: A Laboratory Manual*, CSHL Press, NY, 2006.
- [438] E. Lottspeich, Ed, *Bioanalytik*; Springer Spektrum Verlag, **2012**.
- [439] T. B. Fitzpatrick, N. Amrhein, P. Macheroux, *Characterization of YqjM, an Old Yellow Enzyme homolog from Bacillus subtilis involved in the oxidative stress response*, J. Biol. Chem. **2003**, 278(22), 19891–19897, DOI: 10.1074/jbc.M211778200.
- [440] B. J. Smith, *SDS Polyacrylamide Gel Electrophoresis of Proteins*, Methods Mol. Biol. **1984**, 1, 41–55, DOI: 10.1385/0-89603-062-8:41.
- [441] W. Kabsch, *XDS*, Acta Crystallogr. D Biol. Crystallogr. **2010**, 66(Pt 2), 125–132, DOI: 10.1107/S0907444909047337.
- [442] M. D. Winn, C. C. Ballard, K. D. Cowtan, E. J. Dodson, P. Emsley, P. R. Evans, R. M. Keegan, E. B. Krissinel, A. G. W. Leslie, A. McCoy, S. J. McNicholas, G. N. Murshudov, N. S. Pannu, E. A. Potterton, H. R. Powell, R. J. Read, A. Vagin, K. S. Wilson, *Overview of the CCP4 suite and current developments*, Acta Crystallogr. D Biol. Crystallogr. **2011**, 67(Pt 4), 235–242, DOI: 10.1107/S0907444910045749.
- [443] A. J. McCoy, R. W. Grosse-Kunstleve, P. D. Adams, M. D. Winn, L. C. Storoni, R. J. Read, *Phaser crystallographic software*, J. Appl. Crystallogr. **2007**, 40(Pt 4), 658–674, DOI: 10.1107/S0021889807021206.
- [444] P. D. Adams, P. V. Afonine, G. Bunkóczi, V. B. Chen, I. W. Davis, N. Echols, J. J. Headd, L.-W. Hung, G. J. Kapral, R. W. Grosse-Kunstleve, A. J. McCoy, N. W. Moriarty, R. Oeffner, R. J. Read, D. C. Richardson, J. S. Richardson, T. C. Terwilliger, P. H. Zwart, *PHENIX*, Acta Crystallogr. D Biol. Crystallogr. **2010**, 66(Pt 2), 213–221, DOI: 10.1107/S0907444909052925.
- [445] P. Emsley, K. Cowtan, *Coot*, Acta Crystallogr. D Biol. Crystallogr. **2004**, 60(Pt 12 Pt 1), 2126–2132, DOI: 10.1107/S0907444904019158.
- [446] V. B. Chen, W. B. Arendall, J. J. Headd, D. A. Keedy, R. M. Immormino, G. J. Kapral, L. W. Murray, J. S. Richardson, D. C. Richardson, *MolProbity*, Acta Crystallogr. D Biol. Crystallogr. **2010**, 66(Pt 1), 12–21, DOI: 10.1107/S0907444909042073.
- [447] Huang, C. C, Couch, G.S, Pettersen, E.F, Ferrin, T.E, *Chimera: An Extensible Molecular Modeling Application Constructed Using Standard Components*, Pacific Symposium on Bio-computing **1**, 1996(724).
- [448] E. Vázquez-Figueroa, J. Chaparro-Riggers, A. S. Bommarius, *Development of a thermostable glucose dehydrogenase by a structure-guided consensus concept*, ChemBioChem **2007**, 8(18), 2295–2301, DOI: 10.1002/cbic.200700500.
- [449] W. L. F. Armarego, C. L. L. Chai, *Purification of laboratory chemicals*; Elsevier/Butterworth-Heinemann, Amsterdam, Boston, **2009**.

Literature

- [450] D. R. Laplace, B. Verbraeken, K. van Hecke, J. M. Winne, *Total synthesis of (+/-)-frondosin B and (+/-)-5-epi-liphagal by using a concise (4+3) cycloaddition approach*, *Chem. Eur. J.* **2014**, 20(1), 253–262, DOI: 10.1002/chem.201303273.

Curriculum Vitae Sabine Düwel

Geburtsdatum/-ort 21.01.1992, in Saarbrücken

Nationalität deutsch

Ausbildung

09/2015 - 11/2018 **Promotion** im Bereich der Chemischen Biologie, Fachbereich Chemie, Philipps-Universität Marburg, Arbeitskreis Dr. S. Höbenreich „Directed Evolution of an Fe^{II}-Dependent Halogenase for Asymmetric C(sp³)-H Chlorination“

10/2013 - 07/2015 **M. Sc. in Chemie**, Philipps-Universität Marburg, Abschlussnote 1.0
Masterarbeit im Bereich der Biokatalyse, Arbeitskreis, Dr. S. Höbenreich „Exploring the Evolvability of Ene-Reductases TsER, DrER and RmER towards Activity“

10/2010 - 09/2013 **B. Sc. in Chemie**, Universität des Saarlandes, Abschlussnote: 2.2
Bachelorarbeit im Bereich der Biochemie, Arbeitskreis Prof. Dr. E. Heinzle: „Synthese von Luminmiden mit permeabilisierten Zellen von *E. coli*“

08/2002 - 06/2010 **Abitur**, Gymnasium am Schloss, Saarbrücken, Abschlussnote 2.1